Fruiting body development of *Coprinopsis cinerea*: Cytology and regulatory factors

Dissertation
In Partial Fulfillment of the Requirements for the Degree
Doctor rerum naturalium (Dr. rer. nat.)
Within the doctoral program Faculty of Forest Sciences and Forest Ecology of the Graduate Forest and Agriculture Science (GFA)
Georg-August-Universität Göttingen

Submitted by
Shanta Subba
from Sikkim, India

Göttingen, 2022

Thesis committee

Prof. Dr. Ursula Kües
Georg August University Göttingen
Büsgen-Institut
Abt. Molekulare Holzbiotechnologie und Technische Mykologie
Büsgenweg 2, 37077 Göttingen, Germany

Prof. Dr. Stefanie Pöggeler
Georg August University Göttingen
Institute of Microbiology and Genetics
Dept. Genetics of Eukaryotic Microorganisms
Grisebachstr.8, 37077 Göttingen, Germany

PD Dr. Markus Euring
Georg August University Göttingen
Abt. Holztechnologie und Holzwerkstoffe
Büsgenweg 2
37077 Göttingen

Members of examination board

1st Examiner
Prof. Dr. Ursula Kües

2nd Examiner
Prof. Dr. Stefanie Pöggeler

Further members of examination board

Prof. Dr. Oliver Gailing
Georg-August-University Göttingen
Büsgen-Institute
Forest Genetics and Forest Tree Breeding
Büsgenweg 2, D-37077 Göttingen

PD Dr. Markus Euring

1. Gutachter: Prof. Dr. Ursula Kües

2. Gutachter: Prof. Dr. Stefanie Pöggeler

Tag der mündlichen Prüfung: 5th May 2021

In memory of my loving dad

Table of Contents

Acknowledgement

Firstly, I want to express my sincere gratitude to my advisor Prof. Dr. Ursula Kües for giving me an opportunity to work in her group and thank her for support, patience and motivation during my PhD study. Her guidance helped me throughout my research time and writing of this thesis. Besides my advisor, I would like to thank my previous and current thesis committee members Prof. Dr. Stefan Schütz, Prof. Dr. Stefanie Pöggeler and PD Dr. Markus Euring for their insightful comments and encouragement during my committee meetings and also being members of my examination board. My sincere thanks to Prof. Oliver Gailing for accepting to be a member of my examination board.

I would like to thank Dr. Bastian Dörnte, Dr. Kiran Kumar Lakkireddy and Mr. Weeradej Khonsuntia for their precious support in the molecular biology lab. Without their support it would not be possible to conduct this research. I wish to thank Late Mrs. Karin Lange for her technical support in microscopy. I also want to thank Dr. Andrzej Majcherczyk, Dr. Bastian Dörnte and Mr. Mojtaba Zomorrodi for the proteomics work and Dr. Botond Hegedüs and Dr. László Nagy for performing whole genome sequencing of the two dark stipe mutant strains 7K17 and B1918 at the Institute of Biochemistry in Hungary.

Further, I thank all my former and current fellow lab mates and also the former colleagues who worked with *Coprinopsis cinerea*. In particular, I am grateful to Mr. Marco Winkler for doing outstanding sectioning and staining work. I want to thank Mr. Michael Unger for correcting my German version of summary.

Lastly, I would like to thank my parents, my boyfriend and my friends for supporting me spiritually throughout my PhD and my life in general.

Summary

Coprinopsis cinerea, the gray shagged ink-cap, is a saprotrophic edible basidiomycete that naturally grows on horse dung. Despite richness in nutrients, the typical fast autolysis of the cap of the mushroom during maturation lowers the potential consumption value. In the field of science, for more than a century the fungus served as an excellent model mushroom for studying fungal sex and mating types, the fruiting body developmental process, hyphal growth with asexual sporulation (oidiation) on primary and secondary mycelia (sterile monokaryons and fertile dikaryons), physiology and general genetics in basidiomycetes.

Fruiting body development in *C. cinerea* takes place on dikaryons (mycelia after mating of two compatible monokaryons) at 25 °C and follows a conserved scheme defined by day and night phases, with well predictable distinct stages over the time. It thus takes 7 days to complete the fruiting pathway. The differentiation process starts with the formation of initial hyphal aggregations called primary hyphal knots (Pks) generated in the dark on Day 0 of the fruiting pathway, followed by light-induced compact aggregates, termed secondary hyphal knots (Sks) on Day 1 in which subsequently primordial stipe and cap tissues differentiate. When no light signal is received, Pks will be differentiated into multicellular dormant resting bodies called sclerotia instead of developing into a light-induced fruiting body. Primordium development starting from Sks over the stages P1 to P5 takes five days to culminate on Day 6 of development in karyogamy and meiosis within the basidia and subsequent basidiospore production which parallels fruiting body maturation (stipe elongation and cap expansion). Mature fruiting bodies autolyze on Day 7 of the standard fruiting pathway to release the basidiospores in liquid droplets to the ground.

Primordia of *C. cinerea* are the complex multicellular structures during which the formation, the differentiation and the degeneration of various types of cells and tissues take place over the time of development to form a complete and complex multicellular fruiting structure from a simple hyphal knot. Such a fruiting process is strictly controlled by various environmental and genetic factors that have a direct influence on the morphological characteristics of the fungus. Despite extensive work in the past, it is still mostly unknown what constitutes the complex multicellularity of the fungus. The self-compatible homokaryotic strain AmutBmut with an established genome sequence was used to conduct the experiments in this thesis. The strain is well accessible to classical and molecular genetics, by transformation of asexual spores (oidia) produced in light. By mutations in the two mating-type loci *A* and *B* it mimics a dikaryon and is therefore able to fruit without mating to another compatible monokaryon. Individual genes in the process of fruiting bogy development can thus be studied in a throughout homogenic haploid background.

This research focuses on understanding the complexities in fruiting body formation, using histochemical and microscopy techniques. The study provides detailed morphological

descriptions on the initial hyphal knot stages and the different primordial stages (P1 to P5) which proceed to form a mature mushroom were exactly defined regarding time scale and morphology. Within a typical culture, hundreds of Sks are initiated. During the further developmental processes, at every stage substantial parts of structures abandon in development and only few reach fruiting body maturation. Abortive structures with slightly grayish dry caps can be distinguished from continuing structures by pinkish, fresh looking caps excreting liquid. Furthermore, to understand the complex cytological processes during stipe and cap development, fresh ongoing stages P1 to P5 primordia were identified, harvested and provided for a first proteome pilot study that detected many proteins known to contribute to specific steps in the development. Further, liquid droplets excreted from the actively growing primordia were collected and provided for a proteomic analysis which revealed within the droplets many secreted proteins with potential defense functions against bacteria, fungi, small animals and viruses.

This study in addition examined how environmental factors such as light and dark, and aeration and CO_2 control the entire fruiting process. Changes in these factors can alter the normal phenotypes of the primordial stages in the standard fruiting pathway. In the dark and under increased CO_2, homokaryon AmutBmut as wildtype strain will form so-called “dark stipes” with length-extended stipes and underdeveloped caps. Four mutants in genes *dst1*, *dst2*, *dst3* and *dst4* produce such dark stipes under standard fruiting conditions and were analyzed in morphology. *dst1* and *dst2* are UV and REMI mutants and were already known to have defects in the WC1 photoreceptor and a FAD/FMN-containing dehydrogenase, respectively. These mutants are blind at the Sk stage and form dark stipes under standard fruiting conditions and are also blind with respect to loss of light-induced oidiation. UV mutant 7K17 (*dst3*) and REMI mutant B1918 (*dst4*) of homokaryon AmutBmut have dark stipe defects initiating formation later in the development at the stages P3 and P4, respectively, with dark stipes seen at the stages P4 and P5. However, light regulation of oidia production was normal in mutant B1918 and also still active in mutant 7K17 but with lower effectivity, indicating that these mutants were not per se blind. Whole-genome sequencing identified each two interesting mutations in these strains related to TCA (tricarboxylic acid) cycle, in pyruvate dehydrogenase (PDH) and acetolactate synthase (ILV2) in 7K17 and in a citrate synthase and in subunit CSN5 of the Cop9 signalosome in B1918. Both mutants, therefore, are possibly blocked in feeding acetyl into the TCA cycle. The Cop9 (for constitutive photomorphogenesis 9) signalosome coordinates light and respiratory activities with developmental processes and is conserved in all eukaryotes.

A further focus was given to genes participating in initiation of the fruiting pathway and primordial tissue formation, with a specific family of *NWD2* genes for small NTPase. *NWD2* genes encode proteins with a NACHT domain, an evolutionarily conserved domain that serves in signal transduction and is named after four different types of P-loop NTPases found in

animals and fungi (NAIP, CIITA, HET-E, and TP1). Genome searches in *C. cinerea* found in total 36 different *NWD2* genes which cluster into 7 different subgroups (A to G) in an evolutionary tree of all the encoded NWD2 proteins. Few other individual *Agaricomycetes* (*Amanita muscaria*, *Agaricus bisporus*, *C. cinerea*, *Galerina marginata*, *Gymnopus luxurians*, *Hebeloma cylindrosporum*, *Hypholoma sublateritium*, *Hypsizygus marmoreus*, *Laccaria amethystina*, *Moniliophthora roreri*, and *Laccaria bicolor*) from different families have related genes while their proteins cluster in species-specific manner. Accordingly, duplication and modification of genes of NWD2 proteins have taken place within the fungi. Presence of transposable elements, location of the duplicated genes in the unconserved regions of chromosomes close to telomeres and accumulation of a maximum number of genes in the *C. cinerea* shortest, little conserved and likely youngest chromosome together with the random distribution in a few other fungal species suggest horizontal gene transfer during evolution at the level of speciation. In previous studies, one specific *NWD2* gene from subgroup A was found by transformation to suppress the fruiting defect and other unusal phenotypes in a *pkn* defective mutant Proto159. This mutant, was isolated of AmutBmut after protoplasting and regeneration of oidia, is unable to produce Pks, has a slower and thinner mycelial growth than homokaryon AmutBmut and stains the agar with submerged mycelium of cultures brown. The introduction of other *NWD2* genes of subgroup A into mutant Proto159 by transformation in this study variably altered mutant mycelial properties, blocked the brown staining of submerged mycelium and the agar, and, most importantly, induced primary hyphal knot and sclerotia formation in the vegetative mycelium and also lead to the production of fruiting bodies.

Zusammenfassung

Coprinopsis cinerea, der wollstielige Tintling, ist ein saprotropher essbarer Basidiomycet, der natürlicherweise auf Pferdemist wächst. Trotz seines guten Nährstoffgehaltes reduziert die arttypische schnelle Autolyse der Hüte des Pilzes während seiner Reifung einen potenziellen Verbrauchswert. Auf dem Gebiet der Wissenschaft dient der Pilz seit mehr als einem Jahrhundert als ausgezeichneter Modellpilz für Studien über sexuelle Prozesse und Kreuzungstypen von Pilzen, Entwicklungsprozesse des Fruchtkörpers, Hyphenwachstum mit asexueller Sporulation (Oidiation) von primären und sekundären Myzelien (sterile Monokaryen und fertile Dikaryen), Physiologie und allgemeine Genetik bei Basidiomyceten.

Die Entwicklung des Fruchtkörpers in *C. cinerea* erfolgt an Dikaryen (Myzel nach Paarung zweier kompatibler Monokaryen) bei 25 °C und folgt einem konservierten Schema, das durch Tag- und Nachtphasen definiert ist, mit gut vorhersagbaren definierten Stadien über die Zeit. Es dauert insgesamt sieben Tage, um den Prozess der Fruchtkörperentwicklung zu vollenden. Der Differenzierungsprozess beginnt mit der Bildung von anfänglichen Hyphenaggregaten, die primäre Hyphenknoten (Pks) genannt und am Tag 0 der Entwicklung im Dunkeln erzeugt werden, gefolgt darauf von der Bildung lichtinduzierter kompakter Aggregate am Tag 1, die als sekundäre Hyphenknoten (Sks) bezeichnet werden und anschließend in ihrem Innern primordiales Stiel- und Hutgewebe differenzieren. Wenn kein Lichtsignal empfangen wird, werden die Pks in vielzellige Dauerstadien, sogenannte Sklerotien, ausdifferenziert, anstatt sich in lichtinduzierte Fruchtkörper zu entwickeln. Die Primordiumentwicklung von Sks über die primordialen Stadien P1 bis P5 dauert fünf Tage, um dann am 6. Tag der Entwicklung in Karyogamie und Meiose innerhalb der Basidien mit anschließender Basidiosporenproduktion zu gipfeln, die parallel zur Fruchtkörperreifung (Stielstreckung und Hutöffnung) verläuft. Reife Fruchtkörper autolysieren ihre Hüte am Tag 7 des Standardentwicklungsweges, um die Basidiosporen in zu Boden fallenden flüssigen Tröpfchen freizusetzen.

Primordien von *C. cinerea* sind komplexe vielzellige Strukturen, in denen die Bildung, Differenzierung und Degeneration verschiedener Arten von Zellen und Geweben im Laufe der Entwicklung stattfinden, um aus einem einfachen Hyphenknoten eine vollständige komplexe vielzellige Fruchtkörperstruktur zu bilden. Ein solcher Fruchtungsprozess wird in strikter Weise durch verschiedene Umwelt- und genetische Faktoren gesteuert, die einen direkten Einfluss auf die ablaufenden morphologischen Entwicklungen des Pilzes haben. Trotz umfangreicher Untersuchungen in der Vergangenheit sind die biologischen Grundlagen für die komplexe Vielzelligkeit des Pilzes noch weitgehend unbekannt. Der sequenzierte selbstkompatible homokaryotische Stamm AmutBmut wurde in dieser Arbeit für Untersuchungen eingesetzt. Der Stamm ist für klassische Genetik und molekular durch DNA-Transformation von im Licht produzierten asexuellen Sporen (Oidia) gut zugänglich. Durch Mutationen in den beiden Kreuzungstyporten

A und *B* imitiert der genetisch einheitliche Stamm ein Dikaryon und kann daher Fruchtkörper produzieren, ohne sich mit einem sexuell-kompatiblen Monokaryon paaren zu müssen. Individuelle Gene des Prozesses der Fruchtentwicklung können somit in einem einheitlichen haploiden Hintergrund untersucht werden.

Die Forschung dieser Arbeit konzentriert sich auf das Verständnis der Komplexität bei der Bildung von Fruchtkörpern unter Verwendung von histochemischen und mikroskopischen Techniken. Die Studie liefert detaillierte morphologische Beschreibungen der anfänglichen Hyphenknotenstadien, und der folgenden verschiedenen primordialen Stadien (P1 bis P5), die weiter zur Bildung eines reifen Pilzes führen und die hinsichtlich ihres Zeitpunkts und ihrer Morphologie genau definiert wurden. Typischerweise werden innerhalb einer normalen Kultur Hunderte von Sks initiiert. Während der weiteren Entwicklungsprozesse geben in jeder Phase wesentliche Anteile an Strukturen ihre Entwicklung auf und nur wenige reifen am Ende zu vollständigen geöffneten Fruchtkörpern. Abortive Strukturen unterscheiden sich von den sich noch weiterentwickelnden aktiven Strukturen durch leicht graugefärbte und trocken erscheinende Hüte im Vergleich zu leicht rosafarbenen und frisch wirkenden Hüten, die Flüssigkeit ausscheiden können. Um die komplexen zytologischen Prozesse während der laufenden Entwicklung von Stiel- und Hutgeweben zu verstehen, wurden die aktiven Primordienstadien P1 bis P5 identifiziert, geerntet und für eine erste Proteom-Pilotstudie bereitgestellt, mit der eine Reihe von Proteinen nachgewiesen wurden, von denen bekannt ist, dass sie zu bestimmten Entwicklungsschritten beitragen. Ferner wurden Flüssigkeitströpfchen, die von aktiv wachsenden Primordien ausgeschieden wurden, gesammelt und für eine Proteomanalyse bereitgestellt, die in ihnen viele sekretierte Proteine mit potenziellen Abwehrfunktionen gegen Bakterien, Pilze, Kleintiere und Viren entdeckte.

In dieser Studie wurde außerdem untersucht, wie Umweltfaktoren wie Licht und Dunkelheit sowie Belüftung und CO_2 den gesamten Fruchtkörperentwicklungsprozess steuern. Änderungen dieser Faktoren können die normalen Phänotypen der Primordienstadien im Standardfruchtkörperentwicklungsweg verändern. Im Dunkeln und unter erhöhter CO_2-Konzentration bildet Homokaryon AmutBmut als Wildtyp-Stamm sogenannte „dark stipes“ mit verlängerten Stielen und unterentwickelten Hüten. Vier Mutanten mit den Genen *dst1*, *dst2*, *dst3* und *dst4* produzieren solche abnormalen Stiele unter Standardfruchtungsbedingungen und wurden in ihrer Morphologie analysiert. *dst1* und *dst2* sind UV- und REMI-Mutanten mit bekannten Defekten im WC1-Photorezeptor bzw. in einer FAD/FMN-haltigen Dehydrogenase. Diese Mutanten sind im Sk-Stadium blind und bilden „dark stipes“ unter Standardfruchtungsbedingungen und sie sind blind in Bezug auf den Verlust der lichtinduzierten Oidiation. Die UV-Mutante 7K17 (*dst3*) und die REMI-Mutante B1918 (*dst4*) von Homokaryon AmutBmut wiesen „dark stipe“-Defekte auf, die die Bildung abnormaler Stiele in der Entwicklungskette in den Stadien P3 bzw. P4 initiieren, wobei die „dark stipes“ dann später in den Zeitpunkten der

Stadien P4 und P5 zu sehen sind. Die Lichtregulation der Oidia-Produktion war degegen in der Mutante B1918 normal und auch in der Mutante 7K17 noch aktiv, jedoch mit geringerer Wirksamkeit, was darauf hinweist, dass diese Mutanten per se nicht blind waren. Die Sequenzierung ihrer Genome identifizierte jeweils zwei interessante Mutationen in diesen Stämmen, die mit dem TCA-Zyklus (Tricarbonsäurezyklus) zusammenhängen, in der Pyruvatdehydrogenase (PDH) und der Acetolactat-Synthase (ILV2) in Stamm 7K17 und in einer Citrat-Synthase und in der Untereinheit CSN5 des Cop9-Signalosoms in Stamm B1918. Beide Mutanten sind daher möglicherweise im Einspeisen von Acetyl in den TCA-Zyklus blockiert. Das Cop9 (für „constitutive photomorphogenesis 9“) Signalosom koordiniert Licht- und Atmungsaktivitäten mit pilzlichen Entwicklungsprozessen und ist in allen Eukaryoten konserviert.

Ein weiterer Schwerpunkt in dieser Arbeit lag auf Genen, die an der Initiierung des Fruchtkörperentwicklungsweges und der Bildung von Primordiengewebe beteiligt sind, speziell auf einer spezifischen Familie von *NWD2*-Genen für kleine NTPasen. *NWD2*-Gene codieren für Proteine mit einer NACHT-Domäne, einer evolutionär konservierten Domäne, die der Signalübertragung dient und nach vier verschiedenen Arten von P-Loop-NTPasen benannt ist, die in Tieren und Pilzen gefunden werden (NAIP, CIITA, HET-E und TP1). Bei einer Suche im Genom wurden in *C. cinerea* insgesamt 36 verschiedene *NWD2*-Gene gefunden, die in einem phylogenetischen Baum aller kodierten NWD2-Proteine in sieben verschiedenen Untergruppen (A bis G) clustern. Nur wenige andere einzelne Agaricomyceten (*Amanita muscaria*, *Agaricus bisporus*, *C. cinerea*, *Galerina marginata*, *Gymnopus luxurians*, *Hebeloma cylindrosporum*, *Hypholoma sublateritium*, *Hypsizygus marmoreus*, *Laccaria amethystina*, *Moniliophthora roreri* und *Laccaria bicolor*) besitzen Familien mit ähnlichen Genen, während die codierten Proteine in phylogenetischen Analysen in artspezifischer Weise gruppTieren. Dementsprechend haben Duplikationen und Modifikationen von Genen von NWD2-Proteinen innerhalb der Pilzarten stattgefunden. Vorhandensein transponierbarer Elemente, Positionen der duplizierten Gene in den nicht konservierten Regionen von Chromosomen in der Nähe von Telomeren und die Akkumulation einer höchsten Anzahl von solchen Genen im kürzesten, wenig konservierten und wahrscheinlich jüngsten Chromosom von *C. cinerea* zusammen mit einer nicht konservierten Verteilung in einigen anderen Pilzarten deuten auf einen horizontalen Gentransfer während der Evolution auf der Ebene der Artenentstehung hin. In früheren Arbeiten wurde durch Transformation festgestellt, dass ein spezifisches *NWD2*-Gen aus Untergruppe A einen Defekt in der Initiation der Fruchtkörperbildung und andere ungewöhnliche Phänotypen in einer *pkn*-defekten Mutante Proto159 unterdrückt. Diese Mutante, die nach Protoplastierung von Oidien des Stammes AmutBmut und ihrer Regeneration isoliert wurde, kann keine Pks produzieren, hat ein langsameres und dünneres Myzelwachstum als das Eltern-Homokaryon AmutBmut und färbt den Agar mit submersem Myzel von Kulturen braun. In dieser Studie veränderte die Einführung anderer *NWD2*-Gene der Untergruppe A durch Transformation verschiedentlich die mutierten Mycel-Eigenschaften in der Mutante Proto159,

blockierten verschiedentlich die Braunfärbung des submersen Myzels und des Agars und, in dieser Arbeit sehr wichtig, induzierten verschiedentlich die Bildung von primären Hyphenknoten und Sklerotien im vegetativen Myzel und führten auch zur Herstellung von Fruchtkörpern.

Chapter 1

Introduction

Contribution to this chapter
Input into scientific discussion: S. Subba and U. Kües
Manuscript writing: S. Subba
Manuscript reviewed by U. Kües

1.1. *Fungi* in general

The kingdom of *Fungi* constitutes a varied group of eukaryotic organisms that play various significant roles to sustain equilibrium on earth. The organisms under this kingdom are very numerous and very diverse, most of which are not yet discovered. Yet, it has been estimated that there are probably a minimum of 2.2 to a maximum of 5.1 million species of *Fungi* that exist on earth (Blackwell 2011; Hawksworth and Lücking 2017). Of these, only about 120,000 to 144,000 have been described (Mueller and Schmit 2007; Willis 2017), with over 8000 species that are known to be harmful to plants and at least 300 that can be pathogenic to humans (Gracia-Solache 2010). *Fungi* live everywhere, from soil to rocks, in water, and on and in plants to animals including the human body, over the whole range of latitudes and climates. The occurrence of *Fungi* on earth was estimated to start at least around 400 million years ago from the discovery of a fossil of 8-meter tall terrestrial fungus falling under the genus *Prototaxiste* (Hueber 2001).

From baker's or brewer's yeast and mushroom for food to lethal pathogenic and toxic *Fungi* and to the life-saving antibiotic penicillin, *Fungi* have been a part of life of humans since their existence. Moreover, *Fungi* together with bacteria help to decompose and recycle organic materials and degrade both biotic and abiotic materials such as wood or rocks (Gadd 2007). Besides, *Fungi* are vitally important for the good growth of most plants, including crops, through the development of mycorrhizal symbiosis (Bonfante 2003). Advances in science helped to investigate and characterize fungal enzymes that have benefits in biotechnical applications (Ravalason et al. 2008; Witayakran et al. 2009; Wilson 2009).

The kingdom of *Fungi* is classified into 12 phyla, among which the phylum *Basidiomycota* is considered as an advanced member of this kingdom. The *Basidiomycota* together with the Ascomyctoa form the subkingdom of Dikarya which includes some of the most iconic fungal species such as from single-celled yeast to the gilled mushrooms (Hibbert et al. 2007, James et al. 2020). The phylum *Basidiomycota* is grouped into three subphyla (i) *Pucciniomycotina* (ii) *Ustilagomycotina* and (iii) *Agaricomycotina*. The subphylum *Agaricomycotina* includes most of the mushroom-forming *Fungi* containing about 20,000 species and is further sub-divided into five classes *Wallemiomycetes*, *Dacrymycetes*, *Tremellomycetes*, *Geminibasidiales*, *Bartheletiomycetes* and *Agaricomycetes* (Hibbert et al. 2007; Mishra et al. 2018). Mushrooms are the fleshy, spore-bearing fruiting body of a fungus, more typically produced above ground, on soil, or on its food source (wikipedia.org/wiki/Mushroom). About 98 % of mushroom-forming *Fungi* including the bracket *Fungi* and puffballs fall under class the *Agaricomycetes* (Hibbert et al. 2007; James et al. 2020).

Fruiting bodies of *Agaricomycetes* are the most complex fungal structures which exist on earth and the fungal multicellularity, tissue formation, and cell differentiation are so far little

understood (Kües and Navarro-González 2015; Kües et al. 2018; Nagy et al. 2018, 2020). In order to understand the process of tissue differentiation in fungal development, it is important to recognize and define the successive stages of development that a mushroom has to go through to reach maturity. Two species mainly serve as a model fungus for studying fruiting body development in the class *Agaricomycetes*, they are (i) *Coprinopsis cinerea* commonly known as an ink cap mushroom that grows on horse dung in nature (Kües 2000; Stajich et al. 2010) and *Schizophillum commune* commonly called split-gill mushroom and which is considered a wood-rotting fungus (Ohm et al. 2010; Riley et al. 2014, Floudas et al. 2015; Kües and Navarro-González 2015). In this thesis, the main focus of the study is on the fruiting body developmental process of *C. cinerea*.

1.2. History on *Coprinopsis cinerea* as a model organism

For more than a century, studies on the existence of species under the class *Agaricomycetes* have gained much attention to the researchers. Yet, the knowledge on the development of numerous edible mushroom-forming *Fungi* is restricted due to their growth and fruiting limitations under laboratory conditions. Nevertheless, *C. cinerea*, commonly known as gray shag ink cap mushroom, was found by Brefeld (1877) to be of great study value and served since then as a model organism in the field of research due to its short life cycle of about 1-2 weeks and minimum cultivation requirements under laboratory conditions (Fig. 1) (Binninger et al.1987; Moore 1998; Walser et al. 2001).

Fig. 1. Mature fruiting body of *C. cinerea* on YMG/T medium on a Petri dish in the laboratory. (*Photo by Wassana Chaisaena*)

C. cinerea is a saprotrophic edible fungus that naturally grows on horse dung (Buller 1924; 1931; Moore 1998; Kües 2000). Despite richness in nutrients, the fast autolysis of the cap of a mushroom during maturation lowers the potential consumption value (Arora 1986). However, the fungus is cultivated in Asian and African countries like Thailand where they are harvested before maturation and are then blanched to sell in a pickled form (Fig. 2) (Kües 2007). In the field of science, the fungus served as an excellent model mushroom for studying fungal sex and mating types, the fruiting body developmental process and general genetics in basidiomycetes (Moore 1998; Kües 2000; Kües and Navarro-González 2015).

Fig. 2. Pickled form of primordia of *C. cinerea* ready to be sold in the market of Thailand. (*Photo by Wassana Chaisaena)*

The genome sequence for *C. cinerea* became available in 2010, revealing a haploid genome size of 37.5 Mbp (Stajich et al. 2010). The accessibility of the whole genome opened the door to study the fungus better at the molecular level through various molecular biology methods and now also through proteomics techniques (Moore and Pukkila 1985; Binninger et al. 1987; Granado et al. 1997; Cummings et al. 1999; Stajich et al. 2010; Plaza et al. 2014; Muraguchi et al. 2015; Majcherczyk et al. 2019). This organism is used as a host for the expression of various genes for interesting enzymes which can be useful in the biotechnological applications (Kilaru 2006; Rühl et al. 2013; Cheng et al. 2009; You et al. 2014). Laccase, for example, is a lignin-modifying enzyme (Cohen et al. 2002) secreted by various *Fungi* including *C. cinerea* and can play a role in the degradation of lignin which has uses in the paper and pulp industry, in textile industries and also in application in bioremediation of contaminated water or soil (Durán and Esposito 2000; Pointing 2001; Wesenberg et al. 2003; Husain 2006). Furthermore, in the year 2014, scientists from Switzerland discovered a novel

protein ``Copsin´´ with antibiotic properties that acts as a fungal defensin as antibiotic against Gram-negative bacteria and many other microbes (Sabotic et al. 2016).

The fungus needs simple and minimum conditions to grow in the laboratory on simple artificial media (Kües 2000; Kües and Navarro-González 2015; Kües et al. 2016). On rich medium under specific environmental conditions, in about 12 days, the fungus grows over a whole plate and forms mature fruiting bodies with sexual basidiospores, which can germinate into new monokaryotic mycelia with one type of haploid nuclei in its cell. Fruiting occurs after mating of two compatible monokaryons with each other having different mating type, then the resulting dikaryon has two different haploid nuclei in its cells. The optimal condition for the growth of vegetative mycelia is at 37 °C in the dark whereas the fruiting body development takes place at around 25 °C in a 12-16 h light/8-12 h dark rhythm (Buller 1924, 1931; Granado et al. 1997; Moore and Pukkila 1985; Kües 2000; Kües et al. 2016). After vegetative mycelial growth of the dikaryon, it takes about 7 days to grow from the first stages of fruiting body development, i.e., primary (Pk) and secondary hyphal knot (Sk) formation, respectively to the mature mushroom (Buller 1931; Kües 2000; Kües and Navarro-González 2015; Kües et al. 2016).

The research on *C. cinerea* had already been begun more than 100 years ago (Brefeld 1877; Buller 1909) and was conducted in the past under various names such as *Coprinus lagopus*, *Coprinus fimetarius*, *Coprinus cinereus* and currently *Coprinopsis cinerea* (Redhead et al. 2001). The short life cycle and an ease to cultivate and fruit in a synthetic media allowed studying the fungus using various approaches such as cytological, physiological, genetical, molecular and recently proteomics techniques. Below in Table 1 researches are listed as conducted and accomplished on *C. cinerea* by various scientists.

Table 1. An overview on the progression on the researches conducted on *C. cinerea*

❖ **Please note that the names of the *C. cinerea* have been written in the table as mentioned in the respective research papers.**

Researchers	Years of research	Achievements in *Coprinopsis cinerea* research
J O Brefeld[1]	1871-1877	• Produced the first fruiting body in a culture of various isolates collected under species name *Coprinus lagopus*. • Documented mycelial growth and arrangement, hyphal branching and formation of rod-shaped spores which he named oidia. Showed tissues arrangement in the pileus of mushrooms grown on the horse-dung-extract medium through his outstanding drawings and therefore, he concluded that the primordia of various species of *Coprinus* originated from a single hyphal cell.
M Bensaude[2]	1918	Proved through her mycelial mating experiments and gave definition to monokaryotic (having a single nucleus) and dikaryotic mycelia (having two nuclei), thus explaining the term heterothallism in the fungus.
I Mounce[3]	1922	Studied homothallism and heterothallism in four species of *Coprinus* and concluded that monosporous mycelia of *C. sterquilinus* and *C. stercorarius* produce clamp-connections and fruiting bodies and termed them as homothallic species while *C. lagopus* and *C. niveus* were termed as heterothallic species as they form clamp-connection on mated mycelium, resulting to fruiting body formation only when the primary mycelia were mated.
WF Hanna[4]	1925	Made studies on the sex of *C. lagopus* collected from Canada and England and tested mating.
HJ Brodie[5]	1931 and 1932	Showed the diploidization process in oidial and basidiospore mycelia having different mating types in *C. lagopus.*
AHR Buller[6]	1909-1941	Book series: Researches in *Fungi* • Buller's phenomenon (di-mon mating).

		• Fruiting body development of *C. cinerea* in detail. Buller's drop: liquid droplets that helps basidiospores for ejection upon cap maturity.
HLK Whitehouse[7]	1949	Studied multiple-allomorph heterothallism in *Fungi*.
AHR Buller[6]	1909-1941	Book series: Researches in *Fungi* • Buller's phenomenon (di-mon mating). • Fruiting body development of *C. cinerea* in detail. Buller's drop: liquid droplets that helps basidiospores for ejection upon cap maturity.
U Mittwoch[8]	1951	Produced the first X-ray induced mutants to study genetics of *C. lagopus.*
M F Madelin[9]	1956	Described that stored mycelial glycogen was transferred to the developing gills of mushrooms during the fruiting process.
G Goodway[10], T Kamada[11] S Yuan[12]	1974, 1975, 1983, 1991, 1993, 2014, 2018	Studied stipe development, chitin synthesis and chitin microfibrils in the stipe cell wall of *C. cinerea.*
T Ishikawa[13]	1973, 1974, 1978, 1985	Studied stipe formation in mushrooms, fruiting-inducing substances, glycogen and cAMP regulation in fruiting.
Y Oda[14], BC Lu[15], T Kamada[16]	1973, 1974, 1978	Studied effects of light on basidiocarp initiation, mitosis, hymenium differentiation and maturation.

S Swamy[17]	1984	Obtained a self-compatible mutant (AmutBmut) with genetic defects in both mating-type loci which mimics dikaryon in all phenotypic characters including fruiting body development.
DJ McLaughlin[18]	1985	Studied glycogen storage in hymenia and subhymenia, and basidiospore formation.
T Kanda[19]	1986, 1989	• Isolation of recessive mutants *C. cinerea*. Genetic analysis of primordium-less mutants in *C. cinerea.*
D Moore[20]	1971, 1976, 1981, 1996	• Dedikaryotization of *Coprinus lagopus.* • Studied enzymes involved in nitrogen and glycogen metabolism. • Development of multicellular sclerotia and chlamydospores. Gravitropism of fruiting body of *C. cinerea.*
PJ Pukkila[21]	1987	• Invented DNA-mediated transformation through protoplasts of uninuclear oidia.
E Polak[22]	1997, 2001	• Asexual sporulation in *C. cinerea.* • Showed morphological variation in oidium formation.
BC Lu[23]	2000, 2003	Meiosis progression by light and dark cycle. • White-cap mutant and meiotic apoptosis.
PJ Pukkila[24], M Zolan[25], K Sakaguchi[26]	1992, 1995, 2003	Studied *C. cinerea* using cytological and genetic methods on the occurrence of karyogamy, meiosis and basidiospores formation.
D. Moore[27], U. Kües[28]	1998, 2000	Reviews on morphology, cytology and physiology in fruiting body development.

LA Casselton[29], U Kües[30]	1998, 2002, 2015	Discovered mating type genes as the master regulator in fruiting body development of *C. cinerea*.
M Aebi[31], U Kües[32]	1998, 2000	Discovery of Galectins in initial hyphal knot and primordia of *C. cinerea*.
M Aebi[33], M. Zolan[34]	1997, 1999	Mutants in fruiting pathway generated by REMI (Restricted Enzyme Mediated Integration).
SA Readhead[35]	2001	Concluded through molecular ITS sequencing that the former family *Coprinaceae* with the former genus *Coprinus* were sub-divided into three genera *Coprinellus*, *Coprinopsis* and *Parasola* under the new family *Psathyrellaceae* and a genus *Coprinus* in the family of *Agaricaceae*. This is how *Coprinus cinereus* became *Coprinopsis cinerea.*
H Muraguchi and T Nakazawa[36]	1998, 2000-2017	Characterized several central genes in the fruiting pathway of *C. cinerea.*
K Sakaguchi[37], M Aebi and M Künzler[38], AM Bailey[39], GD Foster[40]	2005, 2006, 2007, 2008	Invented RNA-silencing methods.
AM Bailey[41], GD Foster[42], PJ Pukkila[43], B Dörnte and U Kües[44], Y Honda[45],	2005, 2009-2010, 1987, 2017, 2015, 2017	• Gene Marker in *C. cinerea*. • Reporter marker. • Selection marker. Marker recycling.
T Kamada[46]	2011	Studied mutants *ku70* and *lig4* for knocking-out genes in the genomes of the fungus.

Stajich[47], P Pukkila[48] H Muraguchi[49], M Zolan[50], M Aebi and M Künzler[51], Hoi-Shan Kwon[52]	2010, 2015, 2012, 2014, 2013, 2015, 2021	• Provided complete genome of strains Okayama 7 and AmutBmut. • Genome construction • Published big data on first transcriptomics.
M Aebi and M Künzler[53]	2016	• Defensive proteins in fruiting bodies against microbes.
K Osakabe[54]	2017	• Applied CRISPR/Cas9 in *C. cinerea.*
D Moore[55], YB Kwack[56]	1996, 2017	• Effect of gravity on fruiting of *C. cinerea.*
LG Nagy[57]	2019	• Complexity in *Fungi* through transcriptomic data.

*[1] JO Brefeld 1877; [2] M Bensaude 1918; [3] I Mounce 1922; [4] WF Hanna 1925; [5] HJ Brodie 1931, 1932; [6] AHR Buller 1909-1941; [7] HLK Whitehouse 1948; [8] U Mittwoch 1951; [9] MF Madelin 1956; [10] G Gooday 1974, 1975; [11] T Kamada et al. 1983, 1991, 1993; [12] WM Zhang et al. 2014, J Zhou et al. 2018; [13] I Uno and T Ishikawa 1973, 1974, 1978; S Swamy et al. 1985; [14] N Morimoto and Y Oda 1973; [15] BC Lu 1974a; [16] T Kamada et al. 1978 ; [17] S Swamy et al. 1984; [18] DJ McLaughlin et al. 1985; [19] Kanda et al. 1986, 1989; [20] D Moore and GR Stewart 1971; D Moore and JO Ewaze 1976; JO Ewaze et al. 1978; D Moore 1981, D Moore et al. 1996; [21] DM Binninger et al. 1987 [22] Polak et al. 1997, 2001[23] BC Lu 1974b, 2000; BC Lu et al. 2003 [24] PJ Pukkila et al. 1992, 1995; [25] E Anderson et al. 2012; [26] S Iishi et al. 2008; H Sugawara 2009; [27] D Moore 1998; [28] U Kües 2000; [29] LA Casselton and NS Olesnicky 1998; [30] U Kües et al. 2002, U Kües 2015; [31] RP Boulianne 1998; [32] RP Boulianne et al. 2000; [33] LD Granado et al. 1997; [34] WJ Cummings et al. 1999; [35] SA Readhead et al. 2001; [36] H Muraguchi and T Kamada 1998, 2000; T Arima et al. 2004; K Terashima et al. 2005; H Muraguchi et al. 2008; M Kuratani et al. 2010; T. Nakazawa et al. 2011; Y. Ando et al. 2013; T Shioya et al. 2013; T Nakazawa et al. 2016, 2017; R Masuda et al. 2016; [37] SH Namekawa et al. 2005; [38] MA Wälti et al. 2006; [39] MN Henegahn et al. 2009; [40] AMSB Costa et al. 2008; [41] Burns et al. 2005; [42] MN Henegahn et al. 2009; CM Collins et al. 2010; [43] DM Binninger et al. 1987; [44] B Dörnte and U Kües 2017; [45] T Nakazawa and Y Honda 2015; [46] T Nakazawa et al. 2011; [47] JE Stajich et al. 2010;[48] P Pukkila; [49] H Muraguchi et al. 2015; [50] Burns et al. 2010; E Anderson et al. 2012; [51] DF Plaza et al. 2014; [52] CK Cheng et al. 2013; XJ Cheng et al.

2015; Xie et al. 2021 [53] J Sabotic et al. 2016; [54] SS Sugano et al. 2017; [55] D Moore et al. 1996; [56] JS Kim et al. 2017; [57] K Krizsán et al. 2019.

1.3. Life cycle of *C. cinerea*

C. cinerea is a heterothallic fungus, meaning that it needs a mating process of two distinct compatible mycelia for sexual reproduction. *C. cinerea* produce two types of mycelia, monokaryotic mycelia with a single nucleus and dikaryotic mycelia with two different types of nuclei in a hyphal cell (Casselton 1995). The mating of two compatible monokaryons gives rise to the dikaryon (Casselton 1995, Kües 2000).

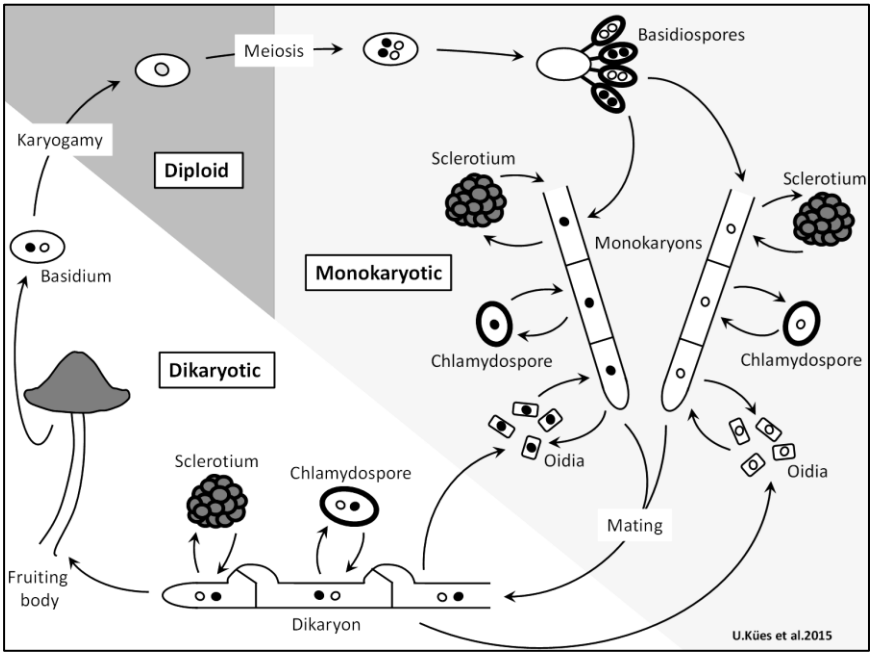

Fig. 3. Life cycle of *Coprinopsis cinerea*.

The three different shades show the three phases the fungus goes through to complete its life cycle. Black and white-colored nuclei in the hyphal cells, oidia, chlamydospores, basidium, and basidiospores indicate genetically different types of nuclei. The bi-nucleate dikaryon produces uni-nucleate oidia by the process of dedikaryotization. Post-karyogamy, the diploid phase is very short and is quickly followed by meiosis which ultimately produces four basidiospores, each with two nuclei as a result of a post-meiotic mitosis (Kües et al. 2015)

The life cycle of *C. cinerea* covers three phases; monokaryotic, dikaryotic and a short diploid phase which quickly leads into meiosis and the formation of tetrads of non-identical haploid nuclei (Fig. 3). The monokaryotic phase starts after meiosis with four haploid bi-nucleate basidiospores on each basidium which further germinate into monokaryotic hyphae containing a single haploid nucleus in its cell, hence the name the monokaryon. Monokaryons do not differ in their basic hyphal characteristics but they can differ in mating capabilities with each other. Mating types are physiological conditions which are analogous to the morphological sexes (male and female) in other eukaryotes. Mating types are controlled by two sets of genes, the *A* mating-type gene and the *B* mating-type genes, that encode two types of homeodomain transcription factors (HD1 and HD2) and pheromone–pheromone receptors, respectively (Kües et al. 1992, Kües 2000).

For successful mating of two monokaryotic strains, after their hyphal fusion HD1 and HD2 transcription factors from different parental origin need to dimerize with each other to bind to promoters of genes controlling dikaryon formation. HD1 and HD2 proteins from the same mating type background cannot do that. In conclusion, here is a key-to-lock-principle that only proteins of foreign mating-type origin fit each other. Likewise, there is a key-to-lock-principle in the interaction between pheromones and pheromone receptors. Compatible interactions are crosswise between pheromones and pheromone receptors from the two mating partners, but there is no interaction between pheromones and pheromone receptors coming from the same nucleus. Compatible interactions between pheromones and pheromone receptors are required to form a stable dikaryon (Kües et al. 1992; Kües 2000). In *C. cinerea*, the two mating-type loci *A* and *B* control differentiation and growth of the dikaryon (Casselton and Olesnicky 1998; Kües 2000). *C. cinerea* is a tetrapolar organism, producing four basidiospores in each basidium having four different mixture of mating types from meiosis: *AxBx*, *AxBy*, *AyBx* and *AyBy*, where *x* and *y* represent the different mating-type specificities of the parental haploid nucleus (Kües 2000). When two compatible monokaryons with different *A* and *B* specificities fuse, *B* mating-type genes control nuclear migration in mating monokaryons and fusion of clamp cells with sub-epical cells. *A* mating-type genes regulate clamp formation in dikaryotic mycelia and also synchronized nuclear division and septation.

Dikaryons develop thus upon a hyphal fusion of two mating-compatible monokaryons, thereby entering a dikaryotic phase (Fig. 3). The morphological appearance and the rate of growth greatly vary in the cultures of parental monokaryons and the dikaryon (Polak et al. 1997). The dikaryon grows much faster than the monokaryons. Moreover, the dikaryon has two distinct haploid nuclei in its cells, one from each parental monokaryon. Furthermore, at all hyphal septa, there are clamp cells fused to the sub-apical hyphal cells, formed as a mechanism to equally

distribute dividing daughter nuclei of both nuclear types to hyphal cells during cell division (Casselton and Olesnicky 1998, Kües 2000).

During the colony development, both monokaryon and dikaryon produce asexual spores called oidia in their mycelia (Fig. 3). Oidia are produced on the tips of the specialized aerial structures called oidiophores. Oidia production in the monokaryons is constitutive, i.e. under all environmental conditions and growth media. The dikaryons, in contrast, produce oidiophores and oidia only after the induction by light (Polak et al. 1997; Kertesz-Chaloupková et al. 1998; Liu 2001; Göbel 2003). The formation of oidiophores starts with the bulging of young oidiophores on a hyphal cell in the aerial mycelia which then is followed by septation, elongation, and budding of young oidia at the oidiophores tip. Oidia are highly hydrophilic and get engulfed in water droplets at the tips of oidiophores (Kemp 1977; Polak et al. 1997). The separation and finally the release of oidia take place by a process of schizolysis (Kendrick and Watling 1979) that splits the cell walls between two cells for the release of individual spores into the liquid droplets (Polak et al. 1997). Due to the hydrophilic nature of oidia, they stick to flies and other insects and can thereby be carried away with the insects to a new place for germination (Brodie 1931; Kües 2000).

Under suitable environmental conditions, a dikaryon forms a fruiting body and in the gills beneath the cap region, basidiospore-producing-cells called basidia are present. Each basidium undergoes karyogamy forming a diploid cell and is then followed by meiosis for again entering the monokaryotic phase through forming four basidiospores on each basidium. This way the cycle is repeated with the germination of monokaryotic hyphae.

Other multicellular structures such as sclerotia (Moore 1981) and single-celled chlamydospores are also produced by the mycelia during the life cycle of *C. cinerea* (Kües et al. 1998a; Kües 2000). Sclerotia are oval or globular, symmetrical, multi-cellular resting bodies of about 0.1 mm to 0.5 mm that have been noticed in both mono- and dikaryons within aerial and submerged mycelia. The mature sclerotium is comprised of an outer uni- or multi-layered rind or cortex, as it is also named, with light to the dark brown stained cell walls (Waters et al. 1972). The rind is built of compact cells. The internal medulla of sclerotia is described to be composed of large, ovulate and globular cells with non-stained cell walls that resemble chlamydospores (Waters et al. 1975a and 1975b; Kües et al. 1998a). Chlamydospores are large, thick-walled mitospores with condensed cytoplasm (Lewis 1961; Anderson 1971; Kües et al. 1998a). They are seen in variable forms in submerged mycelia and may be a round, oval or of irregular shape. The origins of such kinds of spores are not well documented, yet two possibilities were assumed for chlamydospores generation (Kües et al. 1998a). The first is that such type of structures might have internally arisen within the cells of hyphae followed by compression of cytoplasm. The

second is that they might have transferred by compressed cytoplasm from hyphal cell towards as bud (blastocyst) emerging from the end of the hyphal cell (Clémençon 1977; Kües 2000).

1.4. Fruiting body development

Fruiting body formation is a very complex and synchronized process which in *C. cinerea* follows a highly conserved scheme defined through light regulation by day and night phases (Morimoto and Oda 1973; Kamada et al. 1978; Kües 2000; Lu 2000; Navarro-González 2008, Chaisaena 2009, Subba et al. 2019). The competent vegetative mycelia grow faster at 37 °C for 5 days under constant dark but for the induction and the further development of fruiting require 12 h light and 12 h dark phases at 25 °C for 7 days as indicated by days D0 to D7 of the fruiting pathway (Fig. 4) (Kües 2000; Navarro-González 2008; Kües et al. 2016).

Fruiting of *C. cinerea* begins with loosely aggregated primary hyphal knots (Pks) formed on Day 0 (the day on which fungal cultures are transferred to the fruiting conditions) in the vegetative mycelium in the dark as the first differentiated structures in the pathway of fruiting body development (Kües et al. 1998a; Boulianne et al. 2000). They are however not committed to the fruiting and will transfer into the multicellular brown-rinded sclerotia as resting bodies when kept further in the dark (Moore 1981). In contrast, a light signal induces the formation of the compact aggregates termed secondary hyphal knots (Sks) to appear on Day 1 in the pathway of fruiting body formation in which stipe and cap tissues of a fruiting body will start to differentiate (Matthews and Niederpruem 1972, 1973; Moore 1995). Sks are thus the first developmental structures that are specific to the pathway of fruiting (Muraguchi et al. 1999; Boulianne et al. 2000). Subsequently to Sk formation, further light signals are required to coordinate the further tissue development in the fruiting body primordia and then for induction of karyogamy and meiosis in the basidia when all basic tissues are formed at the later primordial stage. On Day 2 with the availability of light, white round P1 stage primordia appear with a clear differentiation of an internal cap and stipe (Morimoto and Oda 1973; Moore et al. 1979). Lack of light at the Sk stage leads to failure to form normal P1 stage primordia and, instead elongated stipes with an under-developed cap called ‘dark stipes’ are formed (Tsusué 1969; Lu 1974a; Kües 2000; Chaisaena 2009). A pear-shaped primordium stage P2 is formed on Day 3 with an internally distinguishable cap, stipe, and basal regions. Gill rudiments are formed at the P2 stage (Moore et al. 1979). On Day 4, a primordium stage P3 attains a terete shape and primary and secondary gills arise from the gill rudiments. The primordium at stage P4 on Day 5 appears in a dumbbell shape where all main tissues are established which is ready to receive a light signal to induce karyogamy in the basidia (Lu 1972; Kamada et al. 1978). Karyogamy (K) occurs at the fully established light-bulb-shaped primordium stage P5 on Day 6. Meiosis (M) and basidiospore production follow over the day. In parallel to sporulation, rapid stipe elongation and cap expansion take place (Lu 1972; Kamada et al. 1978; Lu 2000). On the last

Day 7 of the fruiting pathway, fruiting bodies (FB) are fully matured shortly after midnight in the next night phase and then autolyze in the morning the caps to release the spores in black liquid droplets (Moore 1984; Kües 2000; Navarro-González 2008).

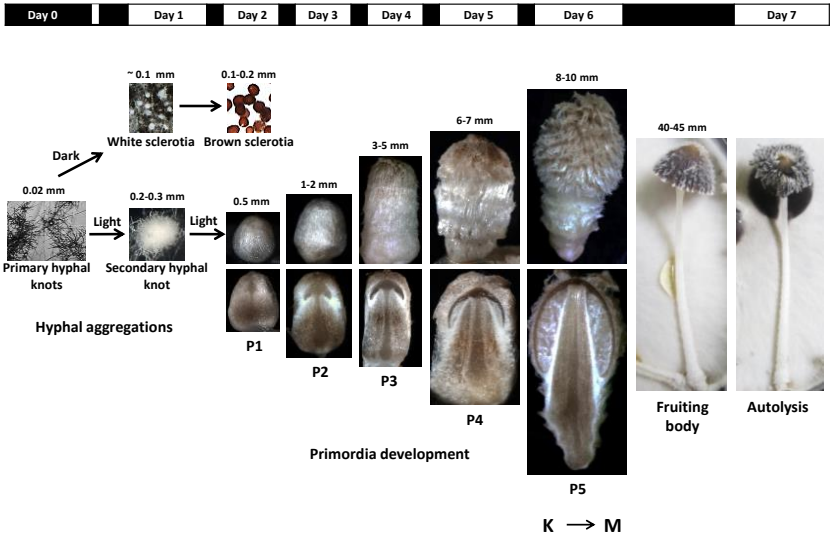

Fig. 4. Fruiting pathway of *Coprinopsis cinerea.*

The bar above the fungal structures presents with white and black boxes refer to the dark and light phases in course of incubation. Day 0 refers to the last day of cultivation for mycelial growth at 37 °C in the dark, prior to transfer of cultures into standard fruiting conditions (alternating 12 h light/12 h dark incubation at 25 °C). P1 to P5 refer to primordia stages. Sizes in mm refer to height of structures. K and M refer to karyogamy and meiosis, respectively. Modified after Navarro-González 2008 and Subba et al. 2019.

1.5. Genetic and environmental regulators in the fruiting process

The development of a complex fruiting body in *C. cinerea* is genetically regulated by mating types which are regarded as the master regulatory genes (Casselton and Olesnicky 1998; Kües 2000; Kües and Navarro-González 2015). Together with the mating-type genes, interactions between various genes and environmental conditions are required for the initiation and the development of the complex multi-cellular fruiting body structure of *C. cinerea* (Moore et al. 1979, 1998; Kües 2000; Stajich et al. 2010; Xie et al. 2021).

A mating-type genes control fruiting body initiation at the stages of primary and secondary hyphal knot formation. However, light plays a crucial role at this stage whether to continue further development or to enter the alternate pathway of sclerotia formation (Lu 1972; Morimoto and Oda 1973; Kamada et al. 1978; Kües et al. 1998a, 1998b). Light also regulates asexual sporulation in *C. cinerea*, as monokaryons produce oidia constitutively in dark but in dikaryons production of oidia is light-dependent as compatible oidiation-repressing *A* mating type genes are themselves repressed by light in dikaryons (Polak et al. 1997; Kertesz-Chaloupková et al. 1998; Kües et al. 1998a). In the fruiting pathway, a short exposure to the light is enough to give rise to round compact 3-dimensional secondary hyphal knots (Sks) (Morimoto and Oda 1973; Lu 1974b; Kües et al. 2016) which are the first structures committed to fruiting that may further develop to form a mature mushroom under a 12 h light and 12 h dark regime. Light signals are required for the differentiation of tissue within growing primordia (Lu 1972; Chaisaena 2009). Without light so-called ``dark stipes´´ are formed instead from Sks with largely extended stipes and underdeveloped caps (Tsusué 1969). In contrast, with constant light, the developmental process of fruiting body formation delays and eventually arrests maturation at diffuse diplotene in meiotic prophase I basidia (Lu 1974b; Kamada et al. 1978). Under standard fruiting conditions with day and night changes, the control of fruiting by the *A* mating-type genes is activated, and the light-induced steps in the fruiting pathway end at the P5 state after light-induction of karyogamy in the basidia at stage P4. Furthermore, the activation of the *B* mating-type genes is required for karyogamy within basidia and the subsequent opening the cap and autolyzing for the spore dispersal (Kües et al. 1998; Lu 2000; Lu et al. 2003). Defects in later stages of meiosis after diplotene in prophase I however do not block subsequent opening the possible spore less caps which remain light-colored and are known as “white caps” (Lu et al. 2003).

1.6. Self-compatible AmutBmut and other mutants

In the past, many mutants were generated from a wildtype dikaryon in order to isolate genes involved in the fruiting process. Since fruiting bodies are typically only produced by the dikaryon with two distinct genomes, it was not expected to identify both dominant and recessive mutations in the dikaryon mutants. However, a high natural accumulation of recessive alleles in native *C. cinerea* populations resulted then in nevertheless also high numbers of recessive mutations in the

fruiting pathway (Takemaru and Kamada 1972; Moore 1981). However, an invention of the self-compatible strain AmutBmut with defects in both mating type loci and a resulting phenotype with dikaryon properties such as formation of clamp cells and an ability to produce fruiting bodies without mating was a big achievement for studying the complex fruiting body development (Swamy et al. 1984; Pukkila et al. 1995; Moore 1995; Polak et al. 1997; Kertesz-Chaloupková et al. 1998). AmutBmut abundantly produces haploid single-nuclear single-celled oidia that can germinate again into colonies with a dikaryon-like phenotype. Oidia have thus been used to generate mutants from AmutBmut by UV and REMI [Restricted Enzyme-Mediated Integration of (DNA)] mutagenesis (Granado et al. 1997). Because of the single haploid genome in the fruiting-capable strain, all possible mutations, both recessive and dominant, can be detected in AmutBmut unbiased from those recessive mutations in genes already appeared before in functional dikaryons in nature (Kanda and Ishiwaka 1986; Granado et al. 1997).

Table 2. Mutants of AmutBmut (Kües, Granado and others, unpublished; data kindly provided by U. Kües)

Phenotype		Mutants	
		UV	REMI
No primary hyphal knots		147	141
No secondary hyphal knots		83	70
Arrest after	Secondary hyphal knots	12	0
	P1	12	9
	P2	8	8
	P3	25	47
	P4	46	49
	P5	67	25
Defect in	Stipe elongation	3	8
	Cap expansion	10	8
	Sporulation	73	0
Bonsai mushrooms		0	2
Other phenotypes		9	0
General Fitness affected		250	230

By UV and REMI mutagenesis, around 1500 mutants were generated from the AmutBmut (Granado et al. 1997; Kües et al. unpublished) (Table 2). Interestingly, mutations do not evenly distribute over the pathway of fruiting body development. High numbers of mutants are available from the early developmental stages up to stage Sks, comparably few in the subsequent primordial steps and again high numbers after stage P2 in the later developmental stages of primordia formation (P3 to P5), correlated basidium maturation, karyogamy and meiosis and subsequent basidiospore development occurring normally on Day 6 for fruiting body maturation and sporulation (Table. 2). The complexity of specific steps in fruiting can be detected from the generation of a varied number of the mutants with defects at different stages of fruiting.

The majority of mutants simply blocks in specific steps of fruiting body development. However, other mutants show morphological aberrations (Srivilai 2006; Chaisaena 2009). For instance, specific mutants *dst1*, *dst2*, *dst3,* and *dst4* form ``dark stipes´´ under standard fruiting conditions. Defects in four distinct genes (*dst1* to *dst4*) cause such phenotypes. *dst1* and *dst2* mutants with "dark stipes" with caps developed up to the P2 stage (Chaisaena 2009; own classification, chapter 5.2 in this thesis) were characterized in Japan and are known to have defects in the WC1 (White Collar 1) photoreceptor and a FAD/FMN-containing dehydrogenase (Flavin adenine dinucleotide/Flavin mononucleotide), respectively (Terashima et al. 2005; Kuratani et al. 2010). These mutants are blind and form dark stipes under standard fruiting conditions at the Sk stage. They also lost the light-induced production of oidia (Chaisaena 2009). The other two dark stipe mutants with defects in *dst3* and *dst4* (Chaisaena 2009) look phenotypically more mature than *dst1* and *dst2* mutants in that the caps appear more advanced, resembling best standard P3 and P4 caps (own classification, chapter 5.2 in this thesis), respectively. However, they still produce abundant numbers of oidia induced by light (Chaisaena 2009), indicating that they are not generally blind. Whole-genome sequencing of two *dst3* and *dst4* strains, established in cooperation with Botond Hegedüs and László Nagy at Institute of Biochemistry in Hungary identified each two interesting mutations related to the TCA cycle (tricarboxylic acid cycle) and possibly interrelated ROS (Reactive oxygen species) in these mutants (Kües and Subba unpublished; further information in chapter 5.2).

Besides, proteins for NTPases acting as potential regulators in the fruiting body development are focus of this research. NTPases are the family of enzymes that are involved in binding and hydrolysis of phosphate group which induces conformational changes in the molecule. (wikipedia.org/wiki/Nucleoside-triphosphatase; Romero et al. 2018). Among NTPases, Ras is a protein that belongs to the class of small GTPases proteins that can be switched on and off by hydrolysis of the GTP bound nucleotide changing it to GDP. A cloned *ras* gene (XP_001836360.2) has been transformed as wildtype and in mutant forms in the past in *C. cinerea* (Bottoli 2001; Srivilai 2006). Especially the introduction of a constitutively activated ras^{val19} allele altered mycelial growth in monokaryotic transformants and mated dikaryons formed dwarf

primordia and mushrooms that also produced a much lower number of basidiospores. Most of the basidiospores produced were unstained and many had a smaller spore size (Bottoli 2001; Srivilai 2006).

Another interesting gene for an uncharacterized NTPase that belongs to *the NWD2* family showed a suppressor effect on the transformed Pks-defective mutant Proto159, isolated before by protoplasting and regeneration of oidia (Granado et al. 1997). Proto159 is an AmutBmut mutant that has an unidentified defect in primary and therefore also in secondary hyphal knot formation and can thus not form fruiting bodies. Beneath its mycelium, massively produced Proto159 pigments stain the agar dark-brown, unlike its non-producing parental strain AmutBmut. The suppressor *NWD2* gene has been isolated from a cosmid library of AmutBmut genomic DNA (Bottoli et al. 1999). Sequencing of this gene in the mutant Proto159 did not reveal any point mutations, deletion or insertion within this gene but the insertions of further copies of gene *NWD2* into the genome of Proto159 showed suppressor effects on the defect (Yu. et al. unpublished). The suppression effect of a mutation in fruiting body initiation in *C. cinerea* by an *NWD2* gene suggests that their presence is influential in the regulation of developmental pathways. *NWD2* genes encode proteins with a NACHT domain (NAIP, CIITA, HET-E, and TP1), an evolutionarily conserved domain that serves in signal transduction and is named after four different types of P-loop NTPases (Koonin and Aravind 2000). Genome searches in *C. cinerea* found in total 36 different *NWD2* genes which cluster in 7 groups at different positions in an evolutionary tree of fungal NWD2 proteins (chapter 6 in this study). Accordingly, duplication and modification of NWD2 proteins have taken place in the fungus. Developmental defects of mutant Proto159 were found to be variably suppressed by the transformation of different cloned genes that belong to the NWD2 family. The introduction of *NWD2* genes altered mycelial properties, blocked the brown staining of mycelium and the agar, and, most importantly, induced primary hyphal knot and sclerotia formation in the vegetative mycelium and also production of mature fruiting bodies.

C. cinerea has in total >13600 predicted genes, many of which are differentially expressed such as for the purpose of fruiting body production, karyogamy, meiosis and spore formation (Stajich et al. 2010; Burns et al. 2010; Cheng et al. 2013; Plaza et al. 2014; Cheng et al. 2015; Muraguchi et al. 2015; Krizsán 2019). To date, not many genes involved in the process of fruiting of *C. cinerea* are known (Kües et al. 2002). Nevertheless, few numbers of genes that have regulation in fruiting body development are listed in the Table. 3.

Table 3: Some of the known genes with characterized functions in the fruiting process in *C. cinerea*

Genes	Functions in Fruiting	References
ich1	Pileus formation	Muraguchi and Kamada 1998
dst1 and dst2	Suppression of dark stipes	Terashima et al. 2005 and Kuratani et al. 2010
cfs1	Secondary hyphal knot formation	Liu et al. 2006
eln2	Primordia development	Muraguchi and Kamada 2000
eln3	Stipe elongation	Arima et al. 2004
cdc3	Stipe elongation	Shioya et al. 2013
wc-2	Suppression of dark stipes	Nakazawa et al. 2011
cag1	Gill formation	Masuda et al. 2016
exp1	Pileus expansion and autolysis	Muraguchi et al. 2008
ras	Fb regulation, spore production	Bottoli 2001, Srivilai 2006
matA	Inducing secondary hyphal knot	Kües 2015
matB	Inducing karyogamy	Kües 2015

Various environmental and genetic signals act as regulators that control the development process of the fruiting body in the fungus, the modification of which can change the morphology of the fruiting body. In the past, various molecular biological, genetic, cytological and physiological techniques have been used to gain knowledge of the developmental process of the fruiting body of *C. cinerea*. The knowledge gained so far on the development process of *C. cinerea* would be the template for the generation of further data in the near future in order to better understand the complexity of the fungus, using modern molecular techniques, including transformation, proteomics and transcriptomics techniques.

1.7. Aims of the study

Studies on *C. cinerea* have been increasingly popular in science for more than a century in order to understand the complex mechanism underlying the multicellular fruiting bodies of the fungus. Despite extensive work in the past, it is still mostly unknown what constitutes the complex multicellularity of a fungus (Kües and Navarro-González 2015; Kües et al. 2018).

This thesis addresses this very broad question, with the specific aims of this PhD thesis in the fruiting body development pathway of *C. cinerea* listed below:

- To introduce the reader into the complexity of developmental processes and fruiting body development of *C. cinerea* as background knowledge for this thesis (**Chapter 1; see here**

also publications Kües et al. 2018a and 2018b and Khonsuntia et al., in revision for further detailed reading).

- To study the two alternative routes of the early stages of multicellular development leading to sclerotia or fruiting **(Chapter 2; see also former master thesis Subba 2015).**

- To define crucial developmental stages over the time to best characterize the complete fruiting pathway and to define methods for the cytological evaluation on the tissues and cells that appear during the developmental stages in the fruiting process of *C. cinerea*. **(Chapter 3; publications Kües et al. 2016, and Subba et al. 2019).**

- To describe in detail the cytological processes and formation of stipe and cap tissues over the whole process of primordia development, as useful for further research such as applied in a first proteomics study **(Chapter 4; publication Majcherczyk et al. 2019 with shared first authorship).**

- To study the effect of environmental signals such as, light and aeration in the fruiting process of *C. cinerea* **(Chapter 5).**

- To study genes that belong to the *NWD2* family, as potential candidates involved in regulation of mycelial growth and fruiting of *C. cinerea* **(Chapter 6).**

1.8. Outcome of the study

The self-compatible homokaryotic strain AmutBmut with an established genome sequence (Muraguchi et al. 2015; Xie et al. 2021) was used to conduct the experiments in this thesis as strain well accessible to classical and molecular genetics (Prayook 2006; Stajich et al. 2010; Dörnte et al. 2020) and able to fruit without mating to study individual genes in a throughout homogenic haploid background (Swamy et al. 1984; Boulianne et al. 2000) and to asexually sporulate on light induction (Kertesz- Chaloupková et al. 1998). The strain thus combines all advantages from monokaryons (mating, oidia formation, transformable with strain-dependent suitable selection markers) with those specific of dikaryons (fruiting with karyogamy and meiosis, regulation of developmental processes by environmental cues).

The work started on the one hand on deepening and completing microscopy observations made before during my former master thesis (Subba 2015) on the very initial stages of blue light-induced fruiting body development and the alternate formation of sclerotia in the dark. This lead to a better understanding and descriptions of timing, series and type of events during Pks and Sks formation, and sclerotia, respectively, and when mycelia have competency for these developments and how it completes, in strain AmutBmut, with oidia formation.

On the other hand, work started with the principle knowledge of major steps in the further fruiting process of strain AmutBmut under standard fruiting conditions (12 h light and 12 h dark at 25 °C) and that it takes 7 days to complete fruiting after transfer of fully grown plates from 37 °C into standard fruiting conditions (Navarro-González 2008; Kües and Navarro-González 2015; Kües et al. 2016). However, it became clear that for reasons of a constant ongoing of further development over the fruiting pathway and of the high complexity in tissue formation in stipe and cap and coordination of events, exact reference points on the daily clock of fruiting under standard environmental conditions were needed to be defined to which other events can than easily timewise be related. We chose to set the moment light switches on in the culture room under standard fruiting conditions as h zero. Other time points on the same day can then easily be also exactly marked as Day X, + Y h (Kües et al. 2016; Subba et al. 2019). Also, for highest reliability in the fruiting process providing Sks at Day 1, primordial stages P1 to P5 at Day 2 to Day 6, and the mature fruiting body with basidiospores and autolysis at Day 7, it was worked out that cultures on freshly made YMG/T medium should be inoculated in the afternoon hour ca 6 pm and plates be transferred after 5 days at 37 °C at 9 h into a fruiting chamber at 25 °C (Kües et al. 2016).

Technically, different histological stainings were tested on primordia tissues and the combination of dyes PAS (Periodic acid–Schiff) and Mayer's hemalum was found out to be most suitable for differentiating cells and tissues in primordia based on PAS staining is used to detect polysaccharides such as glycogen and hemalum is known to stain basophilic materials such as DNA (Subba et al. 2019, posters titled `` How complex is a mushroom?´´ presented at 9$^{th}$ International Medicinal Mushroom Conference 2017, Palermo Italy and ``Tissue staining to study fruiting process of *Coprinopsis cinerea*´´ presented at 9th International Conference on Mushroom Biology and Mushroom Products November 2018, Shanghai and Zhangzhou China and at 3rd Symposium of the VAAM special group september 2019, Göttingen Germany; see posters in appendix). This technique was subsequently used further to describe in all recognized details of the structure of AmutBmut primordia at stages P1 (Day 2, 0 h), P2 (Day 3, 0 h), P3 (Day 4, 0 h), P4 (Day 5, 0 h) and P5 (Day 6, 0 h). In the further study in descriptions of individual structures during this thesis, the focus was laid always at h zero of each day of development. Observations of stained primordia dissections revealed for the first-time generation of types of hyphae and distinct tissues in stipe and cap, their differentiation and in part also degeneration from stages P1 to P5. Overall, more than 35 cell types and tissues were observed. Previously, Lu (1974b) and Moore and coworkers (1979, 1984, 1985, 1995) concentrated particularly on hymenium development and stipe development on likely the P4 to P5 stage, and on processes in later stages during young fruiting body development and maturation. Matthews and Niederpruem (1972, 1973) on the other hand provided momentary views in individual Pks (called their stage I as lattice formation), Sks (called there as stage II as hyphal aggregation) and a view on P1 formation. Descriptions of these authors were found back in this study while they were timewise more

exactly defined and with more cellular details described. Furthermore, the stages P1, P2 and P3 in the primordial development were for the first time described in microscopic details and new details were added to P4 and P5 structures (chapter 4.1 in this study).

Fruiting body development in fresh cultures usually start with hundreds of Sks, of which only parts will continue and enter the P1 stage, and every further day more structures will abandon development, at every stage from P1 to P2, P2 to P3, P3 to P4, P4 to P5 (Kües et al. 2016, chapter 4). The exact definition of developmental stages, active and senescent, is for example essential for finding proteins contributing to specific steps in development by proteomics. As a first step forward to this target, primordia stages were carefully collected at times zero, and first results showed that proteomes between primordia stages differed and that there were proteins known to contribute to fruiting at stages expected (chapter 4.2 in this study, Majcherczyk et al. 2019; Poster titled ``Insights into protein functions during primordia development of *Coprinopsis cinerea* through proteomics analysis´´ presented at 30th Fungal Genetic Conference march 2019, Asilomar CA USA and at 3rd Symposium of VAAM special group september 2019, Göttingen Germany, see poster in appendix)).

Identification of structures actively growing into the next primordial stage had to be first learned by multiple repeated cultivation and fruiting observation cycles with series of plates. It took about one year to be fully confident in recognizing the needed structures. Parameters identified and used were a whitish (P1) and then slightly pinkish fresh looking cap appearance with firm veil cells versus slightly greyish drier cap appearances with drier looking more tousled veil cells. Moreover, actively growing primordia always excrete liquid from cap between veils cells that run down on the structures to collect at the stipe bases. This phenomenon was for the first time described in this study (chapter 4.1 in this study). Liquid droplets were collected during this work and conferred to Dr. Majcherczyk for proteomics analysis. First data revealed these droplets to contain many proteins with fungal defense function against other microbes (bacteria and *Fungi*) and nematodes (Poster titled ``Insights into protein functions during primordia development of *Coprinopsis cinerea* through proteomics analysis´´ presented at 30th Fungal Genetic Conference march 2019, Asilomar CA USA and at 3rd Symposium of VAAM special group september 2019, Göttingen Germany, see poster in appendix). Fruiting bodies of *C. cinerea* in nature emerge clean looking from horse dung with massive microbial and small animal populations which the fungus must defeat. The droplets may help in necessary cleaning by effects such as the lotus effect and proteins killing harmful opponents (chapter 4.1 in this study).

This study covers from chapter 2 to 5 step by step the whole fruiting process of strain AmutBmut, including fruiting body maturation and autolysis. In chapter 5, experiments are presented in which light effects and aeration on distinct steps in the pathway are observed and analyzed. Light and dark experiments largely confirmed former studies by Tsusué 1969, Lu 1974b, and Chaisaena

2009. In total, there are six light-dependent steps from Pk to P4 in the pathways and while once karyogamy is induced (at P4) there is no further need for another light signal and dark-dependent steps are at Pk to P5 stages (chapter 5.1 in this study). Fully new in this study are the findings on block of aeration (chapter 5.2 in this study, poster titled ``Environmental and genetic control of the coordinated process of fruiting body development in *Coprinopsis cinerea´´* presented at 29th Fungal Genetic Conference march 2017, Asilomar CA USA, see poster in appendix). These studies were motivated by *dst3* and *dst4* mutants that distinguished from the blind *dst1* and *dst2* mutants in that light-regulated steps in asexual sporulation and early fruiting up to P3 were still normally be performed under standard fruiting conditions before a dark stipe production started. Dark stipes of *dst3* and *dst4* mutant had therefore more advanced caps than *dst1* and *dst2* dark stipes and this can be further confirmed in the future by microscope analyses of respective primordia sections. Blockage of aeration at different cultural ages showed that mycelial growth stopped, that Sks could not be produced, that P1 was blocked in further development, that elongated "dark stipes" were formed from P2, P3, P4 and P5 structures and that basidiospore staining was also blocked. Genome sequencing suggested for the *dst3* and *dst4* mutants possible links to CO_2 production and the TCA cycle and subsequently possibly regeneration of ROS by the light-related activities of the Cop9 signalosome (Poster titled ``Complexity in mushroom formation´´ presented at 3rd Symposium of VAAM special group september 2019, Göttingen Germany, see poster in appendix). Practically, this can be proven in the future by cloning respective wildtype genes and transforming them alone or together into the mutants with following fruiting tests.

A further mutant handled in this work was strain Proto159 with a defect in primary hyphal knot (*pkn*) formation (Posters titled ``The family of NWD2 proteins in *Coprinopsis cinerea*: roles in development´´ presented at Annual Congress Biotechnology 2020+ 2016, Jena Germany and ``P-loop NTPases in developmental process of *Coprinopsis cinerea´´* presented at 14th European Conference on Fungal Genetic 2018, Haifa Israel, see appendix for posters). Also in this mutant, whole genome sequencing of the mutant might help to get insight in crucially mutated gene(s). Former work by other researchers has indicated a suppressing effect of an *NWD2* gene in transformants of the strain. This could be repeated in this study, together with transformation of six of seven other related *NWD2* genes while more data in the future should be generated for substantiating the observations. A remarkable observation in this work was that time schemes in the normal fruiting process of AmutBmut were not restored in Proto159 transformants and they were speeded up on many transformants of homokaryon AmutBmut. For one, an effect of complementation in transformation of the *pab*$^{+}$*1* deficiency in strain AmutBmut is responsible but there seems to be further speeding up effect by introduced *NWD2* genes. In the future, exact time course of PABA supplemented AmutBmut cultures should be documented and of time courses of NWD2 transformants. For the few observations so far, it appears that especially development at P3 and later speeded up, suggesting interesting possible changes e.g., in the

premeiotic S-phase and prekaryotic and karyotic processes in the basidia (for detailed description see Lu and Jeng 1975) from stage P4 to stage P5.

The discussion of the work of this thesis at the end of chapter 1 intended to give an overview on the most important results and observations of this thesis and to show how the individual chapters logically interconnect to each other. For the interest of the reader, all chapters have their own discussions focusing on more distinct results and details on specific morphological and regulatory steps in the fruiting process of homokaryon *C. cinerea* AmutBmut.

1.9. References

Anderson, E., Burns, C. and Zolan, M. E. (2012) Global gene expression in *Coprinopsis cinerea* meiotic mutants reflects checkpoint arrest. *G3: Genes Genomes Genetics*, *2*, pp.1213-1221.

Anderson, G. E. (1971) The life history and genetics of *Coprinus lagopus*. A practical introduction to biochemical genetics. *The life history and genetics of Coprinus lagopus. A Practical Introduction to Biochemical Genetics.*

Ando, Y., Nakazawa, T., Oka, K., Nakahori, K. and Kamada, T. (2013) *Cc.snf5*, a gene encoding a putative component of the SWI/SNF chromatin remodeling complex, is essential for sexual development in the agaricomycete *Coprinopsis cinerea*. *Fungal Genetics and Biology*, *50*, pp.82-89.

Arima, T., Yamamoto, M.., Hirata, A., Kawano, S. and Kamada, T. (2004) The *eln3* gene involved in fruiting body morphogenesis of *Coprinus cinereus* encodes a putative membrane protein with a general glycosyltransferase domain. *Fungal Genetics and Biology*, *41*, pp.805-812.

Arora, D. (1986) *Mushrooms Demystified*. Ten Speed Press, 80, 959 p.

Bensaude, M. (1918) Recherches sur le cycle évolutif et la sexualité des Basidiomycetes. Nemours: Imprimerie Nemourienne, Henri Boley. (in French)

Binninger, D. M., Skrzynia, C., Pukkila, P. J. and Casselton, L. (1987) DNA-mediated transformation of the basidiomycete *Coprinus cinereus*. *The EMBO Journal*, *6*, pp.835-840.

Blackwell, M. (2011) The Fungi: 1, 2, 3… 5.1 million species? *American Journal of Botany*, *98*, pp.426-438.

Bonfante, P. (2003) Plants, mycorrhizal fungi and endobacteria: a dialog among cells and genomes. *The Biological Bulletin*, *204*, pp.215-220.

Bottoli, A. P. F. (2001) *Metabolic and environmental control of development in Coprinus cinereus* (Doctoral dissertation, ETH Zurich).

Bottoli, A. P., Kertesz-Chaloupkova, K., Boulianne, R. P., Aebi, M. and Kües, U. (1999) Rapid isolation of genes from an indexed genomic library of *C. cinereus* in a novel *pab1*$^{+}$ cosmid. *Journal of Microbiological Methods*, *35*, pp.129-141.

Borris, H., (1934) Beiträge zur Wachstums- und Entwicklungsphysiologie der Fruchtkörper von *Coprinus lagopus*. *Planta*, 22, pp.28-69. (in German)

Boulianne, R. P. (1998) The molecular and biochemical characterization of two novel galectins from the mushroom *Coprinus cinereus* (Ph. D. Degree Year: 1997, Institute: University of Guelph).
Boulianne, R. P., Liu, Y., Aebi, M., Lu, B. C. and Kües, U. (2000) Fruiting body development in *Coprinus cinereus*: regulated expression of two galectins secreted by a non-classical pathway. *Microbiology, 146*, pp.1841-1853.
Brefeld, O. (1877) Botanische Untersuchungen über Schimmelpilze. III. Basidiomyceten. Leipzig: Arthur Felix. (in German)
Brodie, H. J. (1931) The oidia of *Coprinus lagopus* and their relation with insects. *Anatomy of Botany*, 45, pp.315-344.
Brodie, H. J. (1932) Oidial mycelia and the diploidization process in *Coprinus lagopus*. *Anatomy of Botany*, 46, pp.727-732.
Buller, A. H. R. (1909) The rate of fall of fungus spores in air. *Nature*, *80*(2059), pp.186-187.
Buller, A. H. R. (1922) Researches on Fungi. Volume II. *Longmans, Green and Co*.
Buller, A. H. R. (1924) Researches on Fungi. Volume III. London: *Longmans Green and Co*.
Buller, A. H. R. (1931) Researches on Fungi. Volume IV. London: *Longmans Green and Co*.
Buller, A. H. R. (1933) Researches on Fungi. Volume V. London: *Longmans Green and Co*.
Buller, A. H. R. (1930) The biological significance of conjugated nuclei of *Coprinus lagopus* and other Hymenomycetes. *Nature*, 126, pp.686-689.
Buller, A. R. (1941) The diploid cell and the diploidisation process in plants and animals, with special reference to the higher fungi. *The Botanical Review*, *7*, pp.335-387.
Burns, C., Gregory, K. E., Kirby, M., Cheung, M. K., Riquelme, M., Elliott, T. J., Challen, M. P., Bailey, A. and Foster, G. D. (2005) Efficient GFP expression in the mushrooms *Agaricus bisporus* and *Coprinus cinereus* requires introns. *Fungal Genetics and Biology*, *42*, pp.191-199.
Burns, C., Stajich, J. E., Rechtsteiner, A., Casselton, L., Hanlon, S. E., Wilke, S. K., Savytskyy, O. P., Gathman, A. C., Lilly, W. W., Lieb, J. D. and Zolan, M. E. (2010) Analysis of the Basidiomycete *Coprinopsis cinerea* reveals conservation of the core meiotic expression program over half a billion years of evolution. *PLoS Genetics*, *6*, p.e1001135.
Casselton, L. A. (1995) Genetics of *Coprinus*. In *Genetics and Biotechnology* (pp.35-48). Springer, Berlin, Heidelberg.
Casselton, L. A. and Olesnicky, N. S. (1998) Molecular genetics of mating recognition in basidiomycete fungi. *Microbiology and Molecular Biology Reviews*, *62*, pp.55-70.
Chaisaena, W. (2009) Light effects on fruiting body development of wildtype in comparison to light-insensitive mutant strains of the basidiomycete *Coprinopsis cinerea*, grazing of mites (*Tyrophagus putrescentiae*) on the strains and production of volatile organic compounds during fruiting body development (Doctoral dissertation, Göttingen University).

Cheng, C. K., Au, C. H., Wilke, S. K., Stajich, J. E., Zolan, M. E., Pukkila, P. J. and Kwan, H. S. (2013) 5'-Serial Analysis of Gene Expression studies reveal a transcriptomic switch during fruiting body development in *Coprinopsis cinerea*. *BMC Genomics*, *14*, pp.1-17.
Cheng, S., Yang, P., Guo, L., Lin, J. and Lou, N. (2009) Expression of multi-functional cellulase gene mfc in *Coprinus cinereus* under control of different basidiomycete promoters. *Bioresource Technology*, *100*, pp.4475-4480.
Cheng, X., Hui, J. H. L., Lee, Y. Y., Wan Law, P. T. and Kwan, H. S. (2015) A "developmental hourglass" in fungi. *Molecular Biology and Evolution*, *32*, pp.1556-1566.
Clémençon, H. (1977) Die Strukturen der Basidiosporenwand und des Apikulus, und deren Beziehung zur Exogenisation der Spore. *Persoonia-Molecular Phylogeny and Evolution of Fungi*, *9*, pp.363-380.
Cohen, R., Persky, L., Hazan-Eitan, Z., Yarden, O. and Hadar, Y. (2002) $Mn2^{+}$ alters peroxidase profiles and lignin degradation by the white-rot fungus *Pleurotus ostreatus* under different nutritional and growth conditions. *Applied Biochemistry and Biotechnology*, *102*, pp.415-429.
Collins, C. M., Heneghan, M. N., Kilaru, S., Bailey, A. M. and Foster, G. D. (2010) Improvement of the *Coprinopsis cinerea* molecular toolkit using new construct design and additional marker genes. *Journal of Microbiological Methods*, *82*, pp.156-162.
Costa, A. M., Mills, P. R., Bailey, A. M., Foster, G. D. and Challen, M. P. (2008) Oligonucleotide sequences forming short self-complimentary hairpins can expedite the down-regulation of *Coprinopsis cinerea* genes. *Journal of Microbiological Methods*, *75*, pp.205-208.
Cummings, W. J., Celerin, M., Crodian, J., Brunick, L. K. and Zolan, M. E. (1999) Insertional mutagenesis in *Coprinus cinereus*: use of a dominant selectable marker to generate tagged, sporulation-defective mutants. *Current Genetics*, *36*, pp.371-382.
Dörnte, B. and Kües, U. (2017) Split *trp1+* gene markers for selection in sequential transformations of the Agaricomycete *Coprinopsis cinerea*. *Current Biotechnology*, *6*, pp.139-148.
Dörnte, B., Peng, C., Fang, Z., Kamran, A., Yulvizar, C. and Kües, U. (2020) Selection markers for transformation of the sequenced reference monokaryon Okayama 7/# 130 and homokaryon AmutBmut of *Coprinopsis cinerea*. *Fungal Biology and Biotechnology*, *7*, pp.1-18.
Duran, N. and Esposito, E. (2000) Potential applications of oxidative enzymes and phenoloxidase-like compounds in waste water and soil treatment: a review. *Applied Catalysis B: Environmental*, *28*, pp.83-99.
Ewaze, J. O., Moore, D. and Stewart, G. R. (1978) Co-ordinate regulation of enzymes involved in ornithine metabolism and its relation to sporophore morphogenesis in *Coprinus cinereus*. *Microbiology*, *107*, pp.343-357.
Floudas, D., Held, B. W., Riley, R., Nagy, L. G., Koehler, G., Ransdell, A. S., Younus, H., Chow, J., Chiniquy, J., Lipzen, A. and Tritt, A. (2015) Evolution of novel wood decay mechanisms in

Agaricales revealed by the genome sequences of *Fistulina hepatica* and *Cylindrobasidium torrendii. Fungal Genetics and Biology*, *76*, pp.78-92.
Gadd, G. M. (2007) Geomycology: biogeochemical transformations of rocks, minerals, metals and radionuclides by fungi, bio weathering and bioremediation. *Mycological Research*, *111*, pp.3-49.
Garcia-Solache, M. A. and Casadevall, A. (2010) Global warming will bring new fungal diseases for mammals. *MicroBiology*, *1*(1).
Gooday, G. W. (1974) Control of development of excised fruit bodies and stipes of *Coprinus cinereus*. *Transactions of the British Mycological Society*, *62*(2), pp.391-399.
Gooday, G. W. and Anne, D. R. (1975) Properties of chitin synthetase from *Coprinus cinereus*. *Microbiology*, *89*, pp.137-145.
Granado, J. D., Kertesz-Chaloupková, K., Aebi, M. and Kües, U. (1997) Restriction enzyme-mediated DNA integration in *Coprinus cinereus*. *Molecular and General Genetics MGG*, *256*, pp.28-36.
Hanna, W. F. (1925) The problem of sex in *Coprinus lagopus*. *Annals of Botany*, *39*, pp.431-457.
Hawksworth, D. L. and Lücking, R. (2017) *Fungal diversity revisited*: 2.2 to 3.8 million species. *The Fungal Kingdom*, pp.79-95.
Heneghan, M. N., Porta, C., Zhang, C., Burton, K. S., Challen, M. P., Bailey, A. M. and Foster, G. D. (2009) Characterization of serine proteinase expression in *Agaricus bisporus* and *Coprinopsis cinerea* by using green fluorescent protein and *the A. bisporus* SPR1 promoter. *Applied and Environmental Microbiology*, *75*, pp.792-801.
Hibbett, D. S., Binder, M., Bischoff, J. F., Blackwell, M., Cannon, P. F., Eriksson, O. E., Huhndorf, S., James, T., Kirk, P. M., Lücking, R. and Lumbsch, H. T. (2007) A higher-level phylogenetic classification of the Fungi. *Mycological Research*, *111*, pp.509-547.
Hueber, F. M. (2001) Rotted wood–alga–fungus: the history and life of *Prototaxites* Dawson 1859. *Review of Palaeobotany and Palynology*, *116*, pp.123-158.
Husain, Q. (2006) Potential applications of the oxidoreductive enzymes in the decolorization and detoxification of textile and other synthetic dyes from polluted water: a review. *Critical Reviews in Biotechnology*, *26*, pp.201-221.
Ishii, S., Koshiyama, A., Hamada, F. N., Nara, T. Y., Iwabata, K., Sakaguchi, K. and Namekawa, S. H. (2008) Interaction between Lim15/Dmc1 and the homologue of the large subunit of CAF-1–a molecular link between recombination and chromatin assembly during meiosis. *The FEBS Journal*, *275*, pp.2032-2041.
James, T. Y., Stajich, J. E., Hittinger, C. T. and Rokas, A. (2020) Towards a fully resolved fungal tree of life. *Annual Review of Microbiology*, *74*, pp.291-313.
Kamada, T., Kurita, R. and Takemaru, T. (1978) Effects of light on basidiocarp maturation in *Coprinus macrorhizus*. *Plant and Cell Physiology*, *19*, pp.263-275.

Kamada, T. and Takemaru, T. (1983) Modifications of cell-wall polysaccharides during stipe elongation in the basidiomycete *Coprinus cinereus*. *Microbiology*, *129*, pp.703-709.
Kamada, T., Takemaru, T., Prosser, J. I. and Gooday, G. W. (1991) Right and left handed helicity of chitin microfibrils in stipe cells in *Coprinus cinereus*. *Protoplasma*, *165*, pp.64-70.
Kamada, T. and Tsuru, M. (1993) The onset of the helical arrangement of chitin microfibrils in fruit-body development of *Coprinus cinereus*. *Mycological Research*, *97*, pp.884-888.
Kanda, T. and Ishikawa, T. (1986) Isolation of recessive developmental mutants in *Coprinus cinereus*. *Journal of General and Applied Microbiology*, 32, pp.541-543.
Kanda, T., Goto, A., Sawa, K., Arakawa, H., Yasuda, Y. and Takemaru, T. (1989) Isolation and characterization of recessive sporeless mutants in the basidiomycete *Coprinus cinereus*. *Molecular and General Genetics MGG*, *216*, pp.526-529.
Kemp, R. F.O. (1977) Oidial homing and the taxonomy and speciation of basidiomycetes with special reference to the genus *Coprinus*. In *The Species Concept in Hymenomycetes* (6, pp.259-274). Hirschberg J. Cramer.
Kendrick, B. and Walting, R. (1979) Mitospores in basidiomycetes. *The Whole Fungus*, 2, pp.473-545.
Kertesz-Chaloupková, K., Walser, P. J., Granado, J. D., Aebi, M. and Kües, U. (1998) Blue light overrides repression of asexual sporulation by mating type genes in the basidiomycete *Coprinus cinereus*. *Fungal Genetics and Biology*, *23*, pp.95-109.
Kilaru, S. (2006) Identification of fungal multi-copper oxidase gene families: Overexpression and characterization of *Coprinopsis cinerea* laccases for applications in biotechnology. *Cuvillier Verlag*, Göttingen.
Kim, J. S., Kwon, Y. S., Bae, D. W., Kwak, Y. S. and Kwack, Y. B. (2017) Proteomic analysis of *Coprinopsis cinerea* under conditions of horizontal and perpendicular gravity. *Mycobiology*, *45*, pp.226-231.
Koonin, E. V. and Aravind, L. (2000) The NACHT family–a new group of predicted NTPases implicated in apoptosis and MHC transcription activation. *Trends in Biochemical Sciences*, *25*, pp.223-224.
Krizsán, K., Almási, É., Merényi, Z., Sahu, N., Virágh, M., Kószó, T., Mondo, S., Kiss, B., Bálint, B., Kües, U. and Barry, K. (2019) Transcriptomic atlas of mushroom development reveals conserved genes behind complex multicellularity in fungi. *Proceedings of the National Academy of Sciences*, *116*, pp.7409-7418.
Kües, U. (2000) Life history and developmental processes in the Basidiomycete *Coprinus cinereus*. *Microbiology and Molecular Biology Reviews*, 64, pp.316-353.
Kües, U. (2007) Molecular wood biotechnology–defining a new field of research. *Wood Production, Wood Technology, and Biotechnological Impacts*, pp.15-40.

Kües, U., Granado, J. D., Hermann, R., Boulianne, R. P., Kertesz-Chaloupková, K. and Aebi, M. (1998a) The A mating type and blue light regulate all known differentiation processes in the basidiomycete *Coprinus cinereus*. *Molecular and General Genetics MGG*, *260*, pp.81-91.

Kües, U., Granado, J. D., Kertesz-Chaloupková, K., Walser, P. J., Hollenstein, M., Polak, E., Liu, Y., Boulianne, R. P., Bottoli, A. P. F. and Aebi, M. (1998b) Mating types and light are major regulators of development in *Coprinus cinereus*. In *Proceedings of the Fourth Meeting on the Genetics and Cellular Biology of Basidiomycetes.* (pp.113-118). Horst, The Netherlands: Mushroom Experimental Station.

Kües, U., Walser, P., Klaus, M. and Aebi, M. (2002) Influence of activated *A* and *B* mating-type pathways on developmental processes in the basidiomycete *Coprinus cinereus*. *Molecular Genetics and Genomics*, *268*, pp.262-271.

Kües, U. (2015) From two to many: multiple mating types in Basidiomycetes. *Fungal Biology Reviews*, *29*, pp.126-166.

Kües, U., Polak, E., Bottoli, A. P. F. (2002) Vegetative development in *Coprinus cinereus*. *Molecular Biology of Fungal Development*, pp.133-163. Basel: Marcel Dekker.

Kües, U. and Navarro-González, M. (2015) How do Agaricomycetes shape their fruiting bodies? 1. Morphological aspects of development. *Fungal Biology Reviews*, *29*, pp.63-97.

Kües, U., Subba, S., Yu, Y., Sen, M., Khonsuntia, W., Singhaduang, W., Lange, K. and Lakkireddy, K. (2016) Regulation of fruiting body development in *Coprinopsis cinerea*. *Mushroom Science*, *19*, pp.318-322.

Kües, U., Richardson, W. V., Tymon, A. M., Mutasa, E. S., Göttgens, B., Gaubatz, S., Gregoriades, A. and Casselton, L. A. (1992) The combination of dissimilar alleles of the *A* α and *A* β gene complexes, whose proteins contain homeodomain motifs, determines sexual development in the mushroom *Coprinus cinereus*. *Genes & Development*, *6*, pp.568-577.

Kües, U., Khonsuntia, W., Subba, S. and Dörnte, B. (2018a) Volatiles in communication of Agaricomycetes. In *Physiology and Genetics* (pp.149-212). Springer, Cham.

Kües, U., Khonsuntia, W. and Subba, S. (2018b) Complex fungi. *Fungal Biology Review* 32: pp.205-218.

Kuratani, M., Tanaka, K., Terashima, K., Muraguchi, H., Nakazawa, T., Nakahori, K. and Kamada, T. (2010) The *dst2* gene essential for photomorphogenesis of *Coprinopsis cinerea* encodes a protein with a putative FAD-binding-4 domain. *Fungal Genetics and Biology*, *47*, pp.152-158.

Lewis, D. (1961) Genetical analysis of methionine suppressors in *Coprinus*. *Genetics Research*, *2*, pp.141-155.

Liu, Y. (2001) *Fruiting body initiation in the basidiomycete Coprinus cinereus* (Doctoral dissertation, ETH Zurich).

Liu, Y., Srivilai, P., Loos, S., Aebi, M. and Kües, U. (2006) An essential gene for fruiting body initiation in the basidiomycete *Coprinopsis cinerea* is homologous to bacterial cyclopropane fatty acid synthase genes. *Genetics*, *172*, pp.873-884.

Lu, B.C., Gallo, N. and Kües, U. (2003) White-cap mutants and meiotic apoptosis in the basidiomycete *Coprinus cinereus*. *Fungal Genetics and Biology*, *39*, pp.82-93.

Lu, B. C. (1972) Dark dependence of meiosis at elevated temperatures in the basidiomycete *Coprinus lagopus*. *Journal of Bacteriology*, *111*, pp.833-834.

Lu, B. C. (1974a) Genetic recombination in *Coprinus*. IV. A kinetic study of the temperature effect on recombination frequency. *Genetics*, 78, pp.661-677.

Lu, B. C. (1974b) Meiosis in *Coprinus*. V. The role of light on basidiocarp initiation, mitosis, and hymenium differentiation in *Coprinus lagopus*. *Canadian Journal of Botany*, *52*, pp.299-305.

Lu, B. C. and Jeng, D. Y. (1975) Meiosis in *Coprinus* VII. The prekaryogamy S-phase and the postkaryogamy DNA replication in *C. lagopus*. *Journal of Cell Science*, *17*, pp.461-470.

Lu, B. C. (2000) The control of meiosis progression in the fungus *Coprinus cinereus* by light/dark cycles. *Fungal Genetics and Biology*, *31*, pp.33-41.

Lu, B. C., Gallo, N. and Kües, U. (2003) White-cap mutants and meiotic apoptosis in the basidiomycete *Coprinus cinereus*. *Fungal Genetics and Biology*, *39*, pp.82-93.

Madelin, M. F. (1956) Studies on the nutrition of *Coprinus lagopus* Fr., especially as affecting fruiting. *Anatomy of Botany*, 20, pp.307-330.

Majcherczyk, A., Dörnte, B., Subba, S., Zommorodi, M. and Kües, U. (2019) Proteomes in primordia development of *Coprinopsis cinerea*. *Acta Edulis Fungi*. 26: pp.37-50.

Masuda, R., Iguchi, N., Tukuta, K., Nagoshi, T., Kemuriyama, K. and Muraguchi, H. (2016) The *Coprinopsis cinerea Tup1* homologue *Cag1* is required for gill formation during fruiting body morphogenesis. *Biology Open*, *5*, pp.1844-1852.

Matthews, T. R. and Niederpruem, D. J. (1972) Differentiation in *Coprinus lagopus*. Springer, Archiv *für Mikrobiologie*, *87*, pp.257-268.

Matthews, T. R. and Niederpruem, D. J. (1973) Differentiation in *Coprinus lagopus*. Springer, *Archiv für Mikrobiologie*, *88*, pp.169-180.

McLaughlin, D. J., Beckett, A. and Yoon, K. S. (1985) Ultrastructure and evolution of ballistosporic basidiospores. *Botanical Journal of the Linnean Society*, *91*, pp.253-271.

Mishra, B., Choi, Y. J. and Thines, M. (2018) Phylogenomics of *Bartheletia paradoxa* reveals its basal position in *Agaricomycotina* and that the early evolutionary history of basidiomycetes was rapid and probably not strictly bifurcating. *Mycological Progress*, *17*, pp.333-341.

Mittwoch, U. (1951) Studies in the genetics of some X-ray induced morphological mutants in *Coprinus lagopus. Journal of Genetics*, 50, pp.202-205.

Moore, D. (1981) Developmental genetics of *Coprinus cinereus*: genetic evidence that carpophores and sclerotia share a common pathway of initiation. *Current Genetics*, *3*, pp.145-150.

Moore, D. (1998) Fungal morphogenesis. Cambridge: Cambridge University Press.
Moore, D. (1995) Tissue formation. In *The Growing Fungus* (pp.423-465). Springer, Dordrecht.
Moore, D. (1984) Developmental biology of the *Coprinus cinereus* carpophore: Metabolic regulation in relation to cap morphogenesis. *Experimental Mycology*, *8*, pp.283-297.
Moore, D., Elhiti, M. M. Y., Butler, R. D. (1979) Morphogenesis of the carpophore of *Coprinus cinereus*. *New Phytologist*, 83, pp.695-722.
Moore, D. and Stewart, G. R. (1971) Dedikaryotization of *Coprinus lagopus* following growth with 2-deoxy-D-glucose. *Transactions of the British Mycological Society*, *56*, pp.311-313.
Moore, D., Hock, B., Greening, J. P., Kern, V. D., Frazer, L. N. and Monzer, J. (1996) Gravimorphogenesis in agarics. *Mycological Research*, *100*, pp.257-273.
Moore, D. and Ewaze, J. O. (1976) Activities of some enzymes involved in metabolism of carbohydrate during sporophore development in *Coprinus cinereus*. *Microbiology*, *97*, pp.313-322.
Moore, D. and Pukkila, P. J. (1985) *Coprinus cinereus*: an ideal organism for studies of genetics and developmental biology. *Journal of Biological Education*, *19*, pp.31-40.
Morimoto, N. and Oda, Y. (1973) Effects of light on fruit-body formation in a basidiomycete, *Coprinus macrorhizus*. *Plant and Cell Physiology*, *14*, pp.217-225.
Mounce, I. (1922) Homothallism and heterothallism in the genus *Coprinus*. *Transactions of the British Mycological Society*, 7, pp.256-269.
Mueller, G. M. and Schmit, J. P. (2007) Fungal biodiversity: what do we know? What can we predict? *Biodiversity and Conservation*, *16*, pp.1-5.
Muraguchi, H., Umezawa, K., Niikura, M., Yoshida, M., Kozaki, T., Ishii, K., Sakai, K., Shimizu, M., Nakahori, K., Sakamoto, Y. and Choi, C. (2015) Strand-specific RNA-seq analyses of fruiting body development in *Coprinopsis cinerea*. *PLoS One*, *10*, p.e0141586.
Muraguchi, H., Fujita, T., Kishibe, Y., Konno, K., Ueda, N., Nakahori, K., Yanagi, S. O. and Kamada, T. (2008) The *exp1* gene essential for pileus expansion and autolysis of the inky cap mushroom *Coprinopsis cinerea* (*Coprinus cinereus*) encodes an HMG protein. *Fungal Genetics and Biology*, *45*, pp.890-896.
Muraguchi, H., Takemaru, T. and Kamada, T. (1999) Isolation and characterization of developmental variants in fruiting using a homokaryotic fruiting strain of *Coprinus cinereus*. *Mycoscience*, *40*, pp.227-233.
Muraguchi, H. and Kamada, T. (1998) The *ich1* gene of the mushroom *Coprinus cinereus* is essential for pileus formation in fruiting. *Development*, *125*, pp.3133-3141.
Muraguchi, H. and Kamada, T. (2000) A mutation in the *eln2* gene encoding a cytochrome P450 of *Coprinus cinereus* affects mushroom morphogenesis. *Fungal Genetics and Biology*, *29*, pp.49-59.
Nagy, L. G., Kovács, G. M. and Krizsán, K. (2018) Complex multicellularity in fungi: evolutionary convergence, single origin, or both? *Biological Reviews*, *93*, pp.1778-1794.

Nagy, L. G., Varga, T., Csernetics, Á. and Virágh, M. (2020) Fungi took a unique evolutionary route to multicellularity: Seven key challenges for fungal multicellular life. *Fungal Biology Reviews*, *34*, pp.151-169.

Namekawa, S. H., Iwabata, K., Sugawara, H., Hamada, F. N., Koshiyama, A., Chiku, H., Kamada, T. and Sakaguchi, K. (2005) Knockdown of LIM15/DMC1 in the mushroom *Coprinus cinereus* by double-stranded RNA-mediated gene silencing. *Microbiology*, *151*, pp.3669-3678.

Nakazawa, T., Ando, Y., Kitaaki, K., Nakahori, K. and Kamada, T. (2011) Efficient gene targeting in *ΔCc.ku70 or ΔCc.lig4* mutants of the agaricomycete *Coprinopsis cinerea*. *Fungal Genetics and Biology*, *48*, pp.939-946.

Nakazawa, T., Ando, Y., Hata, T. and Nakahori, K. (2016) A mutation in the *Cc.arp9* gene encoding a putative actin-related protein causes defects in fruiting initiation and asexual development in the agaricomycete *Coprinopsis cinerea*. *Current Genetics*, *62*, pp.565-574.

Nakazawa, T., Izuno, A., Horii, M., Kodera, R., Nishimura, H., Hirayama, Y., Tsunematsu, Y., Miyazaki, Y., Awano, T., Muraguchi, H. and Watanabe, K. (2017) Effects of *pex1* disruption on wood lignin biodegradation, fruiting development and the utilization of carbon sources in the white-rot Agaricomycete *Pleurotus ostreatus* and non-wood decaying *Coprinopsis cinerea*. *Fungal Genetics and Biology*, *109*, pp.7-15.

Nakazawa, T. and Honda, Y. (2015) Absence of a gene encoding cytosine deaminase in the genome of the agaricomycete *Coprinopsis cinerea* enables simple marker recycling through 5-fluorocytosine counter selection. *FEMS Microbiology Letters*, *362*, pp. fnv123-fnv123.

Navarro-González, M. (2008) Growth, fruiting body development and laccase production of selected coprini (Doctoral dissertation, Göttingen University).

Ohm, R. A., De Jong, J. F., Lugones, L. G., Aerts, A., Kothe, E., Stajich, J. E., De Vries, R. P., Record, E., Levasseur, A., Baker, S. E. and Bartholomew, K. A. (2010) Genome sequence of the model mushroom *Schizophyllum commune*. *Nature Biotechnology*, *28*, pp.957-963.

Plaza, D. F., Lin, C. W., van der Velden, N. S. J., Aebi, M. and Künzler, M. (2014) Comparative transcriptomics of the model mushroom *Coprinopsis cinerea* reveals tissue-specific armories and a conserved circuitry for sexual development. *BMC Genomics*, *15*, pp.1-17.

Pointing, S. (2001) Feasibility of bioremediation by white-rot fungi. *Applied Microbiology and Biotechnology*, *57*, pp.20-33.

Polak, E., Aebi, M. and, Kües, U. (2001) Morphological variations in oidium formation in the basidiomycete *Coprinus cinereus*. *Mycological Research*, *105*, pp.603-610.

Polak, E., Hermann, R., Kües, U. and Aebi, M, (1997) Asexual sporulation in *Coprinus cinereus*: structure and development of oidiophores and oidia in an AmutBmut homokaryon. *Fungal Genetics and Biology*, *22*, pp.112-126.

Pukkila, P. J., Shannon, K. B. and Skrzynia, C. (1995) Independent synaptic behavior of sister chromatids in *Coprinus cinereus*. *Canadian Journal of Botany*, *73*, pp.215-220.

Pukkila, P. J., Skrzynia, C. and Lu, B. C. (1992) The *rad3-1* mutant is defective in axial core assembly and homologous chromosome pairing during meiosis in the basidiomycete *Coprinus cinereus*. *Developmental Genetics*, *13*, pp.403-410.

Ravalason, H., Jan, G., Mollé, D., Pasco, M., Coutinho, P. M., Lapierre, C., Pollet, B., Bertaud, F., Petit-Conil, M., Grisel, S. and Sigoillot, J. C. (2008) Secretome analysis of *Phanerochaete chrysosporium* strain CIRM-BRFM41 grown on softwood. *Applied Microbiology and Biotechnology*, *80*, p.719.

Redhead, S. A., Vilgalys, R., Moncalvo, J. M., Johnson, J. and Hopple Jr, J. S. (2001) *Coprinus* Pers. and the disposition of *Coprinus* species sensu lato. *Taxon*, *50*, pp.203-241.

Riley, R., Salamov, A. A., Brown, D. W., Nagy, L. G., Floudas, D., Held, B. W., Levasseur, A., Lombard, V., Morin, E., Otillar, R. and Lindquist, E. A. (2014) Extensive sampling of basidiomycete genomes demonstrates inadequacy of the white-rot/brown-rot paradigm for wood decay fungi. *Proceedings of the National Academy of Sciences*, *111*, pp.9923-9928.

Romero, M. L. R., Yang, F., Lin, Y. R., Toth-Petroczy, A., Berezovsky, I. N., Goncearenco, A., Yang, W., Wellner, A., Kumar-Deshmukh, F., Sharon, M. and Baker, D. (2018) Simple yet functional phosphate-loop proteins. *Proceedings of the National Academy of Sciences*, *115*, pp.E11943-E11950.

Rühl, M., Majcherczyk, A. and Kües, U. (2013) Lcc1 and Lcc5 are the main laccases secreted in liquid cultures of *Coprinopsis cinerea* strains. *Antonie van Leeuwenhoek*, *103*, pp.1029-1039.

Sabotič, J., Ohm, R.A. and Künzler, M. (2016) Entomotoxic and nematotoxic lectins and protease inhibitors from fungal fruiting bodies. *Applied Microbiology and Biotechnology*, *100*, pp.91-111.

Shioya, T., Nakamura, H., Ishii, N., Takahashi, N., Sakamoto, Y., Ozaki, N., Kobayashi, M., Okano, K., Kamada, T. and Muraguchi, H. (2013) The *Coprinopsis cinerea* septin *Cc.Cdc3* is involved in stipe cell elongation. *Fungal Genetics and Biology*, *58*, pp.80-90.

Srivilai, P. (2007) Molecular analysis of genes acting in fruiting body development in basidiomycetes (Doctoral dissertation, Göttingen University).

Stajich, J. E., Wilke, S. K., Ahrén, D., Au, C. H., Birren, B. W., Borodovsky, M., Burns, C., Canbäck, B., Casselton, L. A., Cheng, C. K. and Deng, J. (2010) Insights into evolution of multicellular fungi from the assembled chromosomes of the mushroom *Coprinopsis cinerea* (*Coprinus cinereus*). *Proceedings of the National Academy of Sciences*, *107*, pp.11889-11894.

Subba, S. (2015) Morphological and anatomical study of growth and fruiting body developmental stages in *Coprinopsis cinerea*. (Master Thesis, Molecular Wood Biotechnology and Technical Mycology, Göttingen University).

Subba, S., Winkler, M. and Kües, U. (2019) Tissue staining to study the fruiting process of *Coprinopsis cinerea*. *Acta Edulis Fungi*, *26*, p.29.

Sugano, S. S., Suzuki, H., Shimokita, E., Chiba, H., Noji, S., Osakabe, Y. and Osakabe, K. (2017) Genome editing in the mushroom-forming basidiomycete *Coprinopsis cinerea*, optimized by a high-throughput transformation system. *Scientific Reports*, *7*, pp.1-9.

Sugawara, H., Iwabata, K., Koshiyama, A., Yanai, T., Daikuhara, Y., Namekawa, S. H., Hamada, F. N. and Sakaguchi, K. (2009) *Coprinus cinereus* Mer3 is required for synaptonemal complex formation during meiosis. *Chromosoma*, *118*, pp.127-139.
Swamy, S., Uno, I. and Ishikawa, T. (1984) Morphogenetic effects of mutations at the A and B incompatibility factors in *Coprinus cinereus*. *Microbiology*, *130*, pp.3219-3224.
Swamy, S., Uno, I. and Ishikawa, T. (1985) Regulation of cyclic AMP metabolism by the incompatibility factors in *Coprinus cinereus*. *Microbiology*, *131*, pp.3211-3217.
Takemaru, T. and Kamada, T. (1972) Basidiocarp development in *Coprinus macrorhizus*. *The Botanical Magazine= Shokubutsu-gaku-zasshi*, *85*, pp.51-57.
Terashima, K., Yuki, K., Muraguchi, H., Akiyama, M. and Kamada, T. (2005) The *dst1* gene involved in mushroom photomorphogenesis of *Coprinus cinereus* encodes a putative photoreceptor for blue light. *Genetics*, *171*, pp.101-108.
Tsusué, Y. M. (1969) Experimental control of fruit-body formation in *Coprinus macrorhizus*. *Development, Growth & Differentiation*, *11*, pp.164-178.
Uno, I. and Ishikawa, T. (1973) Purification and identification of the fruiting-inducing substances in *Coprinus macrorhizus*. *Journal of Bacteriology*, *113*, pp.1240-1248.
Uno, I. and Ishikawa, T. (1974) Effect of glucose on the fruiting body formation and adenosine 3′, 5′-cyclic monophosphate levels in *Coprinus macrorhizus*. *Journal of Bacteriology*, *120*, pp.96-100.
Uno, I. and Ishikawa, T. (1978) Effect of cyclic AMP on glycogen synthetase in *Coprinus macrorhizus*. *The Journal of General and Applied Microbiology*, *24*, pp.193-197.
Walser, P. J., Hollenstein, M., Klaus, M. J. (2001) Genetic analysis of basidiomycete fungi. Molecular and cell biology of filamentous fungi: *A Practical Approach*, pp.59-60. Oxford: Oxford University Pres.
Wälti, M. A., Villalba, C., Buser, R. M., Grünler, A., Aebi, M. and Künzler, M. (2006) Targeted gene silencing in the model mushroom *Coprinopsis cinerea* (*Coprinus cinereus*) by expression of homologous hairpin RNAs. *Eukaryotic Cell*, *5*, pp.732-744.
Waters, H., Butler, R. D. and Moore, D. (1972) Thick-walled sclerotial medullary cells in *Coprinus lagopus*. *Transactions of the British Mycological Society*, *59*, pp.167-IN25.
Waters, H., Butler, R. D. and Moore, D. (1975a) Structure of aerial and submerged sclerotia of *Coprinus lagopus*. *New Phytologist*, *74*, pp.199-205.
Waters, H., Moore, D. and Butler, R. D. (1975b) Morphogenesis of aerial sclerotia of *Coprinus lagopus*. *New Phytologist*, *74*, pp.207-213.
Wesenberg, D., Kyriakides, I. and Agathos, S. N. (2003) White-rot fungi and their enzymes for the treatment of industrial dye effluents. *Biotechnology Advances*, *22*, pp.161-187.
Whitehouse, H. L. K. (1948) *Genetics of Ascomycetes* (Doctoral dissertation, Cambridge).
Willis, K. J. (2017) *State of the world's plants report-2017*. Royal Botanic Gardens.
Wilson, D. B. (2009) Cellulases and biofuels. *Current Opinion in Biotechnology*, *20*, pp.295-299.

Witayakran, S. and Ragauskas, A. J. (2009) Synthetic applications of laccase in green chemistry. *Advanced Synthesis & Catalysis*, 351, pp.1187-1209.
Xie, Y., Zhong, Y., Chang, J. and Kwan, H. S. (2021) Chromosome-level de novo assembly of *Coprinopsis cinerea* A43mut B43mut pab1-1# 326 and genetic variant identification of mutants using Nanopore MinION sequencing. *Fungal Genetics and Biology*, *146*, p.103485.
You, L. F., Guo, L. Q., Lin, J. F., Ren, T. and Wang, J. R. (2014) Overproduction of geranylgeraniol in *Coprinopsis cinerea* by the expression of geranylgeranyl diphosphate synthase gene. *Journal of Basic Microbiology*, *54*, pp.1387-1394.
Zhang, W., Wu, X., Zhou, Y., Liu, Z., Zhang, W., Niu, X., Zhao, Y., Pei, S., Zhao, Y. and Yuan, S. (2014) Characterization of stipe elongation of the mushroom *Coprinopsis cinerea*. *Microbiology*, *160*, pp.1893-1902.
Zhou, J., Chen, L., Kang, L., Liu, Z., Bai, Y., Yang, Y. and Yuan, S. (2018) ChiE1 from *Coprinopsis cinerea* is characterized as a processive exochitinase and revealed to have a significant synergistic action with endochitinase ChiIII on chitin degradation. *Journal of Agricultural and Food Chemistry*, *66*, pp.12773-12782.

Chapter 2

Two alternative routes of development: early decisions

Contribution to this chapter

data from master studies are applied and extended to interpret the analysis
Input into scientific discussion: S. Subba and U. Kües
Manuscript writing: S. Subba
Manuscript reviewed by U. Kües

Subchapter 2.1. Pathway committed to fruiting: secondary hyphal knot formation

2.1.1. Abstract

Fruiting bodies are mainly formed by dikaryons, a mycelium with two distinct haploid nuclei in its cell. The two nuclei were received from mating of two distinct parental monokaryons, which are mycelia with only one type of haploid nuclei and which germinated from meiotic basidiospores. Unlike the dikaryon, a monokaryon cannot form fruiting bodies. Fruiting body development in *C. cinerea* begins with a simple vegetative hyphal growth followed by specific hyphal interactions to form a mycelial network on which dark-dependent primary hyphal knots are generated by loose hyphal aggregations of multiple short hyphal side-branches. In the absence of illumination, primary hyphal knots transform to the dark pigmented dormant structures named sclerotia which have a distinctive brown-colored outer rind. With induction of light, clusters of primary hyphal knots grouped together to form a 3-dimensional globular structure called secondary hyphal knot that can further develop under favorable conditions into a fruiting body primordium with distinctive cell tissues. With the supply of sufficient amount of light and nutrient conditions in a 12 h light/12 h dark rhythm, a young primordium in due course of time (7 days) can develop into a mature mushroom which eventually undergoes autolysis shedding black basidiospores. In this study, secondary hyphal knot formation by the self-compatible homokaryon AmutBmut and the fertile dikaryon with were observed.

2.1.2. Introduction

The morphogenetic pathway of fruiting body development in *C. cinerea* begins with a simple vegetative hyphal growth and branches, followed by specific hyphal interactions for aggregation, with a sequential formation and differentiation of several structural stages in cap and stipe formation, to grow into a mature carpophore. Environmental and physiological conditions and nutrient status play crucial roles in the production of the hyphae to branch and aggregate into a compact multi-cellular hyphal structure, with specific differentiations which then lead to the formation of fruiting body primordia with characteristic cap and stipe cell tissues (Kües 2000). Apart from mating-type genes as master regulators, the genetic factors that influence the development of the initial fruiting body are so far little known (Kües 2000).

It has been reported that two types of hyphal knots, primary (Pk) and secondary hyphal knots (Sk) are formed in the fruiting process of *C. cinerea*. Dark-dependent primary hyphal knots are generated by loose hyphal aggregations and arise from localized formation of multiple short hyphal side-branches. In absence of light, primary hyphal knots are transformed into darkly pigmented multicellular compact resting structures called sclerotia with a characteristic outer rind (Moore 1981; Clémençon 1997; Kües et al. 1998, Chapter 2.2). With reception of a light signal, primary hyphal knots transfer instead into compact aggregated secondary hyphal knots. The 3-dimensional globular secondary hyphal knots under favorable conditions (around 25 °C and dark/light phases), further develop into fruiting bodies primordia followed by a mature fruiting body over the time. The formation of the primary hyphal knot has been described in the literature in past studies. It usually results from a single hypha that branches and sub-branches to form the multiple short branches that interconnect with each other and fuse with the neighboring hyphae by the process called anastomosis, thereby forming easily recognizable hyphal aggregates within the hyphal lattice of vegetative mycelium (Matthews and Niederpruem 1972; Kües et al. 1998, 2000; Liu 2001; Velagapudi 2006). So far, however, little has been written about the further developmental process towards secondary hyphal knots.

There has always been a speculation on the origin of secondary hyphal knots as fruiting body initials whether it forms from a single hypha or multiple hyphae. Are they formed from a group of primary hyphal knots linked together on a mycelial matrix to create a globular tightly woven 3-dimensional (3D) structure, or does the formation of a secondary hyphal knot begin with a single primary hyphal knot on the mycelial surface, which within the hyphal lattice turned into a tightly woven structure as secondary hyphal knot or initial as called in older literature (Matthews and Niederpruem 1972), which subsequently then turns into a primordium (Matthews and Niederpruem 1972).

In this study, the window technique developed by Liu (2001) with cultures in agar medium in Petri dishes was used to investigate how primary and secondary hyphal knots were formed on the

vegetative mycelial surface of *C. cinerea* during the course of development. Further in this study, we followed up the transformation process from primary hyphal knot to secondary hyphal knot formation through observations at different intervals of time.

2.1.3. Materials and methods

2.1.3.1. Strains, media and standard cultivation conditions

C. cinerea strains used in this study were homokaryon AmutBmut (*A43mut, B43mut, pab1*$^{+}$) (Swamy et al. 1984) and dikaryon PS1X2 generated by mating from the coisogenic monokaryon PS001-1 (*A42, B42*) and PS002-1 (*A3, B1*) (Srivilai 2006).

YMG/T medium per liter: 4 g yeast extract, 10 g malt extract, 0.1 g tryptophan and 10 g agar were dissolved to 950 ml distilled water and 4 g glucose to a 50 ml distilled water and separately autoclaved (Granado et al. 1997). After autoclaving, solutions were mixed and poured into 9 cm sized Petri dishes. Plates were inoculated with a small agar block of fungal mycelium (dimensions 0.2 mm X 0.2 mm) onto the solidified agar in the middle of the plates.

Inoculated Petri dishes were placed into a light-proof ventilated black box which had been previously cleaned with 70 % ethanol. Moist tissue was placed inside the black box to create a moisture condition for good growth of the hyphae. The black box was then kept for 5 days in an incubator at 37 °C in dark condition.

2.1.3.2. Cultivation for the study of primary hyphal knots and microscopy

For microscopy studies, on the 5th day of incubation rectangular observation windows of 7 mm X 5 mm of dimensions were cut out of agar overgrown with fungal mycelia, close to the growth front at the edge of a 3 cm Petri dish. Cultures were then further incubated at 28 °C dark for 24 h to allow hyphae to grow onto the floor of the observation window. The hyphal developments within windows were monitored by using an Axiovert photomicroscope 25 (Zeiss, Göttingen, Germany) at different time intervals. During the course of study, certain modifications were done with respect to the selection of Petri dishes for the convenience in undertaking photographic evidences. Hyphal growth on the floor of the windows was photographed targeting the hyphal knot formation. A 30 mm yellow filter placed onto the light beam was used to avoid arrest to hyphal growth and hyphal knot development caused by blue light coming from the light source of the microscope (Liu 2001).

2.1.3.3. Cultivation for the observation of secondary hyphal knots, primordia and mature carpophores

For the microscopy of secondary hyphal knots, plates were inoculated and incubated as described above.

When growth of the fungal mycelia on the 5th day of incubation at 37 °C reached the region of about 1 mm close to the edge of 9 cm Petri dishes, rectangular observation windows of larger dimensions of 2 cm x 1 cm were cut out of the YMG/T agar plates to give sufficient space for the production of larger secondary hyphal knot and if possible, also for fruiting body primordia. The plates were further incubated for 24 h at 37 °C in the dark in an inverted position to prevent water condensation within the window for a clear observation of the hyphal growth onto the plastic floor of the window. The further incubation of the culture plates at 37 °C after cutting out windows will enable more hyphal growth onto the surface of the plastic window floor. After 24 hours of incubation at 37 °C in the dark, the fungal cultures with the windows were shifted to a fruiting chamber and incubated further in upright position at 25 °C under a 12 h light/12 h dark rhythm.

2.1.3.4. Photography

Samples were inspected underneath a Zeiss Stemi 2000-C binocular and a Zeiss Axiophot 2 photomicroscope (Goettingen, Germany) with 30 mm yellow filter at different enlargements. The binocular and the microscope were equipped with a Soft Imaging Color View II Mega pixel digital camera, linked to a computer. Photos were taken and analyzed with Analysis Software program (Soft Imaging System, Münster, Germany).

2.1.4. Results

2.1.4.1. Primary hyphal knot formation in dark

To investigate the formation of the primary hyphal growth, inoculated agar culture plates of the homokaryotic AmutBmut and the dikaryotic PS1X2 mycelium were incubated in a ventilated black box at 37 °C under dark conditions. When mycelia covered whole plates on 5th day of incubation, observation windows of 7 mm x 5 mm were made and the plates were further incubated at 28 °C. While hyphal growth and in much higher numbers, the Pk formation occurs in the windows also at 37 °C in the dark. This lower temperature condition was chosen due to the fact that hyphae grow more slowly at 28 °C than at 37 °C, with only a few hyphae penetrating into the free space on the window floor, which makes the documentation of hyphal development easier to understand. Hyphal growth was monitored at various time intervals.

After incubation for 24 hours at 28 °C in complete darkness, the growth of the hyphae was monitored and cataloged for both the homokaryon and the dikaryon on the bottom of a plastic Petri dish. A yellow filter was inserted into the light beam microscope to document Pk formation, as the fungus is sensitive to blue light (Kües et al. 1998), which can alter development to stop further differentiation.

In the homokaryon, seen at higher magnification at 48 h, hyphae branched from a main hypha which formed a primary hyphal knot were short and strongly branched with clamp cells (Fig. 1, series A). The short hyphae have restricted tip growth and were partially twisted and connected to the neighboring hyphae by anastomosis (Fig. 1, series A, marked by the red arrows). The hyphae appeared loosely held together. They further branched and sub-branched and at 60 h, they differentiated to form inner loosely interwoven structure of plectenchymatous nature, with a number of short hyphae extending freely outwards from the core (Fig. 1, series A).

In the dikaryon, the first recognized specialized characters were seen 24 hours after the windows were cut. At this point, one or more main hyphae locally formed many branches and short, high-density side branches in the mycelium to give a "bush-like" structure easily distinguishable from other hyphae growing over the plastic base of the window (Fig 1, series B, 24 h, the red arrow shows anastomosis). After 48 hours, there were more side branches and the main hyphae and the earlier side branches of the main hyphae became slightly longer and fused at the side position with some neighboring side hyphae forming a primary hyphal knot (Fig. 1, series B, 48 h, the red arrow shows anastomosis). After 72 hours, the hyphae branched further and formed a dense accumulation of hyphae with a dense core (Fig. 1, series B, 72 h).

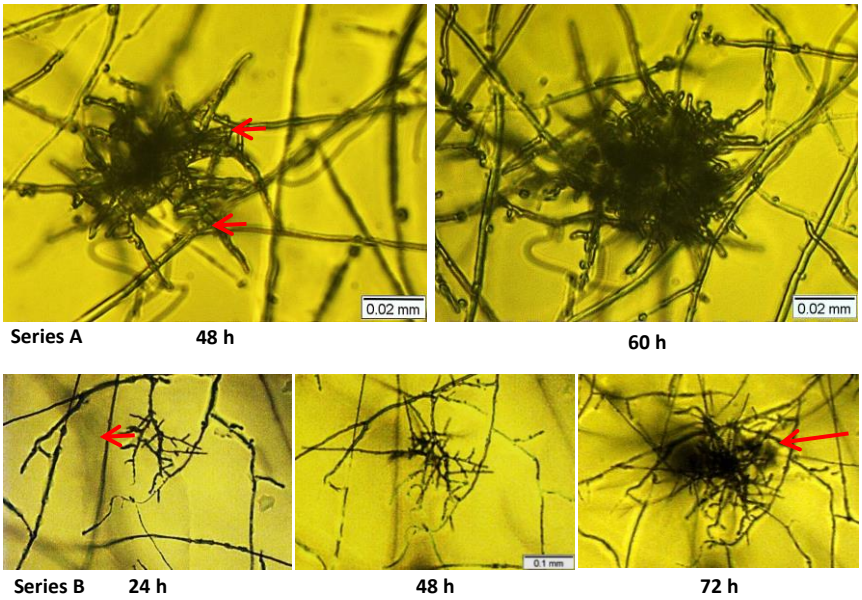

Fig. 1. Primary hyphal knot formation from a simple short hyphal branching.

Series (A) shows an individual primary hyphal knot at 48 h and the same compact hyphal aggregation established at 60 h in the homokaryon AmutBmut. Series (B) shows hyphal growth of dikaryon PS1X2 at 28 °C in dark over the time 24 h to 72 h of incubation documenting the development of a primary hyphal knot from the very young stage of hyphal branching and sub-branching to a mature primary hyphal knot. The red arrows show anastomosis.

2.1.4.2. Light induced secondary hyphal knot formation

Experiments were carried out using as strains homokaryon AmutBmut and dikaryon PS1X2 to observe on cut windows in agar plates the formation of secondary hyphal knots from vegetative mycelium. After 24 hours of incubation at 37 °C in the dark, growth of the vegetative mycelial network onto the plastic floor of the windows was observed, firstly macroscopically with the naked eye and secondly microscopically the details under the binocular. At this time of cultivation, a hyphal network of mycelium with fused hyphae was observed (photos not shown).

The next observation was made after further incubation of the cultures of homokaryon AmutBmut in the climate chamber at 25 °C for 24 h with a 12 h light/12 h dark regime. The observation under the binocular showed that on the plastic floor of cut windows, of the homokaryon AmutBmut, characteristic bright white 3-dimensional round mycelial aggregations (0.2 mm to 0.3 mm in diameter) were formed on the surface of the established vegetative mycelium (Fig. 2A). A photo of the same structure was also taken at higher magnification from the inverse light microscope (Fig. 2B, top Sk). These round hyphal aggregations were secondary hyphal knots. At the same time, similar secondary hyphal knots of same sizes were also observed on the upper agar edges of the window (photo not shown) and on the agar at the edge of the Petri dish as seen with the naked eye (Fig. 2D).

One of the secondary hyphal knots shown in the window in Fig. 2A grew further in size and differentiated into a globular fruiting body primordial structure (P1, Subba et al. 2019) at 48 h (Fig. 2C top). After 48 h, the structure aborted in further development, possibly due to non-availability of nutrients for the mycelium on the plastic floor of the Petri dish. P1 was the maximum stage in development a primordium could reach in all of window experiments done.

Window cultures made in the experiments of the AmutBmut nearly always gave Sks in the windows. In experiments performed with dikaryon PS1X2, Sk formation were also observed in the cut windows but only in about half of all cases. Similarly, only half of the numbers of Sks were obtained on the overgrown agar at the edges of Petri dishes (Fig. 2E) compared to that of homokaryon AmutBmut. Even with lower frequencies of Sk formation in the windows by dikaryon PS1X2, in both the strains, the window technique is found ideal for the observation of the formation of Sks.

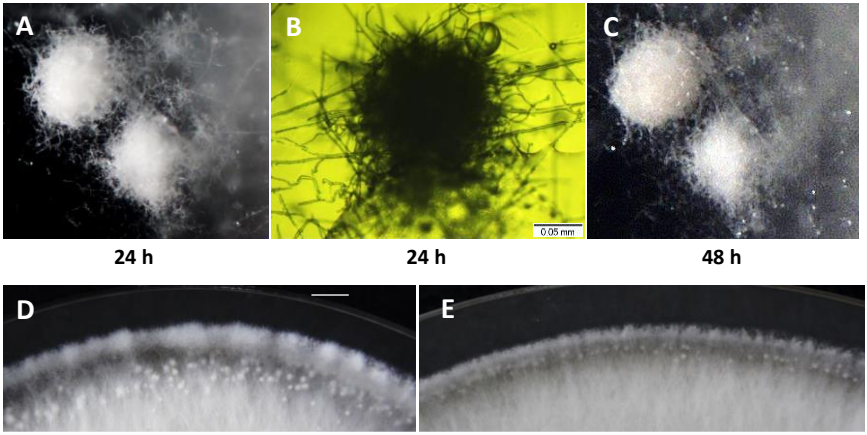

Fig. 2. Secondary hyphal knot formation on the plastic floor and on the agar plate at 25 °C. (A) Secondary hyphal knots formed by homokaryon AmutBmut on the plastic floor of the Petri dish at 24 h of incubation at 12 h light/12 h dark, (B) the same structure (top Sk) photographed underneath the inverse microscope, and (C) the same structure observed after 48 h of incubation. Secondary hyphal knots formed on the agar surface around the edges of Petri dish with YMG/T agar of (D) homokaryon AmutBmut and (E) dikaryon PS1X2 at Day 1of the fruiting pathway incubated in standard fruiting conditions. The scale bars on images A and C measures 0.1 mm.

2.1.4.3. Detail observations on Sk formation

In more detailed observations of further plates of the homokaryon AmutBmut, after 24 hours of incubation at 25 °C in a 12-hour /day 12-hour night rhythm, a lattice of hyphal mat with several cores of localized tightly packed hyphae were formed onto two neighboring locations in a window on the plastic floor of a Petri dish (Fig. 3, series A). After 48 hours, cores of aggregates with more localized hyphae and multiple branches were seen, forming a large oblong-shaped 3-dimensional secondary hyphal knot (0.3 mm, marked by red arrows in one of the places) and a small underdeveloped round Sk (0.2 mm) in the other. Water droplets appear to have been excreted from the mature fused secondary hyphal knots at the left side of the photo (Fig. 3, series A, 48 h to 96 h, marked by the blue arrows). The large secondary hyphal knot grew further in size within the next 72 h whereas the underdeveloped Sk on the right side remained unchanged. Further incubation lead to no further changes in the morphology, with the exception of a color change to a light-brown appearance of the larger secondary hyphal knot arrested in development (Fig. 3, series A). The brown color is a sign of aging (Moore 1981).

Series B in Fig. 3 shows many hyphal accumulations of the homokaryon AmutBmut on the surface of plastic floor at 24 h which led to the formation of several secondary hyphal knots at

various locations at 48 h. Some hyphal aggregations formed as more flat, dense mycelium (marked by yellow arrows) instead of a fluffier hyphal tuft that turned into 3D Sks and may have sacrificed further aerial growth in favor of neighboring Sks (Fig. 3, series B).

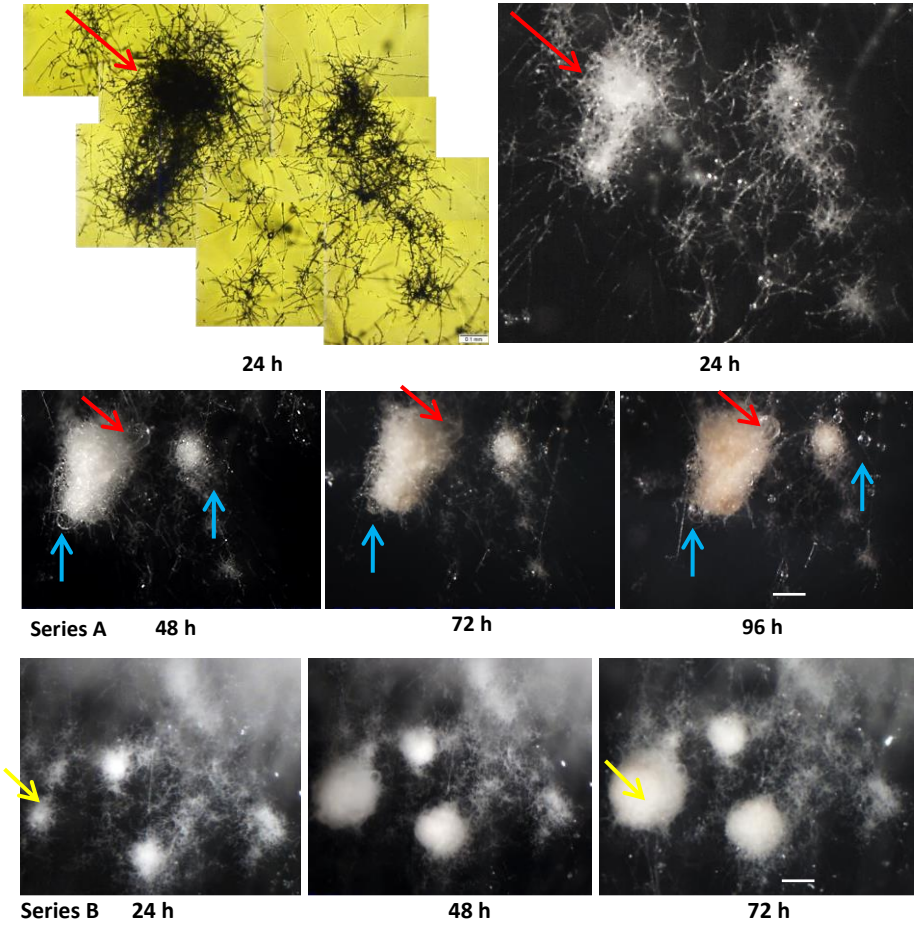

Fig. 3. Secondary hyphal knot formation by the homokaryon AmutBmut in two different windows of an agar culture of the same Petri dish. A mass of a 3-dimensional mycelial network with several loose hyphal aggregates (Pks) was formed after 24 h of incubation at 25 °C in the day/night rhythm on the plastic floor of a window. Series (A) shows that some of the structures further developed at 48 h to two neighboring secondary hyphal knots, a larger one (0.3 mm) and the smaller one that remained

underdeveloped (0.2 mm). Both knots at 72 h showed no further development. Similarly, at 96 h both the knots did not grow further, however, changed in color from white to light brown. Series (B) presents the process of secondary hyphal knot formation at 24 h, 48 h and 72 h in another window of the same plate. The photo of series (A) at 24 h was taken from the plate underneath the inverse microscope and the other photos were taken underneath a binocular 500 KL fitted with a white light from above. The scale bars measure 0.1 mm.

Similarly like in homokaryon AmutBmut, other series (A and B) presented in Fig. 4 show several secondary hyphal knots that formed by the dikaryotic strain PS1X2. In series A, two neighboring somewhat loose round hyphal aggregations were formed on the plastic floor of the Petri dish (Fig. 4, series A, 24 h). These two hyphal balls after incubating in the next 24 h further grew in size through hyphal branching and they fused together to give a compact dumbbell-like structure (Fig. 4, series A, 48 h). They stopped their growing further and remained the same for the next 24 hours (Fig. 4, series A, 72 hours). The arrest in development was confirmed by the further observation after 24 h (no photo taken).

In a parallel progress, series B photos in Fig. 4 were taken from another window on the same plate showing the formation of other secondary hyphal knots at different time intervals. Of the initial, of about seven loosely aggregated hyphal cores on the plastic floor, only three developed further into secondary hyphal knots of different size. The variation in arrest in the development in the size of the secondary hyphal knots was likely due to the lack of sufficient mycelial networks for the transport of sufficient nutrients and water. This contrasts the situation on the plate covered with agar and dense mycelium in which many more Sks were formed at the edges of the Petri dish but faster by one day (24 h after transfer to day/light condition due to the earlier established mycelia on the agar which is more reliable in time compared to the one that appear on the plastic floor depending on how fast the mycelia grow on the plastic floor, controlled by humidity).

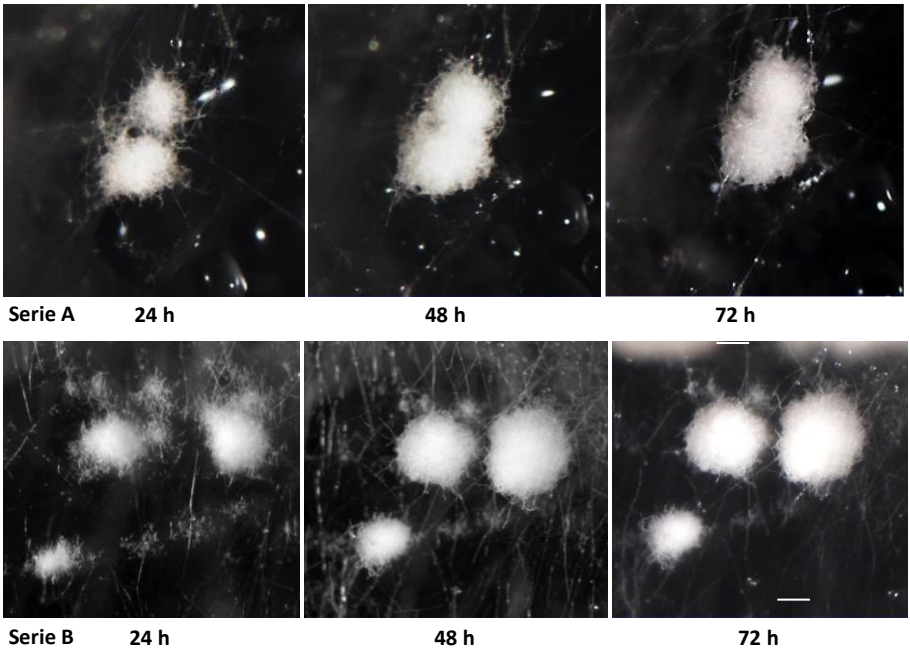

Fig. 4. Secondary hyphal knot formation of the dikaryon PS1X2 in two different windows of an agar culture of the same Petri dish. Series (A) shows two neighboring secondary hyphal knots formed at 24 h of incubation at 25 °C in day/night rhythm on the plastic floor of a window cut into the YMG/T agar. The two secondary hyphal knots at 48 h were observed to grow together and to fuse to give a dumbbell-like structure (series A, 48 h). The structure maintained this appearance for the next 24 h (series A, 72 h). Similar observations were cataloged in the photos shown in series (B) at 24 h and 48 h, respectively from another window of the same plate. The photos were taken from binocular 500 KL fitted with a white light from above. The scale bars measure 0.1 mm

2.1.4.4. Secondary hyphal knot formation in homokaryon AmutBmut and dikaryon PS1X2 at 25 °C under a normal day-night rhythm, observed first at 12 h after putting the plates into fruiting conditions

When analyzing the early developmental sequence in *C. cinerea*, it was observed that a primordium arises from a secondary hyphal knot (Fig. 2 and Fig. 3), but the emergence of a secondary hyphal knot in its very first step was still an unsettled issue. The next experiment with the homokaryon and the dikaryon was therefore to more specifically investigate the origin of the secondary hyphal knot and to observe the early process of growth of mycelia to form the secondary hyphal knots. For this purpose, the experimental process was repeated as before, with

the homokaryon and dikaryon growing at 37 °C and cutting windows in the agar and growing at 37 °C for another 24 hours until the entire experimental set-up was transferred to the climate chamber at the onset of light period and incubated at 25 °C in a 12-hour day/12-hour night rhythm. Initially, observations were made in all four window cuts of a same agar plate and then the decision was made after 12 h of incubation to focus the observation and the documentation in a one window cut which appear to me most promising by finding loose hyphal aggregation for easy observation after 12 h of incubation. After 12 h, documentations were then made at 16 h, 20 h and 50 h of further incubation.

2.1.4.4.1. Observations for the homokaryon AmutBmut

Observations of hyphal growth on the plastic bottom of the four windows cut into the YMG/T agar plate of the homokaryon AmutBmut were carried out under the microscope as well as under the binocular to detect any minute changes in hyphal growth. The first documentation was made after the day period (light period) of 12 hours incubation at 25 °C in the climate chamber. At this point, a vigorous 3-dimensional mycelial network that would develop to primary hyphal knots with a couple of hours was visible on the plastic floor of a window when it was observed under the binocular (Fig. 5, 12 h). However, consecutive photographs under the microscope over the whole mycelial areas on the plastic floor could not be taken because doing this would consume too much time that would be needed by the fungus to proceed in development of the primary hyphal knots. As an extra observation, a few small water droplets of oidia at the tips of oidiophores were also seen at this time point. In AmutBmut oidiation is light-induced which explains the formation of oidiophores.

The next observation was done on the same window floor after further 4 h, i.e. at 16 h of incubation at 25 °C, four of which were in the dark period of 12 h light/12 h dark. During this time, a dense fluffier hyphal growth was seen underneath the binocular compared to before and some hyphal aggregations (one encircled), which could be followed over the time was now recognizable within the mycelial network on the window floor (Fig. 5, 16 h). When observed under the inverse microscope, many primary hyphal knots with restricted hyphal length appeared in clusters on the plastic floor (Fig. 5, 16 h). Again, at this time of observation, also only a part of mycelial network on the window floor surface was documented focusing on areas of hyphal knot development (Fig. 5, 16 h). In addition, numerous oidia engulfed in large water droplets formed on the heads of the oidiophores were observed.

Concentrating at a small area of a specific hyphal knot formation, the observation under the binocular revealed a 3-dimensional aggregation that appeared as a distinct white, loosely held developing ball of hyphae within the mycelial network (Fig. 5, 16 h). When observed under the inverse microscope, the same structure appeared like a loosely interwoven ball-like aggregate of

hyphae (Fig. 5, 16 h). Since it was expected that here a secondary hyphal knot would generate, the distinctive structure was focused for further observation and followed up in the next time interval. Once secondary hyphal knot development was induced, longer light periods or higher light intensities under the binocular were not anymore harmful. There was no restriction to further growth of the young aggregations into secondary hyphal knots.

At the next time point, i.e., 20 h of incubation at 25 °C, eight of which were in the dark period, the observation revealed that several dense, flat hyphal aggregations were formed at various locations on the plastic floor of a window (Fig. 5, 20 h, marked by arrows). Among them, a distinct 3-D hyphal tuft (encircled at Fig. 5, 16 h) was formed which was also visible with the naked eye due to its bright white color. Underneath the inverse microscope, the structure looked like a compact hyphal ball (Fig. 5, 20 h).

At 50 h, the same window made on the YMG/T agar culture of the homokaryon AmutBmut was again observed. At this time point, generation of two secondary hyphal knots (encircled) was seen at different locations (Fig. 5, 50 h) on the window floor. Amongst these two secondary hyphal knots, one belonged to the hyphal tuft shown in Fig. 5 which was observed and followed up since 16 h (Fig. 5, 16 h, encircled).

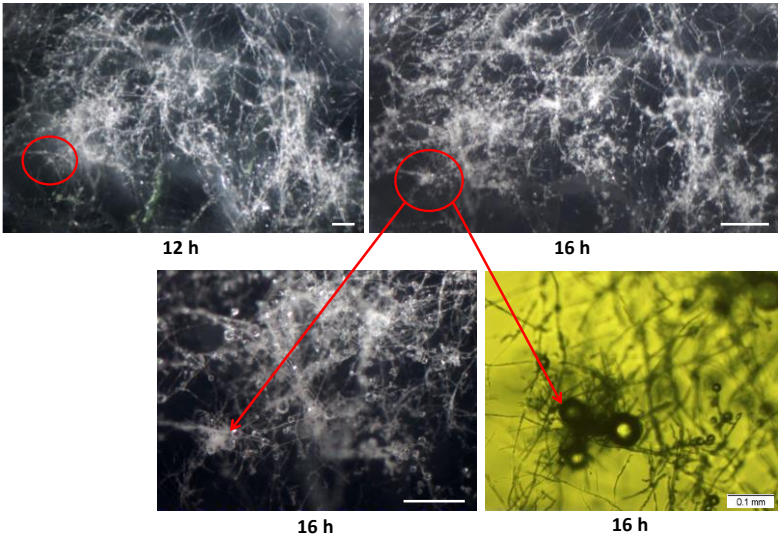

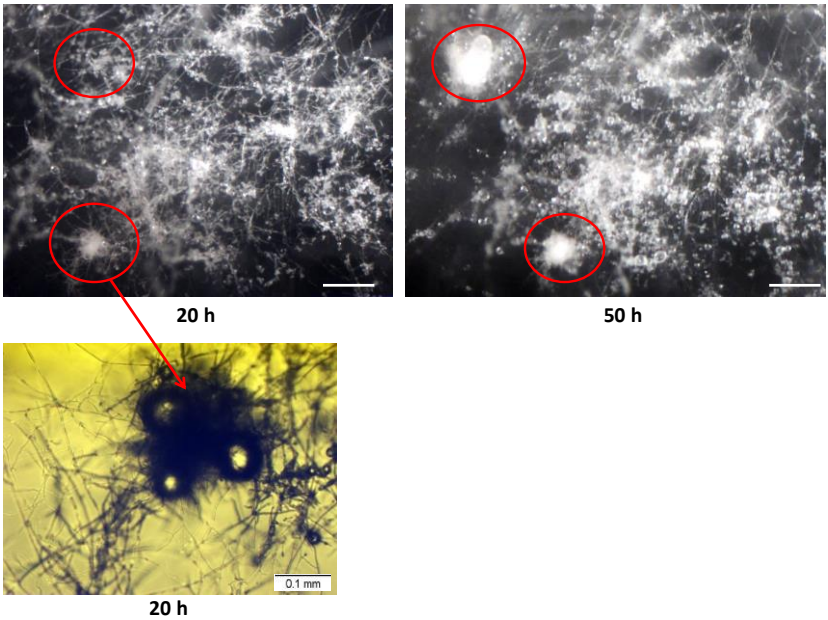

Fig. 5. Observation on the formation of Sks onto the surface of plastic floor of a window cut into an YMG/T agar culture of the homokaryotic strain AmutBmut at different time interval.

Photo at 12 h shows dense mycelial growth onto the surface of plastic floor of a window cut. Same area at 16 h shows fluffy mycelial growth and the hyphal aggregation (encircled) on the plastic floor were observed underneath the inverse microscope and the binocular, respectively. The focused distinct hyphal aggregation (encircled) at 16 h was seen underneath the binocular. Arrows point to the same place of a hyphal knot shown enlarged under binocular and the same structure seen under the inverse microscope. Note that the numerous water droplets represent oidia formation on the tips of oidiophores. The red encircled part in the photo at 20 h shows formation of hyphal tuft on the fluffy mycelial surface viewed under binocular. The red arrow indicates the same structure being focused and enlarged in the photo viewed under the microscope with the light from above using a yellow filter. The numerous water droplets representing oidia formation were increased in numbers and sizes at this time. The observation made after 50 h of incubation revealed the generation of two secondary hyphal knots in the same location on the plastic floor of the window. Note that the secondary hyphal knot represented by the red circle was followed since 16 h until this hour. The scale bas measures 0.1 mm.

2.1.4.4.2. Observation for the dikaryon PS1X2

Similar observations as for homokaryon AmutBmut were done underneath the binocular and the microscope on the four windows of the culture of the dikaryotic strain PS1X2 grown in parallel to the homokaryotic strain AmutBmut. Again, photos of only one window were documented at

12 h, 16 h, 20 h and 50 h following the detection of a more promising hyphal area with aerial mycelial tufts seen at 16 h.

After the day (light) period of 12 h of incubation at 25 °C in the climate chamber, a 2-dimensional mycelial network was seen grown onto the plastic floor of a window when observed underneath the binocular. The hyphal growth at this time was not as vigorous and 3-dimensional as that observed at the same time in the culture of homokaryon AmutBmut. The mycelial network of the dikaryon PS1X2 was dense but restricted to the surface of the plastic floor (Fig. 6, 12 h). Observations through the microscope were not made at this time point, since the only 2-dimensional growth suggested that it was yet too early to start the formation of primary hyphal knots.

The next observation was then done on at 16 h underneath the binocular as before. The mycelial network at this time point did not show much difference in the growth, but many oidia engulfed in water droplets were seen on the tips of oidiophores within the mycelial network (Fig. 6, 16 h). In accordance to that also oidiation is light-induced (Kertesz-Chaloupková et al. 1998). Again, no photographs were made underneath the inverse microscope at this time point to save time for the fungus not to be stressed by the light beam of the microscope.

The next observation time point was at 20 h underneath the binocular. During this time, several dense, flat 2-D hyphal aggregations at a distinct location on the window floor were seen (encircled). These aggregations appeared very bright among the other hyphae and they could be easily seen with the naked eye (Fig. 6, 20 h). The observation of the same area underneath the inverse microscope revealed that a cluster of primary hyphal knots were seen aggregated at this particular location within the mycelial network (Fig. 6, 20 h). Apparently, it took maximum 4 h to produce and aggregate primary hyphal knots at a place that did not show before any sign of further specific development. The distinctive hyphal aggregation was focused on for the further observation and followed up in the next observation, as this structure was expected to transform into secondary hyphal knot. Other than this, at 20 h of incubation, large water droplets engulfing oidia on the head of oidiophores were also observed within the mycelia showing that oidia production continued in the time from 16 h to 20 h of incubation.

At 50 h, several fused secondary hyphal knots at the same location as previously observed at 20 h were detected underneath the binocular (Fig. 6, 50 h). The observations made underneath the microscope revealed that compact structures of hyphae linked with one another were formed within the mycelial network on the plastic surface of the cut window at the specific place focused on for observation over the time (Fig. 6, 50 h).

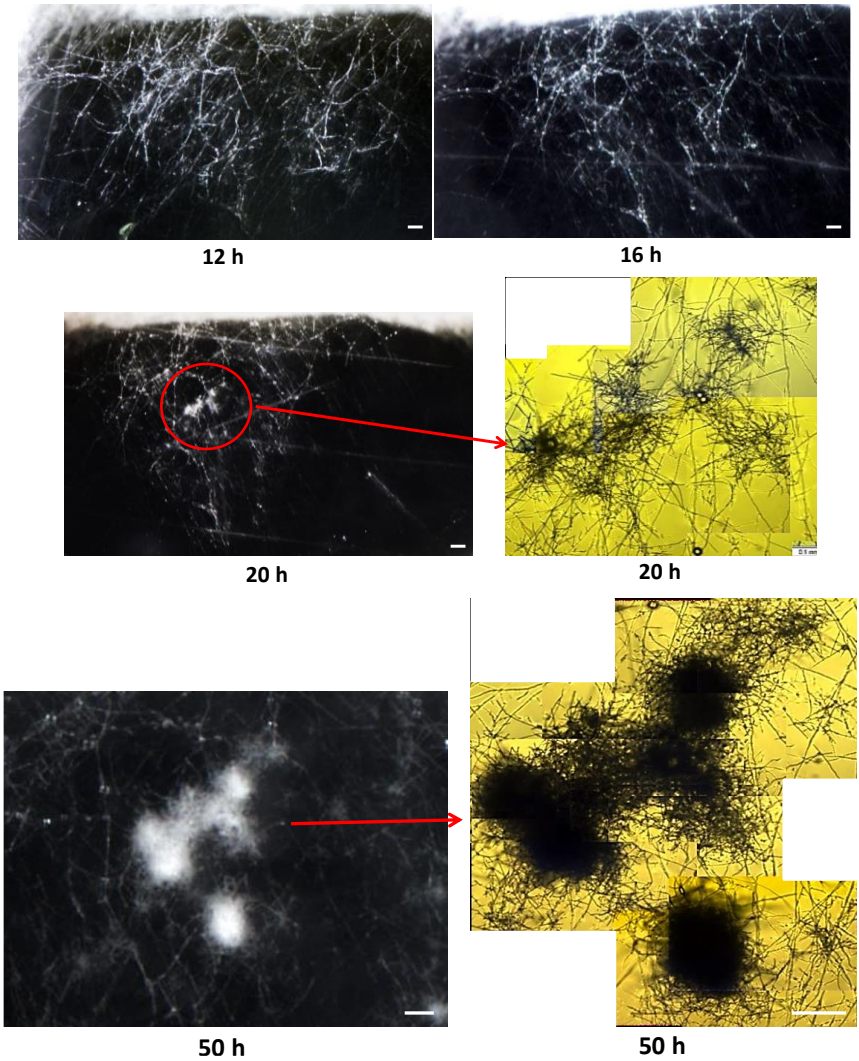

Fig. 6. Observation on the formation of Sks onto the surface of plastic floor of a window cut into an YMG/T agar culture of the dikaryotic strain PS1X2 at different time interval at 25 °C.

Photos at 12 h and 16 h show dense 2-dimensional mycelial growth onto the surface of plastic floor of a window cut. Same area at 20 h shows distinct, dense hyphal aggregations (encircled) on the window floor and arrow shows the enlarged part of the same structure underneath the inverse microscope. The same

location when observed at 50 h showed a cluster of Sks fused together in the distinct place. Underneath the inverse microscope (marked by arrow), several Sks connected to each other by mycelial network. The scale bars measure 0.1 mm.

The overall observations showed that, the general processes of forming a hyphal network and primary hyphal knots and aggregating and converting them to secondary hyphal knots were the same in the homokaryon and the dikaryon. A difference in the set of observation was the timing of the first hyphal aggregation, which was expected in hyphal knot to develop into secondary hyphal knots that appeared at 16 h in the homokaryon AmutBmut and 20 h in the dikaryon PS1X2. The time difference was due to the slower mycelial growth of dikaryon onto the plastic floor on which secondary hyphal knots are formed but once it is started, the timing for the progress in development of Pk and Sk are the same.

2.1.5. Discussion

Most of the studies conducted on *C. cinerea* in the literature are mainly based on the developmental process of fruiting body formation rather than at the initial hyphal growth and aggregation stages prior to specific steps in fruiting body formation. Therefore, this study mainly focuses on the developmental process of the initial hyphal knots, both primary and secondary hyphal knots, which are the foundation for the formation of fruiting bodies.

2.1.5.1. The terms primary and secondary hyphal knots in the literature

The complex process of fruiting in *C. cinerea* begins with a simple hyphal growth as a prerequisite, which continues to branch to form a mycelial matrix leading to the formation of a hyphal aggregation. The formation of hyphal aggregation has been described in the literature as such that a single hypha branch within a mycelial lattice (a network of interconnected hyphae). They further sub-branch to form short branches that are interconnected and merge with the neighboring hyphae and thereby form a hyphal aggregation easily recognizable underneath a microscope, considered as the first step in the initiation (Chapter 2.2), known in younger literature as the primary hyphal knot (Boulianne et al. 2000; Liu 2001; Lakkireddy et al. 2011; Kües et al. 2000). Although primary hyphal knots are considered the first initiation of the fruiting body, they are not specific to fruiting. The presence of a light signal can have a drastic impact on the developmental decision about what can happen on the vegetative mycelium (Lu 1974b, 2000; Kamada et al. 1978; Kamada and Tsuji 1979). With the induction by light, compact 3-dimensional aggregated secondary hyphal knots (Sks) (Velagapudi 2006; Lakkireddy et al. 2011) are formed instead of dormant sclerotia, which are generated from Pks in dark and aging cultures (Moore 1981, Chapter 2.2).

The secondary hyphal knot is the first fruiting body specific structure corresponding to stage 3 in Matthews and Niederpruem (1973) observation (see below). It has a diameter of 0.2 to 0.5 mm and has a compact core with highly branched cells, a plectenchyma that differentiates into cap and stipe in isocarpous manner (Matthews and Niederpruem 1973). The entire structure of a Sk is covered by a young universal veil which is composed of larger outward directed vacuolated hyphae (Matthews and Niederpruem 1972; Liu 2001; Velagapudi 2006; Lakkireddy et al. 2011).

Japanese researchers in the 1970s did not define a clear distinction between primary and secondary hyphal knots and reported hyphal knots as a light-dependent fruiting body initials with a diameter of 0.2 to 0.5 mm (Takemaru and Kamada 1972; Kamada and Takemaru 1977). They divided the development of the fruit body into three phases. Stage 0 was designated as undifferentiated dikaryotic mycelium, stage 1 as hyphal knots and stage 2 as primordia formation (Takemaru and Kamada 1972). Morimoto and Oda (1973) reported that the fruiting body initials appear as a ``fairy ring´´ on a culture incubated for 4 days in the darkness after exposing to the light. ``Fairy ring´´ of primordia formed on the Petri dish were also mentioned by Y.M. Tsusué (1969). This fairy ring is a ring of secondary hyphal knots that forms around the growth front of edges of the Petri dish after being exposed to the light as shown in the literature by Tsusué (1969) and Muraguchi et al. (2015).

2.1.5.2. Techniques to obtain Pks and Sks

The momentary observations were made by Matthews and Niederpruem (1972) from the different areas on the same cover slip on the surface of medium on a Petri dish. They reported that the initial stages of cellular growth and hyphal interactions intensified by anastomoses and resulted in the formation of delicate hyphal lattices upon which aerial hyphae arise to form loose mycelial aggregations which subsequently became more compact and took a shape of an early primordium (Matthews and Niederpruem 1972). In my experiments, I tried to observe the same structure over the time and documented how hyphae interact with each other and form a first hyphal aggregation in the homokaryon AmutBmut and in the dikaryon PS1X2. For this, I used a window technique adopted by Liu (2001) first on a small 3 cm Petri dish by inoculating agar piece at one edge of the plate. On the 5th day of incubation at 37 °C, I observed fungal growth to cover in entire agar area in the Petri dishes. Pks were easily observed and followed over the time, but transformation into Sk was rare on the 3 cm Petri-dish. Therefore, I changed to 9 cm plate which gives more nutrients for the fungal development. As mentioned previously by Velagapudi (2006), the general development of hyphal growth and the formation of the primary hyphal knot at 28 °C in dark was the ideal prerequisite for tracking and documenting the development process, which is why I subsequently moved fungal cultures with windows at 28 °C in the dark. The observation and the documentation were carried out within the window areas using an inverse photo microscope 25 with a yellow filter in order to restrict UV white light and in particular to eliminate the blue light

waves which can harm the hyphal growth and suppress any further development (Kües et al. 1998).

The first sign of primary hyphal knots in my observations were seen at 24 hours of incubation in complete dark after making windows into YMG/T agar cultures of the homokaryon and the dikaryon (Fig. 1 and 2). Matthews and Niederpruem (1973) reported from their individual observation that the time required to produce such hyphal aggregations from the hyphal lattices is about 24-30 h and they divided the initial steps of fruiting process into 4 stages. Stage 1 is the formation of hyphal lattices which are derived from localized interaction between secondary and tertiary branches of dikaryotic hyphae. In stage 2, the up-growth of aerial cells is formed followed by the increase in cell density. In stage 3, the cell growth and tissue organization take place forming a compact mass. In stage 4, hyphal aggregates differentiate into visible cap and stipe tissues with uniform distribution of polysaccharides, which was determined by using the periodic acid Schiff (PAS) reaction. This description clearly explains the sequential development as recognized nowadays from the primary hyphal knot (stage 2) to the secondary hyphal knot (stage 3) and to the primordium (stage 4).

2.1.5.3. Origin of knots from single or multiple hyphae?

Besides hypha-to-hypha connections to form a primary hyphal knot, single-cell origin theories of *C. cinerea*, were proposed by Brefeld (1877) who reported at that time the name under *Coprinus* for a carpophore, a single cell of the dikaryotic mycelium first produced lateral branches rapidly and to then formed irregularly a hyphal knot. Reijnders (1963) however, claimed that the development of a carpophore started from more than a single cell. An involvement of a single cell as an initiation point in the development of sclerotia of *C. cinerea* from the hyphal initials now called as Pk formed in dark was claimed by Moore and co-workers (1976). They further compared sclerotia with primordia and described a close connection between them in the initial growth phase. Finally, Moore (1981) gave genetic evidences that the first step in development (nowadays referred to as primary hyphal knot production) is shared between the pathways of sclerotia development that can occur in dark and in the light-induced pathways of fruiting body development. In my own observation, chapter 2.2 confirms it.

2.1.5.4. Observations on the formation of Sks in the current study

Despite all the studies done in the past, the origin of the secondary hyphal knot has always been an unsettled subject. In more recent years, authors such as Liu (2001), Göbel (2003) and Velagapudi (2006) carried out studies underneath the microscope to observe the initial development process of primary and secondary hyphal knots in window-cuts made in mycelial agar cultures but due to technical difficulties such as undefined needs in light conditions, light

intensity, light timings, sufficient nutrients and humidity, the developmental process could not be observed directly from one structure to another.

In my experiments, I too adopted a window technique to observe the initial development process of secondary hyphal knots on a large 9 cm Petri dish, using strains homokaryon AmutBmut and dikaryon PS1X2. The first sign of hyphal aggregations was seen in the homokaryon AmutBmut at 16 h of incubation (Fig. 5), four of which were in the dark and at 20 h in the dikaryon PS1X2, eight of which were in the dark at 25 °C under normal day-night rhythm (Fig. 6). By the careful observation underneath the binocular as well as underneath the microscope, it was revealed that these hyphal aggregations were formed with a mycelial network as a cluster of primary hyphal knots that became interlinked to one another. Eventually these aggregations grew at 50 h of incubation into a 3-dimensional globular structure named secondary hyphal knot (Fig. 5 and 6) as the first step specific in the pathway to fruiting body development (Navarro-González 2008). Crucially for the development of secondary hyphal knots in the cut windows was that on the one hand light was given to the cultures in the 12 h light/12 h dark rhythm in addition to high humidity, nutrients, temperature of 25 °C. Prior to the decision to form a secondary hyphal knot, the light intensity was an important issue for further development. A too long observation in the white light beam of the microscope and under the binocular was for example harmful for the switch into secondary hyphal knots. Therefore, where possible a yellow filter (in the microscope) was applied to eliminate blue light waves. This was however not possible in observations using the binocular by the external light sources applied. Interesting new observations came from observing secondary hyphal knot development. Once secondary hyphal knot development was induced, longer light periods or higher light intensities under the binocular were not anymore harmful. There was no restriction to further growth of the young aggregations into secondary hyphal knots. This observation in the small windows were reoccurring in the later experiments when full grown plates were exposed continuously to light without dark phase to light (Chapter 2.2).

2.1.5.5. Terminology of hyphal knots

Various terms have been used in the past to define primary and secondary hyphal knots. Moore (1995) used a hyphal tuft to refer to hyphal initials from which both fruiting bodies and sclerotia are created. Clémençon (1997) defined two types of noduli on the initial stages of fruiting body development; a primary nodulus as a woven structure from generative hyphae whose context is loose at first but becomes dense with maturity. Further growth of a primary nodulus leads to the formation of the secondary nodulus with a compact core surrounded by loose hyphae. Both primary and secondary noduli in the initial stages of fruiting body development are now regularly termed as primary and secondary hyphal knots (Boulianne et al. 2000; Kües 2000). However, the primary hyphal knot of Reijnders (1977) was described as a bundle of hyphae that are often found in the various tissues such as in the pileus and at the bottom of stems of a primordium which were

also identified and confirmed in my current observations. He further discussed the morphological difference between the primary and the secondary hyphal in a gilled fungi and termed a secondary hyphal knot as a ``basal plectenchyma´´ found at the base of the stipe. Atkinson (1914b) also described the secondary hyphal knot at the base of stipe in *Amanita* and mentioned that it is not a part of stipe but an independent organ which he named as ``podium´´.

These various nomenclatures given to secondary hyphae knots in the past (see above) reflect the different functions and different locations that lie beneath these terms. In my current analysis of the stained sections of a young stage 1 primordium, I have observed similarities in the hyphae that form Sk and the bundle of hyphae present at the base of stipe of a primordium earlier mentioned by Reijinders (1977) and Atkinson (1914b) which was connected to the mycelia. Such similarity in the morphology of the hyphae leads to speculation that Sks might act as a circulatory mechanism that transports both needed nutrients such as polysaccharides from the mycelium and growth signals through the developing primordia. The secondary hyphal knot, formed from a plectenchyma is meristematic in nature which further grows and differentiates into various tissues of distinct functions. Changes in the mycelia prior to the formation of nodules were first examined in *C. lagopus* by Madelin (1960) and reported that the mycelia are rich in glycogen (Waters et al. 1975a) and are transferred to the initials of the nodules and later to the primordia (Matthews and Niederpruem 1973; Clémençon 1997).

2.1.6. Conclusion

In conclusion from the results of this chapter, for the first time the initiation and the progress of the very early steps in the morphological development of fruiting body of *C. cinerea* were observed over the time and proven at individual structures that could be followed up over the time. It is now possible for me to recognize very early at which places a special structure will appear and this was crucial for following up the progress of individual structures. It is also essential to better define the environmental parameters of cultures during cultivation and during observation periods to ensure the success of individual development. In the coming chapters, later developmental stages from a primordium to the mature fruiting body as described and discussed in detail at different time intervals to understand tissue developments in the mushroom.

2.1.7. References

Atkinson, G. F. (1914b). The development of *Amanitopsis vaginata*. In *Annales Mycology, 12*, pp.369-392.

Boulianne, R. P., Liu, Y., Aebi, M., Lu, B. C. and Kües, U. (2000) Fruiting body development in *Coprinus cinereus*: regulated expression of two galectins secreted by a non-classical pathway. *Microbiology, 146*, pp.1841-1853.

Brefeld, O. (1877) Botanische Untersuchungen über Schimmelpilze. III. Basidiomyceten. Leipzig: Arthur Felix. (in German).
Clémençon, H. (1977) Die Strukturen der Basidiosporenwand und des Apikulus, und deren Beziehung zur Exogenisation der Spore. *Persoonia-Molecular Phylogeny and Evolution of Fungi*, *9*, pp.363-380.
Granado, J. D., Kertesz-Chaloupková, K., Aebi, M. and Kües, U. (1997) Restriction enzyme-mediated DNA integration in *Coprinus cinereus*. *Molecular and General Genetics*, *256*, pp.28-36.
Kamada, T. and Takemaru, T. (1977) Stipe elongation during basidiocarp maturation in *Coprinus macrorhizus*: mechanical properties of stipe cell wall. *Plant and Cell Physiology*, *18*, pp.831-840.
Kamada, T., Kurita, R. and Takemaru, T. (1978) Effects of light on basidiocarp maturation in *Coprinus macrorhizus*. *Plant and Cell Physiology*, *19*, pp.263-275.
Kamada, T. and Tsuji, M. (1979) Darkness-induced factor affecting basidiocarp maturation in *Coprinus macrorhizus*. *Plant and Cell Physiology*, *20*, pp.1445-1448.
Kertesz-Chaloupková, K., Walser, P. J., Granado, J. D., Aebi, M. and Kües, U. (1998) Blue light overrides repression of asexual sporulation by mating type genes in the basidiomycete *Coprinus cinereus*. *Fungal Genetics and Biology*, *23*, pp.95-109.
Kües, U. (2000) Life history and developmental processes in the basidiomycete *Coprinus cinereus*. *Microbiology and Molecular Biology Reviews*, *64*, pp.316-353.
Kües, U. and Navarro-González, M. (2015) How do Agaricomycetes shape their fruiting bodies? 1. Morphological aspects of development. *Fungal Biology Reviews*, *29*, pp.63-97.
Kües, U., Granado, J. D., Hermann, R., Boulianne, R. P., Kertesz-Chaloupková, K. and Aebi, M. (1998) The *A* mating type and blue light regulate all known differentiation processes in the basidiomycete *Coprinus cinereus*. *Molecular and General Genetics*, *260*, pp.81-91.
Kües, U., Walser, P., Klaus, M. and Aebi, M. (2002) Influence of activated *A* and *B* mating-type pathways on developmental processes in the basidiomycete *Coprinus cinereus*. *Molecular Genetics and Genomics*, *268*, pp.262-271.
Lakkireddy, K. K., Navarro-González, M., Velagapudi, R. and Kües, U. (2011) Proteins expressed during hyphal aggregation for fruiting body formation in basidiomycetes. In *Proceedings of the 7th international conference on mushroom biology and mushroom products*.
Liu, Y. (2001) *Fruiting body initiation in the basidiomycete Coprinus cinereus* (Doctoral dissertation, ETH Zurich).
Lu, B. C. (1974b) Meiosis in *Coprinus*: VI. The control of the initiation of meiosis. *Canadian Journal of Genetics and Cytology*, *16*, pp.155-164.
Lu, B. C. (2000) The control of meiosis progression in the fungus *Coprinus cinereus* by light/dark cycles. *Fungal Genetics and Biology*, *31*, pp.33-41.

Madelin, M.F. (1960) Visible changes in the vegetative mycelium of *Coprinus lagopus* Fr. at the time of fruiting. *Transactions of the British Mycological Society*, *43*, pp.105-IN5.
Matthews, T. R. and Niederpruem, D. J. (1972) Differentiation in *Coprinus lagopus*. Springer, *Archiv für Mikrobiologie*, *87*, pp.257-268.
Matthews, T. R. and Niederpruem, D. J. (1973) Differentiation in *Coprinus lagopus*. Springer, *Archiv für Mikrobiologie*, *88*, pp.169-180.
Moore, D. (1981) Developmental genetics of *Coprinus cinereus*: genetic evidence that carpophores and sclerotia share a common pathway of initiation. *Current Genetics*, *3*, pp.145-150.
Moore, D. (1995) Tissue formation. In *The Growing Fungus*, *21*, pp.423-465. Springer, Dordrecht.
Moore, D. and Jirjis, R. I. (1976) Regulation of sclerotium production by primary metabolites in *Coprinus cinereus* (= *C. lagopus* sensu Lewis). *Transactions of the British Mycological Society*, *66*, pp.377-382.
Morimoto, N. and Oda, Y. (1973) Effects of light on fruit-body formation in a basidiomycete, *Coprinus macrorhizus*. *Plant and Cell Physiology*, *14*, pp.217-225.
Muraguchi, H., Umezawa, K., Niikura, M., Yoshida, M., Kozaki, T., Ishii, K., Sakai, K., Shimizu, M., Nakahori, K., Sakamoto, Y. and Choi, C. (2015) Strand-specific RNA-seq analyses of fruiting body development in *Coprinopsis cinerea*. *PLoS One*, *10*, p.e0141586.
Navarro-González, M. (2008) Growth, fruiting body development and laccase production of selected coprini. (Doctoral dissertation, Göttingen University).
Reijnders, A. F. M. (1963) *Les problèmes du développement des carpophores des Agaricales et de quelques groupes voisins*. W. Junk.
Reijnders, A. F. M. (1977) The histogenesis of bulb and trama tissue of the higher Basidiomycetes and its phylogenetic implications. *Persoonia-Molecular Phylogeny and Evolution of Fungi*, *9*, pp.329-361.
Srivilai, P. (2006) *Molecular analysis of genes acting in fruiting body development in basidiomycetes* (Doctoral dissertation, Göttingen University).
Subba, S., Winkler, M., and Kües, U. (2019) Tissue staining to study the fruiting process of *Coprinopsis cinerea*. *Acta Edulis Fungi*, *26*, pp.29-38.
Swamy, S., Uno, I., Ishikawa, T. (1984) Morphogenetic effects of mutations at the *A* and *B* incompatibility factors in *Coprinus cinereus*. *Journal of General Microbiology*, *130*, pp.3219-3224.
Takemaru, T. and Kamada, T. (1972) Basidiocarp development in *Coprinus macrorhizus*. *The Botanical Magazine= Shokubutsu-gaku-zasshi*, *85*, pp.51-57.
Tsusué, Y. M. (1969) Experimental control of fruit-body formation in *Coprinus macrorhizus*. *Development, Growth & Differentiation*, *11*, pp.164-178.

Velagapudi, R. (2006) Extracellular matrix proteins in growth and fruiting body development of straw and wood degrading basidiomycetes (Doctoral dissertation, Georg-August-University of Göttingen).
Waters, H., Butler, R. D. and Moore, D. (1975a) Structure of aerial and submerged sclerotia of *Coprinus lagopus*. *New Phytologist*, *74*, pp.199-205.

Subchapter 2.2. Sclerotia formation as an alternate developmental pathway to fruiting in *Coprinopsis cinerea*

2.2.1. Abstract

The Agaricomycete *Coprinopsis cinerea* can undergo two alternate reproductive pathways on the dikaryotic mycelium, fruiting body development and sclerotia formation. Both processes start with formation of primary hyphal knots in the vegetative aerial mycelium under dark conditions. Light is a decisive factor that can control the fungus to enter an active fruiting process or the path to a dormant sclerotic stage. When no light signal is received, primary hyphal knots will be differentiated into multicellular sclerotia instead of developing into a light-induced fruiting body. Sclerotia are oval or globular, symmetrical, multi-cellular resting bodies whose main function is to survive stressed environmental conditions and germinate when the situation favors this. Here, we describe the cytological process of sclerotia formation. The mature sclerotium is comprised of an outer multi-layered melanized protective rind built of densely arranged short hyphal cells giving a paneled outer appearance. The internal medulla of sclerotia is composed of tightly packed swollen glutinous hyphae and large, ovulate and globular thick-walled cells that resemble mitotic chlamydospores. Such globular cells are known to store carbohydrates such as glycogen as reserve materials.

2.2.2. Introduction

Sclerotia are multicellular resting structures produced by various fungi in order to help them to survive extreme environmental conditions such as drought, freezing, microbial attack or absence of a host and, when the conditions improve, they germinate to reproduce. They are mainly formed by a dense aggregation of hyphal cells. Morphologically, sclerotia of different species may be of variable sizes, globular in shape or irregularly formed structures. Sclerotia usually have an outer protective layer referred to as rind and this layer is probably one of the reasons why sclerotia are often able to survive severe conditions. With maturation, a sclerotium rind commonly changes color from whitish to dark brown by the accumulation of melanin (Chet et al. 1967; Coley-Smith et al. 1979; Smith et al. 2015). A fungal sclerotium may be defined by three distinct layers, the outer rind, an underneath cortex region and the inner medulla. In size-expanding sclerotia, a cortex of compact rounded cells may develop as a pronounced layer under the rind as the sclerotium grows to a full size. Such cortex can be the region for the accumulation and storage of reserve materials. The inner medulla of a sclerotium is formed by interweaving of hyphae as a pseudoplectenchyma with an extracellular matrix (EM) of glutinous material. Like a cortical layer, the medulla may also have similar kinds of storage reserves and wall thickening functions by a compact interweaving of hyphae (Willetts and Bullock 1992).

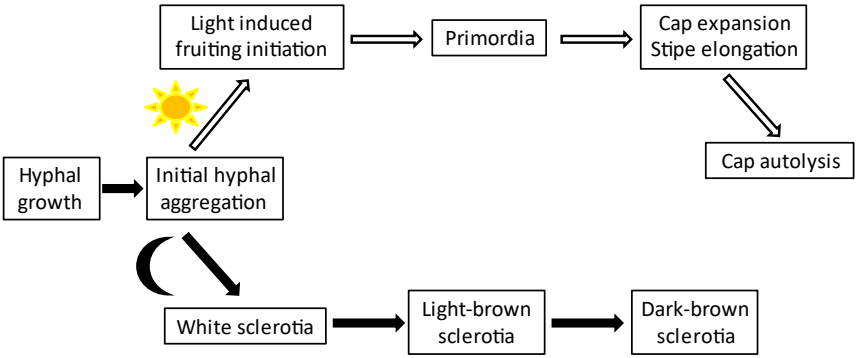

Diagram adapted from Bourne, Chui & Moore (1996)

Fig. 1. Two alternative developmental pathways in the life cycle of *C. cinerea.*

Sclerotia occur in ascomycetes as well as in basidiomycetes (Smith et al. 2015). Morphologies of sclerotia of the Agaricomycete *Coprinopsis cinerea* have been described earlier. Authors reported that sclerotia in *C. cinerea* might be formed in the aerial mycelium and submerged in the mycelium-agar phase in fungal cultures (Volz and Niederpruem 1970; Waters et al. 1975a;

Hereward and Moore 1979). The sclerotia are small, oval or globular, symmetrical, multi-cellular resting bodies (about 0.1-0.5 mm in Ø) comprised of an outer uni- or multi-layered pseudoparenchymatous rind, built of compact cells (Volz and Niederpruem 1970; Waters et al. 1975a). The internal prosenchymatous medulla is described to be composed of large, ovulate and globular cells of chlamydospore-like appearance with non-stained thickened macrofibrillar cell walls (Volz and Niederpruem 1970; Waters et al. 1972, Kües 2000; Badalyan et al. 2011; Watanabe et al. 2011). Waters et al. (1975a and 1975b) studied in phase contrast microscopy the earliest morphogenetic stages of colonies of *C. cinerea* grown on a slide and reported that sclerotia originated from intercalary hyphal cells. Initially for formation, only a single hyphal cell might be involved from which a small hyphal knot arises by branching as an initial for sclerotium formation (Waters et al. 1975b).

By apparently shared transient glycogen stores in early stages of development and by genetic evidences of four recessive sclerotia (*scl*) genes affecting both sclerotia and fruiting, Moore showed that carpophores and sclerotia in *C. cinerea* share a common early developmental pathway (Moore and Jirjis 1976; Moore 1981). While this conclusion found consent by other researchers (Kües et al. 1998, Kües 2000; Boulianne et al. 2000; Xie et al. 2019), conclusive cytological proofs for the alternate developmental transitions were not provided, among due to difficulties in microscopy to follow up individual structures over the time.

The circumstantial evidences suggested that sclerotia and fruiting bodies arise both from small aggregated hyphal knots. However, the first structure in the fruiting pathway recognized by eye was a light-induced compact white hyphal aggregate (about 0.2-0.3 mm in Ø) originally known as fruiting body initial and now termed as secondary hyphal knots (Kües 2000, chapter 2.1). In contrast, generation of the smaller hyphal knots and sclerotium formation happens in the dark (Kües et al. 1998, 2002; Badalyan et al. 2011). Boulianne et al. (2000) therefore distinguished primary hyphal knots as loosely aggregated mycelial structures obtained by intense localized formation of short stunted side branches in the dark form the larger secondary hyphal knots produced in a fertile mycelium upon a light signal as a compact ball of densely arranged undifferentiated hyphae. The authors assumed that it is the primary hyphal knot that potentially can enter alternatively sclerotium formation in the dark or the light-induced fruiting pathway to transfer into a secondary hyphal knot for mushroom production (Boulianne et al. 2000; Kües et al. 2002; Fig. 1). In common light microscopy, these alternatives are impossible to follow up because the blue light wavelengths in the light beam of the instrument will modulate the fungal behavior (Liu 2001; Lakkireddy et al. 2011). Active blue wavelengths however can be excluded by installing a yellow filter into the light beam of the microscope. The postulated path from a vegetative fertile mycelium over primary hyphal knots to secondary hyphal knots in the consecutive development of individual structures have thus been conclusively documented for the first time in a parallel study in the previous chapter 2.1.

Sclerotia in *C. cinerea* are known to be produced by both monokaryotic and dikaryotic mycelia in both aerial and submerged parts of mycelia over the broader range of growth temperatures (such as 25 °C and 37 °C) of the fungus (Waters et al. 1975b; Hereward and Moore 1979; Kües et al. 1998). However, some monokaryotic strains of *C. cinerea* were shown to be unable to form sclerotia on vegetative mycelium when recessive *scl* genes were present (Moore 1981). Transformation of *A*-mating type genes and *B*-mating type genes into monokaryons alone or in combination can enable or increase sclerotia production in the dark (Kües et al. 1998, 2002) suggesting that sclerotia formation is favored as a pathway in fertile dikaryons over sterile monokaryons. In this study, a fertile dikaryon PS1XPS2 and a self-compatible homokaryon AmutBmut that is fertile for fruiting body production by mutations in the *A* and *B* mating type pathways (Swamy et al. 1984; Boulianne et al. 2000) are used to cytologically study the development from primary hyphal knots to sclerotia.

2.2.3. Materials and methods

2.2.3.1. Strains and culture conditions

Dikaryon PS1XPS2 was generated by mating from monokaryons PS001.1 (*A42 B42*) and PS002-1 (*A3 B1*) which are coisogenic monokaryons to the self-fertile homokaryon AmutBmut (*A43mut, B43mut, pab1-1*) (Swamy et al. 1984; Srivilai 2006).

For the observation of hyphal knots and sclerotia, either the monokaryons or the dikaryon or the homokaryotic strain AmutBmut were inoculated onto fresh YMG/T agar (Granado et al. 1997) in plastic Petri dishes (9 cm in Ø) for growth at 37 °C in lightproof ventilated boxes as described (Kües et al. 2016). For microscopy studies, on the 5th day of incubation at 37 °C in the dark when the cultures nearly covered by mycelial growth the whole plates), two to four rectangular observation windows of 8 mm x 6 mm in dimensions were cut out as agar blocks with the mycelial growth fronts, 2 to 3 mm apart from the edges of the Petri dishes. Cultures were further incubated at 28 °C in the dark for 24 h to allow hyphae to grow onto the plastic floors of the observation windows and two further 24-h periods for sclerotia formation. The hyphal developments within windows were monitored 24 h intervals by using an Axiovert photomicroscope 25 (Zeiss, Göttingen, Germany). A 30 mm yellow filter placed onto the light beam was used to avoid arrest to primary hyphal knot and sclerotium development caused by blue light coming from the light source of the microscope (Liu 2001). Microscopy was performed in a dark room. Hyphal growth within windows was documented by photography along the edges of all four sides of the cut windows.

To observe the internal structures of sclerotia, individual mature sclerotia were harvested with the help of a sterilized needle from ageing YMG/T cultures grown for seven days at 37 °C in the dark. Harvested sclerotia were then placed on a microscope slide into a droplet of water used as a mounting media. A cover slip was pressed over the slide to squeeze out the sclerotium contents

for observation of the materials under a microscope Axiovert 5 (Zeiss, Göttingen, Germany) at different enlargements.

Harvesting of sclerotia from fully grown cultures for counting under a microscope were done using a Thoma Hemocytometer.

2.2.3.2. Harvesting, fixation and embedding of the sclerotia for staining

A metal or plastic loop (5 mm in Ø) had proven suitable for gently harvesting larger groups of sclerotia by gently combing the aerial mycelium of cultures with countless sclerotia. If sufficient sclerotia were accumulated on the loops by the combing, they were transferred into a fixation solution (FAE) consisting of 5 ml formaldehyde (37 %), 5 ml acetic acid (100 %) and 90 ml ethanol (70 %). The sclerotia fixed in this manner were stored at room temperature until further use.

For embedding, the sclerotia were freed from acetic acid and formaldehyde residues by each 30 min incubation at room temperature (RT) in an ascending ethanol series with 70 %, 80 %, 90 % and finally 96 % ethanol, respectively, under well mixing the sclerotia with the solutions on a rotating disc during the whole incubation times. Next, the sclerotia were transferred into a 1: 1 mixture of ethanol (96 %) and 2-propanol (99.9 %), and then into pure 2-propanol for incubation on the rotating disc for each 30 min at RT. Then, the sclerotia successively were placed in a 3:1 mixture, a 1:1 mixture and a 1:3 mixture of 2-propanol and Roti®-Histol (Carl Roth, Karlsruhe, Germany) and finally into pure Roti®-Histol for incubation of each 30 min at RT on the rotation drum. Subsequently for penetrating the plectenchyma of the sclerotia with paraffin, the sclerotia were placed into a cold saturated solution of Roti®-Plast (Carl Roth) in Roti®-Histol and left at 56 °C for 3 hours. Then, the samples were embedded in Roti-Plast melted at 56 °C and incubated overnight. Larger samples of sclerotia prepared in this way were then poured into pure paraffin at 56 °C in preheated molds and the samples cooled down.

For cutting of blocks of embedded sclerotia, the solidified paraffin block was warmed to slightly above RT in order to produce a clean-cut image on the microtome. A Leica RM 2265 rotary microtome (R. Jung, Heidelberg, Germany) was used for made in various thicknesses of 5 µm, 10 µm, 15 µm and 20 µm, respectively. Cuts were, softened on slides with a water film heated to about 30 °C on a heating block. The water was sucked off with cotton wool and samples further dried overnight at RT to adhere the plain sections onto the slides. Next, the wax in samples was completely eliminated from the tissue sections by washing them for 3 min at RT with a 100 % xylol solution, which was then removed with a series of ethanol solutions in decreasing concentration (96 %, 80 %, 60 %, and 30 %), each applied for 1 min at RT. The samples were then washed with tap water for 2 min. It is important to proceed carefully so as not to detach all sclerotia sections from the slides. When all wax residues have been removed, the dried slide can

be sealed with transparent resin (DePeX mounting medium (Serva, Heidelberg, Germany) and a cover glass to ensure that the cuts are durable. Alternatively, the cuts can also be subjected to a coloring treatment before sealing. For PAS-periodic acid double staining, a combination of periodic acid and fuchsin sulphurous acid, also known as PAS staining (periodic acid Schiff´s reagent; 0.2 % fuchsin, catalog no. 1358 Merck, Darmstadt, Germany), and Mayer's hemalum stain (hematoxylin + potassium alum) (Bayer, Leverkusen, Germany) were used. Sections were immersed in periodic acid (1 %) at RT for 10 min. Next, slides were dipped into Schiff's reagent for 20 min at RT. Sample were then placed into cold tap water for 1 minute and then into tap water at 40 °C for 5 minutes. Samples were immersed for the second staining into Mayer's hemalum solution for 20 min at RT. To drain the samples, then an ascending ethanol series (30 %, 60 %, 80 %, and 96 %) was run through for 3 min each. After the ethanol evaporated, samples were fixed by putting drops of DIPEX mounting medium (Serva, Heidelberg, Germany) onto the material and the sclerotic sections were sealed by putting cover slips on top.

2.2.3.3. Photography

Photography was done using a Zeiss Stemi 2000-C binocular, a Zeiss Zeiss Axiophot 2 photomicroscope (Goettingen, Germany) with different enlargements. The binocular and the microscopes were equipped with a Soft Imaging Color View II Mega pixel digital camera linked to a computer and photos were taken and analyzed with Analysis Software program belonging to the Color View II camera (Soft Imaging System, Münster Germany).

2.2.4. Results

2.2.4.1. Formation of sclerotia in mycelial cultures

Regularly, formation of masses of sclerotia ($3x10^4$ sclerotia per plate) were observed on YMG/T plates in the outer ca. 2-cm broad mycelial regions of colonies of homokaryon AmutBmut (Fig. 2A) and the dikaryon PS1XPS2 incubated at 37 °C for 9 days in constant dark but none were observed in the parental monokaryons.

When grown for only 5 days at 37 °C in constant dark, cultures of the fertile strains showed no sign of sclerotium formation. When such cultures were transferred to incubate further at 25 °C in constant dark, within 2 days cultures produced similar masses of sclerotia in the outer mycelial regions on the plates (Fig. 2A). In contrast, when the strains were cultured for 5 days at 37 °C in constant dark and were then transferred either into 25 °C and constant light or into 25 °C and at a 12h light/12h dark cycle (standard fruiting conditions, Granado et al. 1997) no or negligible amounts of sclerotia were produced, respectively. Under standard fruiting conditions, such well-grown mycelial cultures of 5 days-transfer age usually formed overnight secondary hyphal knots in the outer periphery of the plates, a part of which will further continue in the fruiting pathway (Subba et al. 2019; Majchercyk et al. 2019).

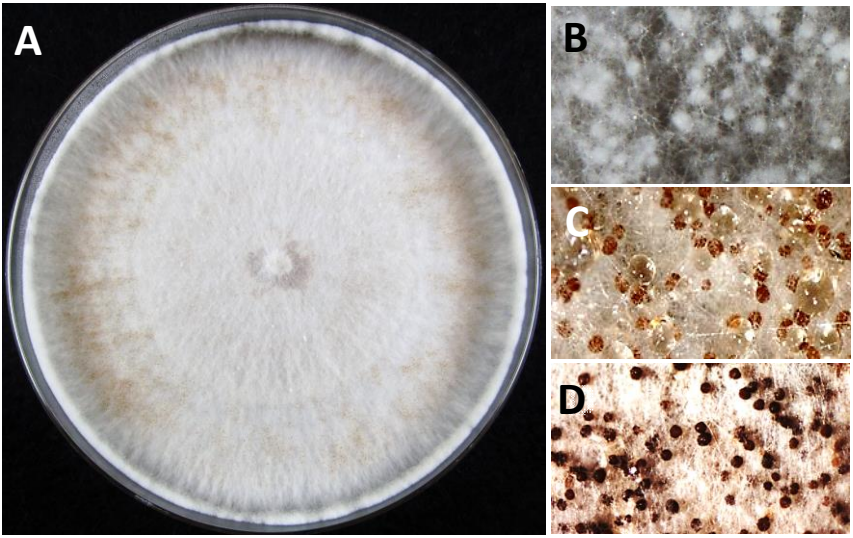

Fig. 2. Sclerotia formed on the mycelial culture plates. (A) Sclerotia formed on the 9 days older AmutBmut culture plate incubated under constant dark at 37 °C, (B) young white sclerotia which turn into (C) light-brown on the next day and then eventually mature into (D) dark brown sclerotia.

Sclerotia however may form mainly in the outer 2-cm regions of colonies when the time of culture transfer from 37 °C into fruiting conditions was too late (after > 5 days incubation at 37 °C in constant dark). Within a day, first white immature sclerotia accompanied by clear water droplets appeared in such cultures (Fig. 2 B) and then the sclerotia were stained light-brown a day after. Clear water droplets transform to pale yellow color at this stage and eventually the sclerotia become dark-brown with the disappearance of water droplets (Fig. 2C and D). Furthermore, when growing cultures during the incubation for 5 days at 37 °C in the dark were repeatedly disturbed, for example by daily exposing cultures during inspections to short periods of light, sclerotia formation was also observed together with some dark stipes instead of normal fruiting after transfer into standard fruiting conditions but in irregular patches over the outer colony regions (not shown).

We conclude from the observations that inner older colony areas formed early during growth periods on nutrient-rich medium are less likely prepared for sclerotium formation unlike outer younger hyphae formed at the end of the period of colony growth. Further, as noted before (Kües et al. 1998, Kües and Liu 2000) growth in constant light is blocking sclerotium formation while distinct temperatures are less important for sclerotium formation.

2.2.4.2. Formation of sclerotia from primary hyphal knots

To study the process of sclerotia formation further, inoculated agar culture plates of *C. cinerea* strains were incubated for 5 days at 37 °C in constant dark and humid conditions within a ventilated black box. When mycelia covered the entire plates, observation windows of dimensions 8 mm x 6 mm were made and the plates were further incubated in ventilated black boxes at 28 °C in constant dark. This temperature condition was chosen for the fact that hyphae grow slower at 28 °C than at the optimum growth temperature of 37 °C, with fewer hyphae entering the free space onto the window floor, making the documentation of hyphal development easier to follow up over the time. Hyphal growth was monitored at 24 h time intervals.

A yellow filter was used while taking photos to avoid arrest of hyphal knot formation caused by blue or white light. In common light microscopy, these alternatives are impossible to follow up because the white light beam of the instrument will modulate the fungal behavior. All dark performed reactions will be blocked while light-induced reactions in fruiting depend on low doses with too much light given also blocking any development (Kües 2000; Kües et al. 1998). Blue light provides the active wave lengths in controlling developmental processes in *C. cinerea* (Lu 1972; Kertesz-Chaloupková et al. 1998). Excluding the active wave length by using a yellow filter in the light beam of the microscope prior to reaching the cultures in observation allows the fungus to proceed towards the sclerotia formation pathway.

24 h after making windows and incubating all strains further at 28 °C in complete darkness, hyphal growth was monitored and cataloged along all sides of the cut windows. The observations revealed that the vegetative mycelia of all strains entered at this time onto the plastic surface of the free window space. Main hyphae branched vigorously and side branches from neighboring main hyphae connected to each other by anastomoses into a mycelial 2-dimensional network on the plastic ground of the Petri dishes (shown for homokaryon AmutBmut in Fig. 3A, 24 h). At 48 hours of incubation after making the windows, young primary hyphal knots were seen as tiny nests of accumulated short hyphae in cultures of homokaryon AmutBmut (Fig. 3B, 48 h) and the dikaryon PS1xPS2 in the form of loose whitish hyphal aggregations formed close to the outer edges of the observation windows. Primary hyphal knots were not formed everywhere but preferentially at the outer window side relative to the Petri dish with the youngest mycelium of the colonies. Individual hyphal knots had a distance of about 0.2 mm $\pm$ 1 (n=15) relative to each other for the both strains.

When the cultures were then further kept in the dark for another 24 h at 28 °C, primary hyphal knots that had previously formed (Fig. 3B, 48 h) were seen to be transformed into the resting structures sclerotia (for homokaryon AmutBmut see Fig. 3C, 72 h). While undertaking the observations, it had also been observed that more primary hyphal knots emerged at 72 h as

compared to 48 h, along with the formations of sclerotia that had been transformed from the previously formed primary hyphal knots.

Further observations of fungal behavior were made in the respective experiment documented in Fig. 3 after 72 h but the fungal cultures showed no remarkable changes. Therefore, no photographic evidences were cataloged after this particular hour, neither for homokaryon AmutBmut nor for the dikaryon PS1XPS2.

In cultures of the monokaryons PS001-1 and PS002-1, mycelial growth into the window cuts into colonies were observed 24 h and more 48 h after (Fig. 3D-3F). Constitutive oidiation (formation of unicellular asexual spores named oidia produced in liquid droplets on specialized aerial hyphae called oidiophores (Polak et al. 1997) was initiated in 48 h old windows with increasing oidial droplet sizes with further spore accumulations over the following 24 h (Fig.3D-3F). Like the hyphal knot and sclerotium production in the cultures of the dikaryon PS1XPS2 and of homokaryon AmutBmut, oidia formation was enhanced on the outer site of the windows with the younger mycelium. In the windows of cultures of PS001-1 and PS002-1, hyphal knots and a sclerotium were only exceptionally seen, indicating that the constitutive oidiation is the favored pathway of reproduction of the monokaryons (Polak et al. 1997).

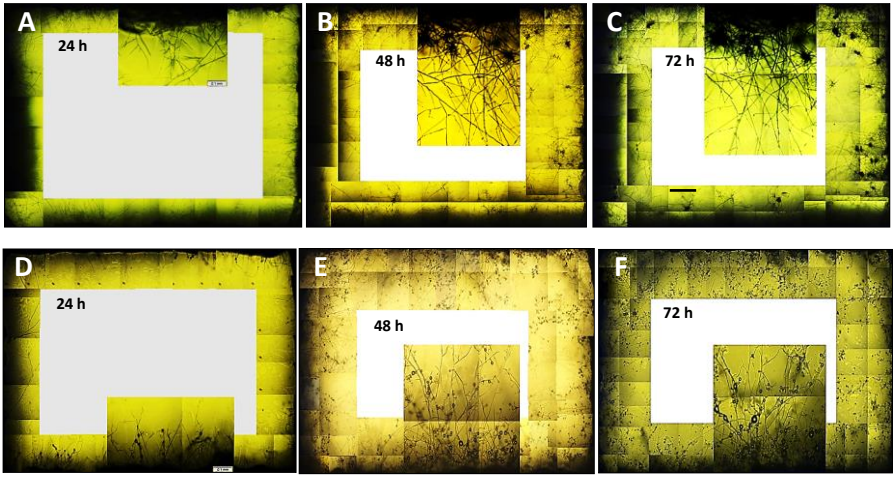

Fig. 3. Hyphal growth of homokaryon AmutBmut (A-C) and monokaryon PS001-1 (D-F) at 28 °C in the dark over the time from (24 h – 72 h) into the free space of the plain plastic surface of a window cut into YMG/T agar plates. (A) At 24 h, the fungus formed first vegetative mycelia with leading (main) hyphae and side branches. (B) At 48 h, few numbers of primary hyphal knots were seen, preferentially at the side of the window which is close to the outer edge of the Petri dish. The enlarged section of the picture

shows a clear view of hyphal growth and hyphal aggregations at the distinct places. (C) At 72 h, sclerotia appeared at the places where primary hyphal knots were detected before and at the same time, more new primary hyphal knots were seen to be emerged around the edges of the window. (D-F) The black spots in the monokaryon culture at 24 h at the side of the window close to the center of the Petri dish and at 48 h and 72 h around all sides of the window represent heads of oidiophores with droplets of oidia. Overlapping photos were taken through a light microscope 25 using a light source from above with magnification of 10 x (objective) and assembled into the larger images. Scale bars in the enlarged section measure 0.1 mm.

The differentiation process from a simple hyphal aggregation to a mature sclerotium on the plastic floor of a window cut into an YMG/T agar culture of AmutBmut at 28 °C at different time intervals are shown in Fig. 4. Among the five aggregations, only three branched further and transformed to the primary hyphal knots at 48 h while the other two directly transformed to sclerotia at this particular hour. Fig. 4 (bottom) shows mature sclerotia with an outer covering rind and the medullary part at the center.

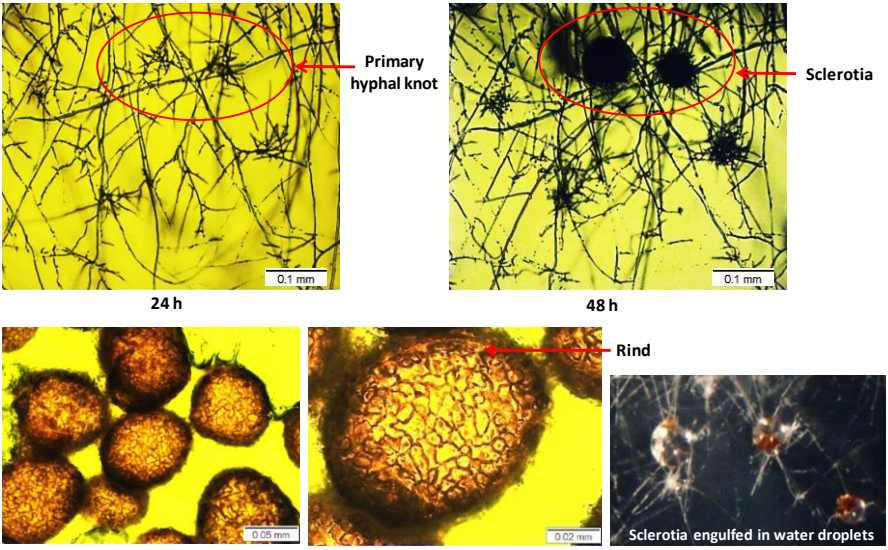

Fig. 4. Sclerotia formation from primary hyphal knots. (Top) The transition process from primary hyphal knots to sclerotia formed on the plastic floor of a window cut into an YMG/T agar culture of the homokaryon AmutBmut when kept at 28 °C in the dark at different time intervals as mentioned beneath each picture. Circled areas indicate the same region in the photos to ease localization of observed structures in the cultures. (Bottom) Mature sclerotia showing the outer rind and the center medulla part. (Bottom right) Sclerotia engulfed in pale yellow water droplets.

2.2.4.3. Chlamydospores -like cells in the medulla of sclerotia

Mature sclerotia were harvested from 9 days older aging cultures of the homokaryon AmutBmut in order to observe their internal contents. For this, the mature brown harvested sclerotia were placed onto a microscope slide and then covered with a cover slip. They were then pressed against the slide to squeeze out the sclerotium contents. Many round to oval to irregular chlamydospores-like structures (Kües et al. 1998) were seen along with many swollen hyphae within the squeezed sclerotia when observed under the microscope at different magnifications (Fig. 5). The chlamydospore-like round to oval cells are characterized by thick cell walls. The swollen cells are filled with condensed cytoplasm and they are believed to be hyphal transversions on the way to give rise to the chlamydospore-like cells. Similarly, white sclerotia were also harvested from the above-mentioned cultures and squeezed in the same way. However, chlamydospore-like cells were not yet formed as observed within ruptured white sclerotia (photos not taken). The hyphae were densely attached to each other so that it was not possible to recognize hyphal cells already that started to swell.

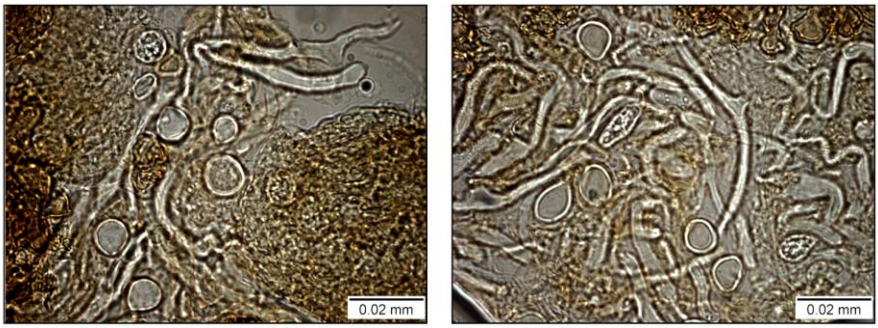

Fig. 5. Chlamydospore-like cells in the medulla of sclerotia. Many round to oval thick-walled chlamydospore-like cells in addition to short swollen hyphal fragments with dense cytoplasm within squeezed and pressed sclerotia harvested from the 9 days older culture of homokaryon AmutBmut, observed with 100 x enlargement.

2.2.4.4. Sectioning and staining of sclerotia to study the cellular composition

We further focused on the cellular composition of mature sclerotia and applied a histochemical method on the sclerotium. Sclerotia were embedded and sectioned in paraffin wax and double-stained using dyes PAS and hemalum. Fig. 6 shows sections of sclerotia of different shapes and sizes of 10 µm thickness without staining process. The thicknesses of the sections kept at 10 µm proved to be better than others because the thinner sections were lost on the slides during the embedding process while details in thicker sections were poorly visible. Sclerotia embedded in

the paraffin wax were randomly oriented and appeared in the cuts from elliptical to egg-shaped to circular (Fig. 6A and 6B).

The section of the sclerotium allowed a clear internal differentiation of the outer melanised rind and the central medullary part (Fig. 6C and 6D). In the Fig. 6, layers of melanised hyphae are seen as an outer cover around the sclerotium corresponding to compact scales as shown in the Fig. 4. Many round cells protrude out of the hyphae around the rind region. The small round cells and the hyphal layers are both melanised and together they form a multi-layered rind of a sclerotium. At the highest magnification, the hyphae with the bloated cells attached can be seen in the Fig. 6C and 6D. The medulla region appeared filled with mucilage material. However, they showed translucent hyphae of low contrast.

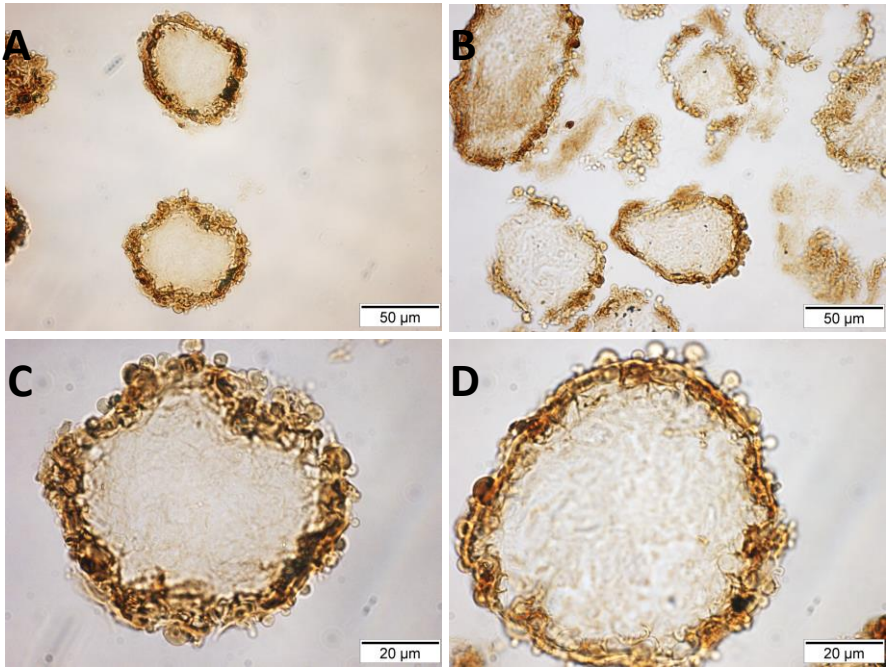

Fig. 6. Sections of sclerotia. A and D are the sections of mature sclerotia without staining showing the medullary and the melanised rind parts. A and B: The shapes of the cuts can be from elliptical to egg-shaped to circular, because of the random orientation during embedding in a paraffin wax. (C and D) A layer of melanised hyphae are seen around the sclerotium section and many round bulbous cells are present within the rind region. C and D: The content of the medullary region is poorly visible, however, a faint view of tightly packed hyphae are seen.

Furthermore, in a double-stained section of sclerotia, the PAS and hemalum combination remarkably stained the sclerotium section, separating the outer rind from the central medulla (Fig. 7). The double-stained sections showed a light-pink to pinkish blue appearance at the medullary part and few round cells marked by yellow arrows and few swollen hyphae marked by blue arrows at the medullary part distinctively stained in magenta color with a dark blue stained cell wall (Fig. 7A-7B). On the other hand, rind with its swollen hyphal layer marked by green arrow and the bloated cells marked by red arrow, were colored in deep-red to wine-red. PAS stain technique is commonly used to identify polysaccharides such as glycogen and polysaccharides are mainly stained by as a magenta color. In our sclerotia stained samples, we observed depositions of glycogen depicted by magenta color in both the rind and the medulla regions (Fig. 7A-7B).

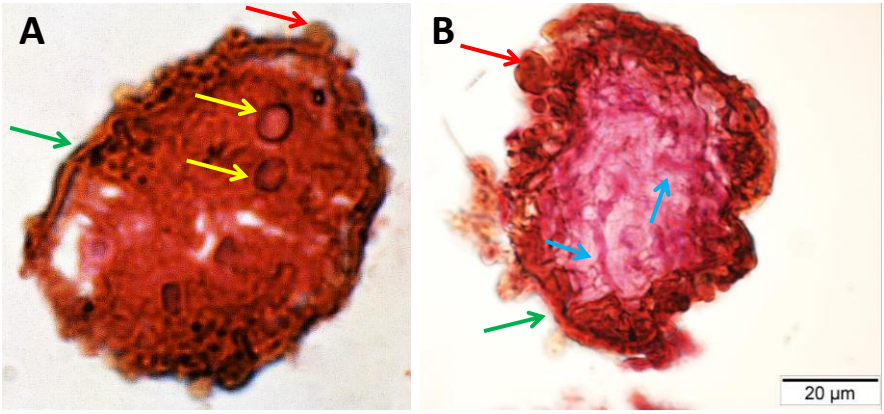

Fig. 7. Double-stained by PAS and hemalum 10 µm sections of the mature sclerotia showing the medullary and the rind parts. The rind with the compartmental layers of hyphae (marked by a green arrow) and the round ballooned cells (marked by a red arrow) are colored with deep-red to wine-red whereas the medulla is colored in light pink to pinkish blue color. Some swollen hyphae in the medulla (marked by blue arrows) are stained as magenta color and few isolated round cells (marked by yellow arrows) are stained in magenta with their cell wall stained as dark blue. These cells serve as storage cells and are rich in glycogen.

2.2.5. Discussion

The term sclerotia is derived from the Greek word skleros = hard. Sclerotia serve as reserve food materials, usually carbohydrate, so that the context becomes hard. However, some sclerotia have a gelatinous medulla eg. *Leucogyrophana pinastri*, therefore, the term may not fully justify the structure (Clemençon et al. 2004; Ginns and Weresub 1976). Sclerotia are the pseudoparenchymatous structures composed of a tightly built dense medulla and a melanised

rind. The main role of sclerotia is to survive under extreme environment which is why the hard outer covering rind is built.

2.2.5.1. Sclerotia in general

Fungal sclerotia are a compact mass of condensed vegetative hyphal cells which become interwoven and aggregate together and are covered by a uni- or multi-layered rind or cortex. Over 100 different species of fungi, both ascomycetes and basidiomycetes, were listed in past studies to produce sclerotia (Lindau 1910). Besides fungi, sclerotia are also produced by myxomycetes such as slime molds under unfavorable conditions which enable them to survive for many years (Chet and Henis 1975). They appear in clusters of hard-walled mono- or multinucleate units called "spherules" (Jump 1954; Chet and Rusch 1969).

Sclerotia-forming fungi include plant pathogens (25 genera) but many other are ectomycorrhizal (11 genera) and saprotrophic (30 genera) (Smith et al. 2015). Investigations on the development and the structure of several types of fungal sclerotia were made almost 100 years ago and it was reported that there are three main types of development referred to as loose, terminal and lateral (Brefeld 1877; Willetts 1972). The loose types are formed by irregular branching of mycelia followed by intercalary hyphal septation and hyphal swelling. They are known to be the most primitive and least common types and are illustrated by *Rhizoctina solani*. In *R. solani*, sclerotia appear with no rind but with a mass of loosely interwoven hyphae (Coley-Smith and Cooke 1971). Such sclerotia become darkly pigmented when matured. The terminal type of sclerotia are formed by hyphal branching at the tip of hyphae, e.g. as in *Botrytis cinerea.* Lateral sclerotia are formed by the interweaving of side branches of one or several main hyphae, e.g., as in *Sclerotium rolfsii*. Besides, sizes of the sclerotia also vary. The sizes of the sclerotia of the air-borne fungal pathogens are variable in size and can attain maximal diameter of 2 cm. The sclerotia of root-infecting fungi are smaller from 1 to 2 mm in diameter. In *S. rolfsii*, sclerotia are composed of four distinct layers: a thick outer skin, a rind made of broad and flattened cells layers, an underneath cortex of thin-walled cells with densely stained cytoplasm and a medulla made of loosely arranged filamentous hyphae.

2.2.5.2. Sclerotia formation in *C. cinerea*

Sclerotia of *C. cinerea* appear to originate laterally by the interweaving of side branches of one or the several main hyphae forming a compact structure (Fig. 2 and 3). They are oval or globular, symmetrical, multi-cellular resting bodies of about 0.1 mm to 0.5 mm that have been noticed in both mono-and dikaryons within aerial and submerged mycelia. The mature sclerotium is covered by an outer rind built with compact cells with usually brown-stained cell walls. The inner of the sclerotia, the medulla is filled by large non-stained round to oval cells with thick cell walls (Waters et al. 1975b). Volz and Niederpreum (1970) reported that mature sclerotia of *C. cinerea*

possessed an outer unicellular rind layer composed of cells with thickened and pigmented walls, which enclose a medulla composed of a compact mass of thin-walled bulbous cells and hyphae. Whereas a later study claimed that sclerotia are found to have a multi-layered rind enclosing a compact medulla composed predominantly of thick-walled cells (Waters et al. 1972, 1975a).

Generally, there are three steps distinguished in the formation and the development of sclerotia as described by various authors (Townsend and Willetts 1954). The first step as an initiation of small distinct initials from the interwoven hyphae, the second step as a development by the increase in size and the third step as maturation (Chet and Henis 1975). The pigmentation of sclerotia is often associated with droplet excretion (Cooke and Mitchell 1969, 1970). Waters et al. (1975b) proposed that sclerotia of *C. cinerea* developed from a single cell and it is very likely that fruiting body primordia which developed from secondary hyphal knots shared the same pathway starting from primary hyphal knots. Similarly, Moore and Jirjis (1976) compared sclerotia with fruiting body primordia and described a close connection between them. Finally, Moore (1981) gave genetic evidences, that first step in the development (primary hyphal knot production) is shared between the pathways of sclerotia development that occurs in dark and fruiting body development induced by light. The formation of the hyphal knot is thus, a decisive stage which can further either develop to a carpophore or a sclerotium (Moore 1981).

2.2.5.3. Types of sclerotia

Two types of sclerotia have been described earlier by Waters, Butler and Moore (1975a and 1975b) on the basis of their anatomical aspects; loosely organized sclerotia formed in the submerged mycelia and compact highly organized sclerotia formed in aerial mycelia. Mature submerged sclerotia were usually larger (0.5 - 1.0 mm) than aerial sclerotia (0.1- 0.5 mm), less regular in shape, and paler. In contrast to aerial sclerotia, their medulla is loosely organized and the thickness of the layer of rind cells was uneven. Mature aerial sclerotia are covered by an outer layer of dead and dying hyphae. Further investigations on phenotype of sclerotia revealed that, two different types of sclerotia were formed by monokaryons, a Z-type and an H-type had been described by Hereward and Moore (1979), on the basis of rind formation. Monokaryon strain H1 produces H-type sclerotia that had rind with many cells thick layer was comparable to the morphology described by Volz & Niederpruem (1970) and monokaryon strain ZBw601/40 produced Z-type that had rind with only one cell thick layer as was described by Waters et al. (1975a). Sclerotia are known to be produced by both monokaryotic and dikaryotic mycelia in both aerial and submerged parts of the mycelium (Hereward and Moore 1979). However, some monokaryotic strains of *C. cinerea* were described to be unable to form sclerotia on the vegetative monokaryotic mycelium (Waters et al. 1975b; Moore 1981). Genetic analysis had shown that four distinct genes (*scl*) were represented, all being recessive to their functional sclerotium-producing alleles (Hereward and Moore 1979).

2.2.5.4. Structure of sclerotia

In this study, we observed that primary hyphal knots differentiated into sclerotia in around 24 h to 48 h to 72 h in the homokaryotic strain AmutBmut in constant darkness (Fig. 3 and 4). Furthermore, sclerotia observed were categorized on the basis of their maturation and color into i) harvestable compact globular structures termed as white sclerotia as a young immature sclerotium stage, ii) upon maturation, they first changed to light brown colored sclerotia and iii) then to dark brown sclerotia with the prominent rind as the outer circumference (Fig. 2 and 4). No further development takes place after this phase. Hence, these structures function as resting bodies whose production are directly related to the dryness of the agar media.

According to Waters et al. (1975a), the medulla is composed of packed tissues of hyaline thick-walled cells. Willetts and Bullock (1992) also reported the presence of mucilage material in the medulla of sclerotium produced by *Sarracenia minor* which is secreted through the hyphal walls and is distinct from the compact cell wall. Therefore, they named this material the extracellular matrix (EM) to describe it. Kües et al. (1998) reported that the internal cells within the medullary part of sclerotia is composed of large, ovulate and globular cells with non-stained cell walls that resemble chlamydospores. In literature, chlamydospores are explained as large, thick-walled mitospores with condensed cytoplasm (Lewis 1961, Kües et al. 1998). They were seen to be variable in form and may be round, oval and of irregular shape. They were found in brown patches present on the submerged mycelia mats of older agar cultures of dikaryons and occasionally on certain monokaryons. The origin of such kind of spores are not well documented, yet two possibilities were assumed for chlamydospores generation, the first being that such type of structures might have internally been arisen within the cells of hyphae through compression of cytoplasm and subsequent cell wall generation around the condensed protoplasts, the second is that they might have been generated by budding and transfer of compressed cytoplasm from hyphal the cells towards the buds (blastocyst) (Clémençon 1997).

During my experiments, many round to oval to irregular chlamydospore-like structures along with many swollen hyphae within the squeezed sclerotia were seen when observed under the microscope at different magnifications (Fig. 5). The chlamydospore-like round to oval cells were characterized by thick cell wall (Fig. 5) and, in some of them, round bodies were seen of probably lipid nature due to the presence of yellow material within the cell (Fig. 5). In addition, there were swollen cells that were filled with condensed cytoplasm and that are believed to be hyphal transversions on the way to give rise to the chlamydospore-like cells (Fig. 5).

2.2.5.5. Sclerotial exudation

Furthermore, there have been many reports on exudation from sclerotia (Colotelo 1978). Exudation is a common phenomenon during the early stages of sclerotium development

(Townsend and Willetts 1954). During sclerotia development, small droplets were produced on the surface of sclerotia and these droplets coalesce to form large droplets when the sclerotia become mature and pigmented (Wong and Cheung 2008). The droplets may remain on the sclerotia from several days to several weeks, with some of the constituents being reabsorbed and probably utilized by the sclerotial tissue (Coletole 1978). The color of the droplets varies from pale to dark brown, probably due to the accumulation of oxidized phenolics (Willetts and Bullock 1992). The composition of droplets may include carbohydrates such as trehalose, mannitol, inositol and glucose and enzymes including polyphenol oxidase, peroxidase, glucosidase and cellulose, amino acids and fatty acids (Cooke and Mitchell 1969; Colotelo 1978). Regarding function of such exudation of sclerotia, different authors have variable suggestions. Some authors have proposed that exudation from sclerotia serves in the maintenance of internal physiological balance (Cooke and Mitchell 1969; Colotelo 1978; Christias 1980). Cooke and Al-Hamdani (1986) suggested that the main function of the exudation from sclerotia is concerned with the release of water along with some nutrients from the interior of sclerotium. Colotelo (1978) concluded that the nutrients in exudation droplets are reabsorbed and utilized by the sclerotia. Other authors suggested exudation as water reservoir for hyphal growth or nutrient reservoir for spore germination (Mcphee and Colotelo 1977; Jennings 1991). In *C. cinerea*, exudation of fluid droplets at the final stages of sclerotium maturation were observed and reported by Waters et al. (1975b) and they mentioned that these droplets soon disappeared from the mature sclerotium, probably evaporated or absorbed during maturing sclerotium. In our experiment, we also observed watery droplets produced around the sclerotia during their development and these droplets disappear once the sclerotia attained maturation (Fig. 2C and 2D, Fig. 4). These droplets are likely to act as a source of nutrients for the maturing sclerotia, and at the same time, these droplets may contain defense proteins against certain bacteria.

2.2.6.6. Histochemical study on sclerotia

As mentioned earlier that the sclerotia can survive for a longer time, so what keeps sclerotia alive for such a long time and then provide them an ability to germinate again after surviving the extremes. To investigate it, many cytological studies were conducted in the past using histological techniques. The identification of sclerotial glycogen as carbon and energy storage material has been reported in many studies in the past (Moore 1995; Willetts and Bullock 1992). Glycogen is present throughout the cytoplasm of the medullary hyphae whereas, cells in the rind region contain much lower quantities of glycogen than the other regions (Wong and Cheung 2008). Granular glycogen deposits were also observed by electron microscopy in the medulla hyphae of sclerotia of *Sclerotinia minor* (Bullock et al. 1980). In *C. cinerea*, cytochemical studies in the past reported that the glycogen is accumulated in a young mycelium and is utilized as the sclerotia mature (Jirjis and Moore 1976). However, the accumulations of amount of glycogen in the *scl* strains which are genetically incapable of producing sclerotia (Waters et al.1975b) were able to

accumulate large quantities of glycogen in hyphal cells. The observation led to the conclusion that although glycogen is utilized for the maturation of sclerotia, there are number of another developmental pathway for which glycogen is synthesized and utilized (Jirjis and Moore 1976). In the histochemical study conducted by Waters et al. (1975a and 1975b), PAS staining gave negative result on the accumulation of glycogen in the cytoplasm of the rind. They also reported that the medullary cells accumulate a glycogen-like polysaccharide in their cytoplasm.

From our staining experiment, we observed in a double-stained section of sclerotia by PAS and hemalum that the rind with its compartmental swollen hyphae and the bloated cells were colored in deep-red to wine-red, while the medullary part of the sclerotium appeared pink to pinkish blue (Fig. 7). In addition, few round cells stained in magenta with a blue stained cell wall and a few swollen hyphae stained in magenta are observed within the medullary region and are shown to store glycogen (Fig. 7). These round cells and the swollen hyphae correspond to the structures we observed earlier on the ruptured sclerotia on the glass slides which we presumed to be chlamydospore-like cells.

2.2.6. References

Badalyan, S. M., Navarro-González, M. and Kües, U. (2011) October. Taxonomic significance of anamorphic characteristics in the life cycle of coprinoid mushrooms. In *Proceed. VII Int. Conf. Mushr. Biol. & Mushr. Prod. Savoie JM, Foulongne-Oriol M., Largeteau M. and Barroso G. Eds*, pp. 140-154.

Boulianne, R. P., Liu, Y., Aebi, M., Lu, B. C. and Kües, U. (2000) Fruiting body development in *Coprinus cinereus*: regulated expression of two galectins secreted by a non-classical pathwayThe GenBank accession number for the sequence reported in this paper is AF130360. *Microbiology*, *146*, pp.1841-1853.

Brefeld, O. (1877) Botanische Untersuchungen über Schimmelpilze. III. Basidiomyceten. Leipzig: Arthur Felix. (in German)

Buller, A. H. R. (1931) Researches on Fungi. Volume IV. London: Longmans Green and Co.

Bullock, S., Ashford, A. E. and Willetts, H. J. (1980) The structure and histochemistry of sclerotia of *Sclerotinia minor Jagger*. *Protoplasma*, *104*, pp.333-351.

Chet, I., Henis, Y. and Mitchell, R. (1967) Chemical composition of hyphal and sclerotial walls of *Sclerotium rolfsii* Sacc. *Canadian Journal of Microbiology*, *13*, pp.137-141.

Chet, I. and Henis, Y. (1975) Sclerotial morphogenesis in fungi. *Annual Review of Phytopathology*, *13*, pp.169-192.

Chet, I. and Rusch, H. P. (1969) Induction of spherule formation in *Physarum polycephalum* by polyols. *Journal of Bacteriology*, *100*, pp.673-678.

Chiu, S. W. and Moore, D. (1996) *Patterns in Fungal Development*. Cambridge University Press.

Christias, C. (1980) Nature of the sclerotial exudate of *Sclerotium rolfsii*. *Soil Biology and Biochemistry*, *12*, pp.199-201.
Clémençon, H. (1997) Anatomy of the Hymenomycetes. *F. Flück-Wirth, Teufen, Switzerland*.
Clémençon, H., Emmett, V. and Emmett, E. (2004) Cytology and plectology of the Hymenomycetes. *Persoonia*, *18*, p.3.
Coley-Smith, J. R. and Cooke, R. C. (1971) Survival and germination of fungal sclerotia. *Annual Review of Phytopathology*, *9*, pp.65-92.
Coley-Smith, J. R., Humphreys-Jones, D. R. and Gladders, P. (1979) Long-term survival of sclerotia of *Rhizoctonia tuliparum*. *Plant Pathology*, *28*, pp.128-130.
Colotelo, N. (1978) Fungal exudates. *Canadian Journal of Microbiology*, *24*, pp.1173-1181.
Cook, R. C. and Al-Hamdani, A. M. (1986) Water relations of sclerotia and other infective structures. *Water, Fungi and Plants*, pp.49-63.
Cooke, R. C. and Mitchell, D. T. (1969) Sugars and polyols in sclerotia of *Claviceps purpurea*, *C. nigricans* and *Sclerotinia curreyana* during germination. *Transactions of the British Mycological Society*, *52*, pp.365-372.
Cooke, R. C. and Mitchell, D. T. (1970) Carbohydrate physiology of sclerotia of *Clavkeps purpurea* during dormancy and germination. *Transactions of the British Mycological Society*, *54*, pp.93-99.
Ginns, J. and Weresub, L. K. (1976) Sclerotium-producing species of *Leucogyrophana* (*Aphyllophorales*), *Memoirs of the New York Botanical Garden*, 28, pp.86-97.
Granado, J. D., Kertesz-Chaloupková, K., Aebi, M. and Kües, U. (1997) Restriction enzyme-mediated DNA integration in *Coprinus cinereus*. *Molecular and General Genetics MGG*, *256*(1), pp.28-36.
Hereward, F. V. and Moore, D. (1979) Polymorphic variation in the structure of aerial sclerotia of *Coprinus cinereus*. *Microbiology*, *113*, pp.13-18.
Jennings, D. H. (1991) The role of droplets in helping to maintain a constant growth rate of aerial hyphae. *Mycological Research*, *95*, pp.883-884.
Jirjis, R. I. and Moore, D. (1976) Involvement of glycogen in morphogenesis of *Coprinus cinereus*. *Microbiology*, *95*, pp.348-352.
Jump, J. A. (1954) Studies on sclerotization in *Physarum polycephalum*. *American Journal of Botany*, pp.561-567.
Kertesz-Chaloupková, K., Walser, P. J., Granado, J. D., Aebi, M. and Kües, U. (1998) Blue light overrides repression of asexual sporulation by mating type genes in the basidiomycete *Coprinus cinereus*. *Fungal Genetics and Biology*, *23*, pp.95-109.
Kües, U. (2000) Life history and developmental processes in the basidiomycete *Coprinus cinereus*. *Microbiology and Molecular Biology Reviews*, *64*, pp.316-353.

Kües, U., Granado, J. D., Hermann, R., Boulianne, R. P., Kertesz-Chaloupková, K. and Aebi, M. (1998) The A mating type and blue light regulate all known differentiation processes in the basidiomycete *Coprinus cinereus*. *Molecular and General Genetics MGG*, *260*, pp.81-91.

Kües, U. and Liu, Y. (2000) Fruiting body production in basidiomycetes. *Applied Microbiology and Biotechnology*, *54*(2), pp.141-152.

Kües, U., Subba, S., Yu, Y., Sen, M., Khonsuntia, W., Singhaduang, W., Lange, K. and Lakkireddy, K. (2016) Regulation of fruiting body development in *Coprinopsis cinerea*. *Mushroom Sci*, *19*, pp.318-322.

Kües, U., Walser, P., Klaus, M. and Aebi, M. (2002) Influence of activated A and B mating-type pathways on developmental processes in the basidiomycete *Coprinus cinereus*. *Molecular Genetics and Genomics*, *268*, pp.262-271.

Lakkireddy, K. K., Navarro-González, M., Velagapudi, R. and Kües, U. (2011) Proteins expressed during hyphal aggregation for fruiting body formation in basidiomycetes. In *Proceedings of the 7th international conference on mushroom biology and mushroom products*.

Lewis, D. (1961) Genetical analysis of methionine suppressors in *Coprinus*. *Genetics Research*, *2*, pp.141-155.

Lindau, G. (1910) Fungi Imperfecti: Hyphomycetes IX. *L. Rabenhorst, Kryptogamenflora. Leipzig*.

Liu, Y. (2001) *Fruiting body initiation in the basidiomycete Coprinus cinereus* (Doctoral dissertation, ETH Zurich).

Lu, B. C. (1972) Dark dependence of meiosis at elevated temperatures in the basidiomycete *Coprinus lagopus*. *Journal of Bacteriology*, *111*, pp.833-834.

Majcherczyk, A., Dörnte, B., Subba, S., Zommorodi, M. and Kües, U. (2019) Proteomes in primordia development of *Coprinopsis cinerea*. *Acta Edulis Fungi* 2019. 26, pp. 37-50.

McPhee, W. J. and Colotelo, N. (1977) Fungal exudates. I. Characteristics of hyphal exudates in *Fusarium culmorum*. *Canadian Journal of Botany*, *55*, pp.358-365.

Moore, D. (1995) Tissue formation. In *The Growing Fungus*. Springer, Dordrecht.

Moore, D. (1981) Developmental genetics of *Coprinus cinereus*: genetic evidence that carpophores and sclerotia share a common pathway of initiation. *Current Genetics*, *3*, pp.145-150.

Moore, D. and Jirjis, R. I. (1976) Regulation of sclerotium production by primary metabolites in *Coprinus cinereus* (= *C. lagopus* sensu Lewis). *Transactions of the British Mycological Society*, *66*, pp.377-382.

Polak, E., Hermann, R., Kües, U. and Aebi, M. (1997) Asexual Sporulation in *Coprinus cinereus*: structure and development of oidiophores and oidia in an Amut Bmut homokaryon. *Fungal Genetics and Biology*, *22*, pp.112-126.

Smith, M. E., Henkel, T. W. and Rollins, J. A. (2015) How many fungi make sclerotia? *Fungal Ecology*, *13*, pp.211-220.
Srivilai, P. (2006) *Molecular analysis of genes acting in fruiting body development in basidiomycetes* (Doctoral dissertation, Göttingen University).
Subba, S.,Winkler, M. and Kües, U. (2019) Tissue staining to study the fruiting process of *Coprinopsis cinerea*. Acta Edulis Fungi 2019. 26, pp. 29-38.
Swamy, S., Uno, I. and Ishikawa, T. (1984) Morphogenetic effects of mutations at the *A* and *B* incompatibility factors in *Coprinus cinereus*. Journal of General Microbiology, 130:3219-3224.
Townsend, B. B. and Willetts, H. J. (1954) The development of sclerotia of certain fungi. *Transactions of the British Mycological Society*, *37*, pp.213-221.
Volz, P. A. and Niederpruem, D. J. (1970) The sclerotia of *Coprinus lagopus*. *Archiv für Mikrobiologie*, *70*, pp.369-377.
Watanabe, T., Tagawa, M., Tamaki, H. and Hanada, S. (2011) *Coprinopsis cinerea* from rice husks forming sclerotia in agar culture. *Mycoscience*, *52*, pp.152-156.
Waters, H., Butler, R. D. and Moore, D. (1972) Thick-walled sclerotial medullary cells in *Coprinus lagopus*. *Transactions of the British Mycological Society*, *59*, pp.167-IN25.
Waters, H., Butler, R. D. and Moore, D. (1975a) Structure of aerial and submerged sclerotia of *Coprinus lagopus*. *New Phytologist*, *74*, pp.199-205.
Waters, H., Moore, D. and Butler, R. D. (1975b) Morphogenesis of aerial sclerotia of *Coprinus lagopus. New Phytologist*, *74*, pp.207-213.
Willetts, H. J. (1972) The morphogenesis and possible evolutionary origins of fungal sclerotia. *Biological Reviews*, *47*, pp.515-536.
Willetts, H. J. and Bullock, S. (1992) Developmental biology of sclerotia. *Mycological Research*, *96*, pp.801-816.
Wong, K. H. and Cheung, P. C. (2008) Sclerotia: emerging functional food derived from mushrooms. *Mushrooms as Functional Foods*, John Wiley & Sons, Inc., pp.111-146.
Xie, Y., Chang, J. and Kwan, H. S. (2019) Carbon metabolism, transcriptome and RNA editome in developmental paths differentiation of *Coprinopsis cinerea*. *BioRxiv*, *143*, pp.1087-1845.

Chapter 3

The process of fruiting body development in *C. cinerea*

Subchapter 3.1. Regulation of fruiting body development in *C. cinerea*

Contribution to this chapter
Input into scientific discussion: S. Subba and U. Kües
Manuscript writing: S. Subba
Manuscript reviewed by U. Kües

Science and Cultivation of Edible Fungi, Baars & Sonnenberg (ed.)
 ISBN 978-90-9029771-2

Regulation of fruiting body development in *Coprinopsis cinerea*

Ursula Kües[1], Shanta Subba[1], Yidong Yu[1,2], Mandira Sen[1], Weeradej Khonsuntia[1],
Wassana Singhaduang[1,3], Karin Lange[1] and Kiran Lakkireddy[1]

[1] *Molecular Wood Biotechnology and Technical Mycology, Georg-August-University Göttingen, Göttingen, Germany*
[2] *Present address: Institute of Microbiology, Universitätsklinikum Erlangen, Erlangen, Germany*
[3] *Present address: Rajamangala University of Technology Lanna, Phitsanulok, Thailand*

ABSTRACT

The edible mushroom *Coprinopsis cinerea* is an excellent model to study the genetics of fruiting body development in the Agaricomycetes. Fruiting follows a conserved scheme defined by day and night phases, with well predictable distinct stages over the time. Fruiting starts with primary hyphal knot formation in the dark, followed by aggregation into compact round secondary hyphal knots in which stipe and cap tissues differentiate. Primordia development (stages P1 to P5) takes five days to culminate on day 6 of development in karyogamy and meiosis within the basidia and subsequent basidiospore production which parallels fruiting body maturation (stipe elongation and cap expansion) during the last day of development. This scheme of development is followed up by normal dikaryons as well as by a self-compatible homokaryon which has mutations in both mating type loci. The *matA* genes control fruiting body initiation at the stages of primary and secondary hyphal knot formation and the decision to enter the alternate pathway of sclerotia formation. *matA* induced steps in fruiting end at the P4 state. Activation of the *matB* genes is required for karyogamy and fruiting body maturation. Further, *matB* activation enhances the frequency of *matA*-induced fruiting. *matB* functions as a mediator between light and nutritional signals and *matA* control of development. We have a large collection of about 1500 mutants in fruiting body development. Mutations do not evenly distribute over the developmental pathway of fruiting body development. High numbers of mutants are available from the developmental stages of primary and secondary hyphal knot formation up to stage P1. Comparably few mutations resulted in defects in the developmental progress from P1 to P4 but high numbers of mutants were found also in the later developmental processes occurring normally on day 6 for fruiting body maturation and sporulation. In our studies, we focus on genes that act at the first stages in fruiting. Mutants with defects in primary and secondary hyphal knot formation helped before by complementation to clone genes *cfs1* and a gene of the *NWD2* family. We study the functions of these and further genes with predicted functions in regulation and light control of early fruiting body development.

Keywords: mating types, light, nutrients, signaling, regulation

INTRODUCTION

Coprinopsis cinerea with a very short life cycle grows very fast on artificial medium and completes its whole life cycle with fruiting body and basidiospore production in Petri dishes in less than two weeks. Fruiting bodies in the wild arise on fertile dikaryons with two types of haploid nuclei which formed by mating of monokaryons germinated from basidiospores of different mating types (Kües, 2000). Monokaryons with only one type of haploid nuclei in their cells are unable to produce fruiting bodies. However, mutations in the two mating type loci can render unmated homokaryons self-compatible, allowing them to produce fruiting bodies with meiotic basidiospores. Fruiting body development of homokaryon AmutBmut (*A43mut*, *B43mut*) is well studied. After mycelial growth on YMG/T medium for 6 days at 37°C and transfer into a standard fruiting regime (25°C room temperature, 12 h dark/12 h light regime at high humidity of 85-90 %; Granado et al., 1997), the complete fruiting pathway takes place in seven days. Distinct stages in primordia development have been defined, for every day one, using as reference point the moment at which the 12-h dark phase (night phase) switches to the 12-h light phase (day phase). First small loose hyphal aggregates (primary hyphal knots, PK) are formed in the dark by local intense sub-branching of length-restricted hyphae. A light signal given at the right time induces production of secondary hyphal knots (SK) which are more compact hyphal ball-like plectenchymatic structures. In these, cap and stipe differentiation for primordia formation initiates. The shape of a mushroom becomes visible at the next day (stage P1). During the next four day-night phases, the primordium grows in size while the cap and stipe further differentiate. Primary and secondary gills are established with a hymenium on their surfaces in which basidia arise (stages P2 to P4). An essential light signal given by the day 5 light phase induces karyogamy in the basidia (accomplished at stage P5), directly followed in the day 6 light phase by meiosis and subsequent basidiospore production. In parallel, the stipe elongates and the cap opens. The fruiting body (FB) is fully matured during the next night phase. At the morning of the seventh day of incubation under standard fruiting conditions, the cap autolyzes to release the basidiospores in liquid droplets (Kües and Navarro-Gonzaléz, 2015; Fig. 1C). Here, we present the fruiting pathway in form of a catalog for a dikaryon with defined hallmarks under the same environmental scheme as applied before for homokaryon AmutBmut, underlining that the mutant strain can be used instead of a dikaryon to define regulatory mechanisms of fruiting and, most importantly, to collect dominant as well as recessive mutants in fruiting body development by mutagenesis of haploid mitotic spores (oidia).

1. Results & Discussion

1.1. Cultural conditions for fruiting body formation

Dikaryon PS1x2 was produced by mating of the AmutBmut co-isogenic monokaryons PS001-1 (*A42*, *B42*) and PS002-1 (*A3*, *B1*) on YMG/T (Granado et al., 1997) agar plates. For fruiting, we inoculate strains with a small agar piece (0.2 x 0.2 mm) from a freshly grown YMG/T pre-culture in the middle of freshly made (!) YMG/T agar plates. For good supply of nutrients and water and for good aeration, the agar layer should be ca 5-6 mm thick leaving above 7-8 mm air space in unsealed Petri dishes (9 cm ø) with cams in the lids; i.e., ca 30 ml

of sterile medium should be poured into the bottom half (8.5 cm in ø) of a dish. For gelling, only 1% agar (Serva 11396) should be used to ensure a low agar water potential. Plates (agar surface top) are incubated at the favored growth temperature at 37°C in lightproof ventilated boxes with a layer of wetted paper tissues at the bottom of the box for maintaining good humidity during the incubation. PS1x2 grows with similar speed on YMG/T at 37°C (7.7 ± 1.0 mm/d during logarithmic growth) as AmutBmut (7.9 ± 0.4 mm/d). By standard, plates are inoculated in afternoon hours (between 2 to 6 pm) for growth at 37°C. Plates are checked for their growth front at similar hours 6 days later. For best results in subsequent fruiting body formation, the front hyphal tips of growing colonies should be close to the edges of the Petri dishes (with 0.5-1 mm of still mycelium-free agar) at the time of transfer into standard fruiting conditions but they should not have yet entered the plastic surfaces of the Petri dishes. By the transfer in the afternoon hours into fruiting conditions (with switching on the 12 h light phase at 9 am), a few hours of illumination are provided to the cultures at the same day at 25°C. Illumination (provided by Osram L40/25 Universal-Weiβ tubes, emission spectrum 295-780 nm; at 30 cm distance above shelfs to provide ca 30-90 µE m^{-2} s^{-1} light to plates which increases the temperature at the plate surfaces to 28°C) serves to induce and synchronize development.

Light-induced initiation of fruiting body formation occurs at the mycelial growth front and likely employs fresh hyphal tips. If a culture is transferred too early from 37°C into fruiting conditions, the vegetative hyphal growth will continue over the still free agar surface but at reduced speed and with a change in mycelial morphology from loose fluffy aerial mycelium at 37°C to a less fluffy mycelium produced at 25°C (Fig. 1A). Due to delayed growth with general culture aging, the mycelium may be less active in induction of secondary hyphal knots and these may be more spread over the outer range of the mycelium produced at 25°C due to a less defined time of light induction of fruiting. When the mycelium in contrast already grew onto the plastic edges of the Petri dish, it likely fails to initiate fruiting but may produce on the plastic a dense mass of mycelium, possibly because of suboptimal water supply for the receptive hyphal tips (Fig. 1B). Several hundred secondary hyphal knots may arise under optimal fruiting conditions along the outer edge of a Petri dish. Once the fruiting process is initiated, every day parts of them will give up development in favor of finally a few that complete the fruiting process (Fig. 1C, Fig. 2).

1.2. The developmental pathway of fruiting in a dikaryon as compared to homokaryon AmutBmut

Under standard fruiting conditions, dikaryon PS1x2 will undergo the same developmental pathway as the co-isogenic homokaryon AmutBmut. Light determines the induction of secondary hyphal knots. If missing, primary hyphal knots will transform into sclerotia as in AmutBmut. Light is further needed for proper primordia development from secondary hyphal knots. If lacking, slender, stipe-like structures with underdeveloped caps (“dark stipes”) grow out of secondary hyphal knots. However, with further day-night phases, cap and stipe tissue development instead proceeds to end with stage P5 in the morning of day 6. During this day, the stipe elongates and the cap opens by cell expansion in parallel to basidiospore production.

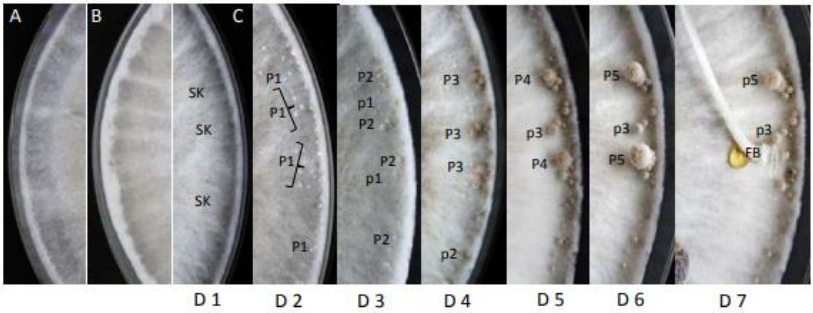

Fig. 1 A. Colony edge of an AmutBmut culture transferred too early and B. of a PS1x2 colony transferred too late into standard fruiting conditions. C. The progress of development (still growing structures: SK, P1 to P5, FB; aborted: p1 to p5) in an AmutBmut culture at the start (when light switches on) of days (D1 to D7) at standard fruiting conditions.

The mushroom is fully matured in the middle of the next night phase (4-5 h in dark). At day 7, the mushroom cap then autolyzes (Fig. 2).

1.3. Regulation of fruiting body development

Previous transformation work showed that the *matA* and the *matB* genes together with light regulate the fruiting pathway. *matA* for homeodomain proteins is most important for induction of fruiting at the secondary hyphal knot stage. Light is needed but too much light is contra-productive. *matB* for pheromones and pheromone receptors can support the *matA* action in induction of fruiting by counteracting negative light effects. *matA*-induced fruiting ends at the P4 state unless *matB* induces further development at the stage of karyogamy (Kües, 2015). By mutations in *matA* and *matB*, AmutBmut performs the light-induced process of fruiting. However, other than dikaryons, the strain produces high numbers of oidia (10^9 versus 10^6 to 10^7 per plate) when cultured in light. This feature of AmutBmut is made use of in mutagenesis of single cells with a single haploid nucleus (Granado et al., 1997). Developmental defects of a large collection of mutants of AmutBmut have so been obtained and assigned to the fruiting pathway shown in Fig. 2. Many mutants are blocked in the formation of either primary or secondary hyphal knots or P1 primordia. Many others are affected in processes of fruiting body maturation at P5 and later whereas few mutants are defective in the developmental progress from P1 to P4. Abundant production of oidia by the mutants in light eases efficient transformation (Granado et al., 1997). Gene *cfs1* for a cyclopropane fatty acid synthase and a gene of the *NWD2* family for a potential regulator in signalling have thus been cloned by restoring defects in hyphal knot formation in AmutBmut mutants (Liu et al., 2006; Yu et al., 2013), showing the value of characterized mutants for studies of regulation of fruiting body development.

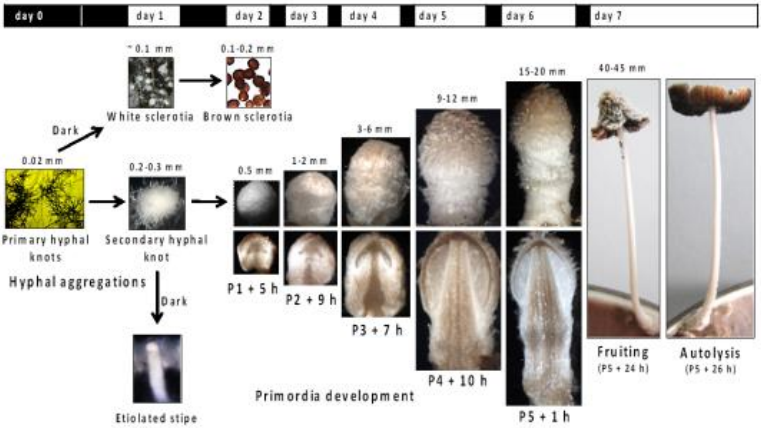

Fig. 2 Fruiting body development in dikaryon PS1x2. Black and white boxes mark dark and night phases (not to scale).

REFERENCES

Granado, J.D., Kertesz-Chaloupková, K., Aebi, M., Kües, U., 1997. Restriction enzyme-mediated DNA integration in *Coprinus cinereus*. *Mol. Gen. Genet.* 256, 28-36.

Kües, U., 2000. Life history and developmental processes in the basidiomycete *Coprinus cinereus*. *Microbiol. Mol. Biol. Rev.* 64, 316-353.

Kües, U., 2015. From two to many: Multiple mating types in Basidiomycetes. *Fungal Biol. Rev.* 29, 126-166.

Kües, U., Navarro-Gonzaléz, M., 2015. How do Agaricomycetes shape their fruiting bodies? 1. Morphological aspects of development. *Fungal Biol. Rev.* 12, 99-107.

Liu, Y., Srivilai, P., Loos, S., Aebi, M., Kües, U., 2006. An essential gene for fruiting body initiation in the basidiomycete *Coprinopsis cinerea* is homologous to bacterial fatty acid synthase genes. *Genetics* 172, 873-884.

Yu, Y., Clergeot, P.-H., Ruprich-Robert, G., Aebi, M., Kües, U., 2013. Transformation of an NACHT-NTPase gene *NWD2* suppresses the *pkn1* defect in fruiting body initiation of the *Coprinopsis cinerea* mutant Proto159. *Fungal Genet. Rep.* 60S, 174.

Subchapter 3.2. Tissue staining to study the primordial stages of *C. cinerea*

DOI: 10.16488/j.cnki.1005-9873.2019.04.005

TISSUE STAINING TO STUDY THE FRUITING PROCESS OF *COPRINOPSIS CINEREA*

SUBBA Shanta, WINKLER Marco, and KÜES Ursula
Molecular Wood Biotechnology and Technical Mycology Institute and Goettingen Center for Molecular Biosciences (GZMB), University of Goettingen, GERMANY

Abstract
The coprophilous *Coprinopsis cinerea* is an edible model mushroom that grows and fruits very fast under laboratory conditions. Fruiting starts with primary hyphal knot (Pk) formation in the dark, followed by light-induced compact aggregates known as the secondary hyphal knots (Sks) in which stipe and cap tissues differentiate. Under defined fruiting conditions, primordium development (P1 to P5) takes five days to culminate on Day 6 of development in karyogamy (K) and meiosis (M) within the basidia and subsequent basidiospore production which parallels fruiting body maturation (stipe elongation and cap expansion). Mature fruiting bodies autolyze on Day 7 to release the spores in liquid droplets to the ground. By applying different histochemical staining techniques for the light microscopy, primordial sections of *C. cinerea* were examined to study different tissues and cell types which appear over the time in the fruiting process. Lactophenol blue, Mayer's hemalum, malachite green and eosin all stained probasidia stronger than other tissues. The pileipellis was best stained by malachite green and lactophenol blue. PAS (periodic acid Schiff) stained the pileipellis better dark and the subhymenium slightly darker as compared to other tissues. All stains were also applied in combinations of two, in both possible orders. In double staining with PAS and hemalum, the subhymenium and probasidia were best differentiated.
Key words: Fruiting body, tissue stains, subhymenium, basidia, glycogen, *Coprinopsis cinerea*

Introduction

Starting in the 19th century to grow *Coprinopsis cinerea* in culture[1], multiple studies on fungal multicellularity and mushroom development have been made over the decades[2-4]. However, fungal multicellularity, tissue formation and cell differentiation is so far still little understood[5,6]. The saprotrophic fungus *C. cinerea*, commonly called gray shag ink cap, occurs in nature on horse dung. It is an excellent model organism for studying developmental processes in Agaricomycetes as it completes its whole life cycle very fast within two weeks and can be easily cultivated on artificial media under laboratory conditions[2,3,6].

In its life cycle, fruiting normally occurs on the dikaryon and follows a conserved morphological scheme with well predictable distinct stages over the time which is defined environmentally by temperature and day and night phases. Fruiting starts with primary hyphal knot (Pk) formation by localized intense formation of growth-restricted short sidebranches on undifferentiated hyphae in the vegetative mycelium in the dark[7]. This is followed by light-induced aggregation of the Pks into compact round secondary hyphal knots (Sks) in which stipe and cap tissues differentiate[8]. Primordia development (stages P1 to P5) takes five days to culminate on Day 6 of development in karyogamy (K) and meiosis (M) within the basidia with subsequent basidiospore production which parallels fruiting body maturation (stipe elongation and cap expansion). Fruiting bodies are fully opened in the middle of the last night phase to shed their spores while at the next morning on Day 7 of development, the cap autolyzes to release the majority of the spores in liquid droplets that fall to the ground[3,4].

Fruiting bodies of the Agaricomycetes are the most complex multicellular structures that occur in the fungal kingdom, with different types of tissues and several kinds of cells of distinct functions. Some estimates have been made on different types of cells which are produced during the fruiting process. In *C. cinerea*, there are probably > 30 cell types that differentiate during different stages of the development[3,4]. We are interested to better define and understand the tissue and cell differentiations during the process of fruiting of *C. cinerea* by studies using

cytological, physiological and genetic methods. Here, we use five different stains to dye sections of primordia for observations by light microscopy. Stains are applied singly and in combinations of each two to mark and identify specific tissues and cells.

Materials and Method

1. Strain and Cultivation

Homokaryon AmutBmut (*A43mut*, *B43mut, pab1-1*) is a self-fertile strain of *C. cinerea* (FGSC 25122) that by mutations in both mating type loci can form fruiting bodies without the need of prior mating to another compatible strain[7,9]. For synchronized fruiting, we inoculated strain AmutBmut at evenings (about 19 h) onto fresh agar plates of YMG/T complete medium[10] for growth at 37°C in lightproof ventilated boxes. Fully grown plates were transferred 5 days later at the respective hour (about 18 to 19 h) into an incubation chamber with set fruiting conditions, i.e. 12 h light/12 h dark at 25 °C and high humidity of 90 %[10], for further cultivation. For practical convenience, light switches on in the incubation chamber daily at 9 o'clock in the morning. The moment of light switches on in the 12 h light/12 h dark cycle in the chamber is arbitrarily considered zero hour of each new day of mushroom cultivation[11].

2. Harvesting and Embedding of Structures

Active primordia stages were harvested on consecutive days at zero hour in the 12 h light/12 h dark cycle of incubation and fixed in series of solutions of 1st 4 % formaldehyde, 2nd 99 % acetic acid and 3rd 70 % ethanol (methylated), each for 24 h at room temperature (RT). For dehydration, the samples were then transferred each time for 1 hour at RT into a series of ethanol (methylated) solutions of increasing concentration (70 %, 80 %, 90 %, and 96 %). This was followed by 3x infiltration using the hydrophobic agent Roti-Histol (Carl Roth, Karlsruhe, Germany) to eliminate alcohol by incubation each time for 45 min at RT and finally by transferring samples into pure Roti-Histol overnight at RT. Next, the samples were transferred into fresh pure Roti-Histol and incubated for 3 hours at RT. Finally, the samples were incubated overnight at 30 °C in a saturated solution of Roti-Plast (Carl Roth) in Roti-Histol. Then, the samples were embedded in Roti-Plast melted at 60 °C and incubated overnight. Embedded samples were cut using a rotation microtome (R. Jung, Heidelberg, Germany) and both longitudinal and transverse sections of primordia of a thickness of 5 µm and of 10 µm were made. 10 µm samples gave better tissue overviews and insight into cells of larger diameter, 5 µm samples allowed better recognition of individual cells of smaller diameter. The sections were floated on warm drops of distilled water (40 °C) placed on clean microscope slides (Menzel, Braunschweig, Germany) and then dried on a hot block. No further treatment of microslides was required to spread and stick samples wrinkle-free onto the slides for subsequent staining.

3. Staining of Sections of Primordia

We used five different stains, (i) lactophenol blue (catalog no. 61335, Sigma-Aldrich, Darmstadt, Germany), (ii) periodic acid-Schiff (PAS), Schiff´s reagent[12] (0.2 % fuchsin, catalog no. 1358 Merck, Darmstadt, Germany) (iii) Mayer's hemalum[12] (catalog no. 51260, Sigma-Aldrich), (iv) 5 % malachite green (Dr. K. Hollborn & Söhne, Leipzig, Germany) and (v) 1 % eosin Y, acidic (catalog no. 230251, Sigma-Aldrich) as a single stain on the sections. Each stain was also used in combination with all others in both possible orders for double staining.

Prior to staining, wax in samples was completely eliminated from the tissue sections prepared as described above by washing them for 3 min at RT with a 100 % xylol solution, which was then removed with a series of ethanol solutions in decreasing concentration (96 %,

80 %, 60 %, and 30 %), each applied for 2 min at RT. The samples were then washed with cold tap water for 2 min.

Before staining with PAS, the samples were put in 1 % periodic acid for 10 min at RT. All other stains were directly applied to samples. Individual stains were applied at RT for either 20 min (5 µm sections) or 30 min (10 µm sections). The samples were then washed with cold tap water for 1 min to wash away the surplus of stains. For PAS and hemalum stainings, samples were afterwards washed with warm tap water (45 °C) for 5 min. For dehydration, all samples except of those of malachite green staining were transferred into a series of ethanol (methylated) solutions of increasing concentration (30 %, 60 %, 80 %, and 96 %), each for 30 sec at RT. The samples were then put into 100 % xylol for 3 min. Samples treated with malachite green were transferred for 3 sec each into 30 % and 80 % ethanol and 100 % xylol. After dehydration, all samples were let drying at RT for a few sec but not to completely dry. The samples were fixed by putting three drops of DePeX mounting medium (a neutral clear viscous solution of polysterene and plasticizers in xylene for use in histology; catalog no. 18243.01, Serva, Heidelberg, Germany) onto them and then a coverslip (2 x 6 cm).

In double staining, the treatment with a first stain was performed as described above including washing with cold tap water for 1 min and, for PAS and hemalum staining, in addition for 5 min with warm tap water. Then, a second stain was applied for the same time as before, samples were twice washed with cold tap water for 1 min and, in case of a PAS or a hemalum staining, additionally with warm tap water for 5 min. Afterwards, samples were transferred into the series of ethanol (methylated) solutions of increasing concentration and 100 % xylol as above, unless malachite green was applied in either one of the two staining steps. In case malachite green was applied 1st, dehydration was done for 3 sec each in 30 %, 80 % and 96 % ethanol, followed by 10 sec in 100 % xylol. When malachite green was applied 2nd, the step of 80 % ethanol was left out.

4. Microscopy and Photography

Samples were inspected underneath a Zeiss Stemi 2000-C binocular and a Zeiss Axiophot 2 photomicroscope (Goettingen, Germany) with different enlargements. The binocular and the microscope were equipped with a Soft Imaging Color View II Mega pixel digital camera, linked to a computer. Photos were taken and analyzed with Analysis Software program (Soft Imaging System, Münster, Germany). Fresh primordia were directly photographed underneath the binocular upon harvest, either complete or cut longitudinally in halves.

Results

1. Fruiting Body Development of *C. cinerea* Strain AmutBmut in Culture

Fruiting body development of *C. cinerea* homokaryon AmutBmut under standard fruiting conditions has been described with details before[4,7,11]. The process is very reliable and always follows in time the same morphological scheme. Fig. 1 gives an overview on the pathway of fruiting body development under standard fruiting conditions after transfer of mycelial cultures on Day 0. Developmental stages Sk and P1 to P5 were defined before by us as those developmental structures which the fungus adopted at the zero hour (when light switches on) on the consecutive days Day 1 to Day 6 of development. Any other time point over the different days can then be unmistaken referenced by the name of the structure plus the further hour[11].

As shown in Fig. 1, fruiting of *C. cinerea* AmutBmut begins with loosely aggregated primary hyphal knots (Pks) formed in the vegetative mycelium in the dark as the first differentiated structures in the pathway of fruiting body development. They are however not committed to fruiting and will transfer into the multicellular brown-rinded sclerotia as resting bodies when cultures are kept further in the dark. In contrast, a light signal induces the formation of the compact aggregates termed secondary hyphal knots (Sks) in which stipe and cap tissues of a fruiting body will start to differentiate. Sks are thus the first developmental structures that

are specific to the pathway of fruiting. Subsequently to Sk formation, further light signals are required in order to coordinate the further tissue development in the fruiting body primordia and for induction of karyogamy and meiosis in the basidia when all basic tissues are formed at the primordial stage P4. Primordia development from Sks over different stages of primordia maturity (P1 to P5) takes place over five days (Day 1 to Day 5) under standard fruiting conditions to reach the stage P5 at the beginning of Day 6 when karyogamy had happened in the basidia. On Day 6, meiosis occurs and also basidiospore production. Stipes start to elongate first slowly over the Day 6 light phase. Later, in parallel to sporulation, stipes elongate and caps expand rapidly with onset of the Day 6 dark phase. The fruiting bodies are fully open in the middle of the Day 6 dark phase. Finally, in the early hours of Day 7, the caps autolyze and thereby shed off the dark-brown basidiospores suspended in liquid droplets which appear stained black by the color of the spores.

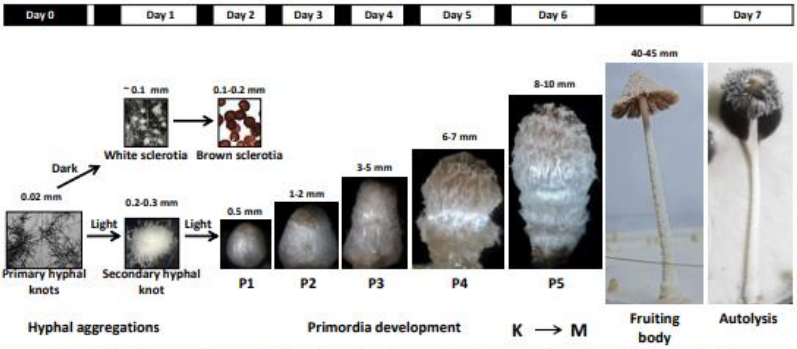

Fig. 1 Fruiting pathway of *Coprinopsis cinerea* strain AmutBmut (modified after[11]).
The bar above the fungal structures presents with white and black boxes the 12 h light and 12 h dark phases alternating in course of incubation, respectively. Day 0 refers to the last day of cultivation at 37 °C in the dark prior to transfer into standard fruiting conditions. The vertical white line refers to the 3 to 4 h light period mycelial plates experience in the climate chamber on Day 0after their transfer. Sizes in mm refer to height of structures.

2. Structural Complexity of Primordia

With proceeding development from stages P1 to P5, the primordia sizes (Fig. 1) and also the inner fungal tissue complexity increase (Fig. 2)[4,5]. A first impression on changing shapes can be obtained from intact freshly harvested primordia (Fig. 1 and 3A) and from views of longitudinal cuts of freshly harvested primordia under the binocular (Fig. 2 and 3B). The primordia cuts reveal further their inner tissue differentiation.

As seen in the figures, stage P1 is about 0.5 mm in size, whitish and more or less round, with a smooth outer veil tissue. Inside, a tiny cap starts to differentiate with gill initiations at the lower edges. The 1 to 2 mm-sized P2 structure is pear-shaped with a broader base and a slender apex. This is because the hyphae in the young stipe elongate in parallel and move the tiny young cap upwards. Internally, young primary gills are formed at the underside of the cap. Stage P3 attains a terete shape (3 to 5 mm tall) covered by a still smooth veil. The cap with primary and secondary gills enlarged in size as compared to P2. A P4 primordium with a further enlarged cap is a dumbbell shaped structure of about 6-7 mm in height covered by a veil of a loose hairy appearance. A longitudinally dissected half reveals a differentiated mushroom structure with a stipe separated from a well-developed cap region with gills, all enclosed by loosened outer veil tissue. Stage P5 has a light-bulb shape (8 to 10 mm high) with a more

disheveled veil. By extension growth of the gills, the cap has now clearly a larger diameter (4-5 mm) than the stipe underneath (3-3.5 mm) which started to slowly increase in length.

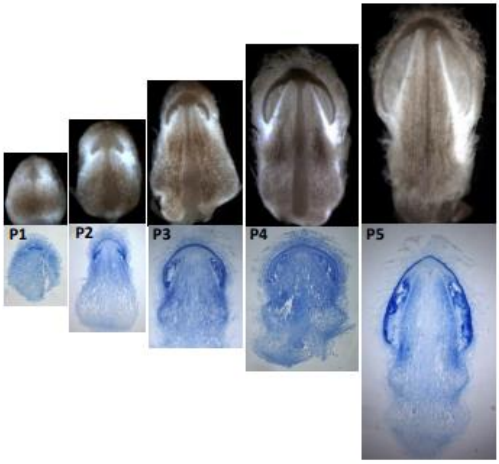

Fig. 2 Primordia stages P1 to P5 cut in halves (upper row) and lactophenol staining of longitudinal 10 µm-thick sections (bottom row), photographed underneath the binocular.
For sizes of structures, please see Fig. 1

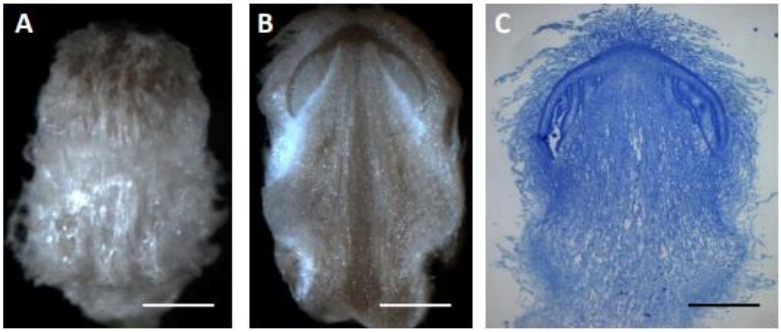

Fig. 3 Structure of primordia at the P4 stage.
(A) Outer view of a P4 stage primordium. (B) Inside view of a mushroom structure with cap and stipe of the same primordium vertically dissected into halves. (C) Lactophenol blue stained longitudinal section (10 µm thick) of a P4 stage primordium showing hyphal tissue differentiation. All photos were taken underneath the binocular. Sizes bars represent 1 mm in length.

In order to study the inner tissue development of *C. cinerea* primordia in more detail, the series of primordial stages from P1 to P5 were harvested, fixed as described in Material and Methods and longitudinally sectioned into cuts of 5 and 10 µm thickness. In microscopy, 10 µm sections were found to be ideal for an overview of a structure as a whole underneath the

binocular (Fig. 2 and 3C) and at lower magnifications under the light microscope (Fig. 4), as this gives a clear differentiation of the arrangement of tissues. On the other hand, a thin 5 µm cut allows better identifying of specific cells and tissues with their morphologies at higher magnifications (Fig. 5), and from that, predictions of possible functions.

However, the unstained fungal tissue by itself has generally little contrast in the cuts of primordia to well observe tissues and cells. Staining is therefore necessary such as by the lactophenol blue staining routinely used in our laboratory[4], as shown in Fig. 2, 3C and 4A. Strikingly, tissues of primordia stained differentially strong with lactophenol blue. Particularly the pileipellis and the gills were always deeper stained. To document this better in detail, a P4 stage cut is shown enlarged in Fig. 3C. The closed layer of the outer veil of larger cells differentiated well in the microscope views by cell sizes and by degree of staining from the pileipellis beneath which is the outer cap layer of smaller densely aggregated hyphae which stained darker blue. Further, the hymenia in the gills were prominently stained as dark blue band indicating well established gill tissue differentiation at this stage of development. Lactophenol blue staining emphasized also the parallel running of upward-growing hyphae in the young stipe.

3. Applying Different Single Stains for Revealing Distinct Tissue Structures

We further concentrated in transverse sections on analysis of caps of the P4 stage at which all main tissues and cells are fully established (Fig. 4)[4]. A transverse section (10 µm thick) of a cap region of a stage P4 primordium stained by lactophenol blue allowed a larger view of the hymenial region under the light microscope with 10x magnification. An arrangement of different tissues in rings is recognized (Fig. 4A).

The loose layer of disheveled larger veil cells is found on the surface of the primordium and, underneath, the darker stained tissue band of small tightly arranged cells of the pileipellis. The inner pileus tissue is made of a broader band with hyphae entangled in a loose plectenchyma which continues by more or less parallel growing hyphae into the inner regions of the primary and secondary gills. Primary gills are attached with uncovered edges via loosely arranged connective tissue to the outer thinner tissue layer of the stipe whereas the shorter secondary gills formed in between primary gills have free edges. The primary gills are partially and the secondary gills fully covered by a rigid band of hymenial tissues of denser hyphae which provides structural support to the probasidia from which later the spores are formed (Fig. 4A). At the P4 stage, the outer hymenial layer is characterized by an uniform layer of similar sized parallel palisade cells (the probasidia) with some intermingled larger inflated cells presenting young facial cystidia (marked by red arrows) protruding into the free gill space (Fig. 4A).

The inner part of the structure represents the stipe (Fig. 4A). A thin more densely aggregated outer tissue ring of narrower hyphae can be discriminated from the inner stipe filling with hyphae of larger diameter. Because the outer and the inner hyphae of the stipe run vertically in parallel over the length of the stipe, any hypha in the stipe is seen in its diameter as horizontally-cut tube.

The same general tissue distributions as found with the lactophenol blue staining are also recognizable in the overview sections of primordia stained with other dyes (PAS, eosin, hemalum and malachite green), while there were however quality differences in individual tissue staining (Fig. 4). Contrasts in sections treated with single dyes were best with the green malachite staining (Fig. 4E), followed by the dark blue hemalum staining (Fig. 4D), the magenta-lilac eosin staining (Fig. 4C), the lactophenol blue staining (Fig. 4A) and the light magenta PAS staining (Fig. 4B).

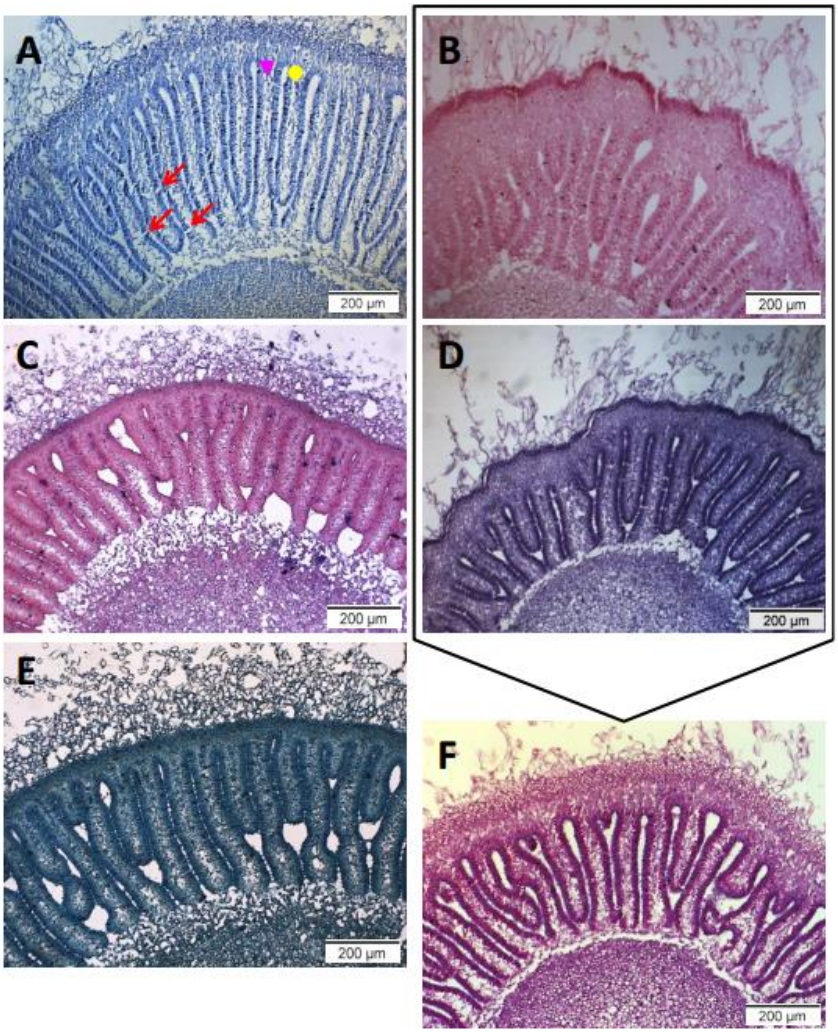

Fig. 4 Cross sections of the cap regions of differentially stained P4 stage primordia.
(A) Lactophenol blue staining of a 10 µm thick section. Primary and secondary gills are indicated by a yellow circle and a pink triangle, respectively. Examples of large protruding cystidia between the layer of probasidia in the hymenium are marked by red arrows. (B) PAS, (C) eosin, (D) hemalum, and (E) malachite green staining of each 5 µm thick sections. (F) A section (10 µm thick) double stained 1st by PAS and 2nd by hemalum shows more explicitly the arrangement of primary and secondary gills in the cap region than either of the single staining shown in (B) and (D) boxed above.

Malachite green (Fig. 4E) and eosin (Fig. 4C) stained the pileipellis and the hymenium on the gills darker than the inner stipe tissue and the veil and the outer stipe tissue. In the stipe, the outer dense hyphal ring and the inner tissue were well distinguishable from each other.

Two distinct colors marked differentially specific tissues in the eosin staining. Stipe tissues and the veil and the pileipellis are seen more lilac as compared to the pileus trama and the hymenium on the gills stained in magenta. Also with eosin, pileipellis and hymenium were stronger stained than other tissues (Fig. 4C).

PAS was the least differentiating stain. The pileipellis was prominently stained while the hymenium was only slightly better magenta stained than all other tissues (Fig. 4B).

4. Double Staining in Differentiating Tissue Structures

Double staining in series was performed of cross sections through P4 caps with all stains in all combinations of two, either as 1st or as 2nd dye. The observations are summarized in Table 1. Double staining mostly resulted in another overall color than exhibited by two dyes when used alone. In tendency, the 2nd stain appeared to contribute more to the final impression. However, for eosin and hemalum it did not as matter whether they were used 1st or 2nd. In contrast, PAS, lactophenol blue and malachite green had always a stronger input when applied 2nd. PAS-hemalum staining was the only double staining which differentiated distinct cells by different colors (Fig. 5H).

Table 1 Comparison of results from single staining of five distinct dyes and combinations of double staining (Cy = cystidia, Pbd = probasidia, Sh = subhymenium).

Single staining, first staining	Second staining				
	Eosin	**PAS**	**Hemalum**	**Lactophenol**	**Malachite green**
Eosin Cherry-red but veil + stipe more lilac, Pbd darker, Cy faint	X	Light pink, Pbd slightly darker	Purple, Pbd darker	Blue, less sharp, Pbd darker, Cy faint	Cyan, Pbd darker, Cy faint
PAS Light pink, Cy faint, Sh faint with internal granules	Rose, Pbd + Sh darker	X	Wine-red, Pbd darker, Sh magenta, Cy with internal magenta patches	Navy blue, Pbd darker, Cy not stained	Blue, Pbd darker
Hemalum Lilac-blue, Pbd darker, Cy faint	Purple, Pbd darker	Light pink, less sharp, Pbd darker, Cy faint	X	Blue, Pbd darker	Blue-gray, Pbd darker
Lactophenol Blue, Pbd darker, Cy with internal blue patches	Lilac, Pbd darker, Sh pink, Cy with internal purple patches	Light pink, Pbd + Sh darker	Lilac-blue, Pbd darker	X	Green, Pbd darker, Cy faint

Malachite green Greenish, Pbd darker, Cy faint	Cherry-red, Pbd darker, Cy with internal cherry-red patches	Pink, Pbd +Sh darker	Gray-blue, Pbd darker	Blue, Pbd darker	X

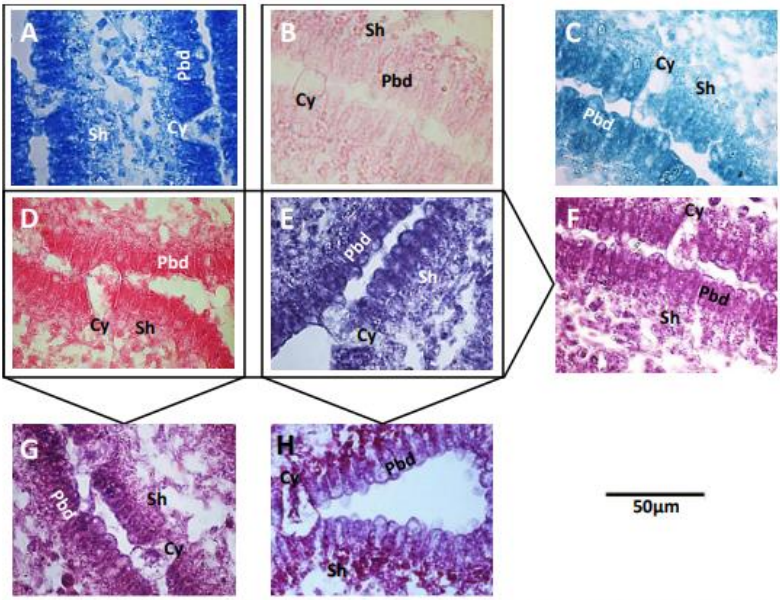

Fig. 5 Cross sections (5 µm thick) of hymenia of P4 stage primordia at higher magnification (100x).

(A) Lactophenol blue, (B) PAS, (C) malachite green, (D) eosin, and (E) hemalum single staining. Single PAS staining shows that the subhymenial (Sh) region is stained somewhat darker by inner granules as compared to the parallel arranged young basidia (Pbd). Large cystidia (Cy) arise in between the probasidia with faintly stained cell walls. Double staining of (F) eosin 1st, hemalum 2nd, (G) lactophenol blue 1st, eosin 2nd and (H) PAS 1st, hemalum 2nd were better in contrast and tissues and individual cells were easier to differentiate than in single staining (combination is boxed) or any other double staining. (H) However, only the PAS-hemalum staining distinguished cell types by different colors. In sections double stained by PAS and hemalum, a clear differentiation in the gills between the subhymenium and the hymenium with the young basidia became evident by wine-red and blue color staining, respectively.

Compared to single staining, contrasts between tissues and also cells were usually not better in double staining or, in the combinations eosin-lactophenol blue and hemalum-PAS, even less good. However, in the combinations lactophenol-eosin (Fig. 5G), hemalum-eosin (not shown but alike Fig. 5F), and eosin-hemalum (Fig. 5F) contrasts of cells and tissues were sharper and in particular probasidia were stronger stained by generating stronger purple or lilac colors. Outstanding was the combination 1st PAS and 2nd hemalum (Fig. 5H). Double staining resulted in much better contrasts and brought up new details in the section which were before

not seen in individual staining or any other double staining. The hymenial region is seen best stained by a stronger lilac color (Fig. 4F and 5H).

Enlarging the views under the microscope to 100x magnification revealed more distinct differentiations (Fig. 5). In the PAS-hemalum double staining, the layer of parallel palisade cells (probasidia) was stained distinctive blue by hemalum (Fig. 5H) and palisade cells were stronger accentuated from the subhymenium than in the single-stained cross section (Fig. 5E). The subhymenium underneath the palisade layer in contrast appeared wine-red (Fig. 5H). Notable were further the young inflated cystidia which arose from the subhymenia within the parallel arrangement of probasidia. In the single staining, they were faint magenta and faint blue stained (Fig. 5B and E), in the double staining they were partially colored wine-red by staining inner granules, comparable to the subhymenium (Fig. 5H). The young cystidia are seen to touch individual palisade cells in the opposing hymenial layer (Fig. 5) which in consequence of this contact are differentiated in the P5 stage to infertile non-meiotic cystesia[13].

Discussion

Tissue differentiation is a complex process in *Coprinosis cinerea* and by applying histochemical techniques we can study formation and behavior of different tissues over the time. *C. cinerea* was first studied by the German Julius Oskar Brefeld[1] in 1877 who concluded that the primordia of various species of the classical genus *Coprinus* (*sensu lato*) originated from a single hyphal cell. We observed that the fruiting process of *C. cinerea* starts from the initiation of primary hyphal knots (Pks) followed by light-induced formation of secondary hyphal knots (Sks) from which then successively primordia stages P1 to P5 form and ultimately the mushroom which autolyzes at maturity for shedding the sexual basidiospores in the form of black droplets[4,7, 8,14,15].

To dissect these processes further in cytology, we applied five different histochemical stains on section cuts of *C. cinerea* primordia. Lactophenol blue as the best known discriminative fungal stain dyes chitin in fungal cell walls[16]. Eosin is also a useful fungal stain that interacts with chitin and chitosan in fungal cell walls[17] and it also stains nuclei and proteins located in the cytoplasm[18]. PAS stains polysaccharides, among glycogen, glycoproteins and glycolipids, why it can be used to stain fungal cell walls and intracellular depositions of glycogen[19,20]. Hemalum is an aluminium-haematein complex that reacts with acidic structures in the cell such as basophilic proteins and nuclei, other polyanions such as glycosaminoglycans and acidic glycoproteins[18]. Malachite green is known to bind to DNA and protein[21] and to stain and adsorb also to polysaccharides such as cellulose[22] and chitin[23]. We can thus expect in our experiments that lactophenol blue stains cell walls of primordia while the other stains may dye cell walls and/or inner cell material.

In all our samples, we recognize cell wall staining e.g. of stipe hyphae (Fig. 4) which suggests that all of the dyes undergo one or another reaction with cell wall polymers. Fungal cell walls consists mainly of chitin and glucans and there might be (glyco) proteins attached to the cell wall layers[24,25]. Cell walls thus could offer specific interphases for respective interactions for all of our stains tested.

Other than the protective pileipellis, staining in our samples in most instances was best of the hymenium (Fig. 4), in accordance to that it should be the most active tissue layer of stage P4 in preparation of karyogamy, meiosis and basidiospore formation[26]. Most interesting appear the cellular views on probasidia and subhymenium double stained by PAS and hemalum. Hemalum stained the inner of the probasidia blue and PAS inner granules of the subhymenium wine-red (Fig. 5H) which implies that quite different metabolic activities happen in these cells. Hemalum indicates presence of basophilic material[26] within the probasidia and this may reflect arrangements of proteins and nuclei in view of the future basidial tasks. PAS stain identifies inner polysaccharides in form of glycogen[19,20]. The staining seen in Fig. 5H thus suggests an accumulation of glycogen in the subhymenial hyphal cells.

Glycogen serves as a form of energy storage in an organism and the involvement of glycogen in the vegetative as well as in the carpophore development has been reported from several past studies. Madelin[28] described that stored mycelial glycogen was transferred to the developing gills of mushrooms during the fruiting process. Such accumulation of glycogen in fruiting structures from the vegetative mycelium begins as early as at the initial primordial stages. According to Matthews and Niederpruem[19], at the P1 stage (our nomenclature) glycogen is spread over the whole primordial structure. The apex of the developing pileus in the young primordia (P2 stage in our nomenclature) and the cells below the stipe are rich in glycogen[19]. However, glycogen depletes at later primordial stages from stipe tissue regions into the cap in favor for an accumulation more at the gills and eventually more specifically in the subhymenia of the P4 stage primordia[29,30]. Bonner *et al.*[20] showed the presence of glycogen at the base of the hymenium and presence of basophilic substances at the outer tips of basidia in two different Coprini mushroom species (*C. cinerea* and *Coprinellus curtus*) by staining with PAS and toluidine blue, respectively. He concluded upon observation of sporulation that both these groups of substances entered the spores and were reserved in there for future germination and growth. Alternative translocation of glycogen from vegetative mycelia to maturing sclerotia was reported by Jirjis and Moore[31]. These authors suggested that such transfer is for the long term storage of polysaccharides also for future germination of the sclerotia. Such transfer of glycogen into sclerotia can happen in case of that fruiting fails when sclerotia are instead generated from primary hyphal knots (Fig. 1).

Along the hymenial layer of probasidia at the P4 stage (Fig. 4 and 5) are some large bulging structures projecting outward from the hymenial region. These structures are cystidia which further grow to touch opposite hymenia and which form a bridge-like structure with the subsequently differentiating cystesia in the opposite hymenium. Cystidia-cystesia bridges serve to prevent opposing hymenial surfaces from touching one another during the development of the basidia and basidiospores[6]. Deposition of glycogen in the cystidia was reported by McLaughlin[32]. In our P4 stage samples, we also saw evidence for glycogen deposits in cystidia by wine-red stained granules (Fig. 5H; Table 1). Probably, this glycogen in the cystidia serves reserving energy for their future growth in size during further development to the P5 stage.

Conclusion

Fruiting body development of *C. cinerea* is a complex process of tissue generation and differentation that follows a strict time course. We used five different histochemical stains, singly and in combinations, to better visualize these processes underneath the microscope. Staining can discriminate tissues and cells in fruiting body primordia from each other and different dyes can variably focus on distinct cells. Of all, best tissue differentiation was achieved in double staining with PAS 1st and hemalum 2nd.

References

[1] BREFELD O. Botanische Untersuchungen über Schimmelpilze. III. Basidiomyceten [M] Leipzig: Arthur Felix, 1877. (in German)

[2] KAMADA T, KURITA R, TAKEMARU T. Effects of light on basidiocarp maturation in *Coprinus macrorhizus* [J]. Plant Cell Physiology 1978, 19:263-275.

[3] KÜES U. Life history and developmental processes in the basidiomycete *Coprinus cinereus* [J]. Microbiology and Molecular Biology Reviews 2000, 64:316-353.

[4] KÜES U, NAVARRO-GONZÁLEZ M. How do Agaricomycetes shape their fruiting bodies? 1. Morphological aspects of development [J.] Fungal Biology Reviews 2015, 12:99-107.

[5] KÜES U, KONSUNTIA W, SUBBA S. Complex Fungi [J]. Fungal Biology Reviews 2018, 32:205-218.

[6] MOORE D. Fungal morphogenesis [M]. Cambridge: Cambridge University Press, 1998.

[7] BOULIANNE RP, LIU Y, AEBI M, *et al.* Fruiting body development in *Coprinus cinereus*: regulated expression of two galectins secreted by a nonclassical pathway [J]. Microbiology 2000,146:1841-1853.

[8] MATTHEWS TR, NIEDERPRUEM DJ. Differentiation in *Coprinus lagopus*. I. Control of fruiting and cytology of initial events [J]. Archives of Microbiology 1972, 87:257-268.

[9] SWAMY S, UNO I, ISHIKAWA T. Morphogenetic effects of mutations at the *A* and *B* incompatibility factors in *Coprinus cinereus* [J]. Journal of General Microbiology 1984, 130:3219-3224.
[10] GRANADO JD, KERTESZ-CHALOUPOVÁ K, AEBI M, *et al.* Restriction enzyme mediated DNA integration in *Coprinus cinereus* [J]. Molecular and General Genetics 1997, 256:28-36.
[11] KÜES U, SUBBA S, YU Y, *et al.* Regulation of fruiting body development in *Coprinopsis cinerea* [J]. Mushroom Science 2016, 19:318-322.
[12] LUNA LG. Manual of histologic staining methods of the Armed Forces Institute of Pathology [M]. New York: McGraw-Hill, 1968.
[13] ROSIN I, MOORE D. Differentiation of the hymenium in *Coprinus cinerea* [J]. Transactions of the British Mycological Society 1985, 84:621-628.
[14] ATKINSON GF. Origin of development of lamellae of *Coprinus* [M]. Botanical Gazette 1916, 41:89-130.
[15] BULLER AHR. Researches on fungi. Vol. IV. Further observations on the Coprini together with some investigations on social organization and sex in the hymenomycetes [M]. New York: Hafner Publishing Co., 1931.
[16] SOLIMAN SSM, GREENWOOD JS, BOMBARELY A, *et al.* An endophyte constructs fungicide-containing extracellular barriers for its host plant [J]. Current Biology, 2015, 25, 2570-2576.
[17] BAKER LG, SPECHT CA, DONLIN MJ, *et al.* Chitosan, the deacetylated form of chitin, is necessary for cell wall integrity in *Cryptococccus neoformans* [J]. Eukaryotic Cell 2007, 6:855-867.
[18] BANCROFT JD, STEVENS A. Theory and practice of histological techniques [M]. 129. Edinburgh: Churchill-Livingstone, 1977.
[19] MATTHEWS TR, NIEDERPRUEM DJ. Differentiation in *Coprinus lagopus*. II. Histology and ultrastructural aspects of developing primordia [J]. Archives of Microbiology 1973, 88:169-180.
[20] BONNER JT, HOFFMAN A, MORIOKA WT. The distribution of polysaccharides and basophilic substances during the development of the mushroom *Coprinus* [J]. The Biology Bulletin 1957, 112:1-6.
[21] BHASIKUTTAN AC, MOHANTY J, PAL H. Interaction of malachite green with guanine-rich single-stranded DNA: preferentially binding to a G-Quadruplex [J]. Angewandte Chemie 2007, 46:9305-9307.
[22] ALEXANDER MP. A versatile stain for pollen fungi, yeast and bacterial [J]. Stain Technology 1980, 55:13-18.
[23] ZHANG L, ZHOU W, TANG HU. Adsorption isotherms and kinetics studies of malachite green in chitin hydrogels [J]. Journals of Hazardous Materials 2012, 209-210:218-225.
[24] BOWMAN SM, FREE SJ. The structure and synthesis of fungal cell wall [J]. Bioessays 2006, 28:799-808.
[25] WESSELS JGH. Wall growth, protein excretion and morphogenesis in fungi [J]. New Phytologist 1993, 123:397-413.
[26] LU BC. The control of meiosis progression in the fungus *Coprinus cinerea* by light/dark cycles [J]. Fungal Genetics and Biology 2000, 31:33-41.
[27] LILLIE D, DONALDSON PT, PIZZOLATO P. The effect of graded 60° C 1 N nitric acid extraction and of deoxy ribonuclease digestion on nuclear staining by metachrome mordant dye metal salt mixtures [J]. Histochemistry 1976, 46:297-306.
[28] MADELIN MF. Visible changes in the vegetative mycelium of *Coprinus lagopus* Fr. at the time of fruiting [J]. Transactions of the British Mycological Society 1960, 43:105-110.
[29] BLAYNEY GP, MARCHANT R. Glycogen and protein inclusions in elongating stipes of *Coprinus cinerea* [J]. Journal of General Microbiology 1977, 98:467-476.
[30] MOORE D, ELHITI MMY, BUTLER RD. The morphogenesis of carpophore of *C. cinerea* [J]. New Phytologist 1978, 83: 695-722.
[31] JIRJIS RI, MOORE D. Involvement of glycogen in morphogenesis of *Coprinus cinerea* [J]. Journal of General Microbiology 1976, 95:348-352.
[32] McLAUGHLIN DJ. Ultrastructural localization of carbohydrate in the hymenium and subhymenium of *Coprinus*. Evidence for the function of the Golgi apparatus [J]. Protoplasma 1974, 82:341-364.

Chapter 4

Studies on primordia of *C. cinerea*

Sub-chapter. 4.1. Cytological study on primordia of *C. cinerea*

4.1.1. Abstract

Coprinopsis cinerea serves as a model fungus for the *Agaricomycetes* to study fruiting body development because it grows and fruits very fast in the laboratory. Under optimal environmental condition, it takes seven days to obtain a matured mushroom from the vegetative mycelium and fruiting is strictly regulated by environmental conditions including nutrients, light, temperature, and aeration. The first initiation of a fruiting body occurs by the formation of primary hyphal knots (Pk) in the dark. Under standard fruiting conditions by fixed light-dark conditions (12 h light/12 h dark) at 25 °C and high humidity, subsequently, secondary hyphal knots (Sks) as a first structure committed to fruiting are formed and subsequently primordial stages P1, P2, P3, P4 and P5 and eventually on the 7^{th} day, the mature mushroom autolyzes its cap for shedding basidiospores in liquid droplet that fall to the ground. In this study, by applying histochemical staining techniques for the light microscopy, primordial sections of *C. cinerea* were examined to study different tissues and cell types that appear over time in the fruiting process.

4.1.2. Introduction

Studies on fruiting body development of *C. cinerea* started over a century ago. Until now studies on the *C. cinerea* fruiting process in Basidiomycetes have been of great interest. The main reason for the extensive studies on *C. cinerea* is the fast growth. The species completes its life cycle under laboratory conditions within two weeks and requires minimal cultivation conditions (Kües 2000; Kües and Navarro-González 2015). Fruiting in *C. cinerea* is a synchronized process that takes from a vegetative mycelium under a normal day/night rhythm seven days (from Day 0 to Day 7) to obtain a mature mushroom (Navarro-González 2008). The process of differentiation begins with a loose formation of a primary hyphal knot (Pk) within the mycelium in dark (Boulianne et al. 2000, chapters 2.1 and 2.2). When a light signal is present, these Pks cluster together on a mycelial lattice and transform into a compact secondary hyphal knot (Sk) (Matthews and Niederpruem 1972, 1973; Moore 1995, chapter 2.1), which otherwise under constant dark turn into multicellular structures of sclerotia (Moore 1981; Kües 2000, chapter 2.2). A light-induced secondary hyphal knot is a structure committed to enter a fruiting body pathway. Stipe and cap tissues start to differentiate in Sks (Kües and Navarro-González 2015; Navarro-González 2008; Subba 2015). After the onset of the Sks, in the following days, under a normal day/night rhythm and at a temperature of 25 °C, development of the primordial stages from P1 to P5 progresses with the induction of karyogamy in basidia in the P5 stage followed after the P5 stage by meiosis. Subsequently, basidiospore production takes place, which parallels the elongation of the stipe and the expansion of the cap for the maturation of the fruiting body. Mature fruiting bodies autolyze on Day 7 to release the spores in liquid droplets (Buller 1924; Navarro-González 2008; Kües and Navarro-González 2015).

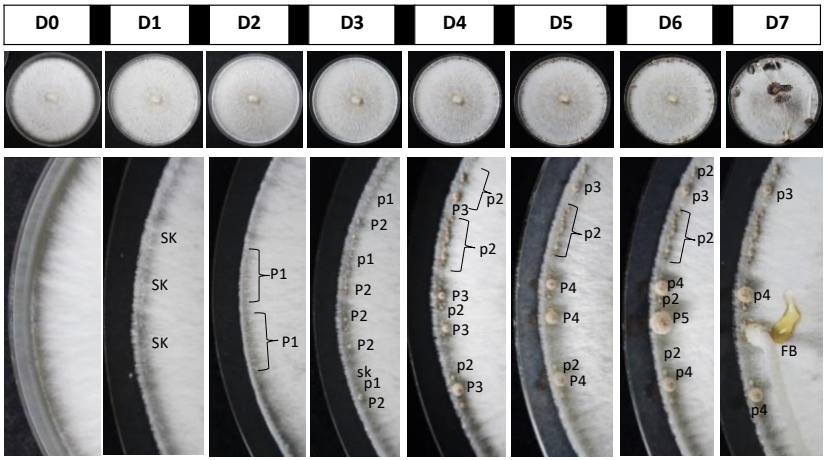

Fig.1. Fruiting body development of homokaryon AmutBmut follows a strict pattern of growth under a 12 h light and 12 h dark regime of incubation under standard fruiting condition at 25 °C and completes in seven days. Many secondary hyphal knots are formed on Day 1. However, because nutrients are restricted, many structures abort development over the time in favor of a few that successfully transform into a complete mushroom. Actively growing structures are marked Sk (secondary hyphal knot), P1 to P5 (primordia stages), FB (fruiting body) and aborted structures in lower case letters p1 to p5. D0 is the day of shifting plates from 37 °C into standard fruiting conditions at 25 °C. D0 to D7 (Day0 to Day7) refer to days of development under standard fruiting conditions. Black and white boxes show the 12 h day and 12 h night regime.

Fig. 1 shows the fruiting pathway of homokaryon AmutBmut on a Petri dish incubated at 25 °C, which begins with the formation of hundreds of initial structures on Day 0 when mycelium is fully grown and transferred into fruiting condition. During the fruiting process, from day-to-day parts of structures are given up in development in favor of just a few each day to finally mature and autolyze on Day 7 of the fruiting pathway. The ongoing developing primordial structures are metabolically active within which formation and differentiation of cells and tissues are continuous. Actively growing structures are therefore, harvested for sectioning by a microtome and staining of the primordial sections for the analysis of various cells and tissues how occur during the developmental stages. The present study thus, gives an insight into a precise definition of the developmental stages of all primordia from stages P1 to P5.

The stages of fruiting body development have been cytologically examined and described in past studies (Buller 1924; Matthews and Niederpruem 1972, 1973; Lu 1974; Moore 1995, 1998; Kües 2000, Kües and Navarro-González 2015). However, the complexity in fruiting body development, including the formation and the differentiation of different types of cells and tissues during the fruiting process, has not yet been fully explained. Previous studies have from mycelium demonstrated transfer and deposition of polysaccharides and basophilic materials into young primordia into stipe and cap regions and finally in subhymenia (Madelin 1960; Matthews and Niederpreum 1973; Bonner et al. 1957; Jirjis and Moore 1976; Blayney and Merchant 1977). Furthermore, in this study here, the complex fungal multicellularity in tissue formation and cell differentiation in the various stages of primordia is identified and analyzed using histochemical techniques over the whole period of primordia development from stages P1 to P5.

4.1.3. Materials and Method

4.1.3.1. Strains and growth conditions

Please refer to chapter 3 section 2 (Chapter 3.2) for details.

4.1.3.2. Harvesting, embedding and staining of primordia

For double-staining, dyes PAS (periodic acid-Schiff, Schiff´s reagent) (0.2 % fuchsin, catalog no. 1358 Merck, Darmstadt, Germany) and Mayer's hemalum (catalog no. 51260, Sigma-Aldrich) were used in combination on the primordial sections (5 µm thick). PAS is commonly used to identify polysaccharides such as glycogen; these macromolecules consist of monosaccharide units that are connected by covalent bonds known as glycosidic bond which can be alpha or beta type. Polysaccharides are mainly stained as magenta in color. The second stain, Hemalum, is the aluminum-hematin complex, which binds to acidic structures in cells such as nuclei, other polyanions for e.g. glycosaminoglycans or acidic glycoproteins, giving always a dark blue color.

Please refer to chapter 3 section 2 (Chapter 3.2) for details in histology techniques.

4.1.3.3. Microscopy and Photography

Samples were inspected underneath a Zeiss Stemi 2000-C binocular and a Zeiss Axiophot 2 photomicroscope (Goettingen, Germany) with different enlargements. The binocular and the microscope were equipped with a Soft Imaging Color View II Mega pixel digital camera, linked to a computer. Photos were taken and analyzed with Analysis Software program (Soft Imaging System, Münster, Germany). Fresh primordia were directly photographed underneath the binocular upon harvest, either complete or cut longitudinally in halves.

4.1.4. Results

4.1.4.1. Initial hyphal knot formations

Under dark conditions, a single hypha branches and a sub-branch to form short-lateral hyphae, which are then interconnected and merged with the neighboring hyphae through the process of anastomosis. They thereby form a hyphal core easily recognizable underneath a microscope, referred to as the primary hyphal knot (Pk) 0.02 mm formed on Day 0 of the fruiting pathway (Fig. 2A). However, Pks are not specific to fruiting and differentiate into multicellular resting bodies sclerotia in constant dark. With the induction by light, a compact 3-D aggregated secondary hyphal knot (Sk) of approx. 0.2 to 0.3 mm (Fig. 2B and C) is formed from the Pks on the Day 1 of the fruiting pathway. In the developing Sk, both cap and stipe tissues begin to differentiate within the structure and the entire body of Sk is covered by an newly formed innate universal veil. After Sk formation, both light and dark phases are required to coordinate further tissue development in the primordia from stages P1 to P5.

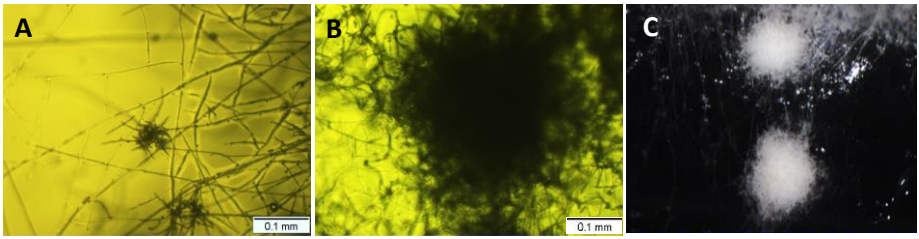

Fig. 2. (A) Primary and (B) secondary hyphal knots observed underneath the inverse microscope and **(C) secondary hyphal knots** observed underneath the binocular formed on the plastic floor of a window of a Petri-dish. The yellow filter is used to block the blue light in order to avoid any kind of disturbance to the developing structures.

4.1.4.2. Primordia development in *C. cinerea*

An overview on the primordial stages from P1 to P5 is shown in Fig. 3. It shows the exterior view of the primordia (top), the interior view of the same primordia, which are cut vertically in halves (center) and the double-stained vertical and cross sections of all stages of the primordia (bottom) in bright-field images (left) and in dark-field images (right). The cytological examinations on the primordial sections made it possible to recognize the formation and differentiation of different cells and tissues that occur in the course of the fruiting process.

In the coming sections, various types of cells and tissues that appear within the growing primordia from stages P1 to P5 from double-stained sections, both longitudinally and vertically are analyzed and described in detail.

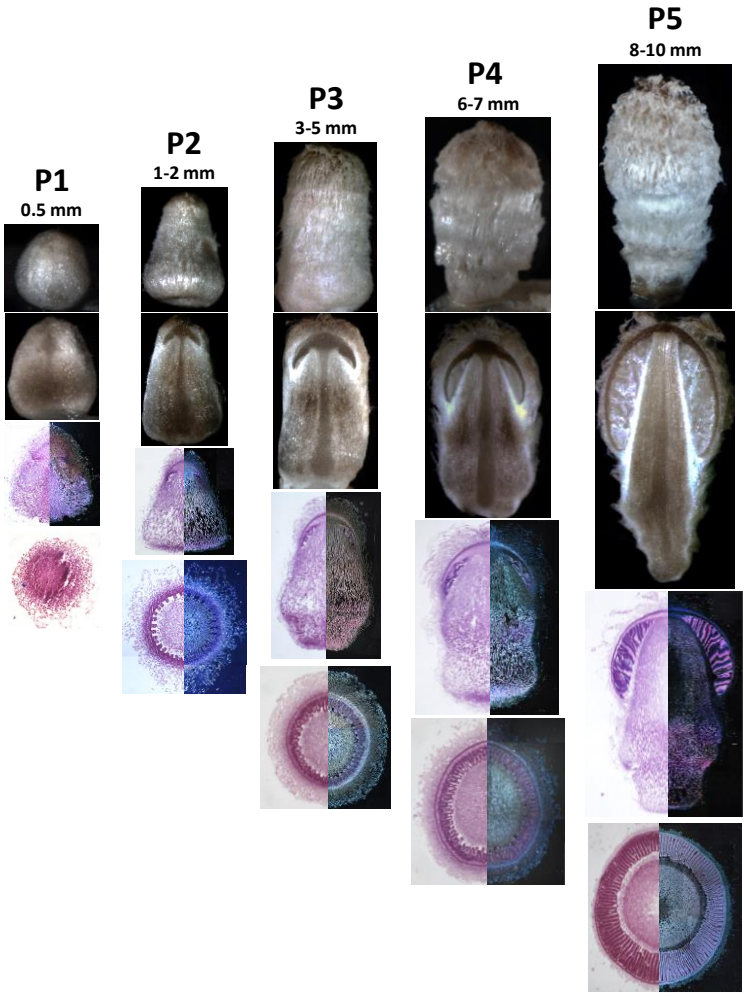

Fig. 3. A morphological overview of the primordia stages from P1 to P5, (top row) outer view of a mushroom structure with cap and stipe of the primordia stages, divided vertically in halves (2nd row), PAS and hemalum double-stained in the longitudinal direction (5µm thick) of the same primordia stages showing the hyphal tissue (3rd row), double stained PAS and hemalum cross-section (5µm thick) of the cap regions of the primordia stages P1 to P5 showing the arrangement of the gill (4th row). Photos of primordia and their halves were taken under the binoculars. Photo of the double-stained sections were taken under the microscope using bright and dark-field techniques, and the photos shown here are the mirror image of each other.

4.1.4.3. Primordium stage 1

The primordium stage P1 develops from a secondary hyphal knot within the next 24 h under standard fruiting conditions fixed to 12 h light/12 h dark at 25 °C. This stage is the first step in the initial development of a carpophore, where cap and stipe tissues started to differentiate within the structure proceeding towards the formation of a complete mushroom (Fig. 4).

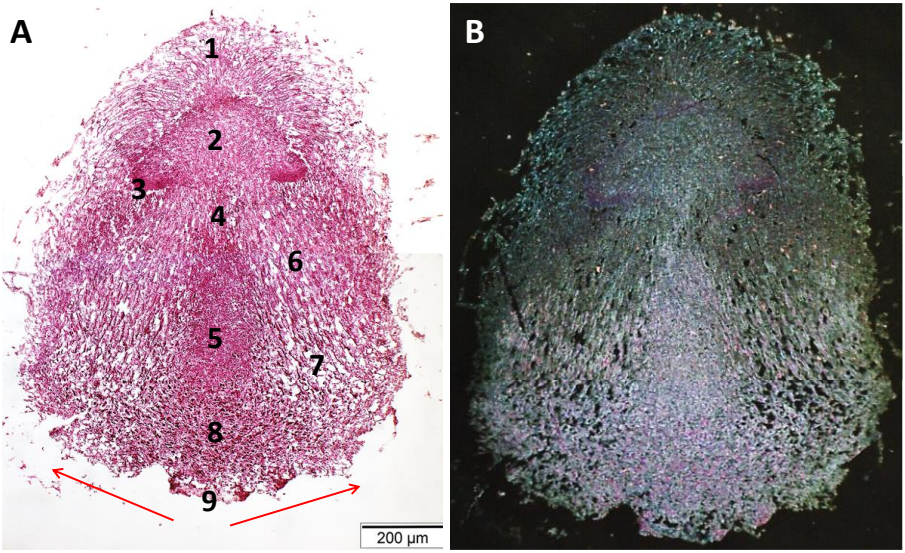

Fig. 4. PAS and hemalum longitudinal stained section showing different tissues and cells of stage P1 primordium, photographed under a light microscope using bright-field (A) and dark-field (B) techniques. Number 1 marks: the universal veil, 2: pileus trama, 3: initial prehymenial palisade with the prehymenial cavity, 4: inner upper stipe tissues at the neck of the stipe joining the cap to the stipe, 5: densely stained narrow inner stipe tissue in the middle of the stipe, 6: inflated hyphae at upper outer part of the stipe, 7: elongated stained hyphae at the lower half of the outer stipe, 8: the round to oval elongated compactly packed darker stained cells at the bottom of the stipe (primordial shaft), 9: the laterally arranged narrow hyphae initiating at the basal part of the primordial shaft and further growing upward to cover the outer part of the stipe found directly underneath the lower part of the universal veil (indicated on image A by the red arrows).

Fig. 4A (bright-field) and 4B (dark-field) shows a longitudinal-section of a P1 stage primordium double-stained by PAS and hemalum. The numbers 1 to 9 in Fig. 4A refer to different types of tissues recognized at the P1 stage. The numbers correspond to the images shown in Fig. 5 and 7 from the same section documented underneath a light microscope at higher magnification in bright-field. The tissue areas that are distinctly stained darker in magenta color in Fig. 4A show

accumulation of glycogen within those tissues. This can be more specifically followed up in the dark-field image (Fig. 4B) which indicates that the lower-half of the stipe, the dense tissue at the inner stipe region and the prehymenial palisades are distinctly stained in pink color. The presence of the pink color by PAS staining indicates an accumulation of glycogen in these areas (Fig. 4B).

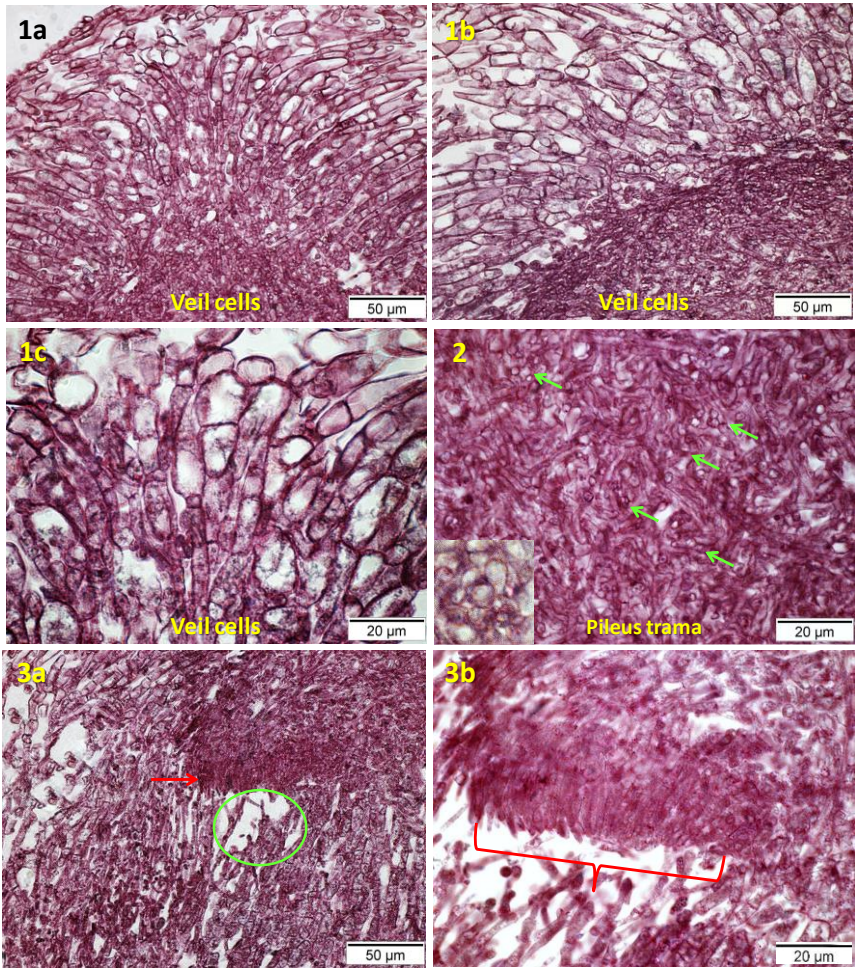

Fig. 5. Enlarged views on the longitudinal section of tissues at the pileus region at higher magnifications at bright-field. The images 1a to 1c show the hyphae of the universal veil emerging from

the pileus trama directly at the tip of the cap (1a) and downwards to the side (1b). Image 2 shows the pileus trama, green arrows mark rosette-like structures (shown enlarged in the inset) indicating the presence of multiple knot-like structures (*sensu* Reinjders 1977) within the pileus trama. 3a and 3b show the prehymenial palisade underside the pileus margin. A thick layer of parallely arranged prehymenial palisade cells (about 35 over the whole width of the palisade) is marked by the red arrow (3a) and a red bar (3b). The prehymenial cavity marked by the circle is generated underneath the prehymenial palisade (3a).

4.1.4.3.1. Pileus development:

The primordial structure at stage P1 is entirely covered by the continuous universal veil but at the base which is attached to the supporting vegetative mycelium (Fig. 4A, marked as 1). At higher magnifications, enlarged LS sections show that multiply segmented rarely branched hyphae for veil formation grow out from the surface and the inner of the pileus trama in a long cell-chain manner and spread outward from the surface of the pileus (1a-1c in Fig. 5). This is further documented in the fountain-like appearance seen in the cross-section shown in Fig. 6A. Veil cell maturation starts at the outer tip of a hypha and goes backward. Outer veil cell segments with increasing age tend to broaden (9.2 µm ±2.2, n=20) and extend in length (18 µm ±5, n=20) by further hyphal extension growth during maturation (1a-1c in Fig. 5). The cell segments in the hyphae closer to the pileus trama possibly undergo secondary segmentation during hyphal development leading to an increase in short cell segments. The young cell segments in the multi-segment veil cells close to the edge of the pileus are short and narrow (length: 8 µm ±3; diameter: 4µm ±1, n=20). In comparison, the oldest veil cells which were already existing on the surface of the secondary hyphal knots are restricted in diameter compared to the newly formed mature veil cells in the P1 stage (length: 10 µm ±3; diameter: 6 µm ±1.4, n=20).

The pileus trama at stage P1 is not distinctly separated from the multiple segmented mostly un-branched hyphae developing into veil cells. The pileus trama underneath the veil consists of tightly inter-woven, heavily branched narrow hyphae (Fig. 4A, marked as 2, and 2 in Fig. 5). There are many small knot-like structures seen localized within the section of the pileus trama appearing in the view of the plectenchyma in rosette-like form (2 in Fig. 5, marked by the green arrows), similarly as described by Reinjders (1977) in the mushrooms of e.g. *Russula fragilis* and *Limacella guttata*. The rosette-like view is a result from the sectioning of the 3D multi-branched knot-like structures.

The prehymenial palisade is located underside the pileus margin (Fig. 4A, marked as 3). In the cross-section, it appears as a closed ring (Fig. 6B). The cells in the prehymenial palisade are densely packed about (35 cells over the palisade width) and are growing in parallel downwards into a free space (3a and 3b in Fig. 5, marked by a red arrow and red bar, respectively). This

gap has been generated beneath the prehymenial palisade and was termed prehymenial cavity by Clémençon (2004) (3a in Fig. 5, marked within a green circle).

Since primordia at stage P1 were just developing from the delicate Sks, the P1 stage is still relatively delicate, especially in the region of the prehymenial cavity where the palisade is growing into. Together with the surrounding loosely connected hyphal veil cells, the region provides reduced stability in microtome cuts. Therefore, a perfect cross-section (Fig. 6B) of the most delicate cap region is difficult to achieve whereas clearer views of the cap region can be seen in the longitudinal-section (Fig. 4A) and in the cross-section of the upper cap region and the lower stipe region (Fig. 6A and 6C). Many cross-sections were performed but in the particular cap ring regions, all were cracked (Fig. 6B, marked by the red arrows).

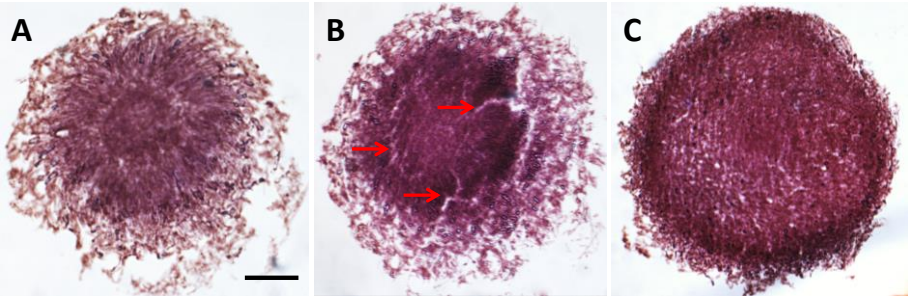

Fig. 6. Bright-field images of cross-sections of a pileus and stipe regions observed underneath a light microscope. The image (A) shows the tip of a cap region, (B) the prehymenial region and (C) shows a transverse cut of a stipe region at the base of the primordium stage P1 above the primordial shaft. The red arrows points to the cracks in the delicate parts of the prehymenial palisade. The scale bar measures 0.1 mm.

4.1.4.3.2. Stipe development:

From the longitudinal cut shown in Fig. 4A and 4B, we recognized an inner conical shape of dense plectenchyma, on the neck of which the cap sits. The cone arises from the primordial shaft at the base of the P1 stage. A thick outer layer of loose inflated hyphae with voids in-between surrounds the inner cone of the stipe. These hyphae arose ring-like (Fig. 6C) from the upper surface of the primordial shaft.

At the basal part before the primordial shaft, many narrow and short branched interlinked hyphae are laterally arranged (Fig. 4A, 9 marked by two red arrows and 9a and 9b in Fig. 7). They resemble very dense, highly branched vegetative mycelium (9a and 9b in Fig. 7). A part of these narrow hyphae began to further grow as a thin layer upward around the stipe region

and covers at stage P1 about the half of the stipe directly underneath the veil. In the CS in Fig. 6C, it is the thin dense outer ring seen underneath the outer loose veil layer. The remaining narrow hyphae located at the basal part of the primordial shaft start to grow upward with massive formation of side-branches and merge with the compact round to oval appearing hyphae with completely magenta stained cytoplasm, already present within the center of the primordial shaft and stained darker in magenta by PAS staining indicates the presence of glycogen in these cells (Fig. 4A marked as 8 and 8 in Fig. 7).

Growing further upward out of the primordial shaft, the narrow hyphae form the darkly stained dense inner cone of the stipe of heavily branched narrow hyphae (Fig. 4A, marked as 5 and 5 in Fig. 7) which continue to grow upward under repeated branching towards the pileus trama with the inner straight growing hyphae reaching the neck of the cone (4a in Fig. 7, shown by red arrows). The narrow hyphae are at the upper-half of inner stipe tapers over the length and consist of vertically oriented main leading hyphae interconnected to each other by laterally branched narrow hyphae under frequent anastomosis (Fig. 4A, marked as 4 and 4a and 4b in Fig. 7, within red bars).

At the outer region over the whole length of the young stipe, the parallel hyphae growing and little branched with some terminal cells are inflated and have voids in-between them and they are loosely connected to each other (Fig. 4A, marked as 7 and 7 in Fig. 7). At the lower-half of the stipe, they are stained partially by magenta-colored granules of glycogen. The hyphae at the upper part of the outer-stipe are inflated, higher segmented and not stained (Fig. 4A, marked as 6 and 6 in Fig. 7). The tissue of the outer part of the stipe is quite fragile due to the presence of many hollow spaces in-between cells and the low networking between hyphae might be the reason for the loose connectivity within neighboring areas.

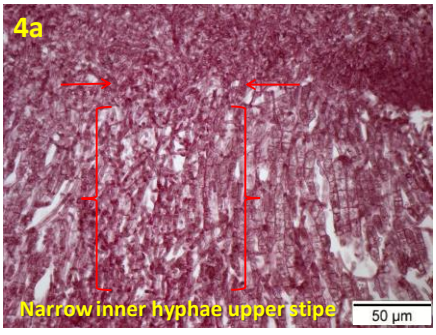
4a
Narrow inner hyphae upper stipe
50 µm

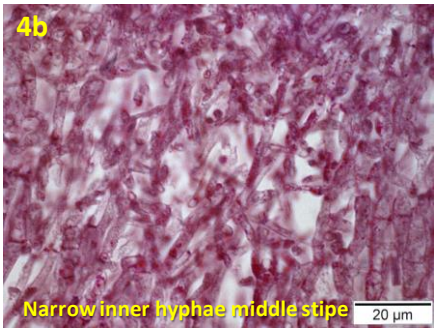
4b
Narrow inner hyphae middle stipe
20 µm

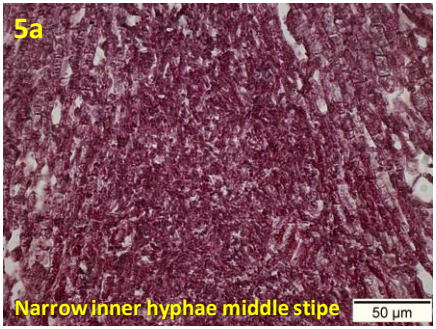
5a
Narrow inner hyphae middle stipe
50 µm


6
Inflated hyphae outer upper stipe
20 µm


7
Inflated hyphaelower part of the outer stipe
20 µm


8
Dense hyphae at center of the primordial shaft
20 µm

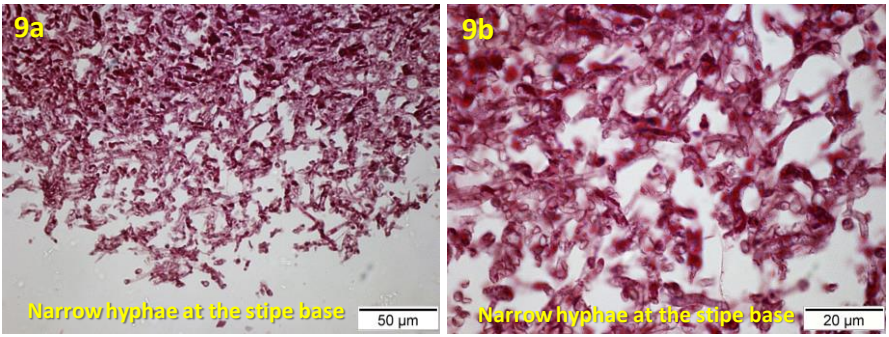

Fig. 7. Longitudinal sections of tissues at the stipe region at higher magnifications of the same areas marked in Fig. 1 observed in bright-field underneath a light microscope. The images 9a and 9b represent the laterally grown narrow hyphae at the base underneath the primordial shaft. Image 8: dense darker stained round to oval appearing hyphae at the center of the primordial shaft. 7: Loosely arranged partially stained in magenta granules inflated hyphae at the lower-half with some terminal cells. 6: Segmented inflated non-stained hyphae at the upper part of outer stipe. 5: dense stained narrow and heavily branched hyphae of the inner cone. 4a and 4b: narrow branched hyphae (within red bars) at the upper-half of inner stipe. The red arrows show connection between the hyphae of inner stipe and pileus trama.

4.1.4.4. Primordia stage 2

After receiving both light and dark signals at 25 °C, stage P1 primordium grows within the next 24 h into a second stage primordium P2 on Day 3 of the standard fruiting pathway (Fig. 8). A P2 primordium is pear-shaped and has a size of approximately 1 to 2 mm with internal clearly distinguishable cap and stipe regions. At this stage, two contexts emerge for the first time: one is a thick tissue band called pileipellis, located underneath the veil in the cap region, and the other are gill rudiments, formed from the prehymenial palisade formed at P1 stage and grown further into young gills. At the apex of the stipe, a new context arose in the connection near the cap. Because it is quite difficult to cut longitudinally through the center a whole structure, the P2 stage primordium shown in Fig. 8A was slightly tangentially captured. Therefore, two more cuts are shown in which the cap region at the connection to the stipe (apex with outer lower pellis) (Fig. 8C, marked by the black arrows) and the inner stipe region are distinctly visible in the central longitudinal view (Fig. 8D).

The dark-field images in longitudinal and cross section of P2 stage primordium highlight the tissues with different colors (Fig. 8B and 8F). The densely packed hyphae at the basal part of the primordium are stained in bright-pink color. Further upwards, most of the tissues in the stipe up till the upper-half region are stained in bright-pink. In the pileus region, gill rudiments are distinctly stained in bright-pink in both longitudinal-and cross-sections (Fig. 8B and 8F). Further the pileipellis is stained in a band of light pink color. The veil cells at the cap and the stipe are stained in blue. The presence of pink color stained by PAS staining and blue color by hemalum indicates the presence of glycogen and basophilic materials, respectively in these tissues.

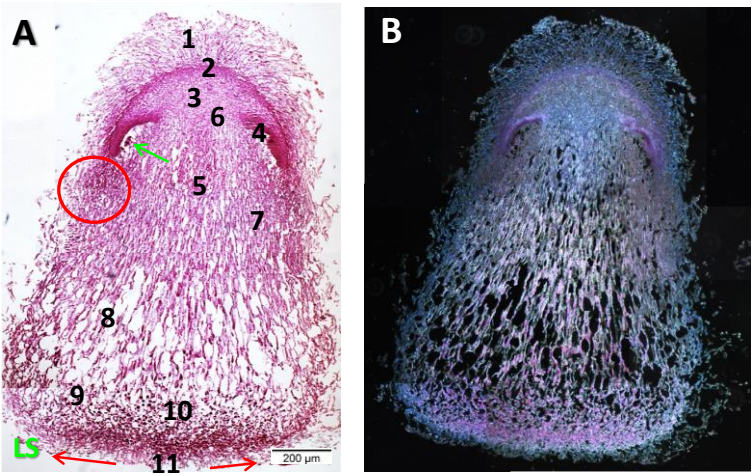

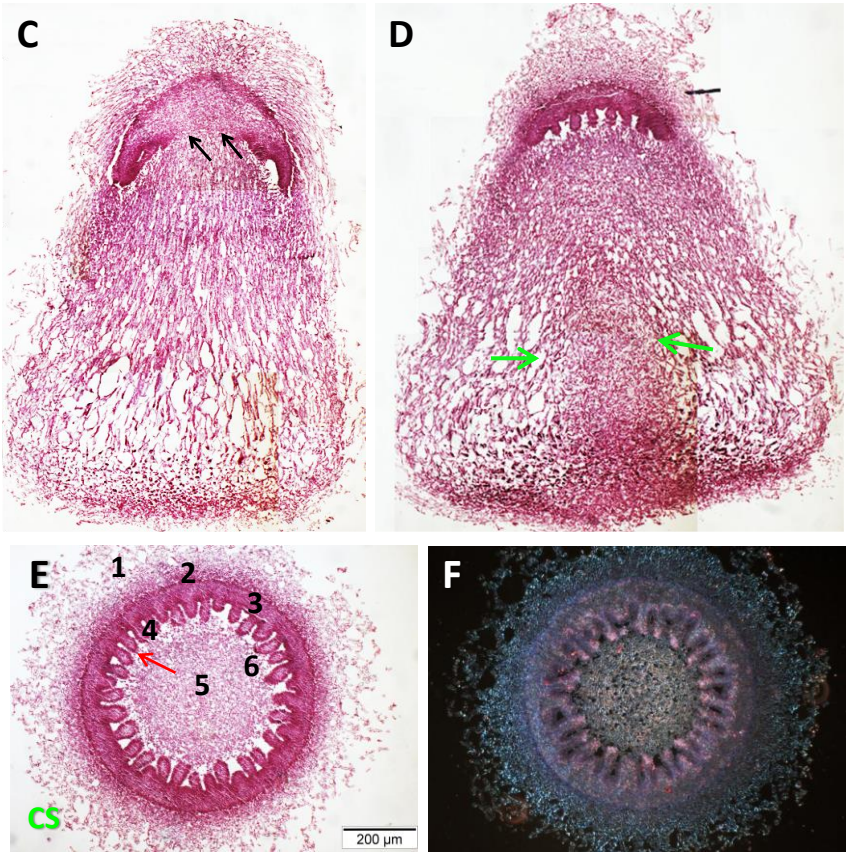

Fig. 8. PAS and hemalum stained longitudinal- (LS) and cross-sections (CS) showing different tissues and cells of stage P2 primordium, photographed under a light microscope using bright-field (A, C, D and E) and dark-field (B and F) techniques. In image (A) the number 1 marks the veil, 2: pileipellis, 3: pileus trama, 4: hymenial tissues, 5: inner stipe tissues, 6: exterior stipe tissue at the apex, 7: inflated and segmented partially stained hyphae at the upper-half of the stipe, 8: inflated and extended hyphae stained darker in magenta granules at the lower-half of the outer stipe, 9: loosely arranged oval to round appearing dark stained hyphae at outer part of primordial shaft,10: dense compact darker stained hyphae at the center of the primordial shaft, 11: narrow highly branched laterally arranged hyphae at the bottom of the primordial shaft further growing upward to cover the outer part of the stipe found directly underneath the lower part of the universal veil (indicated on image A by the red arrows). Note that the inner stipe and the lower pellis were not clearly seen in the image A due to the slightly tangential cut of the section. Therefore, the images C and D are shown as other sections of the same P2 stage primordium in which the lower pellis (marked by the black arrows in C) in the cap region at the connection to the stipe and the inner stipe region

(marked by green arrows in D) are distinctly centrally visible. The green arrows in A and E mark the lipsanoblema interconnecting stipe to the gills and a red circle in A shows the meeting point of the veil from the cap and the stipe region called cleistoblema.

4.1.4.4.1. Pileus development:

The longitudinal- (Fig. 8A-8D) and cross-sections (Fig. 8E and 8F) of a P2 primordium stained by PAS and hemalum were observed underneath a light microscope using bright-field (Fig. 8A, 8C, 8D and 8E) and dark-field techniques (8B and 8F) to analyze tissues and cellular arrangements within the structure. The universal veil which covered the stage P1 primordium differentiated at stage P2 into an upper partial veil covering the cap (termed pileoblema) and a lower partial veil covering the stipe (termed cauloblema), further loosening the tissue at the level where cap and stipe meet. The pileoblema extends from the apex over the whole cap further down along to the edge of the pileus margin where it touches the cauloblema growing out in an upward direction further around the outer stipe. At the edge of the pileus margin, the growing pileoblema and cauloblema intermingle into a newly formed stronger cleistoblema which then stabilizes the structure at the edge of the pileus (Fig. 8A marked in a red circle). The pileus region is now separated from the veil by the generation of the pileipellis, a dense layer of a tightly interwoven plectenchyma of broad highly branched hyphae with cytoplasm stained by PAS in magenta, indicating glycogen within the cells (Fig. 8A, marked by 2, 2 in Fig. 9). At this stage, the chain of veil cells at the pileus region are mostly inflated back to the pileipellis where the chains of veil cells base and, at a larger part, newly originate from the surface of the pileipellis on the enlarging cap (1a-1c in Fig. 9). The young veil cells near the generating hyphae on the surface of the pileipellis measure as 11 µm ± 3 x 5 µm ± 2 (n=20), in the middle part of the chain of veil cells: 25 µm ± 9 x 11 µm ± 2 (n=20) and the older ones at the outer region of the chain: 22 µm ± 7 x 8 µm ± 2 (n=20). Mature veils cells are thus now about 1.4-fold longer and 1.8-fold broader that those at the P1 stage.

The increasing pileus trama (Fig. 8A, marked by 3) underneath pileipellis in appearance is plectenchymous with tightly interwoven, heavily branched narrow hyphae and contains like in stage P1 many knot-like structures seen in rosette-like form in the longitudinal cuts (3 in Fig. 9, marked by the green arrows). A very thin, difficult to spot layer of hyphae (Fig. 8C, marked by the black arrows) referred to as lower pellis is formed at this stage which separates the cap from the outer stipe region (enlarged picture not shown because the hyphae are even more difficult to spot with enlargement by poor optical separation from cap and stipe hyphae).

At the outer lower edges of the pileus, the prehymenial plain palisade formed previously at stage P1 differentiated into gill rudiments with outer palisades and inner gill trama of parallely arranged narrow unbranched hyphae which grew out from the pileus plectenchyma. Gill rudiments continued to grow into young primary gills at stage 2 primordium (Fig. 8, marked as 4 and 4a-4c

in Fig. 9). The young primary gills with the palisades and the inner plectenchymous trama develop by outwards growth at the pileus margin, extending the palisades and incorporation of more parallely growing hyphae as gill trama. Accordingly, gill rudiments enlarge in length by outward growth with the production of more palisade cells at the gill margin (4c in Fig. 9, marked by a red bar). Sporadically, the outer ends of some gill trama hyphae divert laterally into a highly branched and by glycogen granules darkly stained plectenchymous layer representing the young subhymenium (4c in Fig. 9, marked by the red arrows). Some of the trama hyphae form enlarged bulbous cells at their ends. The chleistocystesia push outwards from the gill trama through the subhymenium and the palisades into the free space between neighboring cells and protrude into the direction of the opposite palisades, which base on the prehymenial cavity generated in stage P1 underside the pileus margin (4b and 4c in Fig. 9, marked by a green arrow). The cheilocystidia are also weakly colored by magenta granules (4c in Fig. 9, green arrow).

During gill rudiment formation, the initial palisade cells were lifted up into the prehymenial cavity with the inner end of the young gills splitting into two parallel flanks of palisades. Therefore open, the inner margins of the gills connect loosely to the lipsanoblema emerging from the upper part of the outer stipe (4a-4c in Fig 9). The lipsanoblema is a type of newly generated partial veil that is formed at this stage at the upper-part of outer stipe as much it is covered by the cap. It is marked by a green arrow in the bright-field image of the longitudinal-section (Fig. 8A), and in the cross-section (Fig. 8E). The lipsanoblema is formed as a thin layer of short-branched narrow loose hyphae that connects the upper part of outer stipe to the cap region by intermingling their hyphae to the inner trama hyphae at the outer edges of the developing primary gill rudiments (Fig. 8E, marked by a green arrow). The prehymenial layers at the inner margin edge of the gill rudiment are thus interrupted by the lipsanoblema attachment (4b and 4c in Fig. 9).

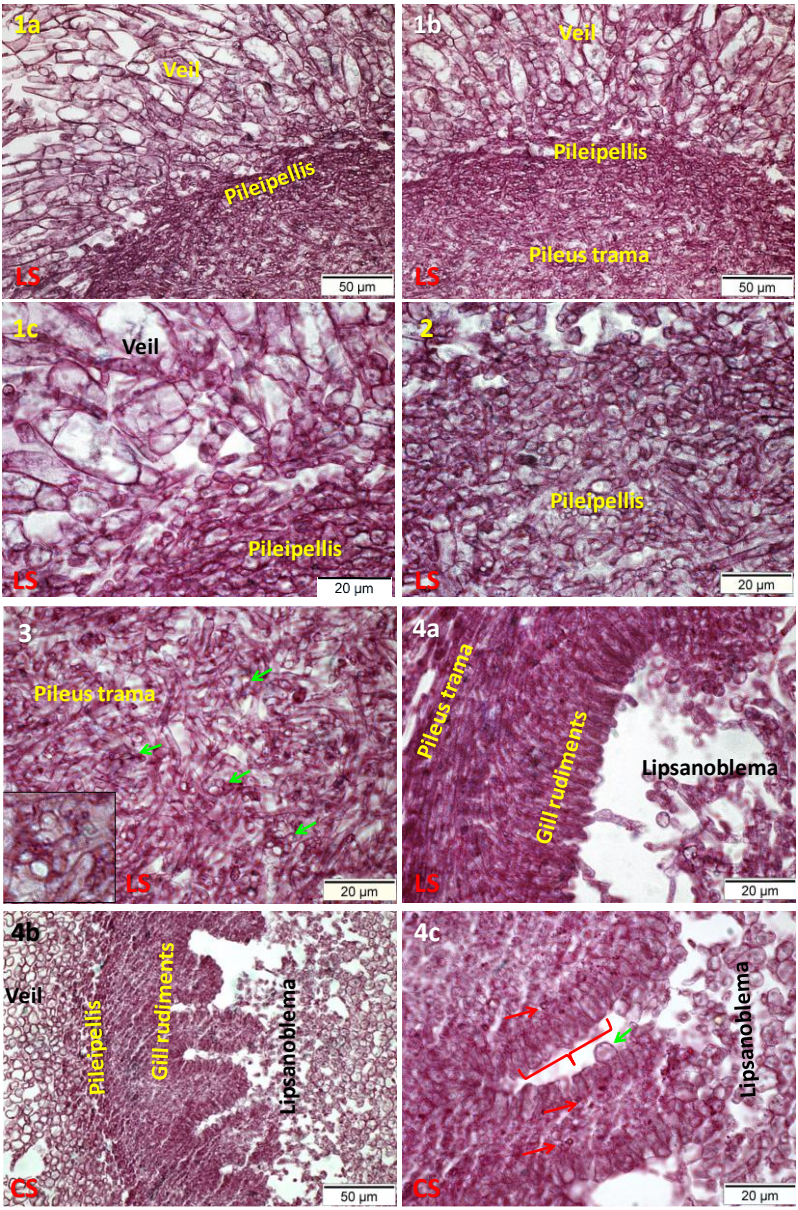
1a
Veil
Pileipellis
LS
50 µm
1b
Veil
Pileipellis
Pileus trama
LS
50 µm
1c
Veil
Pileipellis
LS
20 µm
2
Pileipellis
LS
20 µm
3
Pileus trama
LS
20 µm
4a
Pileus trama
Gill rudiments
Lipsanoblema
LS
20 µm
4b
Veil
Pileipellis
Gill rudiments
Lipsanoblema
CS
50 µm
4c
Lipsanoblema
CS
20 µm

Fig. 9. Enlarged views on longitudinal-and cross-sections of the same primordium at bright-field shown in Fig. 8. The images 1a to 1c show longitudinal sections (LS) of the veil, 2: tightly woven hyphae pileipellis, 3: narrow interwoven hyphae of pileus trama (inset picture shows an enlarged view of rosette-like structure), green arrows mark rosette like structures. The images 4a (LS), 4b and 4c (CS) are the developing gills. A red bar (4c) shows parallely arranged palisade cells in the gill region. The lipsanoblema grows towards the gill rudiment and attached to it at the edge. A thin layer of sub-hymenial layer formed at this stage is marked by the red arrows. A green arrow shows newly formed cheilocystidia (4c) protruding out from the gill trama into the free space.

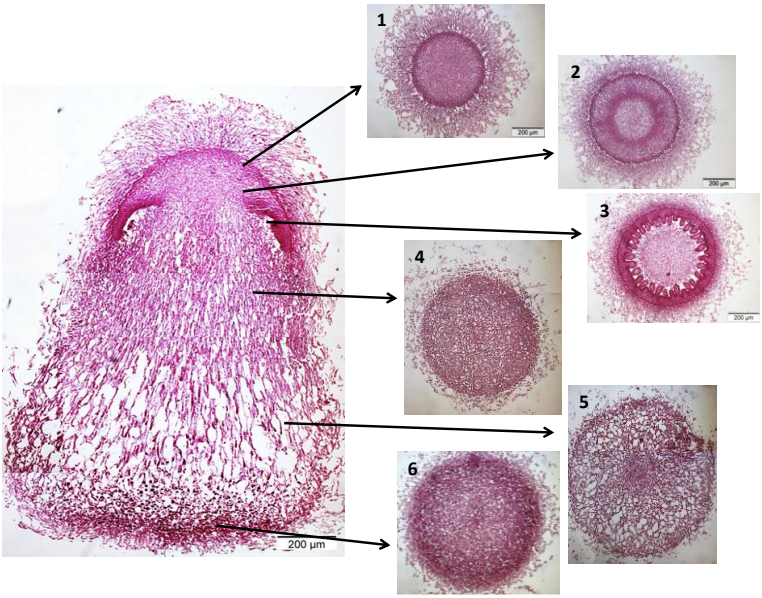

Fig. 10. Cross-sections of the primordium stage P2 marking the respective areas from the tip of the cap to the bottom of the stipe in the longitudinal-section. Cross-sections shown from top to bottom are 1: from the pileus region above the gills, 2: from the cap region with the upper onset of the gills, 3: from a region through the middle of gills, 4: the stipe region directly underneath the cap, 5: the region at the lower part of the stipe, and 6: the region with the primordial shaft.

4.1.4.4.2. Stipe development:

In the longitudinal cut of stage P2 primordium as shown in Fig. 8, dense and compactly arranged plectenchyma hyphae are seen at the primordial shaft similar than in stage P1. Around the primordial shaft at the base of the outer stipe, round to oval appearing, loosely arranged darkly

stained hyphal cells, interlinked by narrow hyphae and both hyphal cells types are interconnected to the outer up-growing inflated hyphae initiating at the lower half of the stipe (Fig. 8A, marked by 9, 9a and 9b in Fig. 11). These outer up-growing inflated hyphae are loosely connected and stretched in cell length between septa, due to which larger hollow spaces were created as compared to stage P1(9a and 9b in Fig. 11). These hyphae are darker stained by magenta granules by PAS (9a and 9b in Fig. 11). The hyphae located at the outer part of the lower stipe directly above the primordial shaft are inflated, partially stained and highly stretched (Fig. 8, marked by 8 and 8 in Fig. 11). In contrast, in their upper parts at the upper half of the stipe, the outer inflated and highly segmented hyphae are relatively closely arranged as compared to the lower half and few small gaps occur in-between them (Fig. 8, marked by 7, 7 in Fig. 11). These upper halves of the hyphae are less stained by PAS. The arrangements of such tissues and degrees of hollow spaces at different stipe levels of the primordium are also seen on the cross-section images in Fig. 10. Directly at the apex of the outer stipe, the still continuing hyphae are at their tips consists of cells that are ovoid to polyhedral shaped and are non-stained (Fig. 8, marked as 6 and 6 in Fig. 11).

The cross-sections also show a layer of densely arranged outer narrow hyphae as outer protective and stabilizing layer underneath the lower partial veil (6 in Fig. 10). This layer goes back to the outer narrow upwards growing hyphae between the former universal veil and stipe discussed before at stage P1. At higher magnification in the longitudinal cut, these narrow laterally-branched hyphae based from the primordial shaft grow further upward and cover now the outer part of stipe up to its apex with the lower pellis (11 in Fig. 11). The hyphae continue underneath the cap into the loose lipsanoblema which connects to the edges of the developing gills (Fig. 8E, marked by a green arrow).

In the center of all cross-sections of stipe regions, an inner dense tissue of equal diameter is recognized, indicating that the former conical inner stipe of upwards growing narrow hyphae has now been developed into a full cylinder (4 to 6 in Fig. 10). At the primordial shaft, these narrow hyphae growing from beneath into the primordial shaft (Fig. 8A, marked by 11, 11 in Fig. 11) and are interconnected to the round to oval appearing darker stained hyphae within the primordial shaft (Fig. 8, marked as 10 and 10 in Fig. 11), forming a dense tissue as already described for the P1 stage. The parallely upwards growing out of the primordial shaft, the hyphae form a vertical bundle of narrow highly branched interlinked hyphae which runs throughout the inner stipe together in the form of a cylinder (Fig. 8D, marked by the green arrows). All hyphae together reached now the central apex of the stipe open to the cap and they eventually got at this position connected to the pileus trama. Within the inner stipe cylinder, over the whole length the narrow-branched hyphae are stained darker in magenta by PAS than the surrounding outer stipe hyphae (Fig. 8A, marked as 5 and 5 in Fig. 11).

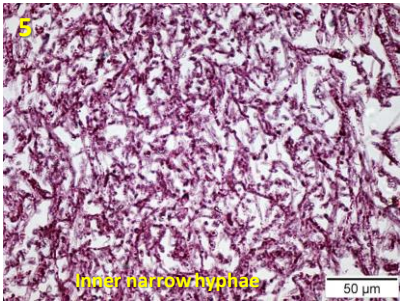
5
Inner narrow hyphae
50 µm

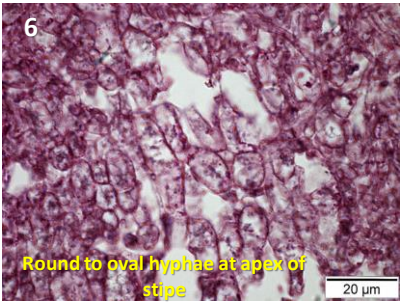
6
Round to oval hyphae at apex of stipe
20 µm

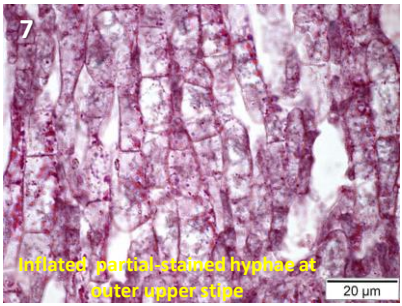
7
Inflated, partial-stained hyphae at outer upper stipe
20 µm

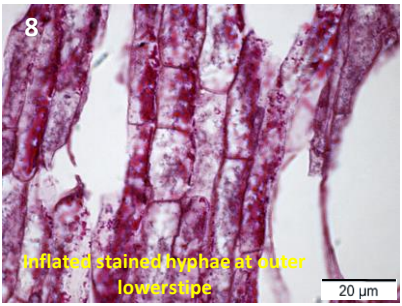
8
Inflated stained hyphae at outer lowerstipe
20 µm

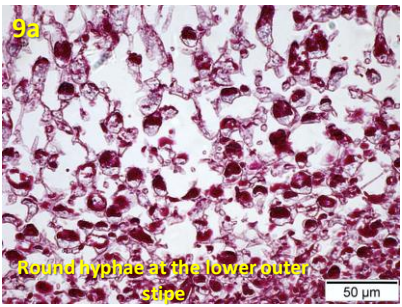
9a
Round hyphae at the lower outer stipe
50 µm

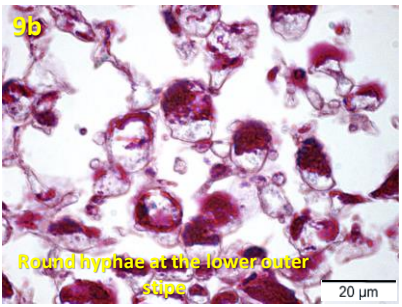
9b
Round hyphae at the lower outer stipe
20 µm

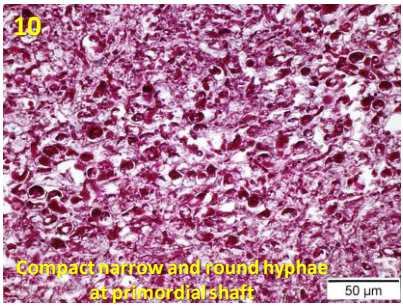
10
Compact narrow and round hyphae at primordial shaft
50 µm

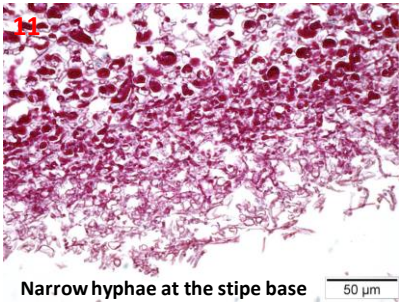
11
Narrow hyphae at the stipe base
50 µm

Fig: 11. Enlarged views on longitudinal-sections of stipe tissues of the same primordium at a bright-field shown in Fig. 8. Image 11 shows the narrow hyphae at the base of the primordial shaft of the primordium, 10: shows densely packed darker stained round to oval appearing hyphal cells in the center of the primordial shaft, 9a and 9b: loosely connected darker stained round to oval appearing hyphal cells at the outer part of the stipe bottom, 8: elongated inflated hyphal cells stained by magenta colored granules at the outer-part of the lower-half of the stipe, 7: inflated, segmented partially stained hyphal cells at the upper-half of the outer stipe, 6: are the non-stained ovoid to polyhedral hyphae at the apex of the stipe, 5: narrow inner hyphae which runs throughout the inner stipe.

4.1.4.5. Primordia stage 3

The pear-shaped stage P2 primordium develops into the terete-shaped stage P3 on Day 4 of the standard fruiting pathway and reaches a complete size of approximately 3 to 5 mm (Fig. 12A and 12B). At this stage, primary and secondary gills grow and arise radially from the underside of the pileus with increasing the size of the basidiome (Fig. 12A and 12C).

In bright-field images (Fig. 12A and 12C), the pileipellis (marked by number 2), the gill region (marked by number 4) and the lower half of the stipe are distinct by darker magenta-stained tissues. In dark-field image (Fig. 12B), the lower-half of the stipe shows densely packed cells which are explicitly stained in bright-pink. Towards the upper-half of the stipe, the tissues are partially stained in bright-pink and further upwards in the cap region, the gills and the pileipellis are stained darker in bright-pink (Fig. 12B and 12D). The darker PAS staining of these tissues at different locations of the P3 primordium in magenta in bright-field and in bright-pink in dark-field indicates accumulation of glycogen in these tissues.

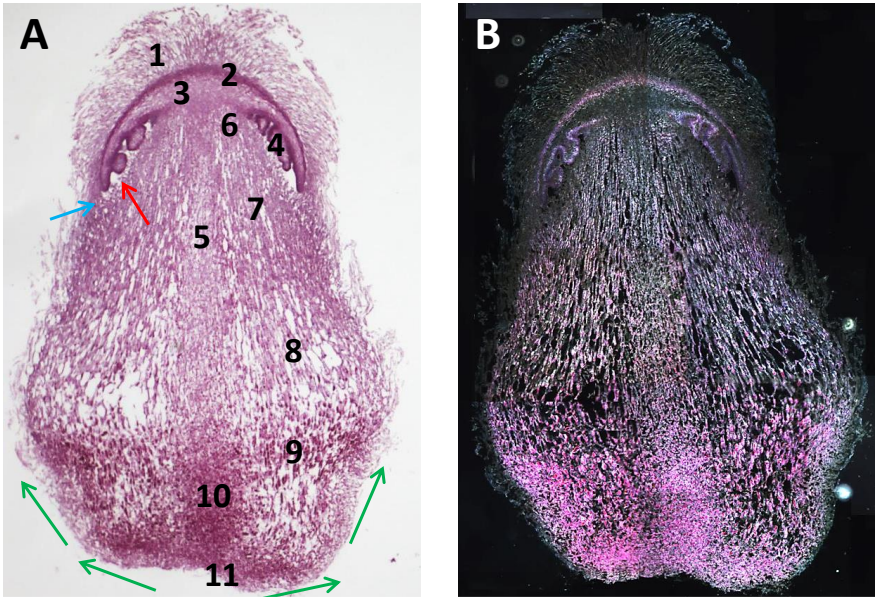

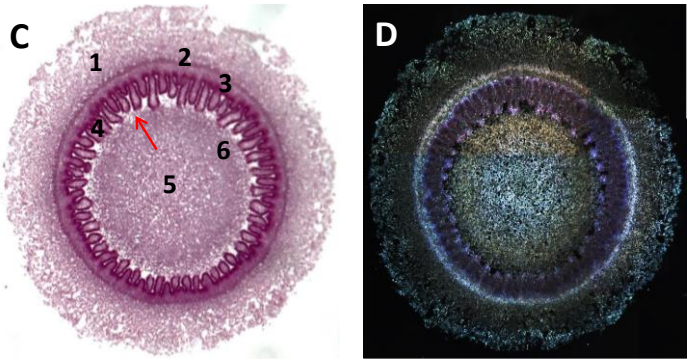

Fig. 12. PAS and hemalum stained longitudinal- and cross-sections showing different tissues and cells of stage P3 primordia, photographed under a light microscope using bright-field (A and C) and (B and D) dark-field techniques. Number 1: veil, 2: pileipellis, 3: pileus trama, 4: hymenial tissues, 5: inner stipe tissues, 6: exterior stipe inflated hyphae at the apex, 7: inflated hyphae at outer stipe, 8: elongated and stretched inflated hyphal cells at the middle of stipe, 9: oval to round dark stained inflated cells at the lower part of stipe and 10: dense hyphae at the middle of primordium shaft, 11: narrow laterally branched hyphae at the base of stipe, the green arrow shows the growth of narrow hyphae upward covering the stipe directly underneath the partial veil. The red arrows show lipsanoblema and blue arrow shows the meeting point between veil from the cap and the stipe region called cleistoblema.

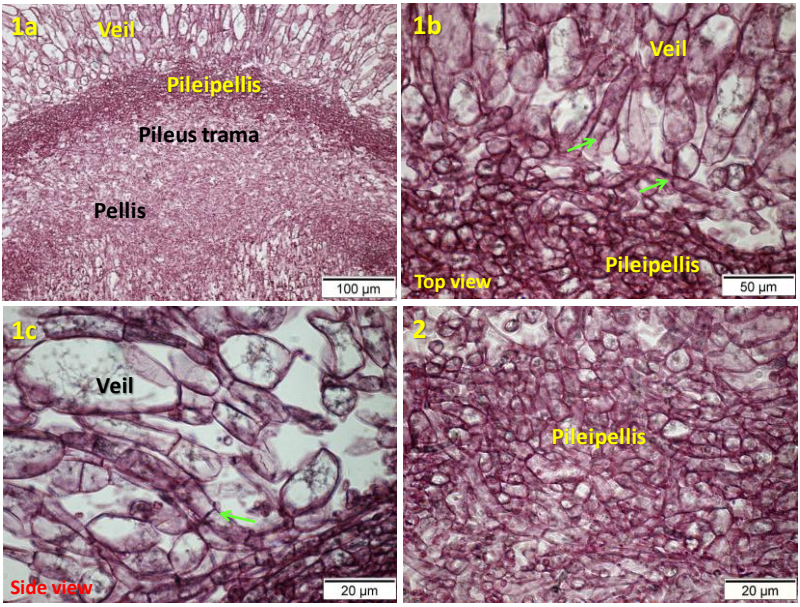

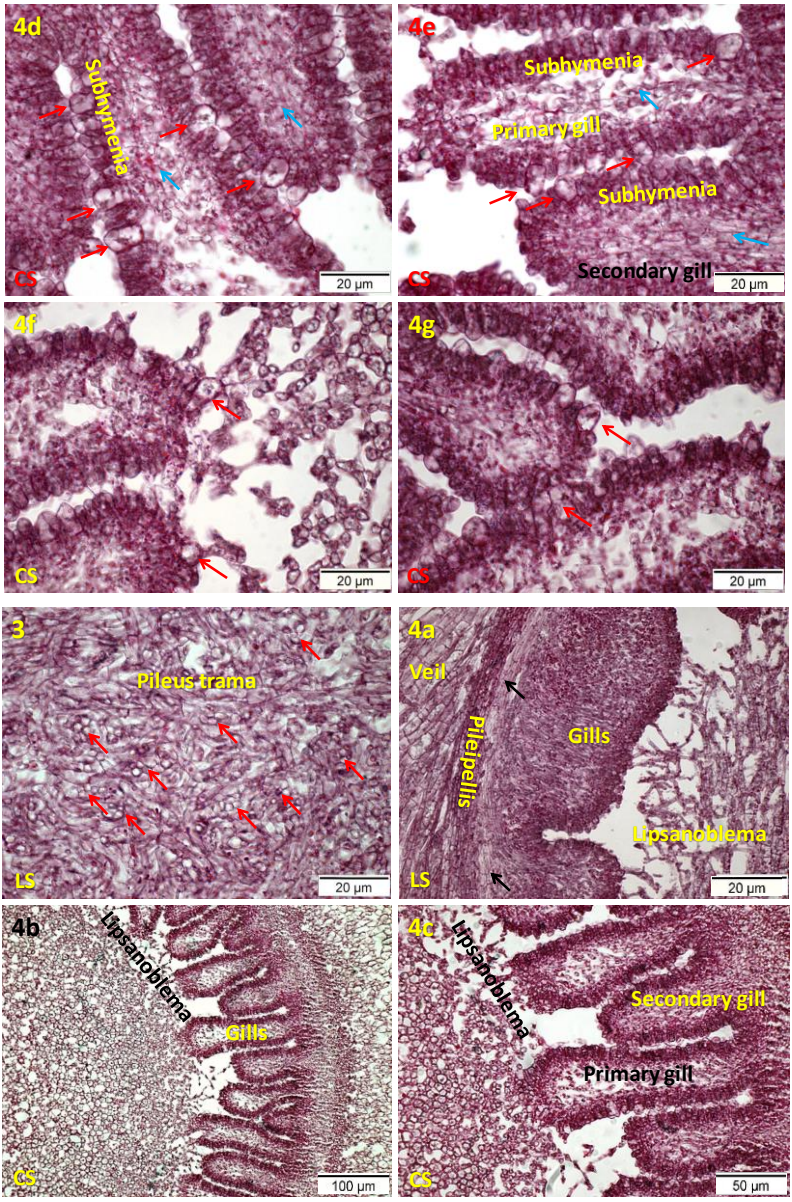
4d
Subhymenia
CS
20 µm
4e
Subhymenia
Primary gill
Subhymenia
Secondary gill
CS
20 µm
4f
CS
20 µm
4g
CS
20 µm
3
Pileus trama
LS
20 µm
4a
Veil
Pileipellis
Gills
Lipsanoblema
LS
20 µm
4b
Lipsanoblema
Gills
CS
100 µm
4c
Lipsanoblema
Secondary gill
Primary gill
CS
50 µm

Fig. 13. Enlarged views on longitudinal- (1-4a) and cross-sections (4b to 4g) of pileus tissues double stained by PAS and hemalum. Image 1a shows four different tissues at the pileus region. 1b and 1c shows veil cells, the green arrows show segmented hyphae near the outer rim of the pileipellis. 2: plectenchymous pileipellis, 3: narrow interwoven hyphae in the pileus trama, the red arrows mark rosette-like cut views of hyphal knot, 4a: parallely arranged gill trama (marked in the black arrows) along the pileus margin and the lipsanoblema attached to the hyphae of a primary gill, 4b and 4c: show primary and secondary gills and the attachment of lipsanoblema to the edges of the inner margin of the primary gill, 4d and 4e: show gill regions at higher magnification with darker stained subhymenia, the hyphae in the gill trama marked by the blue arrows and the pleurocystidia marked by the red arrows, 4f: shows cheilocystidia near the ruptured end of the primary gill marked the red arrows and 4g: shows pleuro-and cheilocystidia and the cystesia marked by the red arrows.

4.1.4.5.1. Pileus development:

As before in the pileus region in stage P3, the pileoblema as the partial veil of the cap (Fig. 12A, marked as 1) grows outwards from the pileipellis and extends downwards, drooping further along the pileus margin. The surface of the pileus extended with increasing cap size by the developing gills beneath which pushed the pileus trama upwards, thereby expanding outwards the pileus margin and thinning the width of the pileus trama. Along, the pileipellis also stretched throughout down to the pileus margin while it became thicker over the whole cap due to continued intruding hyphal branching and growth. In course, new inflated veil cell chains were generated over the whole surface from broader hyphae within the pileipellis to grow out as highly segmented hyphae (1b and 1c in Fig. 13, marked by the green arrows) into the existing pileoblema for getting more inflated veil cells. Seen at higher magnifications, further veil cells emerge in chains directly from meristermoid cells located at the surface of the pileipellis and continue to inflate and lengthen into chains of rounded to oval-lengthy mature cells (1a-1c in Fig. 13). The size of the veil cells further elongated and broadened at this stage as compared to stage P2. The young veil cells at the rim of the pileipellis measure 19 µm ± 8 x 10 µm ± 3 (n=20), the mature cells in the middle of a chain 36 µm ± 12 x 16 µm ± 4 (n=20), and the oldest ones at the outer edge measured 28 µm ± 10 x 9 µm ± 3 (n=20). The young veil cells are about 1.7-fold longer and 1, 6-fold broader, the mature cells in the middle are 1.2-fold longer and 1.3-fold broader and the outer mature veil cells are about 1.3–fold longer and 1.1-fold broader as compared to stage P2.

The layer of the pileipellis underneath the veil is highlighted in the cuts by being stronger stained in dark magenta in light-field (Fig. 12A and 12C, marked as 2) and bright-pink in dark-field images (Fig. 12B and 12D). Higher magnification reveals that the hyphae of pileipellis were dense plectenchymatous and broader in diameter (8.6 µm ± 1.4, n=10) (2 in Fig. 13). The pileus trama (Fig. 12A and 12C, marked as 3) underneath the pileipellis layer consisted of irregularly arranged interwoven thin hyphae which compared to stage P2 were more-loosely packed (3 in Fig. 13). Many more knot-like structures in rosette-like cut views are present within the section of the pileus trama above the stipe than in the previous stages (3 in Fig. 13, marked by the red arrows).

The hyphae within the pileus trama towards the outer pileus margin arranged themselves to grow in parallel (4a in Fig. 13, marked by the black arrows). They diverted at the neck of the growing gills and entered these to form the gill trama as further parallely growing hyphae. The parallely arranged hyphae in the gill trama (4d and 4e in Fig. 13, marked by the blue arrows) continued to the inner edge of the gill, while side-hyphae branched off on the both sides of a gill trama and divert laterally towards the darker stained subhymenia (4d and 4e in Fig. 13). Many more cheilocystidia (cystidia formed at the edge of gills) and pleurocystidia (cystidia formed on the face of gills) originated from the gill trama than at the P2 stage. The pleurocystidia protrude in between the parallel palisades and grow further outward through the free space in between two neighboring gills up to the opposing hymenial tissue (4d and 4e in Fig. 13, shown by red the arrows). In some first cases with the established contact, bulbous cystesia are differentiated from those palisade cells in the opposing hymenial layer to which the pleurocystidia eventually touched to (4d-4g in Fig. 13, marked by the red arrows). Cheilocystidia generated at the edge of the inner margin of the previously closed primary gills at the P3 stage are contacted by hyphae of the lipsanoblema. They may contribute to the splitting of the inner edge of the gills for further contacts of the lipsanoblema with hyphae of the inner gill trama. The hyphae of the gill trama near the rupture appear stretched and partially broken by the attachment to the lipsanoblema, resulting in a loosened trama with larger voids at the gill ends. First secondary gills (4d-4g in Fig. 13) were generated at stage P3, in between some pairs of neighboring primary gills, with an uninterrupted cover of palisade cells over the inner rim the gills and a smooth gill trama of parallel growing hyphae up to the inner end of the gills. Several cheilocystidia grow out from the beneath gill trama into the palisade cell cover at the gill edge of the secondary gills. Depending on space, when primary and secondary gills came closer together, the cheilocystidia attached to palisade cells of the primary gills and transformed them into cystesia upon contact (4g in Fig. 13). Pleuro- and cheilocystidia and the cystesia formed at this stage in both, primary and secondary gills are all partially colored by faded magenta granules.

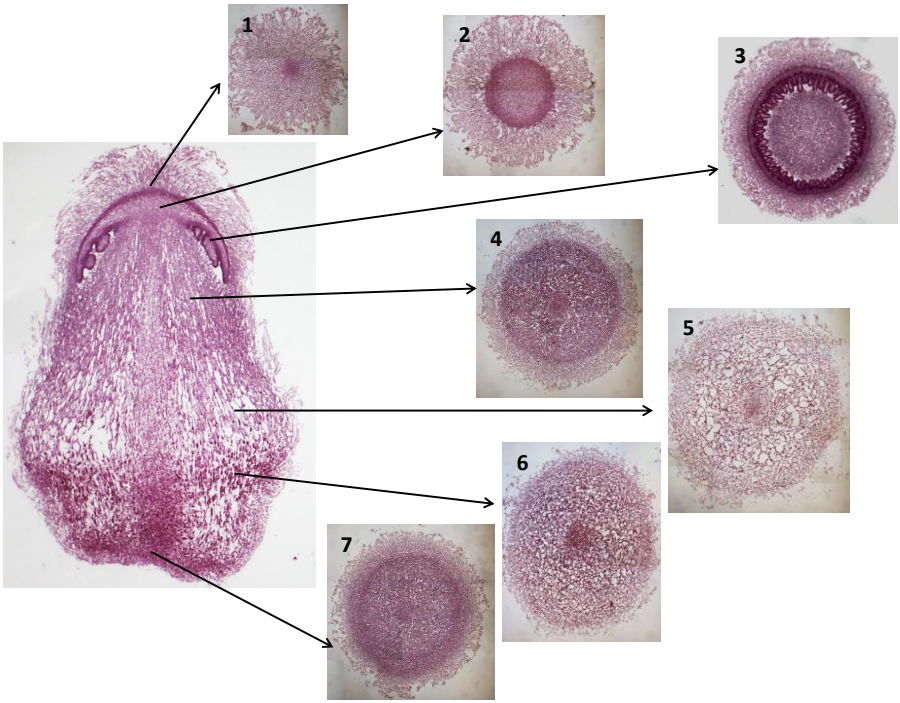

Fig. 14. Cross-sections of the primordium stage P2 marking the respective areas from the apex of the cap to the bottom of the stipe in the longitudinal-section. Cross-sections shown from top to bottom are 1: from the stipe of the pileus region, 2: from the pileus region above the gills, 3: from a region through the middle of gills, 4: the stipe region directly underneath the cap, 5: the region at the middle-stretched part of the stipe, 6: the darker stained region at the lower part of the stipe, and 7: the region within the primordial shaft.

4.1.4.5.2. Stipe development:

As compared to stage P2, the lipsanoblema around the outer part of the stipe apex underneath the cap region is still extending in width by growth of its outer branching and intermingling hyphae in direction to inner edges of primary gills till all will be attached to the lipsanoblema (Fig. 12A and 12C, marked by the red arrows). At the outer edge of the pileus, the pileoblema from above and the cauloblema from below also continue to grow and interconnect with each other. Bridging the gap between the pileus margin and the stipe, a thicker layer of cleistoblema is created that increased the strength of the structure (Fig. 12A, marked by a blue arrow). Over the length of the whole stipe, there was intrusion growth of new narrow veil hyphae into the cauloblema (11c and

11d in Fig. 15, marked by the red arrows), originating from the thin dense layer of narrow heavily branched short hyphae (Fig. 12A, marked as 11, 11a -11d in Fig. 15, marked by a red bar) directly beneath as the outermost coating of the stipe. More short hyphal branching within this coating in random directions deals with the overall surface expansion by increase in structure size.

At the bottom of the stipe, the round to oval cells within the primordial shaft (Fig. 12A, marked as 10, 10a and 10b in Fig. 15) and the surrounding regions (Fig. 12A, marked as 9, 9 in Fig. 15) increased in size by ca 3 fold than those at stage P2. The bottom regions of the stipe appear now darker by massive accumulations of larger magenta-colored granules. At the stipe region above, the difference between inner narrow hyphae (Fig. 12A, marked as 5) and outer inflated hyphae (Fig. 12A, marked as 6) in the longitudinal-section became more evident underneath the light microscope by their dissimilar morphology (Fig. 12A and 12B). At the outer stipe region, the inflated hyphae stretched in length which broke horizontal and vertical neighboring connections and increased and enlarged the hollow spaces in between (Fig. 12A, marked as 8, 8 in Fig. 15). Thereby, the lower half of the outer part of stipe expanded, which gives stipes of the P3 stage a slightly plump-like appearance. The stretching of the inflated hyphae increased their segment lengths and stained more magenta than at stage P2. In contrast, the hyphae at the upper-part of the outer stipe (Fig. 12A, marked as 7, 7 in Fig. 15) remained unstretched, densely segmented and faintly stained as before. They are still relatively intactly attached to each other, with few hollow spaces in-between them (Fig. 12A, marked as 6 and 7). The hyphal cells directly at the apex of the outer stipe (Fig. 12A, marked as 6, 6 in Fig. 15) increased in size but continue to appear ovoid to polyhedral. Hyphal cells now contain very few granules stained in magenta.

The inner cylinder of bundled narrow hyphae (Fig. 12A, marked as 5, 5a and 5b in Fig. 15) continuing from the primordial shaft towards the pileus trama increased in width by further repeated lateral branching in acute angles of vertically oriented main hyphae and at the inner side of primary side branches and an oriented vertically up growth of new primary and secondary side branches. The hyphae are interconnected to each other by random anastomosis (5b in Fig. 15, marked by the blue arrows). The inner cylinder extends in length by hyphal tip growth (Fig. 12A, marked by 5, 5a-5b in Fig. 15). Small granules appearing in the hyphae over whole inner cylinder are stained in magenta.

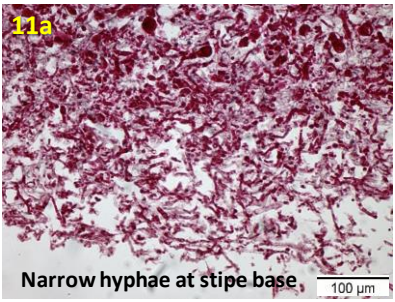
11a
Narrow hyphae at stipe base
100 µm

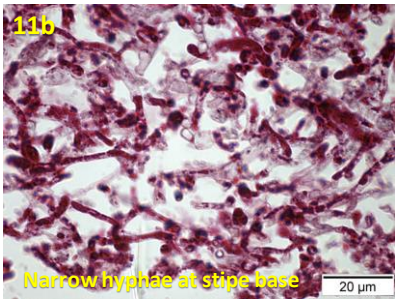
11b
Narrow hyphae at stipe base
20 µm

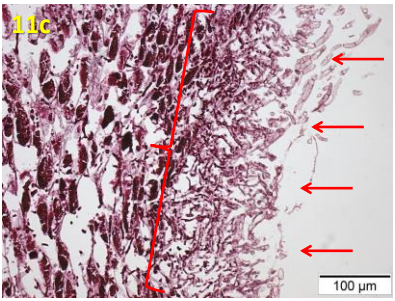
11c
100 µm

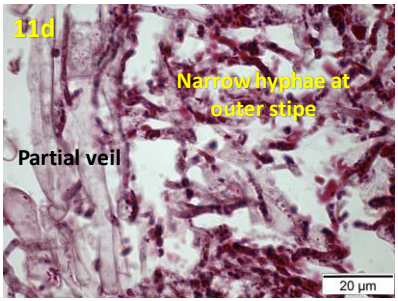
11d
Narrow hyphae at outer stipe
Partial veil
20 µm

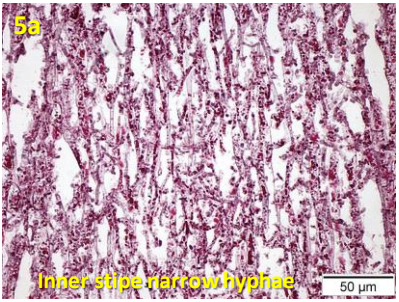
5a
Inner stipe narrow hyphae
50 µm

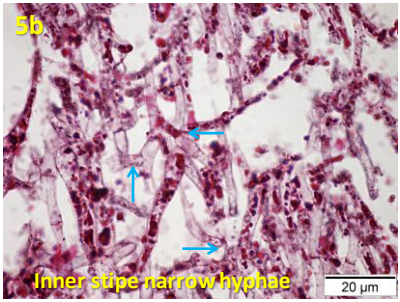
5b
Inner stipe narrow hyphae
20 µm

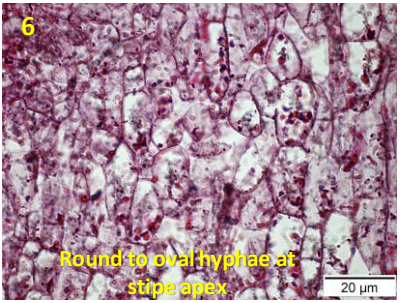
6
Round to oval hyphae at stipe apex
20 µm

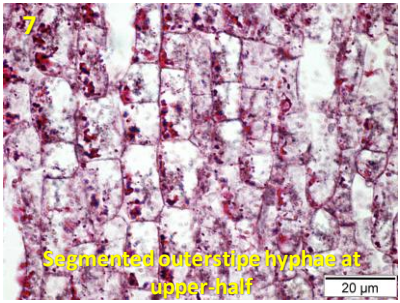
7
Segmented outerstipe hyphae at upper half
20 µm

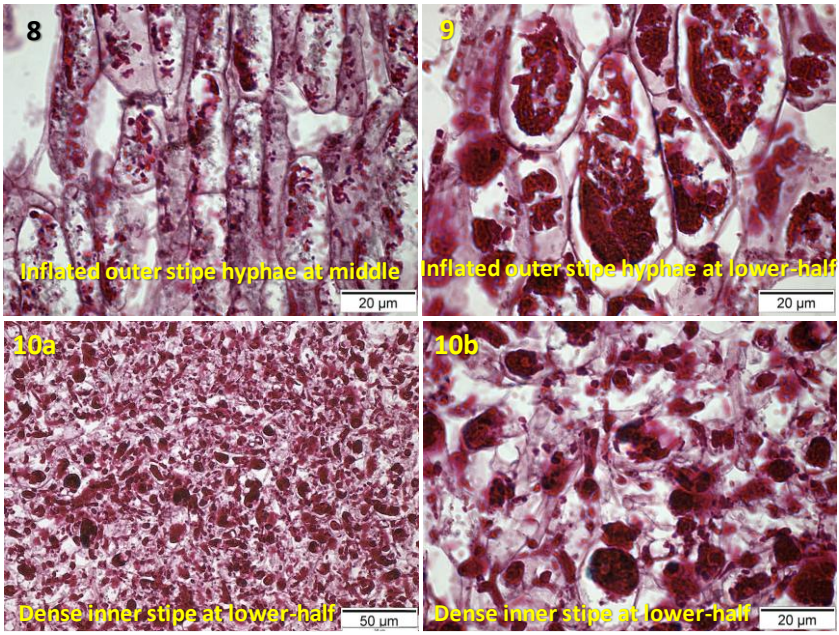

Fig. 15. Enlarged views on longitudinal-sections of the stipe tissues double stained by PAS and hemalum. The images 11a and 11b show laterally-branched narrow hyphae at the bottom of primordial shaft, 11c and 11d: a layer of narrow hyphae (marked by a red bar) at the outer stipe directly underneath the partial veil (marked by red arrows), 10a-10b: dense hyphae in the primordial shaft, 9: large inflated darker stained hyphae at the outer lower stipe, 8: long stretched partially stained inflated hyphae in the middle part of the outer stipe, 7: segmented inflated partially stained hyphae at the upper-half of the outer stipe, 6: round to oval inflated hyphal cells at the apex of the stipe region, 5a-5b: narrow branched stained hyphae at the inner stipe (the blue arrows show anastomosis connections).

4.1.4.6. Primordia stage 4

The dumb-bell shaped primordium stage P4, formed on Day 5 of the standard fruiting pathway is about 6-8 mm in height and the primordium is covered over stipe and cap by the partial veil of loose hairy appearance (Fig. 16A-16D). The upper half of the primordium became broader at this stage due to well-developed lamellae and an increase in secondary gills and the lower half of the stipe region has been stretched.

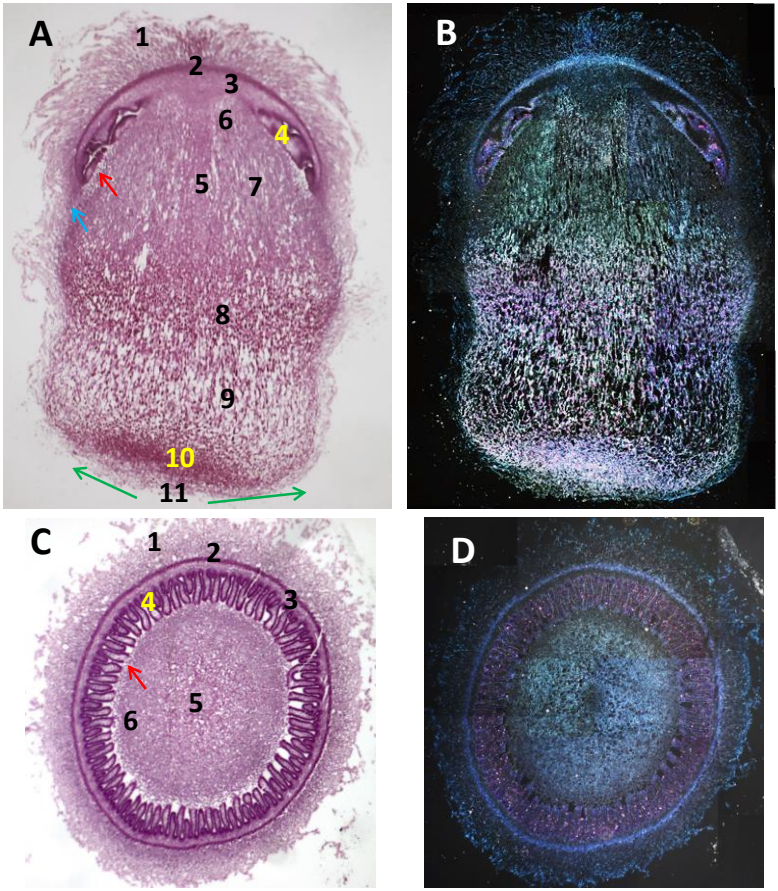

Fig.16. PAS and hemalum stained longitudinal- and cross-sections showing different tissues and cells of stage P4 primordia, photographed under a light microscope using bright-field (A and C) and (B and D) dark-field techniques. Number 1: veil, 2: pileipellis, 3: pileus trama, 4: hymenial tissues, 5: inner

stipe tissues, 6: exterior stipe inflated hyphae at the apex, 7: inflated hyphae at the outer stipe, 8: darker stained elongated and inflated hyphal cells at the middle of the stipe, 9: dark stained inflated and stretched cells at the lower part of the stipe, 10: dense hyphae at the primordium shaft, and 11: narrow laterally branched hyphae at the base of the stipe, the green arrow shows the growth of narrow hyphae upward covering the stipe directly underneath the partial veil. The red arrows show the lipsanoblema and a blue arrow shows the meeting point between partial veil from the cap and the stipe region called cleistoblema.

The densely packed darker in magenta-stained hyphal cells present at the lower half of the stipe in stage P3 have moved more up in the P4 stage by stretching the lower outer stipe tissues as seen in the bright-field image (Fig. 16A). The lower part of the stipe is stretched with many voids in-between them and are darker stained in magenta in the bright field and bright-pink in the dark-field images. The stipe region above appears bright-pink in the dark-field image (Fig. 16B). The pileipellis, hymenial tissues and the primordial shaft continue to appear stained prominently darker, as seen in both LS and CS of the P4 stage primordium (Fig. 16A and 16C).

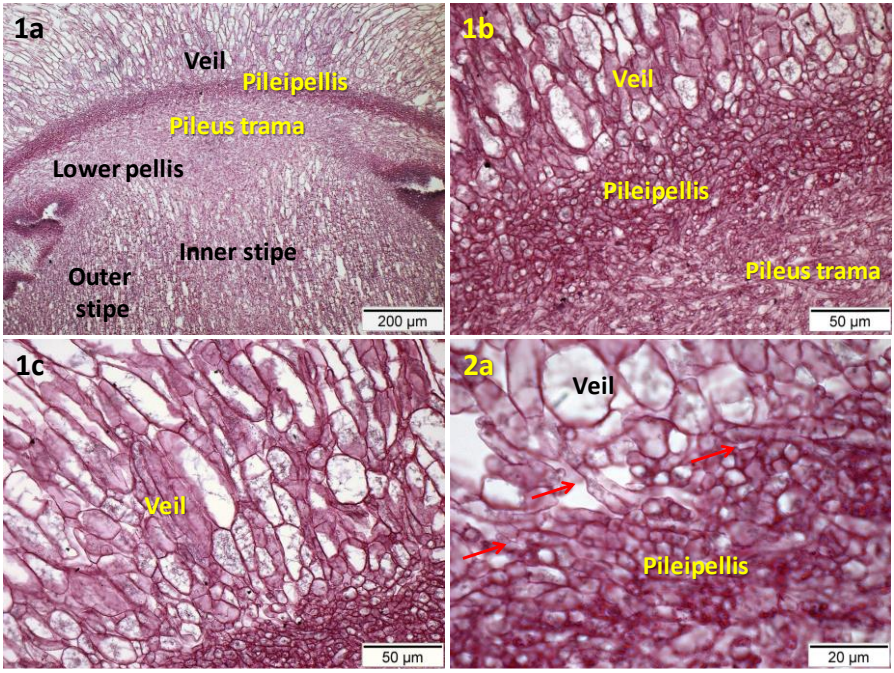

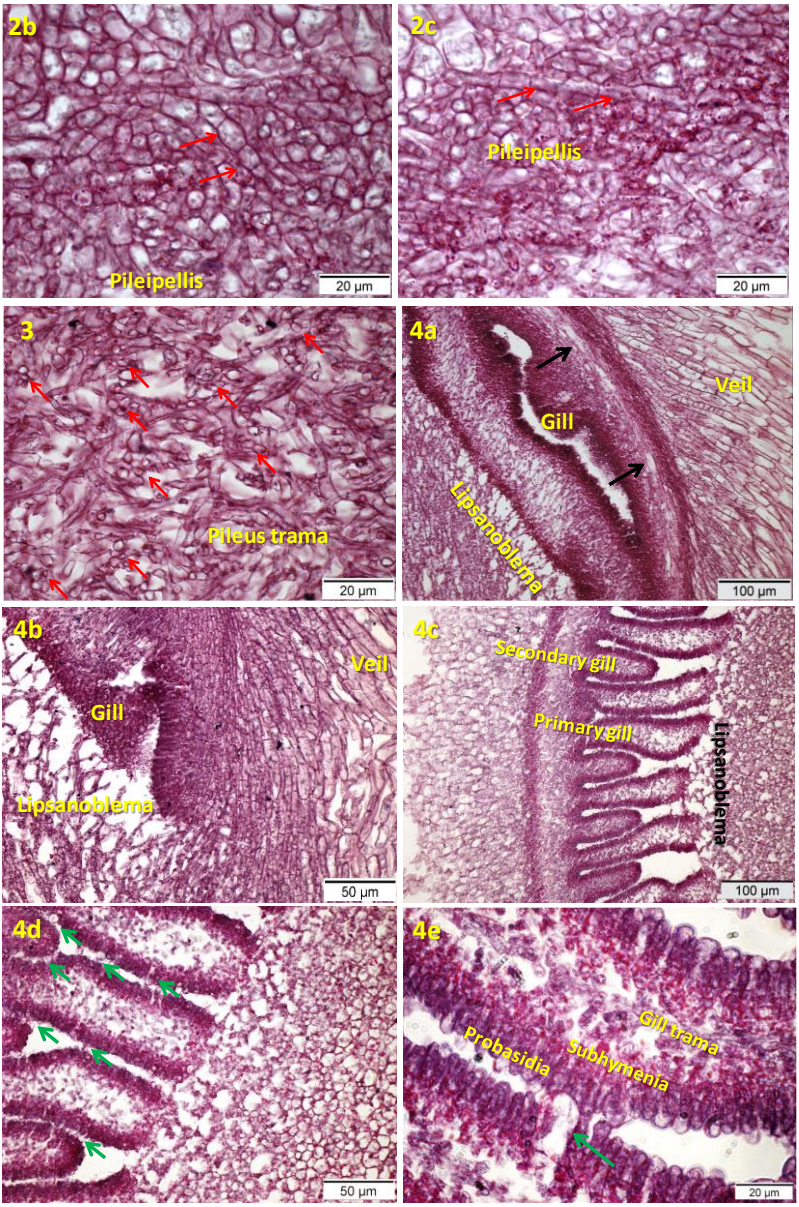
2b
Pileipellis
20 µm
2c
Pileipellis
20 µm
3
Pileus trama
20 µm
4a
Veil
Gill
Lipsanoblema
100 µm
4b
Veil
Gill
Lipsanoblema
50 µm
4c
Secondary gill
Primary gill
Lipsanoblema
100 µm
4d
50 µm
4e
Gill trama
Subhymenia
Probasidia
20 µm

Fig. 17. Enlarged views on longitudinal- (1-4b) and cross-sections (4c to 4e) of pileus tissues double stained by PAS and hemalum. The images 1a and 1b show longitudinal-sections (LS) of veil, pileipellis, pileus trama, lower pellis, outer stipe and inner stipe. 1c: veil, 2: plectenchymous pileipellis, 3: narrow interwoven hyphae in pileus trama, the red arrows mark rosette-like cut view of hyphal knot, 4a and 4b: the lipsanoblema attached to hyphae of the primary gill trama and parallely arranged pileus trama towards the outer pileus margin (marked by the black arrows), 4c and 4d: CS section showing primary and secondary gills, the lipsanoblema attached to the open ends of the primary gills (the green arrows mark the pleuro-and cheilocystidia), the opening represents the hymenial space in-between two neighboring gills, 4e: the hymenial region with darker stained in magenta are the subhymenial layer, dark blue stained are probasidia, a green arrow marks the cheilocystidia and cystesia bridge.

4.1.4.6.1. Pileus development:

Image 1a in Fig. 17 shows in an enlarged view six different tissues, veil, pileipellis, pileus trama and lower pellis in longitudinal-section double-stained in PAS and hemalum of the same primordium as shown in Fig. 16. The observations at higher magnifications revealed that the veil cells (1b and 1c in Fig. 17) continue to grow out from the segmented narrow hyphae of the pileipellis and get inflated and arranged in chains (2a-2c in Fig. 17, marked in by the red arrows). The younger veil cells at the edge of pileipellis measure 36µm ±9 x 22µm ±9 8n=15), and the mature ones at the middle of a chain 125µm ±39 x 40µm ±10 8n=15), and at the outer edge 102µm ±37 x 25µm ±9 (n=15). Compared to those at stage P3, the younger veil were 1.9-fold longer and 2.2-fold broader, the mature ones at the middle are 3.4-fold longer and 2.5-fold broader and the mature ones at the outer edge are 3.6-fold longer and 2.7-fold broader. As seen at larger magnification, the veil cells at the side of the pileus became sparse compared to the ones at the apex. Underneath the whole pileoblema, the plectenchymous pileipellis further extended in length at the pileus outer margins with the increasing width of the cap and was still prominent with a darker stained band of tissues at this stage (Fig. 16A, marked as 2 and 2a-2c in Fig. 17).

The slender layer of pileus trama at the cap apex appeared to be slightly reduced in diameter compared to stage P3 and many larger hollow spaces were present in-between the interwoven highly-branched hyphae (Fig. 16A, marked as 3 and 3 in Fig. 17). Continuously radially outwards growing gills below will push the pileus trama outward, under consumption of parts of pileus trama tissue. More knot-like structures in rosette-like cut view were seen in the central pileus trama at this stage (3 in Fig. 17, marked by the red arrows). The parallely arranged straight hyphae within the pileus trama towards the outer pileus margin continue to increase in length, (4a and 4b in Fig. 17, marked by the black arrows). The arrangements of the tissues at the different level of the pileus above the gills are also seen on the CS images 1, 2 and 3 in Fig. 18.

At the gill region, both primary and secondary gills radially grow further outwards, differentiating as before successively the new hymenial tissues close to the outer edge of the gills (Fig. 16A and 16C, marked as 4). At the inner edge, the lipsanoblema coming from the outer part of the upper

stipe is now attached to the hyphae from the inner trama of all primary gills, interrupting the hymenial layer at the edges of inner margin of the primary gills (4a-4d in Fig. 17 and 4 in Fig. 18). The gill trama at the interaction zone with the lipsanoblema is more loosened at stage P4 than before at stage P3, stretching the edges of the flanking hymenia slightly apart of each other.

The observation of differentiation in tissue formation in the hymenial area became more distinct in the cross-section at higher enlargement (Fig. 16C, marked as 4c-4e in Fig. 17). The outer hymenial layer is characterized by a uniform layer of parallel palisade cells which are the probasidia that later will give rise to spore-bearing cells and paraphyses (hyphidia) of the same look. The thicknesses of the subhymenial regions are increased and are prominently stained in bright field by magenta granules (Fig. 16C, 4d and 4e in Fig. 17) and in dark field bright pink similar than as at stage P3 (Fig. 16D). Both cheilo-and pleurocystidia are partially colored by magenta granules. Pleurocystidia protrude from the gill trama of both primary and secondary gill into the free gill space to bridge the gap and many of them are attached to cystesia at the opposite hymenium (4d and 4e in Fig. 17, marked by the green arrows). Many cheilocystidia arise in the secondary gill and cystidia-cystesia bridges with primary gills (4d in Fig. 2, marked by the green arrows) were formed for appropriate gill spacing and stabilization.

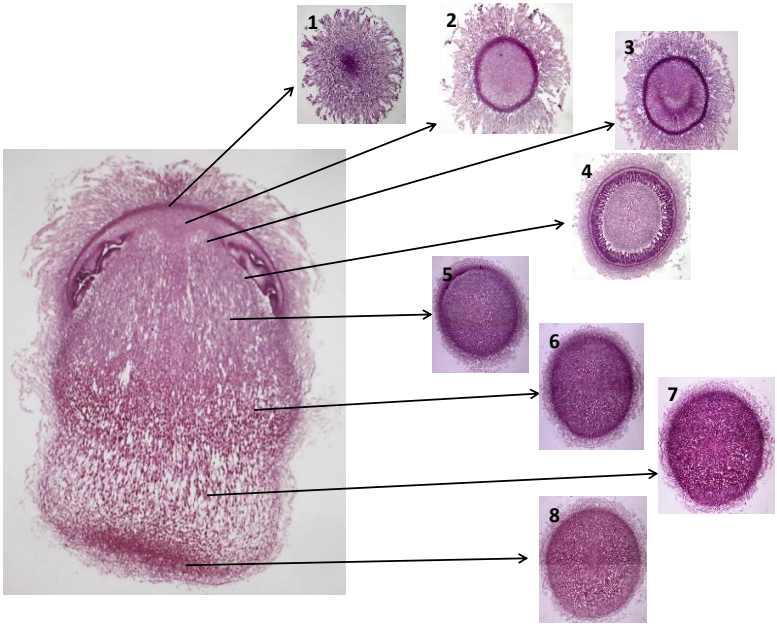

Fig. 18. Cross-sections of the primordium stage P4 marking the respective areas from the apex of the cap to the bottom of the stipe in the longitudinal-section. Cross-sections shown from top to bottom are 1: from the apex of the pileus region, 2: from the pileus trama, 3: from the pileus region above the gills, 4: from a region through the middle of gills, 5: the stipe region directly underneath the cap, 6: the region at the middle dark stained part of the stipe, 7: the darker stained stretched region at the lower part of the stipe, and 8: the region within the primordial shaft.

4.1.4.6.1.2. Stipe development:

Most of the tissues in the stipe area appears as in stage P3 (Fig. 12) and there was not much more differentiation in the tissues other than of the stretching in the outer lower part of the stipe. In consequence, the denser layer of darker stained elongated inflated hyphal cells with massive accumulation of small magenta granules are now shifted up more to the middle part of the stipe (Fig. 16A, marked by 8, 8a and 8b in Fig. 19). The individual stretched inflated hyphae at the lower part of the stipe are darker stained. These are loosely arranged with many enlarged and more voids in between than before in stage P3 and inter-connected by variably stained narrow hypha to each other coming from the primordial shaft (Fig. 16A, marked as 9 and 9a and 9b in Fig. 19). As before, the primordia shaft is densely stained with the mixture of round dark stained cells connected to heavily branched narrow hyphae (Fig. 16, marked as 10, 10a and 10b in Fig. 19). Such arrangements of the tissues at the different level of the stipe above are also seen on the CS images 5 to 8 in Fig. 18.

The inner central cylinder with narrow hyphae (Fig. 16A, marked as 5) throughout the length from the primordial shaft to the stipe apex became denser by further heavily acute branching of hyphae growing upwards and increased in diameter (about 1.0 µm at stage P3 to 2.5 µm at stage P4). Larger hollow spaces now surround the central cylinder at its upper halve caused by stretching of inflated and by magenta granules partially stained hyphae from the innermost layer of the outer stipe (5b in Fig. 19, marked by the red arrows). Other hyphae at the upper-part of the outer stipe are relatively intactly attached to each other (5a and 5b in Fig.19).

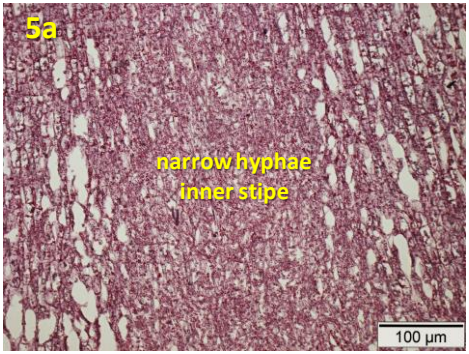
5a
narrow hyphae
inner stipe
100 µm

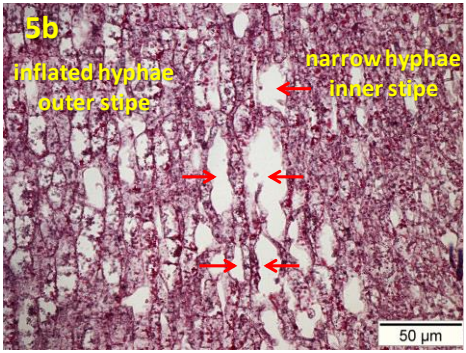
5b
inflated hyphae
outer stipe
narrow hyphae
inner stipe
50 µm

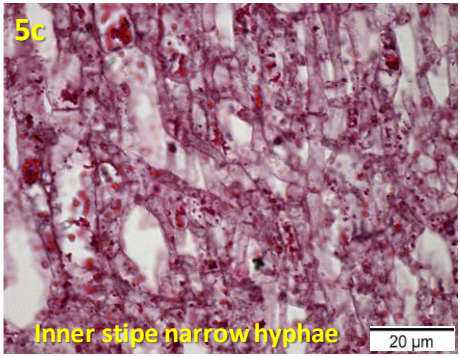
5c
Inner stipe narrow hyphae
20 µm

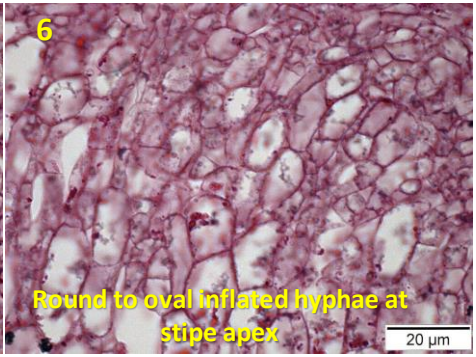
6
Round to oval inflated hyphae at
stipe apex
20 µm

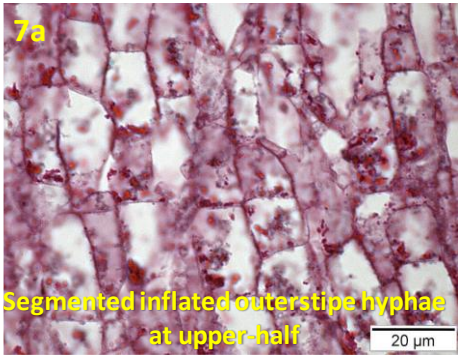
7a
Segmented inflated outerstipe hyphae
at upper-half
20 µm

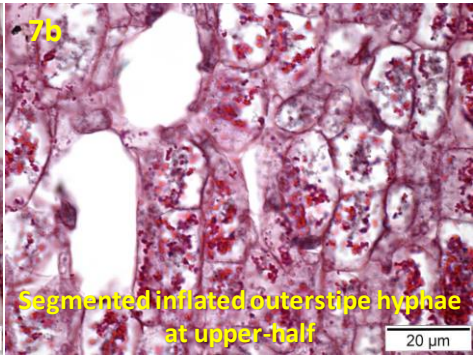
7b
Segmented inflated outerstipe hyphae
at upper-half
20 µm

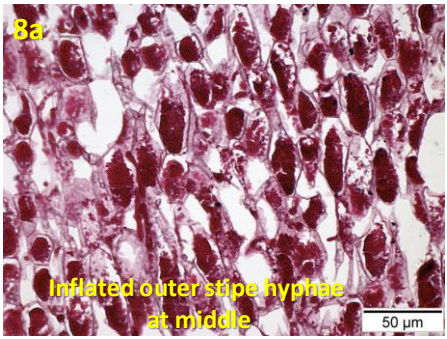
8a
Inflated outer stipe hyphae at middle
50 µm


8b
Inflated outer stipe hyphae at lower-half
20 µm

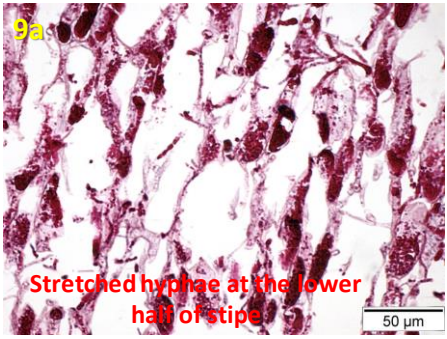
9a
Stretched hyphae at the lower half of stipe
50 µm

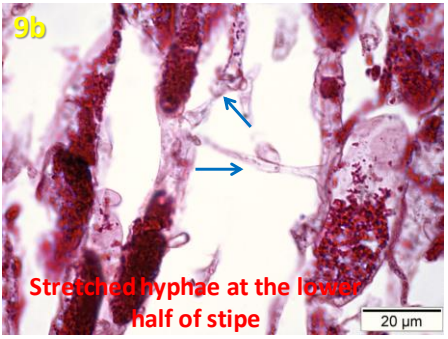
9b
Stretched hyphae at the lower half of stipe
20 µm

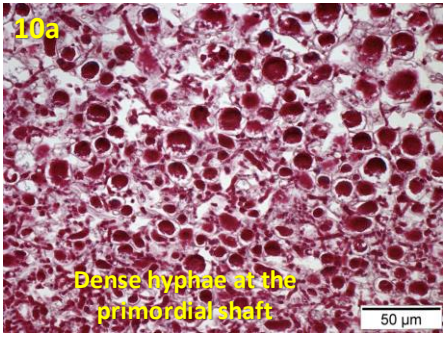
10a
Dense hyphae at the primordial shaft
50 µm

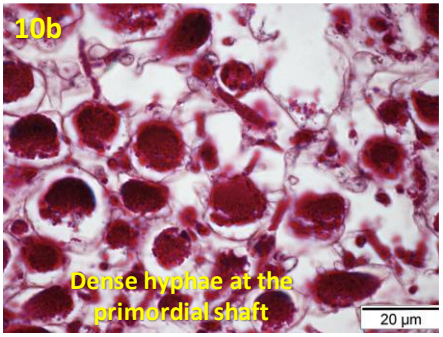
10b
Dense hyphae at the primordial shaft
20 µm

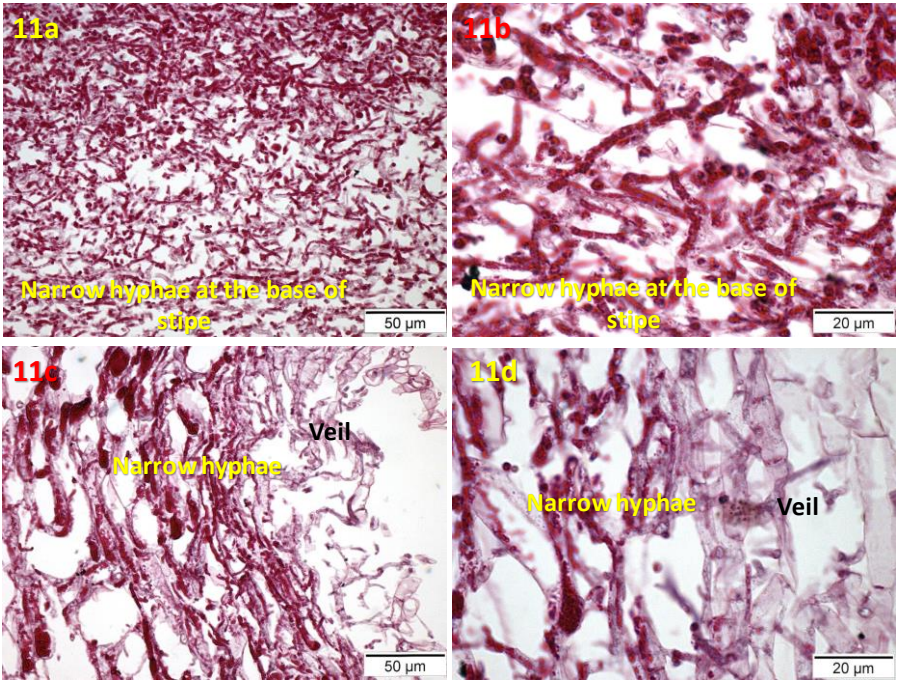

Fig. 19. Enlarged views on longitudinal-sections of the stipe tissues double stained by PAS and hemalum. The images 11a and 11b show laterally-branched narrow hyphae at the bottom of primordial shaft, 11c and 11d: a layer of narrow hyphae at the outer stipe directly underneath the partial veil, 10a and10b: dense hyphae with darker stained round to oval appearing hyphae in the primordial shaft, 9a and 9b: large inflated darker stained hyphae stretched hyphae at the outer lower stipe, 8a and 8b: inflated hyphae massively stained by magenta at the lower part of the outer stipe, 7a and 7b: segmented inflated partially stained hyphae at the upper-half of the outer stipe, 6: round to oval hyphal cells at the apex of the stipe region, 5a-5c: narrow branched stained hyphae in the inner stipe, hollow spaces are generated by stretching of inflated segmented hyphae around the cylinder of narrow hyphae marked by the red arrows..

4.1.4.7. Primordia stage 5

The P5 stage primordium appeared in shape like a light bulb (8-10 mm) at the beginning of Day 6 of the standard fruiting pathway (Fig. 20A and 20B). The main tissue differentiations were completed at this stage. With the induction of a light signal in the light phase of the day before (Lu 2000), karyogamy occurred at stage P5 in the basidia (defined as > 50 % of all basidia contain fused nuclei; Seitz et al. 1996; Navarro-González 2006) and will be followed in the next few hours on Day 6 by meiosis for the subsequent production of the basidiospores (Seitz et al. 1996; Kües 2000; Lu 2000; Navarro-González 2006).

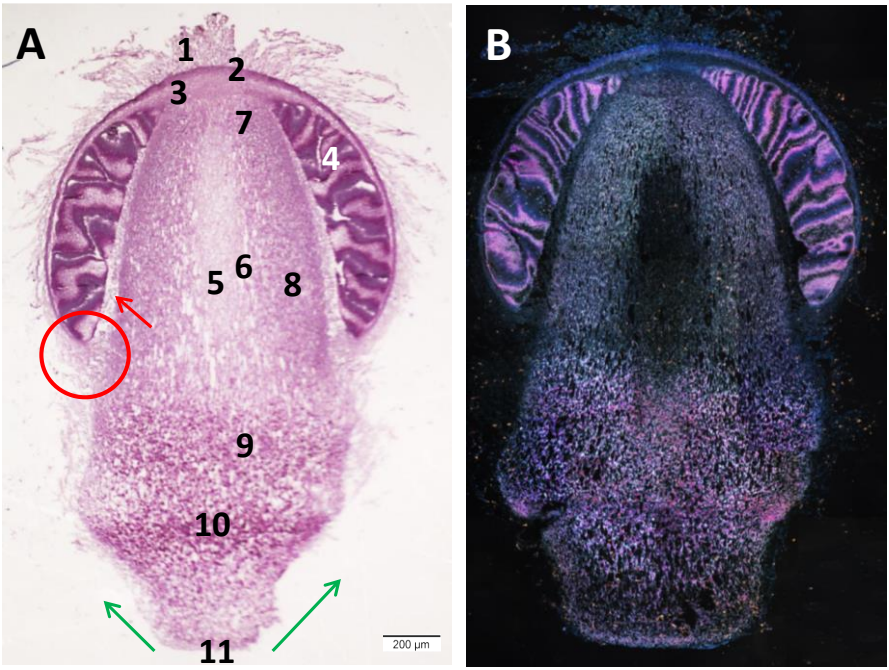

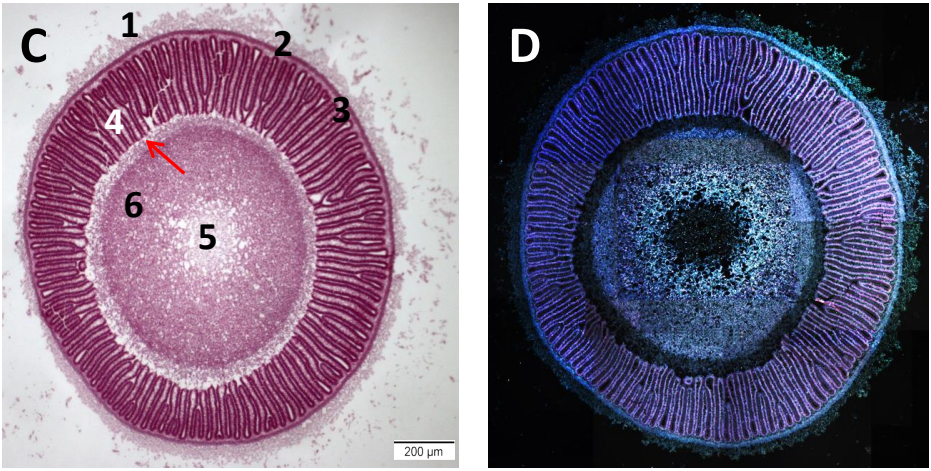

Fig. 20. PAS and hemalum stained longitudinal-and cross-sections showing different tissues and cells of the stage P5 primordium, photographed under a light microscope using bright-field (A and C) and (B and D) dark-field techniques. Number 1 marks the veil, 2: pileipellis, 3: pileus trama, 4: hymenial tissues, 5: stipe tissues at the inner stipe region, 6: marks exterior stipe tissue at the apex, 7: marks inflated segmented hyphal cells, 8: inflated elongated and partially stained hyphae in the middle part of stipe, 9: elongated inflated and darkly stained hyphae at the lower part of the stipe, 10: densely stained compactly packed hyphae at the primordial shaft and 11: narrow short branched hyphae at the base of the primordial shaft, further growing upward to cover the outer part of the stipe found directly underneath the lower part of the partial veil (indicated on image A by the green arrows). A red arrow marks the lipsanoblema and a red circle shows the meeting point of the partial veil from the cap and the stipe region which is called cleistoblema.

In the PAS and hemalum stained sections of stage P5, the fully developed hymenial region and the lower half of the stipe are prominently seen in darker magenta (Fig. 20A and 20C). The same areas are stained in bright-pink in the dark-field images (Fig. 20B and 20D). The veil cells at the pileus region became sparse and the narrow hyphae at the inner stipe became very thin so that they appeared like a barely detectable, faint central cylinder (Fig. 20A and 20B).

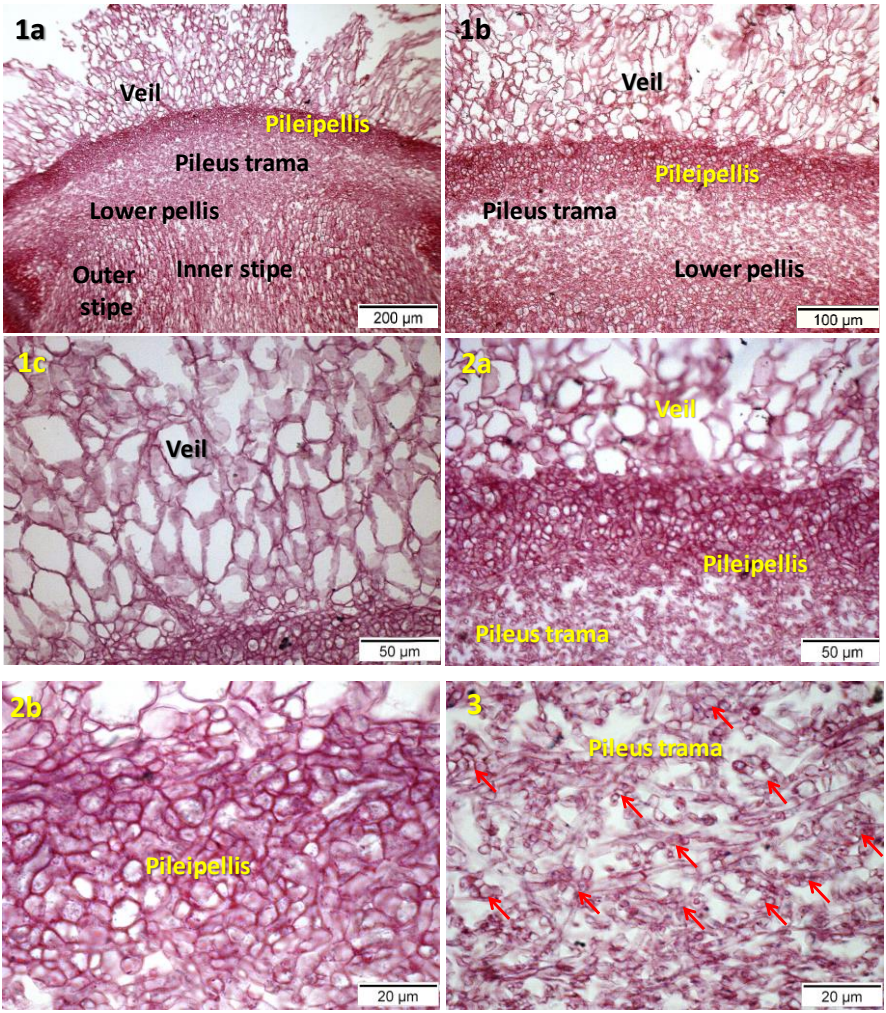
1a
Veil
Pileipellis
Pileus trama
Lower pellis
Outer stipe
Inner stipe
200 µm
1b
Veil
Pileipellis
Pileus trama
Lower pellis
100 µm
1c
Veil
50 µm
2a
Veil
Pileipellis
Pileus trama
50 µm
2b
Pileipellis
20 µm
3
Pileus trama
20 µm

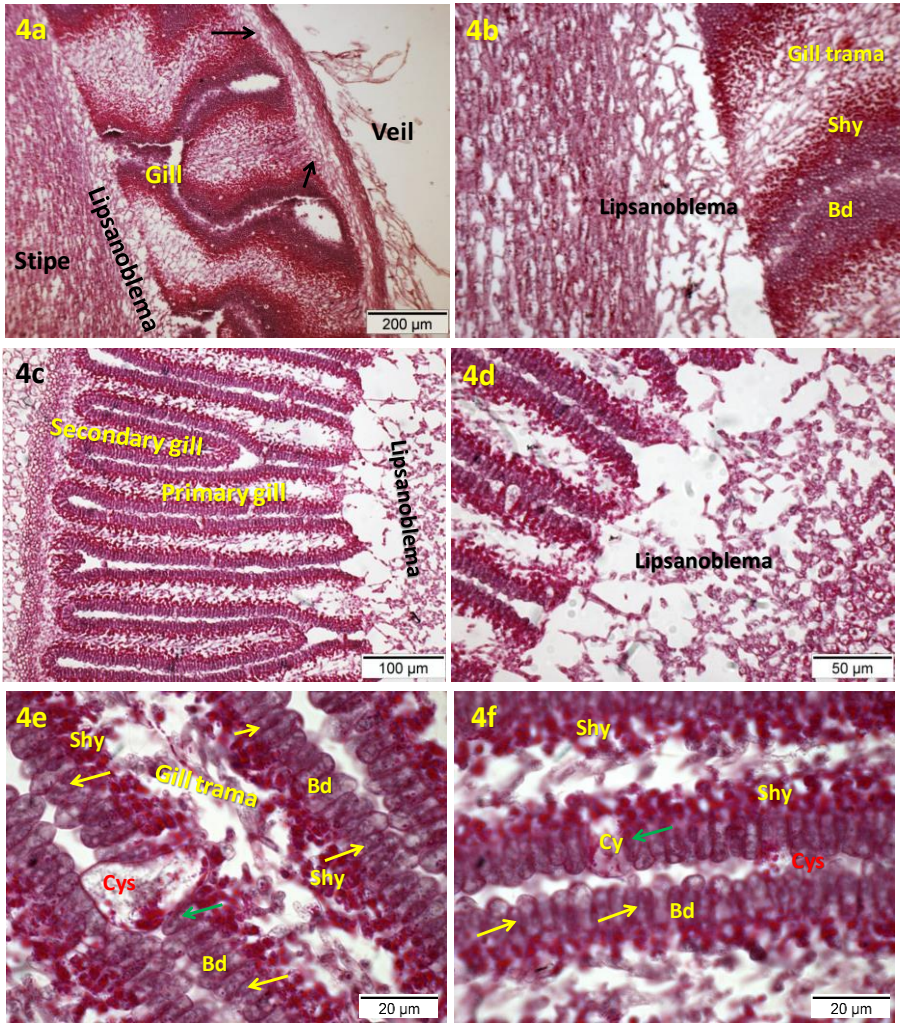
4a
Veil
Gill
Lipsanoblema
Stipe
200 µm
4b
Gill trama
Shy
Lipsanoblema
Bd
4c
Secondary gill
Primary gill
Lipsanoblema
100 µm
4d
Lipsanoblema
50 µm
4e
Shy
Gill trama
Bd
Cys
Shy
Bd
20 µm
4f
Shy
Shy
Cy
Cys
Bd
20 µm

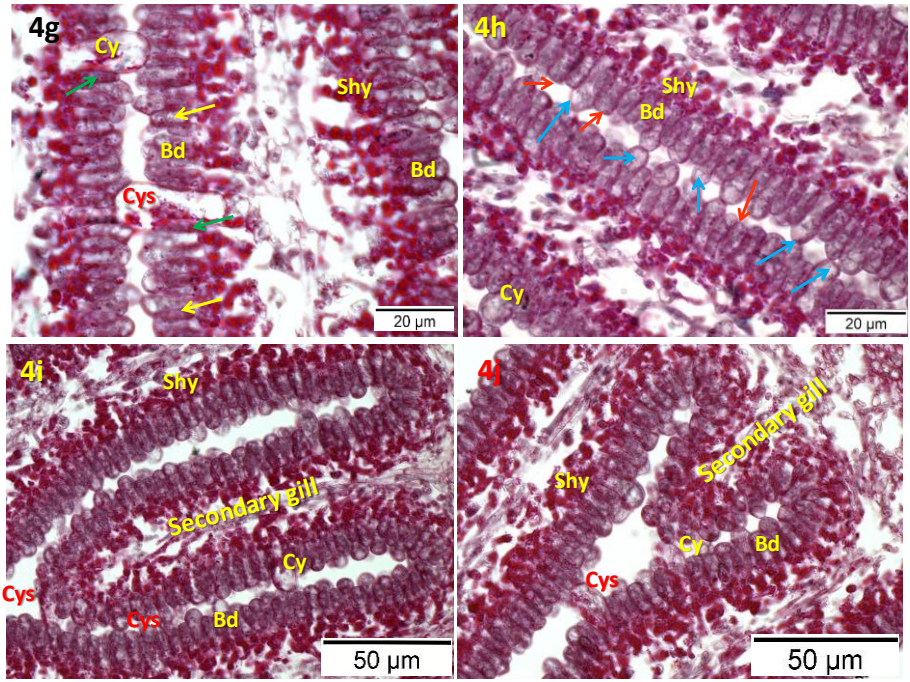

Fig. 21. Enlarged views on longitudinal- (1-4b) and cross-sections (4c to 4j) of pileus tissues double stained by PAS and hemalum. 1a and 1b shows six different tissues at the pileus region, 1c: sparse veil, 2a and 2b: plectenchymous pileipellis, 3: narrow interwoven hyphae in the pileus trama, the red arrows mark rosette-like cut view of hyphal knot, 4a and 4b: lipsanoblema attached to the hyphae of the primary gill trama (Shy: subhymenia, Bd: basidia) and parallely arranged hyphae of the pileus trama are marked by the black arrows, 4c and 4d: radially arranged primary and secondary gills and the lipsanoblema attached to the inner edges of the primary gills, darker stained in magenta are the subhymenia, 4e -4g: enlarged views on gills showing magenta colored granules in the subhymenium (shy), dark-blue colored basidia (Bd), the large cystidia (Cy) emerging from the gill trama and cystesia (Cys) formed upon attachment of cystidia to the opposite hymenia, both the cells are partially stained by magenta granules, the green arrows mark the clasping cells attached to the cystidia and the cystesia and the yellow arrows mark the hyphidia in between basidia, 4h: short (red arrows) and long (blue arrows) dark-blue stained basidia and the darker stained subhymenia in magenta and 4i -4j: secondary gills of the two generations.

4.1.4.7.1. Pileus development:

The pileoblema at the apex and the side of the pileus appeared sparse at this stage (Fig. 20A and 20C, marked by 1, 1a-1c in Fig. 21) by stop of veil cell proliferation and by falling of veil scales. Since the veil running down along the pileus margin is now sparse, the cleistoblema connection appeared loose compared to the previous stages, yet it is still sealed. The edges of the lamellae are now slightly raised up away from the stipe, creating a first small gap as the beginning of the annular cavity around the stipe under stretching and some breakages of the lipsanoblema as attached to the hyphae of the primary gill trama.

The pileipellis (Fig. 20A and 20C, marked by 2, 2a and 2b in Fig. 21) remained as the darker stained band of tissues covering the pileus trama. Over the whole pileus, the pileus trama (Fig. 20A and 20C, marked by 3 and 1b, 2a and 3 in Fig. 21) underneath the pileipellis is significantly reduced in thickness at this stage due to the extension of the growing gills. The plectenchymous hyphal arrangement at the apex is very loose with many more voids in between the hyphae (3 in Fig. 21) as compared to previous stages. Many more rosette-like knots as before became visible (3 in Fig. 21). They were left intact to act as the scaffold for the stability of the remaining hyphal network of the pileus trama.

The arrangements of the tissues at different levels of the cap region above the gills (pileoblema, pileipellis and pileus trama) can be also seen on the CS images 1 and 2 in Fig. 25. The radially arranged primary and secondary gills (Fig. 20C and 20D, 4c and 4d in Fig. 21) beneath were expanded further outwards by pushing the enlarging palisades into the tissue of the pileus trama of parallely growing hyphae, in a manner similar to the opening of a zipper (with the individual palisade cells representing the two rows of teeth of the zipper) (4c in Fig. 21). As a result, the pileus trama at this stage appears very thin in diameter in both longitudinal and -transverse sections (Fig. 20A-20D, marked by 3, 3 and 4 in Fig. 25).

The palisades of the hymenial tissues within the primary and the secondary gills are prominently stained darker in magenta in the bright-field image (Fig. 20A and 20C) and bright-pink in the dark-field image (Fig. 20B and 20D). As seen at higher magnification, the subhymenia stained darker in wine-colored granules within the gills are distinctively differentiated from the dark-blue stained basidia of the hymenium (4e-4j in Fig 21). An alternating arrangement of long (17 µm, blue arrows) and short basidia with swollen ends (13 µm, red arrows) is now visible along the hymenial region (4h in Fig. 21). A configuration of such is for creating an aerial space between the basidiospores from neighboring basidia to avoid overcrowding. At stage P5 as newly appearing cells, slim tips of young growing hyphidia (also called paraphyses) (4e-4g in Fig. 21, marked by the yellow arrows) emerged from the subhymenium over the whole length of the hymenium, moving in between the inflating basidia. In the cross-sections, 3 to 5 pleurocystidia are randomly spread over the individual flanks of primary gills and 2 to 3 over the individual flanks of secondary gills (4e-4g in Fig. 21). The secondary gills carry in addition 1 to 2 similarly

shaped cheilocystidia at their inner edges (4i and 4j in Fig. 21). However, as compared to the stage P4, the frequency of the presence of pleuro-and cheilocystidia in both types of gills were reduced, possibly due to degeneration of parts of the cystidia. Enlarged views revealed darker stained slender, longer clasping cells (4e-4g in Fig. 21, marked by the green arrows) coming from the subhymenium and strongly adhering to both the pleuro- and cheilocystidia. At stage P5, on the hymenia opposite to most pleurocystidia of primary and secondary gills and opposite to some cheilocystidia at the inner edges of secondary gills, cystesia (4e-4g and 4i-4j in Fig. 21) were formed upon contact with the cystidia, bridging the gaps between hymenia of neighboring gills as cystidia-cystesia pairs. The lipsanoblema attachment to the inner edges of primary gill trama is still clearly visible in both the longitudinal- (4a and 4b in Fig. 21) and cross-section (4c and 4d in Fig. 21) images. The trama hyphae were more stretched and broken over about 1/3rd of the primary gills towards the edges of the inner margins with the interrupted hymenial layer to which the lipsanoblema attached. At the outer edge of the primary gills and also of all secondary gills, from stage P4 to P5 there was still comparably dense divergent hyphal growth from the pileus trama as new inner trama into all the gills. The trama hyphae appeared continuously smooth in the secondary gills over their whole length (4c and 4i in Fig. 21).

From the cross-sections in Fig. 22 and Fig. 23, the different lengths of secondary gills non-attached to the stipe suggested that there were about 3 generations of secondary gills formed over the time in the cap. Moreover, there was a splitting of primary hyphal gills as a secondary mechanism of additional gill formation as described before by Moore (1995). To evaluate all their origins better, we decided to follow up 5 µm-thicken cross-sections of a stage P5 primordium cap in 45 µm distances to each other (Fig. 22). From the top to the lower third of the cap, gill numbers increased from 55 to 124 (Fig. 23). While following the different sections of the gills, we observed that, in some cases, primary gills split (marked by the red and the yellow dots on the left side, the black and the white dots on the right side in Fig. 22) within the gill trama by creating internal layers of opposing palisades and eventually forming an aerial space in between. Bifurcation of primary gill happened which resulted in the formation of two second generation of primary gills (marked by the red and the yellow dots in Fig. 22) with their inner edges attached to the lipsanoblema. Splitting may start locally at the gill edges at the lipsanoblema, migrating by bifurcation mainly outwards and upwards into the inner of the existing primary gills (marked by the black and the white dots in images 6 to 9 in Fig. 22). The migrating bifurcation front is sinuate as stated before by Chiu and Moore (1990). This causes that in some views of cross-sections, confined fields of palisades or internal splits become visible within bifurcating primary gills with their the inner and outer edges here still connected to the lipsanoblema and the pileus trama, respectively (marked by the yellow dots in images 7 to 16 and the red dots in images 15 to 16 in Fig. 23). The sinuate gills are also seen on the longitudinal sections of the primordia (marked by the red arrows and the red dots in images A and B in Fig. 24). Secondary gills may originate between established splits at outer ends of primary gills of a second generation, even if they have

not yet been split over their whole length (marked in by the red arrows in images 12 to 16 in Fig. 23). These are the shortest secondary gills of third generation confined to the lower edges of the gills (marked in by the red arrows in images 12 to 16 in Fig. 23). The longest first and the medium-sized second generation of secondary gills originated usually in between un-splitted primary gills (marked by the blue dots in images 1 to 16 in Fig. 23). Secondary gills are over their whole length never connected to the lipsanoblema. First primary gills are connected to their upper ends to the lipsanoblema, along their whole length (marked by the yellow and the green arrows in images 1 to 16 in Fig. 23). Primary gills of split origin are connected at their lower end to the lipsanoblema while their outmost youngest upper ends may not have been connected to the lipsanoblema (marked by the white dots in images 3 to 16 in Fig. 23).

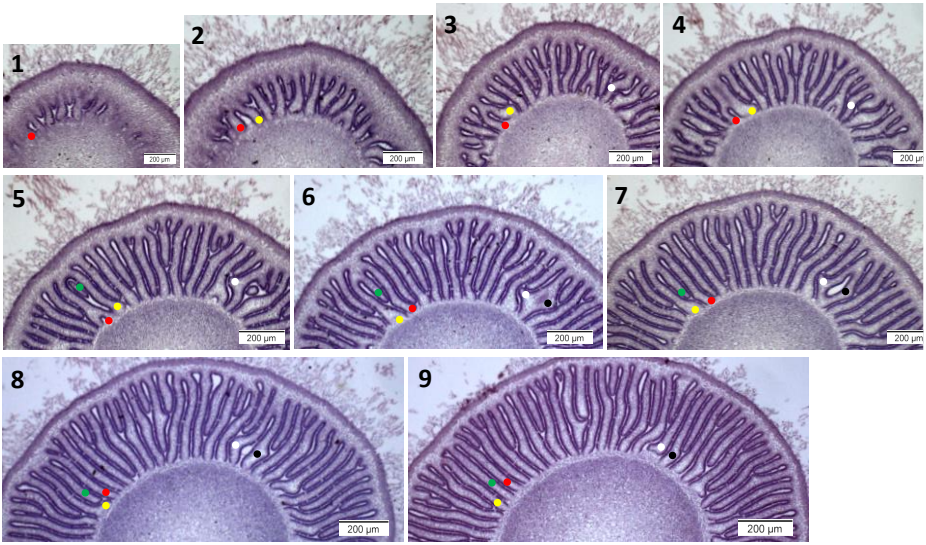

Fig. 22. The images (1 to 9) in series A show CSs stained by PAS and hemalum from top to middle part of the gill regions in the cap. The red and yellow dots on the left side and the black and white dots on the right side of the images mark the splitting of primary gills into two second generation of primary gill. A blue dot marks the third generation of secondary gills generation in-between splits of the primary gills.

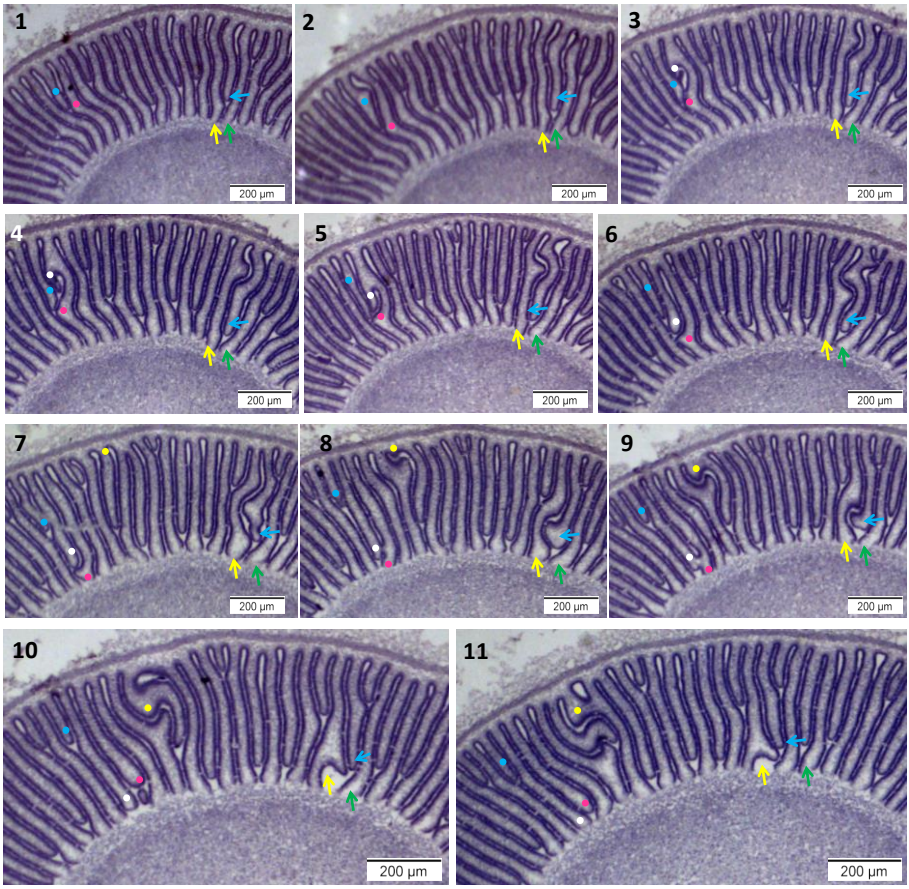
1
200 µm
2
200 µm
3
200 µm
4
200 µm
5
200 µm
6
200 µm
7
200 µm
8
200 µm
9
200 µm
10
200 µm
11
200 µm

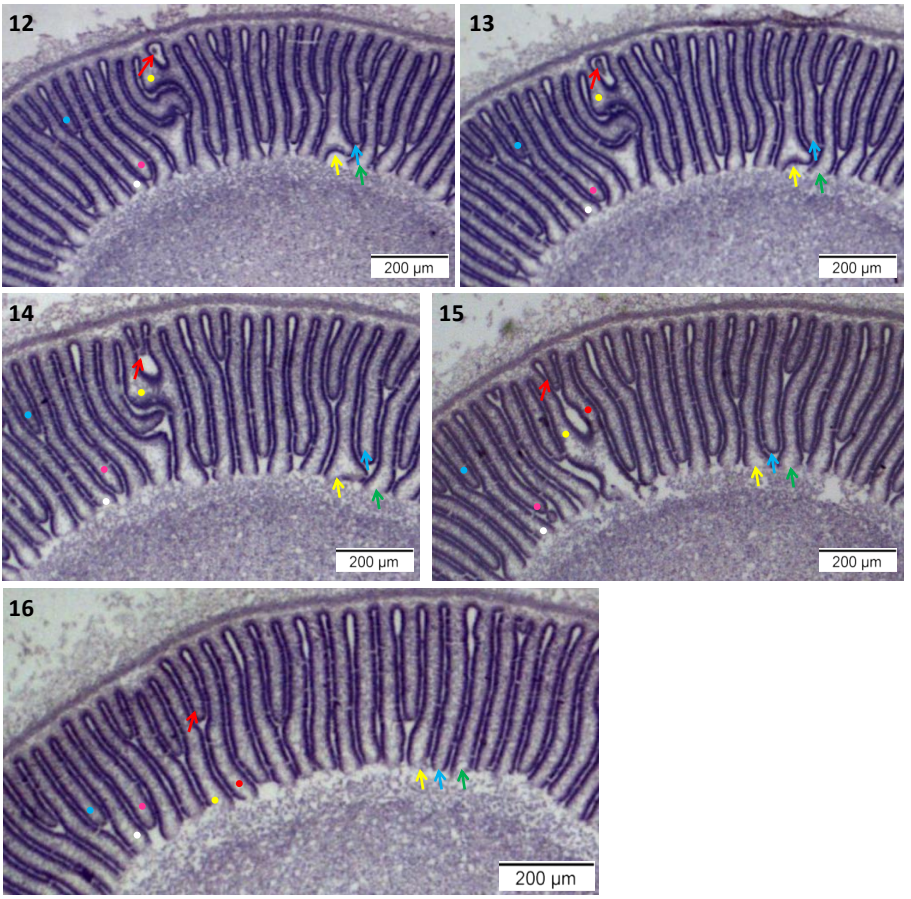

Fig. 23. The images (1 to 16) in series B show CSs stained by PAS and hemalum from middle towards lower part of the cap region. The blue dot in all the images from 1 to 16 shows the 2nd generation secondary gill. The white dot in the image 3 shows the 2nd generation primary gill formed by bifurcation within the gill margin of the 1st generation primary gill marked by pink dot. Towards the lower part of the cap, the same primary gill marked by white dot elongates and eventually touches the lipsanoblema. The yellow and the green arrows in all images marked the 1st generation primary gills and in between them, the generation of 2nd generation primary gill is marked by a blue arrow which eventually touched the lipsanoblema at the lower part of the cap. The red arrows in images 12 to 16 marked the 3rd generation of secondary gill appeared in-between the split of two primary gills.

Series A

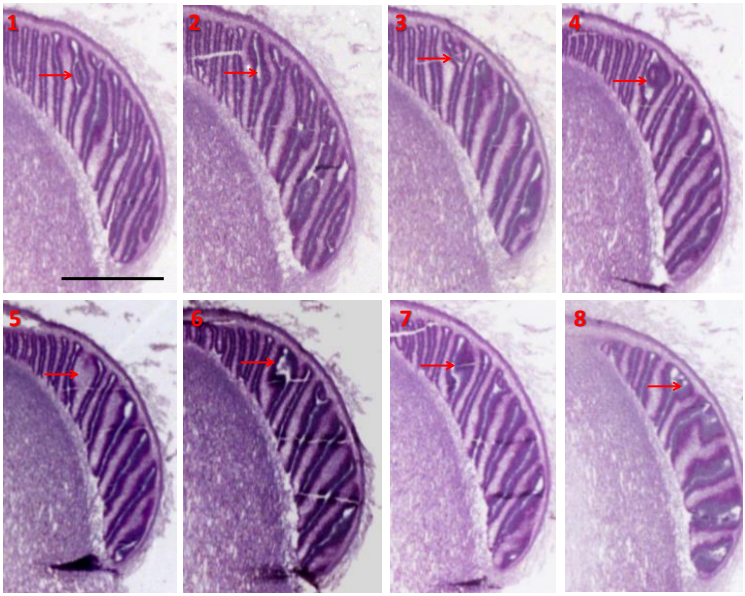

Series B

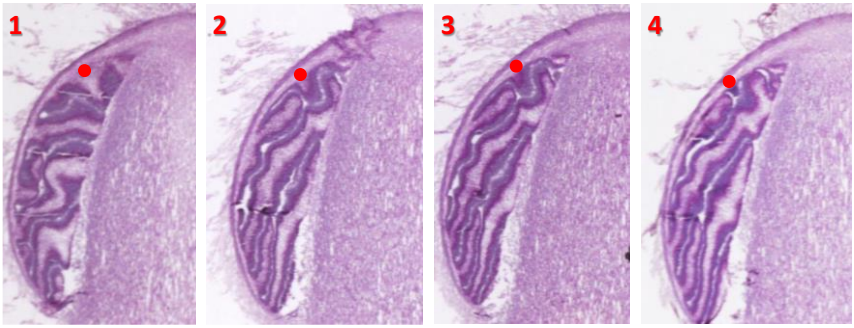

Fig. 24. The images in series A (1-8) and series B (1-4) show LSs stained by PAS and hemalum showing the gill regions from different sections of the cap. The sinuate gills are seen on all the LS images. The red arrows in the series A images followed the splitting of the primary gills and the red dots in the series B images marked the primary gills appearing like secondary gills towards the outer section. The scale bar measures 1 mm.

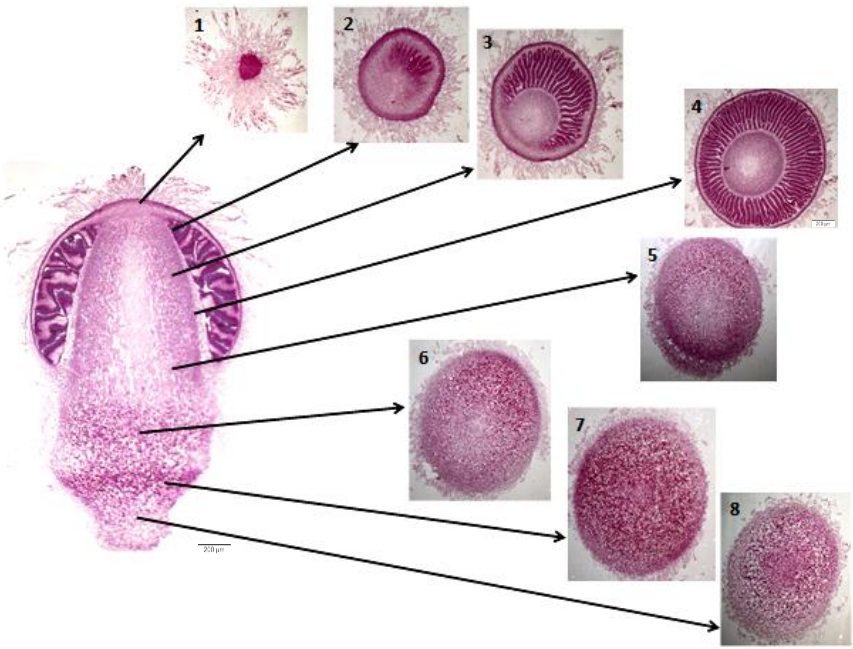

Fig. 25. Cross-sections of the primordium stage P5 marking the respective areas from the apex of the cap to the bottom of the stipe in the longitudinal-section. Cross-sections shown from top to bottom are 1: from the apex of the pileus region, 2: from the pileus trama with small part of gill, 3: from the pileus trama with larger part of gill from the pileus region, 4: from a region through the middle of gills, 5: the stipe region directly underneath the cap, 6: the region at the middle dark stained part of the stipe, 7: the darker stained region at the primordial shaft, and 8: the slightly stretched region at the lower part of stipe.

4.1.4.7.2. Stipe development:

Almost all stipe tissue of the stipe remained the same like before in stage P4 except for some stretching of hyphal cells at the lower half of the stipe and cell proliferation at the upper half of the stipe (Fig. 20A and 20B).

At the basal part of the stipe underneath the primordial shaft and in continuation over the whole outer stipe region, the narrow hyphae (12a in Fig. 26) continue to proliferate by intense branching and appear dense and strongly stained for covering the stipe underneath the partial veil (12b in Fig. 26). The lower part of the primordial shaft was stretched and contained vertically elongated inflated hyphae (11 in Fig. 26) inter-connected by narrow hyphae with hollow spaces in-between them by breaking individual hyphal cells and turning hyphae apart from each other.

Above these stretched part of the primordial shaft, the large inflated hyphal cells present at the lower part of the outer stipe were still darkly stained in magenta by dense masses of granules (10a and 10b in Fig. 26). The elongated partially stained inflated hyphae present above at the upper part of the outer stipe are now slightly stretched (9a and 9b in Fig. 26). They continue upwards as highly segmented partially stained inflated hyphae (8 in Fig. 26) which are still proliferating towards their tips with the extension of the sizes of the gills and slight stretching of cellular segments beneath. In the outmost outer part of the apex of stipe, the dense inflated hyphal cells are always short oval to cuboid or polyhedral (7 in Fig. 26).

The narrow inner hyphae of the central cylinder (5a and 5b in Fig. 26) are surrounded by a new innermost layer of stretched, partially magenta-colored inflated hyphae (6 in Fig. 26) starting at a level just below the cleistoblema from above the shaft continuing to the tip of the outer stipe. Due to this extension of a new outer stipe layer, hollow voids (marked by the red arrows in the images 5a and 6 in Fig. 26) are created around the cylinder of narrow inner hyphae. The inner stipe is continuous from the central pileus trama that runs vertically through the inner part of the stipe with narrow and branched hyphae (5a and 5b in Fig. 26). By stretching and hyphal degeneration, the hyphal tissues appear thinned towards the upper part of the stipe and tend to stretch and are broken in some areas creating hollow spaces (5a in Fig. 26) whereas in the lower half of the cylinder inner hyphae still appeared dense and darkly stained (5b in Fig. 26).

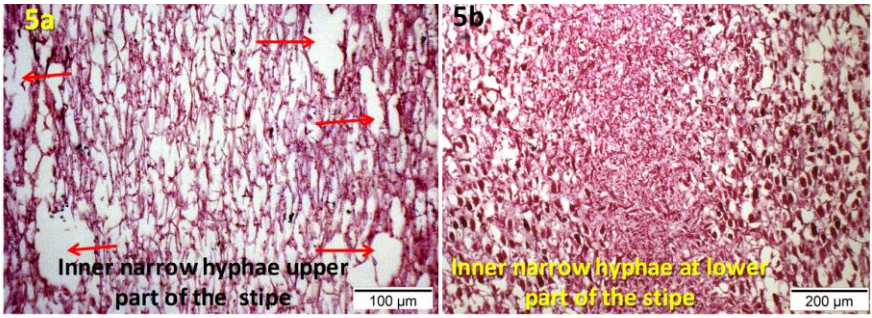

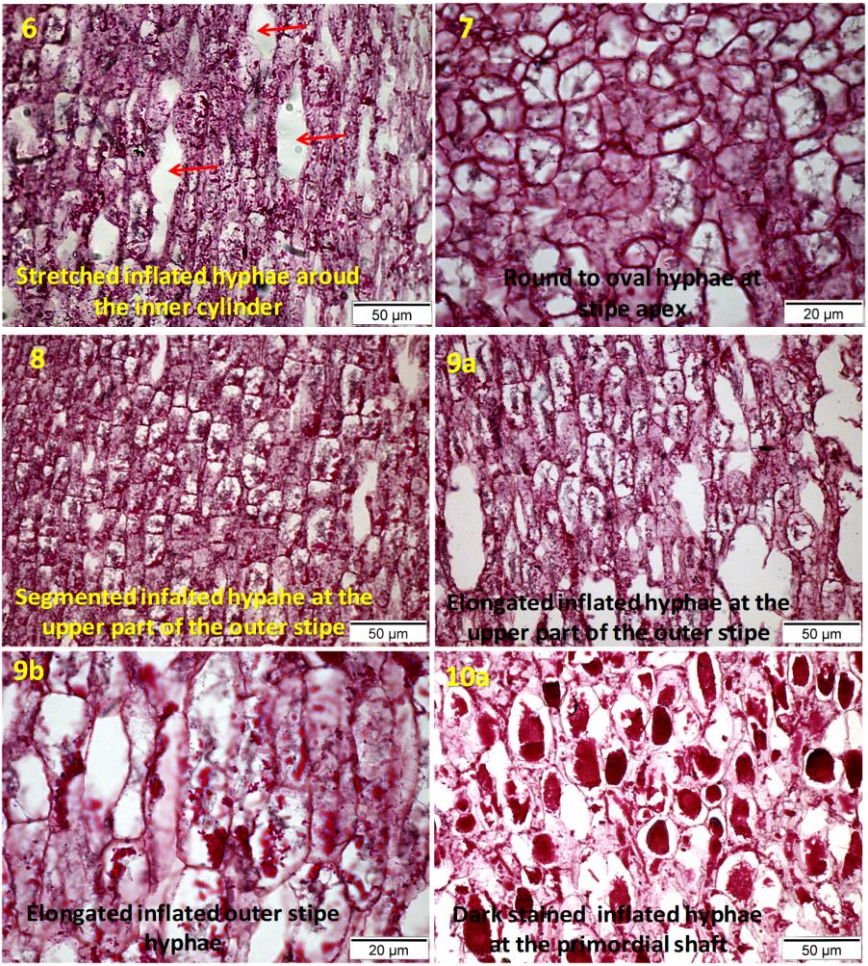
6
Stretched inflated hyphae aroud the inner cylinder
50 µm
7
Round to oval hyphae at stipe apex
20 µm
8
Segmented infalted hypahe at the upper part of the outer stipe
50 µm
9a
Elongated inflated hyphae at the upper part of the outer stipe
50 µm
9b
Elongated inflated outer stipe hyphae
20 µm
10a
Dark stained inflated hyphae at the primordial shaft
50 µm

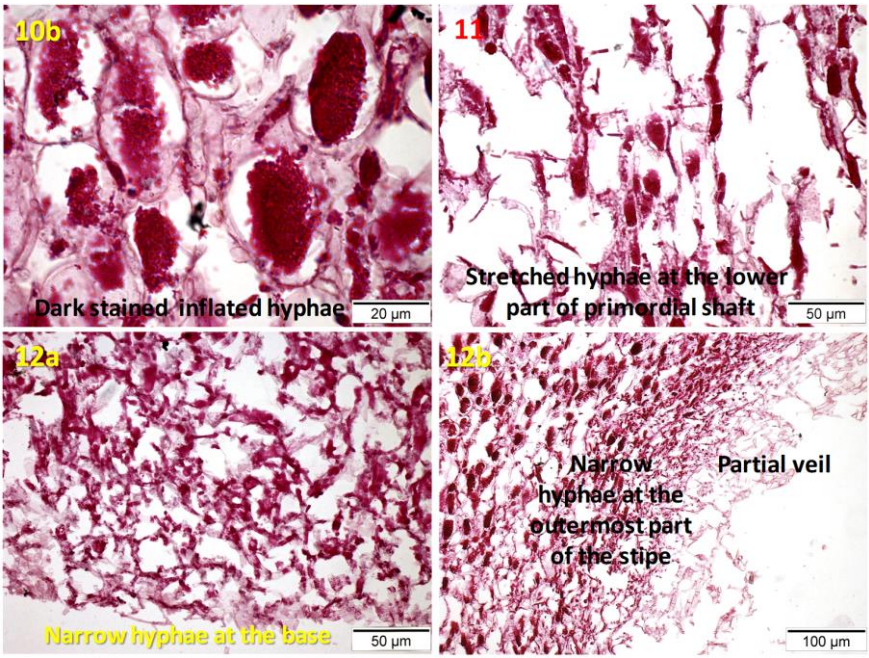

Fig. 26. Enlarged views on longitudinal-sections of stipe tissues double stained by PAS and hemalum. The images 12a and 12b show heavily-branched narrow hyphae at the bottom of primordial shaft and at the outer stipe directly underneath the partial veil, 11: stretched hyphae at the lower part of the primordial shaft, 10a and 10b: darker stained inflated hyphae in the primordial shaft, 9a and 9b: elongated inflated partially stained hyphae at the outer stipe, 8: inflated highly segmented hyphae at the upper-half of the outer stipe, 7: round to oval hyphal cells at the apex of the stipe, 6: long stretched inflated hyphae surrounding the inner cylinder, 5a: narrow partially stained, branched hyphae of the inner cylinder at the upper part of the stipe and 5b: dense n darker stained inner hyphae at the lower half of the inner cylinder.

4.1.5. Discussion

In terms of morphogenesis, *C. cinerea* has been one of the most studied basidiomycetes for more than 100 years due to its minimum cultivation requirements under laboratory conditions and by its coordinated development of fruiting bodies (Brefeld 1877; Buller 1924; Kües 2000; Navarro-González 2006; Kües et al. 2016). The synchronized pathway provides knowledge about the different stages of development as well as on the formation and differentiation of different cells and tissues that occur during the fruiting process.

C. cinerea fruiting development begins with monocentric growth of vegetative hyphae to form a hyphal nodulus (Clémençon 2004), now referred to as primary hyphal knot (Kües 2000). The primary hyphal knot transforms into the more compact secondary hyphal knot and from there, tissue differentiations start and to produce a primordium that continue to develop to form a mature mushroom, which then autolyzes dispersing spores from the cap. However, the process of fruiting body development is not as simple as summarized above, but rather the development process is very complex, in which different types of cells and tissues undergo a series of differentiation processes in the presence of suitable physiological and environmental conditions and ultimately produce a mature carpophore. The coordination between internal and external factors is therefore necessary for the full proceeding of development of a mushroom.

4.1.5.1. From hyphal initials to mature primordia

The initial hyphal growth is the first step in the morphogenesis of *C. cinerea*, provided that the right environmental conditions like temperature, humidity, aeration, and nutrients are given (Kües 2000; Navarro-González 2006; Kües et al. 2016). Light is not essential for the growth of mycelia since all strains can grow in the dark without light. However, the presence of a light signal can have a drastic impact on the developmental decision about what can happen on the vegetative mycelium (Lu 1974, 2000; Kamada et al. 1978; Kamada and Tsuji 1979). Therefore, environmental signals from light and dark periods strongly influence the development process of the fruiting body (Kües 2000; Kües et al. 2016).

Under dark conditions, localized within the mycelial network, usually a single hypha branches and sub-branches intensively to form many short branches. These hyphal branches become laterally interconnected and merged with the neighboring hyphae through the process of anastomosis, thereby forming an easily recognizable primary hyphal knot (Pk) (Matthews and Niederpruem 1972; Boulianne et al. 2000, Kües 2000), which Moore (1995) termed as primary tuft. However, the primary hyphal knots formed on Day 0 of the standard fruiting pathway are not specific to fruiting and require induction of a light signal to differentiate further into a 3-dimensional aggregated secondary hyphal knot (Sk) with inner plectenchyma of loosely interwoven still recognizable individual hyphae (thus a prosenchyma) covered by a thin

preliminary veil of homogenous hyphal nature (Velagapudi 2006; Lakkireddy et al. 2011). In the Sk structure, both stipe and cap tissues of a fruiting body begin to differentiate. Such type of development is known as isocarpous, which means that both structures were formed more or less simultaneously (Reijnders 1986; Clémençon 1997, 2004; Kües 2000).

We observed that, with the induction of a light signal at stage Pk on Day 0, hundreds of secondary hyphal knots (Sks) are formed on Day 1 of the standard fruiting pathway. After Sks are being formed, further light signals are required to coordinate further tissue development in the primordia from stage P1 to stage P5 and ultimately to induce karyogamy, followed by meiosis in the basidia and later to open a cap for autolysis. However, in the absence of light, Sks evolve to form an elongated stipe with a poorly developed cap, and such structures are referred to in the literature as "dark stipes" or "etiolated stipes" (Lu 1974; Morimoto and Oda 1973; Tsusué 1969; Kües 2000; Chaisaena 2009). As the development progressed under standard fruiting conditions from Pks to Sks and further to primordial stages P1 to P5, every day some of the further advancing structures are terminated in favor of a few, that continue in development in order to finally mature into a fruiting body and autolyze on Day 7 (Fig. 1) (Kües and Navarro-González 2015; Kües et al. 2016).

Pks and Sks have been referred to in the past as primary and secondary noduli as the initial steps in the pathway of fruiting body development (Clémençon; 1994b, 1997, 2004), and it is clear that a single Pk or a group of Pks are involved in the formation of Sks (Moore 1981; Kües 2000; Navarro-González 2006; Subba 2015; chapter 2.1). Reijnders (1977) referred to the inner prosenchyma of the Sks as basal plectenchyma because it continues to be located at the base of the stipe throughout primordia development. Atkinson (1914b) called it the podium and reported it to be a basal organ separate of the stipe. From my observations of the sections of secondary hyphal knots and the primordial stages, the upper parts of the inner prosenchymous tissues of the Sk are the foundation for the epinodular formation of the early pileus and stipe tissues. The lower parts of the Sk tissue continue to massively branch and interwove into a then more compact dense and strong plectenchyma found over the P1 to the P5 primordial stages. The successive branching in the plectenchyma gives repeatedly rise to new straight upwards growing narrow hyphae from within the plectenchyma that contribute to the inner and outermost primordial stipe development from stage P1 up to stage P4. These hyphae are probably also transport hyphae and responsible for the translocation of nutrients, throughout the primordial structures during their growth especially also glycogen as suggested from the darker stained basal plectenchyma.

In the past, cytological studies of the primordia development of *C. cinerea* have been performed using histochemical techniques (Matthews and Niederpruem 1973; Moore 1981; Subba et al. 2019) and the formation and the differentiation of various cells and tissues together with the presence of polysaccharides and their transfer from mycelia to growing primordia and from stipe to cap during the development process have been firstly investigated (Madelin 1960; Matthews

and Niederpruem 1973; Blayney and Marchant 1977; Moore et al. 1979). The former observations concentrated majorly in details on stage P4 and subsequent steps in development (Muraguchi et al. 2008; Moore et al. 1979). When earlier structures were considered (Matthews and Niederpruem 1973) there were no accurate time definitions why recognition of early stages remained vague and incomplete, and the timings undisclosed as how long it actually takes from a Pk to a ready primordium stage P5 (Kües 2000). With continuous observations of many cultures in parallel and in many repeats and with photographing distinct developmental steps at distinct days (Navarro-González 2008; Kües and Navarro-González 2015; Subba 2015) and then at distinct times of days of cultivation under defined environmental conditions (Kües et al. 2016; Majcherczyk et al. 2019; Subba et al. 2019), it was possible to document daily progresses in the coordinated pathway of fruiting body development exactly in advancing primordia development and further identify clearly also cases of abortions by loss of freshness leading to brittle drying veils and slight cap color changes from pinkish-beige to light grey-beige at the times of termination (Kües et al. 2016; Majcherczyk et al. 2019; Subba et al. 2019).

As shown in Fig. 1, in total it takes five, six and seven days from formation of a Pk to the stages P4 and P5 and a mature fruiting body releasing its spores by autolysis, respectively (Kües et a. 2016). To have accurate morphological observations, it is necessary to concentrate on exact hours of a day because development will constantly continue with elapsing time. In this study, we concentrated on structures as far as developed at hour 0 of a new day. To mark further developmental steps over the days, due to synchrony in development such could easily be then marked by the name of a stage + additional passed hours of a 24 h-day (Kües et al. 2016).

In this study, we used similar staining techniques as used by Moore et al. (1979) and Subba et al. (2019, chapter 3.2) in all stages of primordia development at hour 0 of a day from stage P1 to P5 and thereby recognized more different types of cells and tissues that are formed during the *C. cinerea* development process than other authors before.

4.1.5.2. Veil

The primary blema is an alternative term used for the innate universal veil (Clémençon 1997), which covers in *C. cinerea* the developing secondary hyphal knot and the primordium stage P1 and serves as a protective layer for the growing structure. Metablema is the term introduced by Clémençon (1997) to describe a type of secondary veil or partial veil that appears secondarily as a protective context during the developmental stage P2 primordium. With the developing primordium, the partial veil is named differently after the organ that produces them. The partial veil produced by the pileus is a termed as pileoblema and a cauloblema is the partial veil formed over its surface by the stipe.

With the increasing size due to primary gill formation in the next stage 2 primordium, the pileoblema appears as a thicker layer by further outwards growth in a manner of chains of heterogeneous elongated veil cells (e.g. see Fig. 9) similar as has been described before for later stages in primordial development (Buller 1924; Muraguchi and Kamada 1998; Morimoto and Oda 1973; Navarro-González 2008). As new observation in this study, the cauloblema from the stipe grows as chains of heterogeneous elongated veil cells in upward direction and meets the pileoblema near the end edge of the pileus margin, forming a meeting point which is called cleistoblema. The formation of the cleistoblema probably has as function to seal the entire primordium to protect the growing primordia from harmful radiation and invasive insect's entry that could damage the structure.

Moreover, it was also observed first time in frame of this PhD study that the formation of the cleistoblema maintains the continued flow of the veil from the pileus to the stem, so that when liquid droplets are generated on the top of the primordium, the droplets roll down along the surface of the entire structure and wash the primordial body instead of falling straight from the cap to the floor (Fig. 27). As can be seen from the photos of P2, P3 and P5, the pale-yellow liquid originates from the pileus underneath the veil. Surface tension analysis if the liquid on the fungal aerial mycelia and parafilm showed that the droplets have a hydrophobic character (Fig. 28) and therefore will keep collected at the different levels of the also hydrophobic cleistoblema formed successively above each other at different primordial stages (Fig. 27, marked by the red arrows). In the past, Knoll (1912) suggested such guttation droplets serve in maintaining high turgor for later stipe elongation. Here, I suggest that this type of practice of droplets running down from the veil is beneficial for wiping away harmful bacteria and adverse fungal spores from the primordial structures. Liquid droplets were collected and provided by me from different actively growing primordial stages (P1 ro P4) for proteomics analysis and the upcoming results indicated that specifically enzymes and various proteins with defense function against bacteria, fungi and small animals were secreted into the droplets (Poster presentation at the 30th Fungal genetics conference Asilomar, US), supporting defense and cleaning functions by these droplets.

Fig. 27. Stages P1 to P5 primordia and FB with multiple liquid droplets (marked by red arrows)

collecting at different levels of cleistoblema and eventually accumulated at the bottom of primordia and the fruiting body.

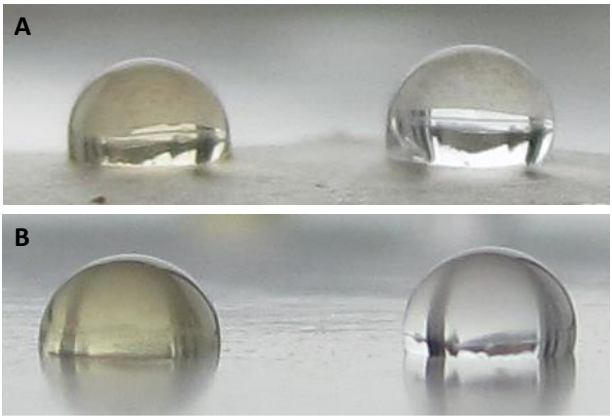

Fig. 28. Liquid droplets collected from P3 (left) and water (right) dropped onto (A) vegetative mycelium and (B) parafilm (each 5 µl volume) indicating different acute angles of attachment to the hydrophobic surfaces. Less acute means more hydrophobic.

4.1.5.3. Pileipellis and pileus trama

Beneath the partial veil at the pileus region, a thick band of compactly woven hyphae, referred to as pileipellis is formed for the first time in the P2 stage. It borders the plectenchymatic pileus tissues. The formation of this protective layer of tissue is to provide protection to the developing hymenial tissues laying underneath the pileus where spores are to be produced in the later developmental stages. The layer of tissues that represents the pileipellis is colored much darker in magenta than the veil above and the pileus trama below, indicating the presence of glycogen in this region. The pileus trama underneath the pileipellis consists of slightly held, narrow, branched interwoven hyphae. The thickness of the pileus trama decreases with increasing cap diameter and gill surface. Lu (1991) reported before from electron-microscope observations of multivesicular bodies and fibrous residual vacuolar bodies in dissolving cells at the outwards moving bases of gill cavities of glutaraldehyde-fixed stage P3 primordia (named Day 0 by Lu) that programmed cell death at the pileus trama resulted in the gills to bifurcate in zipper-like manner into the pileus trama, increasing the length of the outward growing gills. Degeneration of tissue of pileus trama as suggested from the electron-microscope work by Lu (1991) might have happened during pileus stretching and formation of gills diverting by growth from the pileus trama.

Clémençon (2004) further explained that the pileus margin of most young agarics like *Boletellus emodensis* bends downward during development grows towards the stipe and reaches them, forming a secondary hymenial cavity which is defined as claustropileatic mushrooms, while those species that never reach stipe and leave the margin of their downwards bending pileus open are called apertopileate mushrooms. In the primordia of *C. cinerea*, the edge of the pileus margin never touches the stipe, so the term apertopileate fits to this situation. The downwards growth of the *C. cinerea* pileus trama in the stretching cap is achieved from P2 to P4 by long individual narrow hyphae starting at the meristomoid edge of the central pileus trama and running parallely downwards to the pileus margin, some of which diverge off to parallely enter the gills for trama formation within the gills. The plectenchymous trama in the center of the pileus loosens more and more with the growing primordia from P1 to P5 by the stretching of the cap, due to which more and more rosette-like views of small hyphal knots become visible and by many hollow spaces appearing in between. Such rosette-like hyphal knots reported before by Reijnders (1977, 1993) to be present in Agarics within the veil, the pileipellis and the pileus trama of a developing primordial structure. In a longitudinal cut of a growing primordium, bundles of parallel growing while variably twisted hyphae are cut in cross-section direction resulting in the rosette-like views, as pointed out by Reijnders before (1993) in *Russula fragilis*. In *C. cinerea*, such hyphal knots were only seen in the central pileus trama. These hyphal knots *in sensu* Reijnders appear in morphology in the cuts similar to the Pks observed by me underneath a light microscope formed on the mycelial lattice as first possible step towards fruiting. However, the Pks in the vegetative mycelium have stunted hyphal branches (chapter 2.2). Reijnders (1993) mentioned that the main hyphae of the hyphal knots *sensu* Reijnders have an inductive function, directing neighboring hyphae to arrange together to appear rosette-like in transverse cuts of cable-like hyphal agglomerates. Suggested for the first time here, the function of the hyphal knots of *sensu* Reijnders multiply seen in the loosened pileus trama is probably to provide structural stability to the cap of the growing primordia.

4.1.5.4. Hymenophore development

The primordium of the first stage P1 appears white with a kernel rudiment consisting of a tiny inner pileus initial and a rudimentary stipe (Matthews and Niederpruem 1973; Moore 1995; Kües and Navarro-González 2015; Navarro-González 2008). The development of a primordium is endocarp, i.e., the development begins within the shaft or in the matrix that grows out of the secondary nodules (Clémençon 2004). At the P1 stage, at the lower bottom of the cap a dense dark stained annular region appeared with first a few parallel growing palisade cells which is the first sign of a starting prehymenium with an initial small split of tissue beneath (Fig. 4 and 3a in Fig. 5). The P1 stage as defined here corresponds about to the Stage 4 structure published by Matthews and Niederpruem (1973) and a 700 µm-sized structure (not centrally cut) published by Moore et al. (1979), both of which were more tangentially cut in the LS than the P1 structure

presented here (Fig. 4). A developing kernel with an internally distinguishable cap, stipe and basal regions is then clearly visible in a pear-shaped primordium in the P2 stage (Navarro-González 2008; Kües and Navarro-González 2015). At this stage, the first primary gill rudiments originate by outwards invading into the pileus trama and the hyphae of a gill trama at the gill rudiments are attached to the lipsanoblema growing out from the outer layer of the stipe. The very young down-lifted gills at this stage are covered throughout with palisade cells or they are already connected by a first lipsanoblema to the stipe, have a thin layer of subhymenium and inner gill trama and have a few pleurocystidia on their flanks and cheilocystidia their inner edges if these gill edges are yet closed.

According to previous studies, the gill development of *Coprinus* species follows one of three modes (Locquin 1953). Levihymenial development is the normal gill development of most agarics including some inkcap species, where the gill edges are always free and never touch the lipsanoblema, e.g., in *Coprinus comatus* (Reijnders 1979). In the ruptohymenial type, the lipsanoblema are attached to the hyphae of the inner gill margin so that the prehymenial palisade is not continuous, but is interrupted at the edges, as e.g. in *C. cinerea*, *Coprinellus curtus* and *Coprinellus radians* (Reijnders 1979b). The third type is a pseudoruptohymenial development, in which the gill ridges are initially free, but are later associated with the lipsanoblema, as e.g. in *Coprinellus disseminatus* (Kühner 1928).

According to my observations, the categorization of a gill development of *C. cinerea* fits the ruptohymenial type (Reijnders 1979b) to those initiated till stage P2, but the gills are still rudimentary at this point. When the primordium further proceeds to the next stages, primary and secondary gills as two distinct types of gills are formed where trama tissues of the primary gill are attached to the outer layer of the stipe while in the secondary gill, the hymenium remains continuous with a smooth gill edge (Reijinders 1979; Rosin and Moore 1985a and 1985b; Rosin et al. 1985; Moore 1987). The outer layer of the stipe is attached to the hyphae of the primary gill trama with the help of short-branched narrow hyphae of a thin lipsanoblema, whereas in a secondary gill, since the hymenial layer is continuous closing the edge of gill, there is no connection between the secondary gill and the lipsanoblema. It is therefore difficult to state a unique category for all gill development of *C. cinerea*. Notably, Clémençon (2004) and Reijnders (1979) never mentioned two types of gills in the categorization of gill types.

On Day 4 of the standard fruiting pathway, the primordium reaches stage P3, in which more primary gills arise through duplications by a zipper-like outwards-directed bifurcation mechanism and in which first secondary gills are carved out from the pileus trama at the base of gill cavities in between the elongating former gill rudiments (Navarro-González 2008; Kües and Navarro-González 2015). Extension growth of the first primary gills and new primary and secondary gill formation increases the size of the basidiome (Buller 1924; Muraguchi and Kamada 1998). This

includes also a continuous increase in the diameter of the stipe. Moore (1995) explained with his diagrams that during the development process the widening of the stipe is compensated by the gill replication by forming a gill cavity within the trama of a pre-existing primary gill. This gill replication results transiently in a Y-shaped gill structure, anchored at the pileus edge. On the other hand, and more frequently, production of a secondary gill at the outer base of a gill cavity gives a Y-shaped gill cavity which bases with its trunk at the lipsanoblema. He further postulated that there is a defining element, termed by him the gill organizer that appears to be responsible for the gill cavity radially outward towards the pileus to produce a secondary gill. In summary, thus all gills grow radially outwards and extend into undifferentiated tissues of the pileus context. When analyzing our own sample sections, we observed all the different types of gill development and also understood that these types of development result in differentiating gill tissues being pressed into the pileus trama, the thickness of which decreases as the basidiome increases in diameter (4a and 4c in Fig. 21).

For the secondary primary gill formation through gill bifurcation, Chiu and Moore (1990) noted before that this does not occur via a straight moving line of development, but variably sinuate over the length of a gill. Such was followed up and confirmed here in consecutive cross- and longitudinal-sections over the gill lengths for stage P5 primordia (Fig. 22, 23 and 24).

An individual gill as an organ to produce sexual spores in the hymenial out layer can be considered as a hymenophore. Clémençon (2004) has categorized the architecture of hymenophoral trama of the gill fungi. Some of the categories that the mushrooms fall into according to the arrangement of the hyphae in the gill trama are irregular, pachypodial, divergent, bidirectional, regular-irregular trama etc. In *C. cinerea*, the hyphae of the pileus trama line up parallel when entering the gill. Then, the inner hyphae continue growing parallely towards the inner edge of the gill, while the outer hyphae on both sides bend towards the subhymenial layer, presenting then a diverging type of hymenophoral trama. The arrangement of the hyphae in the primary gill trama appears to be stretched and broken towards the ruptured hymenial edge where they get attached to the lipsanoblema, while the arrangement of the hyphae in the secondary gill trama is smooth where the edge with the hymenial layer is continuous.

The fully differentiated *C. cinerea* hymenium consists of highly differentiated cell types, basidia, cystidia and paraphyses, all of which arise from the central layer of a gill, the trama (Rosin and Moore 1985b). According to Moore (1995), there is a defined temporal sequence in the formation of the cells in the hymenium. Moore did not distinguish between parallely organized palisade cells turning into probasidia (to receive a light signal to induce meiotic chromosomal S-replication and karyogamy) and then basidia (karyogamy, then meiosis and basidiospore production happens) unlike Lu (1972) and Kües (2000). According to Moore et al. (1979), basidia appear first at his Primordia stage 1 (now recognized to cover the whole developmental path from

stages P1 up to P5 as defined in Kües et al. 2016 and Subba et al. 2019) and then in his Primordia stage 2 (corresponding to P5 and following hours) paraphyses arise in-between basidia. In my observations, the parallely arranged palisade cells of a stage P3 primordium differentiated into probasidia in the P4 stage primordium, following definitions by Lu (1972). Paraphyses in stage P4 were not yet visible. In the P5 stage primordium however, young paraphyses became firstly visible as thin hyphae pushing themselves from the subhymenium in between the basidia (marked by the yellow arrows in images 4e-4g in Fig. 21). The clasping cells reported by Buller (1924) and Chiu and Moore (1990; for strains of Japanese origin) are also seen adhering to the cystidia in stage P5 (marked by the green arrows in images 4e-4g in Fig. 21) with a suggested function as keeping the pleurocystidia attached to the hymenial surface during cap expansion (Buller 1924). The pleurocystidia, cheilocystidia and the opposing cystesia formed successively during stages P2 to P4 decreased in frequencies in stage P5, probably due to some cell degeneration. Remaining cystidia continue to be attached to their cystesia in the opposing hymenial layer (images 4e-4h in Fig. 21).

4.1.5.5. Stipe development

In *C. cinerea*, tissue formation and differentiation in the stipes are as complex as in the cap region and with the developing primordia stages, the complexity in the stipe tissues also increases.

Earlier studies reported that the stipe tissue of in primordial structures and the mature stipe of *C. cinerea* consisted of both narrow and inflated hyphae (Lu 1974; Hammad et al. 1993b; Kües 2000). The central region at the extreme bases and the apices of pre-rapid elongating stipes are occupied exclusively by narrow hyphae, which are also concentrated on the outside of the stipe (as the lipsanoblema as called by Clémençon 2004) and fringing the central lumen of rapidly elongating stipes and are interspersed between the large inflated hyphae at the outer stipe regions (Hammad et al. 1993b). Hammad et al. (1993b) further added that the narrow hyphae tend to stain more intensively than the inflated hyphae and to have varied spatial arrangements, suggesting distinct functions.

In my observations at younger developmental stages, similar arrangements of narrow long leading hyphae with lateral upwards elongating branches have been observed in all stages from P1 to P5, in which they grow out from the inner of the basal part of the primordial shaft and pass vertically directly along or grow through the inner stipe to enlarge the inner stipe cylinder or, when originating at the outer regions of the primordial shaft, they will cover the outermost part of the stipe. These latter narrow hyphae covering the outer stipe grow out at the apical part of the stipe as enclosed by the cap region to form the lipsanoblema, which is made up of thin-layered, multiple short-branched hyphae which attached to the hyphae of a primary gill trama, disrupting the inner edges of a young, developing primary gills. This event begins at the stage P1 primordium. Due to the outward radially growing gills and the expanding cap, the attachment between the

lipsanoblema and the hyphae of a primary gill trama will constantly be stretched, thereby interrupting the smooth continuation of the trama hyphae in the inner end of the primary gills to which the lipsanoblema is attached. Later during the cap expansion resulting in a mature mushroom, all primary gills detach from the stipe, breaking the connection between the trama tissue and the lipsanoblema (not shown here but refer to Navarro-González (2008) P5 +12 h). The lipsanoblema likely plays an important role in providing structural support to the growing primary gills and may also act as a link between the stipe and the cap for the transmission of nutrients (see below) and, possibly in both directions, of growth signals. Indeed, cap-stipe grafting experiments performed by Kamada and Tsuji (1979) with P5 structures indicated transport of a darkness-induced hormone-like signaling compound from caps into the stipes for induction of stipe elongation.

The inner narrow hyphae below the primordial shaft of the stipe are short and multiple laterally branched, resemble vegetative hyphae as noted before by Borris (1934) and are interconnected but independent of the inflated hyphae of the outer stipe. Such narrow hyphae are densely packed and darker stained in the primordial shaft in the younger primordia. Within the primordial shaft and the lower part of the outer stipe, these narrow hyphae merge with the darker colored, large round to oval inflated hyphal cells. The network of these narrow hyphae has been suggested to act as a nutrient translocator from the mycelium over the stem to the cap region over the whole primordial development (Ji and Moore 1993; Moore 1995). In addition, these narrow hyphae likely transfer glycogen from the mycelium to store them in the round to oval, darker-colored hyphal cells to be used for the later rapid stipe elongation. Some of the glycogen is also likely transferred via narrow hyphae in the inner stipe cylinder to the pileus trama region and from there via gill trama into the subhymenia, or alternatively, in a short cut, from the darker in magenta stained lipsanoblema via gill trama into the subhymenia, where it accumulates in the form of darker stained magenta granules. The deposition of the glycogen at the lower half of the stipe and the hymenial region of the cap in stages of primordia development has been reported by Moore et al. (1979) and Matthews and Niederpruem (1973). Moore et al. (1979) further reported that the glycogen reserves deplete from the stipe after primordia development during fruiting body maturation and accumulates in the cap.

Past studies reported that during the rapid elongation of a stipe of a mature fruiting body, the stipe does not elongate evenly along its entire length, but the extension of the hyphae is mainly limited to the upper part of the stipe enclosed by the lid (Gooday 1974; Cox and Niederpruem 1975; Kamada and Takemaru 1977; Kamada et al. 1978; Moore et al. 1979). In my observations of the primordial stages, the hyphal cell of the lower parts of the outer stipes get generally stretched with an extension of inflated hyphae in all the stages, due to which hollow spaces appeared in-between them. In contrast, the hyphae in the upper part of the stipes are strongly segmented and are intactly connected with a few small cavities in between. At the apex, the presence of the cuboid or

polyhedral inflated hyphal cells and the highly segmented inflated hyphae directly below indicates that cell massive proliferation may have occurred in this region. The subsequent fast elongation of these cells contributes then to the rapid elongation of the stem during rapid expansion of a fruiting body. Reijnders (1977) also mentioned that the proliferation of cells during primordia formation is mainly in the upper part of the stipe and decreases in the lower part. An arrangement of the inflated segmented hyphae in the upper part of the stipe Reijnders (1977) called as meristermoid.

Blayney and Marchant (1977) reported that glycogen and insoluble proteins are degraded in the upper portion of the stipe to provide materials for its elongation. However, Gooday stated from surgeries deleting the caps of immature fruiting bodies and analyses of carbohydrate compositions that polysaccharides do not act as a food reserve during the rapid phase of elongation. He concluded that the stipe elongation is an autonomous endotrophic process which does not require any growth factors, nor connection to mycelia or water or exogenous nutrient but needs chitinases for cell wall extensions (Gooday 1974, 1975). Borris (1934) reported that decapitation of fruit bodies prevented elongation of stipes of younger primordia but not those of later stages. Gooday (1974) also found that the stipe elongation has no requirement for connection either with the cap or the parental mycelia. The same was confirmed by Cox and Niederpruem (1975) on the primordia above 5 mm in height (later stages, probably about stage P4 to stage P5) that were able to elongate after excision and decapitation. These early data suggests that hormone-like factors promoting stipe elongation are probably produced in early phases of development and persist in sufficient amount in the stipe at later phase of elongation (Kamada 1994). Expansion of the stipe is necessary to elevate the pileus into the air for more effective spore dispersal; therefore, the expansion of pileus tissues must happen in co-ordination to the stipe elongation (Hammad et al. 1993a).

Biochemical and light-and electron microscopic studies conducted on an elongation-less mutant (*eln*) with a defect in stipe elongation and the wild type have revealed fundamental aspects of stipe elongation, such as diffuse extension growth of cylindrical stipe cells arranged in segmented hyphae parallel to the stipe axis, causing stipe elongation, helical orientation of chitin micro-fibrils in the cell walls of stipe cells during development, and changes in mechanical properties of the stipe wall parallel with the elongation rate during development (Gooday 1985; Kamada 1994). The content of the chitin increases during the stipe elongation (Gooday 1975). Chitin is the major component of the *C. cinerea* stipe and chitin micro fibrils are predominantly found in the walls of stipe cells in a transverse orientation both before and after elongation (Gooday 1975). Expansion of the cylindrical stipe is axial rather than circumferential and helical and transverse arrangement of chitin and glucans is the reason for such expansion (Kamada 1994). Throughout elongation, the chitin content stays constant and insertion of new chitin microfilaments occurs over the whole length of the cell in a uniform intercalary fashion. Further, genetic analysis also

identified 6 septin genes, 5 of which are heavily transcribed during stipe extension (Shioya et al. 2013). It is known that the cortical septin filaments give localized stiffness to the plasma membrane of stipe cells and allow the stem cells to be cylindrically elongated (Shioya et al. 2013). As environmental factors, light signals play a role in stipe extension. Because the maturation of pilei was favored by light and the stretching of the stipes by darkness (Tsusué 1969), an appropriate duration of the dark phase is necessary for the stretching of the stipes, otherwise a longer exposure leads to the formation of dwarf primordia (Tsusué 1969).

4.1.5.6. Cap expansion and autolysis

The fully developed P5 stage primordium formed on Day 6 of the fruiting pathway, with no further cell proliferation with exception of production of basidiospores, is now ready to attain maturity by the induction of karyogamy (Lu 2000, Kües et al. 2002). The pre-rapid elongation of the stipe mentioned above occurs in parallel to the meiosis followed by spore formation. Up to the end of meiosis (stage P5 + 9 h), the cleistoblema connecting the partial cap and stipe veils is still closed. The cleistoblema loosens with basidiospore production and is fully open at stipe P5 + 12 h (Navarro-González 2008). As the pigmentation of basidiospores takes place, rapid elongation of stipe occurs (Hammad et al. 1993b; Navarro-González 2008). Cap expansion correlates temporally and proportionally with rapid stipe elongation (Moore et al. 1979; Kües 2000). As reported in the past studies, cap expansion happens like an umbrella which starts about 14 h after karyogamy and is completed in about 6 h (Moore 1998: Navarro-González 2008). First, degeneration of loosened pileus tissue underneath the pileipellis and the partial veil of the cap and above the gills proceeds by 3 h rapid cap expansion, creating hollow spaces above the gills, whereas parallely oriented hyphae of the outer pileus trama remain in positions above the gill cavities (Muraguchi et al. 2008). The hollow spaces in the pileus trama create a force that leads to V-shaped cracks by subsequently breaking up also the pileipellis and the pileoblema above the gills as shown by Muraguchi et al. (2008). The opposing orientation of the parallel running hyphae of the pileus trama and those of gill trama appears most optimal for the easy smooth opening of the umbrella, At the start of rapid cap expansion, likely driven by maturation growth and massive inflation of the paraphyses (Moore et al. 1979) invading at stage P5 into the hymenium, each gill splits within the parallel running gill trama from the outside of the cap for opening the umbrella (Muraguchi et al. 2007).

In the 24 h-scheme of fruiting body development, the cap will be fully opened in the night phase of Day 6 at P5 + 18 h (Subba 2015). Basidiospores at first might be released from the caps by ejection from their sterigmata at the basidia through physical forces of Buller´s droplets (Lakkireddy et al. 2011). However, the majority of spores is released in liquid droplets by cap autolysis and takes about 4-5 h on Day 7 (P5 + 21-26) (Kües 2000; Kües and Navarro-González 2015). Degeneration of the whole cap starts with the basidiospores release. Autolysis initiates

from the edge of the gill closest to the stipe towards the outer edge of the cap and from the cap margin towards the apex (Rosin and Moore 1985b), following the same pattern of direction of generation of gills, expansion of palisades and different hymenial cell formations. Chitinases (Iten and Matile 1970) and glucanases (Miyake et al. 1980a) are responsible for the cell wall degradation that cause cap autolysis. In the early hours of the next light phase (0-1 h in this study) of Day 7, the cap autolysis is fully completed, thereby ending the life cycle of the fungus (Navarro-González 2008; own observations shown in Fig. 1).

4.1.6. Conclusion

The multicellular nature of mushrooms by its complexity and variability is difficult to understand (Kües et al. 2018). In this chapter, however, we have attempted to identify and describe the development of various types of cells and tissues of the model basidiomycete *C. cinerea* that form during different primordial stages, which are defined to occur at 0 hour of consecutive days of the standard fruiting pathway of *C. cinerea*. By defining the different stages from P1 to P5, this study identifies and reports different types of new cells and tissues as they are formed and differentiated over the course of the development. A summarizing map shown in Fig. 29 is created for an overall overview and specific orientation. It shows the different cells and tissues identified in this study in the different primordial stages represented by different colors, to give an overview insight into the dynamics of successive and parallel cellular events occurring in the multicellularity in fruiting body development of *C. cinerea*.

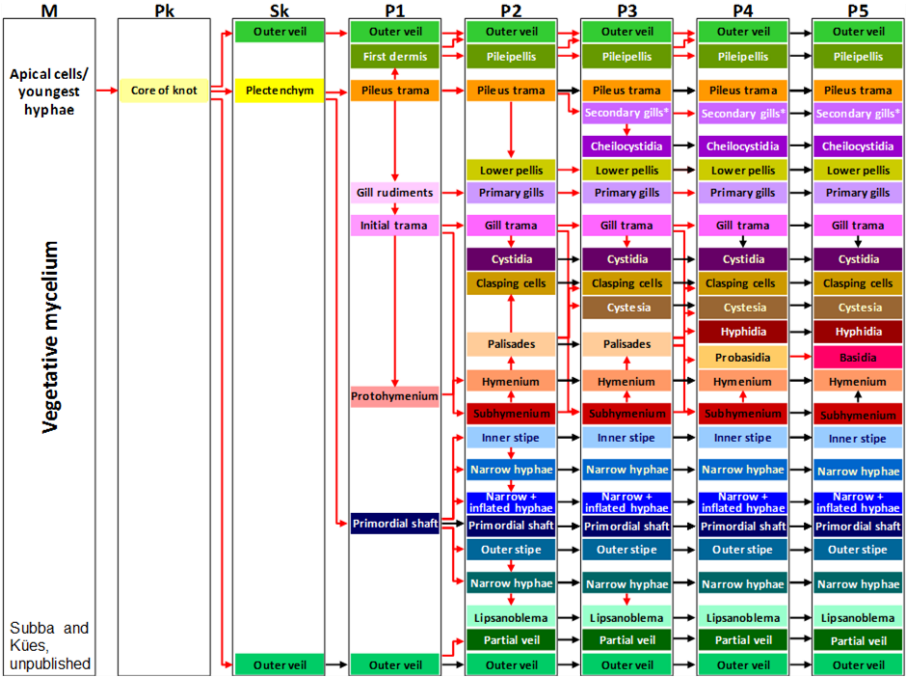
M
Pk
Sk
P1
P2
P3
P4
P5
Apical cells/ youngest hyphae
Vegetative mycelium
Subba and Kües, unpublished
Core of knot
Outer veil
Plectenchym
First dermis
Pileus trama
Gill rudiments
Initial trama
Protohymenium
Primordial shaft
Pileipellis
Secondary gills*
Cheilocystidia
Lower pellis
Primary gills
Gill trama
Cystidia
Clasping cells
Cystesia
Hyphidia
Probasidia
Basidia
Palisades
Hymenium
Subhymenium
Inner stipe
Narrow hyphae
Narrow + inflated hyphae
Outer stipe
Lipsanoblema
Partial veil

4.1.7. References

Atkinson, G. F. (1914b) The development of *Amanitopsis vaginata*. *Annales Mycology*, *12*, pp.346-356

Blayney, G. P. and Marchant, R. (1977) Glycogen and protein inclusions in elongating stipes of *Coprinus cinereus. Journal of General Microbiology*, *98*, pp.467-476.

Borriss, H. (1934) Über den Einfluss äusserer Faktoren auf Wachstum und Entwicklung der Fruchtkörper von *Coprinus lagopus*. *Planta*, *22*, pp.28-69 (in German).

Boulianne, R. P., Liu, Y., Aebi, M. (2000) Fruiting body development in *Coprinus cinereus*: regulated expression of two galectins secreted by a non-classical pathway. *Microbiology*, *146*, pp.1841-1853.

Brefeld, O. (1877) Botanische Untersuchungen über Schimmelpilze. III. Basidiomyceten Leipzig: Arthur Felix, (in German)

Buller, A. H. R. (1924) Researches in fungi III. The production and the liberation of spores in hymenomycetes and Uredineae. Hafner Publishing Co., New York, NY.

Chaisaena, W. (2009) Light effects on fruiting body development of wildtype in comparison to light-insensitive mutant strains of the basidiomycete *Coprinopsis cinerea*, grazing of mites (*Tyrophagus putrescentiae*) on the strains and production of volatile organic compounds during fruiting body development. (Ph.D thesis. Georg-August-University Göttingen).

Chiu, S. W. and Moore, D. (1990) A mechanism for gill pattern formation in *Coprinus cinereus*. *Mycological Research*, *94*, pp.320-326.

Clémençon, H. (1994b) Der Nodulus and die Organogenese während der frühen Fruchtkörperentwicklung von *Psilocybe cyanescens*. Z. *Mykology*, *60*, pp.49–68.

Clémençon, H. (1997) Anatomie der Hymenomyceten. Eine Einführung in die Cytologie und Plectologie der Krustenpilze, Porlinge, Keulenpilze, Leistlinge, Blätterpilze und Röhrlinge. F. Flück-Wirth, Teufen, Switzerland.

Clémençon, H. (2004) Cytology and plectology of the Hymenomycetes. *Bibliotheca Mycological*, 199, pp.1-488.

Cox, R. J. and Niederpruem, D. J. (1975) Differentiation in *Coprinus lagopus* III. Expansion of excised fruit-bodies. *Archiues of Microbiology*. *105*, pp.257-260.

Gooday, G. W. (1974) Control of development of excised fruit bodies and stipes *of Coprinus cinereus. Transactions of the British Mycological Society*, *62*, pp.391–399.

Gooday, G. W. (1975) The control of differentiation in fruiting body in *Coprinus cinereus. Reports Tottori Mycological Institute*, *12*, pp.151-160

Gooday G. (1985) Elongation of the stipe of *Coprinus cinereus*. *Developmental Biology of Higher Fungi*, Manchester, England, pp.311-331.

Granado, J. D., Kertesz-Chaloupová, K., Aebi, M. (1997) Restriction enzyme mediated DNA integration in *Coprinus cinereus*. *Molecular and General Genetics*, *256*, pp.28-36.

Hammad, F., Watling, R. and Moore, D. (1993a) Cell population dynamics in *Coprinus cinereus*: co-ordination of cell inflation throughout the mature basidiome. *Mycological Research*, 97, pp. 269–274

Hammad, F., Watling, R. and Moore, D. (1993b) Cell population dynamics in *Coprinus cinereus*, narrow and inflated hyphae in the basidiome stipe. *Mycological Research, 97*, pp. 275–282.

Iten, W. and Matile, P. (1970) Role of chitinase and other lysosomal enzymes of *Coprinus lagopus* in the autolysis of fruiting bodies. *Microbiology, 61*, pp.301-309.

Ji, J. and Moore, D. (1993) Glycogen metabolism in relation to fruit body maturation in *Coprinus cinereus*. *Mycological Research, 97*, pp.283–289

Jirjis, R. I., and Moore D. (1976) Involvement of glycogen in morphogenesis of *Coprinus cinereus*. *Journal of General Microbioogy, 95*, pp.348–352.

Kamada, T. (1994) Stipe elongation in fruit bodies. *Growth, Differentiation and Sexuality*, *1*, pp. 367-379. Springer, Berlin, Heidelberg.

Kamada, T., Kurita, R. and Takemaru, T. (1978) Effects of light on basidiocarp maturation in *Coprinus macrorhizus*. *Plant and Cell Physiology*, *19*, pp.263-275.

Kamada, T. and Takemaru, T. (1977) Stipe elongation during basidiocarp maturation in *Coprinus macrorhizus*: mechanical properties of the stipe cell wall. *Plant Cell Physiology,18*, pp.831–840.

Kamada, T. and Tsuji, M. (1979) Darkness-induced factor affecting basidiocarp maturation in *Coprinus macrorhizus*. *Plant Cell Physiology 20*, pp.1445–1448.

Knoll, F. (1912) Untersuchungen über Bau und die Funktion der Cystiden und verwandler Organe. Borntraeger, Gebrüder, *50*, pp.453–501.

Kües, U. (2000) Life history and developmental processes in the basidiomycete *Coprinus cinereus*. *Microbiology and Molecular Biology Reviews*, *64*, pp.316-353.

Kües, U., Khonsuntia, W. and Subba, S. (2018) Complex fungi. *Fungal Biology Reviews, 32*, pp.205-218.

Kües, U. and Navarro-Gonzalez, M. (2015) How do Agaricomycetes shape their fruiting bodies? 1. Morphological aspects of development. *Fungal Biology Reviews*, *29*, pp.63-97

Kües, U., Subba, S., Yu, Y., Sen, M., Khonsuntia, W., Singhaduang, W., Lange, K. and Lakkireddy, K. (2016) Regulation of fruiting body development in *Coprinopsis cinerea*. *Mushroom Science, 19*, pp.318-322.

Kühner, R. (1928) Le dévelopment et la position taxonomique de I' *Agaricus disseminates Pers. Le Botaniste, 20*, pp.147-156.

Lakkireddy, K. K., Navarro-González, M., Velagapudi, R. and Kües, U. (2011) Proteins expressed during hyphal aggregation for fruiting body formation in basidiomycetes. *Proceedings of the 7th international conference on mushroom biology and mushroom products,* Arcachon, France, *2*, pp. 82-95

Liu, Y. (2001) *Fruiting body initiation in the basidiomycete Coprinus cinereus* (Doctoral dissertation, ETH Zurich).
Locquin, M. (1953) Reserches sur I'organisation et le dévelopment des agaric, des bolets et des clavaires. *Bulletin de la Société Mycologique de France, 69*, pp.389-402
Lu, B. C. (1972) Dark dependence of meiosis at elevated temperatures in the basidiomycete *Coprinus lagopus*. *Journal of Bacteriology*, *111*, pp.833-834.
Lu, B. C. (1974) Meiosis in *Coprinus.* V. The role of light on basidiocarp initiation, mitosis and hymenium differentiation in *Coprinus lagopus*. *Canadian Journal of Botany, 52*, pp.299–305.
Lu, B. C. (1991) Cell degeneration and gill remodeling during basidiocarp development in the fungus *Coprinus cinereus*. *Canadian Journal of Botany,69*, pp.1161–1169.
Lu, B. C. (2000) The control of meiosis progression in the fungus *Coprinus cinerea* by light/dark cycles. *Fungal Genetics and Biology*, *31*, pp.33-41.
Madelin, M. F. (1960) Visible changes in the vegetative mycelium of *Coprinus lagopus* Fr. at the time of fruiting. *Transactions of the British Mycological Society*, *43*, pp.105-110.
Majcherczyk, A., Dörnte, B., Subba, S., Zommorodi, M. and Kües, U. (2019) Proteomes in primordia development of *Coprinopsis cinerea*. *Acta Edulis Fungi, 26*, pp.37-50.
Matthews, T. R., and Niederpruem, D. J. (1972) Differentiation in *Coprinus lagopus*. I. Control of fruiting and cytology of initial events. *Archives of Mikrobiology*, *87*, pp.257–268.
Matthews, T. R., and Niederpruem, D. J. (1973) Differentiation in *Coprinus lagopus*. II. Histology and ultrastructural aspects of developing primordia. *Archives of Mikrobiology, 88*, pp.169–180.
McLaughlin, D. J. (1974) Ultrastructural localization of carbohydrate in the hymenium of *Coprinus*. Evidence for the function of the Golgi apparatus. *Protoplasma, 82*, pp.341–364.
Miyake, H., Takemaru, T. and Ishikawa, T., 1980. Sequential production of enzymes and basidiospore formation in fruiting bodies of *Coprinus macrorhizus*. *Archives of Microbiology*, *126*, pp.201-205.
Moore, D. (1981) Developmental genetics of *Coprinus cinereus*: genetic evidence that carpophores and sclerotia share a common pathway of initiation. *Current Genetics*, *3*, pp.145–150.
Moore, D. (1987) The formation of agaric gills. *Transactions of the British Mycological Society, 89*, pp.105–114.
Moore, D. (1995) Tissue formation. *The Growing Fungus*. N. A. R. Gow and G. M. Gadd (eds.). Chapman & Hall, London, United Kingdom. pp.423–466.
Moore, D. (1998) Fungal morphogenesis. Cambridge University Press, Cambridge, United Kingdom, Chapter 21, pp. 423-465.
Moore, D., Elhiti, M. M. and Butler, R. D. (1979) Morphogenesis of the carpophore of *Coprinus cinereus*. *New Phytologist*, *83*, pp. 695-722.

Morimoto, N. and Oda, Y. (1973) Effects of light on fruit body formation in a basidiomycete, *Coprinus macrorhizus. Plant Cell Physiology*, *14*, pp.217–225.
Muraguchi, H., Fujita, T., Kishibe, Y., Konno, K., Ueda, N., Nakahori, K., Yanagi, S. O. and Kamada, T. (2008) The *exp1* gene essential for pileus expansion and autolysis of the inky cap mushroom *Coprinopsis cinerea* (*Coprinus cinereus*) encodes an HMG protein. *Fungal Genetics and Biology*, *45*, pp.890-896.
Muraguchi, H. and Kamada, T. (1998) The *ich1* gene of the mushroom *Coprinus cinereus* is essential for pileus formation in fruiting. Development *125*, pp.3133–3141.
Navarro-González, M. (2008) Growth, fruiting body development and laccase production of selected coprini. (Doctoral dissertation, Göttingen University).
Reijnders, A. F. M. (1977) The histogenesis of bulb and trama tissue of the higher Basidiomycetes and its phylogenetic implications. *Persoonia-Molecular Phylogeny and Evolution of Fungi*, *9*, pp.329-361.
Reijnders, A. F. M. (1979) Development anatomy of *Coprinus*. *Persoonia*, *10*, pp.383-424.
Reijnders, A. F. M. (1986) Development of the primordium of the carpophore. *The Agaricales in Modern Taxonomy*, R. Singer (ed.). Koeltz Scientific Books, *4*, pp.20-29.
Reijnders, A. F. M. (1993) On the origin of specialized trama types in the Agaricales. *Mycological Research*, *97*, pp.257-268.
Rosin, I. V. and Moore, D. (1985a) Origin of the hymenophore and establishment of major tissue domains during fruit body development in *Coprinus cinereus*. *Transactions of the British Mycological Society*, *84*, pp.609–619.
Rosin, I. V. and Moore, D. (1985b) Differentiation of the hymenium in *Coprinus cinereus*. *Transactions of the British Mycological Society*, 84, pp.621–628.
Rosin, I. V., Horner, J. and Moore, D. (1985) Differentiation and pattern formation in the fruit body cap of *Coprinus cinereus*. Moore, D., Casselton, L.A., Wood, D.A. and Frankland, J.C (eds.). *Developmental Biology of Higher Fungi: Symposium of the British Mycological Society Held at the University of Manchester April 1984*, Cambridge University Press, *10*, pp.333–352.
Shioya, T., Nakamura, H., Ishii, N., Takahashi, N., Sakamoto, Y., Ozaki, N., Kobayashi, M., Okano, K., Kamada, T. and Muraguchi, H. (2013) The *Coprinopsis cinerea* septin *Cc.Cdc3* is involved in stipe cell elongation. *Fungal Genetics and Biology*, *58*, pp.80-90.
Subba, S. (2015) Morphological and anatomical study on growth and fruiting body developmental stages in *Coprinopsis cinerea*. (Master thesis in the dept. of Molecular Wood Biotechnology and Technical Mycology, Göttingen University).
Subba, S., Winkler, M., and Kües, U. (2019) Tissue staining to study the fruiting process of *Coprinopsis cinerea*. *Acta Edulis Fungi*, *26*, pp.29-38.
Swamy, S., Uno, I., Ishikawa, T. (1984) Morphogenetic effects of mutations at the *A* and *B* incompatibility factors in *Coprinus cinereus*. *Journal of General Microbiology*, *130*, pp.3219-3224.

Tsusu´e, Y. M. (1969) Experimental control of fruit body formation in *Coprinus macrorhizus. Development Growth Differientiation, 11*, pp.164–178.
Velagapudi, R. (2006) Extracellular matrix proteins in growth and fruiting body development of straw and wood degrading basidiomycetes (Doctoral dissertation, Georg-August-University of Göttingen).

Subchapter 4.2. Studying formation of primordia stages of *C. cinerea* through proteomics

PROTEOMES IN PRIMORDIA DEVELOPMENT OF *COPRINOPSIS CINEREA*

MAJCHERCZYK Andrzej*, DÖRNTE Bastian*, SUBBA Shanta*, ZOMORRODI Mojtaba, and KÜES Ursula†

Department of Molecular Wood Biotechnology and Technical Mycology, Büsgen-Institute and Goettingen Center for Molecular Biosciences (GZMB), University of Goettingen, Büsgenweg 2, 37077 Göttingen, GERMANY

* Equal contributors

† Corresponding author: ukuees@gwdg.de

DOI: 10.16488/j.cnki.1005-9873.2019.03.005

Abstract

Fruiting body formation of *Coprinopsis cinerea* takes place at 25 °C under a 12 h day/12 h night regime. It starts by intense local hyphal branching with production of primary hyphal knots in the dark. A first light signal induces then the transfer into the compact secondary hyphal knots. In these, cap and stipe tissue begin to differentiate which underlies distinct patterns of light- and dark-regulated events during primordia development over the following five days in order for the mushrooms to mature on the next day. To gain insight into the complex cytological processes during the cap and stipe tissue development we isolated total proteomes from distinct primordia stages for MS/MS analysis. Between 1672 and 2663 proteins were detected in the different samples and 1401 proteins in overlap between all samples (with at least two peptides with confidence of 99%). Known proteins in primordia development were identified in the samples.

Key Words: Hyphal knots, primordia, fruiting bodies, protein functions, proteomics, mass-spec

Introduction

The edible coprophilous mushroom *Coprinopsis cinerea* is the ideal Agaricomycete to study fruiting body development in the laboratory[1,2]. The complete fruiting process takes places at 25 °C and needs only 7 days. It follows a strict scheme of events which are synchronized by light and dark signals given by day and night shifts[2-4]. Studies in culture address fundamental developmental and physiological questions such as environmental regulation of fruiting including light, temperature, humidity and nutrition, differentiation of cap and stipe tissues, tissue interactions and tissue regeneration abilities, contributions of specific enzymes to steps in development and basidiospore shedding, roles of intracellular carbohydrates (e.g. glycogen) and nitrogen compounds (ammonium, nitrate), metabolic exudates, osmotic turgor regulation and more[1-4].

Fruiting body development is genetically controlled by the mating type loci *A* and *B*[5,6]. Therefore, fruiting bodies typically form on the dikaryon[1]. However, Swamy et al.[7] obtained a self-compatible mutant (*Amut Bmut*) with genetic defects in both mating type loci which is able to fruit without mating to another strain. This fertile mutant is of exceptional value for research on the complex fruiting body development. Detailed morphological descriptions of the fruiting pathway have concentrated on this mutant[2-4,8]. Because of a single haploid genome, it is possible to obtain from the strain both dominant and recessive mutations in the fruiting pathway[1,9-10] and to characterize mutated genes by cloning and transformation[11-19]. More recently, the sequence of the genome of the strain[20] has been provided in addition to that of the formerly sequenced monokaryon Okayama 7[21]. This started a new age of research of 'omics' investigations on transcriptomes[20-25] and proteomes[25,26]. So far, two initial publications on proteomes of an early primordial stage[25] and on effects of gravity on fruiting[26] are available. Here, we present a first proteomic insight over the consecutive process of tissue development in physiologically active primordia.

Material and Methods

1. Organism and Culture Conditions

C. cinerea AmutBmut (*A43mut*, *B43mut*, *pab1*) is a self-fertile homokaryotic mating-type mutant that easily forms fruiting bodies with meiotic basidiospores[7,8] on fresh artificial YMG/T medium (per l: 4 g yeast extract, 10 g malt extract, 4 g glucose, 100 mg tryptophan, 10 g agar) under standard fruiting conditions (25 °C, 12 h light, 12 h dark; high humidity[10]). Following inoculation of a small mycelial piece in the center of a plastic Petri dish (9 cm in Ø) at the end of a working day, the fungus is cultured for 5 days at 37 °C under high humidity in the dark (warranted by growing in dark ventilated boxes on wet paper tissues) until the

mycelium nearly reaches the edges of the plate (at < 1 mm distance to the plastic edge; Fig.1A) which takes about five times 24 h[3.4]. Fruiting is then induced by transferring the mycelial plates on Day 0 (Fig. 1A) into a climate chamber run under standard fruiting conditions ('light-switched-on' at 9 o'clock of a working day, 'light-switched-off' at 21 o'clock of a working day, which allows first illumination of plates for 3-4 h on Day 0). Every subsequent morning, fungal development is newly synchronized in the climate chamber by 'light-switched-on', a moment which is arbitrarily set as 'hour 0' for a fungal development day of 24 h[3,4]. These consecutive 24 h periods are denoted Day 1, Day 2, etc. (Fig. 1). Secondary hyphal knots (Sks) and developing primordia (P1 to P5) for protein analysis were accordingly collected every consecutive day starting at 'hour 0'. Physiologically active structures of same age were collected per plate in a same tube. Collected samples were immediately frozen in liquid nitrogen, weighted in frozen condition and stored at -20°C until freeze-drying for further use.

2. Protein Isolation and Characterization

Lids of Eppendorf tubes with frozen fungal samples were opened, oval glass beads (1.2 x 0.9 cm) positioned vertically onto the opening of the tubes, and samples freeze-dried at -20 °C for 4 days (freeze-drier P4K, **Dieter Piatkowski, Munich, Germany**). All dried samples were ground in Eppendorf reaction tubes with five 4 mm and two 5 mm stainless steel balls in a Retsch Mixer Mill MM400 (Retsch, Haan, Germany) at the temperature of liquid nitrogen. Dry weights of mycelial powder were determined with a Cubis MSA2.7S (Sartorius, Göttingen, Germany) balance.

Typically, 4 mg of dry material was extracted for 1 h at 50°C with 150 µl 100 mM NH_4HCO_3 buffer, pH 8.0 with 10 mM DL-dithiothreitol (DTT). After centrifugation, total proteins from 100 µl supernatant aliquots were purified by a chloroform/methanol protocol[27]. Precipitated proteins were digested by trypsin following the standard protocol of the supplier (https://www.serva.de/www_root/documents/37286%20Trypsin%20MS%20approved%20Ver%1216_e_1.pdf; Serva, Heidelberg, Germany). Resulting peptides were purified by StageTips[28] and dissolved in water with 2% acetonitrile and 0.1% formic acid just prior to MS/MS analysis.

Peptides were analyzed by nanoLC (Eksigent 425, Sciex, Darmstadt, Germany) coupled to a TripleTOF 5600+ mass spectrometer (Sciex) (Eksigent 425, Sciex, Darmstadt, Germany) via NanoSource III (Sciex) and controlled by Analyst TF 1.6 software. Samples were dissolved in 20 µl loading buffer (2% aqueous acetonitrile [ACN] with 0.1% formic acid) and 5 µl were concentrated and desalted on self-made trap column (100 µm ID × 25 mm) packed with 5 µm Reprosil-Pur 120 C18-AQ phase (Dr. Maisch, Ammerbuch-Entringen, Germany). After 10 min loading and washing with loading solvent at 10 µl/min, peptides were separated on reversed

phase-C18 (3 µm Reprosil-Gold C18, Dr. Maisch) packed in a capillary column (75 µm ID × 300 mm). Peptides were eluted at 260 nl/min (column temperature 35 °C) in a linear gradient of solvent A (5% ACN in water with 0.1% formic acid) and B (100% ACN with 0.1% formic acid): 40% B in 70 min, 60% B in 20 min, 95% B in 2 min).

LC-MS/MS analysis was performed using a data-dependent acquisition method with Top30 ions with an MS survey scan of m/z 375–1250 accumulated for 350 ms. MS/MS scans of m/z 100–2000 were accumulated for 75 ms. Precursors above a threshold MS intensity of 150 cps with charge states 2+, 3+ and 4+ were selected for MS/MS, the dynamic exclusion time was set to 15 s.

Data were analyzed and identified using program ProteinPilot (v. 5.0.1, Sciex). The protein fasta-file of *C. cinerea* AmutBmut pab1-1 (v1.0) used for data searches was downloaded (https://genome.jgi.doe.gov/Copci_AmutBmut1/Copci_AmutBmut1.home.html) from JGI (DOE, Walnut Creek, CA, USA). Minimum score for protein identification was set to values corresponding to maximum False Discovery Rate (FDR) of 0.05 and at least two identified peptides with confidence of 99%.

For gel-electrophoresis, precipitated undigested proteins extracted as above from equal amounts of 4 mg sample dry weight were dissolved in 30 µl of NuPage-LDS sample buffer (Invitrogen, Carlsbad, MA, USA) and each 10 µl was loaded on a 1 mm Bolt bis-Tris Plus 4-12% gradient gel (Invitrogen), run at 200 V for 20 min and stained with colloidal Coomassie G250[29].

Results

1. Primordia Development

Upon transfer of fully grown YMG/T cultures (Fig. 1A) at Day 0 from 37 °C in the dark into standard fruiting conditions, hundreds of light-induced secondary hyphal knots (Sks) are typically visible as compact but yet undifferentiated hyphal aggregates (Fig. 1B,C) at the start of Day 1 of cultivation within the youngest mycelium at the edges of the colonies (Fig. 1A) where they arise as first fruiting-body-specific structures from primary hyphal knots (Pks) as initial looser hyphal aggregates[3,4,8]. Within subsets of Sks on a plate, cap and stipe tissue differentiation initiates. Already at Day 2 of cultivation, a minute mushroom shape with cap and stipe becomes visible in the smallest primordium stage P1 (Fig. 1B,D). With every further day in cultivation, growing primordia increase in sizes and progress in differentiation of cap and stipe tissues (Fig. 1B). Primary gill rudiments at the lower edges of the cap are seen first at primordium stage P2 (Fig. 1B,E). The gills enlarge quickly in size and secondary gills are initiated in between, in order to be fully established with probasidia in the hymenium[3,4,30] at

primordium stage P4 (Fig. 1B). Here, a light signal induces prekaryotic S1-phase DNA replication and nuclear fusion. Karyogamy is finished at the primordial stage P5[30,31] that is reached on Day 6 of cultivation (Fig. 1B). Meiosis and basidiospore production follow shortly after during the Day 6[1-4,30,31] and are paralleled by stipe elongation and cap opening for fruiting body maturation (not shown here)[1-4].

Development of different structures on a same plate is synchronized by light[1-4,30,31]. Nevertheless, every day during cultivation subsets of structures are abandoned from further development (Table 1). Abandoning of selected structures and further growth of other structures happens regularly distributed over the whole outer edge of a plate (not further shown), suggesting the presence of a developmental program that defines continuation of development of selected structures by relative distances of structures to each other. We counted numbers of actively growing primordial structures on subsets of plates (Table 1). No significant differences in between different series of cultivations were observed in numbers of abandoned and of continuing structures. In total at completion of primordia development (P4 and further at P5; Fig. 1B), there were only about 2% and 1% of all originally initiated structures that continued development up to Day 5 of cultivation (Table 1). Usually, all stages which reach P5 will continue in development into mature fruiting bodies (here not further shown).

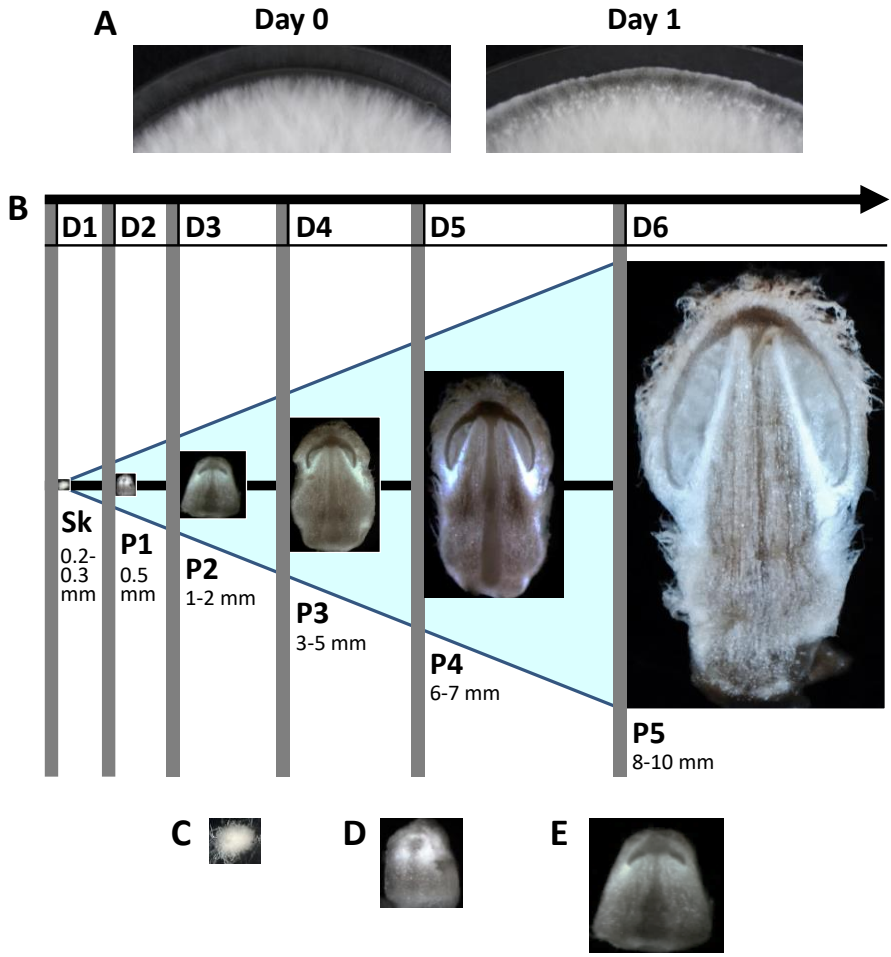

Fig. 1 Fruiting body development of *C, cinerea* AmutBmut.

A. Fully grown YMG/T plate at Day 0 at the time of transfer from 37°C in the dark into standard fruiting conditions and plate at next morning (Day 1 of incubation) with secondary hyphal knots produced at the edge of the mycelium. **B.** Progress in primordia development between Day 1 to Day 5 (D1 to D5) of incubation. Sk (secondary hyphal knot) and P1 to P5 (primordial stages at

Day 2 to Day 6 of incubation when light switches on = 0 h) are defined as those developmental states that are reached at the start of a respective 24 h day[2-4]. Structures are shown in relative size to each other and approximate sizes of structures in mm are added. **C.** Sk and **D.** P1 shown four-fold an **E.** P2 two-fold enlarged as compared to **B.**

Table 1 Physiologically active and senescent primordial structures in cultures of *C. cinerea* homokaryon AmutBmut under standard fruiting conditions (n = 5 plates each from each 5 different experiments, in total 25 plates per case)

Stage	Day	Structures per plate		
		Actively growing	% aborted	
			Compared to day before	Compared to Day 1
Sk	1	273.2 ± 69.5	-	-
P1	2	92.1 ± 25.7	66.3	66.3
P2	3	72.2 ± 22.1	21.6	73.6
P3	4	29.9 ± 8.9	58.5	88.9
P4	5	6.1 ± 1.2	81.7	97.7
P5	6	2.8 ± 1.3	54.0	98.9

2. Harvesting structures

On Day 1 of cultivation, Sks seem morphologically not to differ from each other (Fig. 1B), unlike later primordia structures (P1 to P5) on subsequent days of cultivation. Every morning, with careful observation and good experience it is possible to discriminate among primordia structures those that will continue in development from those that give up and become senescent. Structures with ongoing development have a fresh whitish to light-beige appearance with, in P2 to P5, a light rosy color of the veils at their apex. In contrast, aging structures turn greyish with drying veils which in consequence will appear scrubbier. Also, aging structures somewhat shrink in diameter by desiccation. As a further phenotype of good physiological

activity, small liquid droplets collect on healthy growing structures while they are missing on aging structures (not shown).

Target of the study was to obtain the proteomes of actively growing structures in primordia development. For proteome analyses, all healthy growing structures were therefore selectively collected from individual plates into individual tubes. Sampling times for the multiple tiny Sks and P1 structures per culture (Table 1) took up to 2 h for each 5 in parallel grown plates (under a binocular), about 1 h for P2 and 20 min for P3 structures (also under a binocular) from each 5 plates and about 10 min for P4 and P5 structures which are large enough to be evaluated by the naked eye. Structures per plate were dissected with a sterile needle from the vegetative mycelium, transferred into individual Eppendorf-tubes and directly frozen in liquid nitrogen. Wet weights and after freeze-drying dry-weights were determined from one experiment with five plates each (Table 2).

Table 2 Average wet and dry weights (in mg) of harvests of actively growing structures from cultures of homokaryon AmutBmut under standard fruiting conditions (n = 5 plates per case)

Stage	Day	Wet weight	Dry weight
Sk	1	8.46 ± 3.31	1.38 ± 0.55
P1	2	5.36 ± 1.42	1.15 ± 0.50
P2	3	7.86 ± 2.86	4.81 ± 1.14
P3	4	16.96 ± 0.55	7.22 ± 2.99
P4	5	115.62 ± 34.34	12.08 ± 3.78
P5	6	119.48 ± 41.36	10.74 ± 3.85

3. Characterization of Proteomes during Primordia Formation

Total proteins were isolated from 4 mg dry weight of each harvested stage from Sk to P5, respectively and separated by 1D-gel-electrophoresis as shown in Fig. 2. Overall banding patterns were very similar to each other. In particular the Sk sample appeared to have some bands not seen in other stages (compare lanes in Fig. 2) which might thus be specific to this

early stage in development. Some bands of higher molecular weight appear newly in P samples. There are also some stronger bands of lower molecular weight with increasing staining intensity in all tracks of P samples on the gel (Fig. 2).

So far, only a few proteins were specifically identified from *C. cinerea* primordia. Among are as highly expressed primordia-specific lectins the galectins Cgl1 and Cgl2[8], the galectin-like Cgl3[32] and the β-trefoil proteins Ccl1 and Ccl2[33], the serine protease-inhibitor Cospin[34], and assortments of hydrophobins[35]. All these proteins were shown in the previous works to be secreted with molecular weights analyzed in 1D-gels[8,32-35]. Stronger bands in the 1D-gel shown in Fig. 2 correspond in position to the known molecular weights of the mature proteins (positions are marked at the right border of the gel).

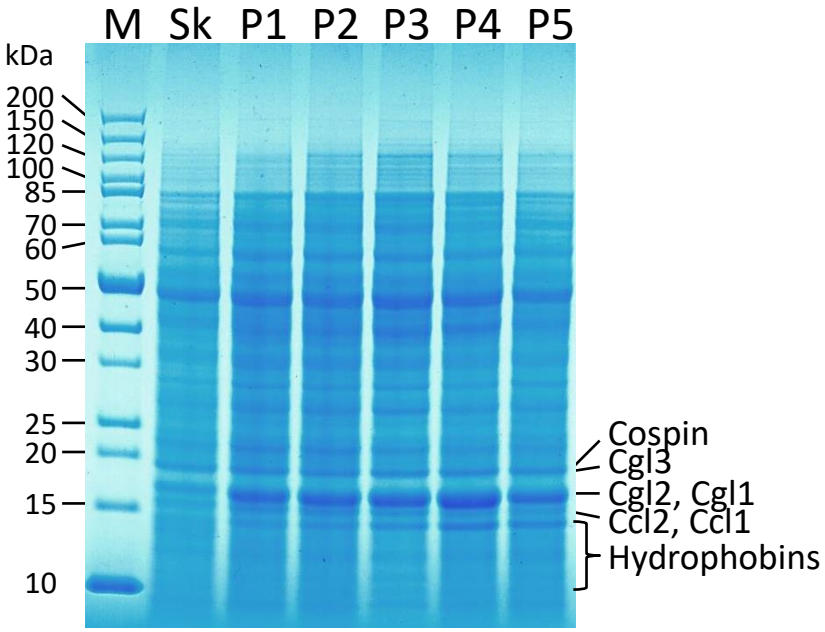

Fig. 2 Coomassie-stained proteomes of secondary hyphal knots (labeled Sk) and primordia of developmental stages P1 to P5 (see Fig. 1) in the process of fruiting body formation of *C. cinerea* AmutBmut.

Expected positions in 1D-gel-electrophoresis of proteins known to be expressed in *C. cinerea* primordia are indicated with names at the right.

To define specific proteins of the individual developmental stages, protein samples of 4 mg powdered dry primordial stages P1 to P4 were trypsin-digested and subjected to MS/MS analysis. From all samples, about 2870 single proteins were identified by the analysis using nanoLC and LC-MS/MS (TripleTOF 5600+) and a stringent cut-off (FDR 0.05, at least two identified peptides with confidence of 99%; Fig. 3). About 2700 proteins were detected in stage P1 and about 2200 proteins in stages P2-P4. More than a half of the proteins (1401) were shared by all stages. Further analysis showed over 550 proteins as unique to the P1 stage and around 20 to 60 proteins unique to samples P2-P4 each (Fig. 3). Using unfiltered MS/MS outputs with less stringent cut-off (at least 1 peptide with 99% confidence), data were about 4000 proteins in P1 (over 700 unique) and 3200 proteins in P2-P4 (in each around 200 unique), with almost half of the proteins (about 2200) shared by all.

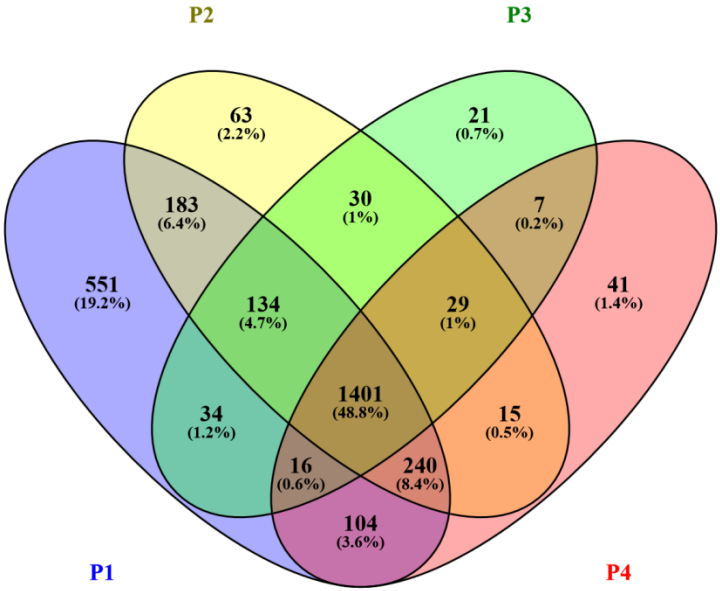

Fig. 3 Venn-diagram of proteins identified by LC-MS/MS in stages P1-P4 with at least two distinct peptides with confidence of 99%

In the following, we searched the unfiltered MS/MS outputs for hits (at least 1 peptide of 99% confidence) of proteins with known functions in fruiting body development. Results in Table 3 are assorted by the developmental process in which they function. Most of the fruiting-body-related proteins were detected in one or more of the four analyzed stages of primordia differentiation, 19 of them by two or more peptides and 11 others by one peptide with 99% confidence while often in several samples.

Transcriptional regulators and signaling proteins required upstream of fruiting body development for induction and progress of Sk formation from Pks (*A* and *B* mating type proteins[21,36], Pcc1[37], Clp1[38], cohesin complex subunit Smc1[14]) and the also critical mitotic cell-cycle checkpoint proteins Atr1 and Chk1[39] were not found in the P1 to P4 protein samples but peptides for proteins Arp9, Snf5, Pex1, Rmtl1 and Csf1 which are needed for primary or secondary hyphal knot formation (Table 3).

Further with regards to stipe development, protein Eln2 for a putative cytochrome P450 with functions in primordial shaft tissue organization[12] and the regulator WC2 (putative partner of

the found photoreceptor Dst1/WC1 for the white-collar transcription factor complex) for light-controlled suppression of dark stipe development (improper proliferation of stipe tissues happening without illumination) and coordination of gill tissue differentiation in the cap[40] were missing, as well as protein Ctg1 which is highly expressed in normal stipe elongation after passing stage P5[41].

Proteins involved in stipe and cap tissue development, Dst1[42], Dst2[43], Eln3[13], Ich1[11], and Exp1[15] were identified in P1 samples and often also in later P samples (Table 3), in accordance to phenotypes of mutants of these proteins based on failures in proper tissue formation and organization likely starting in P1. While essential for gill formation, transcriptional regulator Cag1[19] was an exception with presence in P2 and P4 samples. As a Tup1 homolog, Cag1 might be expected to interact with transcriptional coregulators Ssn6 and McmA[44] which were both detected in all protein samples. We further searched for homologs of transcription factors shown to be involved in fruiting body development in *Schizophyllum commune*[45]. Homologs of Fst3, Fst4 and Bri1 were found (Table 3) unlike homologs for transcription factors Hom1, Hom2 and Gat1.

Regarding highly expressed small secreted proteins, all expected lectins, the serine protease inhibitor cospin and at least 11 different hydrophobins were present in the protein samples (Table 3).

Table 3 Selected proteins identified by LC-MS/MS in stages P1–P4

Gene	JGI protein ID	Putative protein function and morphological effect	Number of peptides found in each primordial stage*				Distinct peptides
			P1	P2	P3	P4	
Primary hyphal knot (Pk) formation							
arp9[47]	185247	SWI-SNF chromatin remodeling complex associated, actin-related; essential for Pks	10	3	1	1	ALQETVGR, AQNESPVLLTLPIPVPSR
snf5[17]	365798	SWI-SNF chromatin remodeling complex, Snf5 subunit; essential for Pks	1	1	-	-	QSFLPSLVSGAR
pex1[48]	471411	Peroxisome biogenesis factor 1; essential for Pks	1	-	-	1	LLTEVFLR
Secondary hyphal knot (Sk) formation							
rmt1[16]	485296	Arginine methyltransferase; essential for Sks	8	6	3	5	AVVTDPYMLK, DLDIGISYK
csf1[18]	365330	Cyclopropane fatty-acid synthase; essential for Sks	2	-	-	-	VGWGAVVR FVNSLSNSR
Stipe tissue differentiation							
eln3[13]	354559	Glycosyltransferase; membrane protein; stipe elongation	1	1	1	1	ALTGTSPGVEVK
cdc3[40] (*eln8*)	416864	Septin family protein (P-loop GTPase); stipe cell elongation	13	9	9	11	ADTLTDEEVAEFK EPLPPSAERPK
cdc1[40]	455217	Septin ring protein CDC10; stipe cell elongation	10	7	10	10	ADSLTLEER AQSYVGFDSITQQIEHK
dst1[42]	369621	WC1-type of photoreceptor and transcription factor; suppression of dark stipe formation	1	-	-	-	FLQSPTGK
dst2[43]	361584	Oxidoreductase activity, FAD binding; suppression of dark stipe formation	7	18	8	14	SLDQDLYDELSSLCRG GPVVLNDDPDFVNYATIFNGNVETR
Cap tissue differentiation							
ich1[11]	545797	*O*-Methyltransferase activity; pileus tissue formation	1	-	-	-	APSSIIDIR
exp1 [15]	421729	HMG1/2-like transcription factor; essential for pileus expansion and autolysis	2	-	-	-	LAPSAWQLYFTDWIQK RENAFRAAQR
cag1[19]	466216	Transcriptional corepressor, Tup1 homolog; essential for gill formation	-	1	-	1	LNENFDVVR
Surface and defense proteins							
cgl1[8]	473274	Galectin; galactose-binding lectin	1	1	2	1	MLYHLFVNNQIK LQDDFK
cgl2[8]	488611	Galectin; galactose-binding lectin	1	1	1	1	LQNDFK
cgl3[32]	539794	Galectin; galactose-binding lectin	2	1	1	1	MFHILR VEGTAIAR
ccl1[33]	456849	β-Trefoil lectin	4	4	4	4	LALTYPGYQR TVYWNAGEAVANTK
ccl2[33]	408852	β-Trefoil lectin	3	3	2	3	LALTYPGR TPVTVSPLDGSSEQAWILR
cospin1 [34]	367957	Serine protease inhibitor	3	4	5	4	GAPVAPQEGK VLPEDNNSGNSWVVEK
coh16[21]	437827	Hydrophobin	1	1	1	1	LEEVTSLNTGVGK
coh17[21]	437809	Hydrophobin	2	2	2	1	ALEWTTTR LIGLLGLDLK
coh18[21]	443707	Hydrophobin	2	2	2	2	SVQSLEWTTK SLLGLLGIDLK
coh21[21]	370922	Hydrophobin	7	3	1	3	LVNLADEVIHVR ITGLLHLDLK
coh22[21]	409790	Hydrophobin	1	1	-	-	WLGFLNINAR
coh23[21]	354674	Hydrophobin	4	3	2	3	VQDSKSLDAGVK TAVNVVGVGGGSH
coh26[21]	47183	Hydrophobin	1	1	1	1	LLNLLNIDVK

coh27[21]	404033	Hydrophobin	3	4	2	2	ADSLDYNTSK KLLGLLNIDVK
coh28[21]	442540†	Hydrophobin	2	1	2	2	SLDQSLTK LLGLLKVDVK
coh30[21]	407897	Hydrophobin	-	1	-	-	LLGLLKVDIK
coh32[21]	445156	Hydrophobin	-	3	1	1	SLDNEVTKLLGHLK LLGHLKIDAK
Other transcriptional regulators of possible importance in fruiting							
mcmA[44]	419006	MADS-box transcription factor	1	1	1	1	LQPLVTQPEGK
ssn6[44]	221461	Transcriptional corepressor of Tup1	4	5	1	1	AYSAYQQALYLLPNPK LWYGIGILYDR
fst3[45]	463573	Fungal specific transcription factor	1	-	-	-	IESLLK
fst4[45]	365344	Zinc finger transcription factor	2	2	1	1	APSTPLAHYALQSLER AAVILPFAGK
bri1[45]	447209	Bright/BRCAA1/RBP1 DNA binding protein	4	1	1	1	QHGFLQGLHNLMAIR LWGTVFQNGGGR

* Only peptides with 99% confidence are listed and only a maximum of two peptides are presented

† CoH28 is given as one hydrophobin possibility. Alternative proteins containing the same peptides: CoH29 (380326), CoH31 (442548), CoH33 (442540), CoH34 (380326)[21].

Discussion

Proteomics work on fruiting body development of *C. cinerea* was so far limited to two studies. Plaza et al.[25] harvested early primordia (presumably P1 to P2 structures but undifferentiated for active and aborted structures) for protein analysis and detected in total 345 proteins in their primordia sample, nearly tenfold less than we found in this study. Of the identified proteins listed in Table 3, only the septin Cdc3, the septin ring protein Cdc10 and the lectin Ccl1 are shared with the study of Plaza et al.[25]. These authors concluded that their analysis was highly biased in detection towards abundant and soluble proteins. Kim et al.[26] concentrated on analysis of 69 differentially expressed stalk proteins of fruiting bodies grown under either normal or perpendicular direction of agar plates. While Cdc10 was also found shared in this study, the work on mature fruiting bodies is of less relevance for our study here.

We have started to dissect the distinct proteomes of physiologically active primordia stages in fruiting body development of *C. cinerea* (Fig. 3). About 2700 (over 3000 under less stringent cut-off) different proteins per stage were identified by MS/MS analysis which now await grouping to functions and pathways and analysis of up and down dynamics in their expression. Primordia of *C. cinerea* are complex structures which undergo over the time many distinct differentiation processes (Fig. 2). It is estimated that >30 different cell types may occur during the process of fruiting body development in *C. cinerea*[2]. Exact microscopic analyses of primordia[4] at defined times in the 12 h light/12 h dark cycle (Fig. 2) are required to link specific sets of proteins to changing morphologies and to functions of distinct cells.

While the protein pattern in the 1-D gelectrophoresis between stages was very similar with only some bands recognisable to be specific (Fig. 2), the proteomics data revealed many unique

proteins in the individual samples (Fig. 3). We present here our first results on protein identification during the process of primordia differentiation. However, further studies are needed to disclose the reliability of protein detection per primordia stage.

High reliability of perfect identification of structures to be analyzed and methods for protein extraction, digestion and MS/MS separation for peptide identification is required for best valuable results. Sampling of structures is very difficult by their tiny sizes, because many of them are abortive (Table 1), and by the fact that active ones will continually develop further which restricts sampling times of physiological active primordia of same age. Samples of small weights are afterwards available for isolation of proteomes. First, we tested 8 mg powdered material in proteome isolation but subsequently several times probes failed in trypsin digestion for the MS/MS analysis. Using only 4 mg dry weight proofed to be effective (Fig. 2). It should be further noted that for a single proteomics run from 4 mg material, it will need complete collections from about three distinct plates at least for *C. cinerea* stages Sk and P1 whereas for stages P2 to P5 the material from a single plate can be sufficient (Table 2).

In the further, it is however difficult to measure the protein amount in the samples. Measurements of concentration in protein samples from fungal mycelium and tissues have been found unreliable due to difficulties in separation of proteins from polysaccharides and metabolites. Classical assays with Bradford Reagent (Coomassie) or BCA for example fails therefore in correct determination of protein amounts[46]. Running gels is the best method for reliable results on protein amounts while it wastes the isolated protein material.

A strategy in proteomics for difficult to collect samples in sufficient amounts for protein isolation (e.g. for the tiny Sks from *C. cinerea* and physiological active primordia of same age) is therefore to optimize the protein isolation protocols to routinely obtain same protein amounts from one isolation optimal for finally one run on a mass spec. In total for this study, we performed three series of parallel proteome isolations from samples Sk to P5 for analysis by 1D-gel-electrophoresis. In the 1st round, the Sk sample was degraded, the P3 sample contained less and the P5 sample more protein than samples P1, P2 and P4 (not shown). In the 2nd and 3rd round, the protein amounts from parallel isolations were more alike as deduced from gel electrophoresis (Fig. 2 and not shown). A final protein isolation using one P3 and five independent P5 collections resulted in gel electrophoresis in five equally stained protein lanes and one slightly stronger stained P5 lane. With more experimental routine, sample preparation seems to become more constant.

We have found in our first proteome analyses of primordial stages of *C. cinerea* generally more proteins than Plaza et al. in their primordia sample[25] and we have identified many more proteins known to act in the primordia differentiation (Table 3) than these authors. Notably, we

have identified also proteins of expected low expression, for example several transcription factors. On the other hand, some expected proteins with functions in fruiting were missing by possible reasons that we might have so far not exactly looked at the respective stages at which these protein are acting, most likely prior to or at stage Sk. In the future, we will need to run sufficient independent biological repeats of digested proteome per all differential stages in mass-spec in order to perform a deeper comparative protein analysis between the different stages.

Conclusions

C. cinerea is an excellent model fungus for studying fruiting body formation in the Agaricomycetes, among due to the unique synchronized fruiting body development which is controlled through daily light and dark phases. Modern 'omics' data suggest that very large groups of genes contribute to the process of fruiting body development. We are studying the proteomes of primordia at distinct stages of development to further define the multiple genetic functions contributing to tissue formation and cellular differentiation during the development. Here, we have explained conditions of good sample collection and proteome preparation which leads to successful identification of large groups of proteins in mass-spec. Our first proteome analysis of distinct primordia sample identified many of those proteins known from mutant analyses to be important for development.

Acknowledgements

Proteomics studies were facilitated through support for a TripleTOF 5600+ mass-spec by the German Science Foundation (DFG grant no. 24946052).

References

[1] KÜES U. Life history and developmental processes in the Basidiomycete *Coprinus cinereus* [J]. Micobiology and Molecular Biology Reviews, 2000, 64:316-353.

[2] KÜES U, NAVARRO-GONZALÉZ M. How do Agaricomycetes shape their fruiting bodies? 1. Morphological aspects of development [J.] Fungal Biology Reviews, 2015, 12:99-107.

[3] KÜES U, SUBBA S, YU Y, *et al.* Regulation of fruiting body development in *Coprinopsis cinerea* [C]. Mushroom Science, 2016, 19:318-322.

[4] SUBBA S, WINKLER M, KÜES U. Tissue staining to study the fruiting process of *Coprinopsis cinerea* [J]. Acta Edulis Fungi, in revision.

[5] KÜES U, GRANADO JD, HERMANN R, *et al.* The *A* mating type and blue light regulate all known differentiation processes in the basidiomycete *Coprinopsis cinerea* [J]. Molecular and General Genetics, 1998, 260:81-91.

[6] KÜES U, WALSER PJ, KLAUS MJ, *et al.* Influence of activated *A* and *B* mating-type pathways on developmental processes in the basidiomycete *Coprinus cinereus* [J]. Molecular and General Genetics, 2002, 268_262-271.

[7] SWAMY S, UNO I, ISHIKAWA T. Morphogenetic effects of mutations at the *A* and *B* incompatibility factors in *Coprinus cinereus* [J]. Journal of General Microbiology, 1984, 130:3219-3224.

[8] BOULIANNE RP, LIU Y, AEBI M, *et al.* Fruiting body development in *Coprinus cinereus*: regulated expression of two galectins secreted by a nonclassical pathway [J]. Microbiology, 2000, 146:1841-1853.

[9] KANDA T, ISHIKAWA T. Isolation of recessive developmental mutants in *Coprinus cinereus* [J]. Journal of General and Applied Microbiology, 1986, 32:541-543.

[10] GRANADO JD, KERTESZ-CHALOUPOVÁ K, AEBI M, *et al.* Restriction enzyme mediated DNA integration in *Coprinus cinereus* [J]. Molecular and General Genetics, 1997, 256:28-36.

[11] MURAGUCHI H, KAMADA T. The *ich1* gene of the mushroom *Coprinus cinereus* is essential for pileus formation in fruiting [J]. Development, 1998, 125:3133-3141.

[12] MURAGUCHI H, KAMADA T. A mutation in the *eln2* gene encoding a cytochrome P450 of *Coprinus cinereus* affects mushroom morphogenesis [J]. Fungal Genetics and Biology, 2000, 29:49-59.

[13] ARIMA T, YAMAMOTO M, HIRATA A, *et al*. The *eln3* gene involved in fruiting body morphogenesis of *Coprinus cinereus* encodes a putative membrane protein with a general glycosyltransferase domain [J]. Fungal Genetics and Biology, 2004, 41:805-812.

[14] MURAGUCHI H, ABE K, NAKAGAWA M, *et al.* Identification and characterization of structural maintenance of chromosome 1 (*smc1*) mutants of *Coprinopsis cinerea* [J]. Molecular Genetics and Genomics, 2008, 280:223-232.

[15] MURAGUCHI H, FIJITS T, KISHIBE Y, *et al*. The *exp1* gene for pileus expansion and autolysis of the ink cap mushroom *Coprinopsis cinerea* (*Coprinus cinereus*) encodes an HMG protein [J]. Fungal Genetics and Biology, 2008, 45:890-896.

[16] NAKAZAWA T, TATSUTA Y, FUJITA T, *et al.* Mutations in the *Cc.rmt1* gene encoding a putative protein arginine methyltransferase alter developmental programs in the basidiomycete *Coprinopsis cinerea* [J]. Current Genetics, 2010, 56:361-367.

[17] ANDO Y, NAKAZAWA T, OKA K, *et al*. *Cc.snf5*, a gene encoding a putative component of the SWI/SNF chromatin remodeling complex, is essential for sexual development in the agaricomycete *Coprinopsis cinerea* [J]. Fungal Genetics and Biology, 2013, 50:82-89.

[18] LIU Y, SRIVILAI P, LOOS S, *et al*. An essential gene for fruiting body initiation in the basidiomycete *Coprinopsis cinerea* is homologous to bacterial cyclopropane fatty acid synthase genes [J]. Genetics, 2006, 172:873-884.

[19] MASUDA R, IGUCHI N, TUKUTA K, *et al*. The *Coprinopsis cinerea* Tup1 homologue Cag1 is required for gill formation during fruiting body morphogenesis [J]. Biology Open, 2016, 5:1844-1852.

[20] MURAGUCHI H, IMEZAWA K, NIIKURA M, *et al.* Strand-specific RNA-Seq analysis of fruiting body development in *Coprinopsis cinerea* [J]. PLOS ONE, 2015, 10:e0141586.

[21] STAJICH JE, WILKE SK, AHREN D, *et al.* Insights into evolution of multicellular fungi from the assembled chromosomes of the mushroom *Coprinopsis cinerea* (*Coprinus cinereus*) [J]. Proceedings of the National Academy of Sciences USA, 2010, 107:11889-11894.

[22] CHENG CK, AU CH, WILKE SK, *et al*. 5‘-Serial analysis of gene expression studies reveal a transcriptomic switch during fruiting body development in *Coprinospsis cinerea* [J]. BMC Genomics, 2013, 14:195.

[23] CHENG XJ, HUI JHL, LEE YY, *et al*. A “developmental hourglass” in fungi [J]. Molecular Biology and Evolution, 2015, 32:1556-1566.

[24] KRIZSÁN K, ALMÁSI É, MERÉNYI Z, *et al.* Transcriptomic atlas of mushroom development reveals conserved genes behind complex multicellularity in fungi [J]. Proceedings of the National Academy of Sciences, 2019, in press.

[25] PLAZA DF, LIN CW, SEBASTIAAN N, *et al*. Comparative transcriptomics of the model mushroom *Coprinopsis cinerea* reveals tissue-specific armories and a conserved circuity for sexual development [J]. BMC Genomics 2014, 15:492.

[26] KIM JS, KWON YS, BAE DW, *et al*. Proteomic analysis of *Coprinopsis cinerea* under conditions of horizontal and perpendicular gravity [J]. Mycobiology, 2017, 45:226-231.

[27] WESSEL D, FLUEGGE UI. A method for the quantitative recovery of protein in dilute solution in the presence of detergents and lipid [J] Analytical Biochemistry, 1984, 138:141-143.

[28] RAPPSILBER J, MANN M, ISHIHAMA Y. Protocol for micro-purification, enrichment, pre-fractionation and storage of peptides for proteomics using Stage Tips [J]. Nature Protocols, 2007, 2:1896-1906.

[29] CANDIANO G, BRUSCHI M, MUSANTE L, *et al.* Blue silver: a very sensitive colloidal Coomassie G-250 staining for proteome analysis [J]. Electrophoresis, 2004, 25:1327-1333.

[30] LU BC. Meiosis in *Coprinus*. V. The role of light on basidiocarp initiation, mitosis and hymenium differentiation in *Coprinus lagopus* [J]. Canadian Journal of Botany, 1974, 52:299-305.

[31] LU BC. The control of meiosis progression in the fungus *Coprinus cinereus* by light/dark cycles [J]. Fungal Genetics and Biology, 2000, 31:33-41.

[32] WÄLTI MA, WALSER PJ, THORE S, *et al.* Structural basis for chitotetraose coordination by CGL3, a novel galectin-related protein from *Coprinopsis cinerea* [J]. Journal of Molecular Biology, 2008, 379, 146-159.

[33] SCHUBERT M, BLEULER-MARTINEZ S, BUTSCHI A, *et al.* Plasticity of the β-trefoil protein fold in the recognition and control of invertebrate predators and parasites by a fungal defense system [J]. PLOS Pathogens, 2012, 8:e1002706.

[34] SABOTIC J, BLEULER-MARTINEZ S, RENKO M, *et al.* Structural basis of trypsin inhibition and entomotoxicity of Cospin, serine protease inhibitor involved in defense of *Coprinopis cinerea* fruiting bodies [J]. Journal of Biological Chemistry 2012, 287:3898-3907.

[35] PEDDIREDDI S, VELAGAPUDI R, HOEGGER PJ, *et al.* Multiple hydrophobin genes in mushrooms [M]. PISABARRO AG, LAMÌREZ L. VI Genetics and cellular biology of Basidiomycetes, pp. 151-163. Pamplona: Universidád Pública de Navarra.

[36] KÜES U. From two to many: Multiple mating types in Basidiomycetes [J]. Fungal Biology Reviews, 2015, 29:126-166.

[37] MURATA Y, FUJUU M, ZOLAN ME, et al. Molecular analysis of *pcc1*, a gene that leads to a-regulated sexual morphogenesis in *Coprinus cinereus*. Genetics, 1998, 149:1753-1761.

[38] INADA K, MOROMOTO Y, ARIMA T, *et al.* The *clp1* gene of the mushroom *Coprinus cinereus* is essential for a-regulated sexual development [J]. Genetics 2001, 157:133-140.

[39] DE-SENA-TOMAS C, NAVARRO-GONZÁLEZ M, KÜES U, *et al*. A DNA damage checkpoint pathway coordinates the division of dikaryotic cells in the ink cap mushroom *Coprinopsis cinerea* [J]. Genetics, 2013, 195:47-57.

[40] NAKAZAWA T, ANDO Y, KITAAKI K, *et al.* Efficient gene targeting in *ΔCc.ku70* and *ΔCc.lig4* mutants of the agaricomycete *Coprinopsis cinerea* [J]. Fungal Genetics and Biology, 2011, 48:939-946.

[41] NAKAZAWA T, KANEKO S, MURATA H, *et al.* The homologue of *Lentinula edodes ctg1*, a target for CDC5 and its interacting partner CIPB, from *Coprinopsis cinerea* involved in fruiting-body morphogenesis of *C. cinerea* [J]. Mycoscience, 2009, 50:331-342.

[42] TERASHIMA K, YUKI K, MURAGUCHI H, *et al*. The *dst1* gene involved in mushroom photomorphogenesis of *Coprinus cinereus* encodes a putative photoreceptor for blue light [J]. Genetics, 2005, 171:101-108.

[43] KURATANI M, TANAKA K, TERASHIMA K, *et al*. The *dst2* gene essential for photomorphogenesis of *Coprinopsis cinerea* encodes a protein with a putative FAD-binding-4 domain [J]. Fungal Genetics and Biology, 2010, 47:152-158.

[44] KEHELER C, REDD MJ, SCHULTZ J, *et al.* Ssn6-Tup1 is a general repressor of transcription in yeast [J]. Cell, 1992, 68:709-719.

[45] OHM RA, DE JONG JF, DE BEKKER C, *et al.* Transcription factor genes of *Schizophyllum commune* involved in regulation of mushroom formation [J]. Molecular Microbiology, 2011, 81:1433-1445.

[46] FRAGNER D, ZOMORRODI M, KÜES U, *et al.* Optimized protocol for the 2-DE of extracellular proteins from higher basidiomycetes inhabiting lignocellulose [J]. Electrophoresis, 2009, 30:2431-2441.

[47] NAKAZAWA T, ANDO Y, HATA T, *et al.* A mutation in the *Cc.arp9* gene encoding a putative actin-related protein causes defects in fruiting initiation and asexual development in the agaricomycete *Coprinopsis cinerea* [J]. Current Genetics, 2016, 62:565-574.

[48] NAKAZAWA T, IZUNO A, HORII M, *et al.* Effects of *pex1* disruption on wood lignin biodegradation, fruiting development and the utilization of carbon sources in the white-rot Agaricomycete *Pleurotus ostreatus* and non-wood decaying *Coprinopsis cinerea* [J]. Fungal Genetics and Biology, 2017, 109:7-15.

[49] SHIOYA T, NAKAMURA H, ISHII N, *et al.* The *Coprinopsis cinerea* septin CcCdc3 is involved in stipe elongation [J]. Fungal Genetics and Biology, 2013, 58-59:80-90.

Chapter 5

Environmental signals in the fruiting of *C. cinerea*

Subchapter 5.1.

Light signals in the fruiting process of *C. cinerea*

Contribution to subchapter 5.1
Experimental planning: U. Kües and S. Subba
Experimental work and data analysis: S. Subba
Sectioning and staining: M. Winkler
Input into scientific discussion: S. Subba and U. Kües
Manuscript writing: S. Subba
Manuscript reviewed by U. Kües

5.1.1. Abstract

Coprinopsis cinerea takes seven days to form a matured mushroom from the vegetative mycelium under a normal day/night rhythm. Fruiting body development in *C. cinerea* is strictly controlled by the environmental conditions including light, temperature, aeration and nutrients. Among all, light but also dark play a significant role in the initiation and the further development of a fruiting body. As a first step towards initiation of fruiting body, however which is not specific to fruiting, development of a primary hyphal knot (Pk) is formed in the dark. Under standard fruiting conditions by fixed light-dark conditions (12 h light/12 h dark) at 25 °C and high humidity, as a first specific step a light-induced secondary hyphal knot (Sk) generates from Pks and subsequently, primordial stages from P1 to P5 are formed and eventually on the 7th day of the fruiting pathway, the mushroom matures and gets autolyzed. Failure in proper light signaling leads to the formation of so-called 'dark stipes' with extended stipe tissues and blocks in cap development. In contrast, when cultures are kept during Sk and primordia formation for longer periods in constant light, tissue development in primordia continues, but primordia abnormally abolish in further development. In this study, we present the morphological characteristics of *C. cinerea* variably cultivated under constant dark and constant light conditions. Light has been found to be required at every step, from Pk to Sk, Sk to P1, P1 to P2, P2 to P3, P3 to P4 and P4 to P5 while once karyogamy is induced (at P4) there is no further need for another light signal. In contrast, dark phases are required to form Pks and for normal tissue differentiation in all subsequent stages. Without, shapes of growing primordia are altered by being retarded in stipe length and more stretched in diameter of flattened caps while gill development is affected after stage P4. In constant light, probably stress-induced, masses of yellow droplets were secreted by all stages of development, from Pks to stipe-retarded P5s, and from the supporting culture mycelium.

5.1.2. Introduction

C. cinerea is an ideal model organism to study the fruiting body development in *Agaricomycetes* and has thus been studied for more than a century due to its synchronized fruiting body developmental process, in which many cells and tissues develop and differentiate over the time of development. The complexity of the fungus begins with the initial formation of primary and secondary hyphal knots and the complexity within the tissue formation increases as the developmental process progresses (chapter 4).

A primary purpose of living organisms in nature is to reproduce and with their offspring continue their legacy. Accordingly, mushrooms also produce spores and naturally distribute them. In case of mushroom-forming fungi such as *C. cinerea*, both the cap and stipe regions contribute equally to construct a mature spore bearing fruiting body. If cap tissues are designed to produce spores, stipe tissues are also engineered in such a way that their extension growth causes the cap to rise into the air for more effective spore dispersion. Therefore, the coordinated development of both the cap and the stipe is essential for the regular growth of a mature fruiting body (chapter 4).

The synchronized development of fruit bodies is regulated by various environmental conditions such as light, temperature, humidity, aeration and nutrients. Light is one of the main factors that play a crucial role in determining the developmental pathway into which *C. cinerea* enters. The production of a dormant sclerotium from a primary hyphal knot, an alternative route taken by the fungus instead of the fruiting-specific route, is the result of a lack of light signals in the Pk stage (chapter 2.2). Similarly, light not only alters the early initiation processes by suppressing Pk formation and in inducing Sk formation from Pk (chapter 2.1), but its absence disrupts the cellular formation of a growing primordium, which has a direct impact on spore production. In the absence of light, the Sks are formed into "dark stipes" with an elongated stipe and a block in the cap development (Tsusué 1969; Lu 1974a; Kües 2000; Chaisaena 2009). The requirement of light for the fruiting body formation in *Basidiomycetes* has been reported by some researches in the longer past (Brefeld 1877; Buller 1924; Madelin 1956). Buller (1924) cultivated *C. cinerea* (then called as *C. lagopus*) in horse dung under complete darkness and reported that its stipes were relatively longer and the gills were narrower with a relatively more pointed narrower pileus. Following that, Tsusué (1969) was first to publish a picture of dark stipes on synthetic media which she explained as malformed fruiting bodies consisting of long stipes and very tiny underdeveloped pilei. 1/2-minute exposure to light is sufficient for the initiation of the fruiting body developmental pathway but for continued normal development and the differentiation of hymenium further light signals are required (Lu 1974b). A type of elongation growth of the stipe but not cap tissue differentiation can continue in the dark.

Therefore, Lu (1974b) suggested that cap and stipe development is initiated by a common light-dependent mechanism but that their further development is under separate control.

Likewise, it has been also observed that the cultivation of the fungus under constant light delays the growth process and eventually arrest maturation of a fruiting body (Chaisaena 2009). A ``dwarf-primordium´´ as termed by Tsusué (1969) with a short stipe and a dome-shaped cap is formed as a result of constant light. In such treated structures seen in strains of South-East Asian origin, unlike in British strains meiosis is permanently arrested at the diffused diplotene, therefore, the fungus fails to produce basidiospores (Lu 2000). This result shows that the fungus, when originating from warmer regions, also requires at least a dark phase of 3 h to complete the fruiting process (Kamada et al. 1978; Lu 2000).

The mechanism of the stipe elongation in a standard fruiting body has been studied in the past which revealed that the normal stipe elongation is a result of diffuse extension of the cylindrical cells which are vertically oriented and are relatively large forming the upper outer layer of the stipe (Kamada 1994; chapter 4). Other studies reported that the stipe elongates due to manifold cell elongation is restricted to the upper-middle region of the stipe rather than by cell division (Borris 1934; Cox & Niederpreum 1975; Kamada and Takemaru 1977a; Gooday 1985, as also observed in this study, chapter 4). Cytological studies found the presence of narrow and wide hyphae with distinct functions in which narrow hyphae have been suggested to act in nutrient translocation from the stipe to the cap (Moore 1987; Chiu and Moore 1988; Ji and Moore 1993; chapter 4). There has also been an increase in the presence of glycogen in the young stipe, which has been reported to gradually decrease in the fully expanded stipe (Kamada and Takemaru 1977b, 1983; Kamada 1994). According to Moore (1995, 1998) and my own observations (chapter 4), this happens in the narrow hyphae.

With priority given to all information from the previous studies, in this chapter, we focus on the morphological characteristics of the self-fertile homokaryotic strain AmutBmut, which has been cultivated under both, either constant darkness or constant light initiated at various stages of development.

5.1.3. Materials and Method

5.1.3.1. Strains and growth conditions

Homokaryon AmutBmut is a self-fertile strain of *C. cinerea* (FGSC 25122) that by mutations in both mating-type loci can form fruiting bodies without the need of prior mating to another compatible strain (Swamy et al. 1984; Boulianne et al. 2000). For synchronized fruiting, we inoculated strain AmutBmut at evenings (19 h) onto fresh YMG/T agar plates (Granado et al. 1997) for growth at 37 °C in lightproof ventilated boxes, on wetted paper tissue to ensure a high humidity in the boxes. Fully grown plates were transferred 5 days later at the respective hour

(19 h) into an incubation chamber with set fruiting conditions, i.e. 12 h light/12 h dark at 25 °C (= 28 °C on the shelfs with plates during the light periods) and high humidity of 90 % (Granado et al. 1997), for further cultivation. For practical convenience, every day light switches on in the incubation chamber at 9 o'clock in the morning as best adjusted to start of time of workdays. The moment of light switches on in the 12 h light/12 h dark cycle in the chamber is arbitrarily considered zero hours of each new day of mushroom cultivation.

For constant dark experiments, every following morning at 9 o'clock after the 5 days of incubation under constant dark at 37 °C up to stage P5, a subset of cultures plates of homokaryon AmutBmut at successive developmental stages (stages Pk to P5) were transferred into ventilated boxes (with wetted paper tissues) for further incubation under constant darkness on shelfs in the growth chamber set at 12 h light/12 h dark and 25 °C (= 28 °C on the shelfs with plates during the light periods). A similar protocol was applied for determining the behavior of fungus under constant light by incubating plates in a lightened Percival DR-36VL growth chamber adjusted to 28 °C. Observations were made for plates transferred into constant darkness for each developmental stage of transfer either after 24 h of further cultivation for photographing or at the end of the Day 7 of the standard fruiting pathway and compared to control plates that in parallel were constantly hold under the standard fruiting conditions. Plates photographed after 24 h incubation in constant dark received for a short phase of ca 10 minutes light but were transferred back for further 24-h periods of incubation in constant dark and were every 24 h newly photographed until the standard Day 7 of incubation. Similarly in the constant light experiments, observations with photographing were made for each successive stage of development after incubating plates in constant light in steps of 24 hours and collectively for all developmental stages at the end of the experiment on the 7th day of the standard pathway. Longitudinal cuts were done for all both, first after incubation of structures after the first 24 h in constant dark or in constant light and then at the end of incubation on Day 7 of the experiment.

Every constant dark incubation and every constant light incubation experiment was 3x performed with per observed stage each 3 individual plates per the two different incubation schemes.

5.1.3.2. Embedding, micro-sectioning and tissue staining

Please refer to chapter 3 section 2 (Tissue staining to study the fruiting process of *C. cinerea.* Subba et al. 2019) for details in histology techniques.

5.1.3.3. Microscopy and Photography

Freshly harvested dark stipes formed at constant light and dark were harvested at times of incubation mentioned above, longitudinally dissected by a sharp razor blade and photographed

beneath a KL 500 binocular. Stained microtome cross-sections of dark stipes were inspected underneath a Zeiss Axiophot photomicroscope (Goettingen, Germany) with different enlargements. The binocular and the microscope were equipped with a Soft Imaging Color View II Mega pixel digital camera, linked to a computer. Photos were taken and analyzed with Analysis Software program (Soft Imaging System, Münster, Germany).

5.1.4. Results

5.1.4.1. Formation of dark stipes (stages Ds1-Ds5) by 24 h of incubation in constant dark

On Day 0 of the standard fruiting pathway, when fully grown culture plates were exposed to light for a few seconds and then reincubated under constant dark, many Sks were observed on Day 1 appearing around the outer edges of a Petri dish (no extra photo shown here but see Fig. 2 in chapter 2.1). Similarly, cultures incubated under constant dark on Day 1 after the formation of Sks formed tiny but slightly elongated white-colored dark stipes (Ds1) having a size of about 1-2 mm height on the next Day 2 (Fig. 1A). This shows an initial elongation of the stipe of early primordial structures resulting in dark stipes instead of forming a round 0.5 mm-sized stage P1 primordium when Sks fail to receive required light signals for regulation of differentiation. Vertically dissected dark stipes at this stage showed just a faint impression of an inner cap region without any prehymenial developments and demarcation from the stipe while stipe hyphae were elongated while not further distinctly differentiated inner and outer stipe tissues (Fig. 1B).

Stage P1 primordia on Day 2 when kept at constant dark for the next 24 h, on Day 3 transformed into white-colored slender dark stipes (Ds2) of 4-5 mm length covered with a smooth veil (Fig. 1A). The dissected halves displayed tiny but not well-differentiated cap initials corresponding to the normal P1 stage and an inner stipe extended by hyphal elongation being embedded within outer stipe trama of elongated hyphae (Fig. 1B). Stage P2 primordia on Day 3, when kept in dark for next 24 hours, formed dark stipes (Ds3) with a length of 5 to 7 mm on Day 4 (Fig. 1A). The partial veils still remained smooth at this Ds3 stage. A clear distinction between the cap and the stipe were seen on the vertically cut halves of the dark stipe (Fig. 1B).

Next, the culture plates when kept in constant dark at stage P3 on Day 4 and stage P4 on Day 5, formed dark stipes (Ds4) of 7 to 10 mm high and (Ds5) 10 to 13 mm high after 24 hours dark incubation, respectively (Fig. 1A). The pilei of the both stages of dark stipes appeared developed with the hymenial tissues (Fig. 1B). The diameters of the dark stipes at these stages became broader in size at the stipe region and the whole structures were covered by overall tousled partial veils.

The last stage P5 primordium on Day 6 when cultivated under constant dark for the next 24 h, matured and autolyzed at the next day on Day 7 in a normal way, shedding spores in black liquid. This observation shows that a exposure of light at the P4 stage prior to karyogamy is enough for the maturation and the autolysis of the mushroom (Fig. 1A and 1B).

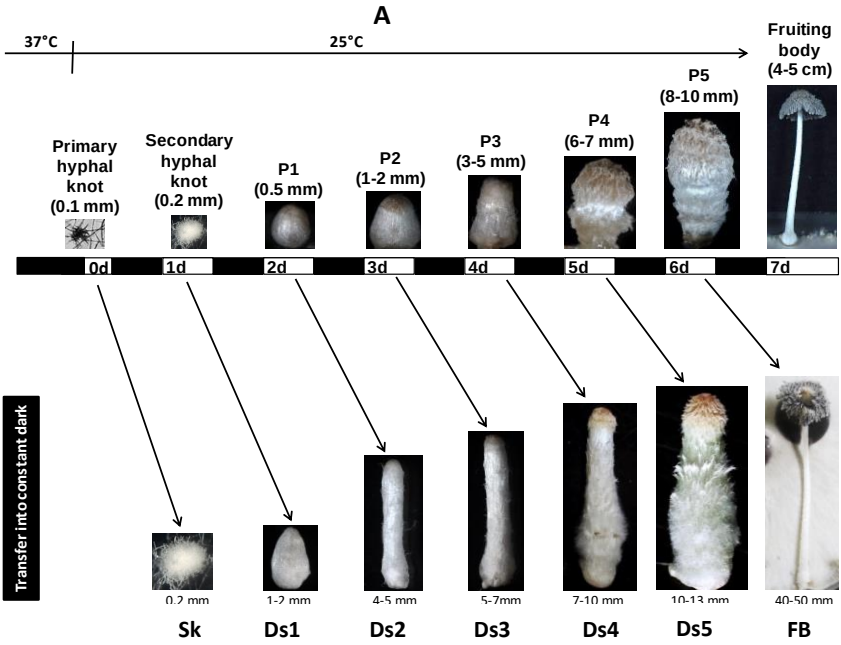

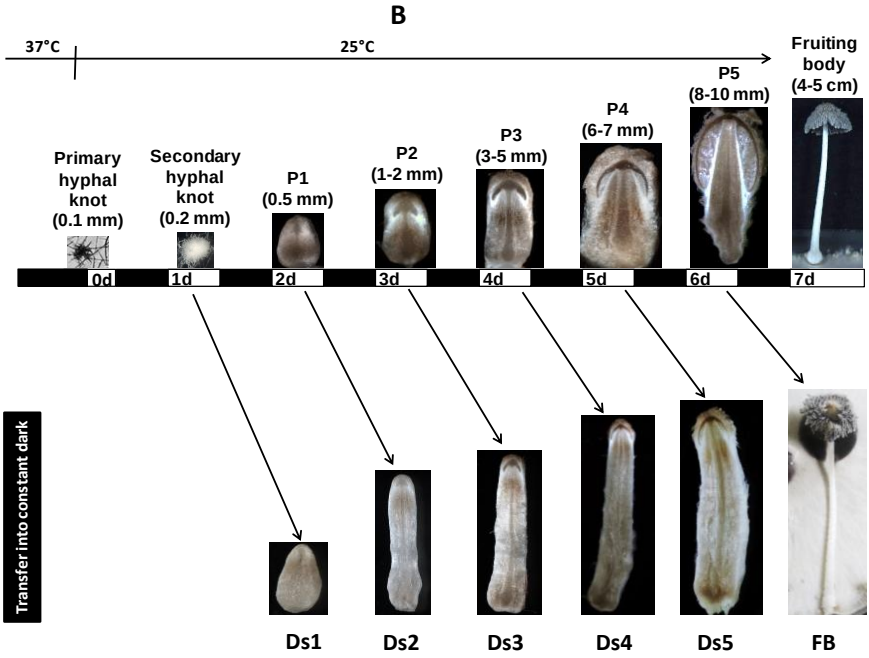

Fig.1. Formation of dark stipes (Ds1 to Ds5) after successive transfer of every primordial stage into darkness with incubation for further 24 h. Figure (A) shows un-dissected dark stipes and figure (B) are their vertically cut halves. The culture plates are incubated at 25 °C (= 28 °C on the shelfs with plates during the light periods) under constant dark.

Further in this study, histochemical stained microtome sections of the dark stipes (Ds1-Ds5) formed after 24 h in the dark were analyzed and compared to the sections of the primordia of same respective age (P1 to P5) as cultivated under standard conditions.

Longitudinal and cross sections of the dark stipes double-stained by PAS and hemalum from stages Ds1 to Ds5 were compared to the sections of primordia P1 to P5 cultivated under standard fruiting (Fig. 2 and 3). In the longitudinal sections, the dark stipes as formed from all into dark transferred stages showed extensively extended hyphae at the 3/4th lower parts of the stipes and extensive cell proliferation at the upper third of the stipes whereas up to transferred P4 structures, the development in the cap regions were blocked at the respective stage earlier of transfer (Fig. 2). An arrest in the further development of the gills were also seen in the cross

sections of the cap area of the dark stipes from stages Ds2 to Ds4, corresponding to the developmental stage at their transfer into dark (Fig. 2 and 3).

Starting from the middle to the lower regions of the stipe in the longitudinal sections of Ds1 to Ds5, the outer and inner inflated and narrow stipe hyphae appeared to be vertically stretched by cell elongation, due to which some of the vertical hyphal continuity has also been broken in stretched areas creating larger hollow spaces in-between them as compared to in the normal structures P1 to P5 (Fig. 2, top). The bottom part of the primordial shaft of the dark stipe in stage Ds5 is predominantly stained darker in magenta whereas such intnese staining were not visible at the lower half in the dark stipes from stages Ds1 to Ds4 (Fig. 2, bottom). This is probably due to incorrect orientation of the specimen while making a microtome cut which causes the missing of the basal parts of the dark stipes (Fig 2, Ds1-Ds4).

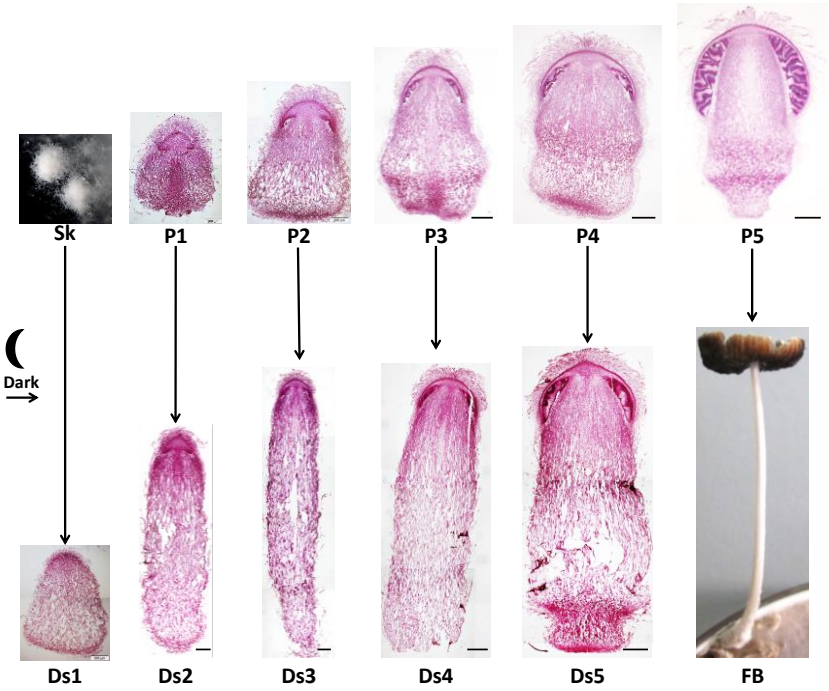

Fig. 2. Comparison between double-stained longitudinal primordia sections cultivated under standard fruiting (top) and dark stipes of same ages formed with 24 h at 25 °C after transfer into constant dark (bottom) conditions. Sk stands for secondary hyphal knot and P1 to P5 are the primordia

stages grown under standard fruiting conditions. Ds1 to Ds5 are the dark stipes formed under constant dark incubation. FB is a fruiting body. The scale bars measure 200 µm.

In the longitudinal sections of the dark stipes, with the exception of the dark stipes at stage Ds1, in which unlike in stage P1 neither the hymenial region nor the veil cells were properly differentiated (Fig. 2 and 3A), the developing gills and the pileipellis in all dark stipes from the stages Ds2 to Ds5 were colored darker compared to the other pileus tissues as in the standard primordia sections (Fig. 3A). The LS of the cap region of the Ds2 stage dark stipe resembled the normal P1 stage primordium where the pileipellis was not clearly differentiated and the initial hymenial palisades were rudimentary (Fig. 3A). Thus, similarity of the Ds2 and the P1 stage primordium were also seen in the CSs in which a darker stained palisade ring was seen (Fig. 3B), indicating that the development had been arrested at stage P1. Furthermore, in all CSs of the Ds3 to Ds5 stages, gill formation seemed to be blocked at the earlier point in time at which structures were transferred into constant dark (Fig. 3B).

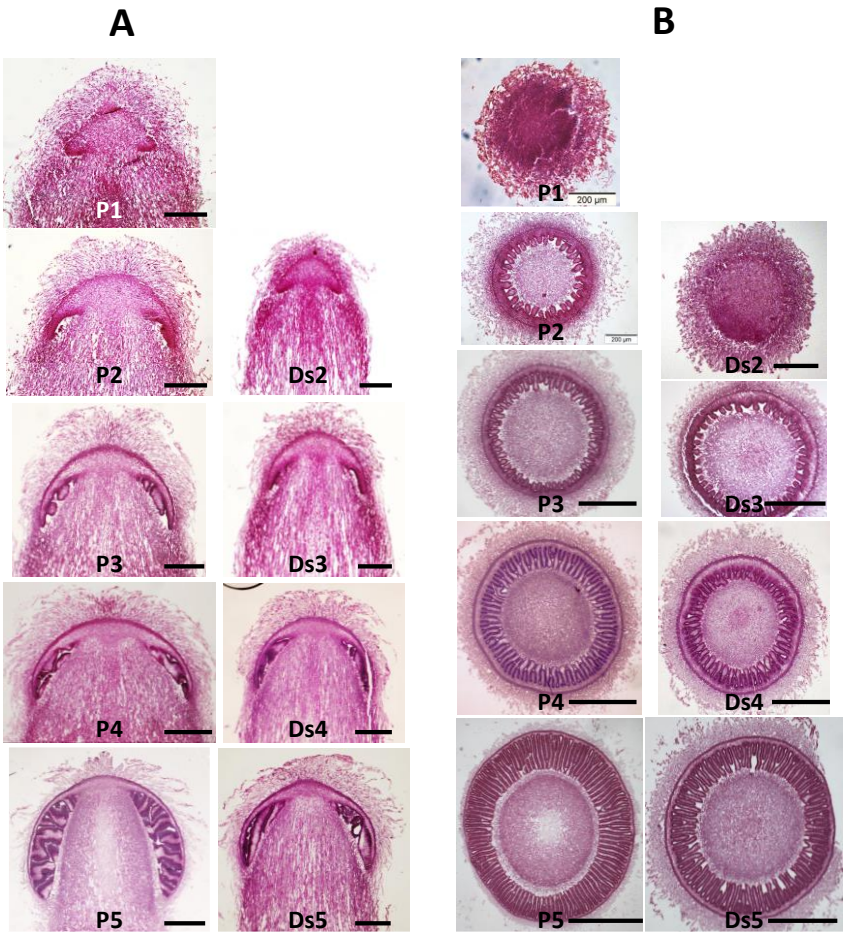

Fig. 3. Comparison between longitudinal (A) and cross sections (B) of the pileus regions double-stained by PAS and hemalum cultivated under standard fruiting (P1 to P5) and under constant dark conditions (Ds2 to Ds5). The LSs of the cap regions and the CSs of the gills for all the stages dark stipes show that they were blocked at earlier stages. The scale bars measure 200 µm.

5.1.4.1.1. Pileus development:

Since the cap region was not fully developed at stage Ds2, the CS photos at higher magnifications were not taken unlike for stages Ds3 to Ds5. At higher magnifications, in the CSs of the cap regions of the dark stipes from stages Ds3 to Ds5, up to the time of transfer both

primary and secondary gills grow and arranged themselves radially as observed in the gill regions of the standard primordia. However, within the 24 h of dark incubation no further development was recognized (Fig. 4A- 4F). The inner ends of the primary gills were attached to the lipsanoblema from dark stipe stages Ds3 to Ds5. A thin layer of darker stained in magenta granules in the subhymenial region is recognized at the Ds3 stage, the thickness of which increased and became more distinct from stages Ds4 to Ds5 (Fig. 4A and 4F). Both cheilo- and pleurocystidia (Fig. 4B, 4D and 4F, marked by the green arrows), along with the few cystesia were present in the hymenia at the stages from Ds3 to Ds5 (Fig. 4D, marker by the yellow arrows). The young paraphyses (Fig. 4F, marked by the red arrows) and the clasping cells (Fig. 4F, shown by the blue arrows) were also recognized at stage Ds5 in-between parallely arranged probasidia and pleurocystidia, respectively.

Like in the hymenial regions of the standard primordia (P2 to P5), bifurcation of primary gill also happened prior to transfer in the pileus of the dark stipes from stages Ds3 to Ds5 resulting in the formation of two second generation of primary gills with their inner edges attached to the lipsanoblema. At CSs from middle to upper parts of the caps, these second-generation primary gills appeared sometimes towards their inner ends like that they were still attached to each other by yet incomplete bifurcation (Fig. 4B and 4E). Secondary gills also originated in-between the outer ends of primary gills of a second generation, even if they had not yet been split over their whole length.

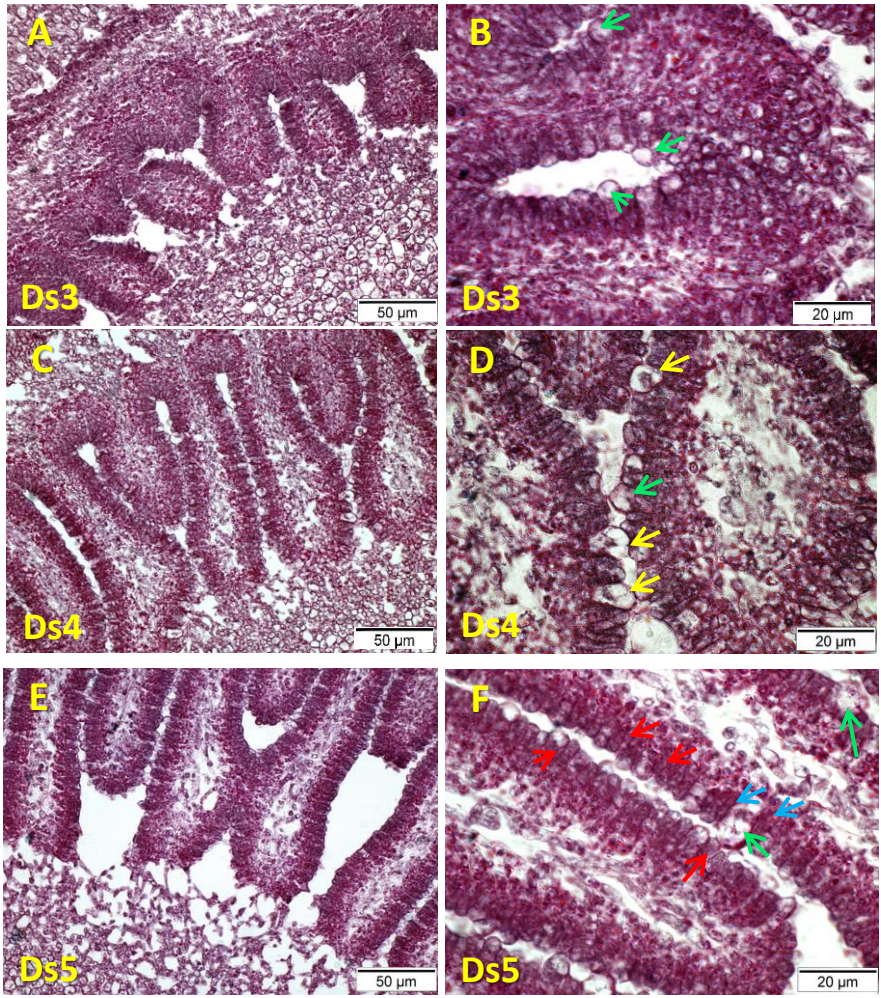

Fig. 4. CSs of the cap regions of the dark stipes from stages Ds3 to Ds5 observed at higher magnifications. The radial arrangement of the primary and secondary gills are seen in all the stages from Ds3 to Ds5. Cheilo- and pleurocystidia marked by the green arrows and cystesia maked by the yellow arrows are present from the stages Ds3 to Ds5. The red arrows and the blue arrows mark the young paraphyses and the clasping cells adhered to the pleurocystidium, respectively.

5.1.4.1.2. Stipe development:

A thin outer layer of partial veil, i.e. the cauloblema covered the entire elongated stipe regions in all the Ds stages. As in normal primordia stages P1 to P5, a layer of narrow hyphae were present at the bottom of the primordial shaft from stages Ds1 to Ds5 which further surrounded the outer part of the primordial shaft but were then limited to that region of the primordial shaft unlike in the standard primordia where these narrow hyphae covered further the lower 2/3rd of the stipe at stage P1 and the entire outer part of the stipe in stages P2 to P5 (Fig. 2). Stipe stretching therefore happened in all the cass in the regions directly above the primordial shaft. As a consequence of stipe stretching, outermost narrow hyphae covering the stipe of normnal primordia directly below the partial veil were torn apart and probably visible as cellular debris irrgularly distributed over the length of the stipe. The dark stained inflated outer stipe hyphae and the narrow hyphae of the inner stipe cylinder originating within the primordial shafts in all the Ds stages were slightly stretched with the primordial shafts as compared to in the standard primordia. Extensive stretching occurred then in the parts of the vertivally up-growing hyphae above the primordial shafts. At the upper ends of the stipes in Ds structures, the lipsanoblema remained as before but below, no narrow hyphae were observed (Fig. 2).

The inflated outer hyphae starting from the middle to the lower half of the elongated dark stipes directly above the primordial shafts from stages Ds2 to Ds5 were extensively stretched unlike in the lower half of the normal stipes of the standard primordia in which the inflated outer hyphae were only slightly extended (Fig. 5E to 5H). Due to the extensive stretching of hyphal cells in stages Ds2 to Ds5, multiple hyphal continuations were vertically broken and larger voids in contrast were created in-between them (Fig. 5E to 5F). The inflated hyphae unstretched at the upper half of the outer part of the dark stipes from stages Ds2 to Ds5 were in contrast highly segmented (Fig. 5A to 5D). These hyphae in the upper half of the dark stipes from all the stages arranged parallely to each other were relatively intactly attached to each other, with few hollow spaces in between them. An alike type of hyphal arragements were also seen in the upper half of the outer stipes in the standard primordial stages. The hyphae at the upper half of the elongated stipes were partially stained by magenta granules (Fig. 5A to 5D), unlike the extensively stretched hyphal parts below (Fig. 5E to 5H). At the upper half of the inner stipe, the cylinder of the narrow highly branched hyphae differentiates clearly from the inflated hyphae of the outer stipe as in the nornal primordia. Towards the middle and the lower part of the inner stipe, the narrow inner hyphae appeared to be stretched and broken along with the stretched outer inflated hyphae and were not any more distinctly visible as forming an inner cylinder (Fig. 2, bottom).

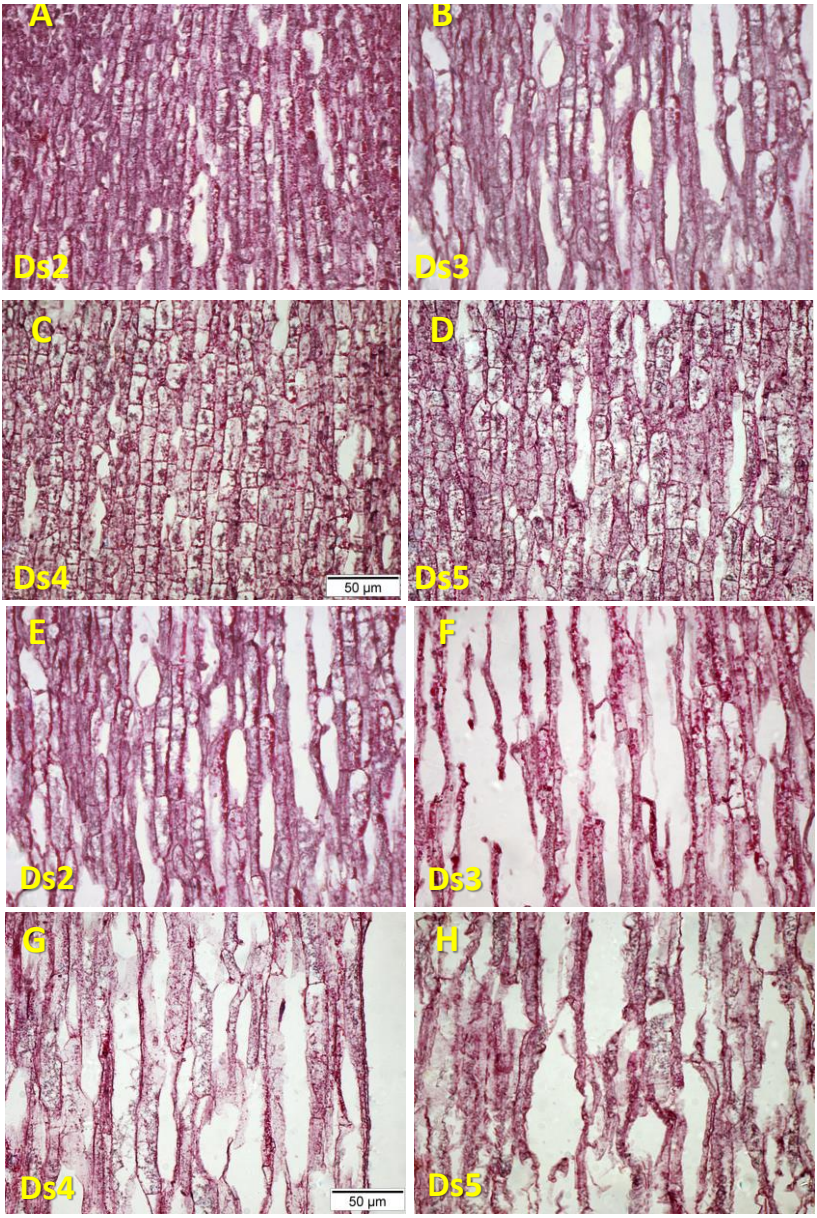
A
Ds2
B
Ds3
C
Ds4
50 µm
D
Ds5
E
Ds2
F
Ds3
G
Ds4
50 µm
H
Ds5

Fig. 5. LSs of the upper (A-D) and the lower (E-H) stipe regions of the dark stipes from stages Ds2 to Ds5 formed at 25 ° C in dark. The images A to D show the inflated highly segmented hyphae at the upper part of the dark stipes from the Ds2 to Ds5 stages. The images E to H show the stretched inflated hyphae at the lower part of the dark stipes from the Ds2 to Ds5 stages.

5.1.4.2. Structure of dark stipes formed from hyphal knots and primordia of different stages after their transfer into continuous dark until Day 7 of incubation

In this section, subsets of culture plates at each stage, starting with Pks, Sks and P1 to P5, were successively placed in constant darkness at 25 °C (= 28 °C on the shelfs with plates during the light periods) on Day 0, Day 1, Day 2 to Day 6, respectively. Progress in the development of dark stipes formed after a sequential transfer of hyphal knot and primordia stages from Pk, Sk and P1 to P5 and continuous cultivation under constant darkness was observed and analyzed collectively on Day 7 of cultivation. The dark stipes thus formed were documented on plates, then harvested and dissected (Fig. 6).

Plates which were put from continuously cultivating at 37 °C in constant dark at the Pk stage on Day 0 into continuously cultivating at 25 °C in constant dark without any exposing to the light formed exclusively masses of sclerotia on the mycelial surface when observed on Day 7 of cultivation at 25 °C, as was expected (chapter 2.2, Fig. 2). All other plates which received at least one or more light signals prior to be transferred for longer cultivation at 25 °C into constant dark however, gave rise to dark stipes but no sclerotia (Fig. 6).

When the culture plates at Day 0 at the Pk stage were exposed to light for few seconds after the 5 days of incubation at 37 °C in the dark and then further incubated at 25 °C for 6 days under constant darkness, on Day 7 of the standard fruiting pathway, they formed secondary hyphal knots in usual numbers at the outer edges of colonies (ca 300 per plate) and in low numbers (2-3/plate) etiolated slender stipes of 13 to 20 mm (n=5) lengths. The pileus region of these dark stipes was poorly developed and when cut in half; a tiny and poorly differentiated imprint of the underdeveloped cap was seen. The development of the primordia caps was probably blocked-in stage P1. The whole interior structure of the dark stipes corresponded to the early Ds2 dark stipes described in section 5.1.4.1. (Fig. 1). Novel at Day 7 of incubation was that dense hairy mycelium grows vertically out at the lower parts of the elongated stipes (Fig. 6).

Culture plates transferred to constant dark at stage Sks formed numerous dark stipes of lengths on Day 7 of 14-27 mm (n=5). On the vertical half-cut, the caps of these dark stipes were distinctly differentiable from the extended stipe and resembled the pileus of P2 stage primordia grown under standard fruiting condition. This showed that the further cap differentiation seemed to be blocked at the P2 stage. The continuously elongated stipe below corresponded in

inner structure to a Ds2 stipe of 4-5 mm in length, but had also vertically outgrowing mycelium at the lower stipe half.

Cultures when placed in constant darkness on Day 2 at stage P1 formed dark stipes of longer length (20-30 mm; n=5) and 1 mm wide. The vertically dissected halves showed well-differentiated pileus tissues in the cap region, which resembled the cap of the standard P3 stage primordium and appeared to be arrested at this stage. As in Ds3 structures (5-7 mm), the extended inner stipe tissues were clearly demarcated from the outer stipe trama. At their lower ends, there was also vertical outgrowth of dense white mycelium. Furthermore, cultures of the P2 stage primordial culture plates formed on Day 3 when kept in constant darkness resulted in 30 to 50 mm long and 1 mm wide elongated dark stipes on Day 7 of cultivation. The cap regions of the dark stipes at this stage also resembled the cap of the standard stage P3 primordia and were arrested at this stage. The elongated stipes were similar to the stipes of Ds3 structures (5-7 mm) while being surrounded at the lower end of white outgrowing mycelium.

Further, cultures plates with stage P3 primordia when further incubated at constant dark and observed on Day 7 contained much longer (35-55 mm, n=5) and broader (2 mm diameter) dark stipes as compared to the earlier induced dark stipe stages. The dissected half of the cap region resembled that of a primordium formed under standard conditions after the P3 stage, more or less approaching the P4 stage while the further development was arrested prior to P4. The extensively elongated stipe below resembled in inner structure to a Ds3 stipe of 6-7 mm in length, but had also vertically outgrowing mycelium at the lower stipe half (Fig. 6).

When culture plates at stage P4 formed on Day 5 of cultivation were placed into constant dark, fat dark stipes of about 20-30 mm lengths and 3-3.5 mm (n=5) widths appeared. The lengths of these dark stipes were shorter compared to those formed at previous stages of transfer into the dark. A vertical-half-cut of the cap region shows well-differentiated pileus tissues similar the cap of stage P4 primordia as cultivated under standard conditions. The elongated stipe showed resemblance in inner structure to a Ds4 stipe of 7-10 mm in length with dense mycelium at the lower stipe half (Fig. 6).

In the next successive stage of transfer, when stage P5 primordia formed on Day 6 of the normal fruiting pathway were transferred to constant dark, matured mushrooms were formed on Day 7 that autolyzed by shedding black basidiospores in liquid droplets (Fig. 6). This last observation showed that continuous darkness did not affect the maturation and the production of basidiospores after performance of karyogamy at stage P5, induced after the stage P4 over the light period of Day 5 by sufficient light probably 6 to 16 h prior to karyogamy (Lu 2000).

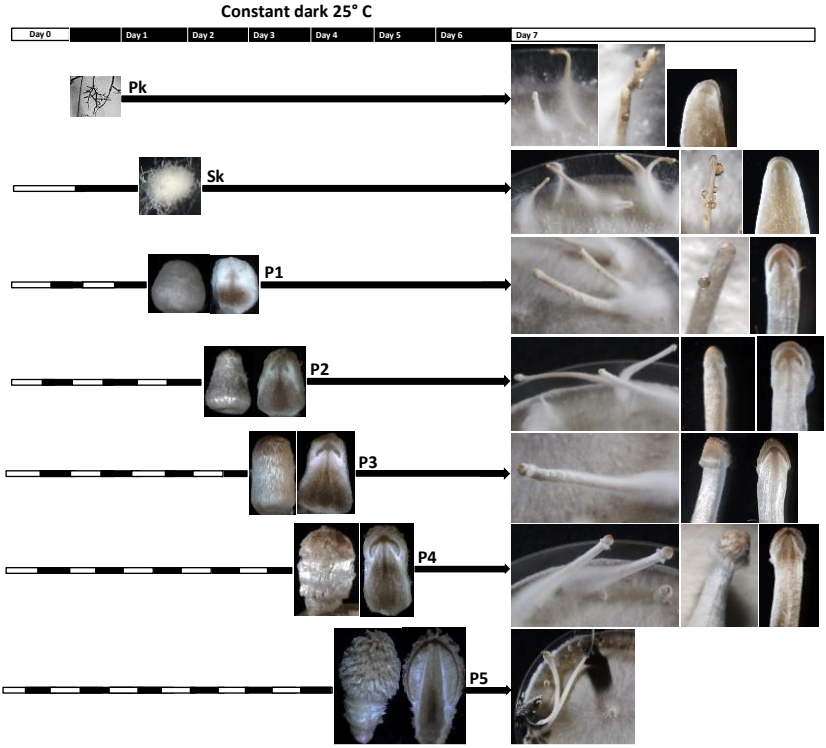

Fig. 6. Structures of dark stipes after cultivation of primordia transferred at different stages of development into constant darkness that were observed collectively on Day 7 of incubation at 25 °C. The culture plates with Pks and Sks formed dark stipes, caps of which resemble stages P1 and P2 primordia, respectively. The culture plates with stages P1 and P2 primordia formed dark stipes, caps of which resemble stage P3 primordia and culture plates with stages P3 and P4 primordia resemble caps of stage P4 primordia. The cultures of stage P5 primordia autolyzed in a normal way, shedding black spores in droplets on Day 7 of the fruiting pathway.

To sum up these observations of the formation of dark stipes obtained by blocking light at different stages of hyphal knot and primordia development show that, the longer the culture plates were kept in constant dark, the longer the dark stipes grow. Therefore, the culture plates which were kept under constant dark at early stages of development formed dark stipes that were longer than those at later stages. Up to a transfer of structures of stage P4, the further development of the pileus tissues slowed down and eventually arrested. Additionally, always white hairy mycelia of yet unknown function were grown from the base along the lower halves

of the extended stipes of Ds structures. The older the dark stipes were, the denser became the hairy mycelia on the surface of the dark stipes. Also, pale water droplets were seen to be produced at the tip of the dark stipes regardless of age of transfer into dark and with the growing stipes, they rolled down and were collected at the base of the older dark stipes (own observations not further shown).

Fig. 7 shows the complete progression in development of dark stipes under dark condition from Pk to FB stages upon transfer into constant dark, starting from Day 0 to Day 7 of cultivation, respectively. Every day, the culture plates with dark stipes were shortly exposed to light technically needed for the photography and then, they were transferred back into constant dark. The daily short illumination of plates appeared to not or only negligible influence the further development of dark stipes in the subsequent incubation in the dark. The appearance of a hairy mycelia along the lower surface of dark stipes was first observed on Day 4 on the culture plates put in dark at the Pk and Sk stages, then on Day 5 on the cultures transferred into the dark at stages P1 and P2, on Day 6 on plates put in dark at the P3 stage and, finally, on Day 7 on plates put in dark at the stage P4.

Numbers of dark stipes formed are influenced by the initiation of number of Sks after the induction of light for a short period in a culture plate and then further elongation of the stipes from the actively growing Sks.


25° C
Day 0
Day 1
Day 2
Day 3
Day 4
Day 5
Day 6
Day 7
Pk
Sk
P1
P2
P3
P4
P5
FB

Fig. 7. The overall progression in development of dark stipes under dark condition at 25 °C successively transferred from stages Pk to FB at Day 0 to Day 7 respectively into constant dark. The same culture plates were followed up over the time of development. The culture plates were exposed to light for a short period of time for the photography and then again were cultivated under constant dark.

5.1.4.3. Effects of constant light on the developmental process of *C. cinerea* primordia

To observe the effect of constant light on the primordial development, experiments were carried out where agar plates were inoculated using the self-compatible AmutBmut for 5 days in the dark at 37 °C. When the cultures plates were fully grown on the Petri dish on 5th day of incubation, they were transferred to the fruiting chamber with 12 h light and 12 h dark at 25 °C and 90 % humidity. According to the normal fruiting pathway of *C. cinerea*, the day on which fully grown cultures were transferred to the fruiting condition was marked as Day 0. Every day, a subset of culture plates at each stage of development from Pk, Sk, and P1 to P5 were transferred to the constant light incubator with a temperature of 28 °C and the observations were made after every 24 hours of incubation at constant light for every stage. In addition, the progress in developing primordia individually starting from stages Pk to P5 to FB in incubating in constant light was followed up and documented every day from Day 0 to Day 7.

Culture plates at stage Pk when transferred to constant light on Day 0 produced within the next 24 h many Sks as seen on the outer range of the plates on Day 1 of cultivation (Fig. 9). Subsequently, with prolonged incubation in constant light, there was no further change up to Day 7 of incubation (Fig. 8).

Sks developed on Day 1 under standard fruiting conditions were able under further incubation in constant light to develop to P1(L) stage primordia (0.5 mm) on Day 2 which showed an internal differentiation of a pileus and a stipe. However, compared to the normal P1 stage, the whole structures were dumpier and covered by a thick smooth veil; the caps were wider with the pileus margins with gill rudiments slightly extended downwards, as seen in the half-cuts in Fig. 8. Upon further incubation in the light, there was no further development of these structures than that they aged and turned brown (Fig. 8).

In the next stage of transfer into continuous light of normal stage P1 primordia on Day 2, on Day 3 the structures differentiated into oval-shaped primordia of about 1-2 mm heights and were also covered by a thick smooth veil. The vertical-half-cut showed distinct differentiations between the cap and the stipe regions, more than in the normal P2 stage. The pileus trama above the gills was also increased, gills were extended and thereby up-lifted top give an ``rabbit's ears´´ impression, and the inner stipe as the lipsanoblema both appeared thicker. These P2(L) slightly grow in size on the next day and then arrest further development and aged and turned brown (Fig. 8).

Transfer of P2 stage primordia on Day 3 of normal development into constant light resulted 24 h later into a dome-shaped primordia (2-3 mm height, 1.5-2.0 mm width) with a thick upper partial veil. The pileoblema, the partial veil on the top of the pileus appeared tousled giving a messy look to the primordia and the cauloblema, the partial veil arising from the stipe region also became more distinct at this stage since thicker than at normal P2. The vertical-cuts of P2(L) revealed the well-differentiated pileus and the stipe regions. The pileus stretched in width and reduced in thickness as compared to the normal P3 stage and the gills underneath were well developed in length and width with still a rabbit's ear appearance and connected with the stipe via a thicker lipsanoblema. The stipes appeared broader in diameter by thicker outer stipe tissues. These P3(L) also slightly grow in size on the next day and then arrest further development (Fig. 8).

Another set of the culture plates when transferred to constant light at stage P3 on Day 4, gave rise within 24 h on Day5 to primordia (3-6 mm high) with a dome-shaped cap with a short not-much-changed stipe attached to it. The pileoblema and the cauloblema appeared dense and messy veil covering the entire primordial body, similarly than in stage P4. The longitudinal half-cut showed that the pileus margins on both sides were more extended downwards, resulting again in a look like a rabbit's ear by overall enlarged gill surfaces. While the gills at this stage were larger, they somewhat resembled in longitudinal extended shape the gills of the standard P4 stage primordia. These P4(L) structures, upon further incubation in the light, no further development of these structures took place (Fig. 8).

In the next stage P4 on Day 5, when constant light was applied to the cultures, after some initial size increase (9-12 mm high) by cap, gill and stipe growth, a permanent arrest in the development took place prior to reaching the normal primordial stage P5. Nevertheless, only the outer veil coving the primordia continued to grow and appeared messier than before as compared to standard primordium stages P4 and P5. Again, these P5(L) structures showed no further development upon further incubation in the light. These primordia were retarded and turned brown with aging (Fig. 9).

When a subset of culture plates was transferred to the constant light incubator on Day 6 at the P5 stage, on the next Day 7 the P5 primordia reached maturation by elongating stipes and autolyzed in a normal way (Fig. 8). Thus, the P5 stage was thus the only one which could continue to completeness and did not need any dark phase for this as reported before by Kamada et al. (1978) and Lu (2000), unlike all other earlier structures that required phases of dark for proper continuation.

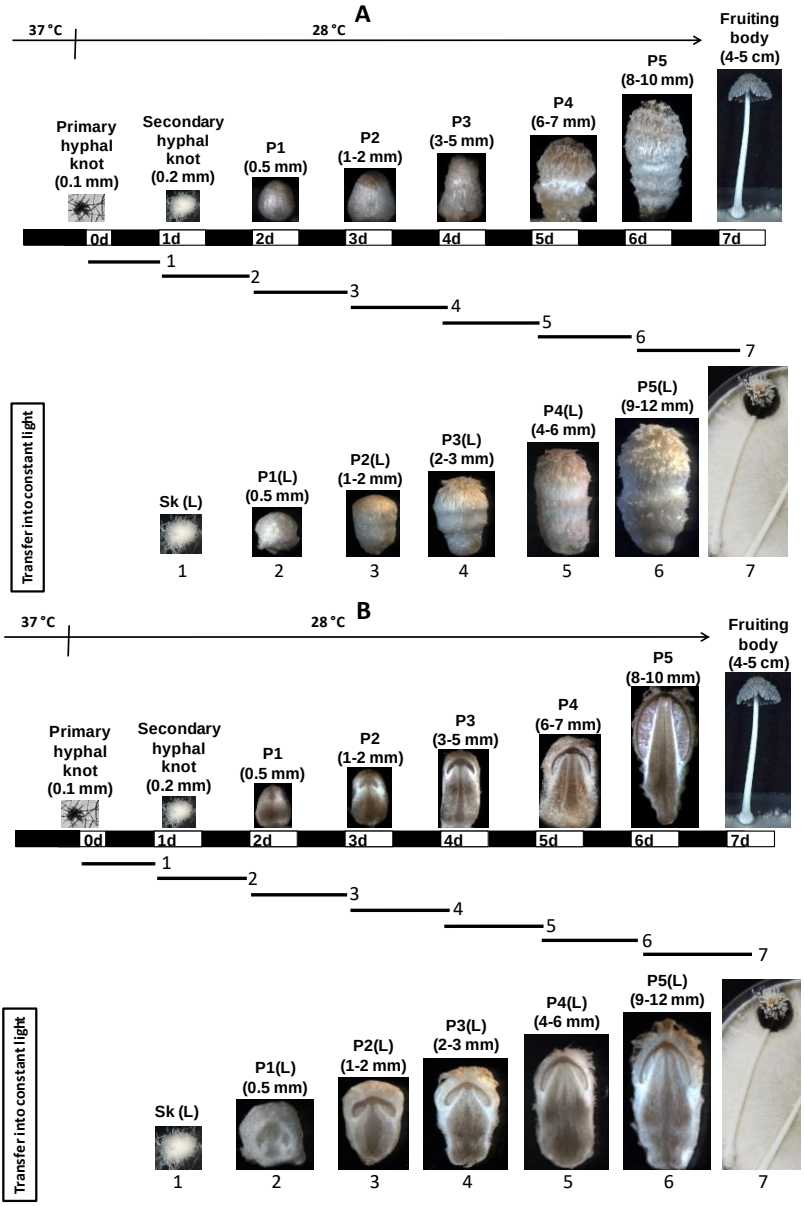
A
37 °C
28 °C
Fruiting body (4-5 cm)
P5 (8-10 mm)
P4 (6-7 mm)
P3 (3-5 mm)
P2 (1-2 mm)
P1 (0.5 mm)
Secondary hyphal knot (0.2 mm)
Primary hyphal knot (0.1 mm)
0d
1d
2d
3d
4d
5d
6d
7d
1
2
3
4
5
6
7
Transfer into constant light
Sk (L)
P1(L) (0.5 mm)
P2(L) (1-2 mm)
P3(L) (2-3 mm)
P4(L) (4-6 mm)
P5(L) (9-12 mm)
B
37 °C
28 °C
Fruiting body (4-5 cm)
P5 (8-10 mm)
P4 (6-7 mm)
P3 (3-5 mm)
P2 (1-2 mm)
P1 (0.5 mm)
Secondary hyphal knot (0.2 mm)
Primary hyphal knot (0.1 mm)
0d
1d
2d
3d
4d
5d
6d
7d
1
2
3
4
5
6
7
Transfer into constant light
Sk (L)
P1(L) (0.5 mm)
P2(L) (1-2 mm)
P3(L) (2-3 mm)
P4(L) (4-6 mm)
P5(L) (9-12 mm)

Fig. 8. Development of primordia P1(L) to P5(L) under 24 h at constant light at 28 °C. Comparison of whole primordia (top A) and their vertical halves (bottom B) grown under standard fruiting conditions with the primordia and their vertical halves formed at different stages of development transferred for 24 h under constant light condition into an incubator. Numbers 2 to 6 refers to primordia structures formed after 24 h of incubation under constant light.

Fig. 9 summarizes a complete pathway of primordia development displaying progress in development under longer incubation times of plates in constant light. Subsets of plates were transferred at distinct stages of normal fruiting body development, i.e. either Pk, or Sk, P1 up to P5, for further incubation into constant light for a maximum of up to seven days. With the increase in the number of days exposed to the constant light, two important observations were made. One is, the earlier the moment of transfer of plates was (and in consequence the longer the exposure time of cultivation to the constant light), the shorter was the stipe and the primordia appeared dumpy. This leads to conclude that too much light suppresses at several primordial stages, from P1 to P4, also normal stipe elongation and further tissue differentiation in the cap. The other observation shown in Fig. 9 refers to the likely stress-related excretion of light-yellow droplets during constant light cultivation, the volume of which increased with the increasing exposure time and became golden yellow on the aged mycelium surface and on the retarded and then aged primordia.

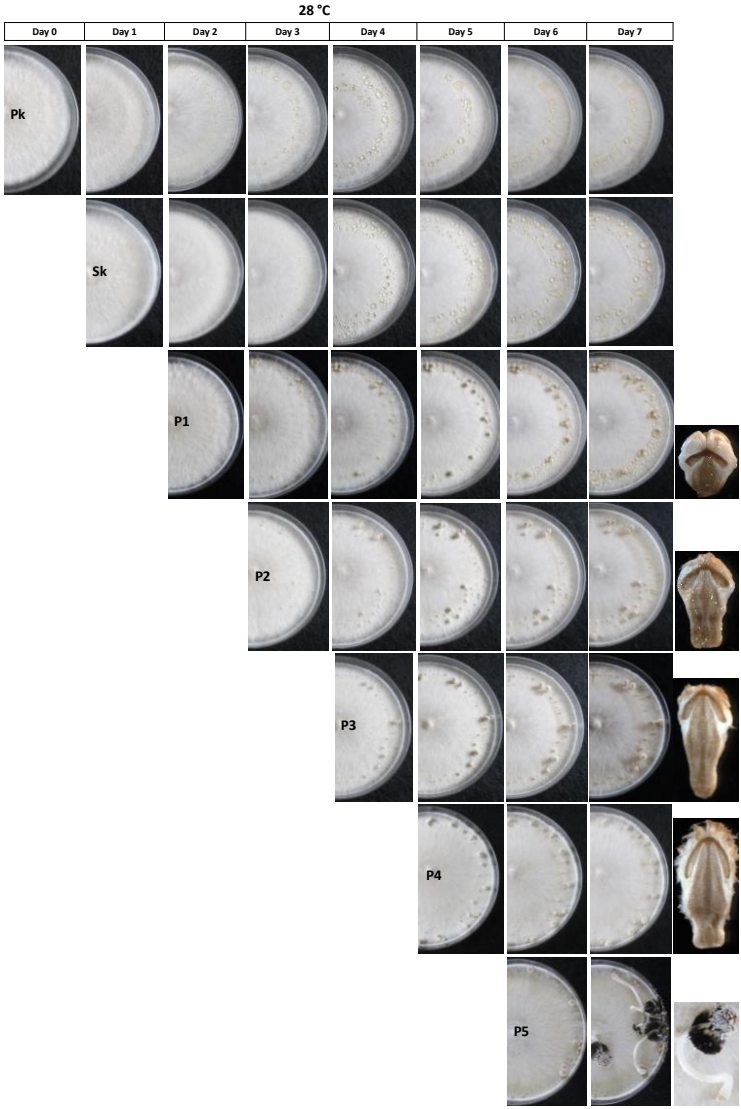

Fig. 9. Progression in development of primordia under constant light at 28 °C when subsets of plates from every stage of development from Pk, Sk, P1 to P5 were successively transferred from standard fruiting conditions into constant light. The cut-half of the primordia from the stages P2(L) to P5(L) progressed in development up till Day 7 were shown on the extreme right side of this figure

whereas half-cut of P1(L) could not be achieved due to destroy of the retarded and aged tiny specimens while cutting.

5.1.5. Discussion

Light is an important environmental factor that regulates the circadian rhythm of organisms. In most *Agaricomycetes*, light enables the organism to enter the various pathways of sexual and asexual reproduction and most often it is necessary for the formation of fruiting bodies. Fruiting body development in *C. cinerea* is genetically controlled by mating-type genes (Kües 2000). However, environmental factors such as light, temperature, humidity, nutrient, and aeration are equally necessary for the synchronized development of the fruiting bodies (Kües 2000). Among all, light is one of the decisive factors, a short exposure of which is sufficient to induce secondary hyphal knot initiation (Lu 1972, 1974a; Morimoto and Oda 1973; Kamada et al. 1978), or else under constant dark, multicellular dormant structures sclerotia are formed from Pks (Moore 1981). Light is not only important for the initiation of fruiting, but also for the synchronized development of the primordial stages that eventually mature into a spore-shedding mushroom and autolyze the caps for the spore dispersal. But in absence of light upon secondary hyphal knot formation, an altered structure called ``dark stipe´´ with an elongated stipe and an under-developed cap results (Tsusué 1969; Lu 1972, 1974b; Morimoto and Oda 1973; Kamada et al. 1978; Lu 2000). Furthermore, induction of light is also necessary for oidiation in the mycelia of dikaryons and the self-fertile homokaryon AmutBmut (Polak et al. 1997, 2001; Chaisaena 2006) and, in the process of fruiting body formation, also at the later stages of primordia development for the progress of gill formation, the induction of karyogamy and meiosis in the basidia and then cap expansion (Kamada et al. 1978; Kües 2000).

Formation of extended slender structures under constant dark were studied by many researchers in the past and are known under various names such as etiolated stipes (Kües 2000), dark stipes (Tsusué 1969; Terashima et al. 2005), pseudorhizal stipes (Blayney and Marchant 1977), oversized stipes (Lu 1974b) or long slender stalks (Morimoto and Oda 1973). Although light plays an important role in the morphogenesis of fruiting bodies, light signals are not always beneficial for the fungal growth because strong light or a long exposure time inhibit vegetative growth as well as fruiting body initiation in *C. cinerea* (Kamada et al. 1978; Lu 2000). Likewise, prolonged exposure to light blocks or delays the tissues differentiation and the maturation of the primordia which means both the light and the dark phases are equally necessary for the regular development of a fruiting body and the maturation of a fungus (result in this study).

5.1.5.1. Dark observations

Successive stages of primordia development were transferred from standard fruiting conditions to constant dark. My observations revealed that after 24 h in darkness all transferred plates but those of P5 stages contained Ds structures with elongated stipes while a longer duration of

incubation under constant darkness resulted by further stipe growth and length expansion in Ds structures with longer stipes. The culture plates that were kept in constant darkness at early developmental stages i.e. Pk, Sk, P1, P2 and P3 formed Ds structures longer than those obtained from transfer of the later stage at P4 (Fig. 6). Cultivation under constant darkness not only lengthened the stems, but also inhibited the further development of the hymenial tissue of a pileus. The longer the primordia were cultivated under constant darkness by transfer at the earlier stages, the poorer the development of the pileus tissue was, which led to Ds structures with longer stipes and rudimentary pileus tissues on Day 7 at the end of the standard fruiting pathway (Fig. 6). Plates transferred at the Pk stage into constant darkness for example reached a maximum cap development at about stage P1. Likewise, cultivation under constant darkness at stage Sks led to the development of structures, caps of which were blocked at stage P2. Cultivations of cultures under constant darkness at stages P1, P2 and P3 led to the termination in the development of caps of the Ds structures at stage P3 whereas constant darkness at stage P4 stopped further development of the caps of the Ds structured prior to P5 and did not mature. However, the incubation under constant darkness for just 24 h at the last primordial stage P5 did not appear to have any influence on the maturation of the fungus; thus, on Day 7, primordia matured into fruiting bodies and autolyzed shedding spores in a dark liquid (Fig. 1). This result indicates that the exposure of light at stage P4 is enough to induce karyogamy and undergo meiosis in the basidia in stage P5, resulting then in the production of basidiospores and the autolysis of a mature mushroom. Thus, the darkness after the P5 stage has no influence on the maturation of the fungus and the production of basidiospores. This latter conclusion confirms earlier observation by Kamada et al. (1978) and Lu (2000).

Furthermore, while observing the entire developmental pathway of the primordia cultivated under constant darkness, hairy mycelia were noticed to grow along the surface of the extended stipes of the dark stipes (Fig. 7). The older the dark stipes were, the denser was the hairy mycelia on the surface of the dark stipes. Formations of such hairy mycelia along the dark stipes were mentioned in the past literature as the result of prolonged cultivation in dark (Tsusué 1969; Morimoto and Oda 1973).

Cox and Niederpruem (1975) reported for normal rapid stipe elongation of mature primordia (after stage P5 after meiosis) that the stipe does not elongate equally over its whole length and that generally the upper mid-region of stipes is the most active zone of elongation and the lower region the less active whereas the cells at the apex and the base do not extend much. This differs in part from the stipe elongation processes observed in Ds structures. In longitudinally stained sections of the dark stipes from stages Ds1 to Ds5, we observed that the hyphal cells in the upper part of the stipes were heavily segmented, similar to the normal primordial stages and that these cells did not extend in length and their cell proliferation contributed little to the dark-stipe elongation. In contrast, the hyphae at the middle and particularly at the lower parts of the

Ds structures were extensively elongated due to which some of longitudinal and also lateral connections of both inflated and narrow hyphae of the outer and inner stipe were broken, creating large voids (Fig. 2 and Fig. 5). During the longer Ds structure development, proliferation of cells happens at the upper end of the Ds structures to replace below those cells that elongated while this provides only a minor contribution to the overall dark-stipe elongation.

The stained cross-sections of the Ds structures (Ds1 to Ds5) after 24 h of incubation under constant dark clearly showed that the development of the cap areas was blocked or delayed for transferred Sks at the P1 stage and for the P1 to P3 at their stages of transfer and for the P4 stage somewhat shortly before to P5, due to lack of light signals (Fig. 3). The hymenial regions of Ds5 structures consisted of darkly stained subhymenia in magenta and beneath were the blue-stained probasidia, similar to the cap regions of the standard primordia P4 (Fig. 4). In contrast, large cheilo- and pleurocystidia protruded from the subhymenium into the parallely arranged probasidia, with cystesia-bridges interlinking to the opposite hymenia as in stage P5. In-between the parallely arranged probasidia, young paraphyses were present as in stage P5 (Fig. 4). The P4 stages prior to transfer into constant dark received some minutes of light at the morning of Day 5. However, this light signal was apparently too early for confer the last required light signal to the structures needed for induction of karyogamy in the basidia. According to Lu (2000), induction of nuclear fusion needs a light signal 16 to 6 h prior to karyogamy (as per definition by Lu: 5 % of all basidia contain diploid nuclei) to take place at the start of the dark phase in a 16 h light/8 h dark incubation scheme (happening in the 12 h light/12 h dark regime within the dark phase of Day 6; Navarro-Gonzaléz 2008). Therefore, only P5 stage primordia with karyogamy in basidia have taken or taking place (>70 % of all basidia contain diploid nuclei; Navarro-Gonzaléz 2008) when transferred into constant dark matured with meiosis and basidiospore formation and resulting fruiting bodies autolyzed for shedding black spores in a normal way.

5.1.5.2. Light observations

On the contrary to the formation of Ds structures cultivated under constant darkness, the culture plates when incubated under constant light starting at successive standard stages from Sks to P4, the development of the transferred structures continued but produced primordia structures P1(L) to P5(L) with a short stipe and a dome-shaped cap which could not mature to form a mushroom and autolyze (Fig. 8). A developed primordium with a short stipe and a bulky head was named as a dwarf fruit-body by Tsusué (1969) which in her study was the result of the combination of constant light and high temperature effects on the fruiting process. Such dwarf primordia aborted their further development and never matured to a mushroom.

The vertical half-cut of the primordia from stages P1(L) to P4(L) formed after 24 h of incubation under constant light showed increased veil tissue and pileus trama at the cap region and

developed gills comparable to the normal primordia (Fig. 8). The appearance of the pileus in the longitudinal cut-half of the primordia stages from P2(L) to P4(L) resembled ``pairs of rabbit's ears´´ with their gills at either side of the pileus cuts (Fig. 8B). Similar types of dwarf and rabbit's ear-like phenotypes were observed under standard fruiting conditions on a transformed dikaryon with the defect in a *ras* gene (*ras*^{Val19}) resulting in the constitutively activated Ras^{Val19} protein. Primordia of this dikaryon attained maturation, forming a short height mushroom with thin caps and thin stipes (about 1-1.5 cm in height, with cap and stipe parameters reduced comparably in size) that either lacked basidiospores or, if some were formed, they were partially reduced in size and/or missing pigmentation (Srivilai 2006). The author further commented in his PhD thesis that chemical communication between cap and stipe tissues have to occur in order to elongate stipes and expand the caps in a normal development (Kamada 1994; Kües 2000) and he suggested further that disturbance in this communication might contribute to the minute fruiting body sizes. However, in the experiments by Srivilai (2006) it became clear that, despite the defect in the *ras* gene, the mutant dikaryotic transformants managed under standard fruiting conditions to further differentiate cap tissues, elongate stipes and eventually mature into tiny mushrooms that autolyzed, suggesting the continued presence of an interactive while possibly modified communication between the cap and the stipe during the primordial growth process. In chapter 4, communication between cap and stipe tissues was postulated to occur through the interlinking lipsanoblema in stages P2 to P5 by providing the shortest path for communication. In the present study, we observed a major control of both, light and dark signals, on the development process of the fungi, the absences of which led to the formation of Ds structures or dwarf primordia, respectively. Again, this could suggest that the communication between the caps and the stems of the primordia stages P2 to P4 was possibly disturbed under such different conditions. At stage P5, the stipe is still connected via the lipsanoblema to the gills until about the end of the 12 h light phase (Navarro-González 2008) further allowing communication. However, past experiments on stipe removal and decapitation of the standard primordia indicated that in later stages of the primordia development after all light-and dark-dependent phases (stage P5 or later), the cap had no influence in the lengthening of the stems, as the stems extended even if the cap was removed from the primordia whereas in younger stages, this was not the case (Borris 1934; Gooday 1975).

The short-sized fat primordia were also described in the past study by Muraguchi and Kamada (2000) and named them as dumpy primordia. Such morphology is caused by the mutation in the *elongationless2* (*eln2*) gene that encodes a novel type of microsomal cytochrome p450 enzyme (CYP502) thereby causing dumpy primordia which culminate in mature fruit-bodies with short stipes (Muraguchi and Kamada 2000). According to their results, the reduction in the stipe length in mutant fruit bodies is not due to a defect in cell extension but due to reduction in the numbers of stipes cells. A next study conducted later in the year 2013 by Shioya et al.,

showed that the defect in the gene encoding septin protein, a homolog of *S. cerevisiae Cc.cdc3*, which are highly transcribed during stipe elongation in the wild type resulted in the formation of dumpy primordia which eventually matured to a short height mushroom and autolyzed. This study suggested that cortical septin filaments provide the localized rigidity to the plasma membrane of stipe cells and allow stipe cells to elongate cylindrically (Shioya et al. 2013).

5.1.6. Conclusions

In our study, formation of Ds structures with different stipe lengths and with much delayed cap tissue development due to the non-availability of light over longer durations and the blocks in tissue differentiation in the P(L) structures due to absence of dark phases was investigated. The observations speculate that there were apparently disturbances in the circadian rhythm of the *C. cinerea*. Studies performed with the model ascomycete *Neurospora crassa* and the model mucoromycete *Phycomyces blakesleanus* showed that several proteins, notably FRQ (Frequency Clock Protein) as the circadian oscillator and WC1 (White Collar 1) and WC2 (White Collar 2) as blue light-receptor and transcription factor complex, are responsible for controlling the circadian rhythms with day lengths and mechanisms for responding to environmental cues including light and the C-source glucose (Gyöngyösi et al. 2017; Poliano et al. 2017; Brody 2019, 2020). The *band* (*bd*) mutation in *N. crassa* causing daily banding in asexual condition of the fungus and the *madC* mutation in *P. blakesleanus* were identified to encode Ras and GTPase activating protein for Ras, respectively, and are types of genes involved in fine tuning of the circadian clock such as to light and to nutritional cAMP-regulation (Poliano et al. 2017; Gyöngyösi et al. 2017). Dark stipe and dwarf phenotypes as described above could indicate regulatory mechanisms by light and by Ras analogously to *N. crassa* and *P. blakesleanus*. *C. cinerea* has been shown before to contain *wc1* and *wc2* genes (i.e. *dst1* and *dst2*) whose defects lead to dark-stipe formation under standard fruiting conditions (Kamada et al. 2010; Kuratani et al. 2010). Brody (2019) reported before that *C. cinerea* has no *FRQ* gene. However, he also demonstrated the generally poor conservation between FRQ-type proteins from fungi and also from insects (Brody 2019, 2020). Blasting on the NCBI homepage (Brody 2019) the *C. cinerea* proteome under low stringency with *Sordaria fimicola* FRQ (AAA20825.1) identified also a potential FRQ protein also in *C. cinerea* (EAU82421.2) with very short shared motifs as described by Brody for other FRQ and PER (period) protein combinations (Brody 2019).

5.1.7. References

Blayney, G. P. and Marchant, R. (1977) Glycogen and protein inclusions in elongating stipes of *Coprinus cinerea. Journal of General Microbiology*, *98*, pp.467-476.

Borriss, H. (1934) Über den Einfluss äusserer Faktoren auf Wachstum und Entwicklung der Fruchtkörper von *Coprinus lagopus*. *Planta*, *22*, pp.28-69.
Boulianne, R. P., Liu, Y., Aebi, M., Lu, B. C. and Kües, U. (2000) Fruiting body development in *Coprinus cinereus*: regulated expression of two galectins secreted by a non-classical pathway. *Microbiology*, *146*, pp.1841-1853.
Brefeld, O. (1877) Botanische Untersuchungen über Schimmelpilze. III. Basidiomyceten Leipzig: Arthur Felix. (in German)
Brody, S. (2019) Circadian rhythms in fungi: Structure/function/evolution of some clock components. *Journal of Biological Rhythms*, *34*, pp.364-379.
Brody, S. (2020) A Comparison of the *Neurospora* and *Drosophila* clocks. *Journal of Biological Rhythms*, *35*, pp.119-133.
Buller, A. H. R. (1924) Researches in fungi III. The production and the liberation of spores in hymenomycetes and Uredineae. Hafner Publishing Co., New York, NY.
Chaisaena, W. (2006) Light effects on fruiting body development of wildtype in comparison to light-insensitive mutant strains of the basidiomycete *Coprinopsis cinerea*, grazing of mites (*Tyrophagus putrescentiae*) on the strains and production of volatile organic compounds during fruiting body development. (PhD Thesis, Georg-August University of Göttingen).
Chiu, S. W. and Moore, D. (1988) Ammonium ions and glutamine inhibit sporulation of *Coprinus cinereus* basidia assayed in vitro. *Cell Biology International Reports*, *12*, pp.519-526.
Cox, R. J. and Niederpruem, D. J. (1975) Differentiation in *Coprinus lagopus* III. Expansion of excised fruit-bodies. *Archives of Microbiology*, *105*, pp.257-260.
Gooday, G. W. (1975) The control of differentiation in fruiting body in *Coprinus cinereus*. Reports Tottori *Mycological Institute 12*, pp.151-160.
Gooday G. (1985) Elongation of the stipe of *Coprinus cinereus*. *Developmental Biology of Higher Fungi*, Manchester, England, pp.311-331.
Granado, J. D., Kertesz-Chaloupková, K., Aebi, M. and Kües, U. (1997) Restriction enzyme-mediated DNA integration in *Coprinus cinereus*. *Molecular and General Genetics*, *256*, pp.28-36.
Gyöngyösi, N., Szőke, A., Ella, K. and Káldi, K. (2017) The small G protein RAS2 is involved in the metabolic compensation of the circadian clock in the circadian model *Neurospora crassa*. *Journal of Biological Chemistry*, *292*, pp.14929-14939.
Ji, J. and Moore, D. (1993) Glycogen metabolism in relation to fruit body maturation in *Coprinus cinereus*. *Mycological Research*, *97*, pp.283-289.
Jirjis, R. I., Moore, D. (1976) Involvement of glycogen in morphogenesis of *Coprinus cinerea*. *Journal of General Microbiology 95*, pp.348-352.
Kamada, T. (1994) Stipe elongation in fruit bodies. *Growth, Differentiation and Sexuality*, *1*, pp.367-379. Springer, Berlin, Heidelberg.
Kamada, T., Kurita, R. and Takemaru, T. (1978) Effects of light on basidiocarp maturation in *Coprinus macrorhizus*. *Plant and Cell Physiology*, *19*, pp.263-275.
Kamada, T., Sano, H., Nakazawa, T. and Nakahori, K. (2010) Regulation of fruiting body photomorphogenesis in *Coprinopsis cinerea*. *Fungal Genetics and Biology*, *47*, pp.917-921.

Kamada, T. and Takemaru, T. (1977a) Stipe elongation during basidiocarp maturation in *Coprinus macrorhizus*: mechanical properties of the stipe cell wall. *Plant Cell Physiology*, *18*, pp.831–840.
Kamada, T. and Takemaru, T. (1977b) Stipe elongation during basidiocarp maturation in *Coprinus macrorhizus*: changes in polysaccharide composition of stipe cell wall during elongation. *Plant Cell Physiology*. *18*, pp.1291–1300.
Kamada, T. and Takemaru, T. (1983) Modification of cell-wall polysaccharides during stipe elongation in the basidiomycete *Coprinus cinereus*. *Journal of General Microbiol*, *129*, pp.703–709.
Kües, U. (2000) Life history and developmental processes in the basidiomycete *Coprinus cinereus*. *Microbiology and Molecular Biology Reviews*, *64*, pp.316-353.
Kües, U., Granado, J. D., Kertesz-Chaloupková, K., Walser, P. J., Hollenstein, M., Polak, E., Liu, Y.,
Kuratani, M., Tanaka, K., Terashima, K., Muraguchi, H., Nakazawa, T., Nakahori, K. and Kamada, T. (2010) The *dst2* gene essential for photomorphogenesis of *Coprinopsis cinerea* encodes a protein with a putative FAD-binding-4 domain. *Fungal Genetics and Biology*, *47*, pp.152-158.
Lu, B. C. (1972) Dark dependence of meiosis at elevated temperatures in the basidiomycete *Coprinus cinereus*. *Journal of Bacteriology*, *111*, pp.833–834.
Lu B. C. (1974a) Meiosis in Coprinus: VI. The control of the initiation of meiosis. *Canadian Journal of Genetics and Cytology*, *16*, pp.155-164.
Lu, B. C. (1974b) Meiosis in *Coprinus.* V. The role of light on basidiocarp initiation, mitosis and hymenium differentiation in *Coprinus lagopus*. *Canadian Journal of Botany*, *52*, pp.299–305.
Lu, B. C. (2000) The control of meiosis progression in the fungus *Coprinus cinerea* by light/dark cycles. *Fungal Genetics and Biology*, *31*, pp.33-41.
Madelin, M. F. (1956) The influence of light and temperature on fruiting of *Coprinus lagopus* Fr. in pure culture. *Annals of Botany*, *20*, pp.467-480.
Moore, D. (1981) Developmental genetics of *Coprinus cinereus*: genetic evidence that carpophores and sclerotia share a common pathway of initiation. *Current Genetics*, *3*, pp.145–150.
Moore, D. (1987) The formation of agaric gills. *Transactions of the British Mycological Society*, 89, 105–114.
Moore, D. (1995) Tissue formation. N. A. R. Gow and G. M. Gadd (ed.), *The Growing Fungus*. Chapman & Hall, London, United Kingdom. pp.423–466
Moore, D. (1998) Fungal morphogenesis. Cambridge University Press, Cambridge, United Kingdom.
Morimoto, N., and Oda, Y. (1973) Effects of light on fruit body formation in a basidiomycete, *Coprinus macrorhizus. Plant Cell Physiology, 14*, pp.217–225.

Muraguchi, H. and Kamada, T. (2000) A mutation in the *eln2* gene encoding a cytochrome P450 of *Coprinus cinereus* affects mushroom morphogenesis. *Fungal Genetics and Biology*, *29*, pp.49-59.
Navarro-Gonzaléz, M. (2006) Growth, fruiting body development and laccase production of selected coprini. (PhD Thesis, Georg-August University of Göttingen).
Polaino, S., Villalobos-Escobedo, J. M., Shakya, V. P., Miralles-Durán, A., Chaudhary, S., Sanz, C., Shahriari, M., Luque, E. M., Eslava, A. P., Corrochano, L. M. and Herrera-Estrella, A. (2017) A Ras GTPase associated protein is involved in the phototropic and circadian photobiology responses in fungi. *Scientific Reports*, *7*, pp.1-12.
Polak, E., Hermann, R., Kües, U. and Aebi, M. (1997) Asexual sporulation in *Coprinus cinereus*: structure and development of oidiophores and oidia in an *AmutBmut* homokaryon. *Fungal Genetics Biology*, *22*, pp.112–126.
Polak, E., Aebi, M., and Kües, U. (2001) Morphological variations in oidium formation in the basidiomycete *Coprinus cinereus*. *Mycological Research*, *105*, pp.603-610.
Shioya, T., Nakamura, H., Ishii, N., Takahashi, N., Sakamoto, Y., Ozaki, N., Kobayashi, M., Okano, K., Kamada, T., Muraguchi, H. (2013) The *Coprinopsis cinerea* septin *Cc.Cdc3* is involved in stipe cell elongation. *Fungal Genetics and Biology*, *58*, pp.80-90.
Srivilai, P. (2006) Molecular analysis of genes acting in fruiting body development in basidiomycetes. (PhD Thesis, Georg-August University of Göttingen).
Subba, S., Winkler, M., and Kües, U. (2019) Tissue staining to study the fruiting process of *Coprinopsis cinerea*. *Acta Edulis Fungi*, *26*, pp.29-36
Swamy, S., Uno, I., Ishikawa, T. (1984) Morphogenetic effects of mutations at the *A* and *B* incompatibility factors in *Coprinus cinereus*. *Journal of General Microbiology*, *130*, pp.3219-3224.
Terashima, K., Yuki, K., Muraguchi, H., Akiyama, M. and Kamada, T. (2005) The *dst1* gene involved in mushroom photomorphogenesis of *Coprinus cinereus* encodes a putative photoreceptor for blue light. *Genetics*, *17*, pp.101-108.
Tsusu´e, Y. M., (1969) Experimental control of fruit body formation in *Coprinus macrorhizus*. *Development Growth Differentiation*, *11*, pp.164–178.

Sub-chapter 5.2. Effect of CO_2 in fruiting body development of *C. cinerea* and dark stipe mutants

Contribution to subchapter 5.2
Experimental planning: U. Kües and S. Subba
Experimental work and data analysis: S. Subba
Whole genome sequencing of strains 7K17 and B1918: Botond Hegedüs and László Nagy
Analysis of defects in strains 7K17 and B1918: U. Kües
Manuscript writing: S. Subba
Manuscript reviewed by: U. Kües

5.2.1. Abstract

Fruiting body development in *Coprinopsis cinerea* follows a conserved developmental scheme of 7 days that starts with formation of loose aggregates (primary hyphal knots, Pks) in the mycelium in the dark. Upon a light signal, these Pks turn into compact secondary hyphal knots (Sks) in which stipe and cap tissues differentiate. Primordia development from stages P1 to P5 takes 5 days to follow on Day 6 by fruiting body maturation. Basidiospores production subsequent to karyogamy and meiosis in the basidia parallels stipe elongation and cap expansion. Mature fruiting bodies autolyze on Day 7 to release the spores in liquid droplets. This pathway is controlled by mating-type genes along with the environmental conditions including nutrients, light, temperature, and, as presented in this chapter, also aeration. Sensitive phases in the developmental fruiting body pathway were at the stages of primary and secondary hyphal knots (Pks and Sks) as well as at the primordial stages P1 to P5. Arrest at Pk formation by block of aeration in a normal 12 h light/12 dark scheme resembles what was observed before in constant light. A block of transfer of Sks into stage P1 primordia however was not observed before. As failure in light signaling under constant, lack of aeration at the P1 to P4 stages lead to the formation of 'dark stipes', under the proliferation of stipe tissues and blocks in cap development. After the P5 stage, as a new phenotype normal shaped fruiting bodies but with white caps with unpigmented basidiospores arose which did not autolyze. Scavenger experiments of CO_2 with KOH recovered the normal phenotypes in fruiting body development (Sk development, normal continuation at P1 to P4 of primordial development, dark spore pigmentation and autolysis) as well as that active mycelial growth was restored with KOH under block of aeration. Accordingly, increase in concentration of CO_2 resulted in abnormal phenotypes and not a lack of oxygen.

We have a collection of mutants with defects in fruiting. In the mutant collection, defects in fruiting do not evenly distribute over the complete pathway which reflects the complexity in a fruiting process. Among are two mutants (*dst3*, *dst4*) with P3- and P4-induced 'dark stipe' phenotypes under standard fruiting conditions with light and aeration. Genome sequencing revealed defects linked to the citrate cycle, production of branched amino acids, and the Cop9 signalosome suggesting links to CO_2 and possibly light regulation. Defects in formerly described genes *dst1* (*wc1*), *dst2* (*wc2*) in contrast caused P1-induced phenotypes by defects in blue-light receptors and a FAD/FMN-binding dehydrogenase of the GlcD superfamily.

5.2.2. Introduction

Fruiting body development in the saprotrophic fungus *C. cinerea* follows a conserved scheme defined by day and night phases, with well predictable distinct stages over the time (Kües 2000, Kües and Navarro 2015). Fruiting initiation starts on complete YMG/T medium in Petri dishes with hundreds of initial structures, but every day some will be given up in development in favor of only a few to eventually mature. Fruiting formation primarily begins with a primary hyphal knot (Pk) formed in the dark, followed by light-induced compact aggregates, a secondary hyphal knot (Sk), in which the stem and the cap tissues differentiate (Buller 1931; Kües 2000; Kües and Navarro-González 2015; Kües et al. 2016). In presence of adequate light and dark rhythms, primordia progress from stages P1 to P5 which takes five days to culminate on Day 6 of development in karyogamy (K) and meiosis (M) within the basidia and subsequent basidiospore production which parallels fruiting body maturation (stipe elongation and cap expansion). Mature fruiting bodies autolyze on Day 7 to release spores in the liquid droplets (Kües 2000; Navarro-González 2008).

Environmental factors such as light, temperature, humidity, aeration and nutrients strongly influence the fruiting process and thus, regulate the path of development of the fungus (Moore et al. 1979; Moore 1998; Kües 2000). A light signal is one of the important factors which is essential at the different stages of fruiting body developmental process such as for the initiation of Sks, for the differentiation of tissues within the growing primordia and at the later stages for the induction of karyogamy within the basidia and the subsequent opening of the cap for the autolysis (Morimoto and Oda 1973; Lu 1974b; Kües et al. 2016). Without light, elongated stipes with underdeveloped caps termed "dark stipes or Ds structures" that neither mature and nor undergo autolysis are formed from the Sks (chapter 5.1, Buller 1924; Tsusué 1969; Morimoto and Oda 1973; Lu 1974a; Kamada and Takemaru 1977; Chaisaena 2009). Shown for the first time in this chapter, comparable dark stipes with elongated stipes and poorly developed caps are formed under non-aerated conditions which appear similar to the Ds structures formed in the aerated cultures that after inducing light signals are cultivated completely in dark (chapter 5.1). Furthermore, blocking of air to vegetatively growing mycelial cultures also inhibits radial colony extension growth. In fully grown cultures, lack of aeration stops Sk initiation. Instead, fluffy mycelium is formed at the edges of the Petri dishes. However, keeping KOH that traps accumulated CO_2 in sealed culture plates helped to restore the mycelial growth induced Sk formation and stopped out-growth of elongated stipes. Such alteration in the growth of mycelia and the phenotype of primordia under unaerated conditions appeared to be caused by the increased concentration of CO_2 thus, indicated the establishment of a CO_2 sensing system in *C. cinerea*.

In fungi, carbon dioxide is sensed via carbonic anhydrase and adenylyl cyclase pathways where cAMP signaling cascades are involved which are directly or indirectly responsible for the growth, morphology, sporulation, mating and the virulence in various fungi (Elleuche and Pöggeler 2009; Martin et al. 2017). In *C. cinerea*, cAMP plays an important role in fruiting

body induction by activating cAMP-dependent kinases that may target proteins involved in sexual morphogenesis (Uno et al. 1974; Uno and Ishikawa 1981; Swamy et al. 1985). With changes in environmental conditions, however, the regulation of the cAMP can also change, which probably has a direct impact on the morphological development of an organism.

Accordingly, with the accessibility of the external conditions, the internal responses are respectively triggered by which different types of genes are activated to participate in the process of constructing a complex body of a mushroom. Early genetic studies also revealed that several later developmental steps such as meiosis, basidiospore formation, cap expansion and autolysis could operate independently of each other (Takemaru and Kamada 1972; Pukkila and Casselton 1991). Newer studies revealed transcriptomes during steps of the primordia pathway (Muraguchi et al. 2015; Cheng et al. 2015) and at later stages of karyogamy, meiosis and spore formation (Burns et al. 2010, Krizsán et al. 2019). However, not many genes that contribute to the fruiting process are further characterized till date. Therefore, attempts were made in the past to generate the developmental mutants that can help to unravel the essentials of the fruiting process. Around 1500 mutants were generated by UV and REMI mutagenesis to study the functions of various genes in the fruiting process (Granado et al. 1997; Cummings et al. 1999; Muraguchi et al. 1999). For this task, the self-compatible homokaryotic strain AmutBmut with mutations in the mating-type loci resulting in a fruiting ability without a mating partner proved to be an ideal strain (Swamy et al. 1984). The strain mimics a dikaryon in all behaviors, including the formation of clamp cells at the septa of its hyphae, production of haploid asexual spores upon induction by light, and abundant sclerotia formation (Swamy et al. 1984; Polak et al. 1997; Kertesz-Chaloupková et al. 1998). Haploid oidia of the strain have been used to generate mutants by UV and REMI (restriction enzyme mediated integration) mutagenesis approaches (Granado et al. 1997; Cummings et al. 1999; Muraguchi et al. 1999; Kües 2000). Mutants with defects at different stages of development were generated. However, in the collection of mutants, mutations do not evenly distribute over the complete pathway of fruiting body development which may reflect the complexity of specific steps in fruiting. Among mutants generated from homokaryon AmutBmut are the dark stipe mutants *dst1*, *dst2*, *dst3* and *dst4*, which form dark stipes with elongated stipes and underdeveloped caps under standard fruit conditions. *dst1* and *dst2* are UV and REMI mutants, respectively and are blind at early stages of Sk stage thus and form dark stipes under standard fruiting conditions. These mutants were characterized in Japan and known to have defects in the WC1 white collar 1 photoreceptor and a FAD/FMN-containing dehydrogenase, respectively (Terashima et al. 2005; Kuratani et al. 2010). They are also blind with respect of light-induced oidiation (Chaisaena 2006). A strain 7K17 is a UV mutant and B1918 is a REMI mutant of AmutBmut and they appeared to have defects at the later stages P3 and P4, respectively. Thus, they resulted in dark stipes at the later stages P4 and P5. However, light regulation of oidia production was normal in mutant B1918 and also still active in mutant 7K17 but with lower effectivity (Chaisaena 2009). Whole-genome sequencing performed by Botond Hegedüs and László Nagy (unpublished) identified each two interesting mutations in these mutants (U. Kües, personal communication). By missense

mutations, 7K17 is altered in pyruvate dehydrogenase subunit E1 and in acetolactase synthase ILV2, both of which are thiamine-dependent enzymes and release CO_2 in their biochemical actions on pyruvate. B1918 then has an early-stop mutation in a citrate synthase gene. Both mutants, therefore, are possibly blocked-in feeding acetyl into the TCA cycle (Fig. 10). B1918 has also a defect in the Cop9 signalosome (subunit CSN5; Kües et al. unpublished) which coordinates light and respiratory activities with developmental processes (Christmann et al. 2013; Cárdenas-Monroy et al. 2017; Bramasole et al. 2019). In 7K17, a further interesting mutation (loss of start codon) is in a gene for an Arf1-like protein as a small GTPase-regulatory protein that is directly localized next to gene *cfs1* for a cyclopropane fatty acid synthase shown to be necessary for primary hyphal knot formation. Expression of the *arf1*-like gene is reduced at Pk formation but about twice as high in the vegetative mycelium grown in dark or light and at the tested primordial stages P2 and P4 (Liu et al. 2006).

In this study, investigations were done to determine the effect of aeration on the mycelial growth and in the developing primordial stages of the wild type strain AmutBmut. Furthermore, defects on the dark stipe mutant strains 7K17 and B1918 were analyzed and studied.

5.2.3. Materials and method

5.2.3.1. Strains and culture conditions

All strains used in this study are listed in Table 1.

Strains	**Genotype**	**Type of mycelium, mutagenesis**	**Source/reference**
AmutBmut	*A43mut, B43mut, pab1*	self-compatible homokaryon	Swamy et al. (1984); P. Pukkila (1993); Muraguchi et al. 2015
7K17	*A43mut, B43mut, pab1-1, dst3-1*	compatible AmutBmut mutant obtained by UV mutagenesis	JD. Granado et al. unpublished; K. Kertesz-Chaloupková unpublished
B1918	*A43mut, B43mut, pab1-1, ::pab1+, dst4-1*	compatible AmutBmut mutant obtained by REMI mutagenesis with plasmid pPAB1-2	Granado et al. unpublished; Liu et al. (1999)

The self-compatible *C. cinerea* homokaryon AmutBmut (FGSC 25122) (*A43mut, B43mut, pab1*) forms fruiting bodies without prior mating to another strain and produces oidia in a light-regulated manner (Swamy et al. 1984, Kertesz-Chaloupková et al.1998). Mutant B-1918 (*A43mut, B43mut, pab1, :: pab1+*) is a *Bam*HI REMI-mutant of homokaryon AmutBmut with plasmid pPAB1-2 (Granado et al. 1997, Liu et al. 1999) and mutant 7K17 (*A43mut, B43mut, pab1*) is an UV-mutant of homokaryon AmutBmut (Granado et al. 1997; Liu et al. 1999).

All strains were cultivated by placing small pieces of mycelium (4 x 4 mm) in the middle of 9 cm Ø Petri dishes. Strains were routinely grown on YMG/T complete medium at 37 °C in the dark in ventilated black boxes (Granado et al. 1997). When the mycelia are fully grown on the Petri dishes on Day 5 of incubation in constant dark, they were transferred on the same day at 17 h to the fruiting chamber (Vötsch Industrietechnik GmbH, Balingen, Germany) with 12 h light/12 h dark at 25 °C and high humidity of 90 % (Kües et al. 2016).

For testing CO_2 effects on the mycelial growth, 3 days old half-grown culture plates of homokaryon AmutBmut were air-sealed by 5-6 layers of Parafilm (product number: P7793 Sigma-Aldrich, Inc., USA) and then further incubated at different temperature and light conditions i.e. 37 °C dark (in ventilated boxes with wetted tissue paper), 25 °C dark (in ventilated boxes with wetted tissue paper), 25 °C light/dark (standard fruiting conditions with high humidity of 90 %) and 25 °C light for another 6 days. Effects of 1 N KOH in sealed cultures were tested by cutting out a round piece of agar (2.3 cm) at the edges of Petri dishes of cultures after 3 days of growth at 37 °C in the dark, placing a sterile Flacon tube cap (washed with soap, rinsed with water, then sterilized by washing then for several min in 70 % ethanol and air-dried in a laminar flow cabinet) into the space and carefully adding 1.0 ml of 1 N KOH solution into the cap (without any spilling onto the agar!), prior to that plates were sealed and further incubated at conditions as indicated above. Preliminary tests with 0.1, 0.5 and 1 N KOH showed that, as in *Schizoplyllum commune* (Niederpruem 1963), only 1 N KOH was sufficiently effective to capture released CO_2.

For testing CO_2 effects on development of primordial stages during the normal fruiting pathway, for every stage of development as arising on the subsequent days, a subset of culture plates were sealed when light switches, using 5-6 layers of parafilm. Sealed plates were transferred back into standard fruiting conditions in a growth chamber at 25 °C with 12 h light/12 h dark and high humidity of 90 %. The development of the primordia was monitored on all plates every day until Day 7 of the standard fruiting pathway. 1 N KOH solution in a Falcon tube cap was added to the plates at all stages of development prior to sealing as mentioned above.

5.2.3.2. Harvesting and photography

The dark stipes formed at the different stages of development under unaerated conditions were harvested after 24 h incubation with blocked aeration and inspected underneath a Zeiss Stemi 2000-C binocular (Goettingen, Germany). The binocular was equipped with a Soft Imaging Color View II Mega pixel digital camera (Soft Imaging System, Münster, Germany), linked to a computer. Photos were taken and analyzed with Analysis Software program (Münster, Germany). Fresh dark stipes were directly photographed underneath the binocular upon harvest as whole structurers and longitudinally dissected structures.

5.2.4. Results

5.2.4.1. Observations on mycelia growth under unaerated condition

For analyzing the effects of aeration on mycelial growth of *C. cinerea*, agar culture plates were inoculated by a mycelial block of homokaryotic AmutBmut and incubated at 37 °C in dark condition within a ventilated black box with wetted paper tissue underneath. On the 3rd day of incubation at 37 °C, when mycelial colonies covered in diameter half of the plates (9 cm Ø Petri dishes), fungal cultures plates were sealed using 5-6 layers of parafilm (Fig. 1A). Each 3 replicates of the sealed cultures were then kept at different light and temperature conditions, i.e. at 37 °C dark, 25 °C dark, 25 °C light/dark and 25 °C light for another 6 days. Three replicates of unsealed controls were in parallel grown with the sealed plates at the respective conditions. Cultures with light phases were observed every day of further incubation. Photographic documentation of colony growth on all the sealed and unsealed plates was made on the 6th day of incubation at different light and temperature conditions (Fig.1). In total, the whole experiment was repeated three times, with alike results.

We observed that inhibiting the passage of air into cultures delayed further growth of the fungus at all tested conditions and, as judged from light-incubated plates, eventually after 2 days stopped the fungal growth (Fig. 1A). The aerial mycelium of all dark-grown cultures was dense and fluffy. The aerial mycelium of all cultures that received light was also dense but less fluffy.

The unsealed control plates at 37 °C parallely grown with the sealed plates in constant dark showed dense mycelial growth with production of masses of sclerotia on the surface of fully grown aging mycelia (Fig. 1C). On the other hand, cultures on the unsealed control plates at other conditions (25 °C dark/light and 25 °C light) fully covered the whole plates but their outer regions of additionally grown mycelium appeared thin and lacked sclerotia (Fig. 1C). Altogether, the results suggested that an increase in the CO_2 level blocks the mycelial growth of fungi regardless of the change in light and temperature conditions.

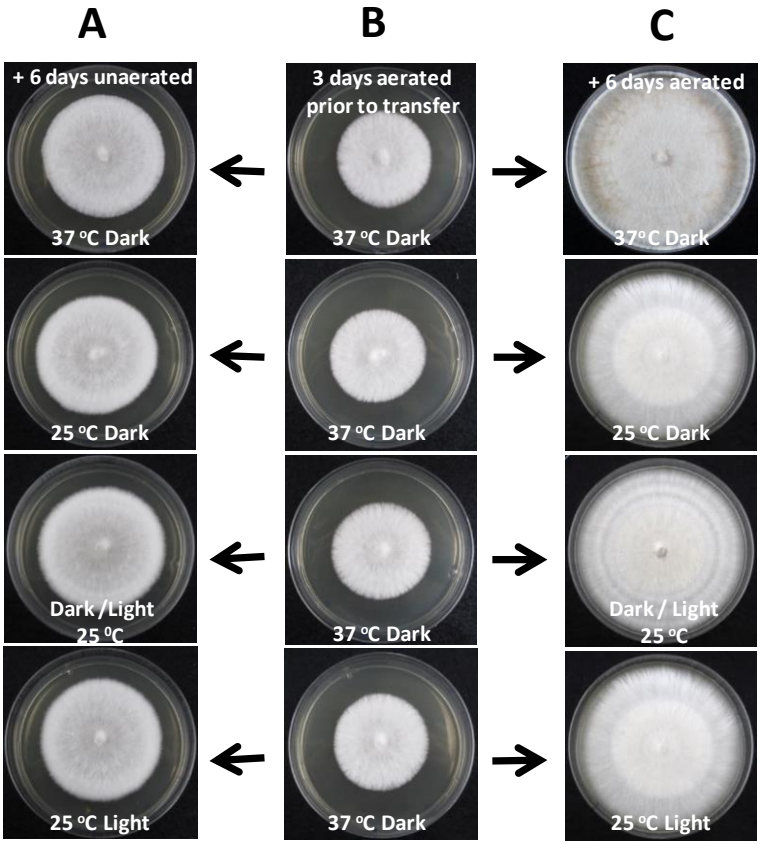

Fig. 1. Mycelial growth under unaerated condition as compared to aeration. (A) Half-grown fungal cultures incubated 3 days at 37 °C at dark condition were air blocked using Parafilm and then kept for further 6 days at different light and temperature conditions. (B) 3 days old cultures incubated at 37 °C at dark condition (C) Unsealed controls were in parallel grown with the sealed plates under the conditions indicated.

5.2.4.2. Observations on primordia development under unaerated condition

In the next part of the study, the effects of absence of aeration were observed on the whole pathway of fruiting body development. For this, inoculation and incubation was done as mentioned in the method and materials section in three series of experiments with always the same observations. Fig. 2 shows then exemplary the entire developmental process under unaerated conditions as subsets of plates were sealed starting from Day 0 to Day 7 of the standard fruiting pathway. This experiment was also repeated three times, with alike results.

On the 5th day of normal incubation under constant dark at 37 °C, when mycelia fully covered the plates, fungal cultures plates were transferred to the fruiting chamber with 12 h light and 12 h dark at 25 °C and 90 % humidity. According to the fruiting pathway of *C. cinerea*, the day on which fully grown cultures was transferred to the fruiting condition is marked as Day 0 (Kües et al. 2016). Every day, when light was switched on in the chamber, subsets of plates were sealed using Parafilm and then put again back into the fruiting chamber. Hindering air entry already on Day 0 before the formation of light-induced Sk fully blocked fruiting initiation. It resulted in the next two days in the formation of fluffy mycelial growth around the edges of a Petri-dish that remained fluffy up to Day 7 of incubation. When plates were sealed at the Sk stage on Day 1, the development arrested at the Sk stage and could not further develop to the P1 stage, up to the end of incubation at Day 7. Block in aeration at P1 to P3 from Day 2 to Day 4, respectively led to the outgrowth of elongated stipes that were morphologically similar to the structures termed "Ds structures" observed in aerated cultures of same age when kept fully at dark (chapter 5.1). The elongated structures continued under block of aeration to grow by stipe length for one further day (elongated P1 structures) to two further days (elongated P2 and P3 structures) and then arrested in development, unlike Ds structures of P1, P2 and P3 that continued in growth (chapter 5.1). When plates were air-sealed on Day 5 at stage P4, on Day 6 stipes extended in length to continue on Day 7 with rapid stipe elongation for fruiting body maturation but the cap of the structures appeared white and remained closed. When plates were then air-sealed on Day 6 at stage P5, fruiting body maturation happened but caps were only partially opened and appeared slight brown by reduced spore numbers and lack of strong pigmentation of spore cell walls, maybe due to disturbances in the process of meiosis (Fig. 2).

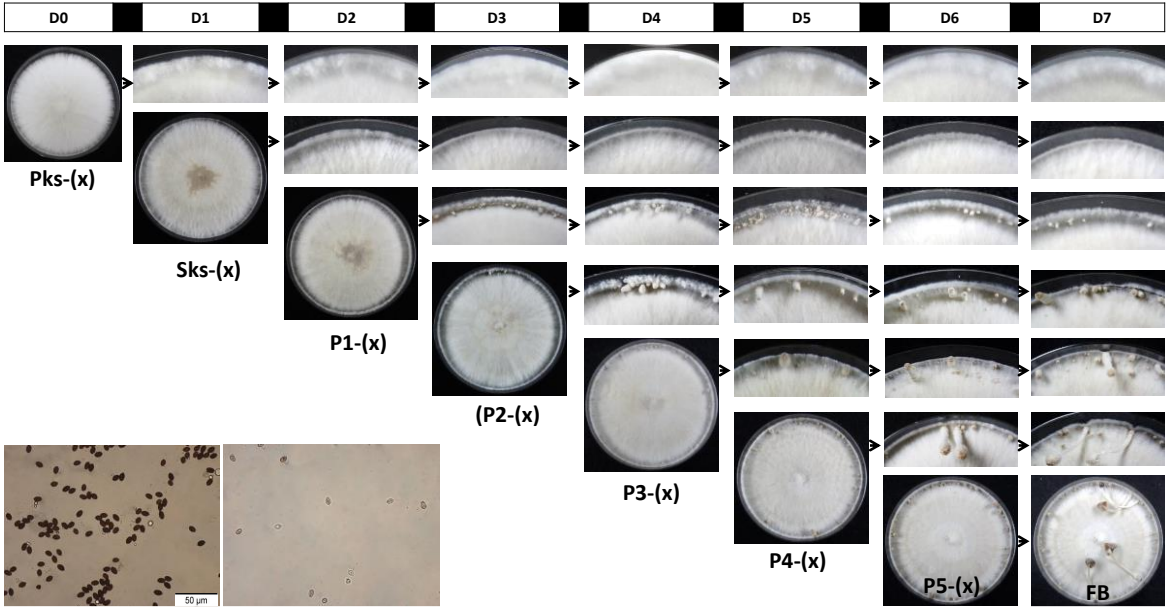

Fig. 3. Formation of mature fruting bodies when unaerated conditions at different stages of development were lifted after 24 h. All stages from Pks to P4 restored normal fruting body after lifting unaerated conditions except for stage P5 primordia which formed closed white cap fruiting bodies, like before in the experiments shown in Fig. 2.

When in other series of experiments unaerated conditions were removed after only incubation for 24 h and plates then were transferred back into the standard fruiting conditions, the fungal cultures closed just for a day at respective stages Pks to P4 all restored their normal development in the following days and formed normal fruiting bodies with open caps and stained basidiospores on day 7 of the standard fruiting pathway but all fruiting bodies had primordial shafts length-stretched by ca 3 mm. When plates were closed for 24 h at the P5 stage, primordia developed into white closed cap fruiting bodies with reduced number of unstained basidiospores and failed in autolysis on Day 7, as in the experiments above (Fig. 3,4).

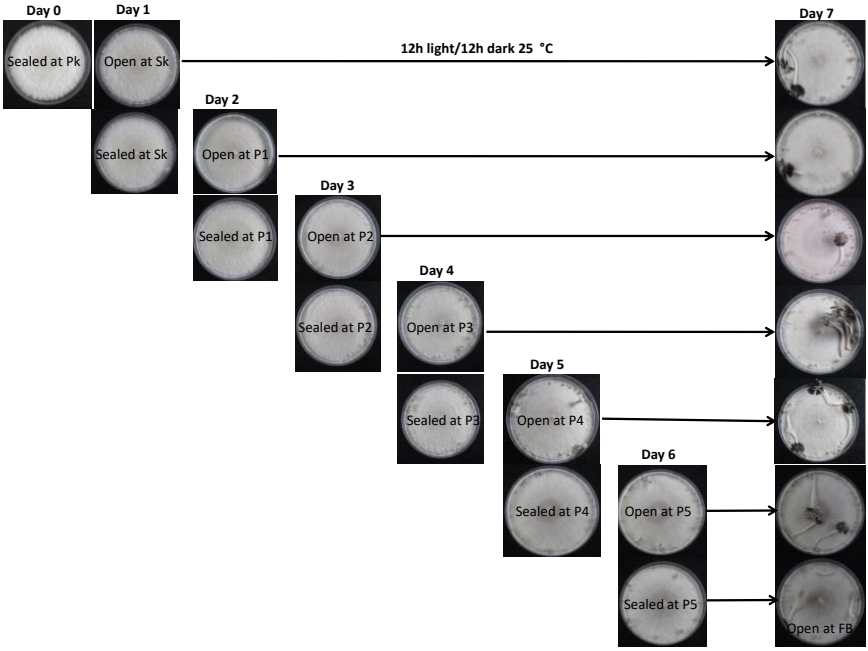

Fig. 4. shows a comparison between the development of primordia at different stages under standard fruiting conditions, aerated constant light, aerated constant dark and unaerated 12 h light and 12 h dark conditions (Fig. 4A and 4B). Under unaerated conditions for 24 h, there was a blokage in the initial stages of the fruting body development at stages Pks and Sks unlike at 24 h in constant light and 24 h in constant dark conditions. The primordial stages from P1 to P4, however, developed in their caps to their next respective stages after 24 hours of incubation under non-ventilated conditions, despite their elongated stipes (Fig. 4B), as recognized by typical changes in sizes and morphologies of caps (Fig. 4A) and by the longitudinal cuts of the primordia at the different stages (Fig. 4B). Also the development of stage P5 primordia when incubated for 24 h in unaerated conditions resulted with the formation of normal shaped fruiting bodies with non-autolysing white caps and a reduced number of partially colored basidiospores. However, such outcome was not comparable to how the primordia at the P5 stage developed when incubated either under constant dark or constant light. In both conditions, under constant dark and constant

light, the P5 stage primordia were fully matured in the normal way and arising fruiting bodies underwent autolysis shedding their stained basidiospores in black droplets (Fig. 4A and 4B).

A

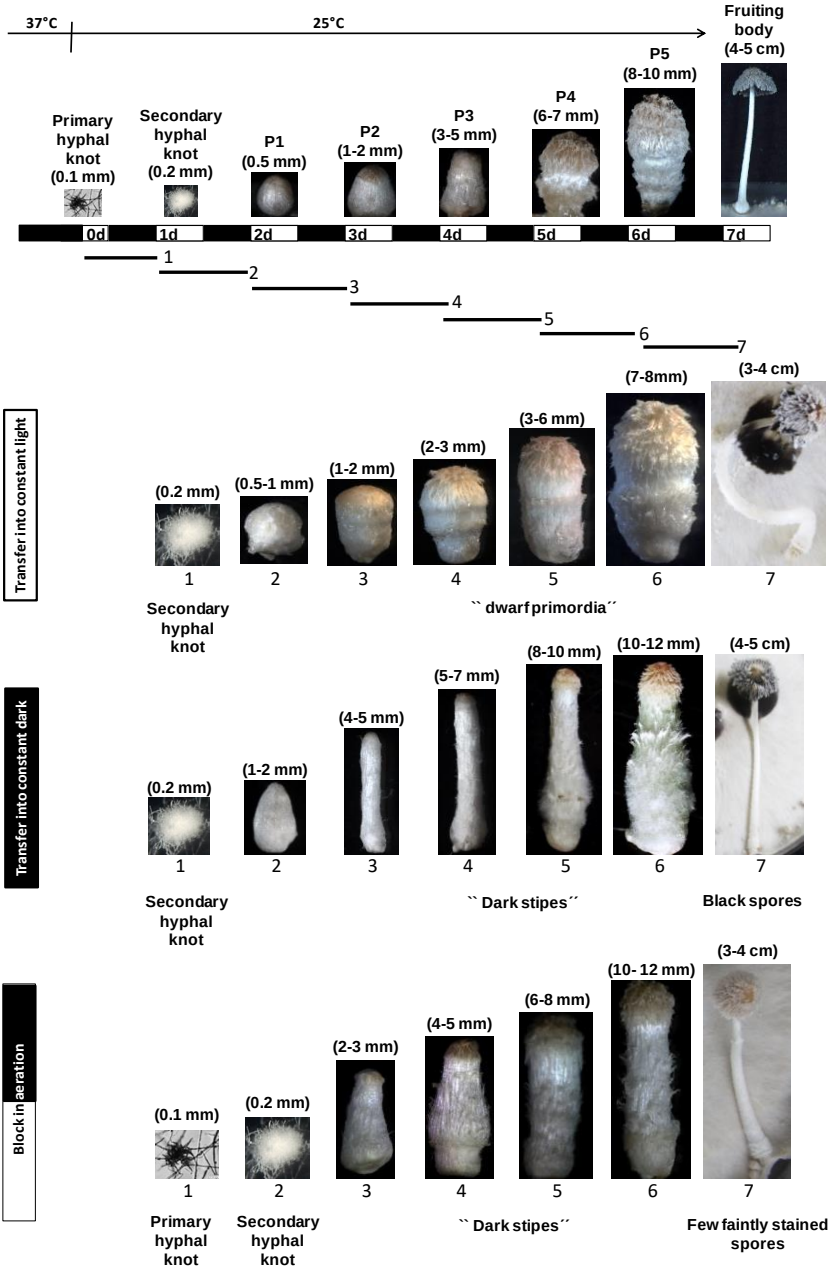
37°C
25°C
Fruiting body (4-5 cm)
P5 (8-10 mm)
P4 (6-7 mm)
P3 (3-5 mm)
P2 (1-2 mm)
P1 (0.5 mm)
Primary hyphal knot (0.1 mm)
Secondary hyphal knot (0.2 mm)
0d
1d
2d
3d
4d
5d
6d
7d
1
2
3
4
5
6
7
Transfer into constant light
(0.2 mm)
(0.5-1 mm)
(1-2 mm)
(2-3 mm)
(3-6 mm)
(7-8mm)
(3-4 cm)
Secondary hyphal knot
`` dwarf primordia´´
Transfer into constant dark
(0.2 mm)
(1-2 mm)
(4-5 mm)
(5-7 mm)
(8-10 mm)
(10-12 mm)
(4-5 cm)
Secondary hyphal knot
`` Dark stipes´´
Black spores
Block in aeration
(0.1 mm)
(0.2 mm)
(2-3 mm)
(4-5 mm)
(6-8 mm)
(10- 12 mm)
(3-4 cm)
Primary hyphal knot
Secondary hyphal knot
`` Dark stipes´´
Few faintly stained spores

B

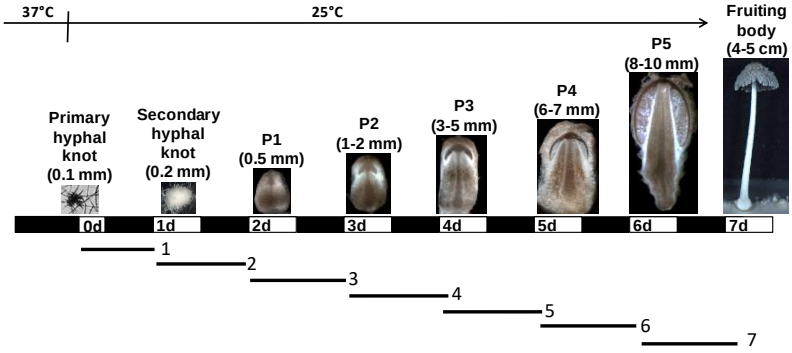
37°C
25°C
Fruiting body (4-5 cm)
P5 (8-10 mm)
P4 (6-7 mm)
P3 (3-5 mm)
P2 (1-2 mm)
P1 (0.5 mm)
Secondary hyphal knot (0.2 mm)
Primary hyphal knot (0.1 mm)
0d
1d
2d
3d
4d
5d
6d
7d
1
2
3
4
5
6
7

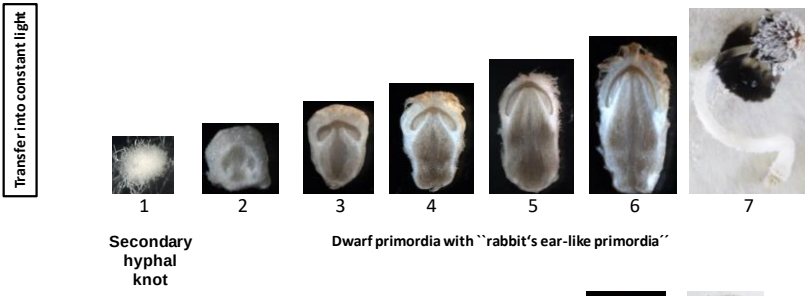
Transfer into constant light
1
2
3
4
5
6
7
Secondary hyphal knot
Dwarf primordia with ``rabbit's ear-like primordia´´


Transfer into constant dark
1
2
3
4
5
6
7
Secondary hyphal knot
`` Dark stipes´´

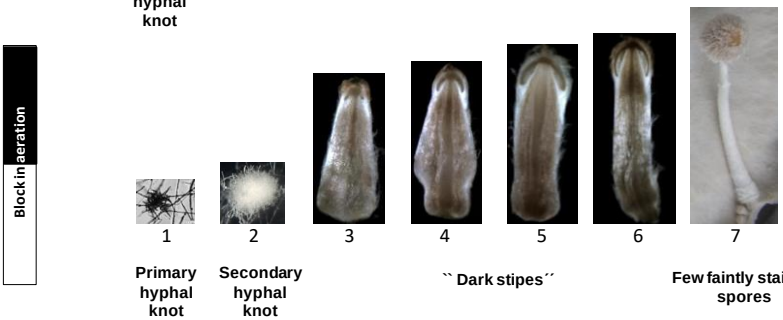
Block in aeration
1
2
3
4
5
6
7
Primary hyphal knot
Secondary hyphal knot
`` Dark stipes´´
Few faintly stained spores

Fig. 5. Comparisons on the process of fruiting body developmental pathways of homokaryon AmutBmut cultivated under different conditions as indicated. (A) Harvested structures 24 h of incubation after changes in environment conditions and (B) their longitudinal halves are compared. Top: standard condition, 2nd: constant light, 3rd: constant dark and. Bottom: unaerated conditions.

5.2.4.3. Effects on mycelial growth and primordia development in cultures cultivated under unaerated condition in presence of KOH

To observe the effects of CO_2 on the mycelial growth and primordia development, agar culture plates were inoculated by a mycelia block of homokaryotic AmutBmut and incubated for 3 days at 37 °C in dark condition with humidity within a ventilated black box. Then, plates were sealed with Parafilm with or without KOH. Experiments were performed three times with each n = 3 plates per test case with comparable results in the three runs.

On 3rd day of incubation at 37 °C, when mycelia covered in diameter half of the plates (Fig. 6, 2nd column), 1 N KOH was added into the fungal cultures and then, they were air-blocked using 5-6 layers of Parafilm as control cultures without KOH. Three replicates of the sealed cultures with KOH were then kept at different light and temperature conditions i.e., 37 °C dark, 25 °C light/dark and 25 °C light for 3 days, and similarly three sealed cultures each without KOH addition. Three replicates of unsealed controls were in parallel grown with the sealed plates at the respective conditions (Fig. 6, 3rd column). Observations made after 6 days of incubation at different light and temperature conditions showed that all sealed plates with KOH restored growth and colonies were fully grown on the sealed culture plates at all tested conditions (Fig. 6, 4th column) unlike the sealed plates without KOH (Fig. 6, 1st column) but similar to the unsealed plates (Fig. 6, 3rd column). However, the further growth in sealed plates with KOH was more vigorous and fluffier than that in the unsealed plates incubated under same conditions.

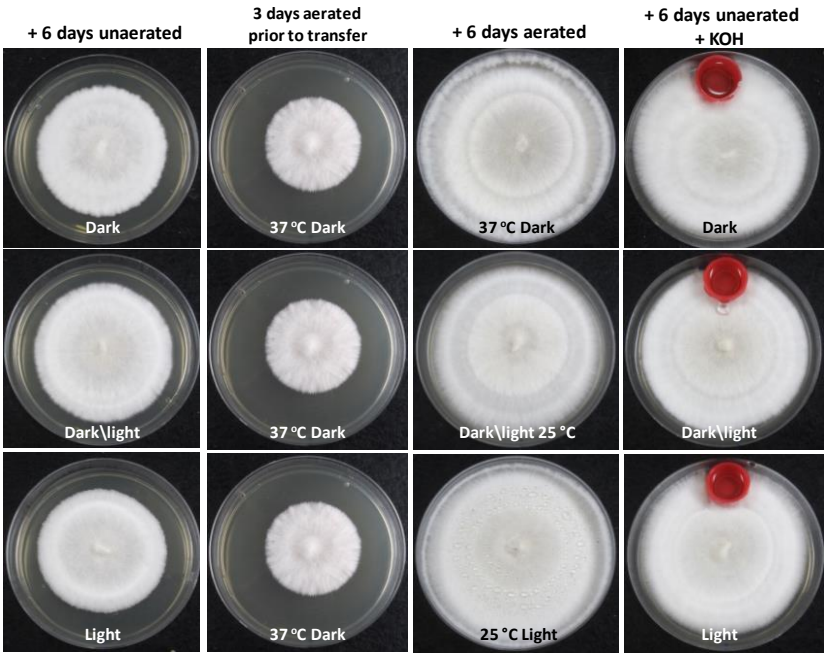

Fig. 6. Growth of mycelia of homokaryon AmutBmut in sealed agar plates without and after the addition of KOH (last column) as compared to unsealed plates. Other growth conditions were as indicated in the figure.

Further, to observe the effect of KOH on the fruiting body developmental pathway, every day at different stages of development from Pk to P5 on Day 0 to Day 6, respectively, 1 N KOH was added into subsets of culture plates and then sealed with layers of Parafilm. The introduction of 1 N KOH at different developmental stages starting from Pk to P5 helped to restore in the next 24 h Sk formation (Fig. 7), normal primordia development and normal autolysis of the caps with pigmented basidiospores at the respective following days as shown in Fig. 8. Afterwards, all development in sealed plates with KOH arrested at the stages shown in Fig. 7 and 8, probably by the consumption of KOH by scavenging CO_2 (photos not shown).

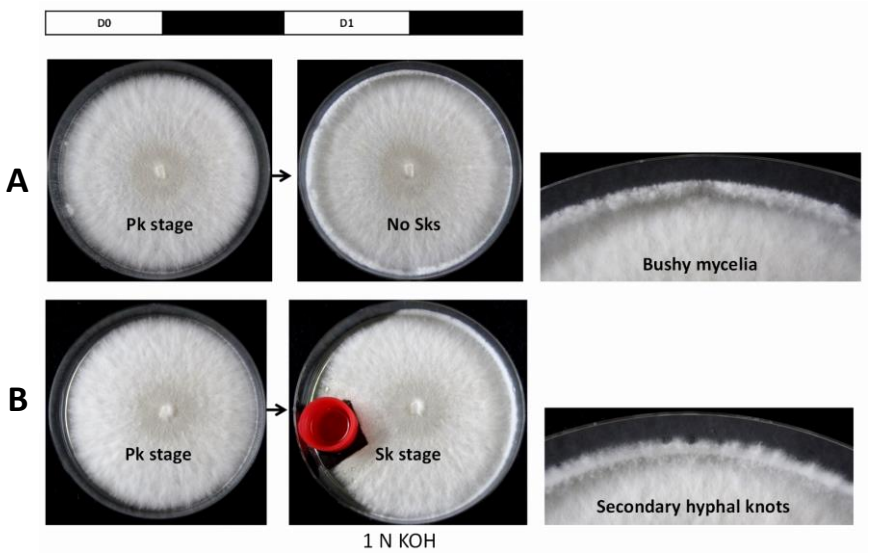

Fig. 7. Effect of initiation of Sks on the cultures of homokaryon AmutBmut on the sealed plates with and without KOH. (A) Culture plates sealed at the Pk stage on Day 0 formed no Sk but instead vigorous aerial mycelia around the outer edges of the plates cultivated at 25 °C under a 12 h light and 12 h dark rhythm. (B) By adding KOH in the sealed plates, Sk formation with less aerial mycelium was achieved. D0 and D1 refer to Day0 and Day1of the standard fruiting pathway. Black and white boxes represent dark and light phases.

Fig. 8 shows the primordia development in culture plates sealed at different primordial stages of development, from P1 to P5, with and without KOH. Elongated primordia with extended stipes were formed within 24 h in the culture plates that were sealed whereas in the sealed culture plates with 1 N KOH further development of primordia for the next 24 h appeared normal. When fungal cultures plates were sealed at the P5 stage, the primordia elongated their stipes but failed to open cap and produced spores. In contrast, with the inclusion of 1 N KOH into the culture plates at the P5 stage enabled fruiting bodies to mature with open caps that produced stained basidiospores as fruiting bodies under standard fruiting conditions (Fig. 8).

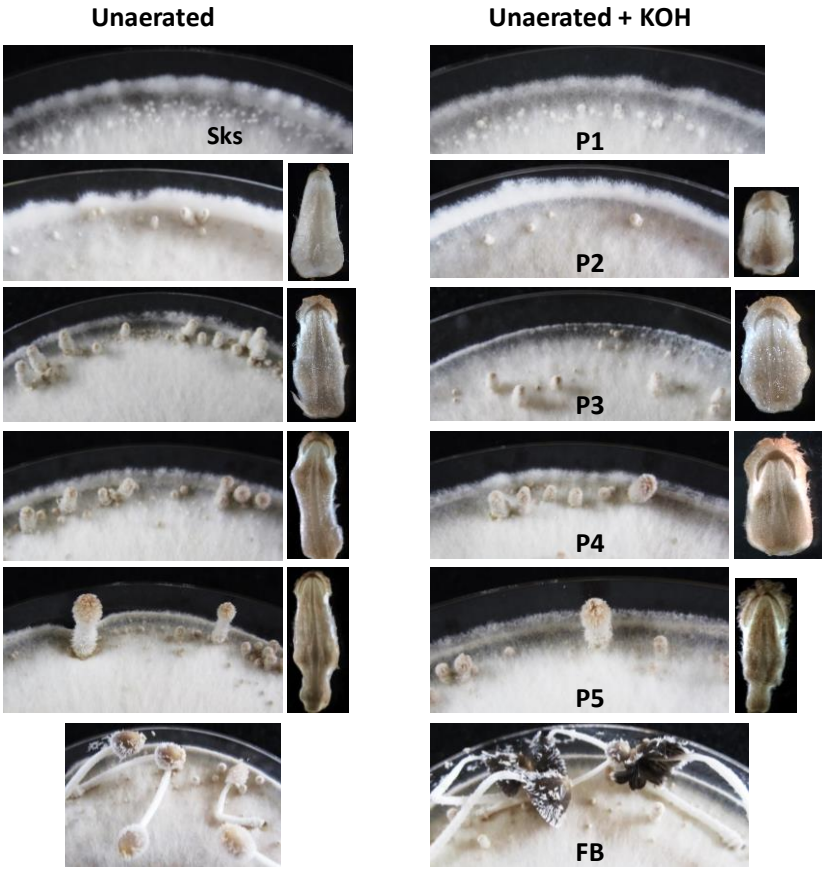

Fig. 8. Primordia development in culture plates of homokaryon AmutBmut sealed at different primordial stages of development (at P1 to P5) with and without KOH after 24 h further incubation at 25 °C. Elongated primordia with extended stipes and were formed under unaerated conditions while addition of KOH in the sealed culture plates restored the normal phenotype of primordia and also the fungus reached maturation with open caps, produced basidiospores and autolyzed as in standard condition.

5.2.4.4. Analyzing the defects in dark stipe mutant strains 7K17 and B1918

Mutants generated from AmutBmut by mutagenesis approaches include the dark stipe mutants *dst1* (REMI generated), *dst2* (REMI generated), *dst3* (UV generated) and *dst4* (REMI generated), which form dark stipes with elongated stipes and underdeveloped caps under

standard fruiting conditions (JD. Granado et al. unpublished; K. Kertesz-Chaloupková unpublished; Liu et al. 1999; Terashima et al. 2005; Kuratani et al. 2010). *dst1* and *dst2* are blind at initial stages of fruiting process thus, they formed dark stipes under standard fruiting condition from Day 2 in standard fruiting conditions onwards, i.e. their defect is effective at Day 1 with the Sk stage. These REMI mutants were characterized in Japan and are known to have defects in the WC1 (white collar 1) photoreceptor and in an uncharacterized FAD/FMN-containing dehydrogenase, respectively (Terashima et al. 2005; Kuratani et al. 2010). Strain 7K17 is a UV mutant and B1918 is a REMI mutant of homokaryon AmutBmut and they appeared to have defects at the later stages P4 and P5, respectively. Thus, they produced dark stipes with defects effective on Day 5 with the P3 stage and Day 6 with the P4 stage of development (Fig. 8, Liu et al. 1999; Chaisaena 2009). *dst1* and *dst2* structures tend to elongate for 6 days while *dst3* and *dst4* structures elongate for all 7 days of the standard fruiting pathway as shown in the Fig. 9 and 10A.

The cultivation of the dark stipe mutants was also tested under constant dark conditions at 25 °C, which led to the formation of elongated stipes in all mutants compared to the dark stipe mutants which were incubated under standard fruiting conditions (Fig. 10B).

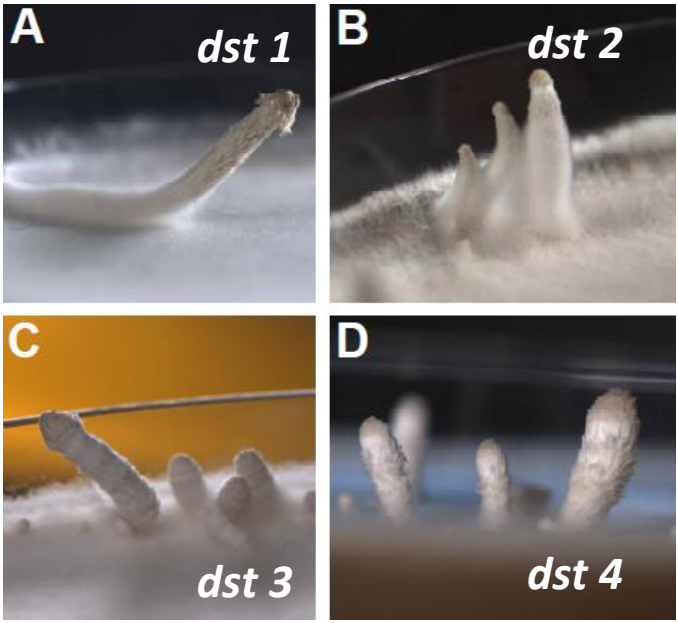

Fig. 9. A-D are the images dark stipes mutants with the defects in 4 genes *dst1* to *dst4* forming dark stipes on YMG/T agar plates at 25 °C. (Photos taken by Wassana Chaisaena 2009)

A

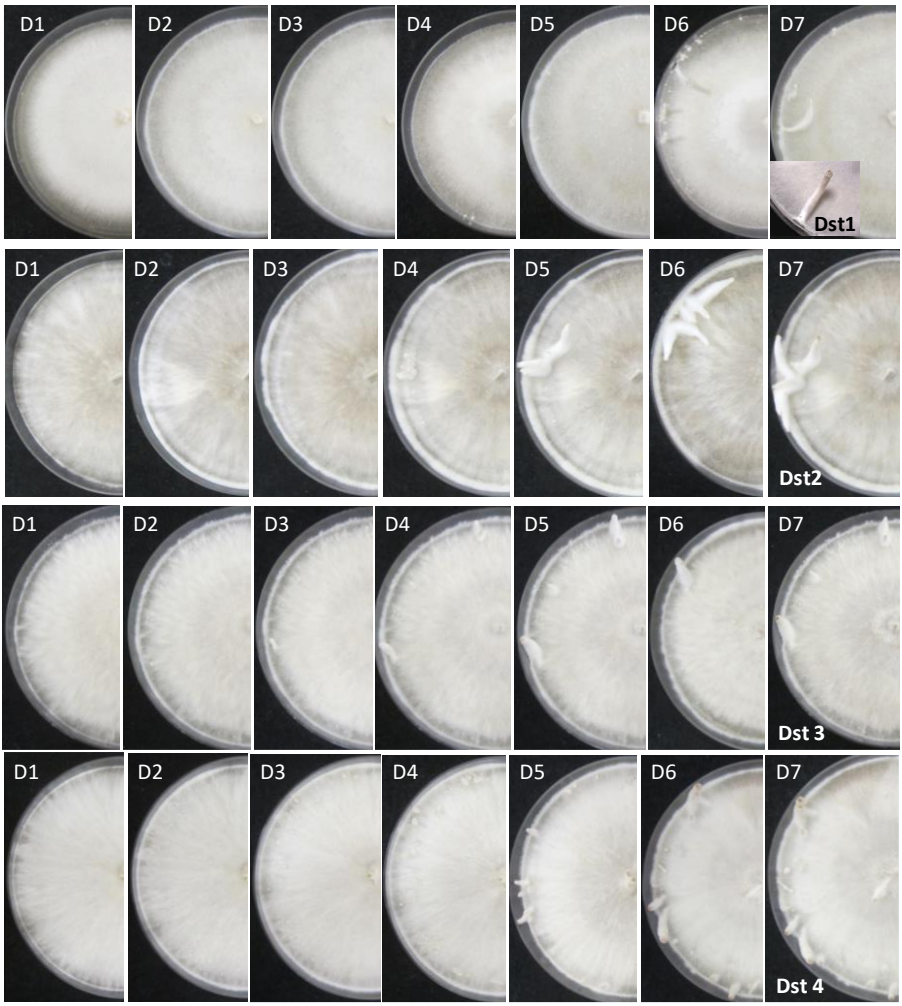
D1
D2
D3
D4
D5
D6
D7
Dst1
D1
D2
D3
D4
D5
D6
D7
Dst2
D1
D2
D3
D4
D5
D6
D7
Dst 3
D1
D2
D3
D4
D5
D6
D7
Dst 4

B

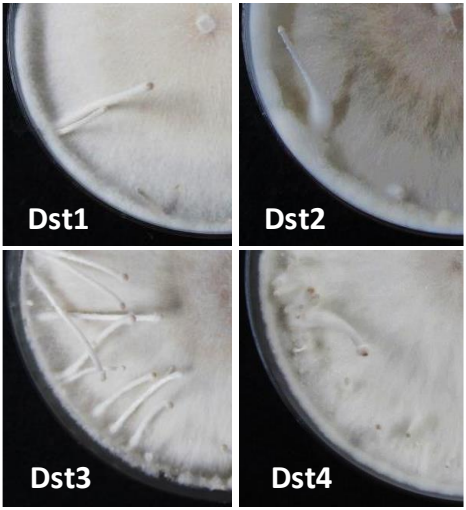

Fig. 10 (A) Developmental pathways of the mutants *dst1*, *dst2*, *dst3* and *dst4* under standard fruiting conditions. (B) Extended stipes of the dark stipe mutants cultivated under constant dark conditions at 25 °C.

Whole-genome sequencing of strains 7K17 and B1918 established in cooperation with Botond Hegedüs and László Nagy identified 64 and 40 different SNPs, respectively in their genomes (single-nucleotide polymorphism; B. Hededüs, personal communication), some of which that correlated with mutations in interesting genes in these mutants (Fig. 11, Kües and Subba, unpublished). Accordingly, 7K17 has missense mutations in pyruvate dehydrogenase subunit E1 (codon 49 CCC changed to ATC, P49I) and in acetolactase synthase ILV2 (codon 49 AAC changed to GAC, N482D), both of which are thiamine-dependent and release CO_2. B1918 has a truncated citrate synthase by a nonsense mutation (codon 230 CGA changed to TGA, R230*) causing loss of the C-terminal membrane retention motif KRVE. Both mutants, therefore, may be hindered in feeding acetyl into the mitochondrial TCA (citric acid) cycle (see Fig. 10). B1918 has also a defect in the Cop9 signalosome (in its subunit CSN5) which coordinates light and respiratory activities in the mitochondria with developmental processes (Christmann et al. 2013; Cárdenas-Monroy et al. 2017; Bramasole et al. 2019). There were three missense mutations in subunit CSN5: codon 73 GAG changed to GGG E73G; codon 97 GTA changed to CTA, V97L; codon 116 GAA changed to GGA, E116G, which are all in the zinc-binding region of the protein and of which at least the first one will block the protein degradation function of CSN5 as shown before in *Schizosaccharomyces pombe* (Ambroggio et al. 2003).

Further in mutant 7K17, the gene for an *arf1* (ADP-ribosylation factor-like protein 1)-like protein (a small GTPase with likely developmental regulator function) has lost its start codon (codon 1 ATG changed to AAG) by a nonsense mutation, Interestingly, this gene localizes in the genome directly next to gene *cfs1* that is essential in the fruiting pathway as the step of Pk formation (Liu et al. 2006). Expression of *arf1* was found reduced at the Pk stage but equally high before in the vegetative mycelium grown in dark and grown in light and in later stages of primordia development (according to the time scheme shown in Fig. 4), P2 and P4 were tested in the study by Liu et al. (2006).

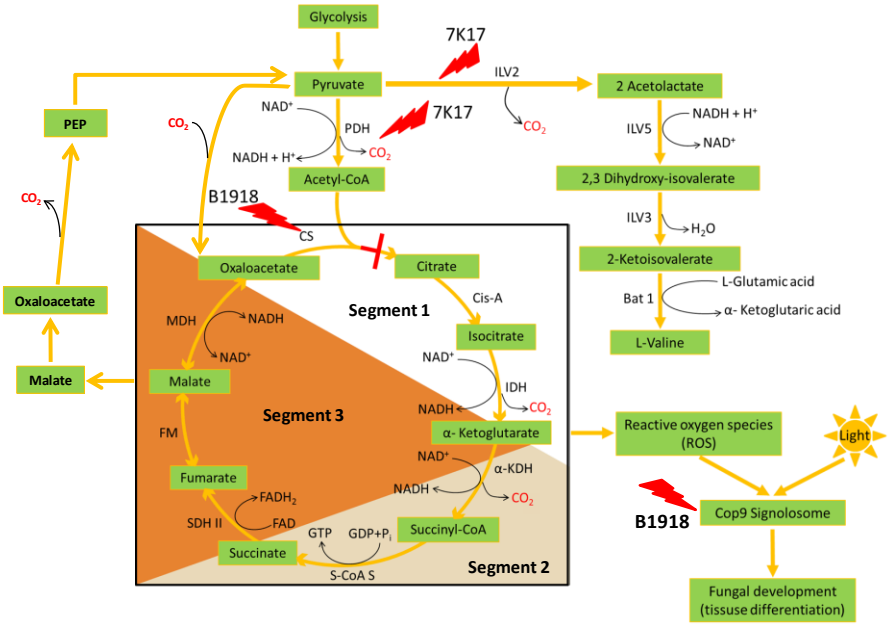

Fig. 11. The citric acid cycle and related pathways. Strains 7K17 (*dst3*) and B1918 (*dst4*) have potential blocks to the entry into the respiratory parts of the TCA cycle which require NAD+ and acetyl-CoA (Segment 1 from oxaloacetate to α-ketoglutarate; Segment 2 from α-ketoglutarate to succinate). Segment 3 from succinate to oxaloacetate may reverse under anaerobiosis (Owen et al. 2002) and under anaplerotic CO_2 fixation (Chinopolous 2013) via carboxylation of PEP (Phosphoenolpyruvate**)** and pyruvate. From our observation of cultures grown under unaerated condition, we assume that such processes might happen in sealed cultures producing ``dark stipes´´.

5.2.5. Discussion

5.2.5.1. CO_2 sensing system in fungi

Carbon dioxide not only plays a key role in the global carbon cycle but also plays an important part in vital organismal processes, such as in photosynthesis in plants and in respiration e.g in animals. All organisms including bacteria and fungi have developed carbon dioxide sensing systems according to the changing environmental CO_2 levels, in order to adapt themselves to such changes (Cummins et al. 2014). For example, many bacterial pathogens demonstrate increased growth potential and virulence when exposed to the elevated CO_2 levels found within mammalian hosts (Cummins et al. 2014).

In fungi, CO_2 is a key factor involved in the fundamental biological processes such as vegetative growth, reproductive development and morphology and, where appropriate, also virulence (Bahn and Mühlschlegel 2006; Martin et al. 2017). Fungi primarily sense carbon dioxide via carbonic anhydrase and adenylyl cyclase pathways (Martin et al. 2017, Fig. 12). Carbonic anhydrases are highly conserved zinc-containing metalloenzymes that enable the fixation of CO_2 by its conversion into bicarbonates (Elleuche and Pöggeler 2009; Martin et al. 2017). Bicarbonates are capable of activation of adenylyl cyclase, thereby inducing the adenylyl cyclase-cAMP pathway which controls various cellular processes such as morphology, mating, and sporulation in fungi (Fig. 11) (Bahn et al. 2005; Bahn and Mühlschlegel 2006). In baker's yeast, such pathway controls various cellular processes including stress response on environmental cues and metabolism (Zippin et al. 2001; Martin et al. 2017). In the fungal pathogens *Candida albicans* and *Cryptococcus neoformans*, such pathways are known to play a central role in virulence and invasion of a human body (Martin et al. 2017). An elevated CO_2 also influences the mating signaling pathway in *C. neoformans*; thereby inhibiting sexual reproduction (Bahn and Mühlschlegel 2006).

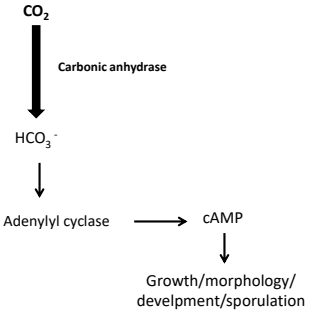

Martin *et al.* 2017

Fig. 12. Enzyme carbonic anhydrase acts as a mediator of CO_2 conversion into bicarbonates which activates adenylyl cyclase- cAMP pathway responsible for triggering various regulatory mechanisms linked to growth, morphology and sporulation.

Besides fungal pathogens, higher mushroom-forming basidiomycetes such as *Schizophyllum commune* (a wood-rotting fungus) can sense CO_2 via cAMP and a high level of CO_2 represses all the developmental stages of fruiting body formation (Niederpruem 1963; Pelkmans 2016). Sca1 and Sca2 are versions of carbonic anhydrase enzymes that are present in *S. commune* and are involved in the conversion of CO_2 to bicarbonate which then induces the adenylyl cyclase-cAMP pathway (Pelkmans 2016). A compatible mating of *S. commune* was carried out in sealed Petri dishes and showed good vegetative growth and clamp-connection formation but fruiting was inhibited. However, by the inclusion of an alkali in the sealed chambers reversed the inhibition (Niederpruem 1963). In our study, a similar kind of CO_2 test was performed by sealing the culture plates of *C. cinerea* using layers of Parafilm. We observed that blocking of the aeration not only blocked mycelial growth but also stopped the initiation and progress of the fruiting body formation in *C. cinerea* at the levels of Pk formation, Sk formation and at P1 stage. Moreover, such sealed cultures have not risen to any sclerotia (multicellular resting bodies, chapter 2.2), even not under prolonged incubation for seven more days as shown on plates in Fig. 2. Sealed cultures formed instead a thick vigorous mycelium around the edges of Petri dishes at the stage of Pk induction. Such growth alterations and developmental inhibitions were restored by the inclusion of KOH into the Petri dishes prior to sealing. This result suggests that the saprotrophic fungus *C. cinerea* senses an elevated level of CO_2 as a result of which altered growth and developmental phenotypes are observed. CO_2 blocks both fruiting body initiation and sclerotia development, indicating that both processes are aerobic and probably responses to oxidative stress.

In *C. cinerea*, not only the initiation of fruiting was affected but the mycelial growth was also completely stopped when the fungal cultures were grown under air-sealed conditions. Various soil fungi show different mycelial growth rates towards an increased CO_2 concentration, for instance, mycelial growth in the ascomycete *Penicillium nigricans* is inhibited whereas in the mucoromycete *Zygorhynchus vuillemin* increased CO_2 levels had less effect on growth (Burges and Fenton 1953). In the mucoromycete *Mucor rouxii*, hyphal growth changes with increasing CO_2 levels into single-celled yeast-like growth (Bartnicki-Garcia and Nickerson 1962). In the mushroom *Agaricus bisporus*, CO_2 produced in the mushroom compost by thermophilic fungi such as *Scytalidium thermophilum* leads to an increased hyphal extension rate of the mushroom mycelium (Wiegant 1992).

Many mushroom forming fungi also exhibited different morphology of fruiting bodies under higher concentration of CO_2, for instance the cap size and the yield of fruiting bodies of *Pleurotus ostreatus* decreased with increase in CO_2 concentration (Jang et al. 2003). An elevated level of CO_2 also has an effect on the morphological structures of *Agaricales*. In *A. bisporus*, high CO_2 concentration has effects on both initial and the later reproductive phases

(Eastwood et al. 2013). Under high CO_2, fluffy chords and early knots were formed on the mycelial network which did not further develop and at the later reproductive stages, yield of the mushrooms were low (Eastwood et al. 2013). Turner (1977) also reported rapid elongation of the stems in *A. bisporus* under high concentrations of CO_2, while the spores matured quickly and the cap and gills expanded upon removal of CO_2.

Other studies also reported malformation of fruiting bodies in the fungi *Flammulina velutipes* and *P. ostreatus* in which pileus expansion was inhibited (Kinugawa et al. 1994; Yan et al. 2019) and heavily damaged by trumpet-like deformation, respectively (Kinugawa et al. 1994). Especially *F. velutipes* is commercially grown under CO_2-rich condition in order to get elongated thin stipes for culinary use which eases harvesting and prolongs shelf-lives whereas in nature the species produce short and thin stipes (Kües and Liu 2000; Sharma et al. 2009). As newly shown in this study, similar types of elongated structures are observed in *C. cinerea* when grown under an unaerated or CO_2-rich environment. On a first overview, they resembled the ``Ds structures (dark stipes) ´´ of *C. cinerea* formed under aerated constant dark conditions. The dark stipes formed under unaerated conditions at 12 h light and 12 h dark from primordial stages P1 to P4, however, developed in their caps to their next respective stages after 24 hours of incubation under non-ventilated conditions unlike in the constant dark conditions where primordia development were arrested at their individual stages (Fig. 5). In addition, the development of stage P5 primordia when incubated for 24 h in unaerated conditions formed normal shaped fruiting bodies on Day 7 of the standard fruiting pathway but with non-autolyzing white caps and a reduced number of partially colored basidiospores. While in constant dark conditions, the P5 stage primordia after 24 h of incubation formed a normal mushroom which autolyzed shedding black spores (Fig. 5).

In summary in *C. cinerea*, we observed higher concentration of CO_2 resulted in the malformation of primordia forming extended stipe structures and further inhibited the expansion of cap thereby blocking autolysis. The CO_2 induced and the repressed stages of development in *C. cinerea* incubated for 24 h at different conditions is compared below in the Table 2 with normal development during the fruiting pathway and with effects of constant dark and of constant light.

Table 2. The CO_2 induced and the repressed stages of development in *C. cinerea* incubated for 24 h at different conditions

25 °C

	Day 0	Day 1	Day 2	Day 3	Day 4	Day 5	Day 6	Day 7
	Pk	**Sk**	**P1**	**P2**	**P3**	**P4**	**P5**	**FB**
☾	Pk induced	Sk repressed Sclerotia induced	P1 rudiment cap and stipe Sclerotia induced	blocked at P1 Sclerotia induced	blocked at P2 Sclerotia induced	blocked at P3 Sclerotia induced	blocked at P4 Sclerotia induced	FB with open cap and black spores, normal autolysis
✸	Pk repressed	Sk induced Sclerotia repressed	P1 cap: advanced stipe: repressed	P2 cap: advanced stipe: repressed	P3 cap: advanced stipe: repressed	P4 cap: advanced stipe: repressed	blocked at P4	FB with open cap and black spores, normal autolysis
12h L/ 12h D	Pk repressed	Sk repressed Sclerotia repressed	P1 repressed	P2 cap: developed stipe: extended	P3 cap: developed stipe: extended	P4 cap: developed stipe: extended	P5 cap: developed stipe: extended	FB with closed cap and partially stanied spores, autolysis repressed

☾ ✸

These symbols represent constant dark, constant light and unaerated conditions, respectively under which at different stages of development were incubated for 24 h.

5.2.5.2. Defects in the dark stipe mutants of *C. cinerea*

In past studies, various mutants were obtained either by conventional UV or chemical mutagenesis or by REMI (restriction enzyme-mediated integration, a technique involving transformation to integrate plasmids into a genome at places opened up by the action of externally added restriction enzymes) for the studies of genes acting in fruiting body development. Among mutants generated from homokaryon AmutBmut by mutagenesis approaches are the dark stipe mutants *dst1*, *dst2*, *dst3* and *dst4*, which form Ds with elongated stipes and underdeveloped caps under standard fruit conditions. The mutations described by Japanese researchers occurred in two independent genes (*dst1* and *dst2*; *dst* = dark stipe). *dst1* and *dst2* mutants are blind at the early stages of hyphal knot formation and form Ds structures under standard fruiting conditions, including a 12 h daily light phase.

Gene *dst1* encodes a protein Dst1 containing two PAS (Per-Arnt-Sim) domains, a coiled-coil structure and a putative, glutamine-rich, transcriptional activation domain (AD). One of the PAS domains has high similarity to the LOV (light-oxygen-voltage-sensing) domains of WC-1 (white collar), VVD (vivid) in *N. crassa* and phototropins in plants (Terashima et al. 2005). As shown by Terashima et al. (2005), the *dst1-1* mutation on chromosome IX has been caused by the truncated putative glutamine-rich AD domain at the C-terminal region. Gene *dst2* located on chromosome V encodes a protein with an FAD-binding-4 domain (flavin adenine dinucleotide) and a BBE (berberine bridge enzyme-like) domain (Kuratani et al. 2010). The result of mutations in these genes caused blind phenotypes in two developmental processes, one in asexual oidia production and the other in sexual fruiting-body photomorphogenesis, suggesting that the two developmental processes share a same light-signal pathway in which the *dst1* and the *dst2* gene are involved (Chaisaena 2009; Kuratani et al. 2010). Observations made in this study add a lack of sclerotia formation in cultures in constant dark as another phenotype to the mutants PUK1 (*dst1*) and PUK2 (*dst2*) (Fig. 9) (Chaisaena 2009). A functional *dst2* gene is thus not required for sclerotia formation. However, it is unclear whether lack of sclerotia formation is due to a defect in one of the *scl* genes needed for sclerotia production (Moore 1981). PUK1 is a F1 progeny of a cross of monokaryon R1428 and homokaryon AmutBmut and PUK2 a F1 progeny of a cross of monokaryon H1-1280 and homokaryon AmutBmut (Chaisaena 2009). While AmutBmut is able to produce sclerotia in the dark (chapter 2.2), these Japanese monokaryons of another origin might not carry responsible sclerotia *scl* genes. Moore (1981) described before that 75 % of *C. cinerea* monokaryons tested lack one or more required *scl* genes.

Further investigations on the involvement of CO_2 in the fruiting body development of *C. cinerea* were carried out in this study using dark stipe UV mutant 7K17 and REMI mutant B-1918 (Liu et al. 1999) with mutations in *dst3* and *dst4*, respectively. Both the mutants were generated from the self-compatible homokaryotic strain AmutBmut and both produce etiolated stipes under standard fruiting conditions (Granado et al. 1997; Liu et al. 1999) and showed morphological defects at the later stages of development; therefore, they cannot make mature fruiting bodies under standard fruiting conditions (Fig. 8). Genomes of these mutant strains were established in cooperation with Botond Hegedüs and László Nagy in Hungary. The whole genome sequencing identified defects linked to the citrate cycle, production of branched amino acids, the Cop9 signalosome and a potential small regulatory GTPase (see result section: 5.2.4.4.), the latter of which is named arf1-like (Liu et al. 2006).

The citric acid cycle, also known as Krebs cycle and shortly TCA, consists of a series of reversible and irreversible biochemical reactions as used by all aerobic organisms to release stored energy through the oxidation of acetyl-CoA derived from carbohydrates, fats, and proteins, into adenosine triphosphate (ATP) and carbon dioxide (Lowenstein 1969; Kay and Weitzman 1987). Even though it is branded as a ``cycle´´, during hypoxia the TCA cycle functions independently in three different segments (Chinopoulos 2013) (Fig. 11). Segment 1 (white underlayed) concerns the tract of the cycle from oxaloacetate to α-ketoglutarate, and the

enzymes citrate synthase to isocitrate dehydrogenase complex. Segment 2 (brown underlayed), the section from α-ketoglutarate to succinate happens during aerobiosis while under anaerobiosis only in presence of sufficient NAD+ and acetyl-CoA and appoints α-ketoglutarate dehydrogenase complex to succinyl-CoA synthetase. Segment 3 (orange underlayed), the path from succinate to oxaloacetate undertaken in aerobic conditions with the enzyme succinate dehydrogenase to malate dehydrogenase, reverses under anaerobiosis because this then generates NAD+ (Chinopoulos 2013). The intermediates of the TCA cycle which are being depleted or consumed are replenished by an anaplerotic reaction, i.e., feeding required intermediates from other sources, thereby preventing the TCA cycle from stopping and at the same time maintaining TCA cycle homeostasis (Chinopoulos 2013).

Strain 7K17 carries mismatch mutations in pyruvate dehydrogenase subunit E1 and in acetolactase synthase ILV2, both of which are thiamine-dependent enzymes and release CO_2. B1918 contains a mutated citrate synthase. Both mutants, therefore, may have blocks to the entry into the respiratory parts of the TCA cycle which require NAD^+ and acetyl-CoA. Due to the possible blockages into the entry of the TCA cycle in the mutants, the cycle may not function in a normal way and only the segment 3 may be functional. In such conditions, segment 3 from succinate to oxaloacetate may reverse even under aerobiosis and under anaplerotic CO_2 fixation via carboxylation of Phosphoenolpyruvate carboxylase (PEP) and pyruvate to give required oxalate. Therefore, effects of such mutations can be seen in the morphology of the mutants producing dark stipes under standard conditions (Fig. 9 and 10), similarly to those produced by the wildtype homokaryon AmutBmut in unaerated plates (Fig. 2 and 4).

In summary, we have presented two distinct scenarios here; one is when the culture plates of the wild-type homokaryotic strain AmutBmut were grown under unaerated conditions, i.e., under increased CO_2 concentration, dark stipes were produced with extended stipes that superficially resembled Ds structures formed under constant dark conditions. On the other hand, similar types of dark stipes were formed by the *dst3* and *dst4* mutants, which are blocked in different steps upon entering the TCA cycle. Due to such blockages in the Dst mutants at the TCA entry points, the TCA cycle could not function normally as the passages from acetyl-CoA to α-ketoglutarate (segment 1) and from α-ketoglutarate to succinate (segment 2) were blocked. Under such conditions of depletion of TCA intermediates, only segment 3 can reverse from succinate to oxaloacetate under aerobiosis and under anaplerotic CO_2 fixation by carboxylation of PEP (phosphoenolpyruvate) and pyruvate, which probably led to the formation of phenotypes with dark stipes in Dst mutants. Similar types of Ds structures were obtained in the sealed plates which led to the assumption that similar types of reactions in which only segment 3 is functional to perform the TCA cycle may have taken place in the sealed culture plates with increased CO_2 concentration generating elongated stipes.

Further, B-1918 also has a defect in the subunit 5 of Cop9 (constitutive photomorphogenesis complex) signalosome (CSN) which is a highly conserved multi-protein complex consisting of 8 subunits CSN1 to CSN8 in higher eukaryotes (Wei et al. 1994; Deng et al. 2000; Wei et al.

2008; Schwechheimer et al. 2010; Braus et al. 2010). The complex was originally identified in plants and subsequently found in all eukaryotic organisms from yeast to humans (Wei et al. 1994, 2008; Schwechheimer et al. 2010). The functions of CSN mainly include regulation of protein degradation, cell signaling pathway, DNA repair, cell differentiation, and development (Wei et al. 2008). The subunit CSN5 is the most studied one and is known to directly bind to numerous target proteins (Wei et al. 2003). CSN5 contains two signature domains, PCI (proteasome cop signalosome initiator) and MPN (Mpr1/Pad1 N-terminal) family domains (Wei and Deng 2003). A JAMM (JAB1/MPN/Mov34 metalloenzyme) motif is present inside the MPN domain of the CSN5 subunit and is responsible for the cleavage of NEDD8-cullin by deneddylation, the process which is mediated by CSN5 (Braus et al. 2010). In *Aspergillus nidulans*, CSND and CSNE show high amino acid identities to CSN4 and CSN5 of higher eukaryotes and have essential regulatory functions in several cellular processes including coloring, cell size, light-dependent signaling and sexual development (Busch et al. 2003). *A. nidulans* senses light by red light receptor and blue light receptors (Blumenstein et al. 2005; Purschwitz et al. 2008) but the sexual cycle (fruiting body formation) is inhibited in light and the fungus forms condiophores for asexual spore production (Purschwitz et al. 2006, 2008; Bayram et al. 2010). In *A. nidulans* mutants, constitutive initiation of the sexual cycle in the presence of light is caused by at least three different single amino acid exchanges within the zinc-coordinating JAMM domain of its CSN5 (Busch et al. 2003, 2007). The E73G as the most N-terminal mutation is the first amino acid of the JAMM domain in the mutated Csn5 of *C. cinerea*, the importance of which for JAMM domain function had been shown before by mutation in *S. pombe* (Ambroggio et al. 2004; see results). In presence of light, the B1918 mutant produces dark-stipes normally in a wildtype repressed by light. In analogy, it is thus possible that the Csn5 mutation in B1918 causes constitutive dark stipe development by lack of light-mediated repression. Asexual sporulation in B1918 is still light-regulated (Chaisaena 2009), suggesting that shared steps in light regulation would not include in asexual sporulation the Cop9 signalosome. In *Alternaria alternata* and *N. crassa*, Csn5 is in contrast essential for conidiation (Wang et al. 2018). Is it in B1918 a coincidence that it has two distinct mutations that may both be a reason for dark stipe formation? Morphologically, the dark stipe phenotype of B1918 resembles rather a CO_2-induced dark stipe than dark stipe produced by a lack-of-light. Transformation of the strain by cloned wildtype genes should help to identify which of the genes is possibly responsible for the phenotype.

Using such a transformation strategy also for 7K17, restoration of the normal wildtype phenotype would likewise identify the responsible dark-stipe mutation, whether it links to the TCA cycle and CO_2 as suggested above, or whether the defect in the afr1-like protein could have a defect in proper regulation of dark stipe repression. In some other fungi, Arf-proteins have functionally been implicated in asexual sporulation for e.g., in *Mucor cirinelloides* Arf proteins regulate important cellular processes such as morphogenesis and virulence (Patino-Medina 2018).

5.2.6. References

Ambroggio, X. I., Rees, D. C. and Deshaies, R. J. (2003) JAMM: a metalloprotease-like zinc site in the proteasome and signalosome. *PLoS Biol*, *2*, pp. e 0113.

Bahn, Y. S., Cox, G. M., Perfect, J. R. and Heitman, J. (2005) Carbonic anhydrase and CO_2 sensing during *Cryptococcus neoformans* growth, differentiation, and virulence. *Current Biology*, *15*, pp.2013-2020.

Bahn, Y. S. and Mühlschlegel, F. A. (2006) CO_2 sensing in fungi and beyond. *Current Opinion in Microbiology*, *9*, pp.572-578.

Bartnicki-Garcia, S. and Nickerson, W. J. (1962) Induction of yeast like development in Mucor by carbon dioxide. *Journal of Bacteriology*, *84*, pp.829-840.

Bayram, Ö., Braus, G. H., Fischer, R. and Rodriguez-Romero, J. (2010) Spotlight on *Aspergillus nidulans* photosensory systems. *Fungal Genetics and Biology*, *47*, pp.900-908.

Blumenstein, A., Vienken, K., Tasler, R., Purschwitz, J., Veith, D., Frankenberg-Dinkel, N. and Fischer, R. (2005) The *Aspergillus nidulans* phytochrome FphA represses sexual development in red light. *Current Biology*, *15*, pp.1833-1838.

Bramasole, L., Sinha, A., Gurevich, S., Radzinski, M., Klein, Y., Panat, N., Gefen, E., Rinaldi, T., Jimenez-Morales, D., Johnson, J. and Krogan, N. J. (2019) Proteasome lid bridges mitochondrial stress with Cdc53/Cullin1 NEDDylation status. *Redox Biology*, *20*, pp.533-543.

Braus, G. H., Irniger, S. and Bayram, Ö. (2010) Fungal development and the COP9 signalosome. *Current Opinion in Microbiology*, *13*, pp.672-676.

Burges, A. and Fenton, E. (1953) The effect of carbon dioxide on the growth of certain soil fungi. *Transactions of the British Mycological Society*, *36*, pp.104-108.

Buller, A. H. R. (1924) Researches on fungi. III. The production and liberation of spores in hymenomycetes and Uredineae. Hafner Publishing Co., New York, N.Y.

Buller, A. H. R. (1931) Researches on fungi, IV. Further observations on the *Coprini* together with some investigations on social organization and sex in the hymenomycetes. Hafner Publishing Co., New York, N.Y.

Burns, C., Stajich, J. E., Rechtsteiner, A., Casselton, L., Hanlon, S. E., Wilke, S. K., Savytskyy, O. P., Gathman, A. C., Lilly, W. W., Lieb, J. D. and Zolan, M. E. (2010) Analysis of the Basidiomycete *Coprinopsis cinerea* reveals conservation of the core meiotic expression program over half a billion years of evolution. *PLoS Genetics*, *6*, p.e1001135.

Busch, S., Eckert, S. E., Krappmann, S. and Braus, G. H. (2003) The COP9 signalosome is an essential regulator of development in the filamentous fungus *Aspergillus nidulans*. *Molecular Microbiology*, *49*, pp.717-730.

Busch, S., Schwier, E. U., Nahlik, K., Bayram, Ö., Helmstaedt, K., Draht, O. W., Krappmann, S., Valerius, O., Lipscomb, W. N. and Braus, G. H. (2007) An eight-subunit COP9 signalosome with an intact JAMM motif is required for fungal fruit body formation. *Proceedings of the National Academy of Sciences*, *104*, pp.8089-8094.

Cárdenas-Monroy, C. A., Pohlmann, T., Piñón-Zárate, G., Matus-Ortega, G., Guerra, G., Feldbrügge, M. and Pardo, J. P. (2017) The mitochondrial alternative oxidase Aox1 is needed to cope with respiratory stress but dispensable for pathogenic development in *Ustilago maydis*. *PLoS One*, *12In*, p.e0173389.

Chaisaena, W. (2009) Light effects on fruiting body development of wildtype in comparison to light-insensitive mutant strains of the basidiomycete *Coprinopsis cinerea*, grazing of mites

(*Tyrophagus putrescentiae*) on the strains and production of volatile organic compounds during fruiting body development. (Ph.D thesis. Georg-August-University Göttingen).
Cheng, X., Hui, J. H. L., Lee, Y. Y., Wan Law, P. T. and Kwan, H. S. (2015) A "developmental hourglass" in fungi. *Molecular Biology and Evolution*, *32*, pp.1556-1566.
Chinopoulos, C. (2013) Which way does the citric acid cycle turn during hypoxia? The critical role of α-ketoglutarate dehydrogenase complex. *Journal of Neuroscience Research*. *91*, pp.1030-1043.
Christmann, M., Schmaler, T., Gordon, C., Huang, X., Bayram, Ö., Schinke, J., Stumpf, S., Dubiel, W. and Braus, G. H. (2013) Control of multicellular development by the physically interacting deneddylases DEN1/DenA and COP9 signalosome. *PLoS Genet*, *9*, p.e1003275.
Cummins, E. P., Selfridge, A. C., Sporn, P. H., Sznajder, J. I. and Taylor, C. T. (2014) Carbon dioxide-sensing in organisms and its implications for human disease. *Cellular and Molecular Life Sciences*, *71*, pp.831-845.
Cummings, W. J. and Zolan M. E. (1998) Functions of DNA repair genes during meiosis. In *Current Topics in Developmental Biology.* 37, pp.117–140.
Cummings, W. J., Celerin, M., Crodian, J., Brunick, L. K. and Zolan, M. E. (1999) Insertional mutagenesis in *Coprinus cinereus*: use of a dominant selectable marker to generate tagged, sporulation-defective mutants. *Current Genetics*, *36*, pp.371-382.
Deng, X. W., Dubiel, W., Wei, N., Hofmann, K. and Mundt, K. (2000) Unified nomenclature for the COP9 signalosome and its subunits: an essential regulator of development. *Trends in Genetics*, *16*, pp.289.
Eastwood, D. C., Herman, B., Noble, R., Dobrovin-Pennington, A., Sreenivasaprasad, S. and Burton, K. S. (2013) Environmental regulation of reproductive phase change in *Agaricus bisporus* by 1-octen-3-ol, temperature and CO_2. *Fungal Genetics and Biology*, *55*, pp.54-66.
Elleuche, S. and Pöggeler, S. (2009) Evolution of carbonic anhydrases in fungi. *Current Genetics*, *55*, pp.211-222.
Granado, J. D., Kertesz-Chaloupková, K., Aebi, M. and Kües, U. (1997) Restriction enzyme-mediated DNA integration in *Coprinus cinereus*. *Molecular and General Genetics*, *256*, pp.28-36.
Jang, K. Y., Jhune, C. S., Park, J. S., Cho, S. M., Weon, H. Y., Cheong, J. C., Choi, S. G. and Sung, J. M. (2003) Characterization of fruit body morphology on various environmental conditions in *Pleurotus ostreatus*. *Mycobiology*, *31*, pp.145-150.
Kamada, T., and Takemaru, T. (1977) Stipe elongation during basidiocarp maturation in *Coprinus macrorhizus*: mechanical properties of the stipe cell wall. *Plant Cell Physiology*, *18*, pp.831–840.
Kay, J., and Weitzman, P. D. J. (1987) "Krebs' Citric Acid Cycle." Half a Century and Still Turning. Cambridge, UK: Biochemical Society.
Kertesz-Chaloupkova´, K., Walser, P. J., Granado, J. D., Aebi, M., and Kües, U. (1998) Blue light overrides repression of asexual sporulation by mating type genes in the basidiomycete *Coprinus cinereus*. *Fungal Genetics Biology*, *23*, pp.95–109.
Kinugawa, K., Suzuki, A., Takamatsu, Y., Kato, M. and Tanaka, K. (1994) Effects of concentrated carbon dioxide on the fruiting of several cultivated basidiomycetes (II). *Mycoscience*, *35*, pp.345-352.

Krizsán, K., Almási, É., Merényi, Z., Sahu, N., Virágh, M., Kószó, T., Mondo, S., Kiss, B., Bálint, B., Kües, U. and Barry, K. (2019) Transcriptomic atlas of mushroom development reveals conserved genes behind complex multicellularity in fungi. *Proceedings of the National Academy of Sciences*, *116*, pp.7409-7418.
Kües, U. (2000) Life history and developmental processes in the basidiomycete *Coprinus cinereus. Microbiol. Mol. Biol. Rev*., *64*, pp.316-353.
Kües, U., Subba, S., Yu, Y., Sen, M., Khonsuntia, W., Singhaduang, W., Lange, K. and Lakkireddy, K. (2016) Regulation of fruiting body development in *Coprinopsis cinerea*. *Mushroom Sci*, *19*, pp.318-322.
Kües, U. and Navarro-Gonzalez, M. (2015) How do Agaricomycetes shape their fruiting bodies? 1. Morphological aspects of development. *Fungal Biology Reviews*, *1*, pp.99-107.
Kües, U. and Liu, Y. (2000) Fruiting body production in basidiomycetes. *Applied Microbiology and Biotechnology*, *54*, pp.141-152.
Kuratani, M., Tanaka, K., Terashima, K., Muraguchi, H., Nakazawa, T., Nakahori, K. and Kamada, T. (2010) The dst2 gene essential for photomorphogenesis of *Coprinopsis cinerea* encodes a protein with a putative FAD-binding-4 domain. *Fungal Genetics and Biology*, *47*, pp.152-158.
Liu, Y., Granado, J. D., Polak, E. and Kües, U. (1999) Crosses with Amut Bmut homokaryons of *Coprinus cinereus*. *Fungal Genetics Reports*, *46*, pp.14-15.
Liu, Y., Srivilai, P., Loos, S., Aebi, M. and Kües, U. (2006) An essential gene for fruiting body initiation in the basidiomycete *Coprinopsis cinerea* is homologous to bacterial cyclopropane fatty acid synthase genes. *Genetics*, *172*, pp.873-884.
Lowenstein, J. M. ed. (1969) *Citric acid cycle* (Vol. 13). Massachusetts, USA: Academic Press.
Lu, B. C. (1974a) Meiosis in *Coprinus.* V. The role of light on basidiocarp initiation, mitosis and hymenium differentiation in *Coprinus lagopus*. *Canadian Journal of Genetics and Cytology*, *52*, pp.299–305.
Lu, B. C. (1974b) Meiosis in *Coprinus*. VI. The control of the initiation of meiosis. *Canadian Journal of Genetics and Cytology*, *16*, pp.155–164.
Martin, R., Pohlers, S., Mühlschlegel, F. A. and Kurzai, O. (2017) CO_2 sensing in fungi: at the heart of metabolic signaling. *Current Genetics*, *63*, pp.965-972.
Moore, D. (1981) Developmental genetics of *Coprinus cinereus*: genetic evidence that carpophores and sclerotia share a common pathway of initiation. *Current Genetics*, *3*, pp.145–150.
Moore, D. (1998) Fungal morphogenesis. Cambridge University Press, Cambridge, United Kingdom.
Moore, D., Elhiti, M. M. and Butler, R. D. (1979) Morphogenensis of the carpophore of *Coprinus cinereus*. *New Phytologist*, *83*, pp.695-722.
Morimoto, N., and Oda.Y. (1973) Effects of light on fruit body formation in a basidiomycete, *Coprinus macrorhizus. Plant Cell Physiology*, *14*, pp.217–225.
Muraguchi, H., Umezawa, K., Niikura, M., Yoshida, M., Kozaki, T., Ishii, K., Sakai, K., Shimizu, M., Nakahori, K., Sakamoto, Y. and Choi, C. (2015) Strand-specific RNA-seq analyses of fruiting body development in *Coprinopsis cinerea*. *PLoS one*, *10*, p.e0141586.

Muraguchi, H., Takemaru, T., and Kamada, T. (1999) "Isolation and characterization of developmental variants in fruiting using a homokaryotic fruiting strain of *Coprinus cinereus*." *Mycoscience, 40*, pp.227-233.
Navarro-González, M. (2008) Growth, fruiting body development and laccase production of selected *Coprini*) (Ph.D thesis. Georg-August-University Göttingen).
Niederpruem, Donald J. (1963) "Role of carbon dioxide in the control of fruiting of *Schizophyllum commune*." *Journal of Bacteriology, 85*, pp.1300-1308.
Ning, W., Chamovitz, D. A., and Deng, X. (1994) "*Arabidopsis* COP9 is a component of a novel signaling complex mediating light control of development." *Cell 78*, pp.117-124.
Owen, O. E., Kalhan, S. C. and Hanson, R. W. (2002) The key role of anaplerosis and cataplerosis for citric acid cycle function. *Journal of Biological Chemistry, 277*, pp.30409-30412.
Patiño-Medina, J. A., Maldonado-Herrera, G., Pérez-Arques, C., Alejandre-Castañeda, V., Reyes-Mares, N. Y., Valle-Maldonado, M. I., Campos-García, J., Ortiz-Alvarado, R., Jácome-Galarza, I. E., Ramírez-Díaz, M. I. and Garre, V. (2018) Control of morphology and virulence by ADP-ribosylation factors (Arf) in *Mucor circinelloides*. *Current Genetics, 64*, pp.853-869.
Pelkmans, J. F. (2016) *Environmental signaling and regulation of mushroom formation* (Doctoral dissertation, Utrecht University).
Polak, E., Hermann, R., Kües, U., and Aebi, M. (1997) Asexual sporulation in *Coprinus cinereus*: structure and development of oidiophores and oidia in an Amut Bmut homokaryon. *Fungal Genetics Biology. 22*, pp.112–126.
Pukkila, P. J. (1993) Methods of genetic manipulation in *Coprinus cinereus*. *Culture, Collection and Breeding of Edible Mushrooms*, pp.249-264.
Pukkila, P. J., and Casselton, L. A. (1991) Molecular genetics of the agaric *Coprinus cinereus*, 127–150. In J. W. Bennett and L. L. Lasure (ed.), *More Gene Manipulations in Fungi*. Academic Press, Inc., San Diego, Calif.
Purschwitz, J., Müller, S., Kastner, C. and Fischer, R. (2006) Seeing the rainbow: light sensing in fungi. *Current Opinion in Microbiology, 9*, pp.566-571.
Purschwitz, J., Müller, S., Kastner, C., Schöser, M., Haas, H., Espeso, E. A., Atoui, A., Calvo, A. M. and Fischer, R. (2008) Functional and physical interaction of blue-and red-light sensors in *Aspergillus nidulans*. *Current Biology, 18*, pp.255-259.
Schwechheimer, C. and Isono, E. (2010) The COP9 signalosome and its role in plant development. *European Journal of Cell Biology, 89*, pp.157-162.
Sharma, V. P., Kumar, S., and Tewari, R. P. (2009) *Flammulina velutipes, the culinary medicinal winter mushroom*. Vol. 6. *Directorate of Mushroom Research, Indian Council of Agricultural Research.*
Swamy, S., Uno, I., and Ishikawa, T. (1984) Morphogenetic effects of mutations at the A and B incompatibility factors of *Coprinus cinereus*. *Journal of General. Microbiology*. *130*, pp.3219–3224.
Swamy, S., Uno, I. and Ishikawa, T. (1985) Regulation of cyclic AMP metabolism by the incompatibility factors in *Coprinus cinereus*. *Microbiology, 131*, pp.3211-3217.
Takemaru, T., and Kamada T. (1972) Basidiocarp development in *Coprinus macrorhizus*. I. Induction of developmental variations. *The Botanical Magazine Tokyo 85*, pp.51–57.

Terashima, K., Yuki, K., Muraguchi, H., Akiyama, M. and Kamada, T. (2005) The dst1 gene involved in mushroom photomorphogenesis of *Coprinus cinereus* encodes a putative photoreceptor for blue light. *Genetics, 171*, pp.101-108.
Tsusue´, Y. M. (1969) Experimental control of fruit body formation in *Coprinus macrorhizus. Development Growth Differentiation 11*, pp.164–178.
Turner, Elizabeth M. (1977) "Development of excised sporocarps of *Agaricus bisporus* and its control by CO*2*." *Transactions of the British Mycological Society 69*, pp.183-186.
Uno, I, and Ishikawa, T. (1974) Effect of glucose on the fruiting body formation and adenosine 39, 59-cyclic monophosphate levels in *Coprinus macrorhizus*. *Journal Bacteriology. 120*, pp.96–100.
Uno, I. and Ishikawa, T. (1981) Control of adenosine 39, 59-monophosphate level and protein phosphorylation by depolarizing agents in *Coprinus macrorhizus*. *Biochim. Biophysica Acta General Subjects, 67*, pp.108–113.
Wang, M., Yang, X., Ruan, R., Fu, H. and Li, H. (2018) Csn5 is required for the conidiogenesis and pathogenesis of the *Alternaria alternata* tangerine pathotype. *Frontiers in Microbiology, 9*, pp.508.
Wei, N., Chamovitz, D. A. and Deng, X. W. (1994) Arabidopsis COP9 is a component of a novel signaling complex mediating light control of development. *Cell, 78*, pp.117-124.
Wei, N. and Deng, X. W. (2003) The COP9 signalosome. *Annual Review of Cell and Developmental Biology, 19*, pp.261-286.
Wei, N., Serino, G. and Deng, X. W. (2008) The COP9 signalosome: more than a protease. *Trends in Biochemical Sciences, 33*, pp.592-600.
Wiegant, W. M., Wery, J., Buitenhuis, E. T. and de Bont, J. A. (1992) Growth-promoting effect of thermophilic fungi on the mycelium of the edible mushroom *Agaricus bisporus*. *Applied and Environmental Microbiology, 58*, pp.2654-2659.
Yan, J. J., Tong, Z. J., Liu, Y. Y., Li, Y. N., Zhao, C., Mukhtar, I., Tao, Y. X., Chen, B. Z., Deng, Y. J. and Xie, B. G. (2019) Comparative Transcriptomics of *Flammulina filiformis* Suggests a High CO_2 Concentration Inhibits Early Pileus Expansion by Decreasing Cell Division Control Pathways. *International Journal of Molecular Sciences, 20*, pp.5923.
Zippin, J. H., Levin, L. R. and Buck, J. (2001) CO_2/HCO_3^--responsive soluble adenylyl cyclase as a putative metabolic sensor. *Trends in Endocrinology & Metabolism, 12*, pp.366-370.

Chapter 6

Genetic regulation: Members of the *NWD2* family are potential candidates involved in the fruiting body development of *C. cinerea*

Contribution to this chapter

Experimental planning: U. Kües and S. Subba
Experimental work: S. Subba
Data analysis: S. Subba
Manuscript writing S. Subba
Manuscript reviewed by U. Kües

6.1. Abstract

Fruiting body morphogenesis of *Coprinopsis cinerea* begins in dikaryotic cultures after simple hyphal growth by localized intense hyphal branching within freshly grown mycelium which leads to hyphal aggregation. A knot-like structure, the primary hyphal knot is formed as a first while not yet committed step in the fruiting process. Under constant dark conditions, primary hyphal knots transform thus into dark brown melanised resting structures sclerotia. Under defined light conditions, primary hyphal knots in dikaryotic cultures may cluster together within the hyphal lattice to form a three-dimensional secondary hyphal knot as the second, now committed step in the process of fruiting body development. The homokaryotic strain AmutBmut with mutations in the *A* and *B* mating type loci is able to fruit despite of having the same type of haploid nuclei in all its cells, thus making AmutBmut a unique strain to study genetics. Proto159 is mutant of strain AmutBmut which has an unidentified *pkn* defect in primary and therefore also in secondary hyphal knot formation. The mutation has been suppressed in previous work by transformation of a gene of the *NWD2* family in the yet unidentified gene encoding a small NTPase. *NWD2* genes encode proteins with an N-terminal NACHT domain. This is an evolutionary conserved domain that serves in signal transduction and is named after four different types of P-loop NTPases (NAIP, CIITA, HET-E and TP1). In *C. cinerea*, 36 genes were found in the sequenced genome for proteins with a conserved NACHT-domain. These genes split further into 7 subgroups (A to G), on the basis of different domains at the C-terminus of encoded proteins – subgroup C has WD-domains while others A, B and D to G have not yet been specifically defined. Genes of the specific *NWD2* family are found only in some of the Agaricomycetes (*Amanita muscaria*, *Agaricus bisporus*, *C. cinerea*, *Galarina maginata*, *Gymnopus luxurians*, *Hebeloma cylindrosporum*, *Hypholoma sublateritium*, *Hypsizygus marmoreus*, *Laccaria amethystina*, *Moniliophthora roreri*, and *Laccaria bicolor*). A phylogenetic tree of the encoded NWD2 proteins from the fungal species indicates that *NWD2* genes were usually multiplied mostly during speciation. The 5' halves encoding the NACHT domain are thereby conserved while they have been fused to variable 3' halves. However, domain functions are not known for most encoded C-termini while tandem WD40 repeats and TRP repeats are present in the C-termini of some NWD2 proteins. The suppression effect of a mutation in fruiting body initiation in *C. cinerea* Proto159 by a *NWD2* gene of the A subgroup suggests that their presence is influential in the regulation of developmental pathways. We have sub-cloned seven different *NWD2* genes of the A subgroup from *C. cinerea* and tested these after transformations of the fungus for effects on sexual and asexual developmental processes. Introduction of cloned genes into mutant Proto159 blocked in some transformants pigmentation, and induced primary hyphal knots and sclerotia and sometimes primordia and fruiting body formation. Transformation into the wildtype homokaryon AmutBmut altered colony phenotypes from poor growth to repeatedly sectoring characterized by irregular growth with parts of colonies collapsing by giving up growth, parts

that may grow out healthy and fluffy AmutBmut-like or fluffy thick, and parts that may grow out as a thin mycelium. Fruiting however speeded up by maturing two days early compared to the normal AmutBmut fruiting and by one day compared to only *pab1*$^{+}$-transformed AmutBmut clones.

6.2. Introduction

The heterothallic Agaricomycetes *C. cinerea* is an excellent model to study fruiting body development. In its life cycle, fruiting normally occurs on the dikaryon and follows a conserved scheme defined by day and night phases, with well predictable distinct stages over time. Fruiting starts with primary hyphal knot formation in dark, followed by light-induced aggregation into a compact round secondary hyphal knot in which stipe and cap tissues differentiate. Primordia development from stages P1 to P5 takes five days to culminate on Day 6 of development in karyogamy (K) and meiosis (M) within the basidia and subsequent basidiospore production which parallels fruiting body maturation (stipe elongation and cap expansion). Fruiting bodies are fully opened in the last night phase to shed their spores, while at the morning on Day 7 the cap autolyzes to release the majority of the spores in liquid droplets that fall to the ground (Navarro-Gonzaléz 2008). Fruiting body development in *C. cinerea* is mainly controlled by mating-type genes in coordination with the environmental signals (Casselton and Kües 1994; Casselton and Olesnicky 1998; Moore 1998; Kües 2000; Kües and Navarro 2015; Chapters 1 to 5 of this thesis).

Strain AmutBmut is a special homokaryotic mutant with defects in the *A* and *B* mating-type loci why it mimics a dikaryon. The strain can fruit like a dikaryon despite having only one type of haploid nuclei in its cells. Like dikaryons, it produces uninucleate haploid oidia upon light-induction (Brodie 1932; Polak et al. 1997; Swamy et al. 1984). Such haploid uninucleate oidia are used to generate collections of mutants by UV and REMI mutagenesis (Granado et al. 1997; Walser et al. 2001). A collection of AmutBmut mutants generated in the fruiting pathway comprises various mutations for every step in the standard fruiting process as morphologically defined in chapters 2 to 4, indicating involvement of many different genes in the fruiting process. *C. cinerea* has a well-established transformation system giving several hundred to one thousand transformants in a single experiment (Binninger et al. 1987; Granado et al. 1997). Some defects in fruiting development in mutants of AmutBmut had been complemented via the transformation of a cosmid with integrated genomic *C. cinerea* DNA (e.g., Liu et al. 2006; Muraguchi and Kamada 1998; Nakazawa et al. 2011). Likewise, complementation tests have been made with AmutBmut mutation Proto159 in fruiting body initiation (*pkn*) through transformations with a cosmid bank of the wild type AmutBmut (Bottoli et al. 1999). A gene belonging to the *NWD2* family repeatedly recovered the defect in fruiting body initiation of the mutant Proto159 after transformation (Ruprich-Robert, Clergeot and Khonsuntia, unpublished experiments). The strain has been isolated after protopasting and regeneration of oidia of strain AmutBmut hence, the name Proto159 (Granado et al. 1997). Proto159 is an AmutBmut mutant that has an unidentified defect in primary and secondary hyphal knot (Sk) formation and can thus not form fruiting bodies. The growth rate of this mutant is slower and with aging, the mutant forms dark pigmentation on the mycelia which diffuses into the agar (Yu et al.

unpublished). Surprisingly, sequencing of the specific *NWD2* gene copy in the mutant Proto159 did not reveal any point mutations, deletion or insertion within this gene. Therefore, it was concluded that the developmental defects of mutant Proto159 were found to be variably suppressed by the transformation of this gene of the *NWD2* family (Yu et al. unpublished).

NWD2 genes encode proteins with a NACHT domain (Fig. 2), an evolutionarily conserved domain that serves in signal transduction and is named after four different types of P-loop NTPases (NAIP, CIITA, HET-E, and TP1) (Koonin and Aravind 2000). NACHT domains are found in fungal, animal and bacterial proteins. However, as reported in this study few species of the Agaricales have genes specific for NWD2 proteins (see below). Genome searches in *C. cinerea* found in total 36 different *NWD2* genes which cluster in 7 different subgroups (A to G) in an evolutionary tree of all the encoded NWD2 proteins. Accordingly, duplication and modification of NWD2 proteins have taken place in the fungus. All the encoded proteins have their NACHT domains at their N-termini while these have been fused to variable C-terminal halves which define the seven subgroups of the NWD2 proteins. Tandem WD40 repeats and TRP repeats are present in the C-termini of some of the NWD2 proteins of subgroups C and D, respectively. Functions for all other of the C-termini are not known. The gene found previously to suppress the fruiting defect in Proto159 belongs to subgroup A. Developmental defects of mutant Proto159 were found to be variably suppressed by the transformation of genes that belong to the subgroup A of the NWD2 family. The introduction of *NWD2* genes variably altered mycelial properties, blocked the brown staining of mycelium and the agar, and, most importantly, induced primary hyphal knot and sclerotia formation in the vegetative mycelium and also lead to the production of fruiting bodies.

Since sequencing showed that a suppressing result of *NWD2* was not defective allele of the gene in the strain Proto159, there are two possibilities to find out how to overcome the *pkn* defect in mutant Proto 159. One would be insertion of further copies of *NWD2* genes into the genome of Proto159 by transformation and characterize the phenotypes of the transformants and the other would be a whole-genome sequencing to identify the responsible defective gene(s) in Proto159, similar as described in chapter 5.2 for mutants 7K17 and B1918. In this study, the former strategy has been applied.

6.3. Materials and methods

6.3.1. Strains, culture condition, transformation and microscopy

For harvesting oidia, Proto159 (*A43mut, B43mut, pab1-1, pkn*) and AmutBmut (*A43mut, B43mut, pab1*$^{+}$) were grown at 37 °C on complete medium YMG/T (Granado et al. 1997). Oidia were used in co-transformation as described by Granado et al. (1997). The yeast-shuttle vector pRS426 was used to integrate *NWD2* genes through homologous recombination in yeast and

constructs were subsequently used in co-transformation of the above-mentioned strains together with pPAB1-1 for selection of positive transformants as described in Dörnte et al. (2020).

Strains Proto159 and AmutBmut were used in transformation. Transformants were picked onto minimal medium (MM) (Granado et al. 1997) and grown at 37 °C in the dark. Colony growth was observed on MM and then they were transferred to the complete medium YMG/T for observing growth rates of colonies. For fruiting tests, when transformants were fully grown on the agar plates, they were transferred to standard fruiting conditions in a fruiting chamber with 12 h light and 12 h dark rhythm at 25 °C and 90 % humidity (Granado et al. 1997).

6.3.2. Plasmids and DNA methods

The *NWD2* gene (XP_001828499) within the 5 kb *Bam*HI-*Hin*dIII fragment NB2 found in a cosmid 27C5 is derived from a genomic library of homokaryon AmutBmut (Bottoli 1999) and was sub-cloned into vector pRS426 in *Escherichia coli* (Khonsuntia, unpublished) and transformed into the primary hyphal knot defective mutant Proto159. Regeneration of transformed oidia was able to restore the defect in fruiting body initiation in Proto159 and altered phenotypes in AmutBmut. Other *NWD2* genes were amplified in this work by PCR with primers listed in Table 1 using Phusion polymerase (New England Biolabs) and the amplified fragments were integrated into yeast vector pRS426 through homologous recombination as described in all details in Dörnte et al. (2020). Inserts with genes *NWD2.4* (XP_001828482.2), *NWD2.5* (XP_001838248.1) in vector pRS426 were fully sequenced for control of the accuracy of the PCR reaction performed at the Department of Forest Genetics, Faulty of Forest Science and Forest Ecology, University of Göttingen, using primers shown in Table 2 and the SnapGene Viewer program (4.2.3) was used to create the whole construct map.

Plasmids pPAB1-1were co-transformed with pRS426 integrated genes (*NWD2*) into Proto150 and AmutBmut. In all transformation experiments, the *pab1*$^{+}$ plasmid pPAB1-1 (Granado et al. 1997) was used as a selection marker in co-transformation of both strains, Proto159 and AmutBmut.

Table 1. Primers for the amplification of the *NWD2* genes

Genes	***NWD2* genes from Group A with Accession numbers**	**Primers Forward and Reverse**
NWD2.1	XP_001840254.2	GTCAGCTTCGGGTTG CTTCATCGTCGAGCTCGG
NWD2.2	XP_001828499.2	CTTTGAACTGTCAGATG GAATTTCGGGTTGAACTG
NWD2.3	XP_001828478.2	CAATCATGGTATCCAAC

		CGAAAGTGTAACCTTGTG
NWD2.4	XP_001828482.2	CTCCAAACACGCAGCATAC CAACAGGTCGGCCCATATC
NWD2.5	XP_001838248.1	GGCTATGCTGTTCCTTC GCGCAACGCTTAACATTG
NWD2.6	XP_001838242.1	GGCCGTCGCATCTATATG CCGTACAGGACGGATTCG
NWD2.7	XP_001838254.2	CACGAGGCTCTGTTTGTC CTAGCACTCCTCCCATCTC
NWD2.8	XP_001838303.2	GCTGACTCTGGATCGAGTG TCTGCATCGTGCTGATTG

Table 2. Primers for sequencing

	Genes	Primer type	Sequence	Length	Temp ° C
1	***NWD2.4***	Forward	CTCCAAACACGCAGCATAC	19	56
2	***NWD2.4***	Forward	GATGTACTGTAGCGTGGC	18	54
3	***NWD2.4***	Reverse	GGTCATCGAGGTAACGG	17	53
4	***NWD2.4***	Reverse	CAGACTGAGGGACTGAGG	18	56
5	***NWD2.4***	Reverse	CAACAGGTCGGCCCATATC	19	57
6	***NWD2.5***	Forward	CGGCCGTCGCATCTATATG	19	58
7	***NWD2.5***	Forward	GTGCCAATTACAACAACG	18	52
8	***NWD2.5***	Forward	GGAAACTTGGCCGCATCG	18	59
9	***NWD2.5***	Reverse	CACGCCGGTCTATCTTAG	18	54
10	***NWD2.5***	Reverse	CCGTACAGGACGGATTCG	18	56

6.3.3. Photography

The growth of the transformants and their fruiting process were photographed using a Color-view MegaPixel-camera (Imaging System program, Münster, Germany) assembled on a Stemi 2000-C Zeiss binocular (Göttingen, Germany), that was linked to a computer equipped with analysis Software program (Münster; Germany).

6.3.4. Protein analysis

Using the reference sequence of gene *NWD2.2* (XP-00182499.2), the NCBI database was screened in protein-protein blast (blastp; default settings) and this identified closer related proteins of *C. cinerea*, *Amanita muscaria*, *Agaricus bisporus*, *Galarina maginata*, *Gymnopus luxurians*, *Hebeloma cylindrosporum*, *Hypholoma sublateritium*, *Hypsizygus marmoreus*, *Laccaria amethystina*, *Moniliophthora roreri,* and *Laccaria bicolor.* Proteins with a NACHT-

domain were downloaded for further analysis. The phylogenetic trees of the NWD2 proteins from the above-mentioned fungal species and of the distinct NWD2 proteins sub-grouped in *C. cinerea* were created using Clustal (X2) and MEGA4 (4.0.2) by the Neighbor-Joining (NJ) method with 500 bootstrap values. The structures of the NWD2 protein models for all the members of the sub-groups in *C. cinerea* with their identified domains and motifs as well as functionally unknown conserved regions were deduced from the function "Identify Conserved Domains" in NCBI and from ClustalW sequence alignments, respectively. Chromosomal localizations of *C. cinerea* genes in the published genome of monokaryon Okayama7/#130 (Stajich et al. 2010) were identified by the pblast function on the JGI (Joint Genome Institute) homepage of the strain (Okayama7/#130).

6.4. Results and discussion

6.4.1. Member XP_001828499 of the NWD2 family has a role in fruiting

Proto159 is mutant of strain AmutBmut which has an unidentified *pkn* defect in primary hyphal knot formation and therefore also in secondary hyphal knot formation and, thus, makes neither any sclerotia in the vegetative mycelium nor that it forms fruiting bodies. The strain has been isolated after protopasting and regeneration of oidia, hence the name Proto159 (Granado et al. 1997). The growth rate of this mutant is slower by two days than the parental strain AmutBmut to fully overgrow a plate. It needs seven days in total at 37 °C (for covering an agar plate fully). Moreover, according to microscopic inspections, it produces a lower number of oidia in light-grown cultures as compared to the wildtype AmutBmut. With aging, Proto159 produced a dark pigmentation which diffuses into the agar. Plates therefore appear dark brown (Fig. 1B). Such pigmentations do not appear in AmutBmut (Fig. 1A).

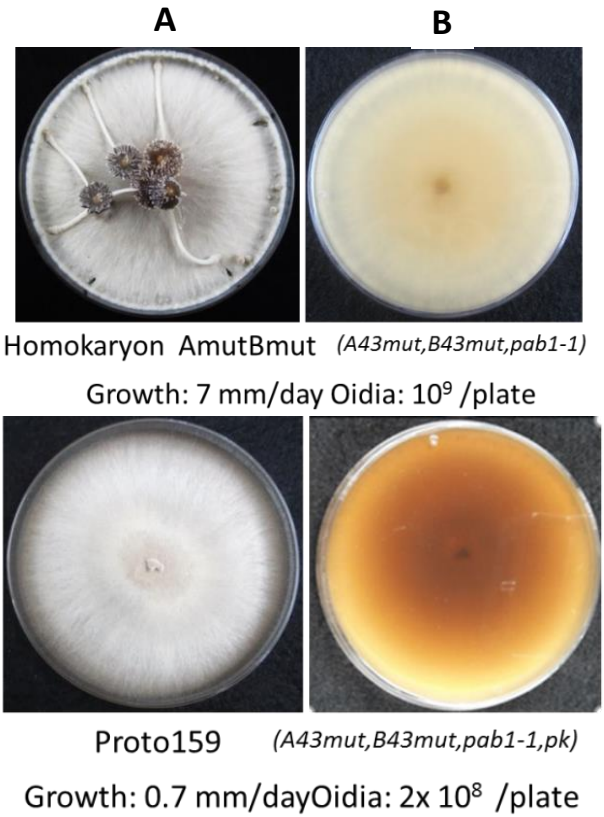

Fig. 1. Images A and B show front and back views of culture plates of homokaryon AmutBmut and Proto159, respectively. AmutBmut produces fruiting bodies (A) that are absent in Proto159 which produces dark pigments which diffuse into the agar (B) and in turn are absent in AmutBmut (A).

Complementation tests have been made with AmutBmut mutant Proto159 in fruiting body initiation (*pkn*) through transformations with a cosmid bank of the wild type AmutBmut (Bottoli et al. 1999). A gene belonging to the *NWD2* family for a protein with a NACHT NTPase domain repeatedly recovered in low frequencies the defects in fruiting body initiation and pigmentation of the mutant Proto159 after transformation (Ruprich-Robert, Clergeot and Khonsuntia, unpublished experiments). Own co-transformation experiments with the cloned gene in vector pRS426 and pPAB1-2 also confirmed the observations of rare phenotype recovery. Co-transformation frequencies were about 2 % of Proto159 transformants, much less than typical co-transformation frequencies in *C. cinerea* (25-43 %) (Dörnte and Kües 2016). The low frequency of recovery may correlate with the suppressor function of the *NWD2* gene of the Proto159 defects suggested by the sequencing work of Yu et al. (unpublished).

6.4.2. NACHT-NTPases – general overview

The *NWD2.2* gene (XP_001828499.2) encodes a protein with a NACHT domain, which is an evolutionarily conserved protein domain and is found in animals in apoptosis proteins as well as in those that are involved in MHC (Major histocompatibility complex) transcription (Koonin and Aravind 2000). The name NACHT stands for NAIP (NLP family apoptosis inhibitor protein), CIITA (C2TA or MHC class II transcription activator), HET-E (incompatibility locus protein from *Podospora anserina*) and TEP1 (that is, TP1 or telomerase-associated protein). The NACHT domain contains 300 to 400 amino acids and is found in variable associations with other domains, such as the CARD domain (caspase activation and recruitment domains), the pyrin domain, the HEAT repeat domain (Huntingtin, elongation factor 3 (EF3), protein phosphatase 2A (PP2A), and the yeast kinase TOR1), the WD40 repeat (beta-transducin repeats), the leucine-rich repeat (LRR) (Koonin and Aravind 2000).

The NACHT NTPases can bind to either GTP or ATP, with preference for GTP over ATP (Leipe et al. 2004). NACHT-NTPases together with ATPases are members of the STAND (signal transduction ATPase with numerous domains) class of proteins and play crucial roles in the signaling cascade of apoptosis and defense responses against pathogens (Aravind et al. 2004; Leipe et al. 2004). The STAND P-loop NTPases, a specific class of P-loop NTPases (phosphate-binding proteins), are longer proteins that contain variably multiple others domains including enzymatic (engaged in several signaling cascades), DNA or protein binding motifs and superstructure-forming repeats (viz toll-like Interleukin (TIR), leucine rich repeat (LRR)) at their amino-termini or carboxyl-termini (Leipe et al. 2004). The STAND AP-ATPase is known to be present in diverse organisms ranging from bacteria to eukaryotes whereas NACHT NTPases are well reported in bacteria, fungi and animalia but to be absent in plants (Arya and Acharya 2016). However, in more recent studies, it has been reported that the putative NACHT STAND NTPases were also present in early green plants; lycophyte (*Selaginella moellendorffii*) and green algae (*Chalmydomonas reinhardtii* and *Coccomyxa subellipsoidea*), the genes of which might have horizontally transferred from cyanobacteria (Arya and Acharya 2016). In this study, we found by pblast analysis of the NCBI database only in few of the Agaricales genes for related NWD2 proteins with a NACHT domain (*Amanitaceae*: *Amanita muscaria*; *Agaricaceae*: *Agaricus bisporus*; *Psathyrellaceae*: *Coprinopsis cinerea*; *Marasmiaceae*: *Moniliophthora roreri*; Omphalotaceae: *Gymnopus luxurians*; Hymenogastraceae: *Hebeloma cylindrosporum*; *Galerina maginata*; Strophariaceae *Hypholoma sublateritium*; *Lyophyllaceae*: *Hypsizygus marmoreus*; Hydnangiaceae: *Laccaria amethystina* and *Laccaria bicolor*. Their phylogenetic relationships are described below.

6.4.3. Detailed structure of the whole NWD2 protein (XP_001828499.2)

The NACHT domain in the NWD2 protein (XP_001828499.2) found before to suppress the defect in Proto159 is located in the N-terminal half of the protein, covering amino acid (aa) 82

to 247 (Fig. 2A). The NACHT domain has the features of a typical NTP binding site (P-loop, Walker A motif, aa), a Walker B motif, a charged amino acid at a specific conserved position, a GRRxE motif, and a GxP motif of STAND NTPases (Koonin and Aravind 2000). The C-terminus of the protein in contrast has no known domain. The suppressor effect by insertion of further copies of gene *NWD2.2* (XP_001828499.2) into the genome of mutant Proto159 is a situation that is somehow reminiscent to the findings in *Schizophyllum commune* where formation of fruiting bodies has been induced in monokaryons upon transformation with the gene *frt1* (Horton and Raper 1991) (Fig. 2B). Gene *frt1* encodes another type of P-loop NTPases (Horton and Raper 1991, 1995) than *NWD2* and both the proteins share a novel short motif of amino acid similarity at their C-terminal ends (IASGQFA, aa 304-310 in *C. cinerea* and LPPGRYS, aa 182-188 in *S. commune* Frt1, Fig. 2).

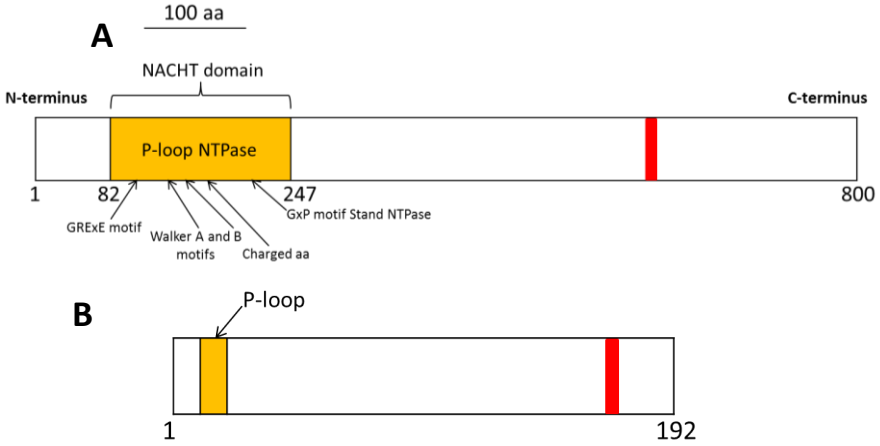

Fig. 2. (A) Structure of NWD2 protein acting as a suppressor in the mutant Proto159 of *C. cinerea*. (B) Structure of Frt1 (for fruit inducing activity 1: Horton and Raper 1995) in *S. commune*. Yellow color denotes domains containing P-loop NTPases at the N-termini and a red color shows short motifs at the C- termini of both proteins. Both colors indicate homology in the sequences in both proteins in both organisms.

Further, the NWD2 protein (XP_001828499.2) of *C. cinerea* also showed 23 % identity/38 % similarity restricted to the P-loop of the vegetative incompatibility protein HET-E (HNWD5) of *Podospora. anserina*. In *P. anserina*, the specific family of HNWD proteins containing a NACHT-domain in the center together with the HNWD-name-giving HET domain at their N-termini and WD-40 repeats at their C-termini are responsible for vegetative incompatibility

reactions (Koonin and Aravind 2000; Chevanne et al. 2009). The *HNWD* family has five members (*HNWD1-5*) in *P. anserina* (Chevanne et al. 2009). It has been reported that the HET-E binds GTP but not ATP, and functions in vegetative incompatibility (Koonin and Aravind 2000).

6.4.4. Grouping of members of the *C. cinerea* NWD2 Family

The suppression effect on the mutation in the fruiting body initiation in *C. cinerea* by a *NWD2* gene suggests that its presence is influential in the regulation of developmental pathways. Through pblast genome searches in this study, total 36 distinct *NWD2* genes in *C. cinerea* are found. 36 different copies of NWD2 proteins are grouped which cluster as 7 subgroups (A to G) at different positions in an evolutionary tree of the NWD2 proteins from *C. cinerea* with between 1 to 10 members in total (Fig. 3). In a larger phylogenetic tree, these proteins cluster also together in between groups of proteins from different *Agaricales* species (Fig. 3 and 4). Species that have NWD2 proteins come mostly from different families of Agaricales (see on section: 6.4.2.), indicating no clearly shared phylogenetic origin. The species-specific grouping of *C. cinerea* and also of other species indicates that *NWD2* genes multiplied late at speciation. Such patterns of enlarging NWD2 families by gene duplications in selected species with lacking genes in other related organisms has been reported to be typical for any specific species, irrespectively of whether being plant, fungi or animals (Van Der Nest et al. 2014). Interpretations for such “defined-species” patterns have been interpreted variously as loss of genes in lines without such genes (Van Der Nest et al. 2014) or been arisen by horizontal gene transfer (HGT) with following gene duplications and diversifications (Arya and Acharya 2016, 2018). Origin from horizontal transfer with later duplication in speciation seems more likely because of the cluster into different groups which bases majorly on the three-domain structure of the proteins, with the conserved NACHT NTPase domain shared by all, but with variable N- and C-terminal domains between clusters of proteins (Arya and Acharya 2006, 2018). Basically, the N- and C-terminal domains appear to be interchangeable modules in the structuring of NWD2 proteins (Van Der Nest et al. 2014).

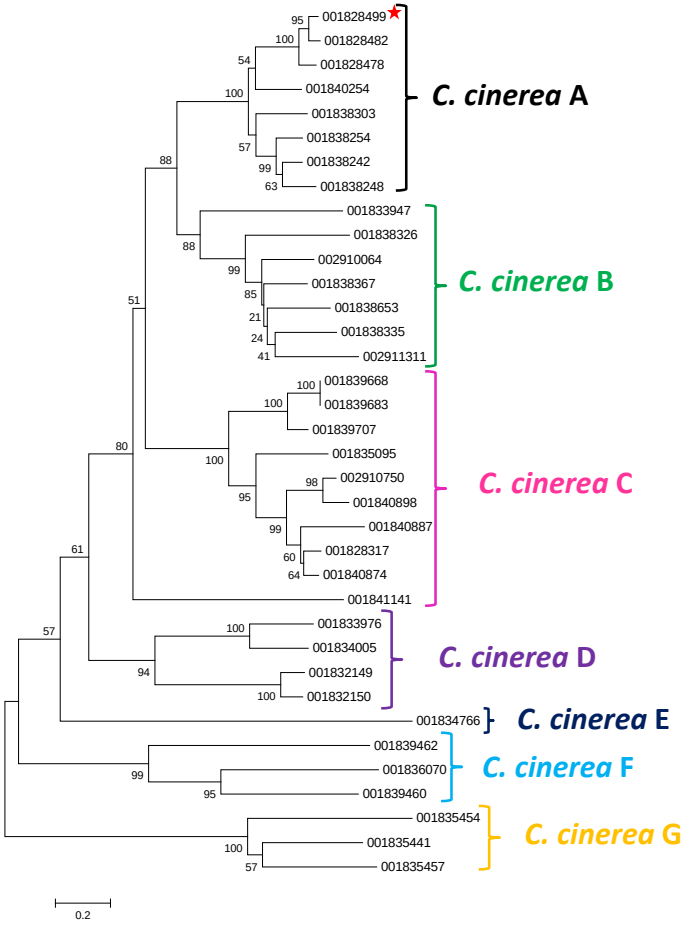

Fig. 3. Phylogenetic tree of NWD2 proteins grouped them into seven different clades (A to G). The original *NWD2* gene found to induce fruiting in mutant Proto159 clusters in subgroup A and is marked by a red star. The different colors of the subgroups correspond to the location of genes in different chromosomes of the fungus shown in Fig. 9.

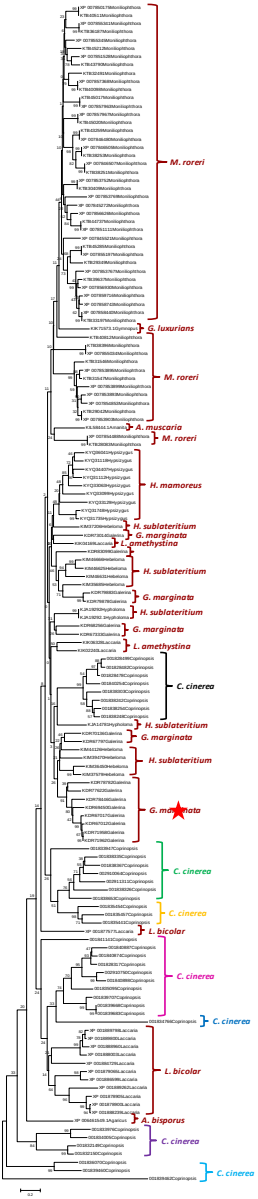
M. roreri
G. luxurians
M. roreri
A. muscaria
M. roreri
H. mamoreus
H. sublateritium
G. marginata
L. amethystina
H. sublateritium
G. marginata
H. sublateritium
G. marginata
L. amethystina
C. cinerea
H. sublateritium
G. marginata
H. sublateritium
G. marginata
C. cinerea
C. cinerea
L. bicolor
C. cinerea
C. cinerea
L. bicolor
A. bisporus
C. cinerea
C. cinerea

Fig. 4. Phylogenetic relationship of NWD2 proteins from different Agaricales as determined by the neighbor-joining method with 500 bootstrap values. Full species names are listed in section: 6.4.2. The different colors of the subgroups of *C. cinerea* correspond to the location of genes in different chromosomes of the fungus shown in Fig. 7.

To emphasize the domain structure of the *C. cinerea* NWD2 proteins further, the models for protein of all seven subgroups were constructed (Fig. 5). Colored regions in the proteins indicate corresponding domains of highly similar sequence (30-84 % identity) while the white areas regions are of variably length and less similar (23-40 % identity) or unique sequence. All the encoded proteins have their NACHT domains at their N-termini while these have been fused to variable N-terminal and C-terminal parts of different lengths. Functions for N-terminal domains and most of the C-terminal parts are not known. However, tandem WD40 repeats are present at the C-terminal of the NWD2 proteins of subgroup C (Fig. 5), and tandem TPR (tetratricopeptide) repeats are present at the C-terminal of NWD2 proteins of subgroup D.

The WD40 repeat (also known as the WD or beta-transducing repeat) is a short structural motif of approximately 40 amino acids, often terminating in a tryptophan aspartic acid (W-D) dipeptide (Neer et al. 1994). Tandem copies having 4 to 16 repeating units form a circularized beta-propeller structure that is called the WD40 domain (Smith et al. 1999; Li and Roberts 2001). WD40-repeat proteins are a large family found in all eukaryotes and are implicated in a variety of functions ranging from signal transduction and transcription regulation to cell cycle control, autophagy and apoptosis (Stirnimann et al. 2010). TPR repeats are present in 4 or more copies in proteins and contain a minimum of 34 amino acids (Blatch and Lässle 1999). TPR motifs have been identified in various organisms, ranging from bacteria to humans (Blatch and Lässle 1999). Proteins containing TPRs are involved in a variety of biological processes, such as cell cycle regulation, transcriptional control, mitochondrial and peroxisomal protein transport, neurogenesis and protein folding (Blatch and Lässle 1999; Scheufler et al. 2000; Gatto et al. 2000).

Group A

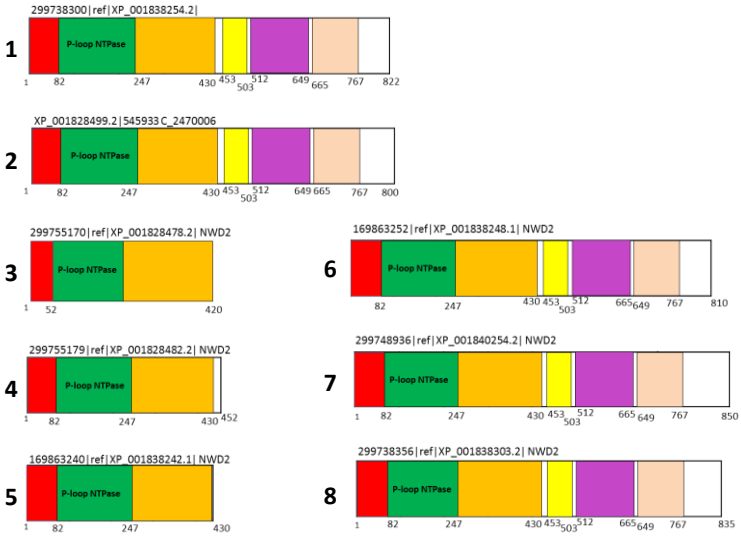

Group B

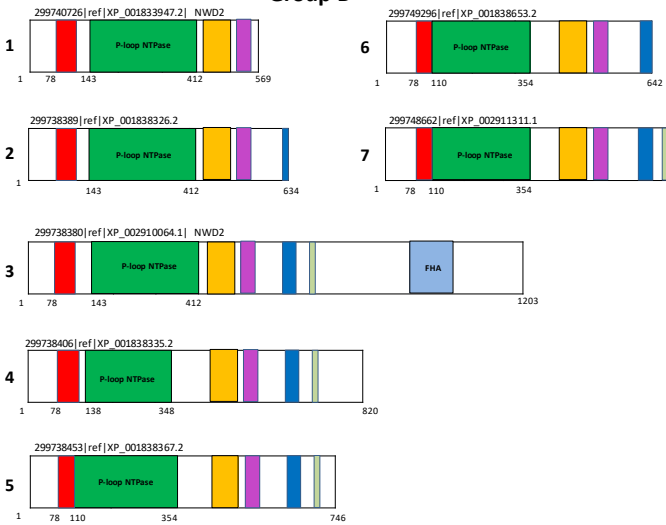

Group C

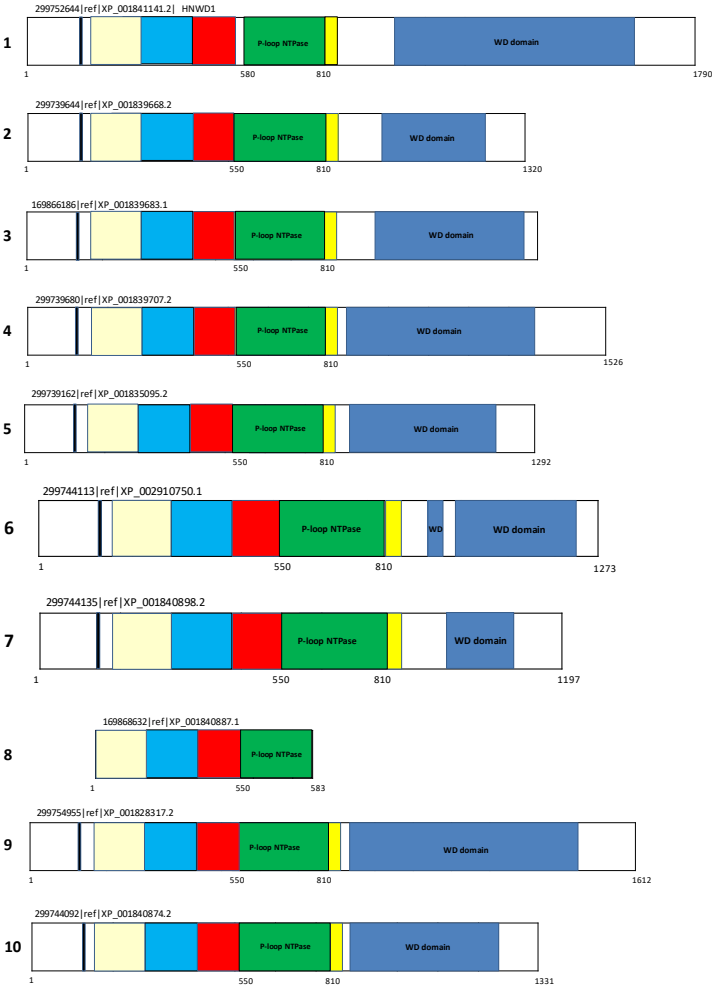
1
299752644|ref|XP_001841141.2| HNWD1
P-loop NTPase
WD domain
1
580
810
1790
2
299739644|ref|XP_001839668.2
P-loop NTPase
WD domain
1
550
810
1320
3
169866186|ref|XP_001839683.1
P-loop NTPase
WD domain
1
550
810
4
299739680|ref|XP_001839707.2
P-loop NTPase
WD domain
1
550
810
1526
5
299739162|ref|XP_001835095.2
P-loop NTPase
WD domain
1
550
810
1292
6
299744113|ref|XP_002910750.1
P-loop NTPase
WD
WD domain
1
550
810
1273
7
299744135|ref|XP_001840898.2
P-loop NTPase
WD domain
1
550
810
1197
8
169868632|ref|XP_001840887.1
P-loop NTPase
1
550
583
9
299754955|ref|XP_001828317.2
P-loop NTPase
WD domain
1
550
810
1612
10
299744092|ref|XP_001840874.2
P-loop NTPase
WD domain
1
550
810
1331

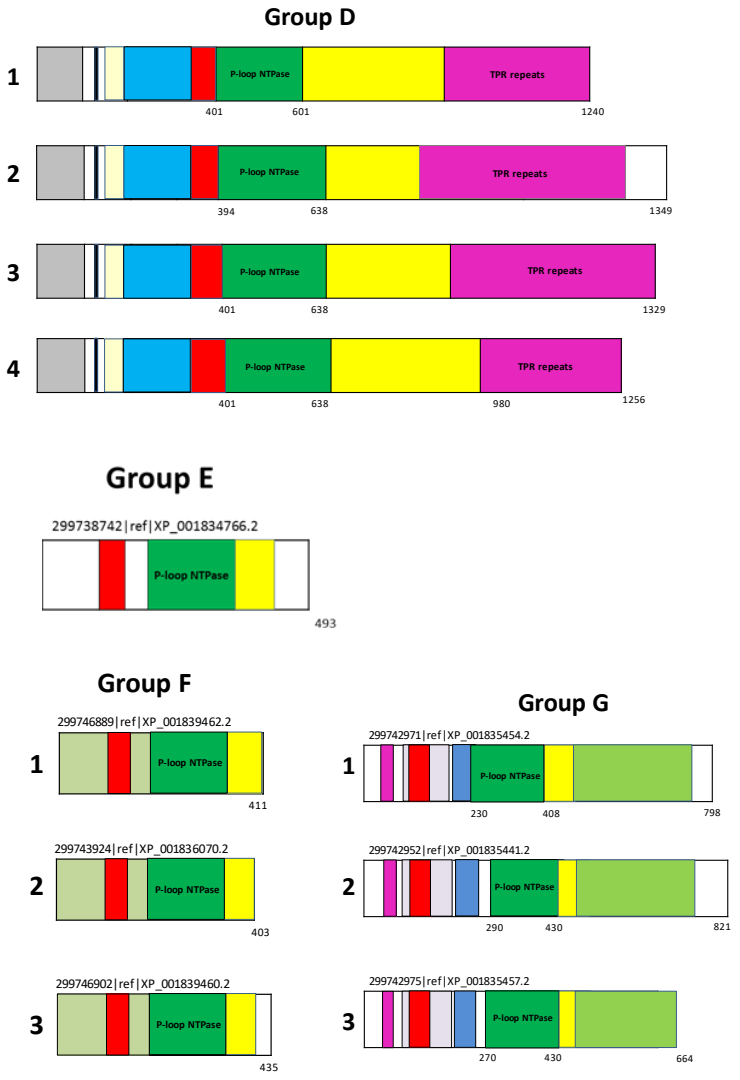

Fig. 5. Structures of NWD2 protein subgroups (A to G) in *Coprinopsis cinerea*. Colored regions indicate corresponding domains of similar sequence, white areas regions of variably unique or less similar

sequence. Green colored boxes are the known P-loop NTPase NACHT domain present in all the proteins. The blue colored boxes of the Group C proteins are the WD domains and the pink colored boxes of the Group D proteins are the TPR domains. Other colors are not identified.

6.4.5. Location of the 36 distinct *NWD2* genes in different chromosomes of *C. cinerea*

The haploid genome size of *C. cinerea* is estimated at 37.5 Mb and assembled into 13 chromosomes (Stajich et al. 2010). Accordingly, duplication and modification of NWD2 proteins have taken place in the fungus during evolution (Fig. 7). The location of 36 distinct *NWD2* genes in the 13 chromosomes of *C. cinerea*) shown in Figure 7. The chromosomal map identified that the distribution of 36 *NWD2* genes is not uniform in different chromosomes of *C. cinerea*, as they are more or less accumulated at the sub-telomeric region of the chromosomes. Cytological evidences indicate that meiotic exchanges are highly enriched in sub-telomeric regions of the 13 chromosomes in *C. cinerea* (Holm et al. 1981; Stajich et al. 2010). The sub-telomeric regions which exhibit an elevated rate of recombination are termed the ``hot´´ regions and the regions within centromere are termed as the ``cold´´ regions which exhibit very little recombination (Stajich et al. 2010). In Fig. 7A, the recombination rates in the 13 chromosomes of *C. cinerea* are shown. White regions in the chromosomes are the unmapped regions, red color depicts the high recombination areas, gray is average recombination and blue color shows low recombination. The 36 *NWD2* genes are represented in Fig. 7A and B by colorful bars in different chromosomes. Ten of the 13 chromosomes carry *NWD2* genes. Same colors of bars indicate genes of a same group, according to the phylogenetic tree. The chromosomal map shows the location of the maximum number of *NWD2* genes within the high recombination regions, covering mostly subtelomeric hot regions of the chromosomes, indicating that the *NWD2* genes might have transferred to the genome through horizontal gene transfer (HGT) and might have subsequently been multiplied during evolution (Fig. 7A), possibly including domain swapping in *C. cinerea*. This is suggested from Fig. 3, because *C. cinerea* proteins of subgroups A to G cluster together, without intermingling of proteins from other species (Fig. 4).

Stajich et al. (2010) provided a map of paralogous gene distributions in general on the *C. cinerea* chromosomes (Fig. 7B). A general investigation on the paralogous family distributions revealed that the various paralogous multicopy genes are found in highly recombining regions, i.e., in ``hot´´ regions, including for example a large family of paralogous genes for protein kinases which control mechanism essential for developmental patterns and a complex organismal structure (Stajich et al. 2010). From our analysis, we found that the clusters of *NWD2* gene copies are mainly located within the areas where paralogous genes in high frequency are present, marked by red color in the chromatograms (Fig. 7B). Furthermore, several of the *NWD2* genes of subgroups A and B are seen to accumulate on the shortest chromosome 13 as compared to others. Chromosome 13 is known to be poorly conserved

among Agaricales and thus is possibly the newest formed chromosome in *C. cinerea*. The newest chromosomes are often prone to get attacked by foreign DNA including transposons (Stajich et al. 2010; see Fig. 6A for chromosomal transposon distributions). In accordance, we found in the shortest 13 chromosome a transposable element in which *NWD2.7* gene (XP_001838254) was incorporated (Fig. 6 and 7B, marked by a black arrow), emphasizing the vulnerability of the chromosome and one manner as how the *NWD2* genes may duplicate.

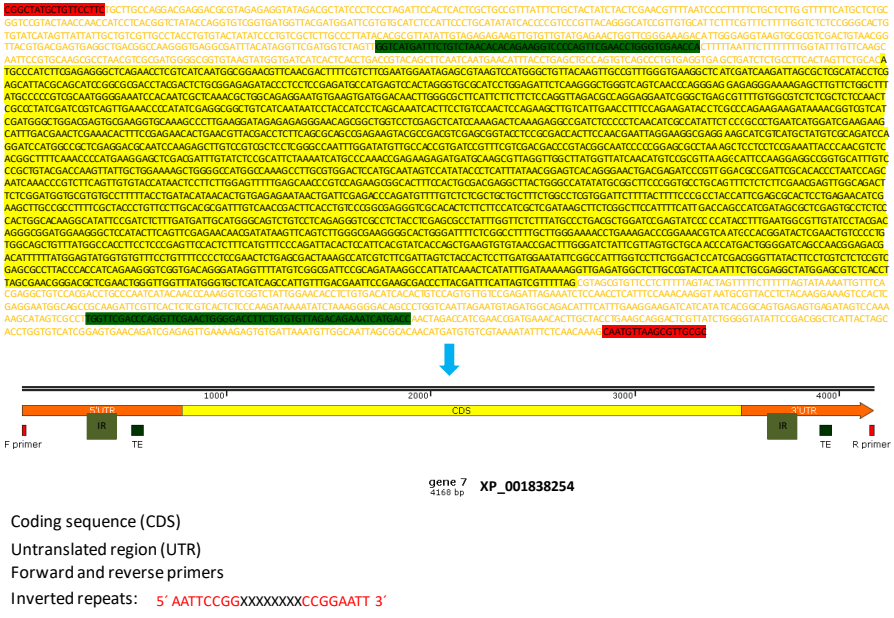

Fig. 6. The image shows the gene map of gene *NWD2.7* (XP_001838254) with its coding region (yellow color), UTR regions (orange color), its forward and reverse primers marked in red colors and the inverted repeats on the both sides of UTR regions marked in green colors. The presence of inverted repeats indicates the presence of transposable element within the gene.

As mentioned earlier only few of the Agaricales have genes for NWD2 proteins, amongst is *L. bicolar* with whom *C. cinerea* shares a common ancestor dated 200 Mya back (Stajich et al. 2010). While comparing the genome of these fungi, Stajich et al. (2010) revealed that the 39 % of the assembled *C. cinerea* genome is syntenic with *L. bicolor* and the syntenic regions are located at both sides next to the centromere regions which are the highly conserved regions of the chromosomes and typically lack any transposable elements (Fig. 7C). This information

directly reflects to the horizontal transfer of the *NWD2* genes which are mostly accumulated at the less conserved sub-telomeric regions of the chromosomes.

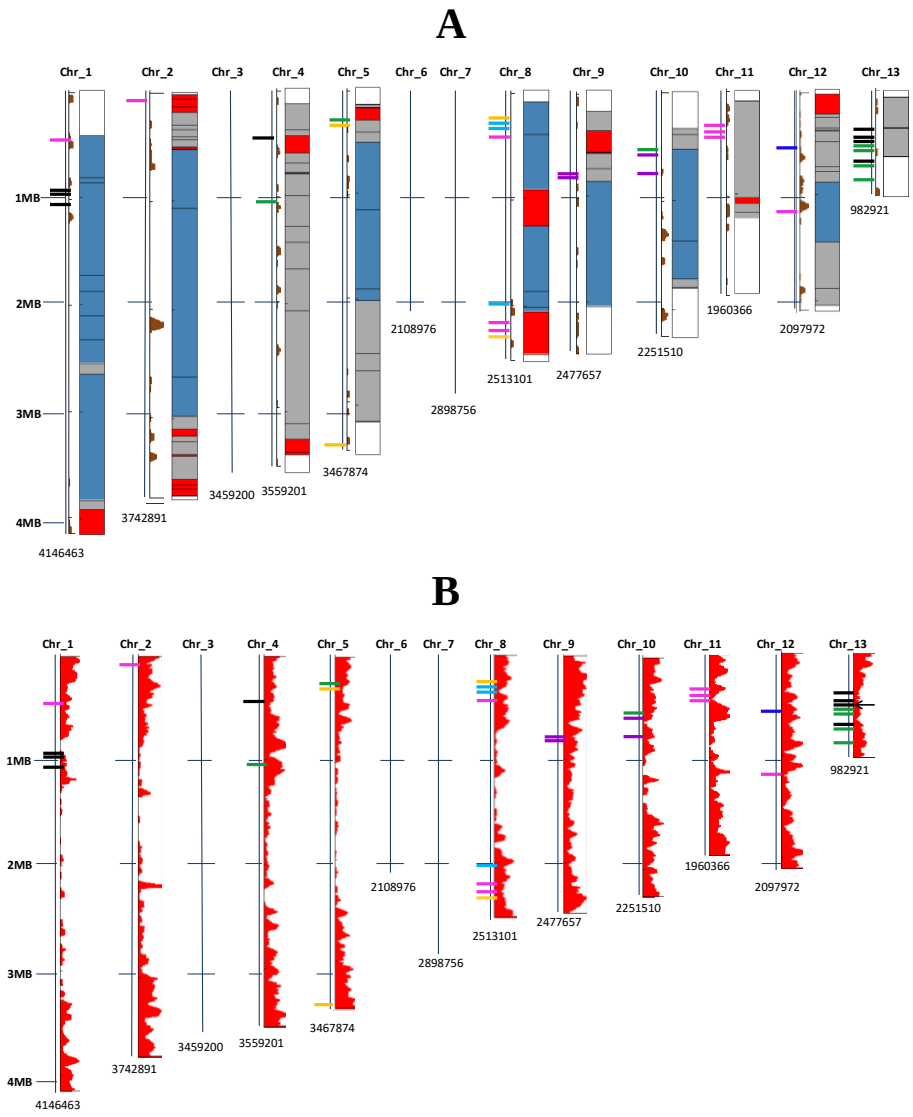

C

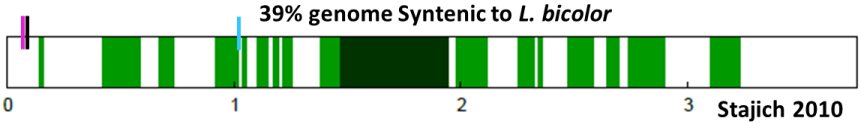

Fig. 7. Location of 36 distinct *NWD2* genes on different chromosomes of *C. cinerea* in relation to (A) recombination rate (red = high, gray = average, blue = low recombination areas) and transposon distributions (marked in brown), and to (B) regions with a high paralogous gene frequency (red area). Bars at different chromosomes of a same color correspond to the color of subgroups of *NWD2* genes in the phylogenetic tree of NWD2 proteins in Fig. 5. The black arrow in the chromosome number 13 shows the black bar of the *NWD2* gene (XP_001838254) with the transposon element. (C) 39 % of the assembled *C. cinerea* genome is syntenic with *L. bicolor*, green regions are syntenic region between *C. cinerea* and *L. bicolar*, dark green color indicates the conserved region (Stajich et al. 2010). The bars pink, black and blue indicate locations of one of the *NWD2* gene (XP_001841141) of subgroup C and the other essential genes *ras* GTPases and *trp1*, respectively. The *trp1* gene lies within the syntenic region colored s light green

6.4.6. Transformations of the *NWD2* genes of subgroup A into mutant Proto159 and the wildtype homokaryon AmutBmut

The transformation of *NWD2* genes into Proto159 has been performed in three independent experiments described below. Similarly, AmutBmut transformation experiments have been independently performed three times. In Table 1 in the method section, the different *NWD2* genes from subgroup A are listed. All the *NWD2* genes from the subgroup A have been cloned and co-transformed with selection vector pPAB1-1 into Proto159 and AmutBmut, except for the 1st gene listed in the Table 1 because a PCR product of the *NWD2.1* could not be obtained unlike the PCR products of the rest of the genes from *NWD2.2 to NWD2.8*. Transformation of the *NWD2.2* construct was only once performed since another colleague was concentrating specifically on characterizing this individual gene.

The blue, green and magenta bars in the graphs (Fig. 9 and 10) indicate 1^{st,} 2nd and 3rd experiments performed in this study for the transformation of the *NWD2* genes from the subgroup A into Proto159 and AmutBmut. In the first experiments, one µg of pNWD2.4 to pNWD2.8 and one µg of pNWD2.3 to pNWD2.8 were co-transformed each with one µg of pPAB1.1 into the mutant strain Proto159 and the wildtype homokaryon AmutBmut, respectively (both experiments shown by blue bars in Fig. 9 and 10). In the second experiments, one µg of pNWD2.2 to pNWD2.8 and one µg of pNWD2.3 to pNWD2.8 were co-transformed each with one µg of pPAB1.1 into the mutant strain Proto159 and the wildtype homokaryon AmutBmut, respectively (both shown by green bars in Fig. 9 and 10). In the third experiments,

one µg of pNWD2.3 to pNWD2.8 and one µg of pNWD2.2 to pNWD2.8 were co-transformed each with one µg of pPAB1.1 into the mutant strain Proto159 and the wildtype homokaryon AmutBmut, respectively (both shown by magenta bars in Fig. 9 and 10).

Numbers of transformants for genes *NWD2.2* and *NWD2.3* in experiment 1 and for gene *NWD2.2* in experiment 3 for mutant Proto159 (Fig. 9) and the numbers of transformants of gene *NWD2.2* in experiments 1 and 2 for the wildtype AmutBmut (Fig. 10) are not shown in the graphs because respective transformation experiments were not performed for these genes by lack of clones at the time. The numbers of the transformants obtained in three independent experiments were counted and the cumulative final numbers are shown together in the graphs (Fig. 9 and 10). In case of transformation of Proto159, the 1st experiment gave only lower amounts of transformants (between 3 to 32), unlike parallel transformations of homokaryon AmutBmut (between 24 or 62), which suggested that the plasmid DNAs were of sufficient quality while protoplasts of AmutBmut were better able to take up the plasmid DNA into its cells and nuclei and regenerated better while protoplasts of Proto159 were only 30% efficient to take up plasmid DNA compared to that of per experiment of AmutBmut and had a less healthy appearance under the microscope (Fig. 9). In the 2nd and 3rd experiments, transformations rates of different plasmids were more alike between plasmids for both strains.

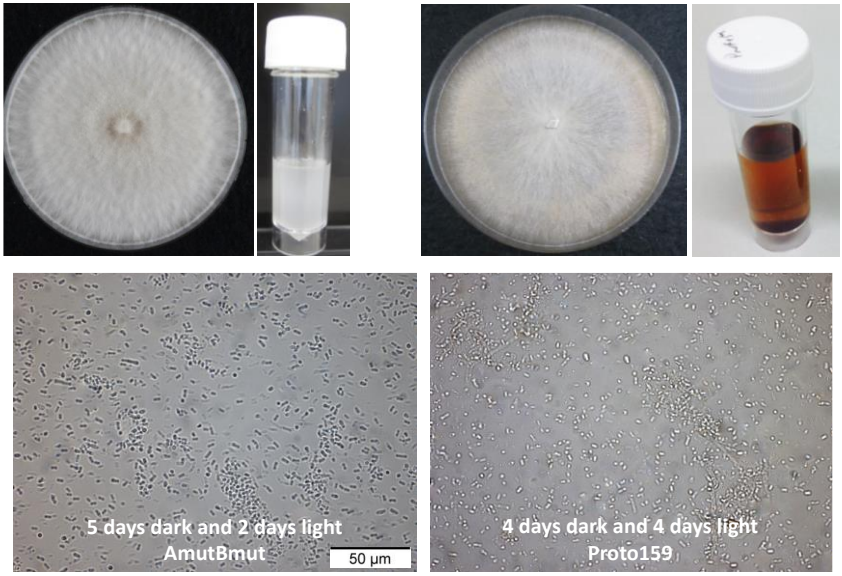

Fig. 8. Protoplasts of AmutBmut and Proto159

Growing transformants per individual experiments were picked from the regeneration agar over 5 consecutive days and transferred to the minimal media for further selection of the *pab1*$^{+}$ gene in the transformants. After incubating transformants for few days, the transformants were further inoculated on the complete medium YMG/T and incubated at 37 °C for 5 days under constant dark for phenotypical observations. Mycelial growth and colony morphology were analyzed and, then, plates were transferred for further incubation into fruiting conditions.

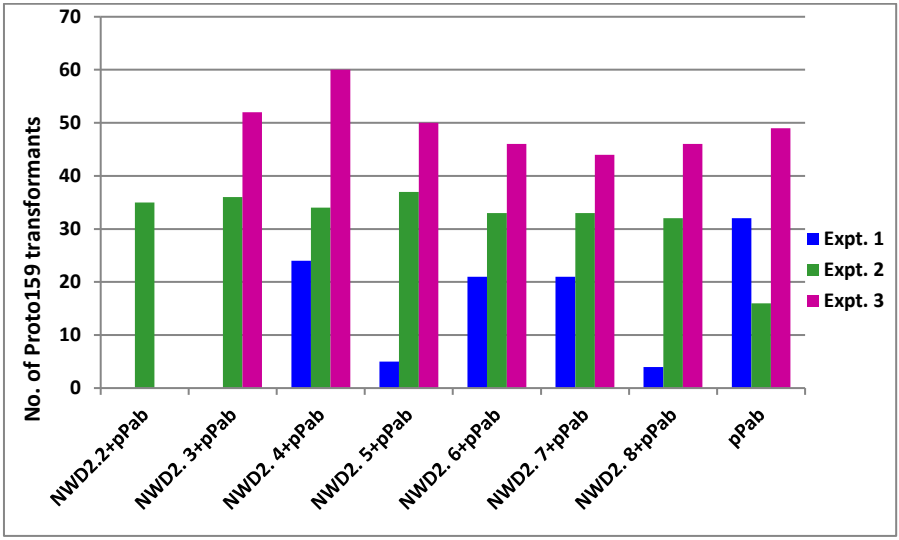

Fig. 9. The graph shows the numbers of Proto 159 transformants in three independent experiments. The missing bars of genes in Expt. 1 and 3 indicate no transformation performed for the respective genes.

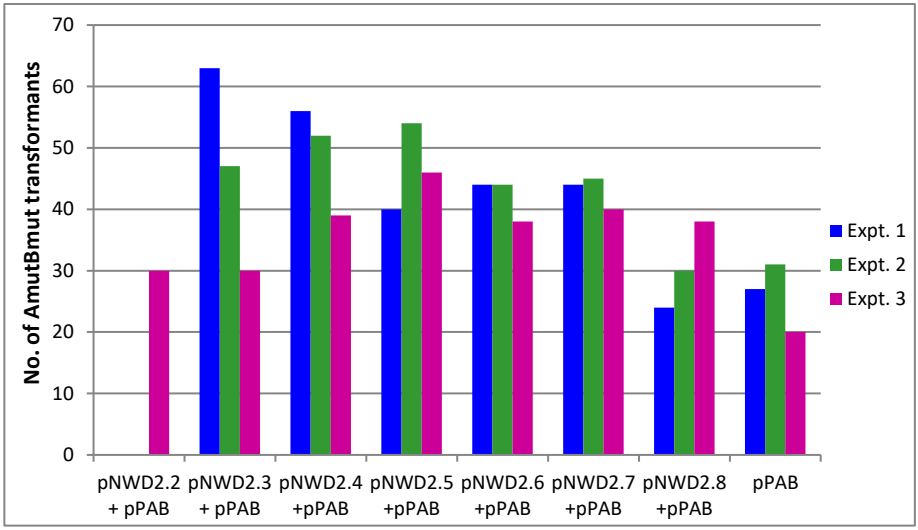

Fig. 10. The graph shows the numbers of AmutBmut transformants in three independent experiments. The missing bars of genes in Expt. 1 and 2 indicate no transformation experiment performed for the respective genes.

6.4.6.1. Proto159 transformants

Various types of phenotypes were observed in the transformants obtained from the mutant Proto159 of genes of the first subgroup A of the *NWD2* family. In the 1st experiment, different transformants showed four types of phenotypes, i.e. poor irregular growth, Proto159-like growth with brownish coloration underneath in the agar, dense colonies with thin white aerial mycelium and a light-brown color underneath in the agar, and AmutBmut-like mycelium (fluffy white mycelium) with no coloration underneath in the agar (Fig. 11). Table 3 reports on quantities of phenotypes for the different transformed plasmids. Amounts of Proto159-like growth varied between 14 % and 100 % of transformants. Poor growth phenotypes were seen in several of the colonies transformed with *NWD2.6* (29 %) and *NWD2.7* (62 %). Phenotypes of thin white mycelia were also shown by *NWD2.6* (55 %) and *NWD2.7* (5 %) transformants. White fluffy mycelia were shown by each one transformants of *NWD2.6* (2 %), *NWD2.7* (5 %) and *NWD2.8* (25 %), but also by one of the pPAB1-2 control (3 %). Further, one colony (4 %) transformed with gene *NWD2.4* showed thin mycelium and formed primary hyphal knots seen underneath the microscope when using the window technique (chapter 2.1). The rest of all other colonies did not produce such Pks in windows cut into the agar medium. Under standard fruiting

conditions, none of the transformants initiated the fruiting pathway and also none produced primary hyphal knots and sclerotia.

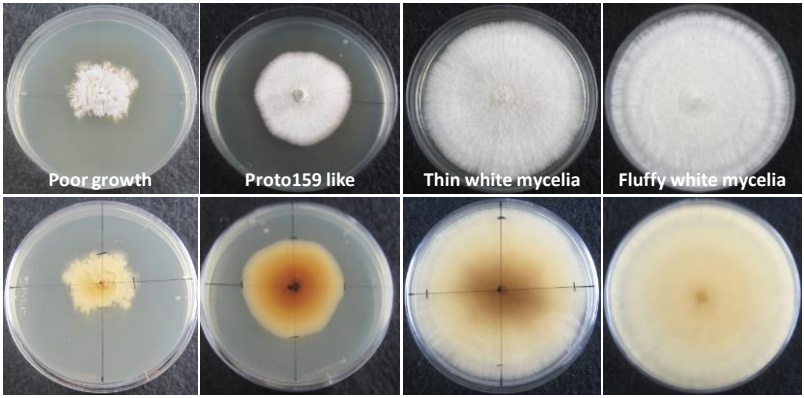

Fig. 11. Four types of phenotypes, poor growth, Proto159 like, thin white mycelium and AmutBmut-like mycelium (fluffy white mycelium) were exhibited by the transformants of Proto159 in the 1st experiment. Same plates were photographed from above and below.

Table 3. Colony phenotypes observed after growth at 37 °C in the dark upon transformation of Proto159 cultivated on YMG/T media in the 1st expt. and behavior after transfer into standard fruiting conditions at 25 °C.

Plasmids	Total transformants	Proto159 like	Poor growth	Thin mycelium	AmutBmut mycelium	Primary hyphal knot
pPAB1.1	**3(100 %)**	31(97 %)	0	0	1(3 %)	0
pPAB1.1 + pNWD2.4	**24(100 %)**	22(92 %)	0	1(4 %)	0	1(4 %)
pPAB1.1 + pNWD2.5	**5(100 %)**	5(100 %)	0	0	0	0
pPAB1.1 + pNWD2.6	**21(100 %)**	3(14 %)	6(29 %)	11(55 %)	1(2 %)	0
pPAB1.1 + pNWD2.7	**21(100 %)**	6(28 %)	13(62%)	1 (5 %)	1(5 %)	0
pPAB1.1 + pNWD2.8	**4(100 %)**	3(75 %)	0	0	1(25 %)	0

In the 2nd experiment, again the same four types of colony phenotypes as above were exhibited by the transformants of mutant Proto159 (Fig. 12). Poor growth phenotypes were shown by all genes in frequencies of transformants between 3 and 21 %, except for the control pPAB (Table

4). No primary hyphal knots were produced by any of the thin white and AmutBmut-like transformants as also tested by the window technique in this experiment. However, AmutBmut-like mycelium (fluffy white mycelium) was formed by transformants with all *NWD2* genes in frequencies of transformants between 3 and 14 %, except for the control pPAB (Table 4). Under standard fruiting conditions, none of the transformants initiated the fruiting pathway and also none produced primary hyphal knots and sclerotia.

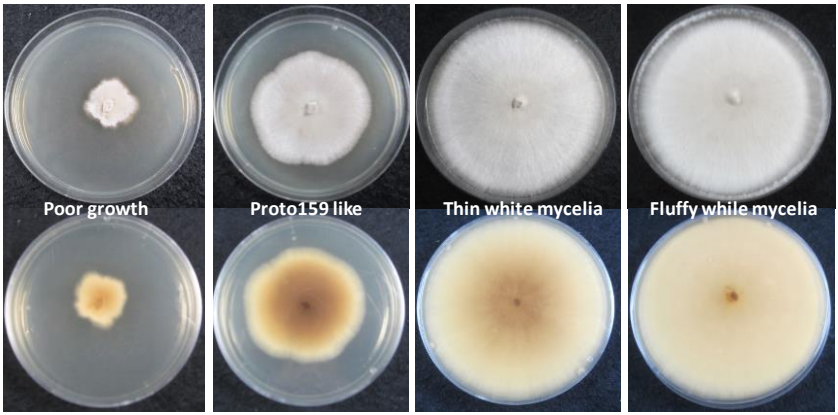

Fig. 12. Four types of phenotypes, poor growth, Proto159 like, thin white mycelium and AmutBmut-like mycelium (fluffy white mycelium) were exhibited by the transformants of Proto159 in the 2nd expt. Same plates were photographed from above and below.

Table 4. Colony phenotypes observed after growth at 37 °C in the dark upon transformation of Proto159 cultivated on YMG/T media in the 2nd expt. and behavior after transfer into standard fruiting conditions at 25 °C.

Plasmids	Total transformants	Proto159-like	Poor growth	Thin white mycelium	AmutBmut-like mycelium
pPAB1.1	**16(100 %)**	13(81 %)	0	3(19 %)	0
pPAB1.1 + pNWD2.2	**35(100 %)**	22(63 %)	3(9 %)	5(14 %)	5(14 %)
pPAB1.1 + pNWD2.3	**36(100 %)**	26(72.5 %	4(11 %)	4(11 %)	2(5.5 %)
pPAB1.1 + pNWD2.4	**34(100 %)**	30(88 %)	1(3 %)	0	3(9 %)
pPAB1.1 + pNWD2.5	**37(100 %)**	33(89 %)	3 (8 %)	0	1(3 %)

pPAB1.1 + pNWD2.6	**33(100 %)**	23(70 %)	5(15 %)	2(6 %)	3(9 %)
pPAB1.1 + pNWD2.7	**33(100 %)**	25(76 %)	7(21 %)	0	1(3 %)
pPAB1.1 + pNWD2.8	**32(100 %)**	26(82 %)	3(10 %)	0	2(8 %)

In the 3rd experiment, transformants of mutant Proto159 exhibited various phenotypes upon the introduction of *NWD2* genes from the subgroup A of *NWD2* family (summarized in Table 5, shown in Fig. 13 and shown as graphs A and B in both in absolute numbers and in percentage, respectively in Fig. 14). Shared phenotypes with the former experiments were again poor growth, Proto159-like phenotype, thin white mycelium, and Pk formation (as tested with the window technique) in AmutBmut-like mycelium (fluffy white mycelium). In the latter group, with Pk formation as a precondition (chapter 2.2), newly observed phenotypes under standard fruiting conditions were formation of white sclerotia and fruiting bodies (Table 5). Fruiting bodies were formed by each one colony transformed with either genes *NWD2.4*, *NWD2.5* or *NWD2.6*. White sclerotia (see chapter 2.1) were formed in 2 to 4 colonies transformed with either genes *NWD2.4*, *NWD2.6*, *NWD2.7* or *NWD2.8*. AmutBmut-like mycelium (fluffy white mycelium) with no agar coloration was seen in all the colonies which made sclerotia and fruiting bodies. Thin white mycelia with no agar coloration were seen in other colonies transformed with genes *NWD2.4*, *NWD2.5*, *NWD2.7*, and *NWD2.8*.

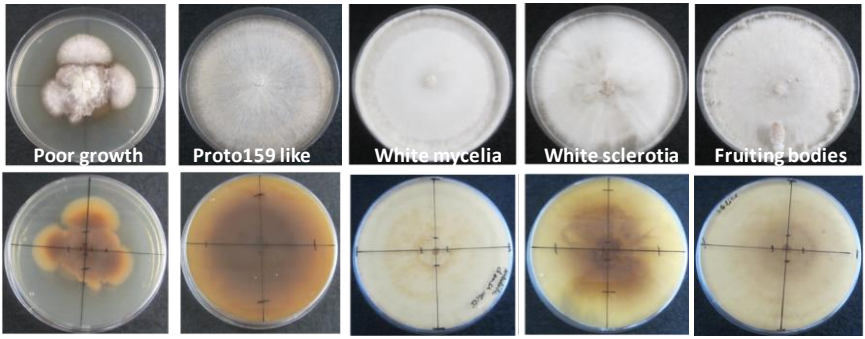

Fig. 13. Six types of phenotypes, poor growth, Proto159 like, thin white mycelium and AmutBmut-like mycelium (fluffy white mycelium) which produced white sclerotia and fruiting bodies were exhibited by the transformants of Proto159 in the 3rd expt. Same plates were photographed from above and below.

Table 5. Colony phenotypes observed after growth at 37 °C in the dark upon transformation of Proto159 cultivated on YMG/T media in the 3rd Expt. and behavior after transfer into standard fruiting conditions at 25 °C.

Plasmids	Total transformants	Proto159-like	Poor growth	Thin white mycelium	AmutBmut-like mycelium	
					White sclerotia	Fruiting body
pPAB1.1	**49(100 %)**	31(63 %)	18(37 %)	0	0	0
pPAB1.1 + pNWD2.3	**52(100 %)**	48(92 %)	4(8 %)	0	0	0
pPAB1.1 + pNWD2.4	**62(100 %)**	48(80 %)	3(5 %)	6(10 %)	4(7 %)	1(2 %)
pPAB1.1 + pNWD2.5	**50(100 %)**	42(84 %)	4(8 %)	3(4 %)	0	1(2 %)
pPAB1.1 + pNWD2.6	**46(100 %)**	39(85 %)	4(9 %)	0	2(4 %)	1(2 %)
pPAB1.1 + pNWD2.7	**44(100 %)**	36(82 %)	4(9 %)	3(7 %)	1(2 %)	0
pPAB1.1 + pNWD2.8	**46(100 %)**	38(83 %)	4(9 %)	2(4 %)	2(4 %)	0

Graph A, Expt. 3

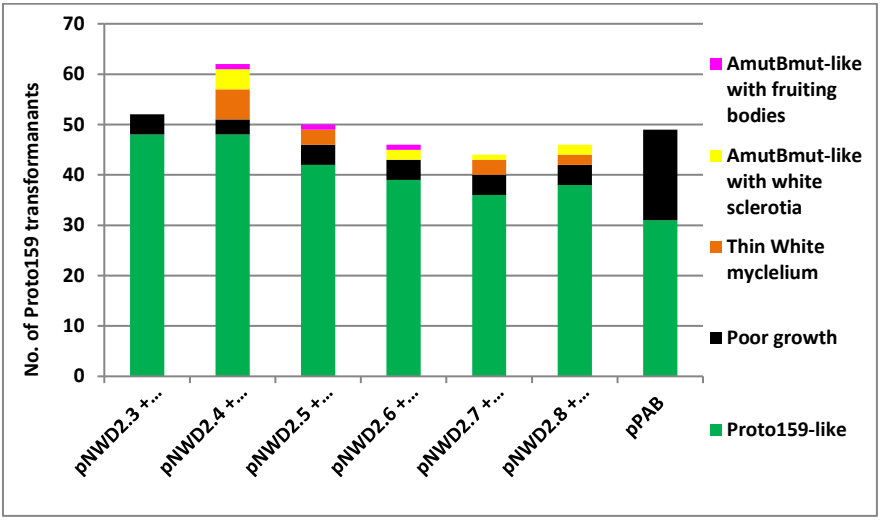

Graph B, Expt. 3

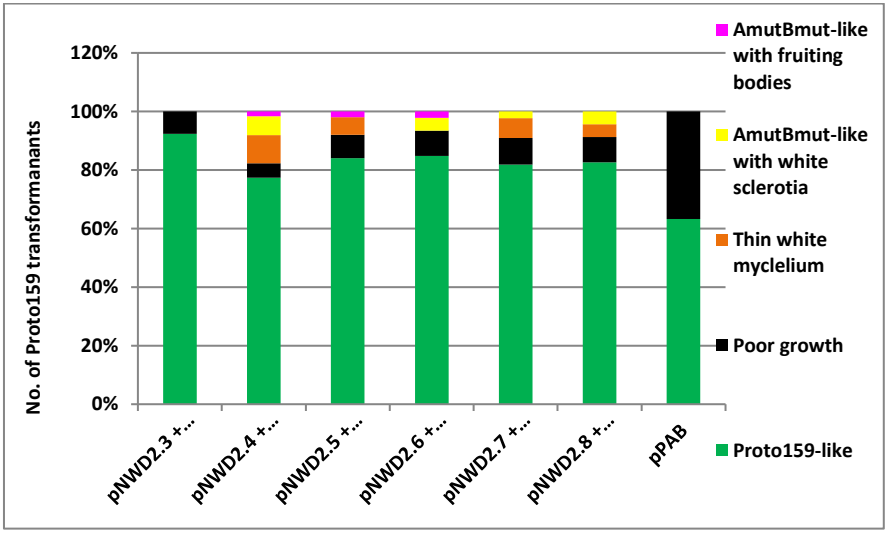

Fig. 14. In the 3rd expt., four types of phenotypes, poor growth, Proto159 like, thin white mycelium and AmutBmut-like myceilum (fluffy white mycelium) were exhibited by the transformtnts of

Proto159. Transformants with AmutBmut-like mycelium also produced white sclerotia and fruiting bodies when incubated under 12h light/12h dark rythmn at 25 °C.

Graph A, Expt. 1, 2 and 3

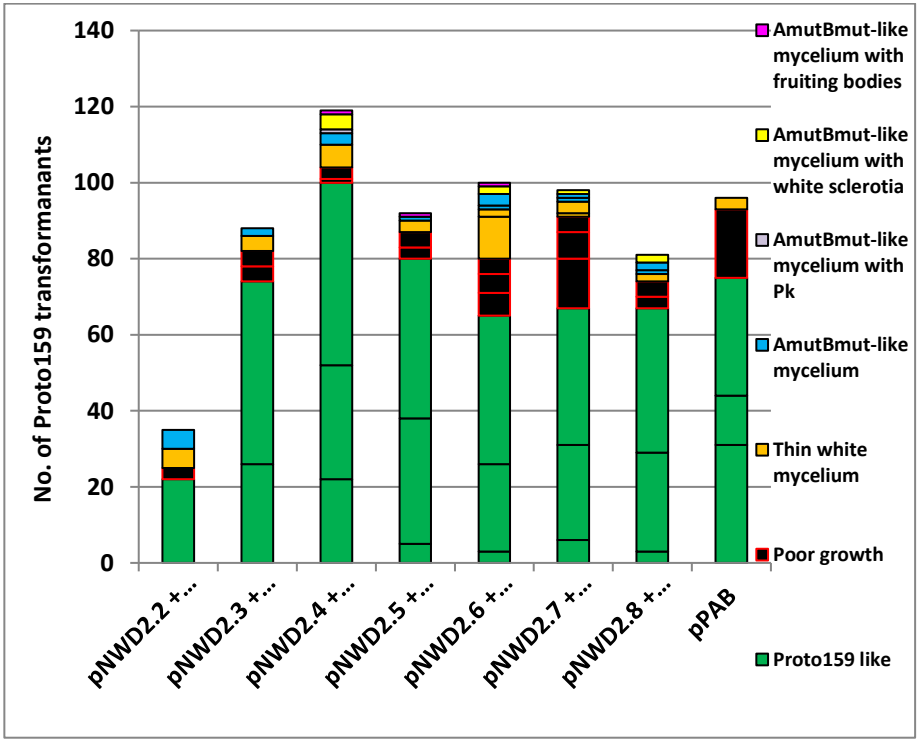

Graph B, Expt. 1, 2 and 3

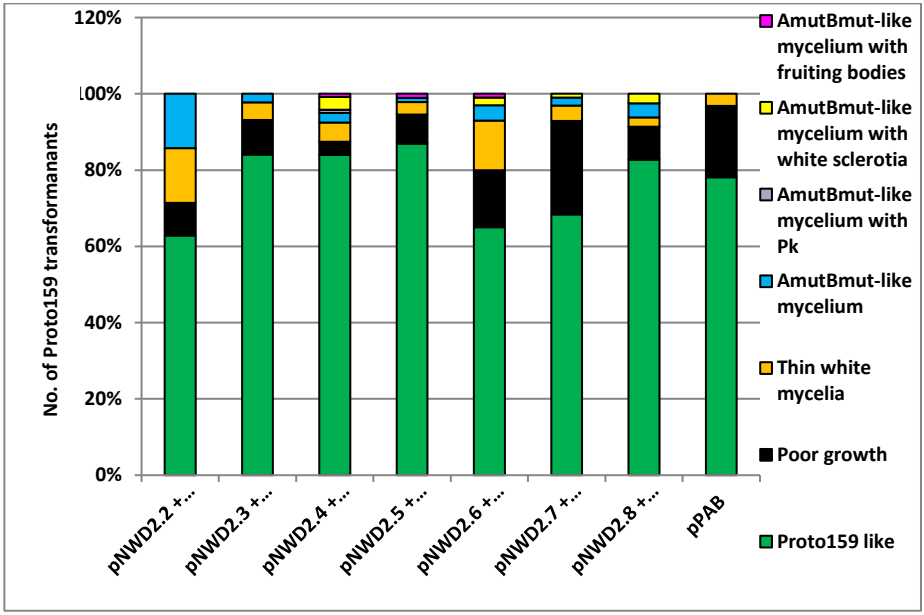

Fig. 15. The graphs A and B show number of Proto 159 transformants in absolute numbers and in percentage exhibiting seven types of mycelial phenotypes in the experiments 1st, 2nd and 3rd, respectively. The black lines saparating each boxes of similar colors on the graph A represent similar type of phenotypes exhibited by transformants in three independent experiments.

To summarize all three above experiments (1, 2 and 3) by adding the phenotypes of all transformants per gene together, in all cases it was observed that there were variations in the phenotypes over the groups of the transformants obtained, such as from poor growth to thin and to AmutBmut-like and further to the production of sclerotia and fruiting bodies (shown in graphs A and B in Fig. 15). Transformation is per se mutagenic e.g. by ectopic DNA integration possibly into functional genes (Granado et al. 1997), which might explain phenotypic changes to poor growth in control transformants of pPAB1 as compared to mutant Proto159. However, transformed *NWD2* genes seem to have had extra effects, while on the one hand phenotypes of different transformants per individual gene were very distinct of each other and while on the other hand distributions of phenotypes between transformant groups of different genes resembled one another (Fig. 15). Co-transformation rates of *NWD2* genes for white mycelia were 1 to 14 %, white sclerotia 1 to 4 % and fruiting 1 % (Fig. 15), adding up per gene to 10 to 20 % of co-transformants. Similar effects of variable to even contrasting growth phenotypes

with co-transformation rates of 25 to 50 % sometimes 40 % were observed before from transformations of monokaryons 218 and PG78 with extra copies of the *ras* wildtype gene and constitutively active *ras*^{val19} and constitutively inactive *ras*^{asn24} mutant genes (Bottoli 2001; Srivilai 2006; Kües, unpublished). Ras is a protein that belongs to a class of small GTPases that can be switched on and off by hydrolysis of the Ras-bound nucleotide GTP changing it to GDP. When Ras is 'switched on' in the GTP-bound form by incoming signals, it subsequently activates by phosphorylation other proteins in signalling cascades, which ultimately turns on genes involved in cell growth, differentiation, and fruiting body formation. Then, Ras is 'switched off' by the de-phosphorylation to GDP, thereby shutting down the activation. Regulation of Ras is determined by the balance between the activity of two proteins, GEF (guanine exchange factor) and GAP (GTPase activating protein). Specific mutations in *ras* genes (*ras*^{val19}) can however lead to the production of permanently activated Ras protein which results in unintended and overactive signaling inside the cells, even in the absence of incoming signals. Similarly, other specific mutations (*ras*^{asn24}) can transfer the protein into a permanentaly inactive stage (Broach and Deschenes 1990; Thevelein 1992). This can be seen in very contrasting phenotypes such as in *C. cinerea* transformants of *ras* mutant phenotypes by very healthy fluffy mycelium growth and by very poor slow growth, respectively. Moreover, random integration of wildtype *ras* can have in lower frequencies of transformants also either positive or negative effects on the growth. This is based on the random integration of gene copies leading to variably increased *ras* gene expression and in consequence changes in the cellular *ras* ^{GTP}-*ras* ^{GDP} balances (U. Kües, personal communication).

The above described situation for Ras cycle reactions is expected to be similar to the regulation of a *NWD2* gene which encodes a type of NTPases that should function like a Ras GTPase with alternative active GTP-bound and inactive GDP-bound stages. Therefore, the random integrations of the copies of the different *NWD2* genes into the genome of Proto159 possibly have caused an imbalance in the cellular control and signalling system leading to the formation of various growth phenotypes of the transformants and an occassional restoration of the fruiting ability.

6.4.6.2. AmutBmut transformants

The phenotypes of the transformants obtained in three series of experiments by introducing *NWD2* genes of the group A of the *NWD2* family into the wildtype strain AmutBmut are shown in the individual experiment graphs (A, B and C) in Fig. 16 and in the cumulative graphs (A and B) in Fig. 17. Mycelial phenotypes were documented from observations in all three experiments whereas fruting tests were done only for the transformants obtained in the 3rd experiment (graphs A and B in Fig. 18).

In the 1st and the 2nd experiments, three types of mycelial phenotypes such as AmutBmut-like mycelium, thick mycelium, and sectors within the mycelial colonies were shown by the transformants (Fig. 16 and Fig. 17). Sector mycelia were seen in all the tranformations except for genes *pab1*$^+$ and *NWD2.7* in the 1st experiment and *pab1*$^+$ and *NWD2.5* in the 2nd experiment (graphs A and B in Fig. 16 and graphs A and B in Fig. 17). In the 3rd series of experiments, colonies of poor growth were in addition detected on frequencies of 10 to 24 % of clones, excluding in the *pab1*$^+$ vector control (graph C in Fig. 16 and graphs A and B in Fig. 17). Importantly, sector mycelia were seen in all the tranformations but in *pab1*$^+$ and *NWD2.3* transformations (graphs C in Fig. 16 and graphs A and B in Fig. 17). Colonies with sector formation were characterized by irregular growth with parts of colonies collapsing by giving up growth, parts that may grow out healthy and fluffy AmutBmut-like or fluffy thick, and parts that may grow out as a thin mycelium (photos not taken).

Graph A, Expt. 1

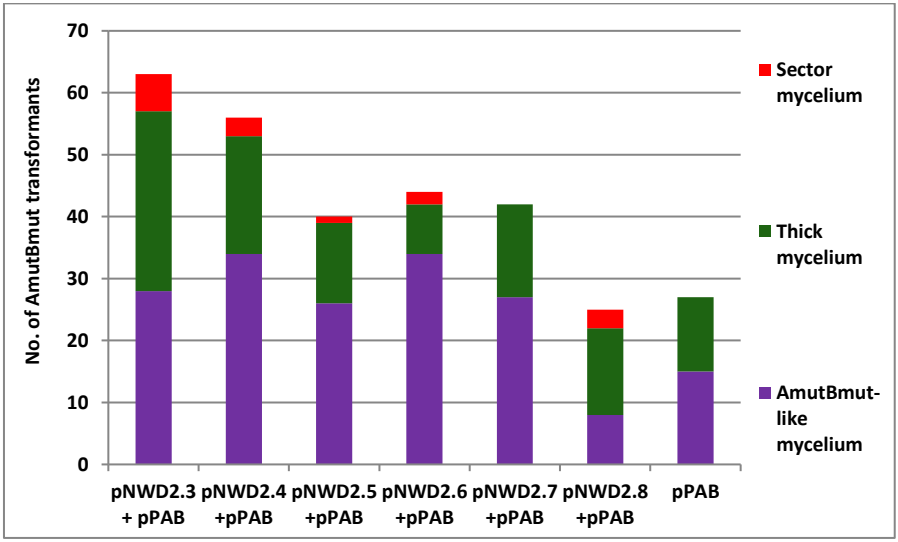

Graph B, Expt. 2

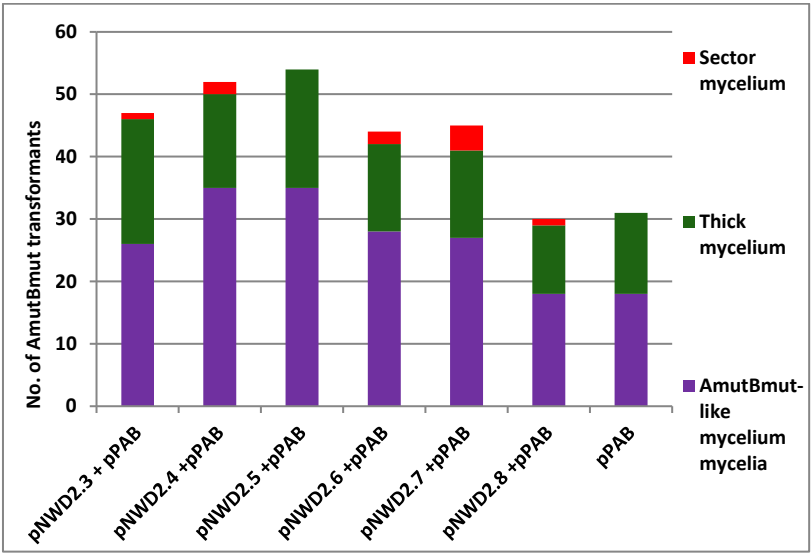

Graph C, Expt. 3

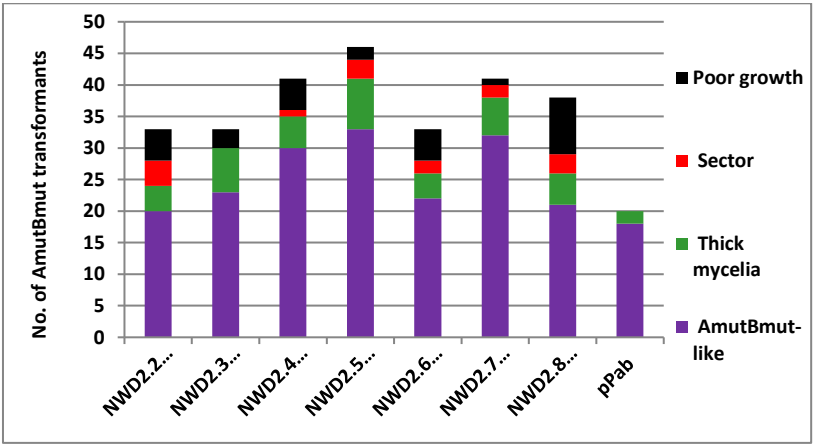

Fig. 16. The graphs A and B show three types of mycelial phenotypes of the AmutBmut transformants in the experiments 1st and 2nd, and the graph C shows four types of mycelial

phenotypes of the AmutBmut transformants in the 3rd experiments. In the 1st and the 2nd experiments, AmutBmut-like mycelium, thick mycelium and sector mycelium were exhibited by the transformants. In the 3rd experiment all above mentioned mycelial phenotypes and additionally poor growth growth were exhibited by the transformants.

Graph A, Expt. 1, 2 and 3

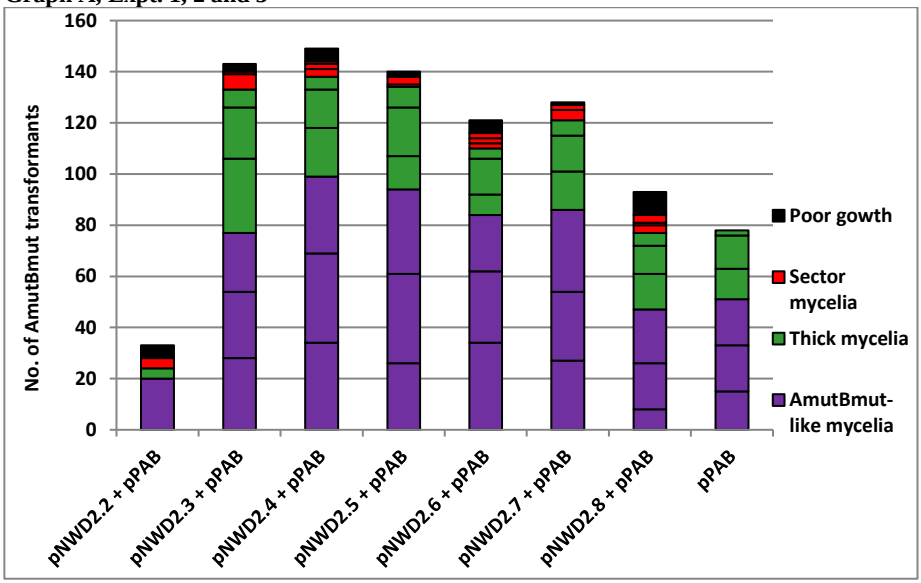

Graph B, Expt. 1, 2 and 3

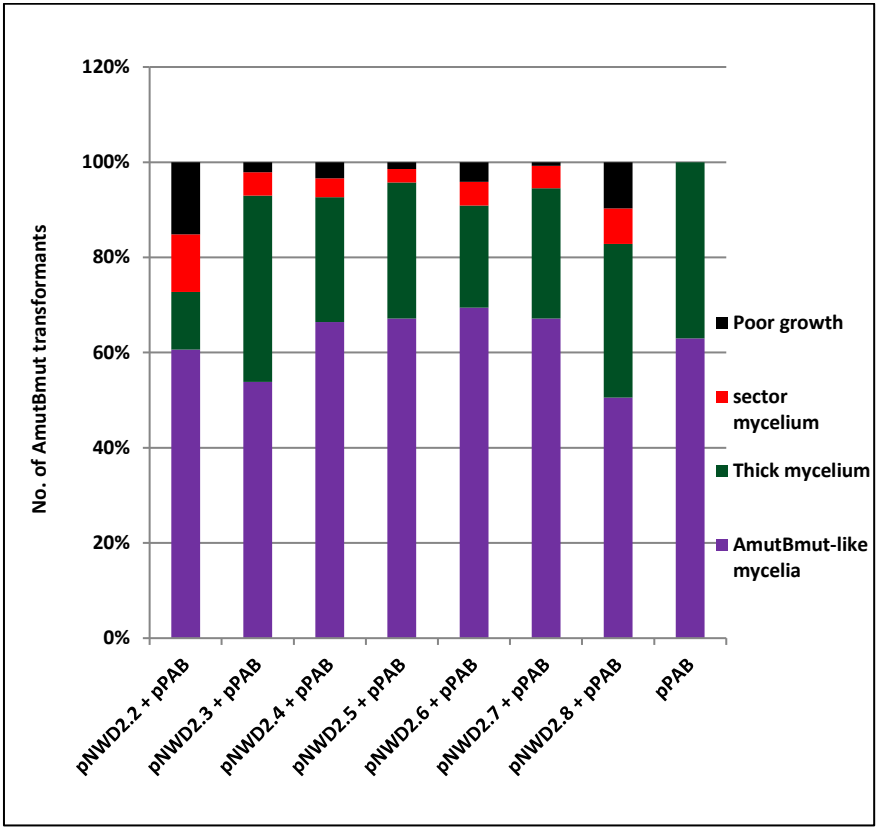

Fig. 17. The graphs A and B show number of AmutBmut transformants in absolute numbers and in percentage exhibiting four types of mycelial phenotypes in the experiments 1st, 2nd and 3rd. The black lines saparating each boxes of similar colors on the graph A represent similar type of phenotypes exhibited by transformants in three independent experiments.

Fruiting tests were carried out for the tranformants in the 3rd experiment (graphs A and B in Fig. 18). For this, after incubation of cultures for 5 days in dark, they were shifted to fruiting conditions at 25 °C with 12h light and 12h dark with 90 % of humidity. In total, 16 of 20 transformants of the *pab1*$^{+}$ control (80 %) intiated and complete fruiting. In groups of transformants of *NWD2* genes, the overall fruiting frequencies were similar with 66 to 88 % of total colonies (graphs A and B in Fig. 18). Unusual in this series of experiments however, the

maturation and the autolysis of fruiting bodies took place on differents days, with some (5 to 18 %) that needed 7 days days for the whole fruiting pathway, and others that completed fruiting after six (39 to 70 %) or, with exception of the pPAB1 control, even five days (6 to 33 %) of incubation under standard fruiting conditions (graphs A and B in Fig. 18). It appears from growing primordia observations on plates of all types of transformants that increase in speed of fruiting was after the P3 stage in the morning of Day 4 of incubation under standard fruiting conditions (photos not taken).

Graph A, Expt. 3

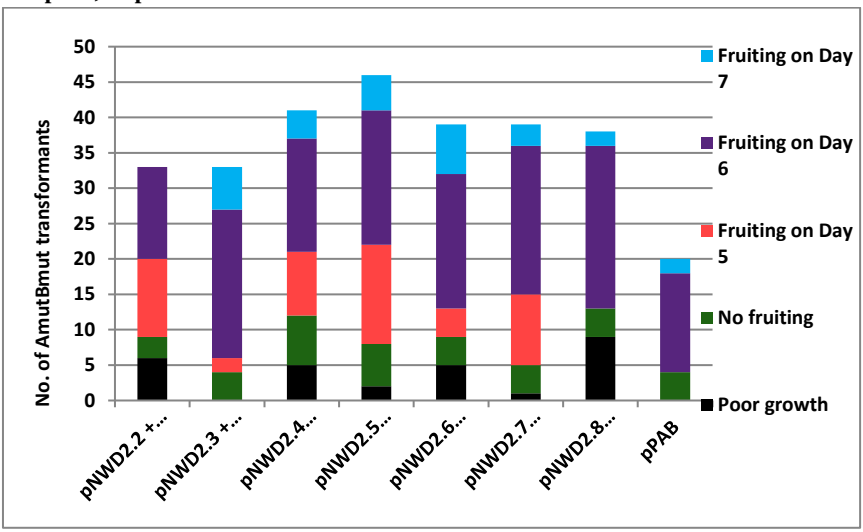

Graph B, Expt. 3

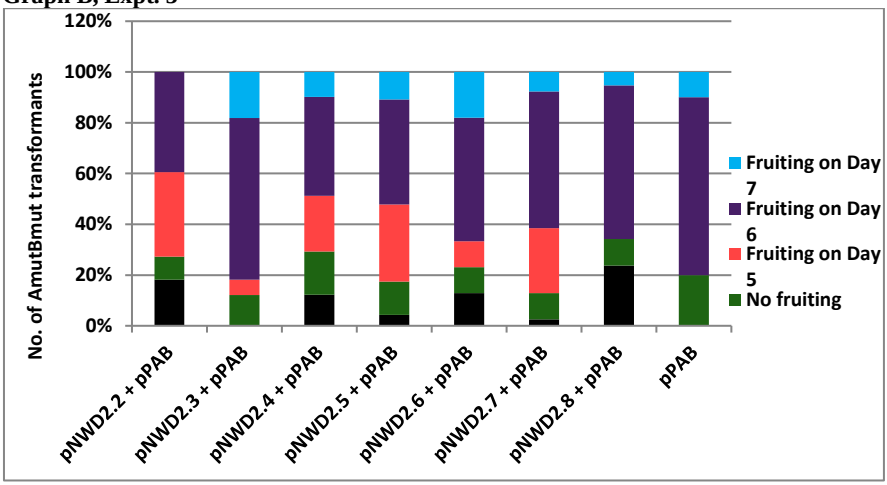

Fig. 18. The graphs A and B show the ability of the AmutBmut transofrmants to fruit and autolyse on the respectives days of the standard fruiting pathway in the 3rd experiment presented in absolute numbers and in percentage, respectively. Fruiting test was done after incubating cultures on YMG/T media for 5 days under dark condition at 37 °C and then transfering cultures to fruiting conditions at 25 °C.

Table 6. Colony phenoptype, non-fruting and ability of AmutBmut transofrmants to fruit and autolyse on the respectives days of the standard fruiting pathway in the 3rd experiment after transfer into standard fruiting conditions at 25 °C.

Genes	Colony phenotype	No fruiting	Day 5	Day 6	Day 7	Total (fruiting)
pNWD2.2 + pPAB	Poor growth	6	0	0	0	**6 (0)**
	with sector	3	0	1	0	**4 (1)**
	thick mycelium	0	4	0	0	**4 (4)**
	Amutbmut-like	0	7	12	0	**19 (19)**
	Total	**9**	**11**	**13**	**0**	**33 (24)**
pNWD2.3 + pPAB	Poor growth	0	0	0	0	**0 (0)**
	with sector	1	0	3	1	**5 (3)**
	thick mycelium	0	2	0	0	**2 (2)**
	AmutBmut-like	3	0	18	5	**26 (23)**
	Total	**4**	**2**	**20**	**6**	**33 (28)**
pNWD2.4 +pPAB	Poor growth	5	0	0	0	**5 (0)**
	with sector	2	1	0	0	**3 (1)**
	thick mycelium	2	1	0	2	**5 (3)**
	Amutbmut-like	3	7	16	2	**28 (25)**
	Total	**12**	**9**	**16**	**4**	**41 (29)**
pNWD2.5 +pPAB	Poor growth	2	0	0	0	**2 (0)**
	with sector	0	0	1	2	**3 (3)**
	thick mycelium	0	4	4	0	**8 (8)**
	Amutbmut-like	6	10	14	3	**33 (27)**
	Total	**8**	**14**	**19**	**5**	**46 (38)**
pNWD2.6 +pPAB	Poor growth	5	0	0	0	**5 (0)**
	with sector	2	0	0	0	**2 (0)**
	thick mycelium	2	1	1	0	**4 (2)**
	Amutbmut-like	0	3	18	7	**28 (28)**

	Total	**9**	**4**	**19**	**7**	**39 (30)**
pNWD2.7 +pPAB	Poor growth	1	0	0	0	**1 (0)**
	with sector	1	0	0	1	**2 (0)**
	thick mycelium	2	0	3	0	**5 (3)**
	Amutbmut-like	1	10	18	2	**31 (30)**
	Total	**5**	**10**	**21**	**3**	**39 (34)**
pNWD2.8 +pPAB	Poor growth	9	0	0	0	**9 (0)**
	with sector	3	0	0	0	**3 (0)**
	thick mycelium	1	0	4	0	**5 (4)**
	Amutbmut-like	0	0	19	2	**21 (21)**
	Total	**13**	**0**	**23**	**2**	**38 (25)**
pPAB	Poor growth	0	0	0	0	**5 (0)**
	with sector	0	0	0	0	**0 (0)**
	thick mycelium	2	0	0	0	**2 (0)**
	Amutbmut-like	2	0	14	2	**18 (16)**
	Total	**4**	**0**	**14**	**2**	**20 (16)**

*Probable funtions of the *NWD2* genes are highlighted in yellow color and the probable funtions of *pab1*$^{+}$ are highlighted in gray color and the non colored parts are normal or unexpected phenotypes.

Graph A

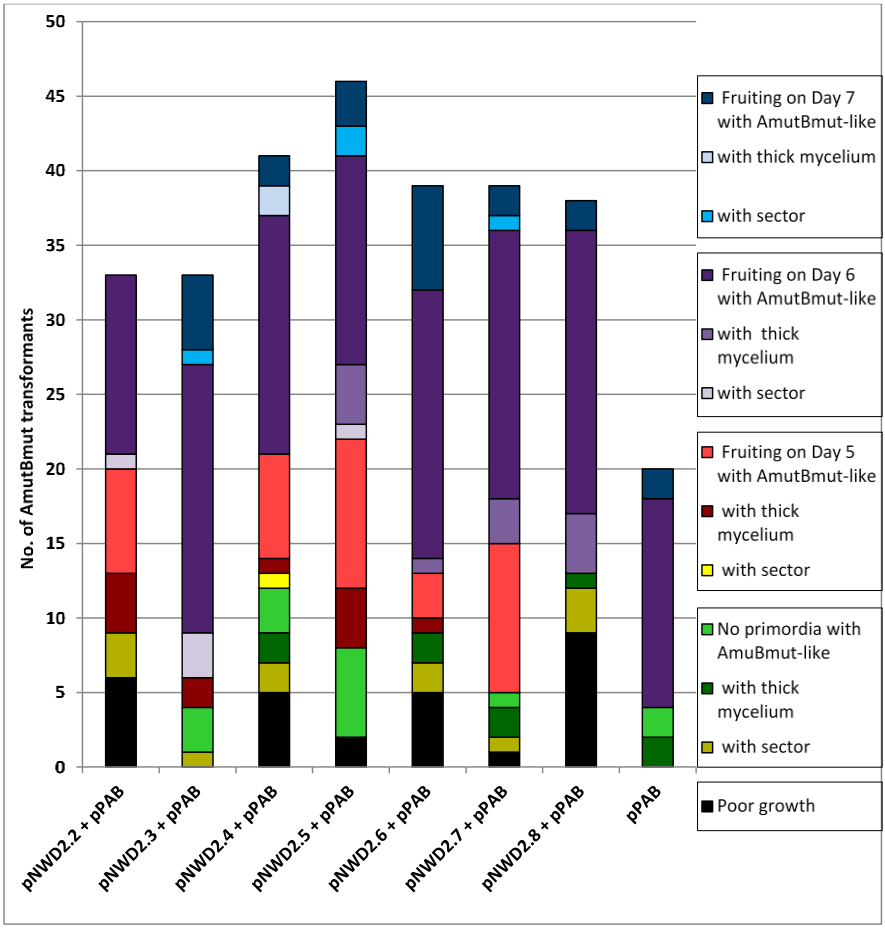
No. of AmutBmut transformants
50
45
40
35
30
25
20
15
10
5
0
pNWD2.2 + pPAB
pNWD2.3 + pPAB
pNWD2.4 + pPAB
pNWD2.5 + pPAB
pNWD2.6 + pPAB
pNWD2.7 + pPAB
pNWD2.8 + pPAB
pPAB
Fruiting on Day 7 with AmutBmut-like
with thick mycelium
with sector
Fruiting on Day 6 with AmutBmut-like
with thick mycelium
with sector
Fruiting on Day 5 with AmutBmut-like
with thick mycelium
with sector
No primordia with AmuBmut-like
with thick mycelium
with sector
Poor growth

Graph B

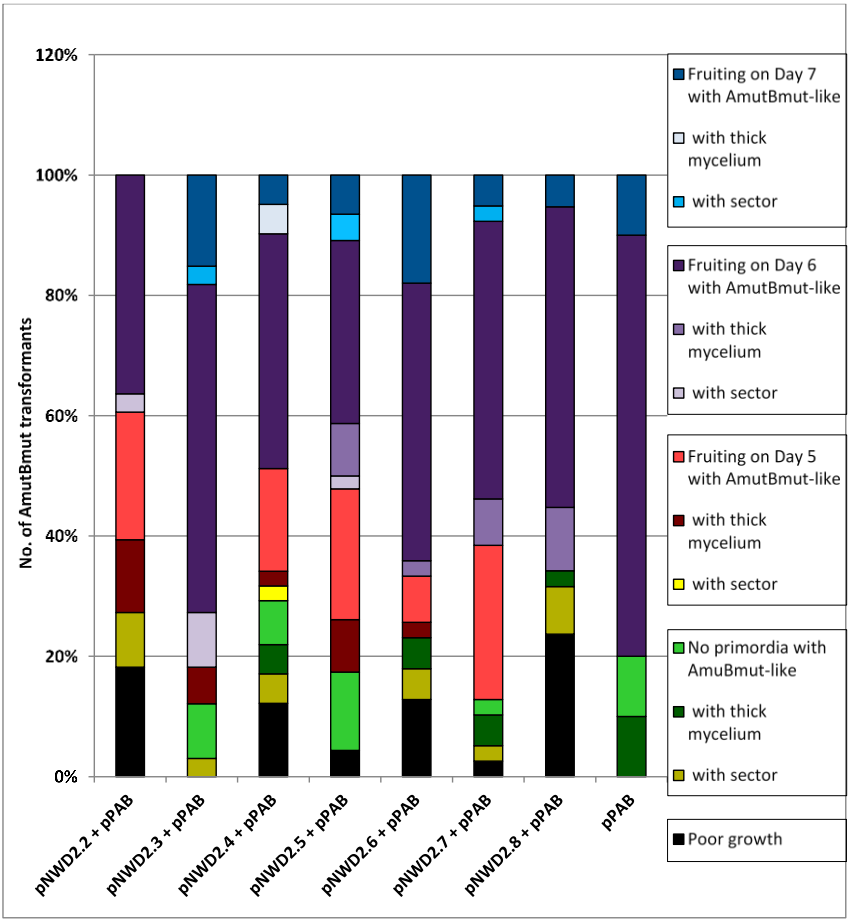

Fig. 19. The graphs A and B show number of transformants in absolute numbers and in percentage exhibiting fruiting abilities by three different types of mycelial phenotypes such as mycelium with sectoring, thick mycelium and AmutBmut-like mycelium in 3rd experiment, respectively. Transformants were cultivated on YMG/T media under standard fruiting condition at 25 °C.

The majority of maturation with autolysis of the fruiting bodies happened for clones on the 6th day of the fruiting pathway for all the genes including of the control gene *pab1*$^{+}$ (Table 6, graphs A and B in Fig. 19, shown in different shades of purple bars). The reason for the speeded-up fruiting is probably because of the ectopic integration of *pab1*$^{+}$ into the genomes with

complementation of the PABA deficiency. Evidence for this idea comes from further experiments of W. Khonsuntia (personal communication) that addition of extra PABA (*para*-aminobenzoic acid) to the medium has a similar effect of speeding up fruiting of homokaryon AmutBmut. PABA is needed in cells for vitamin B5 (pantothenate) production. Vitamin B5 is precursor of biosynthesis of coenzyme A (CoA) that balances the metabolic reactions between carbohydrate and lipid synthesis during glucose oxidation in the TCA cycle and degradation of fatty acid (Leonardi et al. 2005; Leonardi and Jackowski 2007) and is also a required cofactor for the biosynthesis of ketone bodies (McGarry and Foster 1980; Puchalska and Crawford 2017). It is needed at the same steps than vitamin B1 (thiamine) in steps of CO_2 release (see Chapter 5.2 of this thesis). Previously, I reported that increase in CO_2 by lack of aeration in sealed cultures blocked growth and fruiting (see Chapter 5.2 of this thesis). Here, cultures were left open allowing quick release of produced CO_2 from the cultures. From mutant analysis with dark-stipe formation under standard fruiting conditions, connections to the pyruvate metabolism and the TCA cycle for generation of the phenotype in mutants 7K17 and B1918 and a defect in the Cop9 signalosome in mutant B1918 suggests an interrelation with the light regulatory system (see chapters 5.1 and 5.2 of this thesis). Morphological observations of the B1918 phenotype during the fruiting pathway revealed that it was at stage P4 when the CO_2-interlinked dark stipe phenotype was expressed in cultures (chapter 5.2). The timing seems to well correlate between the B1918 phenotype and the putative effect of PABA discovered here.

Other than an apparent effect of PABA on the fruiting might be excretred by the members of *NWD2* gene family A. The transformants of genes from *NWD2.2* to *NWD2.7* that autolyzed very early already on the 5th day of the fruiting pathway might then have been even faster by the introduction of extra *NWD2* gene copies (Table 6, graphs A and B in Fig. 19, shown in red, brown and yellow bars). Notably, early fruiting happened in most transformants with AmutBmut-like mycelium (14 %), in most transformants with thick mycelium and in parts of the sectoring transformants (0.3 to 4 % for all genes together), either within sectors of AmutBmut-like or of thick mycelium (graph B in Fig. 19). This suggests that there might be some correlation between changes in regulation of colony growth and morphology and in fruiting by extra introduced copies of *NWD2* genes. However, the complexity of the combined phenotypes and the fruiting variably at different places within the sectoring colonies makes more concrete conclusions at this time difficult. Variabilities in phenotypes in transformants of homokaryon AmutBmut by introduction of the different *NWD2* genes might again base on distinct changes in balances of the respective NTPase-cycles with NTP-bound and NPD-bound molecules, similar as known from the Ras GTPase cycle (Farnsworth and Feig 199; Downward, J. 2003).

6.5. Conclusions

Mutant phenotypes of clone Proto159 with a defect in fruiting body initiation and specific colony morphologies (slower growth and less aerial growth than the parental AmutBmut, pigmentation of agar) have been suppressed by introduction of gene members of the *NWD2* family of a group A. The tendency towards the suspected potential regulatory functions of 7 cloned out of 8 *NWD2* genes from the 1st group A in the fruiting initiation of the *pnk* defective mutant Proto159 is reported is this chapter. Also, interesting effects such as mycelial sectoring and of early fruiting were seen in transformants of the parental homokaryom AmutBmut. However, experimental series in this chapter were not fully complete and results should still be considered as preliminary. Further experimental analysis and transformations are required to be done in order to complete the story of this chapter. In particular, sufficient numbers of transformants of all genes should be obatained and analyzed in growth and fruiting exactly as described for the optimal fruiting conditions in chapter 2.1 (Kües et al. 2016). Then, morphologiocal dissections and observations should be done over the whole fruting pathway from fruiting-restored Proto159 clones and also from early fruiting transformants of homokaryon AmutBmut. Effects of dark and of light can be tested for such AmutBmut transformants to reveal whether CO_2 and/or light regulation is altered within the transformants, similar as described in chapters 5.1 and 5.2. Further, more attention has to be given to effects of PABA on fruiting and possible links to CO_2 and/or light regulation. Finally, another most interesting scientific approach to be done would be to sequence the whole genome of mutant Proto159 in order to identify by genome comparisons with homokaryon AmutBmut the potentationl mutated gene(s) responsible for the Proto159 phenotypes.

6.6. References

Aravind, L., Iyer, L. M., Leipe, D. D. and Koonin, E. V. (2004) A novel family of P-loop NTPases with an unusual phyletic distribution and transmembrane segments inserted within the NTPase domain. *Genome Biology*, *5*, pp.1-10.

Arya, P. and Acharya, V. (2016) Computational identification raises a riddle for distribution of putative NACHT NTPases in the genome of early green plants. *PLoS One*, *11*, p.e0150634.

Arya, P. and Acharya, V. (2018) Plant STAND P-loop NTPases: A current perspective of genome distribution, evolution, and function. *Molecular Genetics and Genomics*, *293*, pp.17-31.

Binninger, D. M., Skrzynia, C., Pukkila, P. J. and Casselton, L. (1987) DNA-mediated transformation of the basidiomycete *Coprinus cinereus*. *The EMBO Journal*, *6*, pp.835-840.

Blatch, G. L. and Lässle, M. (1999) The tetratricopeptide repeat: a structural motif mediating protein-protein interactions. *Bioessays*, *21*, pp.932-939.

Bottoli, A. P., Kertesz-Chaloupkova, K., Boulianne, R. P., Aebi, M. and Kües, U. (1999) Rapid isolation of genes from an indexed genomic library of *C. cinereus* in a novel *pab1*$^{+}$ cosmid. *Journal of Microbiological Methods*, *35*, pp.129-141.

Bottoli, A. P. F., Boulianne, R. P., Aebi, M. and Kües, U. (2001) Expression of mutant *ras* alleles in *Coprinus cinereus.* (PhD thesis, chapter 3, Zurich)

Broach, J. R. and Deschenes, R. J. (1990) The function of *ras* genes in *Saccharomyces cerevisiae*. *Advances in Cancer Research*, *54*, pp.79-139.

Brodie, H. J. (1932) Oidial mycelia and the diploidization process in *Coprinus lagopus. Annals of Botany*, *46*, pp.727-732.

Casselton, L. A. and Kües, U. (1994) Mating-type genes in homobasidiomycetes. In *Growth, Differentiation and Sexuality* pp.307-321. Springer, Berlin, Heidelberg.

Casselton, L. A. and Olesnicky, N. S. (1998) Molecular genetics of mating recognition in basidiomycete fungi. *Microbiology and Molecular Biology Reviews*, *62*, pp.55-70.

Chevanne, D., Bastiaans, E., Debets, A., Saupe, S. J., Clavé, C. and Paoletti, M. (2009) Identification of the *het-r* vegetative incompatibility gene of *Podospora anserina* as a member of the fast-evolving *HNWD* gene family. *Current Genetics*, *55*, pp.93-102.

Dörnte, B., Peng, C., Fang, Z., Kamran, A., Yulvizar, C. and Kües, U. (2020) Selection markers for transformation of the sequenced reference monokaryon Okayama 7/# 130 and homokaryon AmutBmut of *Coprinopsis cinerea*. *Fungal Biology and Biotechnology*, *7*, pp.1-18.

Downward, J. (2003) Targeting RAS signaling pathways in cancer therapy. *Nature Reviews Cancer*, *3*, pp.11-22.

Farnsworth, C. L. and Feig, L. A. (1991) Dominant inhibitory mutations in the Mg^{+} binding site of RasH prevent its activation by GTP. *Molecular and Cellular Biology*, *11*, pp.4822-4829.

Gatto, G. J., Geisbrecht, B. V., Gould, S. J. and Berg, J. M. (2000) Peroxisomal targeting signal-1 recognition by the TPR domains of human PEX5. *Nature Structural Biology*, *7*, pp.1091-1095.

Granado, J. D., Kertesz-Chaloupková, K., Aebi, M. and Kües, U. (1997) Restriction enzyme-mediated DNA integration in *Coprinus cinereus*. *Molecular and General Genetics*, *256*, pp.28-36.

Holm, P. B., Rasmussen, S. W., Zickler, D., Lu, B. C. and Sage, J. (1981) Chromosome pairing, recombination nodules and chiasma formation in the basidiomycete *Coprinus cinereus. Carlsberg Research Communications*, *46*, pp.305.

Horton, J. S. and Raper, C. A. (1991) A mushroom-inducing DNA sequence isolated from the Basidiomycete, *Schizophyllum commune*. *Genetics*, *129*, pp.707-716.

Koonin, E. V. and Aravind, L. (2000) The NACHT family–a new group of predicted NTPases implicated in apoptosis and MHC transcription activation. *Trends in Biochemical Sciences*, *25*, pp.223-224.

Kües, U. (2000) Life history and developmental processes in the Basidiomycete *Coprinus cinereus*. *Microbiology and Molecular Biology Reviews*, *64*, pp.316-353.
Kües, U. and Navarro-González, M. (2015) How do Agaricomycetes shape their fruiting bodies? 1. Morphological aspects of development. *Fungal Biology Reviews*, *29*, pp.63-97.
Leipe, D. D., Koonin, E. V. and Aravind, L. (2004) STAND, a class of P-loop NTPases including animal and plant regulators of programmed cell death: multiple, complex domain architectures, unusual phyletic patterns, and evolution by horizontal gene transfer. *Journal of Molecular Biology*, *343*, pp.1-28.
Leonardi, R. and Jackowski, S. (2007) Biosynthesis of pantothenic acid and coenzyme A. *EcoSal Plus*, *2*, pp.10-128.
Leonardi, R., Zhang, Y. M., Rock, C. O. and Jackowski, S. (2005) Coenzyme A: back in action. *Progress in Lipid Research*, *44*, pp.25-153.
Li, D. and Roberts, R. (2001) Human Genome and Diseases: WD-repeat proteins: structure characteristics, biological function, and their involvement in human diseases. Cellular and *Molecular Life Sciences* CMLS, *58*, pp.2085-2097.
Liu, Y., Srivilai, P., Loos, S., Aebi, M. and Kües, U. (2006) An essential gene for fruiting body initiation in the basidiomycete *Coprinopsis cinerea* is homologous to bacterial cyclopropane fatty acid synthase genes. *Genetics*, *172*, pp.873-884.
McGarry, J. D. and Foster, D. W. (1980) Regulation of hepatic fatty acid oxidation and ketone body production. *Annual Review of Biochemistry*, *49*, pp.395-420.
Moore, D. (1998) Fungal morphogenesis. Cambridge: Cambridge University Press.
Muraguchi, H. and Kamada, T. (1998) The *ich1* gene of the mushroom *Coprinus cinereus* is essential for pileus formation in fruiting. *Development*, *125*, pp.3133-3141.
Nakazawa, T., Ando, Y., Kitaaki, K., Nakahori, K. and Kamada, T. (2011) Efficient gene targeting in *ΔCc. ku70 or ΔCc. lig4* mutants of the agaricomycete *Coprinopsis cinerea*. *Fungal Genetics and Biology*, *48*, pp.939-946.
Navarro-González, M. (2008) Growth, fruiting body development and laccase production of selected coprini (Doctoral dissertation, Göttingen University).
Neer, E. J., Schmidt, C. J., Nambudripad, R. and Smith, T. F. (1994) The ancient regulatory-protein family of WD-repeat proteins. *Nature*, *371*, pp.297-300.
Polak, E., Hermann, R., Kües, U. and Aebi, M. (1997) Asexual Sporulation in *Coprinus cinereus*: Structure and Development of Oidiophores and Oidia in an Amut Bmut Homokaryon. *Fungal Genetics and Biology*, *22*, pp.112-126.
Puchalska, P. and Crawford, P. A. (2017) Multi-dimensional roles of ketone bodies in fuel metabolism, signaling, and therapeutics. *Cell Metabolism*, *25*, pp.262-284.
Scheufler, C., Brinker, A., Bourenkov, G., Pegoraro, S., Moroder, L., Bartunik, H., Hartl, F. U. and Moarefi, I. (2000) Structure of TPR domain–peptide complexes: critical elements in the assembly of the Hsp70–Hsp90 multichaperone machine. *Cell*, *101*, pp.199-210.

Smith, T. F., Gaitatzes, C., Saxena, K. and Neer, E. J. (1999) The WD repeat: a common architecture for diverse functions. *Trends in Biochemical Sciences*, *25*, pp.181-185.
Srivilai, P. (2007) Molecular analysis of genes acting in fruiting body development in basidiomycetes (Doctoral dissertation, Göttingen University).
Stajich, J. E., Wilke, S.K., Ahrén, D., Au, C. H., Birren, B. W., Borodovsky, M., Burns, C., Canbäck, B., Casselton, L. A., Cheng, C. K. and Deng, J. (2010) Insights into evolution of multicellular fungi from the assembled chromosomes of the mushroom *Coprinopsis cinerea* (*Coprinus cinereus*). *Proceedings of the National Academy of Sciences*, *107*, pp.11889-11894.
Stirnimann, C. U., Petsalaki, E., Russell, R. B. and Müller, C. W. (2010) WD40 proteins propel cellular networks. *Trends in Biochemical Sciences*, *35*, pp.565-574.
Swamy, S., Uno, I. and Ishikawa, T. (1984) Morphogenetic effects of mutations at the *A* and *B* incompatibility factors in *Coprinus cinereus*. *Microbiology*, *130*, pp.3219-3224.
Thevelein, J. M. (1992) The RAS-adenylate cyclase pathway and cell cycle control in *Saccharomyces cerevisiae*. *Molecular Biology of Saccharomyces*, *62*, pp.109-130.
Van der Nest, M. A., Olson, Å., Lind, M., Velez, H., Dalman, K., Durling, M. B., Karlsson, M. and Stenlid, J. (2014) Distribution and evolution of *het* gene homologs in the basidiomycota. *Fungal Genetics and Biology*, *64*, pp.45-57.
Walser, P. J., Hollenstein, M., Klaus, M. J. (2001) Genetic analysis of basidiomycete fungi. Molecular and Cell Biology of Filamentous Fungi: *A Practical Approach*, pp.59-60. Oxford: Oxford University Press.

TISSUE STAINING TO STUDY THE FRUITING PROCESS OF *COPRINOPSIS CINEREA*

Shanta Subba, Marco Winkler, Ursula Kües

Georg-August-University of Göttingen, Molecular Wood Biotechnology and Technical Mycology,

Büsgenweg 2, D-37077 Göttingen, Germany

General introduction

Fruiting bodies of the Agaricomycetes are the most complex multicellular structures that occur in the fungal kingdom, with different types of tissues and several kinds of cells of distinct functions. The coprophilous *Coprinopsis cinerea* is an edible model mushroom for studies on fruiting body development because it grows very fast and fruits within two weeks under laboratory conditions. Some estimates have been made on different types of cells which are produced during the fruiting process. In *C. cinerea*, there are probably > 30 cell types that differentiate during different stages of the development. Here, we apply different histochemical staining techniques with different dyes singly and in combinations to mark and identify specific tissues and cells. Stains help to analyze deposition of protein material (Mayer's hemalum, malachite green), glycoproteins (periodic acid Schiff, PAS), chitin (lactophenol blue, eosin), and other polysaccharides (PAS) in the growing mushroom.

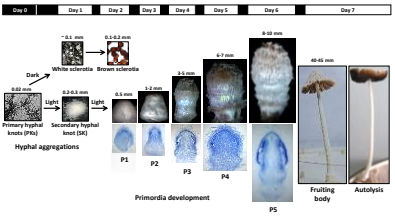

Fig. 1 Fruiting pathway of *C. cinerea*
The bar above the fungal structures presents with white and black boxes to the dark and light phases in course of incubation. Day 0 refers to the last day of cultivation for mycelial growth at 37 °C in the dark, prior to transfer of cultures into standard fruiting conditions (alternating 12 h light/12 h dark incubation at 25 °C). Sizes in mm refer to height of structures.

Stages of fruiting body development in *C. cinerea*

Fruiting formation in *C. cinerea* follows a highly conserved scheme defined through light regulation by day and night phases.

- Day 0: Fruiting starts with loosely aggregated primary hyphal knots **(PKs)** formed in the dark.
- Day 1: A first light-signal induces compact secondary hyphal knots **(SKs)** in which stipe and cap tissues start to differentiate.
- Day 2: First stage white round primordia **P1** appear with an internal clear cap differentiation.
- Day 3: Primordium stage **P2** is pear-shaped with internally distinguishable cap, stipe and basal regions. Gill rudiments are formed at the **P2** stage.
- Day 4: Primordium stage **P3** attained a terete shape. Primary and secondary gills arise form gill rudiments.
- Day 5: At primordium stage **P4,** all main tissues are established. A light signal is received to induce karyogamy in basidia.
- Day 6: Karyogamy **(K)** occurs at the fully established light-bulb-shaped primordium stage **P5**. Meiosis **(M)** and basidiospore production follows over the day. In parallel to sporulation, rapid stipe elongation and cap expansion take place.
- Day 7: Fruiting bodies **(FB)** are fully matured shortly after midnight in the next night phase and autolyze in the morning to release the spores in black liquid droplets.

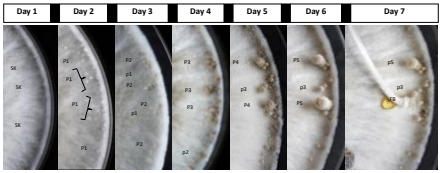

Fig. 2 Primordia development under standard fruiting conditions
C. cinerea initiates fruiting by formation of multiple SK structures. Every day, parts of developing structures are aborted (structures marked **p1** to **p5**) in favor of further actively growing structures (marked **SK**, **P1** to **P5** , **FB**).

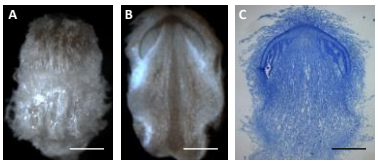

Fig. 3 Structure of primordia at the P4 stage
(A) Outer view, (B) inside view of a P4 stage primordium with a well-developed cap and stipe, vertically dissected into halves. (C) Lactophenol-stained longitudinal section (10 µm thick) of a P4 stage primordium showing hyphal tissue differentiation. Size bars represent 1 mm in length.

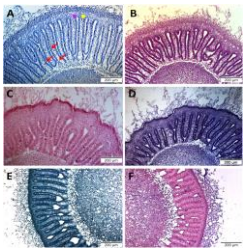

(A and B: 10 µm sections , C to D: 5 µm sections)

Fig. 4 Cross sections of the cap region at the P4 stage
(A) Lactophenol blue staining: A yellow circle and a pink triangle mark primary and secondary gills, respectively, and red arrows large protruding cystidia in the hymenium.
(B) PAS and Mayer's hemalum double-staining shows more explicitly the arrangement of primary and secondary gills in the cap region than
(C) single PAS staining and
(D) single Mayer's hemalum staining.
(E) Differential staining with malachite green and
(F) with eosin.

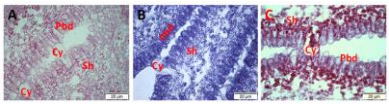

Fig. 5 Cross section of hymenia of a P4 stage primordium at higher magnification (100x)
(A) Single PAS staining shows that the subhymenial (Sh) region is stained somewhat darker as compared to the parallel arranged young basidia (Pbd).
(B) Mayer´s hemalum stains best the probasidia in dark blue.
(C) In a section double-stained by PAS and Mayer's hemalum, a clear differentiation in the gills between the subhymenium and the young basidia becomes evident by wine-red and blue color staining, respectively.

As PAS identifies inner polysaccharides in the form of glycogen, (A) and (C) suggest an accumulation of glycogen in the subhymenial hyphal cells seen, as wine-red stained granules and Mayer's hemalum indicates presence of basophilic material within the probasidia stained as dark blue as shown in (B) and (C).

Conclusion

Fruiting body development of *C. cinerea* is a complex process of tissue generation and differentiation that follows a strict time course. We used five different histochemical stains to better visualize these processes underneath the microscope. Staining can discriminate tissues and cells in fruiting body primordia from each other and different dyes can variably focus on distinct cells.

Appendix

The family of NWD2 proteins in *Coprinopsis cinerea:* roles in development

Shanta Subba, Weeradej Khonsuntia, Ursula Kües

Georg-August-University of Göttingen, Büsgen-Institute, Molecular Wood Biotechnology and Technical Mycology, Büsgenweg 2, D-37077 Göttingen, Germany

The heterothallic basidiomycete *Coprinopsis cinerea* is an excellent model to study fruiting body development in the Agaricomycetes. In its life cycle, fruiting normally occurs on the dikaryon and follows a conserved scheme defined by day and night phases, with well predictable distinct stages over the time. Fruiting starts with primary hyphal knot formation in the dark, followed by light-induced aggregation into compact round secondary hyphal knot in which stipe and cap tissues differentiate. Primordia development (stages P1 to P5) takes five days to culminate on day 6 of development in karyogamy (K) and meiosis (M) within the basidia and subsequent basidiospore production which parallels fruiting body maturation (stipe elongation and cap expansion). Fruiting bodies are fully opened in the last night phase to shed their spores while at the morning on day 7 the cap autolyses to release the majority of the spores in liquid droplets that fall to the ground. Strain AmutBmut is a special homokaryotic mutant with defects in the *MatA* and *MatB* mating type loci why it mimics a dikaryon. The strain is able to fruit like a dikaryon despite of having only one type of haploid nuclei in its cells. This makes AmutBmut an unique strain to study the genetics of fruiting. Mutants in fruiting can easily be generated in this strain.

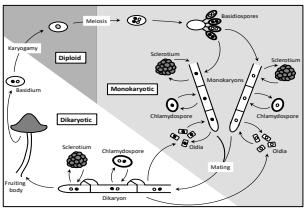

The heterothallic life cycle of *Coprinopsis cinerea*

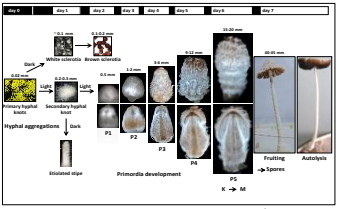

Fruiting body pathway of homokaryon AmutBmut on YMG/T agar plates

AmutBmut

Proto 159

Proto159 is an AmutBmut mutant which has an unidentified defect in primary and secondary hyphal knot formation and can thus not form fruiting bodies. The mutation has been suppressed by the transformation of a gene of the *NWD2* family. *NWD2* genes encode proteins with a NACHT domain, an evolutionary conserved domain that serves in signal transduction and is named after four different types of P-loop NTPases (NAIP, CIITA, HET-E and TP1). NACHT domains are found in fungal, animal and bacterial proteins.

The NACHT domain in the NWD2 protein suppressing the defect in Proto159 is located in the N-terminal half of the protein. The NACHT domain has the typical NTP binding site (P-loop, Walker A motif), a Walker B motif, a charged amino acid at a specific conserved position, a GRRxE motif, and a GxP motif of STAND NTPases.

Genome searches in *C. cinerea* found in total 36 different *NWD2* genes. All the encoded proteins have their NACHT domains at their N-termini while these have been fused to variable C-terminal halves. Functions for most of the C-termini are not known. However, tandem WD40 repeats are present in the C-termini of some of the NWD2 proteins.

The suppression effect of a mutation in fruiting body initiation in *C. cinerea* by a *NWD2* gene suggests that their presence are influential in the regulation of developmental pathways. We have sub-grouped the 36 different copies of NWD2 proteins in *C. cinerea* into 9 different sub-families (A to I) which cluster as groups at different positions in an evolutionary tree of fungal NWD proteins. Accordingly, duplication and modification of NWD2 proteins have taken place in the fungus.

We have sub-cloned so far five of the eight different *NWD2* genes from group A in order to test these after transformations of the fungus for effects on sexual and asexual developmental processes.

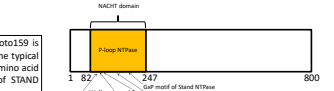

Structure of the NWD2 protein acting as a suppressor in Proto159

Most interestingly, genes of the *NWD2* family are found only in some genomes of the sequenced Agaricomycetes. So far, we observed *NWD2* genes only in Agaricales (*Amanita muscaria, Agaricus bisporus, C. cinerea, Moniliophthora roreri, Galerina marginata, Gymnopus luxurians, Hebeloma cylindrosporum, Hypholoma subtartitrum, Hysizygus marmoreus, Laccaria amethystina* and *Laccaria bicolor).*

The *NWD2* genes do not cluster by phylogeny in the same manner as the fungal species. Therefore, the origin of the *NWD2* genes remains currently unclear. The phylogenetic tree of the NWD2 proteins from the different fungal species indicates that *NWD2* genes were usually multiplied during speciation.

Structures of group A of NWD2 proteins in *Coprinopsis cinerea* (coloured regions indicate corresponding domains, white areas variable regions; the protein with suppressor function in Proto159 is shown at the top left; a star indicates sub-cloned genes)

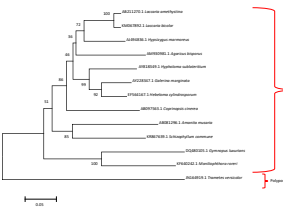

Phylogenetic relationship of fungal species as determined by ITS sequence analysis

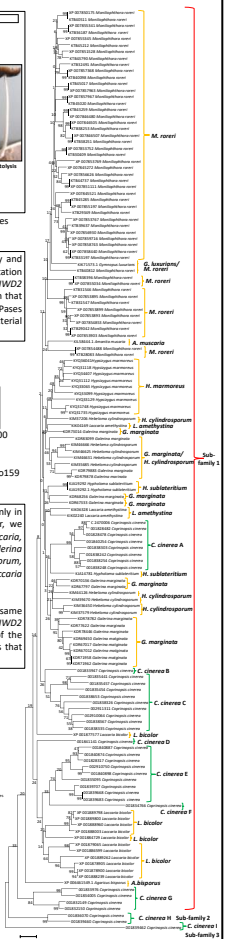

Phylogenetic relationship of NWD2 proteins from Agaricales

Appendix

Environmental and genetic control of the coordinated process of fruiting body development in *Coprinopsis cinerea*

Shanta Subba, Ursula Kües

Georg-August-University of Göttingen, Büsgen-Institute, Molecular Wood Biotechnology and Technical Mycology, Büsgenweg 2, D-37077 Göttingen, Germany

Fruiting body development in the saprotrophic fungus *Coprinopsis cinerea* follows a conserved scheme defined by day and night phases, with well predictable distinct stages over the time. Starting with hundreds of initial structures, every day some will be given up in development in favour of only a few to eventually mature. Fruiting starts with primary hyphal knot (PK) formation in the dark, followed by light-induced formation of compact aggregates, secondary hyphal knots (SKs) in which stipe and cap tissues differentiate. Primary hyphal knots are transformed into oval to globular sclerotia under further incubation in the dark. These are multicellular resting bodies covered by an outer melanized rind and they have an inner medulla with thick-walled chlamydospore-like cells. Primordium development (P1 to P5) takes five days to culminate on day 6 of development in karyogamy (K) and meiosis (M) within the basidia and subsequent basidiospore production which parallels fruiting body maturation (stipe elongation and cap expansion). Mature fruiting bodies autolyse on day 7 to release the spores in liquid droplets. The developmental pathway of the fungus is regulated by factors such as light, temperature, humidity and nutrients. Light signals are essential to induce formation of SKs, differentiation of tissues within the growing primordia and karyogamy within the basidia. Without light, so-called "dark stipes" are formed from SKs with elongated stipes and underdeveloped caps. Aeration is a new key factor we show here to influence the morphological development of the fungus.

Fruiting pathway of *Coprinopsis cinerea*

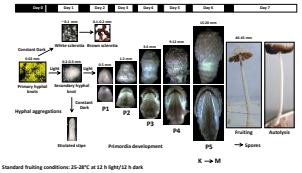

Standard fruiting conditions: 25-28°C at 12 h light/12 h dark

Primordia development under standard fruiting conditions

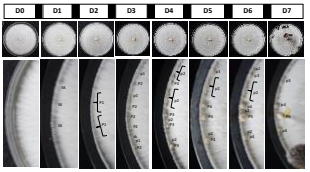

Actively growing structures are marked SK (secondary hyphal knot), P1 to P5 (primordia stages), FB (fruiting body) and p1 to p5 (aborted structures). D0 is the day of shifting plates from 37°C into standard fruiting conditions. D1 to D7 refer to days of development under standard fruiting conditions.

Effect of aeration on mycelial gowth

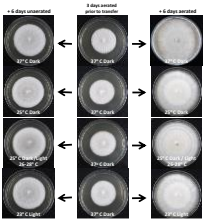

Half-grown fungal cultures incubated 3 days at 37°C at dark condition were air blocked using parafilm and then kept at different light and temperature conditions. Unsealed controls were in parallel grown with the sealed plates.

Inhibiting passage of air into cultures delayed further growth of fungi at all tested conditions and eventually stopped the fungal growth.

Blocking of air effects fruiting development

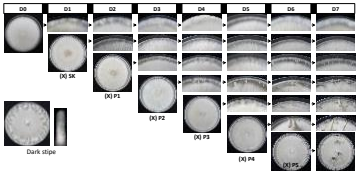

(X) SK and (X) P1 to (X) P5 indicate plates air blocked at secondary hyphal knot and P1 to P5 primordia stages, respectively. D1 to D7 refer to days of development under standard fruiting conditions (12 h light and 12 h dark rhythm). Arrows mark the rows of development over the times (days) in plates after the day of sealing.

Effects of lack of air were observed on the morphology of primordia during their developmental process. 5 days fully grown mycelia on agar plates incubated at 37°C under dark conditions were transferred into standard fruiting conditions. On every day of further incubation, subsets of plates were sealed after 4–6 h in light using parafilm. Hindering air entry before light-induced formation of SKs fully blocks fruiting and results in the formation of fluffy mycelial growth. When SKs have been formed prior to blockage of air, development arrests at the P1 stage. Block in aeration at P1 to P3 leads to outgrowth of elongated stipes that are similar to the structures observed in aerated cultures kept fully in the dark (known as "dark stipes" or "etiolated stipes"). When plates are air-sealed on the day of the P4 or the P5 stage, fruiting body maturation happens but caps are colourless by reduced spore numbers. The observations suggest that meiosis and basidiospore formation following karyogamy will need good aeration.

Primordia grown under standard (A) and air-blocked conditions (B)

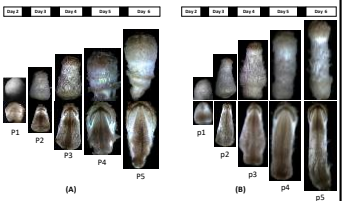

P1 to P5 and p1 to p5 are the primordia developed at aerated and unaerated conditions, respectively
Day 2 to Day 6 refer to days after transfer into standard fruiting conditions:
25-28°C under a 12 h light/12 h dark rhythm

Cultures fully grown at 37°C in dark were transferred into fruiting conditions under a 12 h light and 12 h dark rhythm. Every day after 4-6 h in light, subsets of plates were sealed using parafilm. Sealed plates with SKs arrested further development at P1. When plates were sealed however at the P1 or subsequent P stages, stipes abnormally elongated while the caps arrested in development.

Dark stipe mutants

Phenotype		Mutants	
		UV	60Coγ
No primary hyphal knots		147	141
No secondary hyphal knots		82	70
Arrest after	Secondary hyphal knots	12	0
	P1	17	9
	P2	8	8
	P3	25	47
	P4	45	48
	P5	67	25
Defect in	Stipe elongation	3	8
	Cap expansion	30	8
	Sporulation	73	0
Bonsai mushrooms		0	2
Other phenotypes		9	0
General Fitness affected		250	230

Pictures courtesy of Mamona Elaghamny

Blocks in development can be obtained over the whole fruiting pathway. However, in our collection of 1500 mutants with defects in fruiting, mutations do not evenly distribute in numbers over the complete developmental pathway. The first steps (PK, SK) and the P4 and P5 stages are more sensitive to mutations (see Table), possibly reflecting the complexity of the processes ongoing at these stages. Specific mutants form types of dark stipes under the standard fruiting conditions as wildtype cultures sealed at the P3 (Fig. C) and the P4 stage (Fig. D). They differ at the time in change of morphology from normal to dark stipe development from mutants with defects in light reception (Fig. A and B) which adopt at earlier stages (SK and P1) the abnormal phenotype.

Appendix

THE 9th INTERNATIONAL MEDICINAL MUSHROOMS CONFERENCE

24-28 SEPT 2017 PALERMO, ITALY

University of Palermo
Department of Agricultural, Food and Forest Sciences

How complex is a mushroom?

S. Subba[1], M. Winkler[1], U. Kües[1]

[1] Molecular Wood Biotechnology and Technical Mycology, University of Goettingen, Germany

General introduction

Mushrooms are commonly distinguished into edible, non-edible, medicinal, psychedelic and poisonous species which overlap in their categories and are known to produce a diverse array of bioactive compounds and metabolites of benefit for human health. Production of secondary metabolites and other bioactive molecules with potential pharmaceutical effects are often confined to the fruiting bodies [1,2] and even to specific tissues, cells and stages of development [3-8]. In general, little knowledge has yet been acquired on tissue-specific synthesis of bioactive compounds.

Fruiting bodies of Agaricomycetes are the most complex fungal structures which exist on earth. Mushrooms from different species distinguish very much in morphology, structure, types of tissues, numbers of different cell types produced and in the overall progress of development. However, fungal multicellularity, tissue formation and cell differentiation is so far little understood and observed [9]. Different developmental stages and different cells and tissues within a mushroom likely differ in their physiological conditions. Knowledge on such physiological differences can be crucial for basic exploitation of mushroom productions. To better understand the process of mushroom production and tissue differentiation, it is essential to first define the process of fruiting body development in easier to address species. The model species *Coprinopsis cinerea* is used here to study the cellular complexity during development and maturation of fruiting bodies. More than 10 different cell types are asserted to occur in this species during fruiting [9].

Fruiting pathway in *C. cinerea*

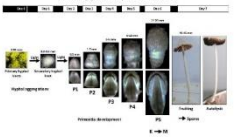

C. cinerea serves as a model fungus for the Agaricomycetes to study fruiting body development since it grows and fructs very fast in the laboratory, it takes seven days to obtain a matured mushroom from the vegetative mycelium under a normal day/night rhythm. Under standard fruiting conditions by fixed light-dark conditions (12 h light/12 h dark) at 25°C and high humidity, it is possible to predict by the hour of the day what is happening within the young developmental stages (secondary hyphal knot and subsequent primordial stages **P1, P2, P3, P4, P5**). We grow our fungus at 37°C for 5 days in the dark to then transfer the cultures in the afternoon into fruiting conditions to start the fruiting time course by a light signal implemented in the environmental shift [10].

Bioactive molecules of *C. cinerea*

C. cinerea is an edible mushroom with a good nutritional chemical composition and has likely also much more to offer in terms of medicinal potential. The fungi is known to produce secondary metabolites and other bioactive molecules [2].

Perennially interesting secondary metabolites of the fungus include sesquiterpenes as one type of volatile terpenes [11]. The violet pigment lagopodin with antimicrobial and human platelet anti-aggregative activities has been isolated from liquid cultures of *C. cinerea* [12, 13]. Microbial cultures of *C. cinerea* were in other studies be reported to give rise to pentalenene, α-muurolene, α-cuparenone (potential precursor of lagopodin) and ß-cadinen as main sesquiterpenes. Cuparene was found in the headspace of maturing fruiting bodies in a collection of 12 other set to identify sesquiterpenes. Six sesquiterpene synthase genes (*copJ* to *copS*) are identified in the sequenced mushroom *C. cinerea*. Encoded enzymes were reported in *Escherichia coli* to yield individual selections of different sesquiterpenes, among α-muurolene (a main compound of CopS, minor product of CopJ and CopQ), α-cuparene (the product of CopR), and ß-cadinen (a main compound of CopJ and CopQ and a minor product of CopS). The product range of CopR was enhanced from α-cuparene to its derivatives α-cuparophenol and α-cuparene by simultaneous expression in yeast of the cytochrome P450 monooxygenases Cox1 and Cox2 [11, 14]. Expression of the *cox1 - cox2* gene cluster on chromosome 9 in *C. cinerea* is in collective negatively controlled by the A mating type locus whereas CopS is expressed at homogamy early meiotic prophase primordia. Karyogamy is the hallmark of the P5 stage in the process of fruiting body development of *C. cinerea*. Upon karyogamy, fruiting bodies mature by stipe elongation and cap expansion [9] during which cuparene is emitted.

The species furthermore produces galectins outer-tissue specific in stipes and caps, ß-galactoside-binding lectins with entomo- and nematotoxic activities. CGL2 is among fruiting-body specific lectin of the species with nematotoxic activities that binds to trisaccharides (N-glycans) [15, 16].

Bioactive compounds produced by *C. cinerea* and their genes			
Names	**Bioactivities**	**Genes**	**Bioactive products**
Volatile sesquiterpenes	Antimicrobial, human platelet antiaggregation activities, antimalarial, antioxidant, antitumor, antiinflammatory, antifungal	Cop1, Cop7	ß-Elemene, ß-cadinene, germacrene D, α-muurolene, α,ß-cuparene
		Cop3	α-Muurolene, ß-elemene, γ-muurolene, germacrene D, α-cuparene, ß-cadinene
		Cop4	ß-Cadinene, ß-cuparene, ß-cadelene, germacrene D, patchoula oxidoxi
		Cop5	
		Cop6	α-Cuparene
		Cop5+Cop1	α-Cuparene, α-cuparene
		Cop5+Cox2	α-Cuparenone, α-cuparophenol, α-cuparene
		Cop6+Cox1+ Cox2	α-Cuparenone, α-cuparophenol, α-cuparene
Galectin	Entomo- and nematotoxic activities	CGL2	ß-Galactoside-binding lectin
ß-Trefoil lectin	Nematotoxic	CCL2	N-Glycan binding lectin

Primordia development under standard fruiting conditions

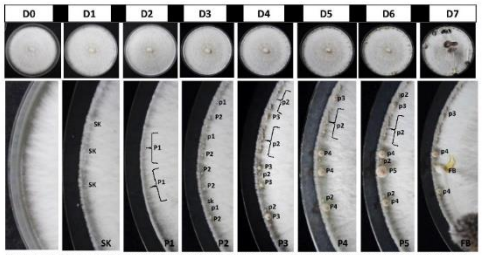

Actively growing structures are marked **SK** (secondary hyphal knot), **P1** to **P5** (primordia stages), **FB** (fruiting body) and aborted structures **p1** to **p5**. **D0** is the day of shifting plates from 37°C into standard fruiting conditions. **D1** to **D7** refer to days of development under standard fruiting conditions.

Stages of fruiting body development in *C. cinerea*

Fruiting body formation is a very complex process which in *C. cinerea* follows a highly conserved scheme defined through light regulation by day and night phases.

Fruiting starts in the compatient vegetative mycelium with loosely aggregated primary hyphal knots (**PKs**) formed in the dark, followed by light-induced compact aggregates called secondary hyphal knots (**SKs**) in which stipe and cap tissues differentiate.

The fruiting body developmental process in *C. cinerea* is endocarpic as primordia with individual cap and stipe tissues develop from the inside of secondary hyphal knots **(D1)**. **SKs** further develop to first stage primordia **P1 (D2)** (approx. 0.5 mm size), round in shape, off white in color and with a clear cap differentiation. When dissected vertically **P1** shows an imprint of a tiny mushroom.

Primordium **P2** stage developed at the next day **(D3)** is pear-shaped, 1-2 mm in size with internally distinguishable cap, stipe and basal regions. Gill rudiments are formed at the **P2** stage.

At day 3 **(D3)**, the primordium stage **P3** attained a teerte shape and looks smooth on the surface. Two types of gills, primary and secondary gills arise form gill rudiments. **P3** primordia grow more rapidly and elongate to reach the **P4** stage on day 4 **(D4)** a size of 2-3 mm.

In structure **P4 (D5)**, all main tissues are established. A light signal is received to induce karyogamy in basidia. Structural **P4** further elongates and grows into a size of about 5-7 mm to look like a clavibelt **(P5 stage)** on the next day **(D6)**.

Karyogamy **(K)** occurs at the fully established light-bulb shaped **P5** stage in the basidia. Meiosis **(M)** follows and basidiospore production. In parallel, rapid stipe elongation and cap expansion take place. Fruiting bodies are fully matured shortly after midnight in the next night phase. Mature fruiting bodies autolyse in the morning on day 7 **(D7)** to release the spores in liquid droplets.

Here we present first overviews on the tissue structures of the **P4** and the **P5** stage.

Tissues at stage P4

A: Longitudinal and B, C: cross sections of the primordial stage **P4**.

At the P4 stage, the primordium is still covered by a closed outer veil of larger cells of a loose hairy appearance. Beneath the veil is the the pileipellis as outer cap layer (stained darker blue) of smaller densely aggregated hyphae. The inner pileus tissue is made of larger hyphae in a loose plectenchyma which continues into the inner regions of the primary and secondary gills. The primary gills are partially and the secondary gills fully covered by a rigid band of hymenial tissues of denser hyphae which provides structural support to the basidia where later the spores are formed. At the P4 stage, the outer hymenial layer is characterized by an uniform layer of similar sized parallel palisade cells (protoxidia) with some intermingled longer inflated cells presenting young fixed cystidia protruding into the free gill space.

A narrow layer of hyphae clearly distinguishes the cap from the apex of the stipe and a loosely arranged tissue overs the stipe and connects the stipe with the uncovered edges of the primary gills. The inner hyphae of the stipe run vertically in parallel over the length of the stipe.

Methods

Cultivation. For synchronized fruiting, we inoculated strain AmutAmut at evenings (12 h) onto YMG/T agar for growth at 37°C in lightproof ventilated boxes. Fully grown plates were transferred 5 days later at the respective hour into fruiting conditions: 12 h light/12 h dark at 25°C [10].

Harvest and embedding of structures. Active primordia stages were harvested in the morning hour (9 h) and fixed in series in solutions of 3*-4% formaldehyde, 2*-99% acetic acid and 3*-70% ethanol each for 1h at RT. For dehydration, the samples were then transferred into a series of ethanol (methylated) solutions of increasing concentration (40%, 60%, 90%, and 96%) and incubated each time for 1 hour at RT. This was followed by 3x infiltration using the hydrophobic agent Rot-Histol to eliminate ethanol, incubating each time for 45 min at RT and finally transferring samples into pure Roti-Histol overnight at RT. Next, the samples were transferred into fresh pure Roti-Histol and incubated for 3 hours. Finally the samples were incubated overnight at 30°C in a saturated solution of Roti-Plast in Roti-Histol. Further, the samples were embedded with melted Roti-Plast at 60°C and incubated overnight. Embedded samples were cut using a rotation microtome (R. Jung, Heidelberg) and both longitudinal and transverse sections of primordia of a thickness of 5 µm and of 10 µm were made. The sections were floated on warm drops of distilled water placed on slides and dried on a hot block. Wax was completely eliminated from the tissue sections with Xylene solution, which was then removed with ethanol. Finally, samples were stained with lactophenol blue. Samples were microscoped and photographed.

Tissues at stage P5

A: Longitudinal and B to E: cross sections of the P5 stage.

At the P5 stage, the cap and stipe are stretched in length and the veil became disconnected between cap and stipe. The stipe increased in diameter by cell inflammation, thereby spreading the gills radially outward. The gills also increased in length and width, with the inner band of loose parallel running hyphae. A closer look at the hymenial regions shows the arrangement of young fertile basidia **(Ba)** and sterile cystidia **(Cd)** on the surface and sterile hyphidia (paraphyses) growing newly from a deeper hymenial tower in between the layer of basidia **(He)**. Cystidia attach to a cell on the surface of the opposite hymenium and this cells converted into cystosia **(Cs)**

References

[1] Wasser (2002) Appl Microbiol Biotechnol 60: 258-274; [2] Kües & Badalyan (2017) In Agrowal (ed) Medicinal plants and fungi - Recent advances in research and development. Springer, Berlin, in press; [3] Hulbert J et al. (1999) Comput Biol Acad Sci Sec III 322: 859-863; [4] Walser et al. (2005) Fungal Genet Biol 42: 293-305; [5] Luan et al. (2010) Fungal Biol 114: 509-606; [6] Plaza et al. (2014) BMC Genom 15: 492; [7] Pfiz et al. (2012) J Sci Food Agric 92: 2564-2567; [8] Liu et al. (2014) Proc Natl Acad Sci USA 11: E4761-E4767; [9] Kües & Navarro-Gonzalez (2015) Fungal Biol Rev 29: 63-97; [10] Kües et al. (2016) In Baars & Sonnenberg (eds) Science and cultivation of edible fungi. Int Soc Mushroom Sci, pp 319-322; [11] Agger et al. (2009) Proc Nat Microbiol 72: 11383-1195; [12] Buchal & Derbyshire (1975) Phytochem 15: 2004; [13] Lorenzen & Anke (1998) Curr Org Chem 2: 329-364; [14] Lopez-Gallego et al. (2015) ChemBioChem 15: 1063-1066; [15] Walser et al. (2004) Structure 12: 689-700; [16] Tito et al. (2009) J Biol Chem 52: 36223-36233.

P loop-NTPases in developmental processes of *Coprinopsis cinerea*

Shanta Subba, Weeradej Khonsuntia, Sarina von Wensierski, Ursula Kües

Georg-August-University of Göttingen, Molecular Wood Biotechnology and Technical Mycology, Büsgenweg 2, D-37077 Göttingen, Germany

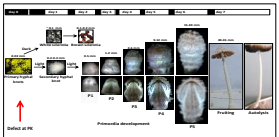

Fruiting body development of *C. cinerea*

The self-compatible homokaryotic strain AmutBmut with defects in both mating-type loci is a mutant of *Coprinopsis cinerea* ideal for studying fruiting body development. Proto159 is a mutant of AmutBmut obtained by protoplasting and regeneration of asexual aerial spores (oidia). It has a defect in the formation of primary hyphal knots (PK) as a step prior to light-regulated fruiting body development and alternatively in sclerotia formation in the dark. Proto159 has a somewhat slower growth rate than AmutBmut. It pigments the mycelium and the agar beneath dark-brown. The mutation in Proto159 was found to be suppressed by transformation of a specific gene that belongs to the *NWD2* family.

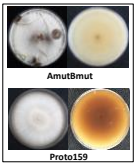

AmutBmut **Proto159**

NWD2 genes encode proteins with a NACHT domain, an evolutionary conserved domain that serves in signal transduction and is named after four different types of P-loop NTPases (NAIP, CIITA, HET-E and TP1). NACHT domains are found in fungal, animal and bacterial proteins. However, few of the Agaricales have genes for NWD2 proteins. Species tend to contain paralogous genes whose products group together in the phylogenetic tree shown to the right.

The NACHT domain in the NWD2 protein suppressing the defect in Proto159 (**protein 2** in group A in the phylogenetic tree below) is located in the N-terminal half of the protein. The NACHT domain has the typical NTP binding site (P-loop, Walker A motif), a Walker B motif, a charged amino acid at a specific conserved position, a GRRxE motif, and a GoP motif of STAND NTPases. The C-terminus of the protein in contrast has no known domain.

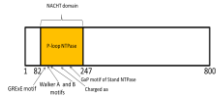

Structure of NWD2 acting as suppressor in Proto159

NWD2 genes in Agaricales	
1	*Amanita muscaria*
2	*Agaricus bisporus*
3	*C. cinerea*
4	*Moniliophthora roreri*
5	*Galerina maginata*
6	*Gymnopus luxurians*
7	*Hebeloma cylindrosporum*
8	*Hypholoma sublateritium*
9	*Hypsizygus marmoreus*
10	*Laccaria amethystina*
11	*Laccaria bicolor*

Genome searches in *C. cinerea* found in total 36 different *NWD2* genes. All the encoded proteins have their NACHT domains at their N-termini while these have been fused to variable C-terminal halves. Functions for most of the C-termini are not known. However, tandem WD40 repeats are present in the C-termini of some of the NWD2 proteins (Group: C).

The suppression effect of a mutation in fruiting body initiation in *C. cinerea* by a *NWD2* gene suggests that their presence are influential in the regulation of developmental pathways. We have grouped the 36 different copies of NWD2 proteins in *C. cinerea* (A to G) which cluster as groups at different positions in an evolutionary tree of fungal NWD2 proteins. Accordingly, duplication and modification of NWD2 proteins have taken place in the fungus.

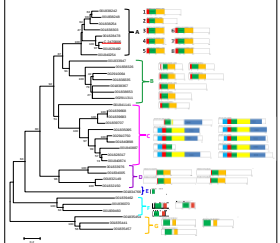

Phylogenetic tree of NWD2 proteins and structures of groups A to G proteins in *Coprinopsis cinerea*
Coloured regions indicate corresponding domains of similar sequence, white areas regions of variably unique sequence.

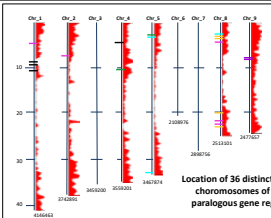

Location of 36 distinct *NWD2* genes on different chromosomes of *C. cinerea* in relation to paralogous gene regions (strain Okayama 7)

Bars at different chromosomes of same color correspond to groups of *NWD2* genes in the phylogenetic tree of NWD2 proteins of *C. cinerea* shown at the left.

Genes are clustered relatively close to the less conserved telomeric regions of different chromosomes, within regions that are rich in paralogous genes. Also, many genes are seen to accumulate on the shortest chromosome 13 which as compared to other Agaricales is a poorly conserved and thus possibly the newest chromosome.

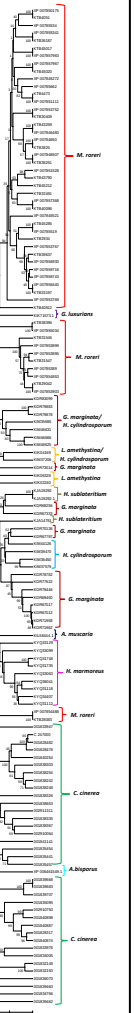

Transformation of Proto159

After addition of pure sterile water to fully grown Proto159 cultures, oidia harvested in the supernatant which is stained brown by fungal pigments. However, the oidia can still be used for transformation using vector pPAB1-2 to complemment the *pab1* auxotrophy of the strain.

Proto159 **Oidia**

All transformed *NWD2* genes led to changes in phenotypes of Proto159.
In particular introduction of genes 2 and 4 of group A (see phylogenetic tree with NWD2 proteins models to the left side) altered mycelial properties, blocked the brown staining of mycelium and the agar, and, most importantly, induced primary hyphal knot and sclerotia formation in the vegetative mycelium.

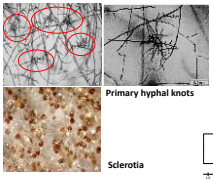

Primary hyphal knots

Sclerotia

Phenotypes of transformants

NWD2 genes transformed	Number of Transformants		
	Proto159	AmutBmut	Growth restricted
pPab (control)	30	1	--
Gene 2	15	15	--
Gene 4	12	2	10
Gene 5	2	--	3
Gene 6	2	12	7
Gene 7	6	2	13
Gene 8	--	1	3

For genes 2 to 8 see phylogenetic tree above

Insights into protein functions during primordia development of *Coprinopsis cinerea* through proteomics analyses

A. Majcherczyk*, S. Subba*, B. Dörnte*, W. Khonsuntia, M. Zomorrodi, M. Winkler and U. Kües

Büsgen-Institute, Section of Molecular Wood Biotechnology and Technical Mycology,Georg-August-Universität Göttingen, Büsgenweg 2, 37077 Göttingen (* equal contributions)

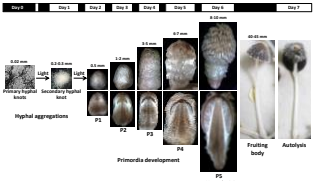

Fig. 1 Fruiting pathway of *C. cinerea* strain AmutBmut

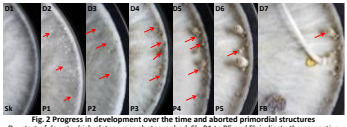

Fig. 2 Progress in development over the time and aborted primordial structures
D = start of day at which plates were photographed. Sk, P1 to P5 and Fb indicate the respective developmental stages reached at photography. Arrows point to structures aborted a day before.

Introduction

Fruiting body development of *Coprinopsis cinerea* takes place at 25 °C under a 12 h day/12 h night regime in a highly synchronized pattern. It starts by intense local hyphal branching with the production of primary hyphal knots (Pks) in the dark which are transferred into hundreds of light-induced secondary hyphal knots (Sks). Subsequent primordium development (P1 to P5) takes five days and is also light controlled. Every day, subsets of structures are given up in development in favour of only a few that continue in development and eventually mature. At stage P5 on day 6 of development, karyogamy (K) and meiosis (M) happen within the basidia followed by basidiospore production and parallel fruiting body maturation (stipe elongation and cap expansion). Mature fruiting bodies autolyse on day 7 to release the spores in liquid droplets.

Primordia are complex multicellular structures with different types of cap and stipe tissues and several kinds of cells of distinct functions. All basic tissues are fully developed at primordial stage P4. Tissues stain differentially strong with lactophenol blue, such as veils, pileipellis, inner pileus, hymenia on gills, and stipe. PAS-Mayer's hemalum double-staining shows more explicitly the arrangement of primary and secondary gills in the cap, with pink-stained subhymenia, paraphyses in bright pink in between the blue-stained prosbasidia. Hemalum further stained veil, pileipellis, pileus and gill trama and the stipe blue.

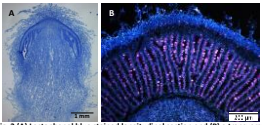

Fig. 3 (A) Lactophenol blue stained longitudinal section and (B) a transverse section double stained by PAS-Mayer's hemalum of a P4 stage primordium

Proteomic analyses during development of primordia stages P1 to P4

Fig. 4 Venn-diagramm of proteins identified by LC-MS/MS in stages P1 to P4 by at least two distinct peptides with confidence of 99%

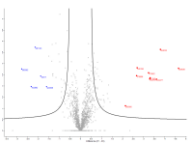

Fig. 5 Volcano plot analysis of label free quantified (LFQ) proteins of stage P1-P2

Proteomic analyses of liquid droplets excreted by primordia

During development, primordia actively excrete liquid from the pileipellis which slowly rolls off the veil cells for possible surface cleaning to collect in droplets at the base of the stipe where they remain and possibly grow during further development until the mushrooms are mature and droplets may roll onto the vegetative mycelium. The droplets contain characteristic proteins. Up to 318 proteins in total and 142 different proteins with N-terminal secretion signals were detected in droplets from stages P1 to P4. Protein analysis shows that these serve or may serve in defense against various biotic threats.

Fig. 6 P1 to P4 primordia with multiple liquid droplets

Fig. 7 Liquid droplets from P3 (left) and water (right) on A. mycelium and B. Parafilm (each 5 µl volume)

Table 3 Number of proteins identified in the droplets from stages P1 to P4

Stage	Total proteins	Proteins with N-terminal secretion signal
P1	187	109
P2	273	131
P3	318	142
P4	232	128

Observations:

- 144 proteins were shared between droplets from all stages of which 121 have an N-terminal secretion signal.
- The three galectins Cgl1, Cgl2 and Cgl3 of *C. cinerea*, Ccl1, Ccl2 and a third lectin of a family of 5, a mucin binding lectin Cml1, serine protease inhibitor copsin 1 and another member of a family of 7 were also found in this group. All these proteins are known defense proteins with effects against either nematodes, insects or bacteria (Sabotic *et al.* 2016).
- Other proteins in the droplets also present members of larger protein families and are also candidates for defense with potential bacterial, fungicidal, insecticidal or nematicidal functions.
- As another hallmark of defense proteins, homologs often distribute irregularly over basidiomycetes or also ascomycetes with no visible pattern of regular evolution.
- Several of the proteins were found induced in vegetative mycelium when confronted with bacteria , e.g. the single WSC domain protein of *C. cinerea* (Kombrink *et al.* 2018).
- Remarkedly, hydrophobins were not found in the droplets.

[Refs.: Sabotic *et al.* (2016) AMB 100:91-111; Kombrink *et al.* (2018) ISME J 13:588-602]

In total, about 2870 single proteins were identified by LC-MS/MS analysis. Most of the fruiting-body-related proteins were detected in one or more of the four analyzed primordia stages. More than one-half of the proteins (1401) were shared by all stages. Using a stage-by-stage volcano-plot analysis showed only minor changes in protein amounts for the majority of detected proteins between stages P1 to P4.
The compact stage P1 with first cap and stipe tissue differentiations had the highest number of unique proteins. Among were proteins linked to basic carbohydrate metabolisms, mitochondria function, vitamin B6 production, nitrogen metabolism, fatty acid metabolism, phosphatases, signaling (MAP2K; G protein subunits), membranes (flotillin), and vesicular transport (Arf6). Several hydrophobins and two fungal proteins of unknown function (DUF4449) are much increased in amounts from P1 to stage P2 when primary gills grow into the gill cavity, air channels arise in loosened stipe and pileus tissues and the veil layer becomes more massy. Very little change in protein amounts was found from P2 to P3 when tissue growth and differentiation continue seemingly unaltered between the two stages. Significant changes in protein amounts were detected again in stage P4 and concerned among other functions putative defense proteins such as a cerato-platanin-like protein, a ricin B-like and a mucin-binding lectin. Mei2 as essential protein for pre-meiotic S-phase (light-induced at P4) and commitment for meiosis was one of the proteins unique to the P4 stage.

ProteinID	Difference	Gene name	Putative function
		P1→P2	
500636	4.647223	-	Fungal, DUF4449
404033	3.786639	*coh27*	Hydrophobin
433477	3.605709	-	Fungal, DUF4449
47183	3.295866	*coh26*	Hydrophobin
443707	3.282811	*coh18*	Hydrophobin
370922	3.22369	*coh21*	Hydrophobin
445156	2.685221	*coh32*	Hydrophobin
380326	2.66575	*coh34*	Hydrophobin
369380	2.132014	-	Rossmann-fold NAD(P)(+)-binding protein
		P2→P3	
440168	1.798962	-	Kynurenine 3-monooxygenase
438486	1.444729	-	DUF4243 (quastin oxidase family)
		P3→P4	
408843	2.568906	-	Cerato-platanin-like
495335	2.479759	-	Ricin B lectin
356460	2.195266	-	ABC transporter, SunT superfamily
439037	2.157768	*cml1*	Mucin-binding lectin 1
370922	2.093503	*coh21*	Hydrophobin
433477	1.911105	-	Fungal, DUF4449
423716	1.787971	-	Linoleate_diol_synthase_like
546783	1.70201	-	*C. cinerea* specific protein
380508	1.58911	-	Chloroperoxidase

Table 1 and 2 Proteins identified on a stage-by-stage analysis with at least three fold difference in protein amounts (red: upregulated, blue: downregulated)

ProteinID	Difference	Gene name	Putative function
		P1→P2	
363062	-2.8	-	Broad spectrum L-amino oxidase 4
422592	-2.3	-	Rare fungal protein fam. 1
481143	-2.2	-	Rare fungal protein fam. 2
10617	-1.9	-	Peptidase (S8 and S53), PA, PsS1_like fungal subtilase
422636	-1.6	-	Rare fungal protein fam. 1
		P2→P3	
500636	-2.0	-	Fungal, DUF4449
376383	-1.6	-	Alpha-trehalase
		P3→P4	
451504	-2.1	-	Putative elongation factor 3
440168	-1.6	-	Kynurenine 3-monooxygenase

Acknowledgements
Proteomics studies were facilitated through support for a TripleTOF 5600+ mass-spec by the German Science Foundation (DFG grant no. 24946052).

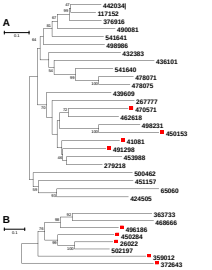

Fig. 8 A. Peptidase M43B and B. fungalysins families
Marked in red: proteins found in liquid droplets

Table 4 Selection of protein families with members present in primordia droplets

Protein type	No. in droplets	Total in *C. cinerea*
Peptidase S8 and S53, subtilisin	3	7
Peptidase M36, fungalysin	5	8
Peptidase M43B	4	25
Chitinase	3	8
Chitin deacetylase	2	16
β-*N*-Acetylhexosaminidase	1	2
Glucan 1,3-β-glucosidase	2	2
Glucan 1,4-β-glucosidase	2	3
FAD-Oxidoreductase, berberine-like	2	17
GMC-oxidase	6	26
Glyoxal oxidase	2	6
Cupredoxin	2	9
Laccase	2	17
Tyrosinase	2	19
Copsin	2	7
Galectins	3	3
Ccl1-like	3	5
Ricin B-like with N-terminal secretion signal	4	17
Cerato-platanin-like	2	5
Rare fungal protein family 1	1	3
Rare fungal protein family 2	1	3
Mannoprotein family	2	4

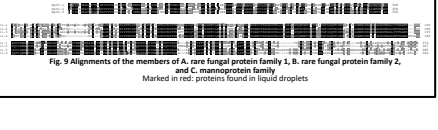

Fig. 9 Alignments of the members of A. rare fungal protein family 1, B. rare fungal protein family 2, and C. mannoprotein family
Marked in red: proteins found in liquid droplets

Appendix

Complexity in mushroom formation

Shanta Subba[1], Weeradej Khonsuntia[1], Botond Hegedüs[2], Andrzej Majcherczyk[1], Bastian Dörnte[1], Mojtaba Zomorrodi[1], Marco Winkler[1], Kiran Lakkireddy[1], Margarita Cemert[1], Laszlo G. Nagy[2], and Ursula Kües[1]

[1]Büsgen-Institute, Section of Molecular Wood Biotechnology and Technical Mycology, Georg-August-Universität Göttingen, Büsgenweg 2, 37077 Göttingen, Germany

[2]Synthetic & Systems Biology Unit, Institute of Biochemistry, Biological Research Center, Hungarian Academy of Science, H-6726 Szeged, Hungary

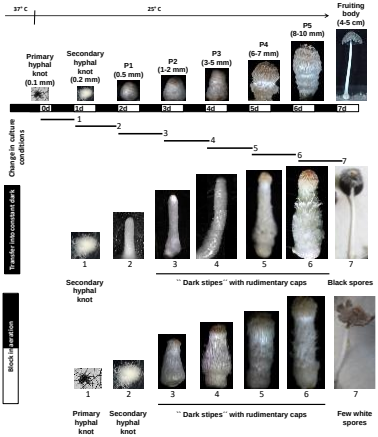

Fig. 1 Top: Fruiting pathway of *C. cinerea* AmutBmut under standard fruiting conditions (25° C, 12 h dark/12 h light, high humidity). Middle: Cultivation in constant dark at different days of development leads to the formation of abnormal stipes with an underdeveloped cap (``dark stipes``). Bottom: Block of aeration at different stages of development results in similar structures. 0d to 7d indicate number of days of cultivation. Lines 1 to 7 mark periods of cultivation change in conditions.

Environmental control of fruiting body developmrnt of *Coprinopsis cinerea*

Fruiting body formation of *Coprinopsis cinerea* follows a conserved developmental scheme defined by day and night phases, with well predictable distinct stages over the time (Fig. 1 Top). The differentiation process starts with the formation of loose aggregates in the mycelium in the dark. Upon a light signal, these primary hyphal knots (Pks) turn into compact secondary hyphal knots (Sks) in which stipe and cap tissues differentiate. Primordium development (P1 to P5) (Fig. 2) takes 5 days to culminate on day 6 of development in karyogamy and meiosis within the basidia. Subsequent basidiospore production parallels stipe elongation and cap expansion for fruiting body maturation. Mature fruiting bodies autolyze on day 7 to release the spores in liquid droplets.

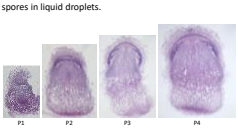

Fig. 2 Longitudinal sections of P1 to P5 primordia stages show tissues formation and differentiation during the course of development. The thickness of sections are 5 µm and are double stained by PAS and Hemalum (for detail of tissue staining please see Poster P59).

Fruiting body development in *C. cinereo* is strictly regulated by environmental conditions including nutrients, light, temperature and aeration. Failure in light signaling or in aeration leads to formation of so-called ``dark stipes``, under proliferation of stipe tissues and blocks in cap development.

Light: Cultivation in dark at different stages of development leads to the formation of abnormally extended stipes with underdeveloped caps. When light is blocked on Day 0 (on the day when Pks are formed and the culture is ready to be transferred into the fruiting conditions) after exposing cultures to light for a short time, Sks are formed on the following Day 1. Block in light at stages Sk, P1 or P2 leads to the formation of elongated stipes with poorly developed caps known as ``dark stipes``. When plates are at P3 and P4, elongated stipes are formed but the caps of the elongated primordia are more developed than those of the stages before. Blocking light at the P5 stage on Day 6 leads to the maturation of mushroom and autolysis happens shedding black stained spores in droplets (Fig. 1 Middle).

Air: Hindering entry of air before light-induced formation of Sks fully blocks fruiting and results in the formation of fluffy mycelial growth. When Sks have been formed prior to blockage of air, development arrests at the Sk stage. Block in aeration at P1, P2 or P3 leads to outgrowth of elongated stipes that are similar to the structures observed in aerated cultures kept fully in the dark. When plates are air-sealed on the day of the P4 or the P5 stage, fruiting body maturation happens but caps are poorly colored by lack of stained spores. Few white spores are produced (Fig. 1 Bottom). Keeping KOH in the sealed cultures restores formation of Sks and stopped out-growth of elongated stipes.

Dark stipe mutants

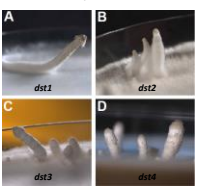

Phenotype		Mutants UV	Mutants REMI
No primary hyphal knots		147	141
No secondary hyphal knots		83	70
Arrest after	Secondary hyphal knots	12	0
	P1	12	9
	P2	8	8
	P3	25	47
	P4	46	49
	P5	67	25
Defect in	Stipe elongation	3	8
	Cap expansion	10	8
	Sporulation	73	0
Bonsai mushrooms		0	2
Other phenotypes		9	0
General fitness affected		250	230

From mutagenesis approaches of the self-compatible strain AmutBmut, high numbers of mutants with blocks in development are available from the early development up to stage P1, comparably few then from P2 to P3. Larger sets of mutants exist for P4 and P5 when karyogamy and meiosis have to occur in the basidia and fruiting body maturation has to be initiated. Mutant numbers may reflect the complexity of specific steps in fruiting. The same tendency is experienced in proteomics work by the number of proteins that changed in expression between the different developmental stages (please refer to Poster P58 for details). Here, we focus on the mutants that form ``dark stipes`` under standard fruiting conditions. Defects in four genes (*dst1* to *dst4*) cause such phenotypes.

Defects in *dst* mutants

The Japanase *dst1* and *dst2* mutants with defects in the WC1 white collar 1 photoreceptor and a FAD/FMN-containing dehydrogenase, respectively[1,2] are blind and form dark stipes under standard fruiting conditions at the Sk stage.

Strains 7K17 (*dst3*) and B1918 (*dst4*) have defects at the later stages P4 and P5, respectively. Whole genome sequencing identified each two interesting mutations in the mutants. 7K17 is defective in pyruvate dehydrogenase subunit E1 and in acetolactase synthase ILV2 , both of which are thiamine-dependent and release CO_2. B1918 lacks a functional citrate synthase. Both mutants therefore are blocked in feeding acetyl into the TCA cycle (see Fig. 3). B1918 has also a defect in the Cop9 signalosome (subunit CSN5) which coordinates light and respiratory activities with developmental processes[3-5] .

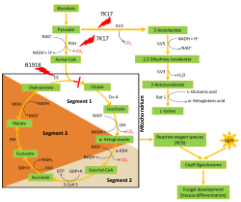

Fig. 3 Strains 7K17 (*dst3*) and B1918 (*dst4*) have blocks to the entry into the respiratory parts of the TCA cycle which require NAD⁺ and actely-CoA (Segment 1 from oxaloacetate to α-ketoglutarate; Segment 2 from α-ketoglutarate to succinate). Segment 3 from succinate to oxaloacetate may reverse under anaerobiosis[6] and under anaplerotic CO_2 fixation[7] via carboxylation of PEP and pyruvate. Such processes might happen in sealed cultures producing ``dark stipes``.

NWD2 genes for small NTPases as a suppressor proteins in an initiation defect of fruiting

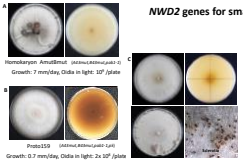

Fig. 4 A. Fruiting culture of homokaryon AmutBmut. B. A derived fruiting-defective mutant Proto159 prior and C. after transformation with an *NWD2* gene. Upon transformation, agar pigmentation is blocked and primordia or alternatively sclerotia might be produced.

Mutant Proto159 has a defect in the formation of primary hyphal knots (Pks) as a step prior to light-regulated fruiting body development and alternatively in sclerotia formation in the dark. Beneath its mycelium, Proto159 pigments agar dark-brown unlike its parental strain AmutBmut (Fig. 4). Developmental defects of mutant Proto159 were found to be variably suppressed by transformation of genes that belong to the *NWD2* family.

NWD2 genes encode proteins with a NACHT domain (Fig. 5), an evolutionary conserved domain that serves in signal transduction and is named after four different types of P-loop NTPases (NAIP, CIITA, HET-E and TP1). NACHT domains are found in fungal, animal and bacterial proteins. However, few species of the Agaricales have genes for NWD2 proteins (see Table 1).

Sequencing showed that a suppressing *NWD2* was not the defective gene in strain Proto159. Whole genome sequencing should be a strategy to identify responsible defective genes in Proto159 as above in mutant 7K17 and B1918.

Fig. 5 Structure of NWD2 protein acting as a supressor in Proto159

Table: 1

NWD2 genes in Agaricales	
1	Amanita muscaria
2	Agaricus bisporus
3	C. cinerea
4	Moniliophthora roreri
5	Galerina marginata
6	Gymnopus luxurians
7	Hebeloma cylindrosporum
8	Hypholoma sublateritium
9	Hydnopolyporus fimbriatus
10	Laccaria amethystina
11	Laccaria bicolor

References

[1] Kazuhisa Terashima et al. 2005; Genetics 171:101-108, [2] Masaki Kuratani et al. 2010; Fungal Genetics and Biology 47:152-158, [3] Martin Christmann et al. 2013; PLoS Genetics 9: e1003275, [4] Cardenas Monroy et al. 2017; PLoS One 12: e1718385, [5] L. Bernaude et al. 2019; Redox Biology 20: 533-543, [6] Oliver E. Owen et al. 2002; 277: 30405-30412 [7] Christos Chinopoulous 2013; 91: 1030-1043.